AD-778 766

ADVANCED, SMALL, HIGH-TEMPERATURE-RISE COMBUSTOR PROGRAM. VOLUME I. ANALYTICAL MODEL DERIVATION AND COMBUSTOR-ELEMENT RIG TESTS (PHASES I AND II)

S. C. Hunter, et al

AiResearch Manufacturing Company of Arizona

Prepared for:

Army Air Mobility Research and Development Laboratory

February 1974

DISTRIBUTED BY:

NTIS

National Technical Information Service
U. S. DEPARTMENT OF COMMERCE
5285 Port Royal Road, Springfield Va. 22151

DISCLAIMERS

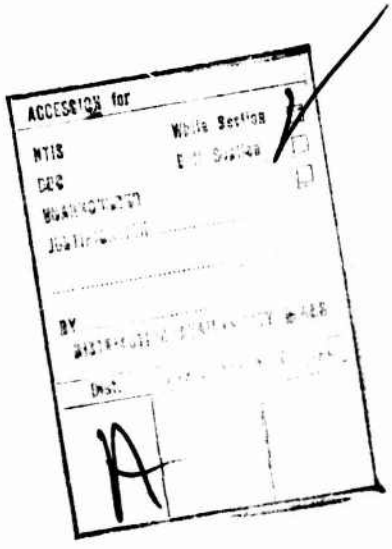
The findings in this report are not to be construed as an official Department of the Army position unless so designated by other authorized documents.

When Government drawings, specifications, or other data are used for any purpose other than in connection with a definitely related Government procurement operation, the United States Government thereby incurs no responsibility nor any obligation whatsoever; and the fact that the Government may have formulated, furnished, or in any way supplied the said drawings, specifications, or other data is not to be regarded by implication or otherwise as in any manner licensing the holder or any other person or corporation, or conveying any rights or permission, to manufacture, use, or sell any patented invention that may in any way be related thereto.

Trade names cited in this report do not constitute an official endorsement or approval of the use of such commercial hardware or software.

DISPOSITION INSTRUCTIONS

Destroy this report when no longer needed. Do not return it to the originator.



16

Unclassified
Security Classification

AD 778 766

DOCUMENT CONTROL DATA - R & D

(Security classification of title, body of abstract and indexing annotation must be entered when the overall report is classified)

1. ORIGINATING ACTIVITY (Corporate author)	2a. REPORT SECURITY CLASSIFICATION
AiResearch Manufacturing Company of Arizona A Division of The Garrett Corporation Phoenix, Arizona	Unclassified 2b. GROUP

3. REPORT TITLE

ADVANCED, SMALL, HIGH-TEMPERATURE-RISE COMBUSTOR PROGRAM
VOLUME I - ANALYTICAL MODEL DERIVATION AND COMBUSTOR-ELEMENT RIG TESTS
(PHASES I AND II)

4. DESCRIPTIVE NOTES (Type of report and inclusive dates)

Final Report

5. AUTHOR(S) (First name, middle initial, last name)

S. C. Hunter H. C. Mongia
K. M. Johansen M. P. Wood

6. REPORT DATE	7a. TOTAL NO. OF PAGES	7b. NO. OF REFS
February 1974	561	62

8a. CONTRACT OR GRANT NO.	9a. ORIGINATOR'S REPORT NUMBER(S)
DAAJ02-70-C-0060 b. PROJECT NO. c. Task 1G162203D14413 d.	USAAMRDL Technical Report 74-3A 9b. OTHER REPORT NO(S) (Any other numbers that may be assigned this report)

10. DISTRIBUTION STATEMENT

Approved for public release; distribution unlimited.

11. SUPPLEMENTARY NOTES	12. SPONSORING MILITARY ACTIVITY
Volume I of a 2-volume report.	Eustis Directorate, U. S. Army Air Mobility Research and Development Laboratory Fort Eustis, Virginia

13. ABSTRACT

This report describes an analytical and experimental study of advanced, small, high-temperature combustors. The objectives of the 32-month program were (a) to develop and validate an analytical design technique for small, high-temperature-rise, low-airflow combustors and related components, and (b) to define the limitations associated with these small combustors and related components and the effects of these limitations on the cycle and the configuration of advanced-technology engines.

Analytical models were developed to predict the characteristics and performance of the basic combustor elements, including fuel injection, primary zone, dilution zone, and liner cooling. Nine combustor element rig test programs were conducted to provide data to update and validate the analytical models. Based on the analysis and rig test results, a full-scale combustor was designed, fabricated, and tested. An ancillary material screening program was conducted to select the most suitable existing material for combustor application. A relatively new material (IN-586) was selected. Material-property tests were conducted to supplement published data for this material.

The analytical models were used to assess combustor design and performance limitations and the applicability of the design techniques over an airflow range of 2 to 5 pounds per second, cycle pressure ratio range of 10 to 16 (including recuperation), and a turbine inlet temperature range of 2300°F to 2700°F.

Reproduced by
NATIONAL TECHNICAL
INFORMATION SERVICE
U S Department of Commerce
Springfield VA 22151

DD FORM 1 NOV 68 1473 REPLACES DD FORM 1473, 1 JAN 64, WHICH IS OBSOLETE FOR ARMY USE.

Unclassified
Security Classification

14. KEY WORDS	LINK A		LINK B		LINK C	
	ROLE	WT	ROLE	WT	ROLE	WT
Gas turbine engine Annular combustor Analytical combustor design Fuel injection						

ia

DEPARTMENT OF THE ARMY
U. S. ARMY AIR MOBILITY RESEARCH & DEVELOPMENT LABORATORY
EUSTIS DIRECTORATE
FORT EUSTIS, VIRGINIA 23604

The research described herein was conducted by AiResearch Manufacturing Company of Arizona, a Division of the Garrett Corporation, under Contract DAAJ02-70-C-0060. The work was performed under the technical management of Captain Frederick S. Sherwin (deceased), Mr. L. E. Bell, SP4 C. R. Roehrig, and Mr. R. G. Dodd, Technology Applications Division, Eustis Directorate, U.S. Army Air Mobility Research and Development Laboratory.

The objective of this contractual effort was to develop and validate analytical design techniques for small, high-temperature-rise, low-airflow gas turbine combustors and related components and to define the design limitations associated with these small advanced combustors. The analytical design models developed under this program were used to design a straight-through annular combustor with a W_a = 3 lb/sec, P_3 = 16 atm, and TIT = 2500°F. Combustor rig tests of this combustor indicate that the design models have the potential for reducing combustor development time and cost significantly.

Appropriate technical personnel of this Directorate have reviewed this report and concur with the conclusions contained herein.

The findings and recommendations outlined herein will be considered in planning future small gas turbine engine and combustor component development programs.

ic

Task 1G162203D14413
Contract DAAJ02-70-C-0060
USAAMRDL Technical Report 74-3A
February 1974

ADVANCED, SMALL, HIGH-TEMPERATURE-RISE COMBUSTOR PROGRAM

Final Report

VOLUME I

ANALYTICAL MODEL DERIVATION AND COMBUSTOR-ELEMENT RIG TESTS (PHASES I AND II)

By

S. C. Hunter
K. M. Johansen
H. C. Mongia
M. P. Wood

Prepared by

AiResearch Manufacturing Company of Arizona
A Division of The Garrett Corporation
Phoenix, Arizona

for

EUSTIS DIRECTORATE
U.S. ARMY AIR MOBILITY RESEARCH AND DEVELOPMENT LABORATORY
FORT EUSTIS, VIRGINIA

Approved for public release;
distribution unlimited.

ABSTRACT

This report describes an analytical and experimental study of advanced, small, high-temperature combustors. The objectives of the 32-month program were

(a) To develop and validate an analytical design technique for small, high-temperature-rise, low-airflow combustors and related components

(b) To define the limitations associated with these small combustors and related components and the effects of these limitations on the cycle and the configuration of advanced-technology engines

Analytical models were developed to predict the characteristics and performance of the basic combustor elements, including fuel injection, primary zone, dilution zone, and liner cooling. Nine combustor element rig test programs were conducted to provide data to update and validate the analytical models. Based on the analysis and rig test results, a full-scale combustor was designed, fabricated, and tested. An ancillary material screening program was conducted to select the most suitable existing material for combustor application. A relatively new material (IN-586) was selected. Material-property tests were conducted to supplement published data for this material.

The analytical models were used to assess combustor design and performance limitations and the applicability of the design techniques over an airflow range of 2 to 5 pounds per second, cycle pressure ratio range of 10 to 16 (including recuperation), and a turbine inlet temperature range of 2300°F to 2700°F.

FOREWORD

The Advanced, Small, High-Temperature-Rise Combustor Program was conducted by the AiResearch Manufacturing Company of Arizona under Contract DAAJ02-70-C-0060, Task 1G162203D14413, with the Eustis Directorate, U.S. Army Air Mobility Research and Development Laboratory. The primary objective of the three-phase, 32-month program was to develop and validate design techniques for advanced, small, high-temperature-rise combustors for gas turbine engines in the 2- to 5-pound-per-second class.

This report is presented in two volumes. Volume I describes the derivation of the analytical models (Phase I) and combustor-element rig tests (Phase II) that were conducted to provide data to validate the models. Volume II describes the design and test (Phase III) of a full-scale combustor that was derived from the results of Phases I and II.

Volume I contains six appendixes, which give abstracts of six of the computer programs derived for combustion system analysis under the contract. Information presented in each abstract includes a brief description of program computation capability, input, computation procedures (including a listing of all computation routines), and a sample output. The programs are coded in Garrett Universal FORTRAN for the Control Data Corporation (CDC) 6400 computer facility. Because of the limited schedule and budget constraints of the contract, the computer programs were not fully developed and debugged; therefore, it can be assumed that some programming errors still remain in some or all of the computer programs.

The Program Manager was Mr. K. M. Johansen. Principal contributing engineers to Phases I and II were Mr. S. C. Hunter (Principal Investigator), Ms. S. L. Trexler (Documentation Engineer), and Dr. M. P. Wood (Element Test Director). Dr. H. C. Mongia (Combustion Engineering) was assigned to the program during Phase II to update the analytical models. Other contributors to the program were Messrs. C. G. Mackay, E. L. Kumm, and J. A. Pyne. Dr. D. E. Metzger of Arizona State University was the major consultant on liner film cooling studies. The program was monitored by Messrs. L. Bell, Jr., R. Dodd, and C. Roehrig from the Eustis Directorate, U.S. Army Air Mobility Research and Development Laboratory.

Preceding page blank

TABLE OF CONTENTS

	Page
ABSTRACT	iii
FOREWORD	v
LIST OF ILLUSTRATIONS	xii
LIST OF TABLES	xxiii
LIST OF SYMBOLS	xxiv
1.0 INTRODUCTION	1
1.1 General Information	1
1.2 Objectives	1
2.0 CYCLE STUDIES AND COMBUSTOR GEOMETRY	4
2.1 Engine Cycle Studies	4
2.2 Combustor Preliminary Sizing Analysis	4
2.2.1 Combustor Volume	7
2.2.2 Combustor Geometry	11
2.2.3 Combustor Open Area	11
2.2.4 Preliminary Combustor Envelope	12
2.3 Engine Schematics	14
3.0 MATERIAL SELECTION	23
3.1 Candidate Materials	23
3.2 Screening Tests	24
3.2.1 Thermal Stability	24
3.2.2 Thermal Fatigue	24
3.2.3 Corrosion	26
3.2.4 Fabricability	29
3.3 Screening Test Results	29
3.4 IN-586 Property Tests	30
3.4.1 Tensile Tests	30
3.4.2 Creep-Rupture Tests	31
3.4.3 Low-Cycle-Fatigue Tests	31
3.4.4 Fabricability Tests	31
3.4.5 Material Property Test Conclusions	37

Preceding page blank

		Page
4.0	FUEL INJECTION	38
4.1	Air-Assist Atomizer	38
4.1.1	Model Definition	38
4.1.2	Atomizer Spray Tests	47
4.1.2.1	Spray Characteristics	47
4.1.2.2	Spray Envelope Tests	50
4.1.3	Conclusions	59
4.2	Pneumatic-Impact Atomizer	59
4.2.1	Model Definition	61
4.2.2	Pneumatic-Impact Spray Tests	64
4.2.2.1	Drop-Size Characteristics	64
4.2.2.2	Circumferential Distribution	68
4.2.2.3	Spray Envelope	68
4.2.3	Conclusions	71
4.3	L-Pipe Injector	73
4.3.1	Model Definitions	74
4.3.2	L-Pipe Injector Tests	76
4.3.2.1	Fuel Flow Distribution	78
4.3.2.2	Film Thickness Measurement	87
4.3.3	Analytical Model Update	92
4.3.4	Conclusions	93
5.0	PRIMARY ZONE	95
5.1	Primary-Zone Recirculation	95
5.1.1	Model Definition	95
5.1.1.1	Gosman Program Solution Technique	96
5.1.1.2	Modifications to the Gosman Program	101
5.1.1.3	Comparison With Well-Stirred Reactor	103
5.1.1.4	Impinging Jet Recirculation	108
5.1.2	Element Tests	118

Page

5.1.2.1 Primary-Zone Element Water Rig Description 118

5.1.2.1.1 Test Procedure 121
5.1.2.1.2 Eddy Viscosity Correlation . . 123
5.1.2.1.3 Double-Entry Rig Experiments 125
5.1.2.1.4 Analytical Prediction 128

5.1.2.2 Two-Dimensional Cold-Flow Air Rig 132

5.1.2.2.1 Test Results 136
5.1.2.2.2 Comparison of Analytical and Experimental Velocity Profiles . 138

5.1.2.3 Two-Dimensional Hot-Flow Rig . . 140

5.1.2.3.1 Test Results 144
5.1.2.3.2 Comparison of Analytical and Experimental Evaporation Rates . 157
5.1.2.3.3 Comparison of Analytical and Experimental Profiles for the Two-Dimensional Hot-Flow Model . 163

5.1.2.4 Three-Nozzle-Sector Primary-Zone Rig 165

5.1.2.4.1 Test Section Description . . . 165
5.1.2.4.2 Test Results 169

5.1.3 Combustor Evaluation Tests . . . 176

5.1.3.1 Temperature Profiles . . . . . 17[illegible]
5.1.3.2 Velocity Profiles . . . . . 1[illegible]
5.1.3.3 Analytical Predictions 177

5.1.4 Conclusions 183

5.2 Primary-Zone Ignition Energy Requirements . 186

5.2.1 Ignition Model Equation 186
5.2.2 Experimental Ignition Energy Requirements 194
5.2.3 Conclusions 197

		Page
6.0	DILUTION ZONE	198
6.1	Model Definition	198
6.1.1	Discharge Coefficient and Efflux Angle Model	198
6.1.2	Annulus Loss Model	201
6.1.3	Jet Trajectory and Mixing Models	207
6.1.3.1	Empirical Trajectory Method	209
6.1.3.2	Analytical Trajectory Methods	212
6.1.3.2.1	Predicted Trajectories	217
6.1.3.2.2	Velocity and Temperature Decay	221
6.2	Rig Tests and Model Update	223
6.2.1	Discharge Coefficient Tests and Model Update	223
6.2.1.1	Rig Tests	223
6.2.1.2	Test Results and Model Update	226
6.2.2	Dilution-Zone Tests and Model Update	238
6.2.2.1	Rig Tests	238
6.2.2.2	Test Results and Model Update	241
6.3	Conclusions	248
7.0	LINER COOLING	251
7.1	Stress Analysis	251
7.1.1	Method of Solution	252
7.1.2	Combustor-Shell Analysis	252
7.1.3	Combustor Wall Temperature Gradient	254
7.2	Combustor Cooling Analysis	254
7.2.1	Film-Cooling Analysis	259
7.2.1.1	Procedure and Apparatus	261
7.2.1.2	Summary of Results and Conclusions	265

Page

7.2.1.2.1 Impingement Film Configuration 273
7.2.1.2.2 Impingement Film With Wiggle-Strip Configuration 276
7.2.1.2.3 Pinched-Impingement Film Configuration 276
7.2.1.2.4 Hole-Step Configuration . . 278
7.2.1.2.5 Correlating Equations . . . 278

7.2.2 Cooling Film Mixing 280

7.2.2.1 Experimental Results 280
7.2.2.2 Analytical Predictions . . . 284

7.3 Radiant Heat-Transfer Analysis 288

7.3.1 Model Definition 288

7.3.1.1 Radiant Interchange With Transparent Media 292
7.3.1.2 Radiant Interchange in Participating Media 292
7.3.1.3 Luminous Radiation 294
7.3.1.4 Radiation Interchange Equation . 294

7.3.2 Element Tests 296
7.3.3 Conclusions 305

8.0 CONCLUSIONS AND RECOMMENDATIONS 307

8.1 Conclusions 307
8.2 Recommendation for Future Analytical Studies 308
8.3 Recommendations for Future Experimental and Development Studies 309

LITERATURE CITED 310

APPENDIXES

I. Air-Assist Pressure Atomizer Computer Program 1527 316

II. Pneumatic-Impact Fuel Injector Computer Program 1528 340

III. Air-Blast Film Vaporizer Computer Program 1529 399

		Page
IV.	Primary-Zone Model Computer Program No. 1338	433
V.	Impingement-Jet, Primary-Zone Recirculation Model Computer Program No. 1526	498
VI.	Dilution-Zone Jet-Trajectory Calculation, Computer Program No. 1530	505
DISTRIBUTION.		528

LIST OF ILLUSTRATIONS

Figure		Page
1	Relationship of QV to Gas Generator Speed (Flight Conditions of Sea Level, Static, and 25,000 Feet, Static, Standard Day.)	8
2	Relationship of QV to Gas Generator Speed (Flight Conditions of 45,000 Feet, 0.85 Mach, Standard Day.)	9
3	Relationship of Combustor Efficiency to Aerodynamic Loading.	10
4	Annular Combustor Configuration	13
5	Annular Combustor Envelope	16
6	Turboshaft Engine Schematic With Two-Stage Centrifugal Compressor, Reverse Annular Combustor, and Radial Turbine.	17
7	Turboshaft Engine Schematic With Two-Stage Centrifugal Compressor, Straight-Through Annular Combustor, and Radial Turbine.	18
8	Turboshaft Engine Schematic With Two-Stage Centrifugal Compressor, Reverse Annular Combustor, and Two-Stage Axial Turbine	19
9	Turboshaft Engine Schematic With Two-Stage Centrifugal Compressor, Straight-Through Annular Combustor, and Two-Stage Axial Turbine.	20
10	Turboshaft Engine Schematic With Two-Stage Centrifugal Compressor, Can Combustor, and Radial Turbine	21
11	Turboshaft Engine Schematic With Two-Stage Centrifugal Compressor, Can Combustor, and Two-Stage Axial Turbine.	22
12	Thermal Fatigue Test Specimen Geometry	27
13	Thermal Cycle Rig Showing Test Specimen in the Ambient Air Jet (Top) and the Oxyacetylene Flame (Bottom).	28

Figure		Page
14	The 0.2 Percent Yield Strength of IN-586 at Various Temperatures	32
15	Parametric Curves for 0.5 Percent (Top) and 1.0 Percent (Bottom) Creep-Rupture Tests of IN-586 Material	33
16	Stress-Rupture Curve for IN-586.	34
17	Low-Cycle-Fatigue Data for IN-586, Hastelloy X, and Haynes 188.	35
18	Air-Assist Atomizer.	39
19	Air-Assist Atomizer.	40
20	Comparison of Measured and Calculated Droplet Trajectories	44
21	Calculated Simplex Trajectories Without Air Assist	45
22	Effect of Ambient Temperature and Pressure on Fuel Penetration	46
23	Drop-Size Distribution Data for Air-Assist Nozzle.	51
24	Fuel-Injection Element Test Rig.	52
25	Fuel-Injection Rig Temperature Profiles	54
26	Comparison of Analytical and Experimental Spray Trajectories for Air-Assist Nozzle	55
27	Pneumatic-Impact Injector Schematic	60
28	Pneumatic-Impact Fuel-Injection System . .	63
29	Pneumatic-Impact Fuel-Injector Nozzle . . .	65
30	Drop-Size Distribution for Pneumatic-Impact Nozzle	67

Figure		Page
31	Pneumatic-Impact Injector Fuel Distribution Test Hardware	69
32	Pneumatic-Impact Injector Test Temperature Profiles	70
33	Comparison of Experimental and Analytical Spray Trajectories From Pneumatic-Impact Atomizer	72
34	L-Pipe Vaporizer Fuel Injector	75
35	Fuel-Film Parameters for L-Pipe Injector at 16 Atmospheres	77
36	L-Pipe Configurations Tested	79
37	L-Pipe Flow Distribution Rig	80
38	Circumferential Distribution of Fuel From Standard L-Pipe With Varying Fuel and Airflow Rates	81
39	Fuel Flow From Standard Discharge L-Pipe	83
40	Fuel Flow From Standard Discharge L-Pipe	84
41	Fuel Flow From Rectangular Discharge L-Pipe	85
42	Fuel Flow From Rectangular Discharge L-Pipe	86
43	Film Thickness Measurement Apparatus	89
44	Straight Fuel Tube Film Thickness Measurements, Air ΔP = 15 Inches of H_2O	90
45	Straight Fuel Tube Film Thickness Measurement, Air ΔP = 0 Inch of H_2O	91
46	Gosman Coordinate System	97
47	Primary-Zone Subelement Reduced Model Efficiency Versus Herbert's Loading Parameter	105

Figure		Page
48	Primary-Zone Subelement Reduced-Model Efficiency Versus Herbert's Loading Parameter	106
49	Primary-Zone Subelement Reduced Model Efficiency Versus Empirical Loading Parameter	107
50	Jet Impingement Segment	108
51	Recirculation Model	109
52	Recirculation Ratio as a Function of Radius Ratio, Temperature Rise, and Dome Flow for Normal Injection and Eight Holes	115
53	Effect of Jet Efflux Angle on Recirculation Ratio	116
54	Recirculation Flow as a Function of Hole Diameter and Number of Holes	117
55	Primary-Zone Water Flow Rig Schematic . . .	119
56	General View of Water Analog Test Section	120
57	Two-Dimensional Primary-Zone Subelement Model	122
58	Water Model Flow Patterns	124
59	Water Model Basic Test Section, Double Entry	126
60	Hardware for Water Model Rig	127
61	Typical Water-Model Flow Pattern	129
62	Velocity Vector Plot for Air-Assist Nozzle Primary Zone	130
63	Typical Water-Model Flow Pattern	131
64	Double-Entry Water-Model Predicted Flow Patterns	133

Figure		Page
48	Primary-Zone Subelement Reduced-Model Efficiency Versus Herbert's Loading Parameter	106
49	Primary-Zone Subelement Reduced Model Efficiency Versus Empirical Loading Parameter	107
50	Jet Impingement Segment	108
51	Recirculation Model	109
52	Recirculation Ratio as a Function of Radius Ratio, Temperature Rise, and Dome Flow for Normal Injection and Eight Holes	115
53	Effect of Jet Efflux Angle on Recirculation Ratio	116
54	Recirculation Flow as a Function of Hole Diameter and Number of Holes	117
55	Primary-Zone Water Flow Rig Schematic	119
56	General View of Water Analog Test Section	120
57	Two-Dimensional Primary-Zone Subelement Model	122
58	Water Model Flow Patterns	124
59	Water Model Basic Test Section, Double Entry	126
60	Hardware for Water Model Rig	127
61	Typical Water-Model Flow Pattern	129
62	Velocity Vector Plot for Air-Assist Nozzle Primary Zone	130
63	Typical Water-Model Flow Pattern	131
64	Double-Entry Water-Model Predicted Flow Patterns	133

Figure		Page
65	Double-Entry Water-Model Predicted Axial Velocity in Cross-Stream Planes	134
66	Two-Dimensional Cold-Flow Rig	135
67	Primary-Zone Flow-Field Schematic	137
68	Two-Dimensional Cold-Flow Subelement Velocity Profiles, Analytical and Experimental	139
69	Hardware for Atmospheric Primary-Zone Rig	141
70	Water-Cooled, Shielded, Platinum/ Platinum 10-Percent Rhodium Thermocouple	142
71	Double-Sonic Venturi Temperature Probe	143
72	Water-Cooled, U-Tube Velocity Vector Probe	145
73	Leeds and Northrup Double Mirror Type Rayotube	146
74	Water-Cooled Emission Measurement Probe	147
75	Two-Dimensional Atmospheric Rig Temperature Distribution	148
76	Two-Dimensional Atmospheric Rig Temperature Distribution	149
77	Velocity Vectors, Two-Dimensional Atmospheric Rig	151
78	Two-Dimensional Atmospheric Rig - Fuel Evaporation, Centerline Thermocouples Only	154
79	Two-Dimensional Atmospheric Rig - Fuel Evaporation, Thermocouples 2.5 Inches Left and Right of Centerline	155
80	Fuel Evaporation Plate	156

Figure		Page
81	Film Evaporation Lengths at 1 Atmosphere	158
82	Film Evaporation Lengths at a Pressure of 4 Atmospheres	159
83	Film Evaporation Lengths at 4 Atmospheres	160
84	Fuel Film Predicted and Measured Temperature	161
85	Comparison of Experimental and Analytical Temperature Profiles at Different Axial Distances Downstream From Inlet Slot	164
86	Comparison of Analytical and Experimental Velocity Profiles at Different Axial Distances Downstream From Inlet Slot	166
87	Pressurized Combustor Primary-Zone Rig Hardware	167
88	L-Pipe Combustor Primary-Zone Sector . . .	168
89	Annular Combustor Primary-Zone Segment for Air-Assist and Pneumatic-Impact Fuel Nozzles	170
90	Air-Assist Fuel Nozzle Assembly	171
91	Pneumatic-Impact Fuel Nozzle	171
92	Radial Swirler System on Modified Pneumatic-Impact/Air-Assist Nozzle Section	172
93	L-Pipe Orientation During Atmospheric Rig and Pressure Rig Test	174
94	L-Pipe Combustor Modified With Air Swirlers	175

Figure		Page
95	Temperature Traverse Data for L-Pipe Plus Swirler Primary Zone (Axial Position is at the Exit Plane)	178
96	Temperature Traverse Data for L-Pipe Plus Swirler Primary Zone (Axial Position is 3.0 Inches in From Exit Plane)	179
97	L-Pipe Primary-Zone Axial Velocity Profiles at 1 Atmosphere (In Line With Swirler)	180
98	L-Pipe Primary-Zore Axial Velocity Profiles at 6 Atmospheres (In Line With Swirler)	181
99	Impingement Jet Profiles	182
100	Primary-Zone "Blockage"	182
101	Primary-Zone Velocity and Temperature Profiles (Predicted)	184
102	Primary-Zone Velocity and Temperature Profiles (Predicted)	185
103	Ignition Energy Versus Fuel-Air Ratio for Jet Fuels	188
104	Evaporation Fraction of Fuel Droplets as a Function of Size and Time	189
105	Predicted Minimum Ignition Energy Requirements for Primary Zone (Mixture Velocity Is 40 ft/sec)	191
106	Predicted Minimum Ignition Energy Requirements for Primary Zone (Mixture Velocity Is 10 ft/sec)	192
107	Combustor Ignition Energy Requirements	193
108	Dilution Port Model Schematic	199

Figure		Page
109	Discharge Coefficient Versus Pressure Drop Parameter, α, and Flow Ratio	202
110	Jet Efflux Angle Versus Pressure Drop Parameter, α, and Flow Ratio	203
111	Orifice Area - Annulus Area Ratio Versus Pressure Drop Parameter, α, and Flow Ratio	204
112	Computer Plot for Annulus Loss Program Output	206
113	Effect of Compressor Exit Flow Swirl on Combustor Pressure Loss and Flow Distribution	208
114	Jet Trajectory Parameter Definition	210
115	Jet Trajectory Momentum Flux Control Volume.	213
116	Spreading Rate Parameter for Published Air Jets	217
117	Jet Trajectories From Several References.	218
118	Effect of Mainstream Profile on Jet Trajectory	219
119	Effect of Mainstream Profile Reversal on Jet Trajectory	220
120	Jet Lateral Spreading for Various Injection Angles and Effective Velocity Ratios	222
121	Jet Profile Parameter for Velocity and Temperatures	224
122	Discharge Coefficient Rig	225
123	Discharge Coefficient Data for the Circular Orifice	229
124	Discharge Coefficient Data Versus Pressure Drop Parameter for Different Orifices	231

Figure		Page
125	Discharge Coefficient Data for Cooling Slot	232
126	Comparison of Jet Efflux Angle Data	234
127	Discharge Coefficient Data for Thin-Walled Circular Orifice	235
128	Jet Efflux Angle Data for Thin-Walled Circular Orifice of 0.5-Inch Diameter	236
129	Jet Efflux Angle Data and Discharge Coefficient Data for Plunged Circular Orifice	237
130	Dilution-Zone Element Test Rig Schematic	239
131	Dilution-Zone Test Rig	240
132	Reduced-Area Transition Duct	242
133	Dilution-Zone Measured and Predicted Jet Centerline Trajectories	245
134	Spreading Rate Parameter	246
135	Updated Measured and Predicted Jet Centerline Trajectories	247
136	Pattern Factor	249
137	Combustor Stress Analysis (Including Temperature and Pressure Distribution)	253
138	Hot-Spot Model Schematic	255
139	Stress Range Versus Temperature Gradient for IN-586	256
140	Combustor Life Versus Temperature Gradient for IN-586	257
141	Combustor Film-Cooling Schematic	260
142	Cooling Slot Geometry Schematics	262
143	Film-Cooling Test Facility Schematic	266

Figure		Page
144	Film-Cooling Test Section	267
145	Typical IF Test Pieces	268
146	Impingement Film Configuration	269
147	Pinched-Impingement Film Configurations	270
148	Impingement Film With Wiggle-Strip Configurations	271
149	Hole-Step Configurations	272
150	$\overline{T}_{ad}$ Correlation Versus ℓ/G for $\overline{W}$ Greater Than 0.6	274
151	ϕ Versus ℓ/G Correlation	275
152	Pinched-Impingement Film Geometry	277
153	Pinched-Impingement Film Geometry Test Results	279
154	Cooling Film Mixing Results ($\overline{W}$ = 1.19)	282
155	Cooling Film Mixing Results ($\overline{W}$ = 2.79)	283
156	Velocity Decay Curves	285
157	Temperature Decay Curves	286
158	Cooling Film Mixing Rates	287
159	Predicted Adiabatic Wall Temperature Versus Axial Distance	289
160	Monochromatic Radiation Intensity Versus Wavelength	291
161	Three-Dimensional Geometry	291
162	Typical Surface and Gas Element	294
163	Test Configuration Schematic for Flame Radiation Measurement (Not to Scale)	297

Figure		Page
164	Combustor/Radiation Port Orientation (Port Number 1)	298
165	Schematic of Unfolded Primary Zone (Top View) Showing Axial and Circumferential Orientation of Radiation Measurement Ports Relative to Fuel Nozzles	299
166	Measured and Predicted Heat Flux	300
167	Measured and Predicted Heat Flux	301
168	Radiant Heat Flux Variation With Fuel-Air Ratio	302
169	Air-Assist Pressure Atomizer Program No. 1527 Input Data	317
170	Pneumatic-Impact Injector Program No. 1528 Input Data	341
171	L-Pipe Air Blast Vaporizer Circular Pipe Geometry	400
172	Film Vaporization Program, Air-Blast; Option A (With L-Pipe), Program No. 1529 Input Data	401
173	L-Pipe Air-Blast Vaporizer Noncircular Pipe	402
174	Film Vaporization Program, Air-Blast; Option B (Without L-Pipe), Program No. 1529 Input Data	405
175	Two-Dimensional Flow, Program No. 1338 Input Data, Sheet 1	434
176	Two-Dimensional Flow, Program No. 1338 Input Data, Sheet 2	435
177	Two-Dimensional Flow, Program No. 1338 Input Data, Sheet 3	436
178	Two-Dimensional Flow, Program No. 1338 Input Data, Sheet 4	437

Figure		Page
179	Two-Dimensional Flow, Program No. 1338 Input Data, Sheet 5	438
180	Grid Line Parameters	440
181	Various Grid Configurations	441
182	Grid Layout Procedure	442
183	Tested Configurations	497
184	Recirculation Model	500
185	Input Data for Program No. 1530, Sheet 1	515
186	Input Data for Program No. 1530, Sheet 2	516

LIST OF TABLES

Table		Page
I	Engine Cycle Parameters	5
II	Calculated Turboshaft Engine Cycle Data	6
III	Chemistry of Materials Evaluated . . .	25
IV	Weld Strength Data for IN-586	36
V	Droplet Size Distributions	41
VI	Air-Assist Atomizer Drop-Size Test Results	48
VII	Pneumatic-Impact Injector Droplet Size Test Points	66
VIII	Spread in Flow Ratios	82
IX	Test Conditions for Film Thickness Measurement	88
X	Terms of the General Elliptic Equation	99
XI	Primary-Zone Subelement Rig Emission Data in the Control Plane	152
XII	Fuel Evaporation Plate Test Conditions, Fuel Insertion Rig	153
XIII	Ignition and Lean-Limit Blowout Data from L-Pipe Plus Swirler Primary Zone .	195
XIV	Ignition Model Predictions	196
XV	Discharge Coefficient Test Configurations	227
XVI	Discharge Coefficient Test Conditions .	228
XVII	Dilution-Zone Test Conditions	243
XVIII	Cooling Film Mixing Test Conditions . .	281
XIX	Radiation Test Conditions, Data, and Results	304

Table		Page
XX	Listing for Program No. 1527	320
XXI	Program No. 1527 Output	336
XXII	Listing of Program No. 1528	344
XXIII	Program No. 1528 Output	387
XXIV	Listing of Program No. 1529	407
XXV	Program No. 1529 Output	430
XXVI	Listing for Program No. 1338	444
XXVII	Number of Iterations Possible	493
XXVIII	Listing of Program No. 1526	501
XXIX	Program No. 1526 Output	504
XXX	Listing of Program No. 1530	506
XXXI	Nomenclature	518
XXXII	Output for Program No. 1530	521

LIST OF SYMBOLS

Symbols

A	Duct area
A_1	Upstream nozzle throat area
A_2	Downstream nozzle throat area
A_B	Frontal area of inserted body
A_e	Combustor annulus area, ft^2
A_{jo}	Jet initial area at the orifice, Eq. (120)
A_o	Flame tube area, Eq. (52)
A_p	Area of jet projected on a plane normal to the cross-flow direction, Eq. (106)
A_s	Total surface area enclosing
A_{sh}	Shroud flow area, $in.^2$
a	Constant in mixing length expression, Eq. (72) or apparent origin of jet, Eq. (117)
a/L	Annulus width change/upstream width
a_ϕ	Convection by fluid flow
B	Mass transfer number
B_{COMB}	Mass transfer number, combustion, Eq. (19)
B_{evap}	Mass transfer number, evaporation, Eq. (18)
B_i	Geometric parameter, Eq. (53)
b	Constant in mixing length expression, Eq. (72)
b/L	Slot width/upstream annulus width
c	Empirical constant for initial droplet velocity, Eq. (28)
C_D	Orifice discharge coefficient
C_d	Coefficient of drag

Symbols

C_f	Surface friction coefficient
C_{pj}	Species j specific heat at constant pressure
C_v	Atomizer velocity coefficient
c	Upstream annulus velocity/slot
c_p	Isobaric specific heat
D	Duct hydraulic diameter
D_{duct}	Duct diameter
D_o	Atomizer exit orifice diameter, in.
D/SMD	Droplet diameter/Sauter Mean Diameter
d	Jet diameter, Eq. (29), or kernel diameter, Eq. (80)
d_o	Injection orifice diameter, Eq. (53)
dw	Injected mass flow, Eq. (91)
dx	Element length
E	Ignition energy, Eq. (84), or radiation flux
FN	Flow number of the injector, Eq. (3)
F_{lig}	Primary-zone fuel-air ratio
F_{vap}	Fuel-air ratio near the igniter, Eq. (85)
F_{12}	View factor, Eq. (139)
f	Wall friction factor
f/a	Fuel-air ratios
f_p	Primary-zone fuel-air mass ratio

Symbols

G	Slot gap width
g	Mass flow through injection-jet holes
g_c	Gravitational constant
h	Convective heat-transfer coefficient
h*	Rippled film heat-transfer coefficient
$\tilde{h}$	Mixture stagnation enthalpy
h_j	Negative of j species heat of formation
IR	Combustor inner radius
$I_{\lambda bn}$	Monochromatic radiation intensity
i	Pounds of air required to burn 1 pound of fuel
J	Local temperature or velocity in defining jet profile parameters (Figure 132)
K	Constant, Eq. (49)
k	Jet spreading rate parameter, Eq. (125)
k	Viscosity exponent, Eq. (12), or turbulence kinetic energy
k	Fraction of mass flow through injection jet holes that flows upstream, Eq. (52)
L	Combustor length or cooling slot cover-plate lengths (wiggle-strip)
L_f	Luminosity factor, Eq. (144)
M	Mach number
M_a	Molecular weight of air
MBL	Mean beam length, ft, Eq. (141)
MMD	Mass median diameter
m_{O_2}	Oxygen concentration in the surrounding gas

Symbols

M_R	Air to fuel mass flow ratio
M_v	Molecular weight of vaporized fuel
m_j	Species mass fraction
m_j	Mass of species j in unit mass of mixture (mass fraction)
N	Generalized constant for species creation rate Eq. (48)
Nu	Nusselt number
Nu_h	Nusselt number for heat transfer, Eq. (7)
Nu_m	Nusselt number for mass transfer, Eq. (8)
$N/\sqrt{\theta_2}$	Gas generator speed
Nu_x	Local Nusselt number (h /k)
n	Annulus upstream flow rate/slot flow rate
n	Constant, Eq. (50)
n	Number of holes, Eq. (53)
OR	Combustor outer radius
P/P	Cycle pressure ratio
PF	Combustor exit pattern factor
P_a	Partial pressure of air
P_{comb}	Combustor internal pressure, psia
Pr	Prandtl number
P_t	Total pressure
P_v	Partial pressure of vaporized fuel
P_1	Upstream total pressure in double sonic probe
P_2	Downstream total pressure

Symbols

P_3	Combustor inlet pressure, psi
p	Hydrodynamic pressure
Q_c	Heat of combustion of fuel
Q_L	Latent heat of evaporation
Q_1, Q_2, Q_3	Loading parameters
q	Dynamic head
$\dot{q}$	Local heat flux
$\dot{q}_{liquid}$	Heat transfer rate with liquid film
$\dot{q}_{g-l}$	Gas radiation flux
$\dot{q}_r$	Radiation flux from the back wall, Eq. (152)
R_j	Rate of j-th species creation, $lb/sec/ft^3$
R_n	Reynolds number
r	Radius, in.
S	Stoichiometric ratio of 0_2
Sc	Schmidt number
SG	Fuel specific gravity
SMD	Sauter Mean Diameter
s	Slot width or fuel sheet thickness
T_{amb}	Ambient temperature
T_{aw}	Adiabatic wall temperature
T_m	Main (hot) stream temperature
T_{max}	Maximum temperature
T_{min}	Minimum temperature
T_{sp}	Spontaneious ignition temperature

Symbols

T_r	Back wall temperature
$\bar{T}$	Normalized temperature, Eq. (129)
T_f	Initial coolant film temperature
T_u	Turbulence intensity at the flame surface
T_w	Droplet surface temperature
T_t	Total temperature
T_1	Geometric calibrated gas temperature in double sonic probe
T_2	Downstream measured temperature in double sonic probe
T_3	Combustor inlet temperature, °R
T_4	Combustor discharge temperature
t	Mixture temperature
U	Mixture velocity, ft/sec
V	Combustor or reaction volume of enclosed gas, ft^3
V	Flow through dome/flow, g, through holes
V_a	Assist-air shroud discharge velocity, ft/sec
V_e	Effective gas velocity, ft/sec
V_f	Fuel sheet velocity, ft/sec
V_{g2}	Free-stream velocity
V_i	Viscosity number
V_R	Air velocity/fuel velocity
$\frac{V^2}{2}$	Kinetic energy of mean motion
W	Duct mass flow
W_a	Assist-air mass flow, lb/hr

Symbols

W_{air}	Shroud airflow, lb/sec
We	Weber number
W_f	Fuel flow rate, lb/hr
W_f/L	Fuel flow rate per unit length
W_g	Mainstream weight flow rate, lb/sec
W_{je}	Weight flow entrained in jet, lb/sec
W_{jo}	Injected jet weight flow rate, lb/sec
W_p	Flow rate of products
$\bar{W}$	Ratio of coolant mass velocity to the mainstream mass velocity
w	Volume flow per unit width, cu ft/sec/ft
x	Radial distance from center of jet
Y+	Normalized distance from the wall
Y_c	Critical depth, in.
y	Cross-stream distance from wall
y	Velocity of injected mass/duct velocity
y_1	Supercritical upstream depth
y_2	Subcritical downstream depth
Z	Wall width, ft
ZrO_2	Rokide-Z coating
α	Spray angle, degrees or pressure drop parameter
α	Angle of jet spreading
$\bar{\alpha}$	Absorptivity
β	Jet efflux angle

Symbols

Γ_j	Exchange coefficient of species j
Γ_h	Exchange coefficient of heat
Γ_k	Exchange coefficient of turbulence kinetic energy
γ	Arc sin $\delta/2\ R_o$, Eq. (54)
ΔP_{air}	Airflow differential pressure, psid
ΔP_e	Effective differential pressure, psid
ΔP_f	Differential fuel pressure, psid
$\Delta P/P$	Maximum pressure drop
$\Delta P/P_3$	Maximum total pressure loss
δ	Effective jet width at the orifice greater than d_o due to jet distortion, Eq. (54)
ε	Recuperative effectiveness
$\bar{\epsilon}$	Gas emissivity
$\bar{\epsilon}_r$	Back wall emissivity
η_B	Combustor efficiency
λ	Wave length, μ
ν	Fuel viscosity, centistokes
ρ	Mixture or air density
ρ_f	Fuel density, lb/ft^3
ρ_g	Gas density, lb/ft^3
ρ_o	Injected air density, lb/ft^3
ρ_r	Hot gas density, lb/ft^3
σ	Effective jet width or Stefan-Boltzmann constant
σ	Square root of the variance of a distribution (stress analysis)
σ_f	Fuel surface tension, dynes per cm

Symbols

ϕ	Dependent variables or rotational angle around circumference of ellipse or ratio of average surface heat transfer with injection to that without injection
ϕ_{fo}	Transformed dependent variable
ℓ_1, ℓ_2	Metric coefficients
ℓ	Length scale of turbulence or finite axial film cooled distance

1.0 INTRODUCTION

1.1 GENERAL INFORMATION

Advanced, small, high-pressure-ratio high-turbine-inlet-temperature turboshaft engines impose conflicting requirements on the various elements of the combustor such as fuel injection and liner cooling.

A large number of insertion points are desirable in order to provide a uniform temperature pattern over a large range of fuel flows. However, nozzle fuel passages should be large in order to tolerate contaminated fuels.

Small engine configurations dictate combustors with relatively high liner surface-to-airflow ratios requiring higher airflow percentages for cooling. Conversely, the liner cooling-air temperature increases with higher pressure ratio and less is available at higher turbine inlet temperatures, due to increased airflow required for combustion and turbine cooling.

Current design procedures for small combustion systems are based largely on empirical correlations and experience derived from numerous APU and propulsion engine combustor development programs. One-dimensional simplified analytical models are included in the current design procedures but are of limited use. Two-dimensional and three-dimensional models are desirable; but due to computer time limitations and limited knowledge of the transport phenomenon in typical combustor flow fields, they have been extremely difficult to apply. The work in this program represents a concerted effort to advance the analytical capabilities available to the combustor designer to deal with these complex problems.

1.2 OBJECTIVES

This report describes a program addressed to the problems of advanced, small, high-temperature-rise combustors. The objectives of the three-phase program were:

(a) To develop and validate an analytical design technique for small, high-temperature-rise, low-airflow combustors and related components

(b) To define the limitations associated with these small combustors and related components and the effect of these limitations on the cycle and configuration of advanced-technology engines

The approach that was employed included analysis and test of combustor elements, followed by the design and test of a complete combustion system. Volume I of this report describes the development of the analytical models and the combustor element rig tests that were conducted to obtain data for updating and validating the design techniques. Volume II describes the design and test of the full-scale combustion system.

The analysis was addressed to combustors and engines having the following characteristics:

(a) Airflow (W_a) = 2 to 5 pounds per second

(b) Cycle pressure ratio (P/P) = 10.0 to 16.0

(c) Turbine inlet temperature (T_4) = 2300°F to 2700°F

(d) Centrifugal last-stage compressor

(e) Axial or radial turbine

(f) Reverse-flow annular, straight-through annular, and single- or multiple-can combustors

(g) Simple or recuperative cycles (recuperative effectiveness, ε, of 65 percent)

Performance goals of combustors derived by the design techniques established by this study include:

(a) Combustion efficiency (η_B) = 99 percent

(b) Maximum total pressure loss ($\Delta P/P_3$) = 3 percent (excluding recuperator)

(c) Maximum combustor exit pattern factor, PF = 0.20

$$PF = \frac{T_{4\ max} - T_{4\ avg}}{T_{4\ avg} - T_{3\ avg}}$$

where T_3 and T_4 are the combustor inlet and discharge temperature, respectively

(d) Stability over a wide range of fuel-air ratios, f/a

(e) Light-off/relight capability up to 25,000 feet altitude, M = 0 (the requirement for relight at an altitude of 45,000 feet, M = 0.85, was also examined)

(f) Multifuel capability including MIL-T-5424, Grades JP-4 and JP-5, MIL-T-83133, Grade JP-8, and Aviation Turbine Fuel, ASTM D1655-67 Type A-1

(g) Contamination tolerance in accordance with MIL-E-5007C

(h) Minimal formation of nitrogen oxides (NO_x), carbon monoxide (CO), and unburned hydrocarbons (UHC) consistent with the system performance goals listed above

(i) Smoke level below the visible limit

The performance goals are applicable to the air path between the compressor discharge and turbine stator inlet.

2.0 CYCLE STUDIES AND COMBUSTOR GEOMETRY

Engine cycle studies and a preliminary combustor sizing study were conducted to define combustor operating conditions and the approximate envelope for can- and annular-combustor configurations. Schematic drawings of several turboshaft engine configurations were prepared to assess the effects of the combustor configuration on the engine envelope.

2.1 ENGINE CYCLE STUDIES

Parametric cycle studies were conducted for a turboshaft engine having the following component configurations:

Compressors: Two-stage centrifugal flow

Gas Generator Turbine: Radial flow (simple cycle)
Two-stage axial flow (simple cycle)
Single-stage axial flow (recuperated cycle)

Power Turbine: Two-stage axial flow

Recuperator: Stationary finned heat exchanger

The component parameters used for the cycle studies are listed in Table I. These parameters were either defined by the contract or derived from AiResearch correlations. Table I also presents the calculated design-point output power and specific fuel consumption for the specified cycles.

Calculated combustor operating conditions for the simple-cycle engine are given in Table II. The table presents engine steady-state operating conditions (idle to maximum rated power) from sea level to 45,000 feet, and engine acceleration characteristics at 25,000 feet, static, and at 45,000 feet, 0.85 Mach number. Engine windmilling conditions at 45,000 feet, 0.85 Mach number are also presented.

2.2 COMBUSTOR PRELIMINARY SIZING ANALYSIS

A preliminary combustor sizing analysis was conducted in order to determine the approximate size and shape of combustors (can, straight-through annular, and reverse annular configurations) that are compatible with the specified engine cycle and combustor performance goals. For this study, the combustor preliminary design is required only to the extent needed to outline the combustor envelope, thus providing a framework for analytical studies. A simplified procedure was used, based on existing empirical correlations utilizing the engine cycle data presented in Table II.

TABLE I. ENGINE CYCLE PARAMETERS

Parameter	Simple Cycle	Recuperated Cycle
Engine total airflow (lb/sec)	3.0*	3.0*
Combustor total airflow (lb/sec)	2.733	2.733
Turbine cooling air (%)	8.9	8.9
Compressor pressure ratio	16.0*	10.0*
Compressor efficiency	0.786*	0.803
Combustor efficiency	0.99*	0.99*
Combustor pressure drop	0.03*	0.03*
Gas generator turbine		
o Inlet temperature (°F)	2500*	2500*
o Efficiency	0.850	0.805
o Cooling flow (%)	6.7	4.5
Power turbine efficiency	0.87	0.87
Recuperator		
o Effectiveness	-	0.65*
o Hot-side pressure drop	-	0.04
o Cold-side pressure drop	-	0.02
Shaft horsepower	644.5	606.4
Specific fuel consumption (lb/hp-hr)	0.431	0.381

*Parameters specified by the contract

TABLE II. CALCULATED TURBOSHAFT ENGINE CYCLE DATA

Engine Condition	Altitude (ft)	Flight Mach Number	Gas Generator Speed, $N_{GG}/\sqrt{\theta_2}$ (%)	Combustor Airflow, W_{a3} (lb/sec)	Combustor Inlet Pressure, P_3 (psia)	Combustor Total Pressure Drop, ΔP (psi)	Combustor Inlet Temperature T_3 (°R)	Turbine Inlet Temperature T_4 (°R)	Fuel Flow, W_f (lb/hr)
Steady-state run line	0	0	100	2.733	235.7	7.10	1290	2960	280.9
			90	2.094	168.0	5.28	1170	2540	166.2
			80	1.632	119.1	4.00	1054	2120	96.3
			70	1.228	83.6	2.89	953	1850	59.2
			60	0.934	59.7	2.09	854	1629	38.5
	25,000	0	109.9	1.186	101.9	2.90	1194	2960	126.6
			98.9	1.085	85.1	2.55	1070	2494	88.8
			87.9	0.815	58.1	1.84	957	2080	50.4
			76.9	0.612	39.8	1.33	853	1735	28.7
			60.5	0.385	22.6	0.77	713	1415	14.1
			55.0	0.331	18.9	0.64	669	1335	11.5
			44.0	0.235	13.3	0.41	592	1250	8.0
	45.000	0.85	107.8	0.730	62.8	1.90	1212	2960	79.7
			102.4	0.707	55.6	1.70	1152	2760	66.7
			97.0	0.645	48.3	1.49	1092	2545	52.0
			91.6	0.549	41.6	1.28	1033	2330	40.4
			86.2	0.478	34.6	1.09	977	2130	30.7
			80.9	0.419	28.8	0.94	921	1920	22.9
			75.5	0.364	23.8	0.81	872	1745	17.1
			70.1	0.315	19.5	0.69	822	1570	12.6
			64.7	0.275	16.2	0.59	775	1420	9.4
			59.3	0.241	13.4	0.50	727	1270	6.8
			53.9	0.211	11.1	0.43	682	1140	5.2
Acceleration line (T_4 limit = 3060°R)	25.000	0	65.9	0.315	27.55	0.58	787	3260	43.9
			55.0	0.221	19.33	0.38	694	3060	31.1
			44.0	0.155	13.68	0.24	607	3060	22.9
	45.000	0.85	60.0	0.162	14.14	0.29	764	3060	23.0
			55.0	0.139	12.18	0.24	720	3060	20.3
			50.0	0.119	10.43	0.20	678	3060	17.6
			40.0	0.087	7.58	0.14	600	3060	13.4
Windmilling line (T_4 T_3)	45.000	0.85	54.6	0.242	10.09	0.57	680	680	0
			50.0	0.214	8.72	0.49	646	646	0
			49.4	0.210	8.50	0.45	640	640	0
			45.0	0.187	7.44	0.42	612	612	0
			40.0	0.162	6.32	0.35	582	582	0

An estimate of overall minimum size requirements of the initial combustion system generally involves three basic considerations: (a) the combustor volume necessary to achieve the established combustion efficiency characteristics, (b) the combustor open area required to satisfy the limitation on allowable pressure drop, (c) the geometric proportions required to attain the required discharge gas temperature characteristics and stability limits within the specified liner pressure drop. To meet these requirements, the approximate combustor geometry was determined by scaled empirical correlations derived from previous well-developed combustors.

2.2.1 Combustor Volume

The minimum combustor volume requirement (V_{min}) was determined by the empirical correlation

$$QV_{min} = \frac{W_{a3}}{(P_3)^2 (T_3)^{1/2}} \qquad (1)$$

where Q is the combustor aerodynamic loading parameter. This is one of many empirical correlations used to relate combustor efficiency with the combustor inlet conditions and minimum volume requirements. Figures 1 and 2 present plots of QV versus gas generator speed ($N/\sqrt{\theta_2}$) for the data listed in Table II.

These plots show that QV increases as the engine speed is reduced but reaches maximum at approximately 27 percent speed and then begins to decrease. Since component performance maps are not accurately detailed in this low-speed regime, the computer program used for the cycle calculations was unable to converge to a solution below a corrected speed ($N/\sqrt{\theta_2}$) of approximately 250 percent. Hence, the component maps were extrapolated to extend the lines below the peak loading. It is apparent that the peak loading (and therefore the combustor volume requirements) increased with increasing altitude starting requirements.

Figure 3 shows a plot of Q versus combustor efficiency (η_B). As the performance of a combustor is improved by development, the slope of the line is decreased. The design line, shown in Figure 3, was selected as a minimum attainable goal within the scope of this program. A combustor efficiency of 80 percent is required to provide acceptable engine acceleration during the start cycle. From Figure 3, this requires a value of aerodynamic loading, Q, of 0.80. Therefore, for engine acceleration at 25,000 feet, Mach 0 (where the peak QV = 0.0107, from Figure 1), the minimum combustor volume is 32.7 cubic inches.

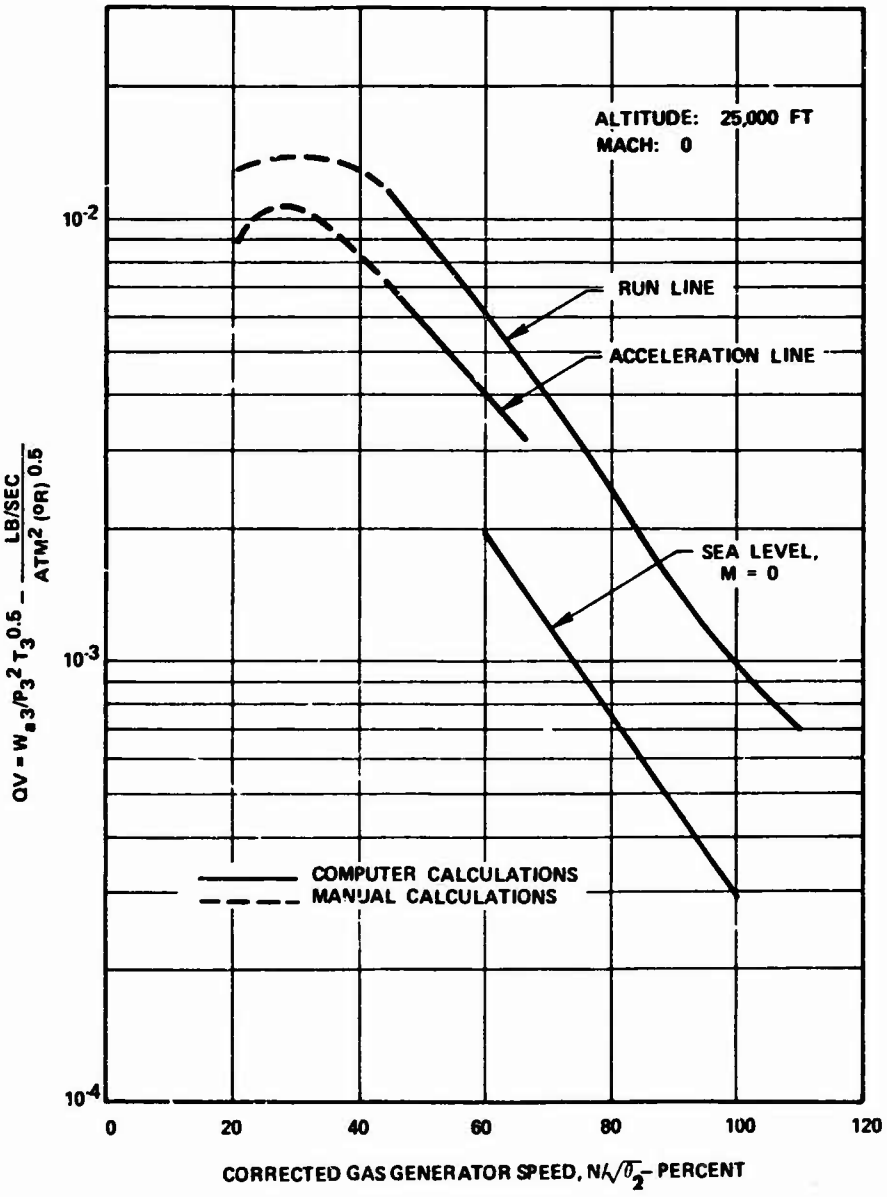


Figure 1. Relationship of QV to Gas Generator Speed (Flight Conditions of Sea Level, Static, and 25,000 Feet, Static, Standard Day).

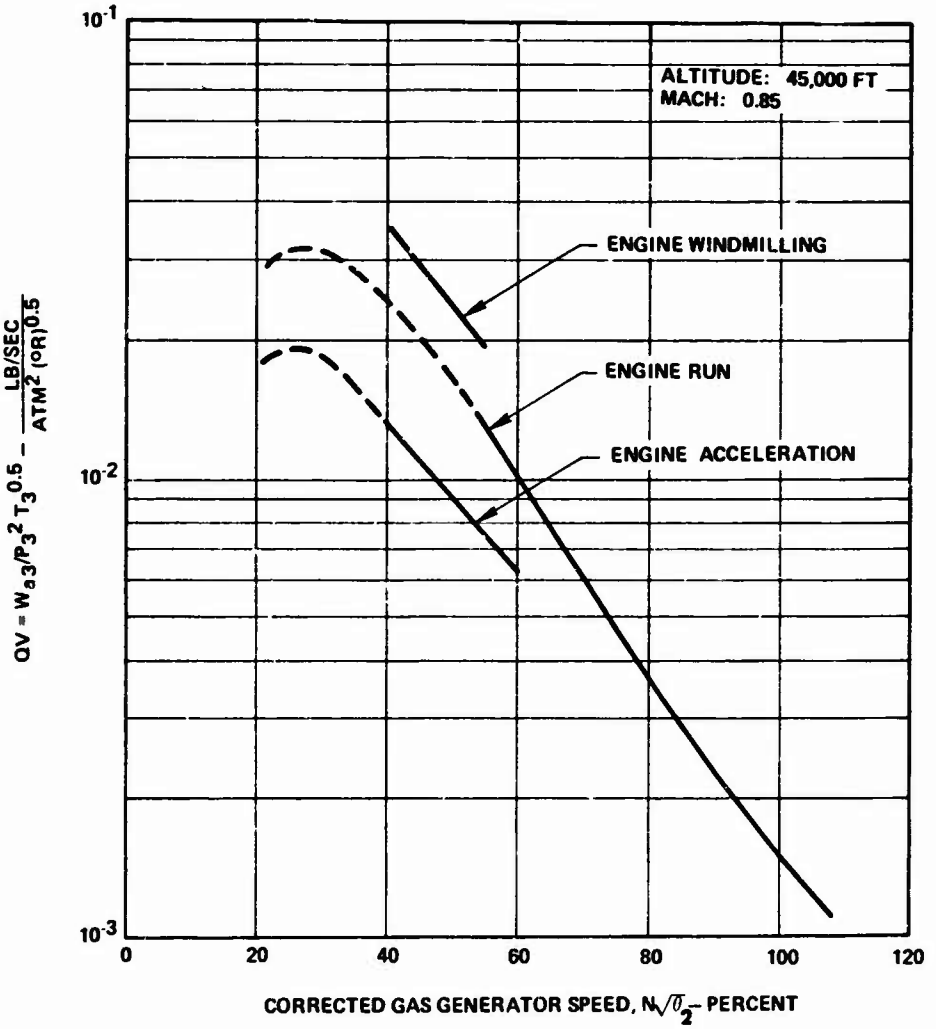


Figure 2. Relationship of QV to Gas Generator Speed (Flight Conditions of 45,000 Feet, 0.85 Mach, Standard Day).

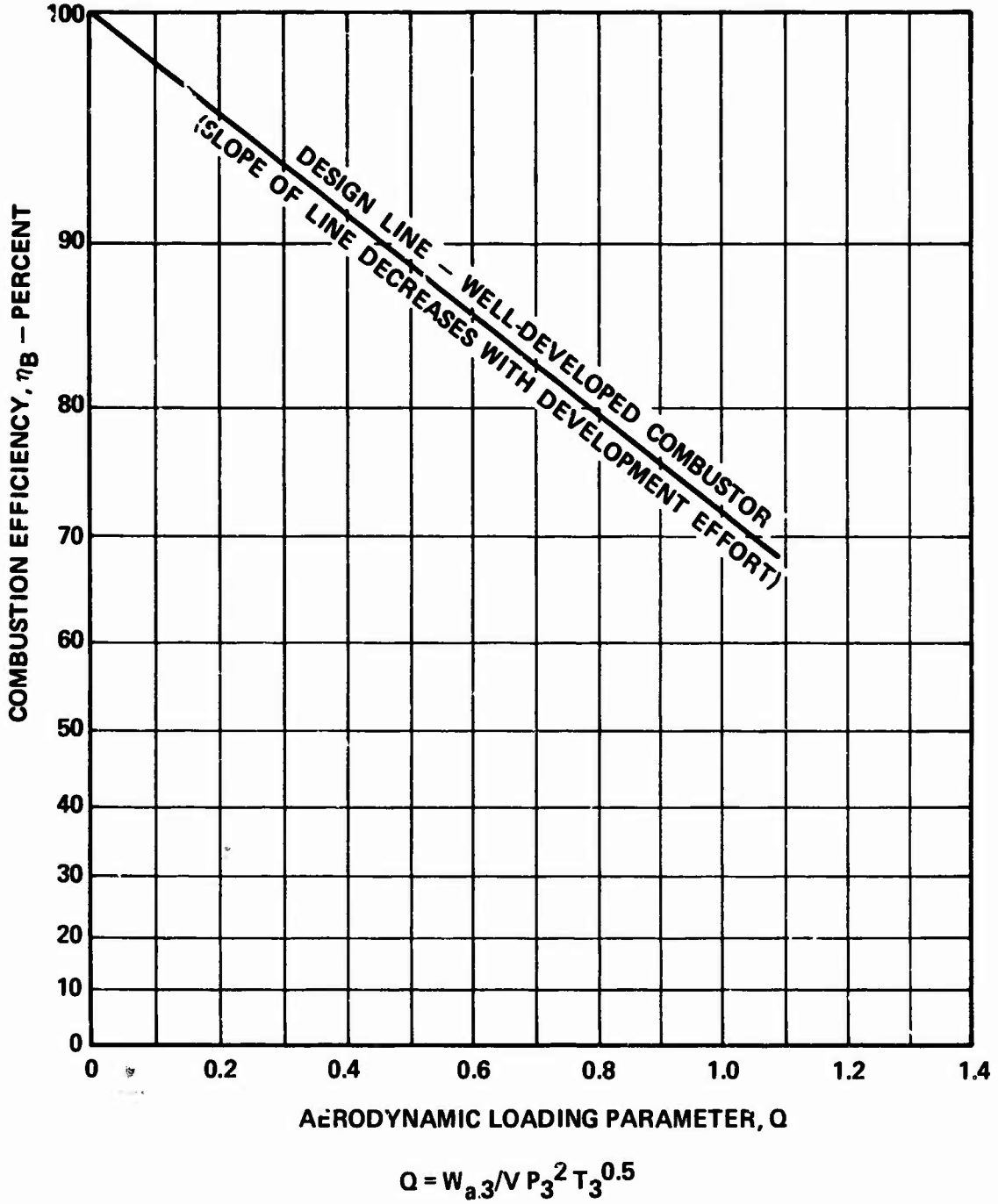


Figure 3. Relationship of Combustor Efficiency to Aerodynamic Loading.

On the run line, the minimum volume is 41.5 cubic inches. Similarly, at 45,000 feet and Mach 0.85, the minimum volume is 94 cubic inches. The primary consideration was relight capability at 25,000 feet, Mach 0. The preliminary sizing analysis was therefore directed toward this goal. The requirements for relight at 45,000 feet, Mach 0.85 will be discussed later.

2.2.2 Combustor Geometry

The combustor length (L) is the sum of the lengths of the primary zone and dilution zone. The primary-zone length must be sufficient to ensure fuel droplet evaporation and primary-zone recirculation. The dilution-zone length is dictated by the length required for inserting the dilution air and mixing to achieve the required pattern factor and radial temperature profile. Experience has shown that combustor length is typically 2.5 times the combustor diameter (can combustor) or annular height (annular combustor).

$$L = 2.5\ D$$
$$L = 2.5\ (OR - IR) \qquad (2)$$

where D, OR, and IR are the combustor diameter, outer radius, and inner radius, respectively.

For an annular combustor, fuel injector spacing is a function of fuel droplet dispersion uniformity as required by discharge temperature objectives and other pertinent combustion parameters. Experience has shown that the number of injectors is determined by the combustor geometry as follows:

$$N = \frac{\pi\ (OR + IR)}{2.5\ (OR - IR)} \qquad (3)$$

2.2.3 Combustor Open Area

The combustor effective open area (Ae) is dictated by the allowable maximum pressure drop ($\Delta P/P_3$), which was specified to be 0.03 for this analysis.

For the small pressure drop across the combustor, this effective open area can be approximated by

$$Ae = \frac{W_{a3}\ \sqrt{\theta_3}}{\delta_3} \left(\frac{1.99}{\Delta P/P_3}\right)^{0.5} \qquad (4)$$

The effective open area is equal to the sum of the orifice physical open area multiplied by the orifice discharge coefficient, C_D, for all liner openings.

These discharge coefficients depend on the type of orifice design and the flow properties at the orifice location. Orifice location and design are dictated by the required fuel-air ratio at any location and the amount of penetration and mixing desired.

2.2.4 Preliminary Combustor Envelope

The geometrical relationships presented above can be used to define an approximate combustor envelope by specifying a minimum or maximum allowable combustor radius. The centrifugal compressor diameter typically establishes the maximum engine diameter, and the annular combustor envelope can usually be tailored to fit above the turbine for a reverse annular combustor configuration or between the compressor and turbine for a straight-through combustor configuration.

From an analysis of several engine schematics that were prepared, the reverse annular configuration appeared to be the optimum for the specified cycle. The maximum combustor diameter was established to be 10.1 inches with the corresponding combustor length and height equal to 1.65 inches and 0.66 inch, respectively. The number of injectors required, based on experience, was 18. This number was considered too large, since the orifice size for each injector would be relatively small and therefore more subject to contamination. The number of injectors can be reduced by holding the length-to-height ratio constant and increasing the volume, as depicted in Figure 4. Approximately eight injectors were considered to be optimum from spacing and fuel contamination considerations. This number results in a volume of 126 cubic inches, which is well in excess of the minimum requirement of 32.7 cubic inches obtained previously. Wall cooling requirements and considerations were deferred until information from heat transfer tests and improved guidelines were available.

The preliminary sizing analysis described thus far was primarily concerned with annular combustor configurations, either reverse or straight-through. The foregoing considerations, however, are generally applicable to both can and annular configurations. The approximate can-combustor geometry was determined as described in the following paragraphs.

The single-can combustor configuration is attractive because the larger fuel passage afforded by a single fuel injector reduces susceptibility to plugging by fuel contamination and fuel-injection system costs are less than annular combustor injector assemblies. However, the configuration is usually difficult to package into an engine envelope because the hot gas torus, which is required to deliver the combustor discharge

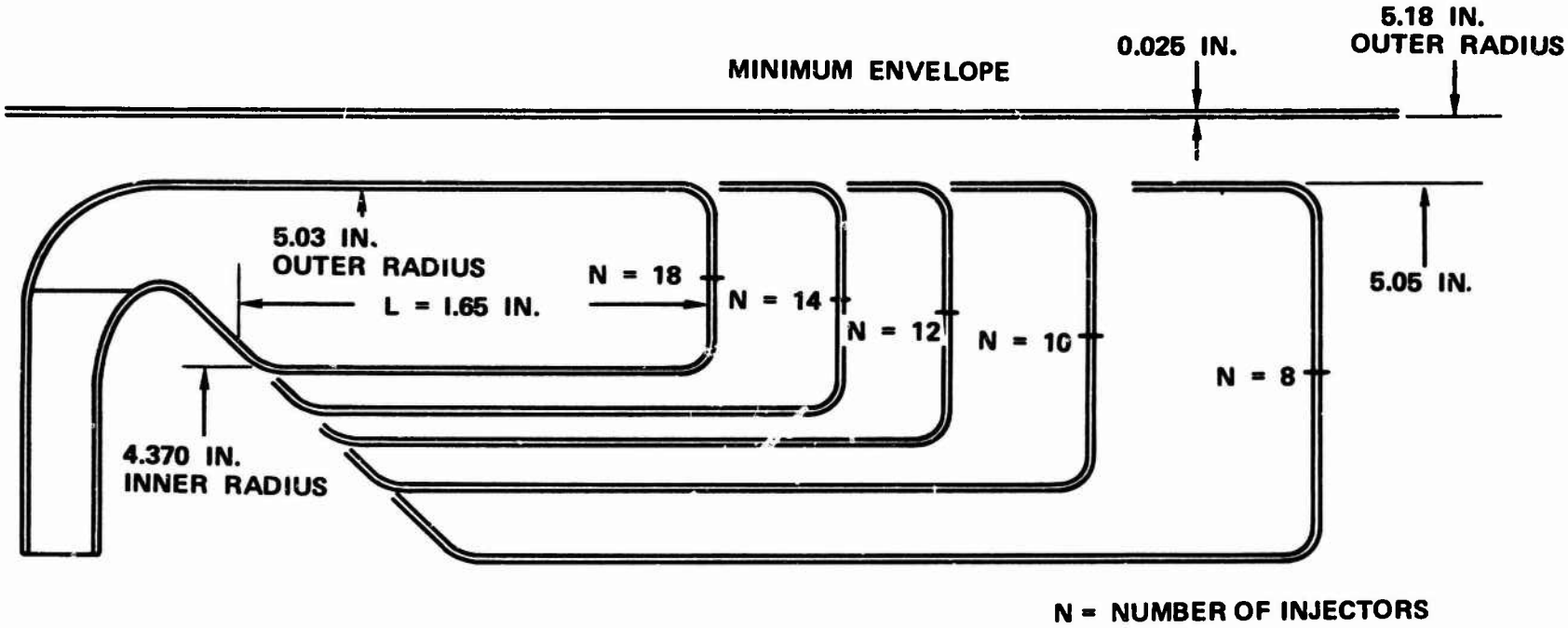


Figure 4. Annular Combustor Configuration.

gas to the turbine, is difficult to cool. In addition, the system pressure drop is typically greater for this configuration, since the dynamic head at the compressor-diffuser exit is lost in the single-can plenum.

The combustor dimensions are determined by the minimum volume requirements, and by a minimum length-to-diameter ratio of 2.0. Thus, for a volume of 41.5 cubic inches, the single-can combustor would require a length of 3.74 inches and a diameter of 1.87 inches.

Efforts were primarily directed toward an annular configuration. For the analyses and element tests, the basic geometry had eight fuel injectors, a height of 1.36 inches and a length of 3.40 inches, as depicted in Figure 5.

2.3 ENGINE SCHEMATICS

Simple-cycle engine schematics were prepared as an aid in determining the size and type of combustor to be used in the analytical studies. The combustors in these schematics were sized by techniques described in Section 2.2. The engine components were based on the cycle parameters in Table I.

The schematics were prepared with both a radial and a two-stage axial gas generator turbine, a two-stage axial power turbine, and three combustor configurations. A single-stage axial gas generator turbine was not included for the simple-cycle engine because of an efficiency penalty, and because the radial location of the turbine inlet (and, thus, the combustor geometry and envelope) would not be significantly affected.

The schematics are shown in Figures 6 through 11. The two schematics that show the shortest engine are the radial turbine with the reverse-flow combustor and the single-can combustor (Figures 6 and 10, respectively). Of these two configurations, the reverse-flow combustor is preferred because it results in the smallest engine diameter and, hence, the most compact engine.

A cursory stress analysis was conducted for the radial turbine with a 0.65-inch-diameter bore for the coaxial power turbine shaft. With a rotational speed of 50,690 rpm, the power turbine shaft will be operating below its first critical speed for lengths less than 8.5 inches. Only the configurations in Figures 7, 9, and 11 would require an increase in power turbine shaft diameter or intershaft bearings to avoid critical speed difficulties.

A more detailed engine design was prepared during Phase II to illustrate the mechanical feasibility of the selected full-scale combustor configuration.

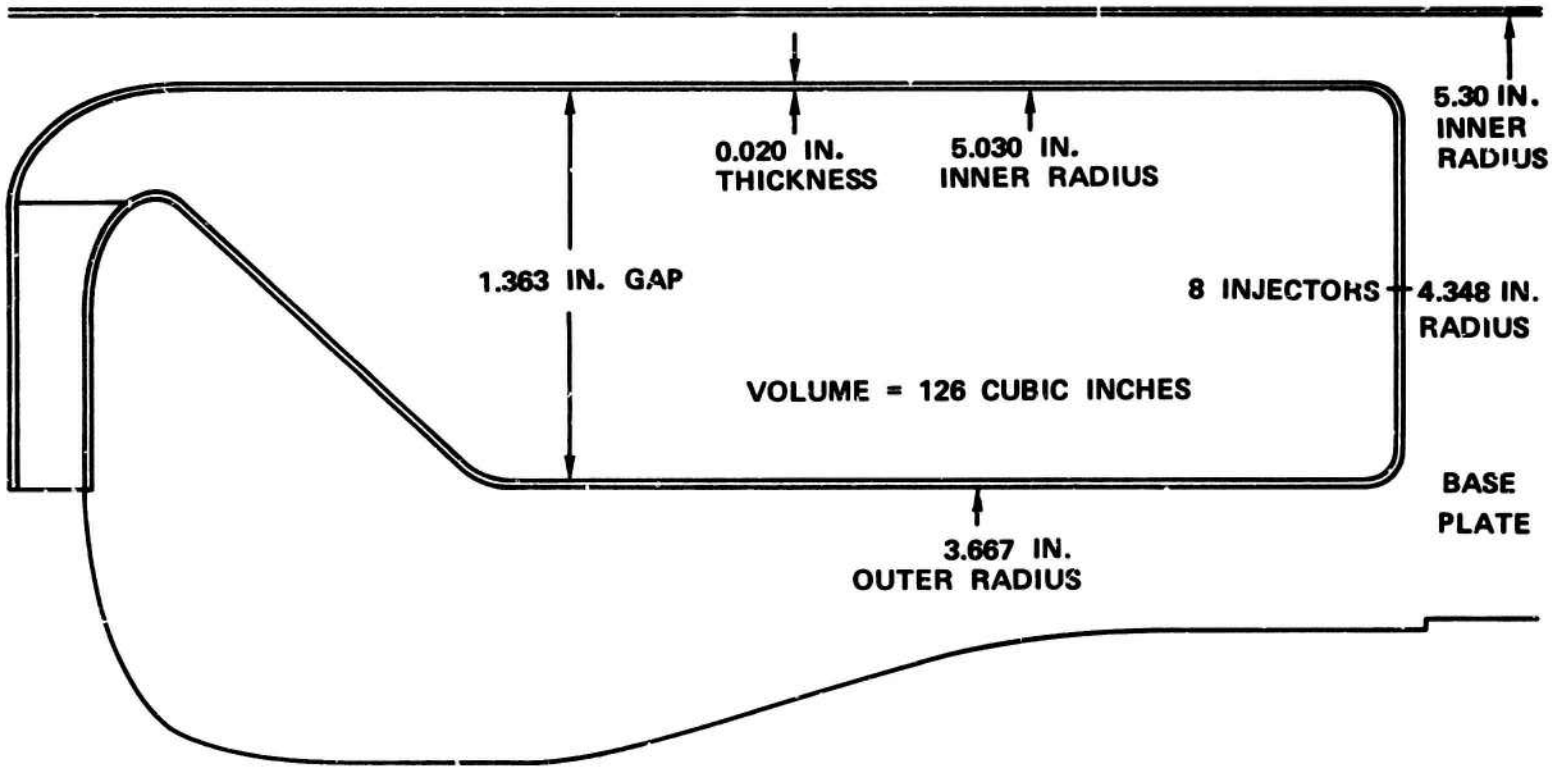


Figure 5. Annular Combustor Envelope.

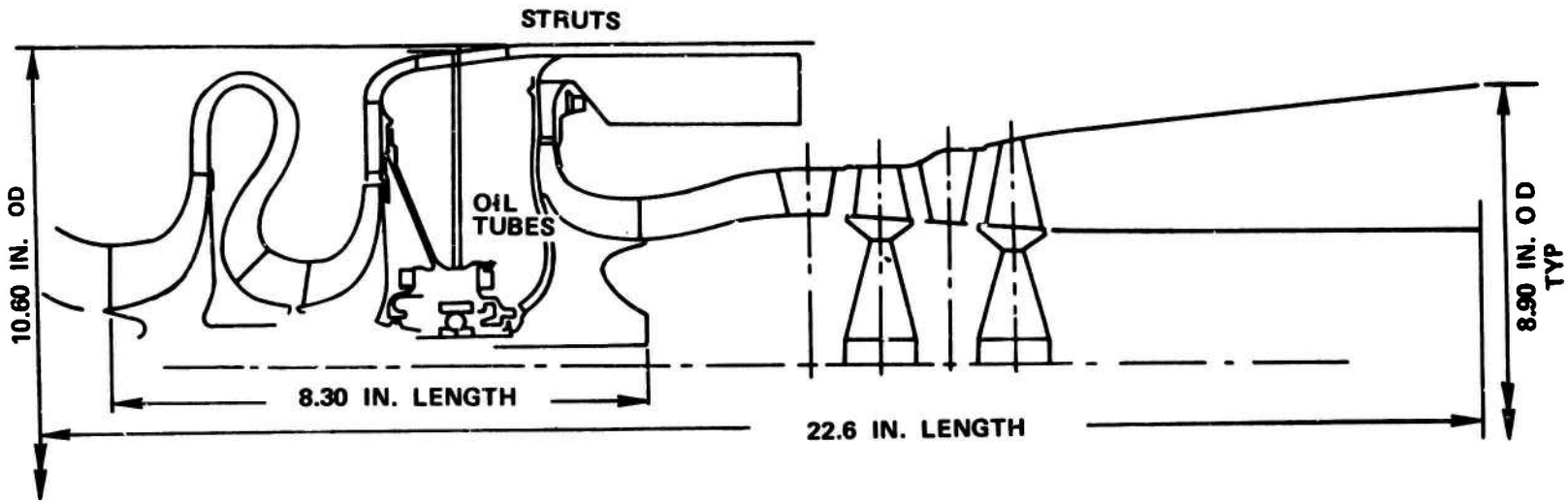


Figure 6. Turboshaft Engine Schematic With Two-Stage Centrifugal Compressor, Reverse Annular Combustor, and Radial Turbine.

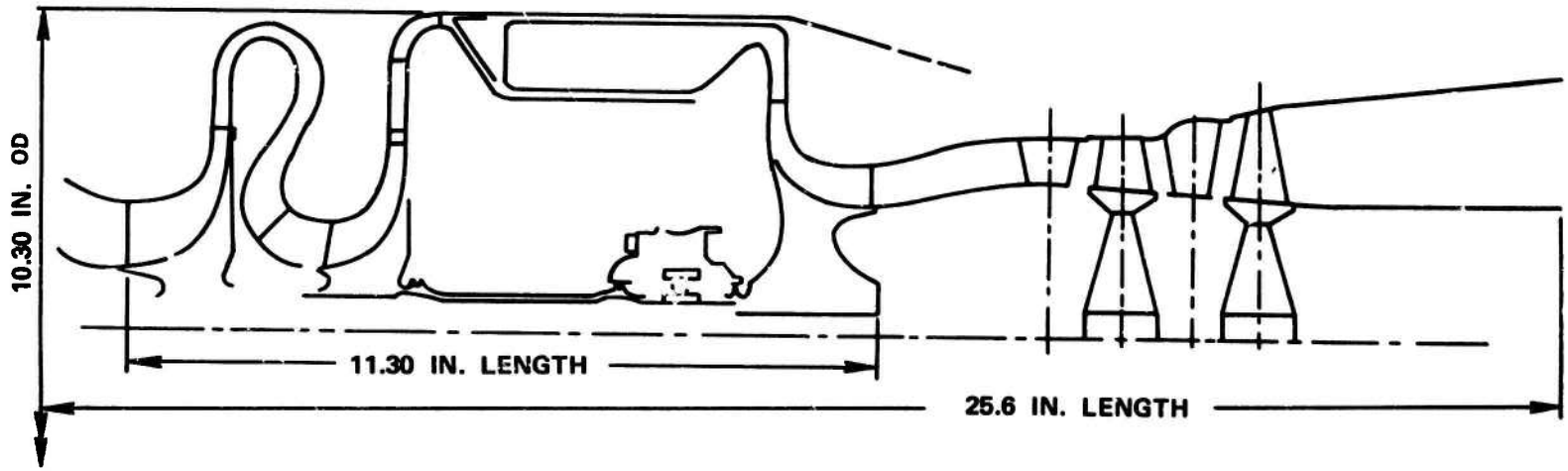


Figure 7. Turboshaft Engine Schematic With Two-Stage Centrifugal Compressor, Straight-Through Annular Combustor, and Radial Turbine.

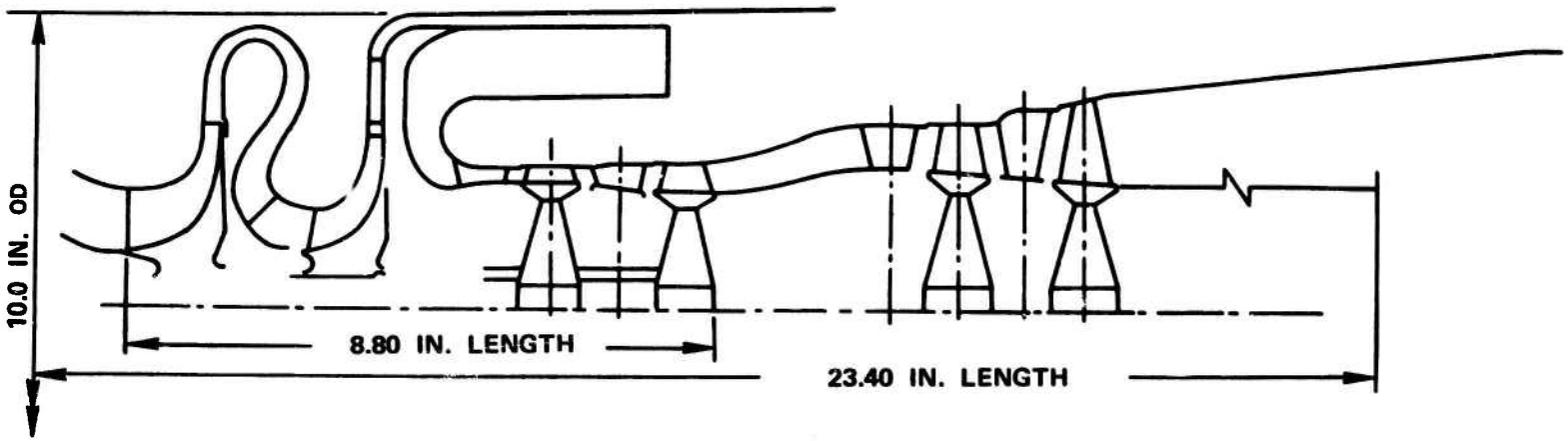


Figure 8. Turboshaft Engine Schematic With Two-Stage Centrifugal Compressor, Reverse Annular Combustor, and Two-Stage Axial Turbine.

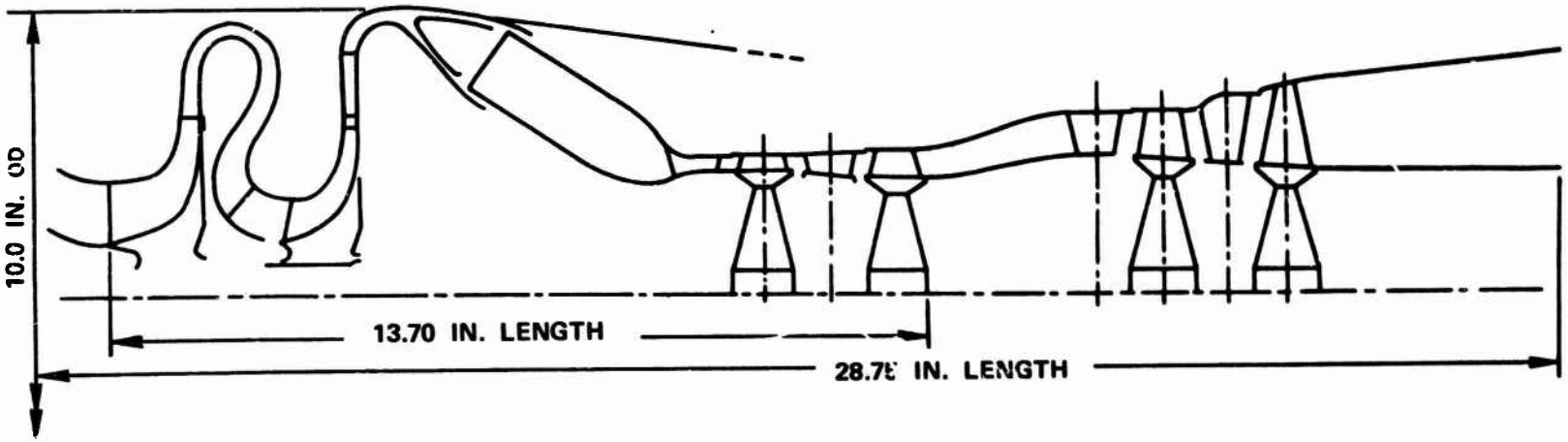


Figure 9. Turboshaft Engine Schematic With Two-Stage Centrifugal Compressor, Straight-Through Annular Combustor, and Two-Stage Axial Turbine.

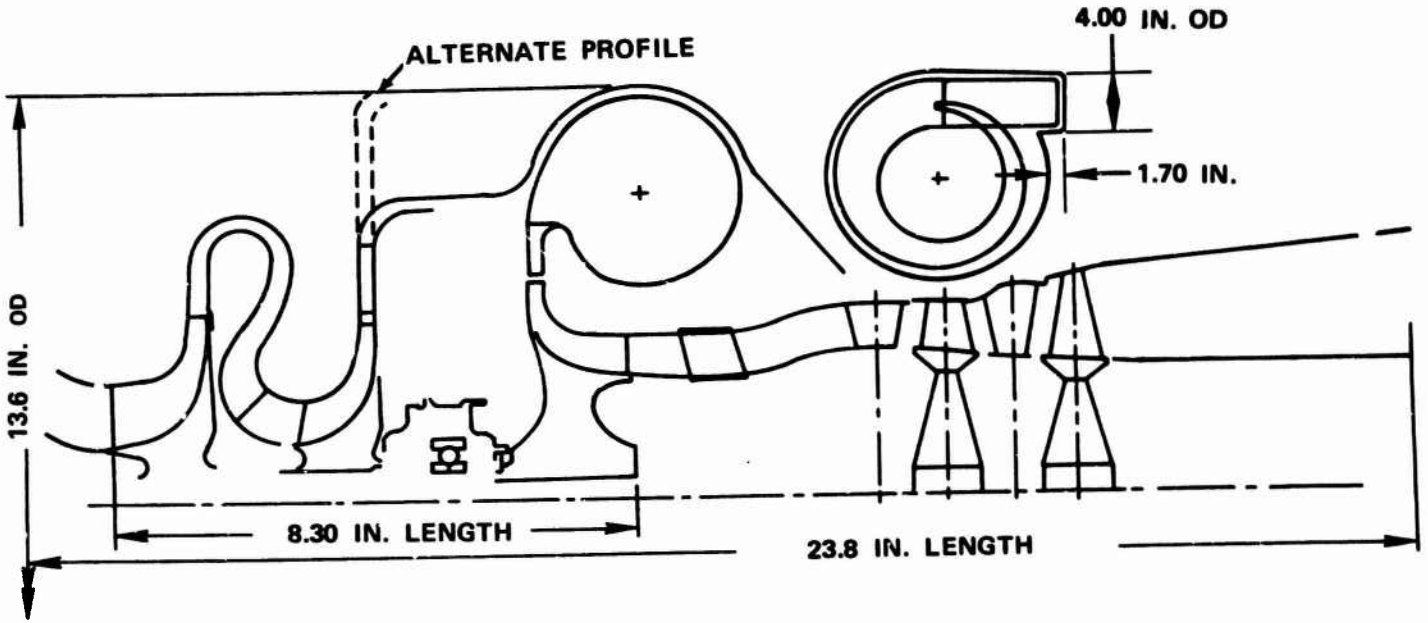


Figure 10. Turboshaft Engine Schematic With Two-Stage Centrifugal Compressor, Can Combustor, and Radial Turbine.

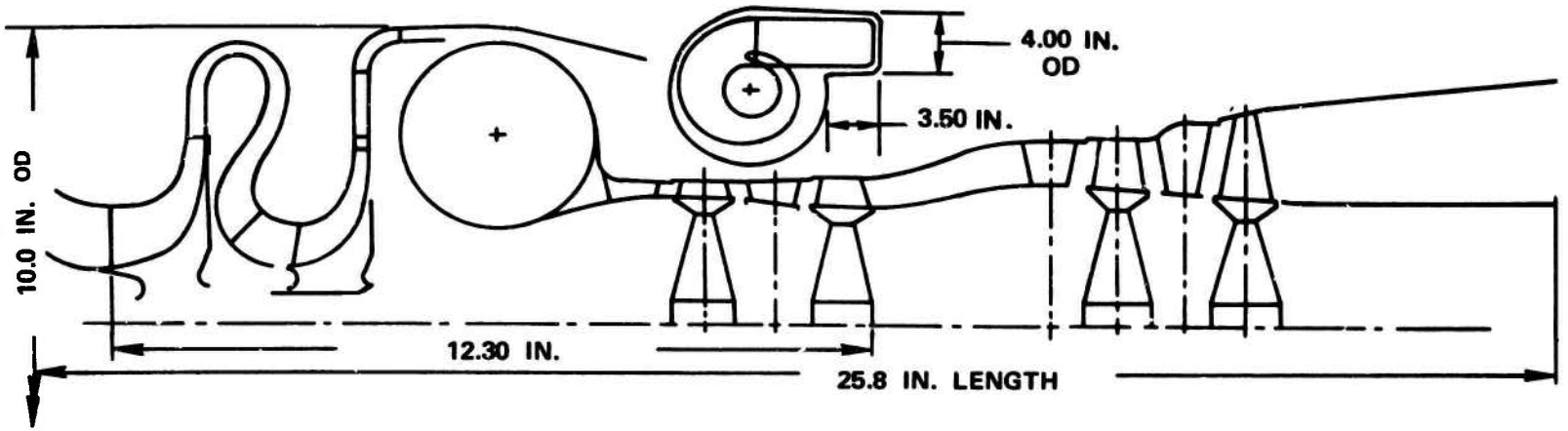


Figure 11. Turboshaft Engine Schematic With Two-Stage Centrifugal Compressor, Can Combustor, and Two-Stage Axial Turbine.

3.0 MATERIAL SELECTION

For small, advanced, high-temperature engine cycles, the cooling-air requirements are considerable because of high combustor air (compressor discharge) temperatures and high surface-to-airflow ratios. In addition, the quantity of cooling air available is severely limited due to primary-zone and dilution-zone requirements. It is therefore necessary to reduce cooling-air requirements by (a) minimizing the liner surface area, (b) optimizing the cooling-element design, and (c) selecting materials with optimum high-temperature properties.

Surface-area and cooling-element design optimization is discussed in subsequent sections of this report. This section describes a series of material screening tests that were conducted to provide a basis for comparing existing materials and for ultimately selecting one material that will provide better properties for an advanced combustor application than those materials currently in use.

Based on a comparison of high-temperature metallurgical stability, corrosion resistance, and fabricability, IN-5/6 was selected. Subsequent to this selection, a series of mechanical-property tests was conducted to supplement the limited published data that was available for this relatively new material.

A brief summary of the test procedures and results is presented here. Two AiResearch reports[1,2] provide detailed test results and data analyses.

3.1 CANDIDATE MATERIALS

Experience has shown that the three principal modes of combustor material failure are cracking, buckling, and hot corrosion. Materials of the Hastelloy X class are currently used for combustors to provide hot-corrosion resistance and high-temperature fretting resistance. The properties of Hastelloy X are well established and thus served as a base line for comparison with other candidate materials in this screening program.

Candidate materials were selected on the basis of one or more properties that were known to be as good as or better than Hastelloy X. The candidate materials were:

- Haynes 188
- AiResist 213

- o Rigimesh wire (L605) with Rokide-Z (ZrO_2) coating
- o TD Ni-Cr
- o IN-586
- o Hastelloy X (base line)

Table III details the chemical composition (required and actual) and thickness of the material specimens used in the program. As noted in the table, the compositions of AiResist 213 and IN-586 were below specifications. Since these discrepancies were small, and because these were the only specimens of these materials available for test within the time limitation of the program, they were included for comparison. The evaluation of test results included a consideration of the effects of these discrepancies.

An attempt was made to obtain all the materials in 0.020-inch-thick sheets. Since IN-586 and AiResist 213 were available only in 0.032-inch sheets, Hastelloy X specimens of this thickness were also tested to ensure a valid comparison.

3.2 SCREENING TESTS

The candidate materials were screened by a series of tests to assess thermal stability (property degradation after prolonged exposure at 1800°F), thermal fatigue, corrosion resistance (oxidation and sulfidation), and fabricability. Where possible, the test results were compared with published data.

3.2.1 Thermal Stability

Tensile properties, at room temperature and 1800°F, and stress-rupture properties at 1800°F were determined before and after 100-hour exposure in air at 1800°F. These tests were conducted in accordance with ASTM Test Methods E8 and E139, respectively.

The stress-rupture tests were conducted with three specimens of each material, one specimen loaded to produce failure in approximately 50, 100, and 150 hours. A Larson-Miller parameter of 52 was arbitrarily selected for rating the stress-rupture properties of the candidate materials. This is equivalent to 1000 hours at 1800°F.

3.2.2 Thermal Fatigue

While a standard thermal-fatigue test procedure has not been established, a test procedure has been previously devised and used at AiResearch for a comparison of the relative thermal-fatigue characteristics of several materials. The data from

TABLE III. CHEMISTRY OF MATERIALS EVALUATED

Material	AiResist 213		Hastelloy X		Haynes 188		IN-586		Rigimesh L605		TD Ni-Cr	
Heat No.			2600-9-4876 BA		1880-0-0154		KND 0980					
Elements	Actual	Required	Actual	Required	Actual	Nominal	Actual	Required	Actual	Required	Actual	Required
C	-	-	0.06	0.05- 0.15	0.07	0.05	0.05	0.03 -0.08	0.08	0.05- 0.15	0.03	0.1 Max
S	-	-	0.005	0.03 Max	0.001	-	-	-	-	-	0.005	0.05 Max
Cr	15.8*	18.0 -20.0	21.77	20.5 -23.0	21.32	22.0	21.2*	24.0 -26.0	19.59	19.0 -21.0	19.45	19.0-23.0
ThO_2	-	-	-	-	-	-	-	-	-	-	2.20	1.5- 3.0
Ni	-	-	Bal	Bal	22.45	22.0	Bal	Bal	10.04	9.0 -11.0	Bal	Bal
Mo	-	-	8.94	8.0 -10.0	-	-	9.0	9.0 -11.0	-	-	-	-
Ce	-	-	-	-	-	-	0.02	0.015-0.05	-	-	-	-
La	-	-	-	-	0.03	0.08	0.002	-	-	-	-	-
Mg	-	-	-	-	-	-	0.0006*	0.01 -0.03	-	-	-	-
Ta	6.2	6.0 - 7.0	-	-	-	-	-	-	-	-	-	-
Zr	0.11	0.10- 0.20	-	-	-	-	-	-	-	-	-	-
Y	0.6	0.05- 0.15	-	-	-	-	-	-	-	-	-	-
Co	Bal	Bal	1.89	0.5 - 2.5	Bal	Bal	-	-	Bal	Bal	-	0.3 Max
Al	3.3	3.2 - 3.7	-	-	-	-	-	-	-	-	-	-
W	-	-	-	0.20- 1.0	13.76	14.0	-	-	14.85	14.0 -16.0	-	-
Fe	-	-	18.96	17.0 -20.0	1.68	1.5	-	-	2.01	3.0 Max	-	-
Si	-	-	0.43	1.0 Max	0.43	0.20	-	-	0.02	1.0 Max	-	-
Mn	-	-	0.67	1.0 Max	0.75	0.75	-	-	1.24	1.0 -2.0	-	-
P	-	-	0.014	0.04 Max	0.005	-	-	-	-	0.4 Max	-	-
B	-	-	0.002	0.01 Max	-	-	-	-	-	-	-	-
Sheet Thickness (inch)	0.032	-	0.021	-	0.021	-	0.038	-	0.009	-	0.020	-

*Below specified Cr minimum

the tests provides a qualitative assessment of material life when compared to a reference material (e.g., Hastelloy X), even though it cannot be directly translated to combustor life.

The test apparatus consists of an automatic indexing mechanism that can cycle test specimens between an oxyacetylene flame and an ambient-air jet. The geometry of the test specimen (shown in Figure 12) allows for minimum mechanical constraint. and therefore the induced stresses are totally caused by the thermal gradients generated during cycling.

Views of the test-rig setup are shown in Figure 13, with a specimen both in and out of the flame.

The maximum metal temperature was 1800°F as measured by a surface thermocouple installed adjacent to the center hole. Thermal cycling of the samples was completed with a cycle time of 5 seconds in the flame and 10 seconds in the ambient-air jet. The first sample of each material was inspected every 25 cycles for cracks. Subsequent samples were run initially until the number of cycles equaled the number accumulated on the first sample before cracking. Subsequent inspections of these additional specimens were then made at intervals of 10 cycles to establish the number of cycles required to initiate a crack. Each specimen was then subjected to an additional 50 cycles to evaluate crack propagation.

3.2.3 Corrosion

Oxidation testing was accomplished by placing duplicate specimens in a furnace at 1800°F for 150 hours. Air circulation was achieved by natural circulation through an open furnace. Both sets of samples were evaluated by weight changes, and one set was mounted for metallographic examination.

Test specimens for the sulfidation corrosion test were placed in a silica retort mounted in a resistance-heated furnace. The retort was heated to 1800°F prior to loading. Initially, the specimens were exposed for 10 minutes in a reducing atmosphere of 76.7 percent N_2, 20.5 percent CO_2, and 2.83 percent H_2S with 1 ppm NaCl. The balance of the atmosphere was N_2 saturated with water at room temperature.

The two-cycle procedure closely simulates a gas turbine start, H_2S being found in the oxygen-starved, initial combustion products and SO_2 during continuous, or oxygen-rich, operation. The 1 ppm of NaCl simulates operating in a marine environment. After the test cycles, the specimens were removed and the corrosion products were cleaned from the surface on one set of

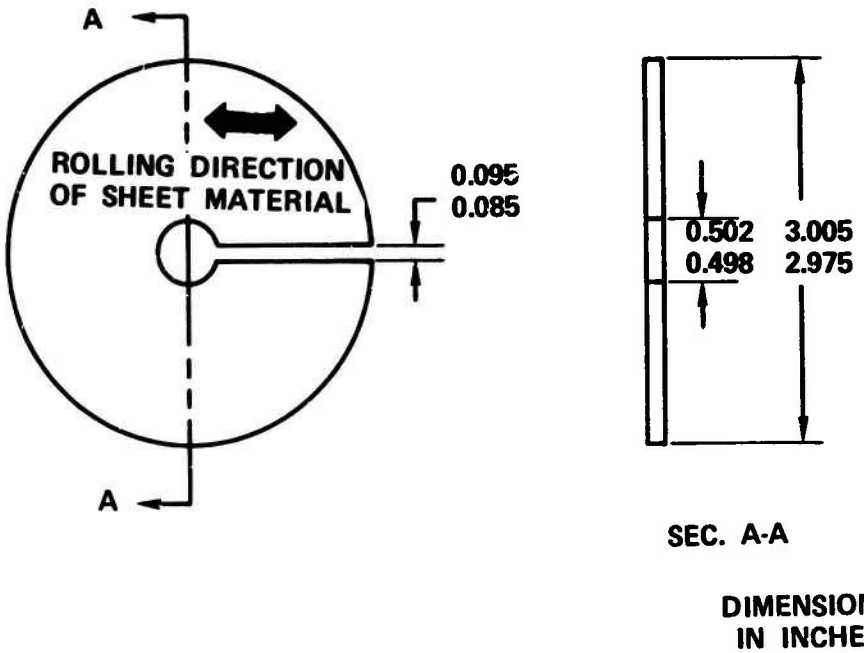


Figure 12. Thermal Fatigue Test Specimen Geometry.

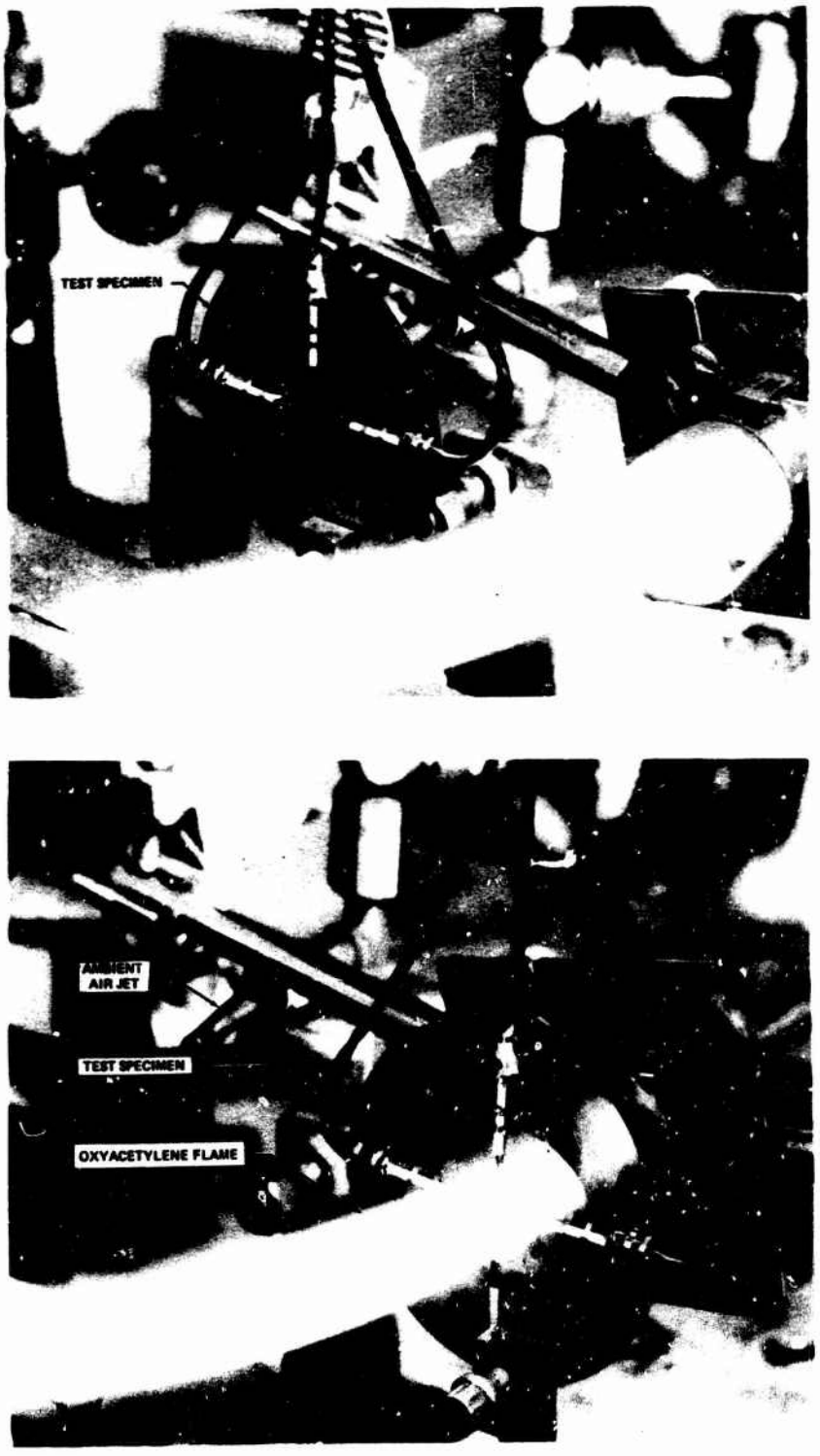


Figure 13. Thermal Cycle Rig Showing Test Specimen in the Ambient Air Jet (Top) and the Oxyacetylene Flame (Bottom).

samples. The evaluation was made on the basis of weight loss in milligrams per initial unit surface area. The duplicate samples were examined by metallography to evaluate the depth of attack.

3.2.4 Fabricability

Fabrication studies were limited to the IN-586 and the Rigimesh material. These consisted primarily of weldability and weld ductility evaluations. The fabricability of the other candidate materials is well documented, including the difficulties involved in handling the dispersion-strengthened alloys. It was not considered necessary to confirm this data.

3.3 SCREENING TEST RESULTS

The screening test results are summarized as follows:

(a) Tensile Property - TD Ni-Cr was rated superior both on an absolute strength level and on retention of properties after exposure. IN-586, Haynes 188, and Hastelloy X rated slightly lower due to the lower strength levels. AiResist 213 was rated lower because of failure to meet published properties.

(b) Stress Rupture - TD Ni-Cr and Haynes 188 were rated superior; IN-586 and Hastelloy X were only slightly lower. AiResist 213 was rated the lowest of the sheet metal alloys.

(c) Thermal Fatigue - IN-586 was rated superior, AiResist 213 second, and TD Ni-Cr third, due to inconsistency of results. Haynes 188 was rated only slightly better than Hastelloy X. The composite structure (Rokide-Z-coated Rigimesh wire) does show promise. In the range of 0.020- to 0.040-inch-thick material, no correction was required.

(d) Oxidation - AiResist 213, Haynes 188, IN-586, and TD Ni-Cr showed equivalent resistance to oxidation. All were rated slightly better than Hastelloy X. Rokide-Z-coated Rigimesh was rated very poor.

(e) Sulfidation - AiResist 213 was rated superior, IN-586 second, and Haynes 188 third, bordering on unacceptable. TD Ni-Cr and Hastelloy X were rated unacceptable.

(f) Fabricability - Both IN-586 and L605 Rigimesh with Rokide-Z coating were easily welded with the use of both the tungsten-inert-gas and resistance welding techniques. The weld ductility was good.

A numerical method of rating the sample materials would be highly arbitrary and was not attempted. The Rokide-Z-coated Rigimesh was eliminated due to oxidation of the L605 wire structure. Some development work could make this a workable structure. Haynes 188 did show some improvement over Hastelloy X but did not rate as high as other candidate alloys in the tests, primarily because of thermal fatigue and sulfidation. The TD Ni-Cr rated higher than the Haynes 188 alloy in most tests but was very poor in sulfidation resistance.

Materials that compared closely were the AiResist 213 and the IN-586. IN-586 was selected due mainly to the excellent thermal-fatigue resistance of the alloy and its ease of fabrication. Also, the actual strength of the IN-586 appeared to be higher at elevated temperatures than the AiResist 213.

3.4 IN-586 PROPERTY TESTS

From the screening test results, it was concluded that IN-586 is well suited for a combustor application. However, since the material is relatively new (International Nickel, 1968), and therefore only limited published data is available,[3] a series of material property tests was conducted to provide more information on the alloy and to define guidelines for combustor design and fabrication.

Additional tensile tests were conducted so that the effect of temperature on the properties could be more fully evaluated. The added stress-rupture tests included creep measurements so that a family of parametric curves could be drawn for several creep extensions and rupture life. Low-cycle-fatigue data was also generated, with comparative specimens of Hastelloy X and Haynes 188. Tensile specimens of both fusion-butt welds and lap-seam welds were tested in both the as-welded and the heat-treated condition.

The property data (curves and tables) presented in the following paragraphs also includes published and screening test data for IN-586. Although some scatter was noted in the tests, the data agreed well with published data for the alloy.

3.4.1 Tensile Tests

Tensile tests were conducted with metal temperatures in the range of 800°F to 2000°F in accordance with ASTM Test Method

E8. The data for 0.2-percent yield strength versus temperature is presented in Figure 14. Lines drawn indicate the approximate envelope of test data. Note that the data from the specimens exposed to air at 1800°F for 100 hours (Screening Tests, Section 3.2) compares well with the unexposed specimen data, confirming the thermal stability of IN-586.

3.4.2 Creep-Rupture Tests

The creep-rupture tests were conducted in accordance with ASTM Test Method E139. The 0.5-percent and 1.0-percent creep-rupture data is presented in Figure 15; the stress-rupture data is presented in Figure 16. A curve fitting computer program was used to obtain both the average and the 3-sigma minimum design curve.

3.4.3 Low-Cycle-Fatigue Tests

The specimen was resistance-heated to 1600°F in the gauge section. The test was conducted using load control, with the strain being continuously monitored. The A-ratio was maintained at less than 1.0 so that compressive strain would be avoided. The cyclic rate was 30 cpm, and data for load versus time, axial strain versus load, axial strain versus time, and lateral deflection versus time was developed. Figure 17 graphically shows the low-cycle-fatigue data obtained for IN-586, Hastelloy X, and Haynes Alloy 188. The superiority of IN-586 is clearly evident.

3.4.4 Fabricability Tests

Fusion-butt and lap-seam welds were made and samples machined to evaluate the tensile strength. The welds were tested in both the as-welded and the stress-relieved condition. The data is presented in Table IV. The butt weld flash was ground to the approximate thickness of the sheet to make the test more severe. Filler material used in making the welds was sheared from the edges of the sheet alloy.

The welded strengths presented in the table may be clouded by the scatter in tensile data noted below 1600°F. The elevated-temperature tests were performed at 1300°F, as the tensile curve began dropping at this point. The data indicates that the material may be better used in the as-welded condition than stress-relieved, and that weld repair should present no particular difficulties on new or engine-run combustors.

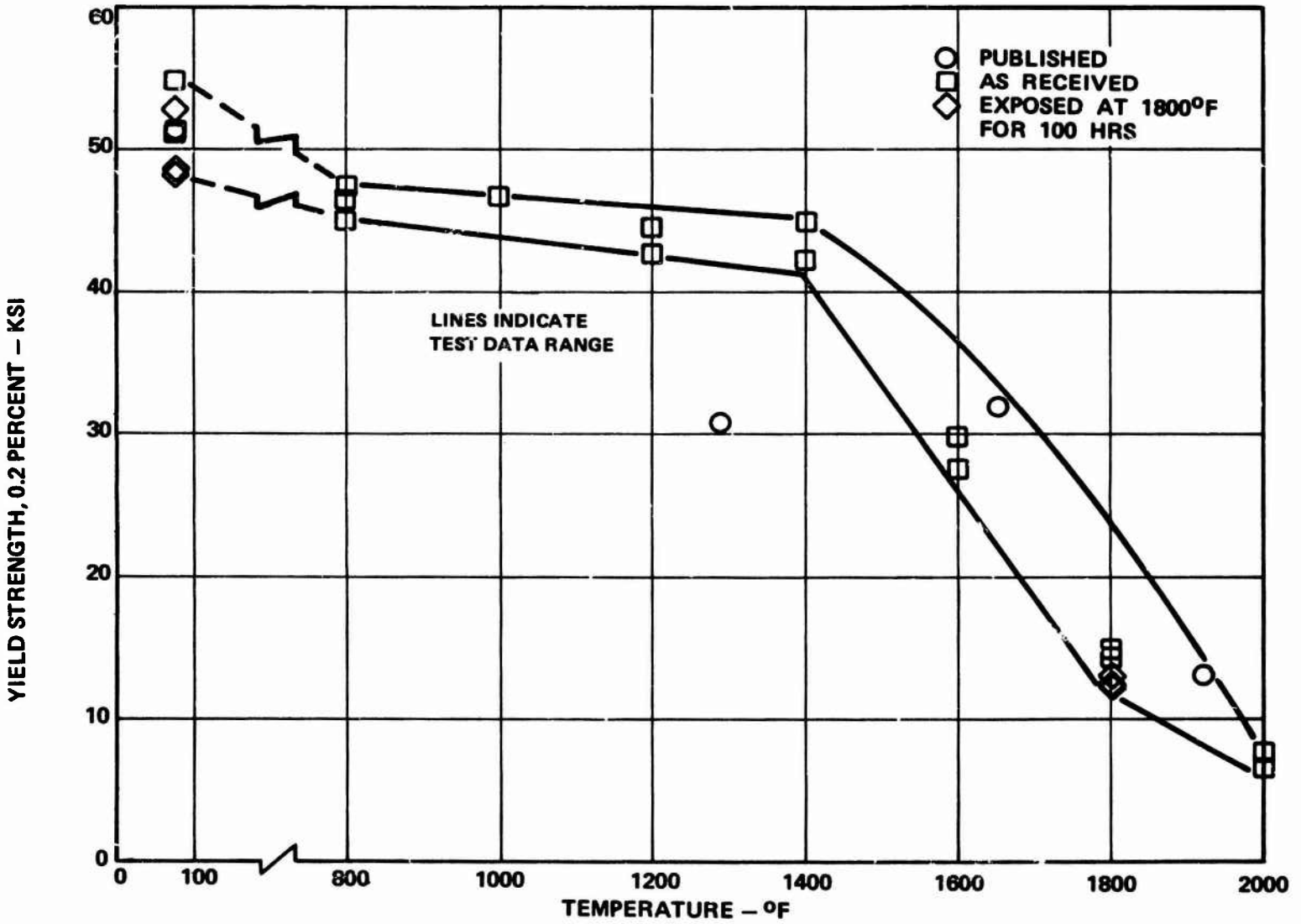


Figure 14. The 0.2 Percent Yield Strength of IN-586 at Various Temperatures.

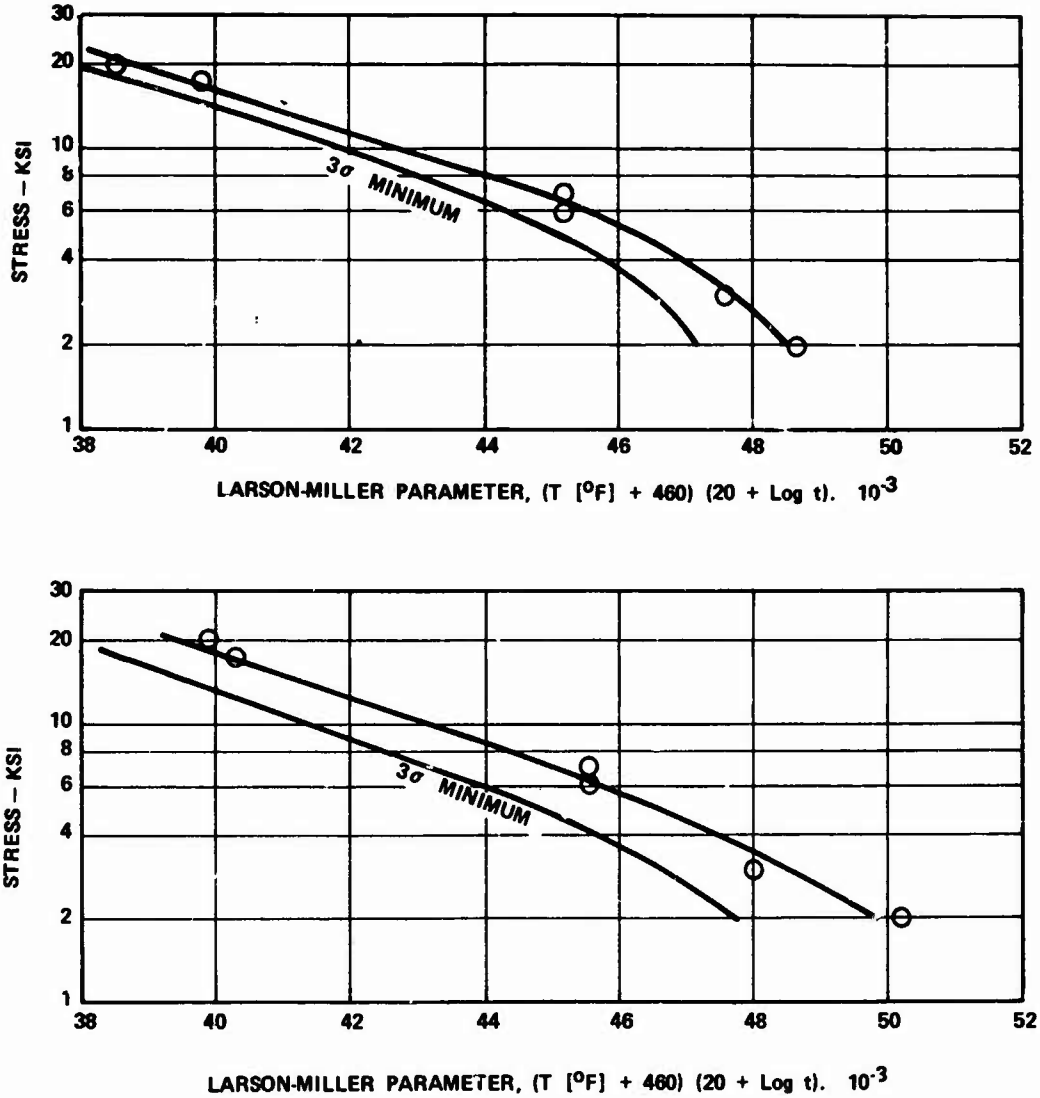


Figure 15. Parametric Curves for 0.5 Percent (Top) and 1.0 Percent (Bottom) Creep-Rupture Tests of IN-586 Material.

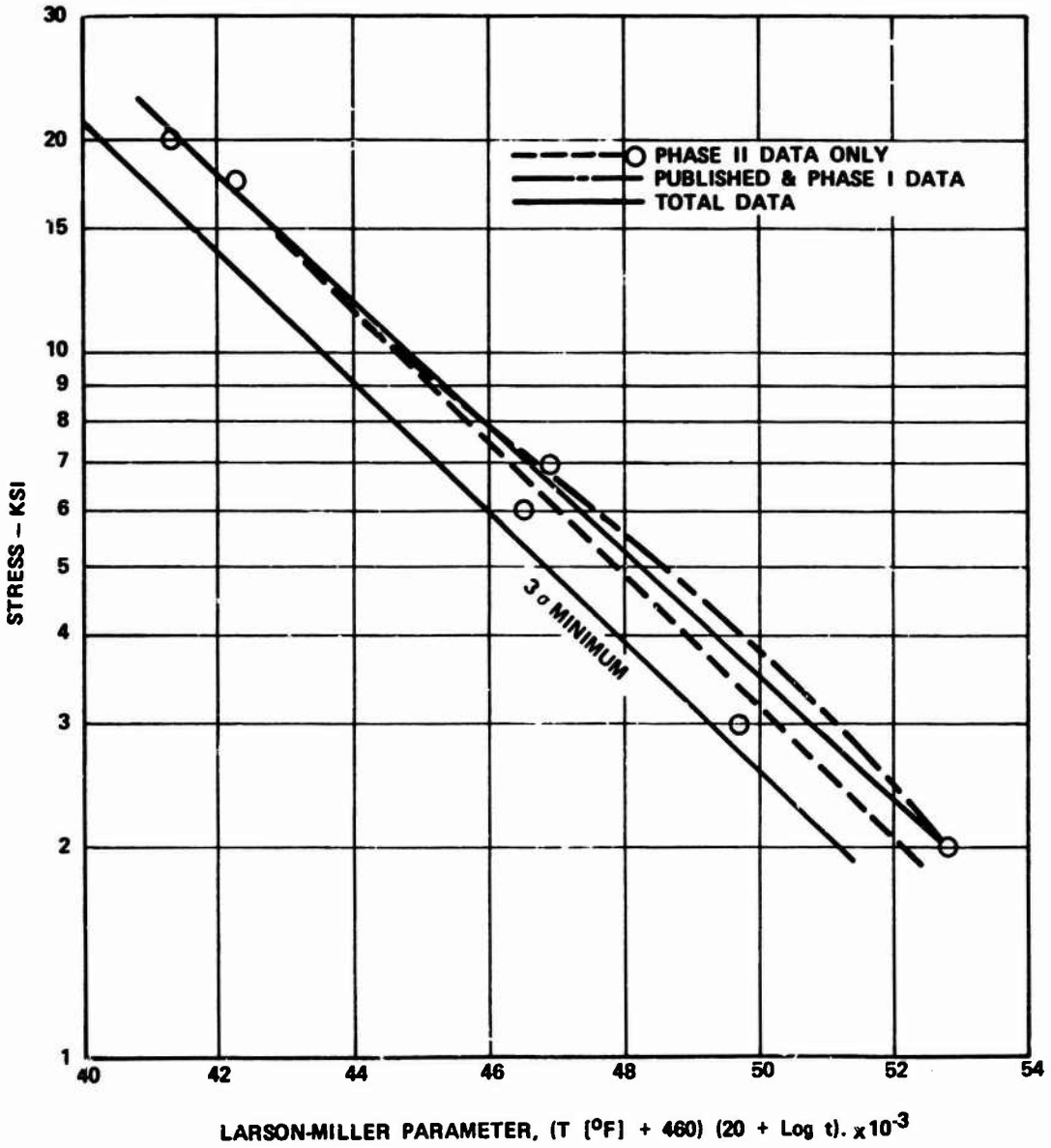


Figure 16. Stress-Rupture Curve for IN-586.

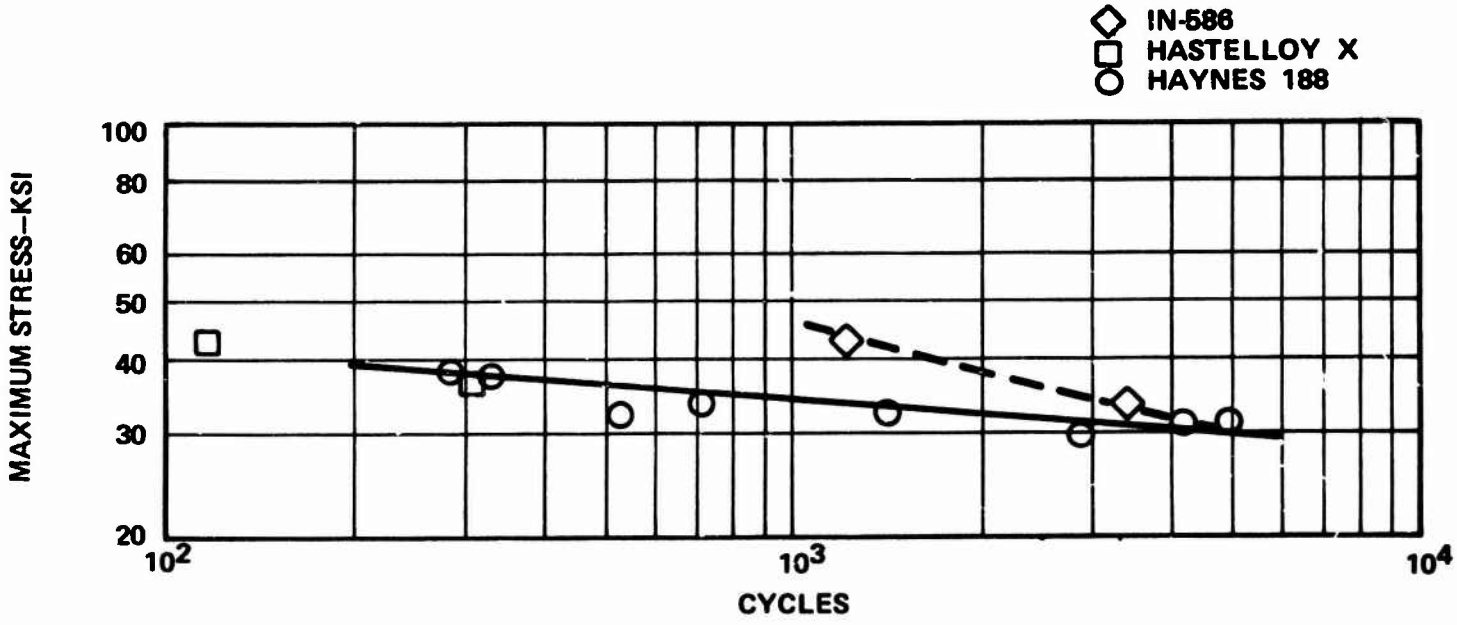


Figure 17. Low-Cycle-Fatigue Data for IN-586, Hastelloy X, and Haynes 188.

TABLE IV. WELD STRENGTH DATA FOR IN-586

Weld Type	Condition	Test Temp (°F)	Strength	
			Ultimate (ksi)	Average (ksi)
Butt Fusion-Group I	As welded	Room Temp	105 110 100	105
Butt Fusion-Group II	Stress-relieved	Room Temp	110.5 104 105	106.5
Butt Fusion-Group III	Stress-relieved	Room Temp	89.2 91.5 91.0	90.6
Butt Fusion-Group IV	Stress-relieved	1300	40 41.5	40.7
Lap - Seam	As welded	Room Temp	121 121.1	121
Lap - Seam	Stress-relieved	Room Temp	110.5 106.5 105 99	105.3
Lap - Seam	Stress-relieved	1300	46.2 45.5	45.9

NOTES: 1. SPECIMENS WERE WELDED IN 3-INCH-WIDE SHEETS AND CUT FOR TENSILE TESTS.

2. STRESS-RELIEF CYCLE WAS 2100°F FOR 15 MINUTES.

3.4.5 Material-Property Test Conclusions

Comparison of the measured design property levels of IN-586 with previously published data indicates better tensile strength than published properties, with some scatter at temperatures below 1600°F. The creep-rupture tests confirm the strength and the oxidation resistance of the alloy and agree well with the published data. The low-cycle-fatigue tests showed that the material can be used with more confidence than Hastelloy X, and possibly Haynes 188.

NOTE

IN-586 is not produced commercially in the United States at this time (the material used for this program was provided at no charge by International Nickel Company of England). A local sales representative for INCO said that IN-617 has similar properties and is available in the United States. He also said that IN-586 would be made available if the marketing demands were sufficient.

4.0 FUEL INJECTION

The fuel-injector design requirements are primarily dictated by the following:

- Fuel-flow range
- Requirement to pass fuel contaminated per MIL-E-5007C
- Combustor chamber design interface requirements

Maximum fuel flow was determined from the cycle analysis, shown in Table II of Section 2.0, to be 280.9 pounds per hour at the design point. For typical gas turbine applications a reasonable minimum fuel flow is 8 to 10 percent of this value (23.0 pounds per hour). Experience indicates that to pass the MIL-E-5007C contamination requirements, all internal fuel flow passages should be larger than 0.030 inch.

Injector types that were selected for analysis included:

- Air-assist atomizer
- L-pipe vaporizer
- Pneumatic-impact atomizer

4.1 AIR-ASSIST ATOMIZER

One of the most conventional combustor fuel injection systems is the pressure atomizer type in which fuel is forced, under pressure, through a swirl chamber and small orifice to achieve atomization. Either one (simplex) or two (dual) orifices can be used, depending on the range of fuel flow (turndown ratio) required. For an air-assist atomizer, shown schematically in Figure 18, a small quantity of air is used to improve atomization and control the spray angle and also to cool and clean the injector.

The analyses described below were generally derived for a simplex atomizer with air assist (shown in Figure 19), but they are also applicable to a dual-orifice nozzle. A brief description of the air-assist pressure atomizer computer program is presented in Appendix I.

4.1.1 Model Definition

The following equations, assumptions, and references were used to develop the initial atomizer analytical model.

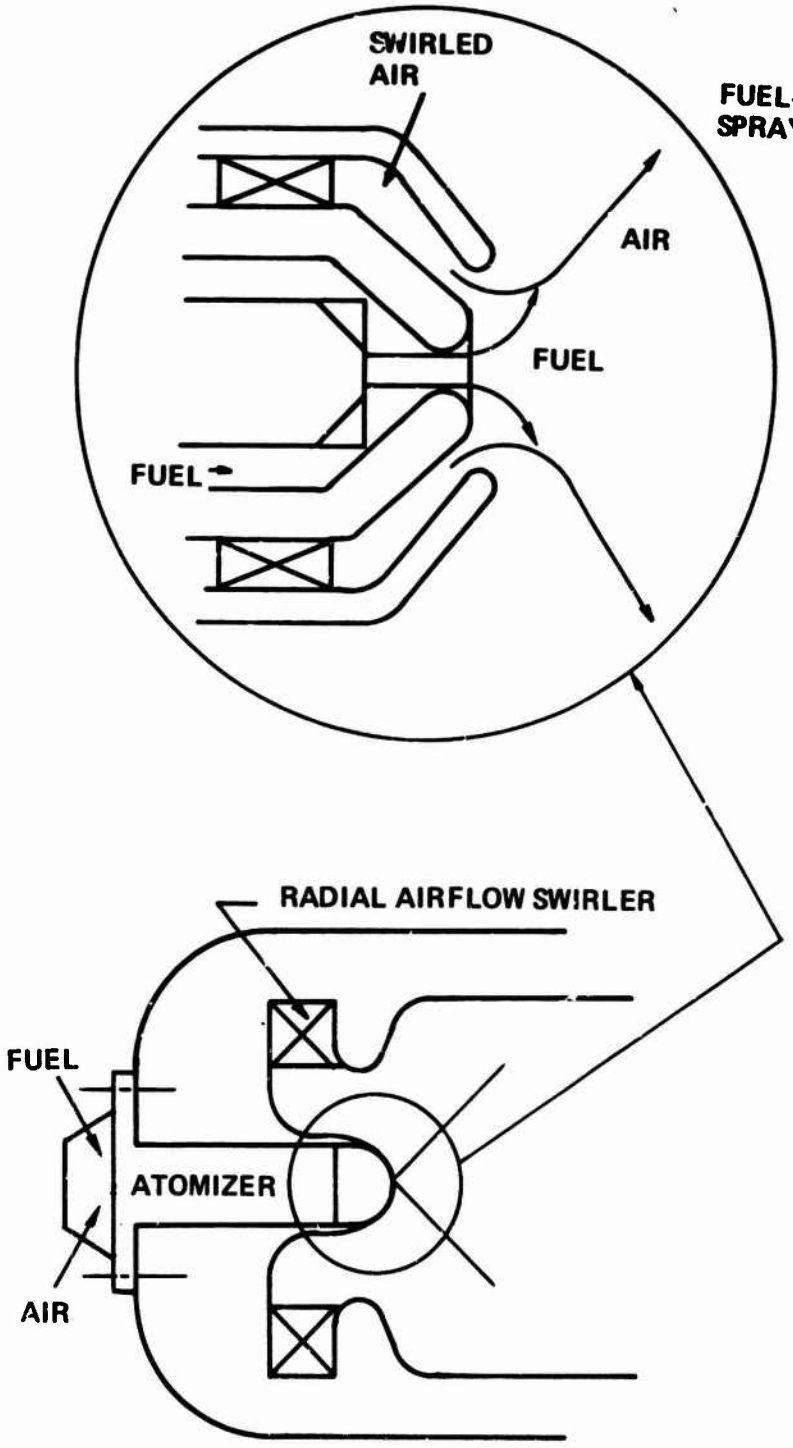


Figure 18. Air-Assist Atomizer.

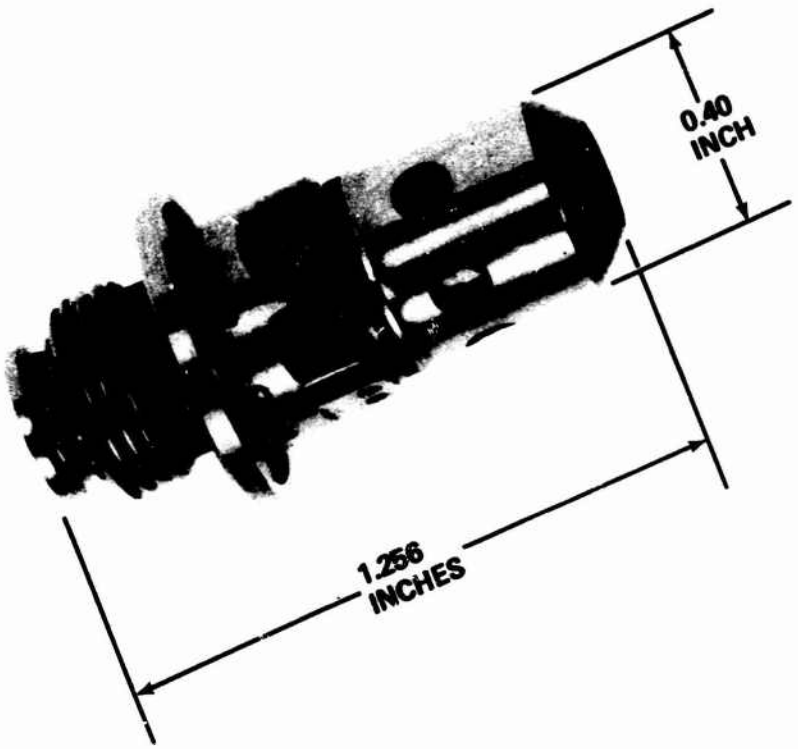


Figure 19. Air-Assist Atomizer.

Fuel droplet atomization is characterized by Sauter mean diameter (SMD) defined as the size of a droplet which has surface to volume ratio equal to that of the collection of the droplets. From Frazer,[4]

$$\text{SMD (microns)} = 220\ (W_f)^{0.209}(\nu)^{0.215}(\Delta P_f)^{-0.485} \qquad (5)$$

where W_f = fuel flow rate per nozzle, lb per hr

ν = fuel viscosity, centistokes

ΔP_f = differential fuel pressure, psid

The fuel flow and pressure drop are related for a given atomizer by a constant flow number (FN) where

$$FN = \frac{W_f}{\sqrt{\Delta P_f}} \qquad (6)$$

The atomized droplet size distributions with and without air-assist were computed and are shown in Table V.

TABLE V. DROPLET SIZE DISTRIBUTIONS

	Volume Percent of Spray				
	0-20	20-40	40-60	60-80	80-100
Size ratio (D/SMD) with air-assist atomizer	0.38	1.00	1.37	1.80	2.40
Size ratio (D/SMD) without air-assist atomizer	0.77	1.05	1.23	1.45	1.75

For a dual-orifice atomizer an energy equation was used to obtain an effective atomizer pressure drop for use in Equation (5). Thus,

$$\Delta P_{effective} = (\Delta P_P W_{fP} + \Delta P_S W_{fS})/(W_{fP} + W_{fS}) \qquad (7)$$

where subscripts P and S refer to primary and secondary fuel orifices, respectively.

Droplet trajectories were calculated based on the following assumptions:

(a) Coefficient of drag, C_d, is 27 $Rn^{-0.84}$ (from Ingebo).[5]

(b) Atomizer velocity coefficient, C_v, is 1.0.

(c) Droplets are atomized exactly at the atomizer exit.

(d) Droplets leave the atomizer at the atomizer cone angle with no dispersion.

(e) Droplets do not interfere with each other.

(f) Ambient pressure level and fuel flow do not change the droplet distribution.

In the trajectory calculations, velocity triangles determine the relative droplet-air velocity at a particular location. The relative velocity then determines the Reynolds number from which the drag and the droplet acceleration are calculated. When the droplet acceleration is in a different direction from the relative velocity vector, the droplet velocity can be calculated at some small increment of distance from a given station. Then, provided that the distance increment is made small enough, an accurate droplet trajectory can be calculated.

Droplet evaporation is based on the empirical relations by Priem and Heidman.[6]

$$\text{Heat transfer, } Nu_h = 2 + 0.6\, Pr^{1/3} Rn^{1/2} \qquad (8)$$

$$\text{Mass transfer, } Nu_M = 2 + 0.6\, Sc^{1/3} Rn^{1/2} \qquad (9)$$

where Rn = Reynolds number

Pr = Prandtl number

Sc = Schmidt number

Nu = Nusselt number

In the calculation, the droplet temperature stabilizes at the "wet bulb" temperature, after which all heat input results in evaporation of some liquid fuel and progressive reduction of droplet mass.

Reynolds, Prandtl, and Schmidt numbers are calculated for gas-vapor properties at averaged temperatures and composition. The average temperature is taken as 1/2 ($T_{air} + T_{fuel}$); the average composition uses fuel-vapor pressure and air pressure to obtain the boundary properties from the properties for air and for fuel vapor. For fuel vapor and air, the properties of interest are thermal conductivity, viscosity, specific heat, molecular weight, density and binary diffusivity; whereas for liquid fuel they are vapor pressure, specific heat, density and latent heat of vaporization. These properties were obtained from Nelson,[7] Wallmer,[8] Gladden,[9] Barnett,[10] Roberts,[11] Maxwell,[12] and Nixon.[13]

Droplet trajectories (Figure 20) were calculated for water atomization with the atomizer used by Mellor.[14] Good agreement was found to exist between the experimental and the calculated trajectories. Calculations of fuel droplet trajectories (JP-4) are shown in Figure 21. Figure 22 shows calculated fuel penetration as a function of ambient temperature and pressure.

Equation (5) for SMD does not include any effect of improved atomization by air assist. The Parker-Hannifin Corporation, Accessories Division, was consulted to determine a technique to account for the effect of the air. As a result of their suggestion, an effective fuel pressure, based on a kinetic energy equivalence of the airflow, was determined:

$$\Delta P_e = \frac{3600\ \Delta P_{air}\ W_{air} + \Delta P_f W_f}{3600\ W_{air} + W_f} \qquad (10)$$

where ΔP_e = effective differential pressure, psid

ΔP_{air} = airflow differential pressure, psid

W_{air} = shroud airflow, lb per sec

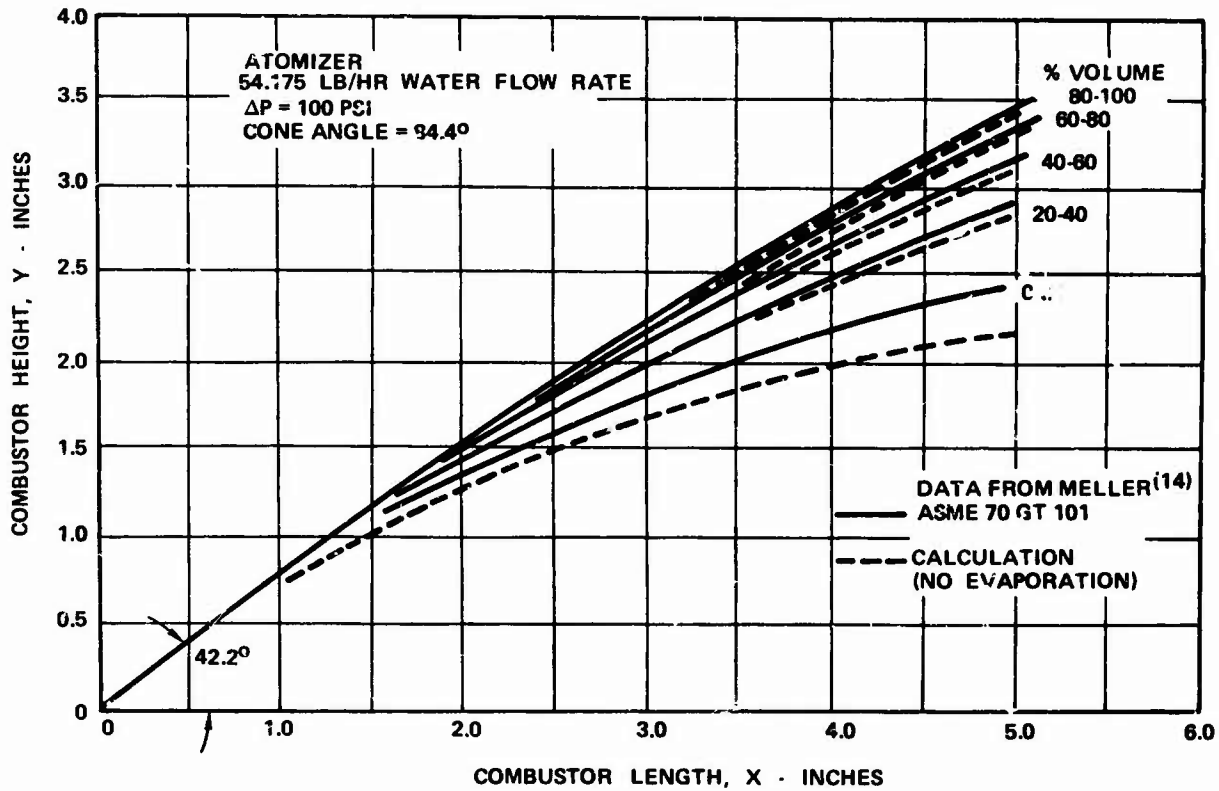


Figure 20. Comparison of Measured and Calculated Droplet Trajectories.

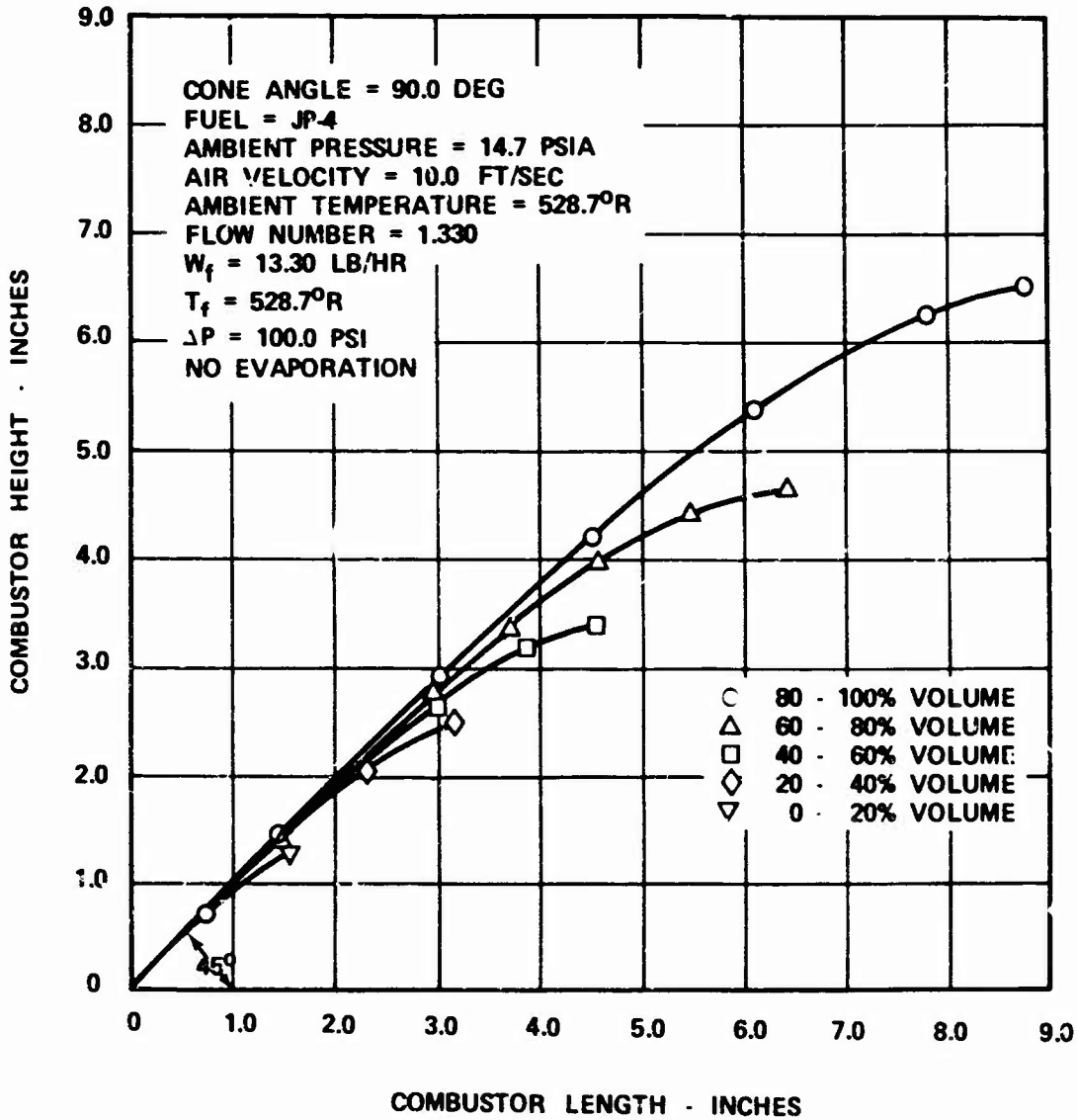


Figure 21. Calculated Simplex Trajectories Without Air Assist.

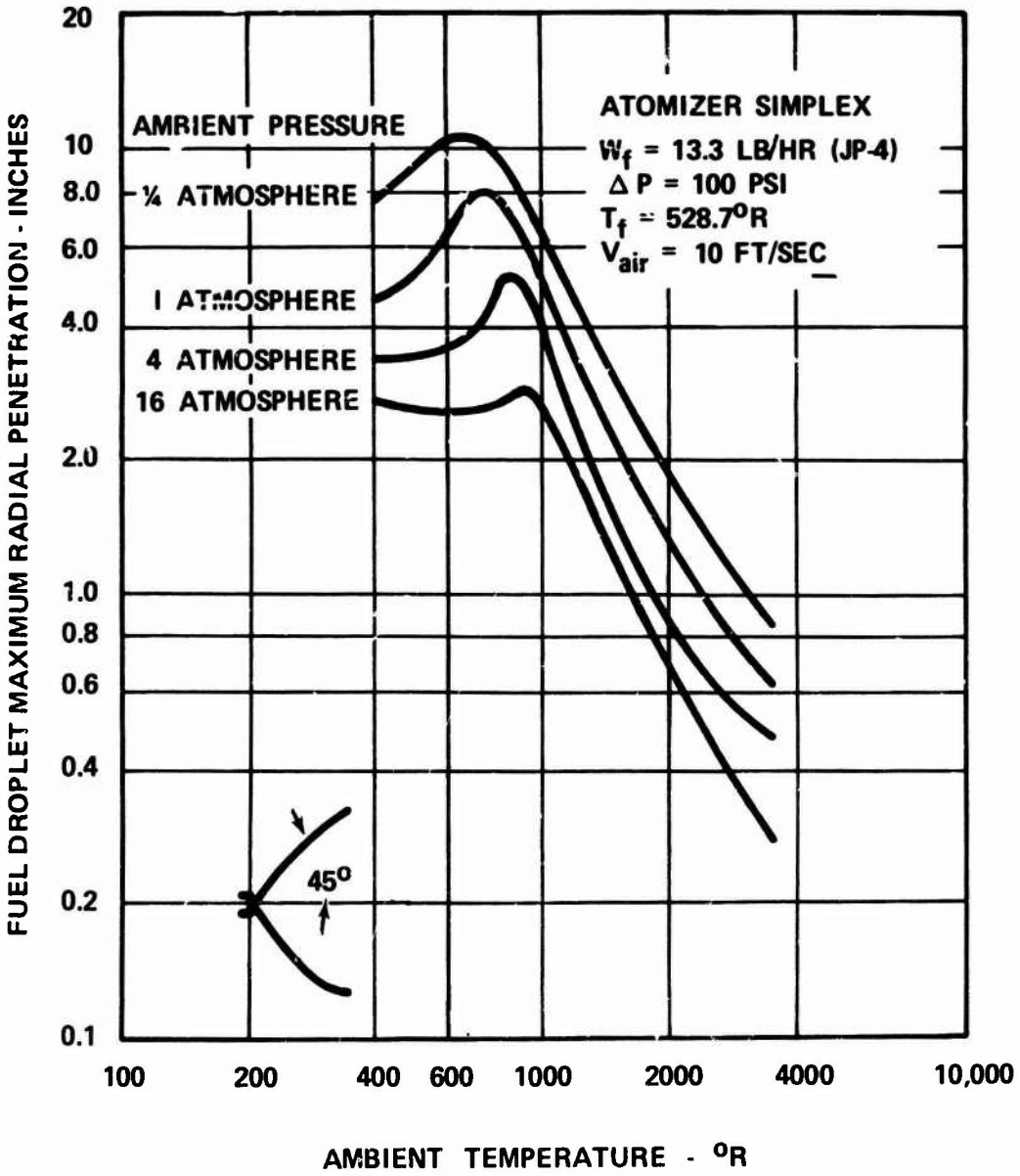


Figure 22. Effect of Ambient Temperature and Pressure on Fuel Penetration.

The shroud airflow is calculated from

$$W_{air} = 1.098\ A_s \sqrt{\frac{\Delta P_{air} P_{comb}}{T_{air}}} \qquad (11)$$

where A_s = shroud flow area, sq in.

P_{comb} = combustor internal pressure, psia

T_{air} = combustor inlet air temperature, °R

4.1.2 Atomizer Spray Tests

The air-assist fuel atomizer was tested (a) by Parker-Hannifin under subcontract to obtain spray characteristics and (b) in a fuel-injection rig to determine spray envelope under varying conditions of air velocity, air temperature, air pressure, and fuel flow rates. The test results were then used to update the analytical models.

4.1.2.1 Spray Characteristics

Calibration testing by Parker-Hannifin consisted of sampling radial droplet distributions in two lines, at right angles, through the spray axis, at a distance of 1 inch from the spray origin. Drop sizes are classified in approximately nine size groups. Data includes the number of drops counted, the relative volume of fuel in each size group, local SMD at each 0.1-inch radius, the overall SMD, and the mass median diameter (MMD). The significance of MMD is that one-half of the fuel volume is contained in droplets less than the MMD, whereas the ratio of SMD to MMD is a measure of droplet uniformity.

Test conditions and experimentally determined SMD values are shown in Table VI. Values calculated from Equation (5) and including the effect of air are shown in Row 1. Because poor correlations were obtained, additional consultation with Parker-Hannifin was necessary, which resulted in a revised equation for prediction of drop size from simplex atomizers without assist airflow. The revised relation is

$$SMD = 225\ \frac{(W_f)^{0.205}}{(\Delta P_f)^{0.354}} \left(\frac{\nu}{1.5}\right)^{0.3} \qquad (12)$$

This relation was developed from extensive data accumulated with the Parker-Hannifin measurement system on a variety of injectors. Compared with the previously presented relation,

Equation (5), the revised relation shows a greater effect of fuel viscosity with the exponent increased from 0.215 to 0.3. The effect of fuel differential pressure is reduced. The overall relation resulted in drop sizes on the order of twice the previous relation, shown in Row 2, Table VI.

TABLE VI. AIR-ASSIST ATOMIZER DROPLET-SIZE TEST RESULTS

Parameter	Test Point				
	1	2	3	4	5
Fuel flow, lb/hr	35.2	10	10	3.6	1.7
Air pressure, psia	0	10	10	10	35
Fuel viscosity, CS	12	1.17	12	12	12
Fuel pressure, psig	211	18	17	2.5	0.95
Airflow rate, lb/hr	0	0.515	0.495	0.585	0.914
SMD, microns	164	150	187	150	107
MMD, microns	216	164	222	179	119
Row 1 - Predicted SMD (original) - with air effect (Eq. 5 + Eq. 10)	58.9	98	167	274	129
Row 2 - Revised Predicted SMD - without air effect (Eq. 12)	131	120	242	395	475
Row 3 - Revised predicted SMD - with air effect (Eq. 12 + Eq. 10)	131	121	244	348	190
Row 4 - Final updated SMD - predictions (Eq. 13 + 14 + 15)	-	148	184	153	105

The revised predictions including the effect of assist air are shown in Row 3. The revised prediction of 131 microns without air assist (Test Point 1) is within 20 percent of the measured 164 microns. Parker-Hannifin stated that 20 percent is the best level of agreement that could be expected, but

could not present any specific improved correlation for the effect of assist air. It was therefore concluded that the air-assist correction factor based on a calculated effective differential pressure was invalid.

An alternate procedure was developed with the use of the basic relation derived by Fraser[15] for the breakup of a liquid sheet into ligaments and then droplets:

$$SMD = 196\ \nu^{k} \sqrt{\frac{\sigma s}{\rho_g V_e^2}} \qquad (13)$$

where σ = fuel surface tension, dynes per cm

ρ_g = gas density, lb per cu ft

V_e = effective gas velocity, ft per sec

k = viscosity exponent

s = fuel sheet thickness, microns

Fuel sheet thickness ,s, is obtained from Giffen[16] by

$$s = \frac{3.359\ FN}{D_o \sqrt{\rho_f}\ (\cos \alpha/2)} \qquad (14)$$

where

FN = atomizer flow number

D_o = atomizer exit orifice diameter, in.

α = spray angle, deg

ρ_f = fuel density, lb per cu ft

The effective gas velocity is the root-mean-square value of the relative velocities on either side of the sheet in the sheet breakup region. This velocity is some fraction of the air velocity at the discharge of the air-assist slots. The following relation, an extension of that used by Fraser, was found to correlate the data:

$$V_e = 0.438\ (W_a/W_f)^{0.1}\ V_a \left[0.5 + (V_f/V_a)^2 - V_f/V_a\right] \qquad (15)$$

where W_a = assist-air mass flow, lb per hr

V_a = assist-air shroud discharge velocity, ft per sec

V_f = fuel sheet velocity, ft per sec

Air and fuel velocities are computed by assuming complete conversion of pressure differential head to kinetic energy.

Equations (14) and (15), together with a viscosity exponent, k, of 0.095, when used in Equation (13), predict measured drop sizes within 2 percent (Row 4, Table VI).

Drop-size distribution data was analyzed and found to be correlated, as shown in Figure 23, on the basis of the square root of the ratio of drop size to MMD as a function of cumulative volume.

The ratio of SMD to MMD was found to be 0.85. Little difference is observed between the distribution with and without the assist air. This data was used to correct the distribution size ratios in the analytical prediction method for the five drop classes given in Section 4.1.1.

4.1.2.2 Spray Envelope Tests

The air-assist atomizer was tested in the fuel-injection rig to determine the spray envelope characteristics. The test section (Figure 24) was an 8-inch-diameter pipe with Plexiglas viewing windows arranged in such a way that at atmospheric pressure the spray envelope could be observed. At higher pressures, steel plates replaced the Plexiglas windows. Two fuel tube bosses were provided at different axial locations; and through these bosses, nozzle support stands could be inserted so that the fuel nozzle was positioned on the test section centerline. Spray envelope location was determined by means of a movable thermocouple traversed through instrumentation ports located along the length of the test section at 3/16-inch spacing.

Testing was conducted at 24 test combinations of duct air velocity, pressure, temperature, and fuel flow:

- Air velocities ranged from 8 to 500 feet per second.
- Air temperatures ranged from 130° to 400°F.
- Air pressures ranged from 1 to 16 atmospheres.
- Fuel flows ranged from 10 to 35 pounds per hour.

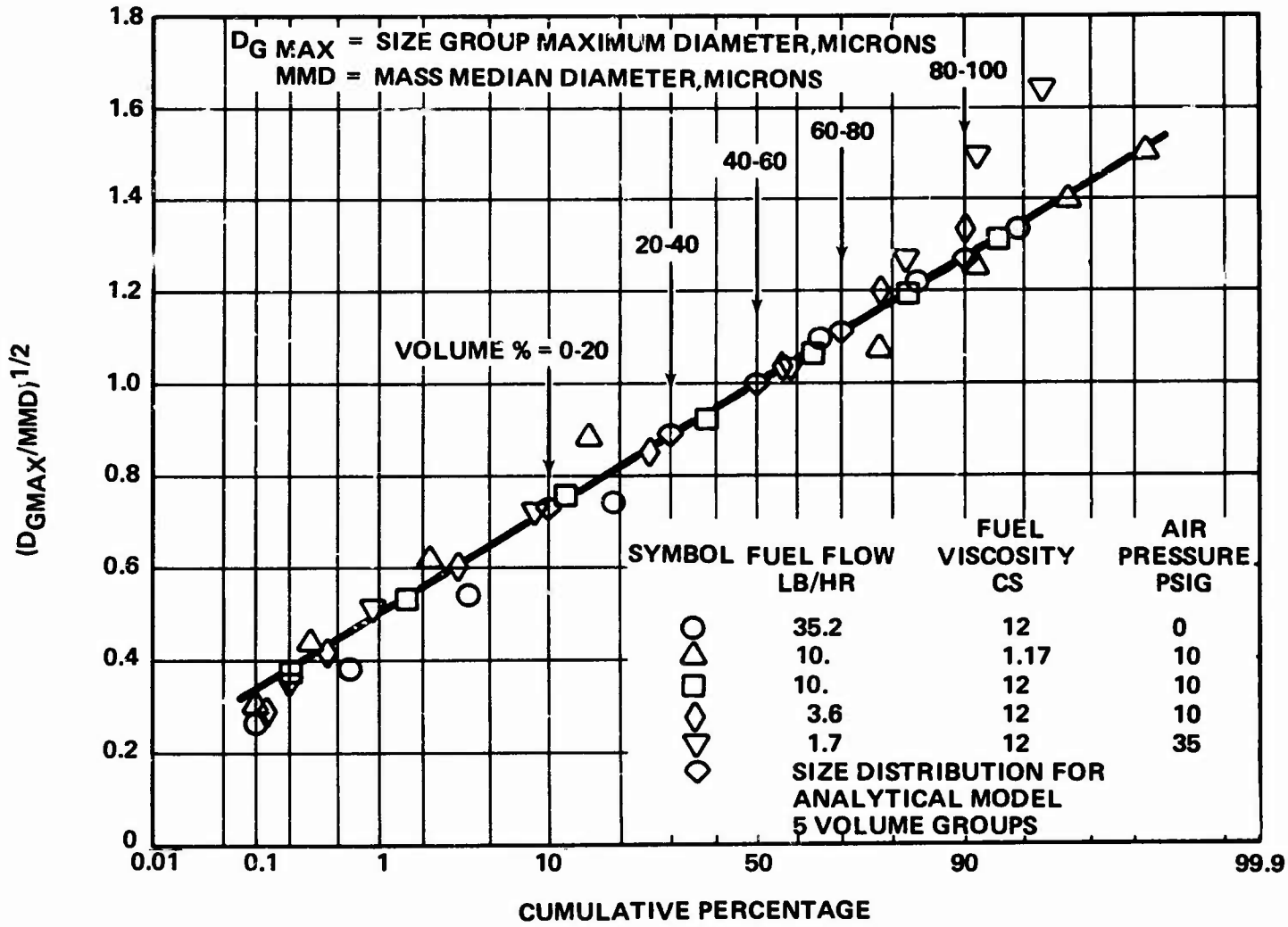


Figure 23. Drop-Size Distribution Data for Air-Assist Nozzle.

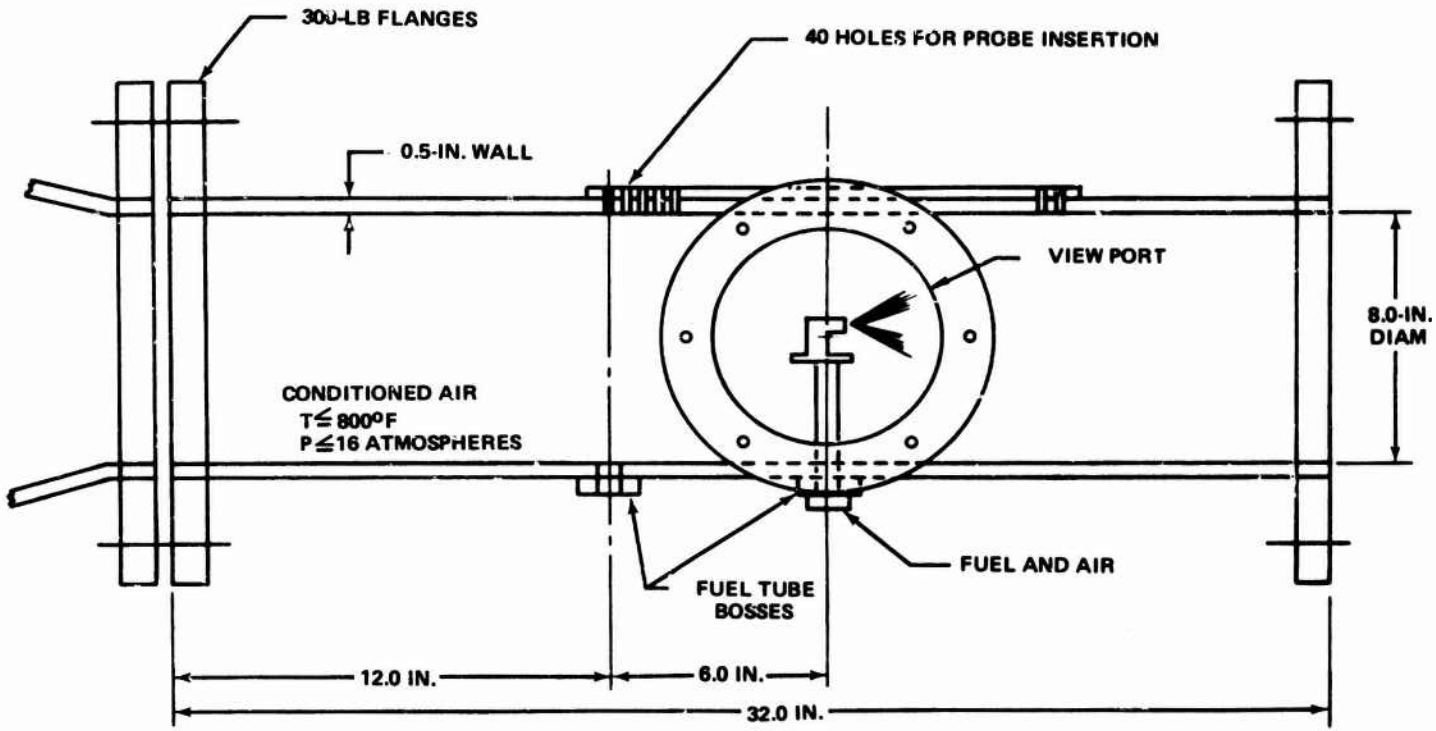


Figure 24. Fuel-Injection Element Test Rig.

The thermocouple probe traverses were made at axial distances of 0.54, 1.2, 1.9, 2.6, 3.3, and 4.3 inches from the face of the atomizer. Observation of the fuel discharge was made with the probe just entering the spray cone; at this point, the probe reading also indicated fuel contact. Similarly, as the probe was observed to pass out of the cone on the far side, the probe output again indicated the cone boundary. This verified the feasibility of the experimental procedure.

Figure 25 shows a plot of temperature profiles typical of those obtained while testing. The plot is made in a manner that allows visualization of the trajectory. Each profile curve represents the differential temperature referenced to the inlet air temperature. A reference air-temperature line for each profile is located a distance from the spray origin equal to the actual traverse position distance from the spray origin. The differential temperatures for each profile are then plotted relative to the particular reference line. Included on this plot are the initial spray trajectory predictions. As expected, the smaller droplets are more rapidly deflected than the larger droplets; the experimental data, however, shows more deflection than predicted.

The updated drop-size correlation (SMD) was incorporated in the fuel-injection model, and this model was used to compute droplet trajectories for the test conditions. Typical comparisons between experimental and analytical trajectories are shown by the solid lines in Figure 26. The experimental nozzle spray cone angle was specified as being between 75 and 90 degrees. An initial specific angle of 85 degrees was used in the predictions. As shown in 26(a) and (c), the experimental data within 1.5 inches of the apex indicated a spray angle somewhat greater than this value and the analytical predictions of inner and outer droplet boundaries. Figure 26(b) shows a comparison of predicted trajectories with cone angles of 85 and 100 degrees. The 100-degree spray angle gave good correlation for the outer boundary (large droplets) up to approximately 1.5 inches of penetration, but the inner boundary (small droplets) did not correlate as well.

Possible reasons for the limited correlation between the experimental and predicted trajectories are:

- Disruption of the airflow around the nozzle and nozzle support within the tunnel--i.e., experimental error.

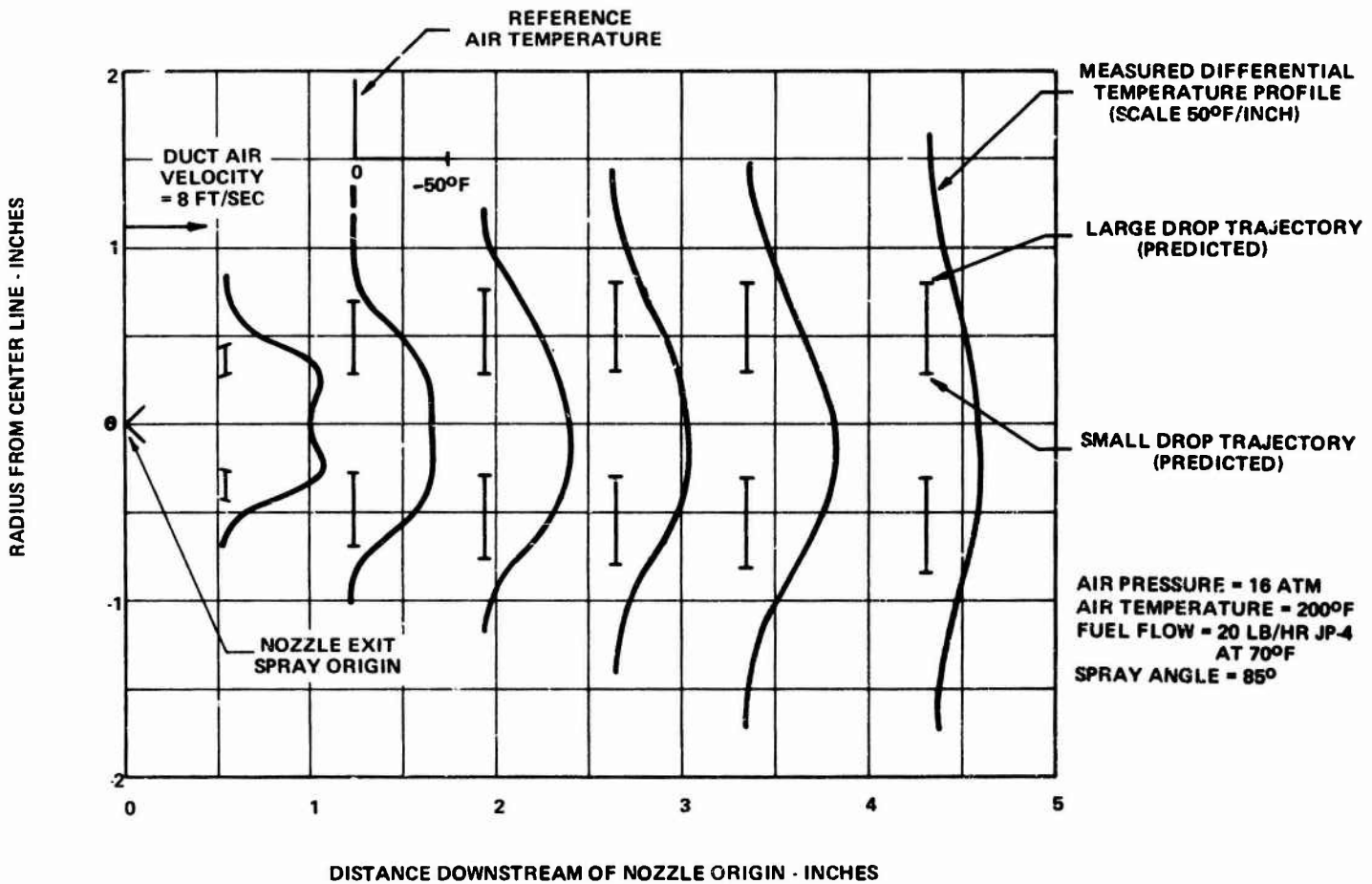
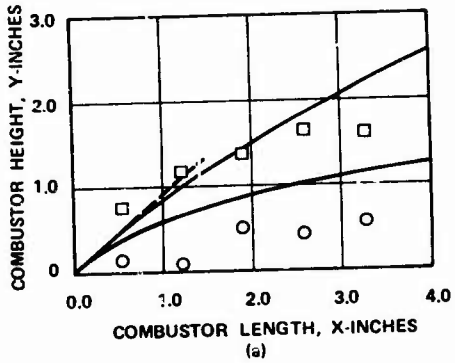
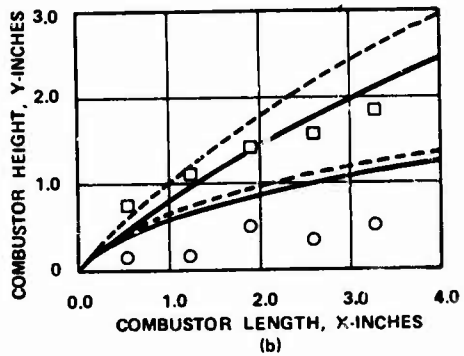


Figure 25. Fuel-Injection Rig Temperature Profiles.

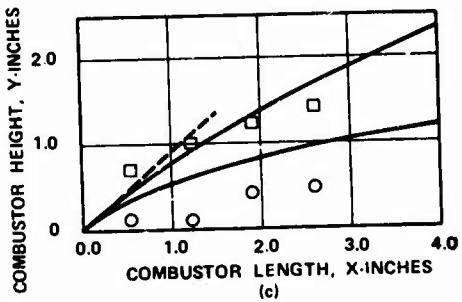


FUEL FLOW RATE = 25 LB/HR
APPROACH AIR VELOCITY = 22.6 FT/SEC
CHAMBER PRESSURE = 1 ATM
CALCULATED SMD = 70.7 MICRONS



FUEL FLOW RATE = 22 LB/HR
APPROACH AIR VELOCITY = 22.6 FT/SEC
CHAMBER PRESSURE = 1 ATM
CALCULATED SMD = 79.04 MICRONS

DROPLET TRAJECTORY RANGE
- - - ANALYTICAL SPRAY CONE ANGLE = 100°
——— ANALYTICAL SPRAY CONE ANGLE = 85°
□ OUTER SPRAY DROPLET BOUNDARIES FROM EXPERIMENTAL RESULTS
○ INNER SPRAY DROPLET BOUNDARIES FROM EXPERIMENTAL RESULTS



FUEL FLOW RATE = 20 LB/HR
APPROACH AIR VELOCITY = 25.3 FT/SEC
CHAMBER PRESSURE = 1 ATM
CALCULATED SMD = 79.04 MICRONS

Figure 26. Comparison of Analytical and Experimental Spray Trajectories for Air-Assist Nozzle.

- Droplets smaller than those accounted for are formed and rapidly deflected, forming the inner cone boundary--i.e., SMD prediction error.
- Aerodynamic shattering of droplets--i.e., assumption error.
- Interaction of individual droplets in the spray--i.e., assumption error.
- Oversimplification of the drag coefficient expression.

A more rigorous mathematical model for predicting spray trajectories should include the effect of particle interaction as well as laws of nucleation (mostly heterogeneous), droplet growth, and disappearance due to evaporation and aerodynamic shattering. Each discrete droplet size trajectory can be described by a partial differential equation of the hydrodynamic flow type with terms for convective transport, diffusive transport, generation, and destruction of droplets. The present spray-trajectory prediction procedure takes into account only acceleration due to aerodynamic drag and fuel evaporation; thus, for complete prediction of spray trajectories, further modifications to the present prediction procedure would be required. Since the main interest is only in the first 2-inch-downstream region, this approach was not pursued.

The empirical drag coefficient used in the predictions is given by

$$C_d = 18.5/(Rn)^{0.6} \tag{16}$$

where Reynolds number, Rn, is based upon relative velocity between droplet and air stream, and droplet diameter. Consideration of experimental work reported by Eisenklam[17] indicates that more realistic coefficients may be available. Their results and recent work reported by Natrajan[18] show that drag coefficient (C_d) of a burning or evaporating droplet can be correlated by

$$C_d = \frac{C_{d,s}}{(1+B)} \tag{17}$$

where $C_{d,s}$ = drag coefficient of a sphere in uniform flow evaluated at mean conditions

B = mass transfer number

The mass transfer numbers with evaporation and combustion (B_{evap} and B_{comb}, respectively) are given by

$$B_{evap} = c_p (T_{amb} - T_w)/Q_L \tag{18}$$

$$B_{comb} = c_p [(T_{amb} - T_w) + M_{O_2} Q_C/S]/Q_L \tag{19}$$

where c_p = ambient gas specific heat

T_{amb} = ambient gas temperature

T_w = droplet surface temperature (equal to wet bulb temperature for evaporating drops and boiling-point temperature for burning drops)

M_{O_2} = oxygen concentration in the surrounding gas

Q_C = heat of combustion of fuel

S = stoichiometric ratio of O_2

Q_L = latent heat of evaporation

From Streeter,[19] $C_{d,s}$ was calculated by the following expressions:

$$C_{d,s} = \frac{24}{Rn}(1 + 3/16\ Rn) \qquad 0 < Rn \leq 0.5$$

$$C_{d,s} = \frac{24}{Rn} + \frac{3.54}{Rn^{0.345}} \qquad 0.5 < Rn \leq 10.0 \tag{20}$$

$$C_{d,s} = \frac{24}{Rn} + \frac{3.09}{Rn^{0.314}} \qquad Rn > 10$$

A typical value of B for the experimental cases that were run is 0.1; consequently, the effect of evaporation on drag coefficient reduction was insignificant.

A comparison of trajectories calculated with use of Equations (16) and (17) showed that spray penetration with C_d given by the latter equation was slightly less than that given by the former.

With regard to droplet shattering, the breakup of a spherical droplet injected into a high-speed stream can take place due to a combination of forces of pressures and surface tension.

When aerodynamic force exceeds the force of surface tension, the large droplets (those having a diameter greater than a "critical" diameter) will shatter. This critical diameter (d_{crit}) is determined by

$$d_{crit} = \frac{K}{U^2} \tag{21}$$

where K = function of fuel viscosity, density, and droplet size as correlated by Lane[20] and Hanson[21]

U = velocity of air relative to the droplet

For the case shown in Figure 26(a), the critical diameter is 120 microns, whereas the outer boundary of the trajectory is calculated with droplet size equal to 134 microns. Therefore, it appears that in the downstream region, poor correlation between theory and experiment can be explained to some extent in terms of the breakup process of the droplet. It is possible to calculate equilibrium droplet diameter and breakup time required by using a formulation from Taylor,[22] Valentas,[23] and Karam.[24]

Aerodynamic shattering of droplets can also be expressed in terms of two dimensionless groups:

$$We = \rho_g U^2 d/\sigma \tag{22}$$

and

$$V_i = \frac{\nu}{\sqrt{\rho_f d\sigma}} \tag{23}$$

where We = Weber number

V_i = viscosity number

ν = fuel liquid viscosity

The greater the Weber number, the greater the deformation of the droplet, until at a critical Weber number, We_{crit}, breakup of the droplet occurs. According to Hinze,[25] for an inviscid

steady flow, We = 13. For viscous fluids, it can be expressed as

$$\frac{We_c}{We} = f(V_i) \qquad (24)$$

From Eisenklam[26] for the case shown in Figure 26(a), the critical diameter is again about 120 microns.

4.1.3 Conclusions

Based on analysis of the data and correlations, the following conclusions were reached:

(a) The updated model for predicting Sauter mean diameters gives good correlation with the experimental data for the particular nozzle tested.

(b) Within the limits of the assumptions and errors outlined in 4.1.2.2, spray envelope trajectories can be successfully predicted.

Contamination problems may limit the use of the air-assist nozzles where many nozzles with small flow rates and small passage sizes are required. This problem may be partially overcome by the use of filters in the fuel lines which would require changing at given intervals.

Separate air pumps increase the cost and complexity of the system, thereby, to some extent, limiting their use.

Recommended use for nozzles of this type are:

- Conditions where compensation is required for poor primary-zone design
- To minimize light-off problems, particularly in the case of cold starts with low pressure drop systems
- In low-cost, state-of-the-art-technology engine applications

4.2 PNEUMATIC-IMPACT ATOMIZER

The pneumatic-impact injector is an air atomizing fuel nozzle that was developed as a result of the U.S. Navy Contaminated Fuels Program[27] and AiResearch developmental activities. As shown schematically in Figure 27, the nozzle consists of a

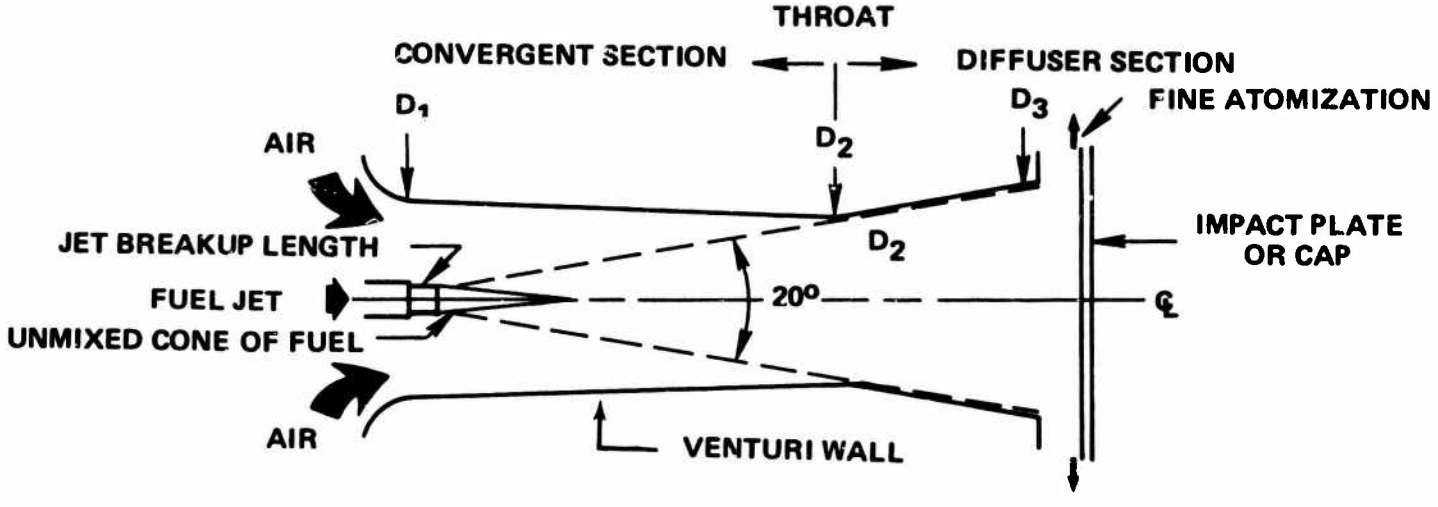


Figure 27. Pneumatic-Impact Injector Schematic.

single fuel jet, a venturi, and an impact plate. The venturi is designed to avoid fuel impingement on the walls of the venturi and to accelerate the fuel to impinge on the impact plate at the highest possible velocity in order to atomize the fuel. The energy for atomization is derived from the combustor pressure drop.

The computer program derived for analysis of the pneumatic-impact fuel injector is briefly described in Appendix II.

4.2.1 Model Definition

The calculation procedures assume coarse jet breakup and acceleration through the venturi accompanied by some droplet evaporation. A film is formed at the impact plate and a fine atomization then takes place at the plate lip.

Jet breakup calculations are based on work by Fraser[15] in which a spinning cup was used to deliver a thin sheet of fuel into an annular air jet where it was then broken up into droplets.

Fraser obtained the correlation

$$SMD = 6 + 20036 \frac{\sigma_f^{1/2} \, (SG \times \nu)^{0.21}}{(\rho_g)^{1/2}} \left(1 + \frac{0.065}{M_R^{1.5}}\right) \left[\frac{S}{V_f^2 \, (0.5 \, V_R^2 - V_R + 1)}\right]^{1/2} \qquad (25)$$

where

SG = fuel specific gravity

M_R = air to fuel mass flow ratio

V_R = air velocity/fuel velocity = V_{air}/V_f

In order to complete the jet breakup model, two other assumptions were made. First, the breakup length was taken to be 2.4 times the SMD, based on an analysis by Rayleigh[28], and second, the fuel spray was assumed to mix into the airstream progressively. This was done with the assumption that all fuel inside a cone (downstream of the breakup point) that is six times the jet diameter in length is not involved in the aerodynamic process.

The net effect of these two assumptions is that as atomization deteriorates, the fuel spray extends farther down the venturi before becoming involved in the aerodynamic process. In the venturi the fuel droplets are accelerated by the aerodynamic forces, while the air is slowed down by droplet drag and duct friction and modified by heat transfer between the fuel and the air.

Droplet correlation is based on Ingebo's[5] drag coefficient data, in which

$$\text{Coefficient of Drag, } C_d, = 27\ Rn^{-0.84} \qquad (26)$$

Heat transfer is calculated by the same method as defined in the air-assist atomizer section.

The effects of drag, friction, heat transfer and change in duct size were calculated from Shapiro[29] in which the calculations are carried in small steps from the duct inlet to the duct outlet and iterated to get the duct exit static pressure to the required value. This allows the calculation of V_{air}, T_{air}, V_{fuel} (five droplet groups) and T_{fuel} at the duct exit. Typical velocities are shown in Figure 28.

Factors that were assumed negligible were:

(a) Heat transfer from the duct wall to the fluid stream was neglected because of the small temperature difference between the duct wall and the fluid.

(b) Secondary flows induced by the drag of the fuel spray were neglected, making the assumption that by the time the fuel spray reaches the diffuser inlet most of the airflow will be mixed with the fuel spray and the one-dimensional analysis will be adequate.

(c) The fact that some air bypasses the fuel spray cone was neglected.

Following coarse atomization and evaporation from the fuel jet, film conditions at the edge of the impact plate were calculated. These were based on the following assumptions:

(a) Average fuel velocity at the venturi exit is equal to the fuel velocity at the edge of the impact plate (i.e., viscous drag on the fuel sheet is counterbalanced by air scrubbing velocity).

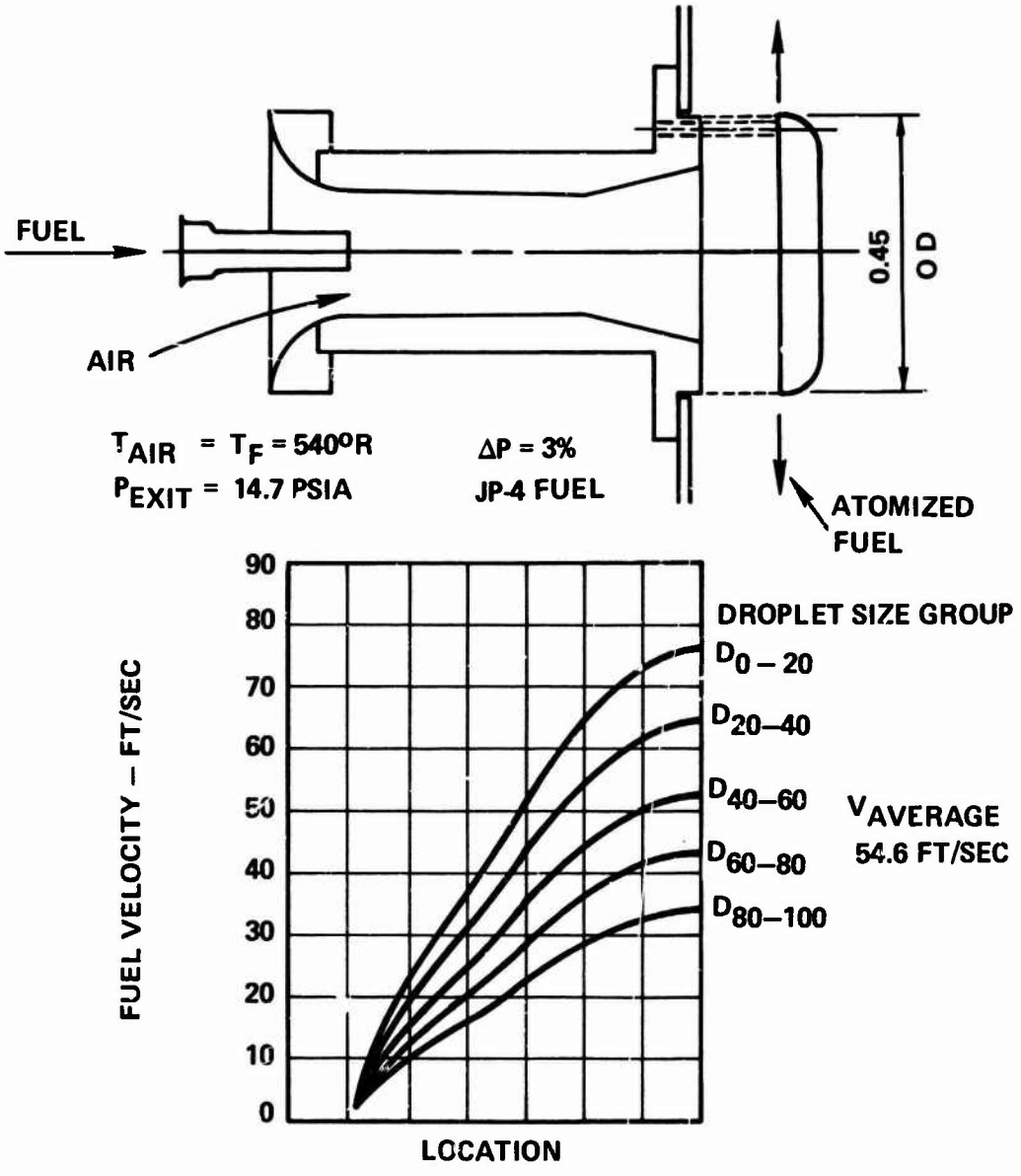


Figure 28. Pneumatic-Impact Fuel-Injection System.

(b) Average fuel temperature at the venturi exit is equal to the fuel temperature at the edge of the impact plate (i.e., no heat transfer from the impact plate to the fuel).

(c) At the edge of the impact plate, the fuel is moving in a thin sheet; this sheet is atomized in the shear layers between the high-velocity air from the venturi and the low-velocity ambient air. Fuel sheet thickness was determined by the method of Kinney et al.[30]

(d) SMD calculations are based on Fraser's correlation, Equation (25).

Droplet evaporation is calculated with the procedure outlined for the atomizer injector, except that the fuel droplets are injected into a velocity temperature-field setup by injector through-flow air. The air leaving the injector was assumed to follow the form of a radial wall jet. The temperature and velocity fields were determined from Ricon[31] and Bakke[32] based on this assumption.

4.2.2 Pneumatic-Impact Spray Tests

The purpose of the pneumatic-impact spray tests was to determine the pneumatic-impact circumferential distribution, the drop-size characteristics and the spray envelope. The injector is shown in Figure 29.

4.2.2.1 Drop-Size Characteristics

The pneumatic-impact nozzle was calibrated by Parker-Hannifin. Test conditions and predicted SMD values are shown in Table VII. The drop size predicted by the original procedure was about one-tenth the measured values. This was attributed to the method used for calculating the fuel sheet thickness and the gas velocity in the sheet breakup region. Fuel sheet thickness was initially computed with the assumption that the sheet velocity at the lip was equal to the fuel velocity at the venturi. Results from the film thickness calculations conducted for the L-pipe injector, discussed later, provided an updated film thickness calculation procedure.

Incorporation of this procedure with a reduction in the air and fuel sheet velocities as they flow radially outward on the impact plate resulted in predicted values in close agreement with those measured. Predictions were within 25 percent of the measured values, with the exception of the third test



Figure 29. Pneumatic-Impact Fuel-Injector Nozzle.

point. The second and third test points tabulated are the same except for increased air pressure drop. The test results indicate that the effect of almost doubling the air velocity results in only a 9-percent decrease in drop size, whereas over a 50-percent reduction was predicted by the original operation.

TABLE VII. PNEUMATIC-IMPACT INJECTOR DROPLET SIZE TEST POINTS

	Test Point Number			
Fuel flow, lb/hr	2	10	10	10
Air pressure, in. of H_2O	4	4	12	12
Fuel viscosity, CS	1.17	1.17	1.17	12
Fuel pressure, psig	0.2	0.9	0.9	1.1
Airflow rate, lb/hr	9.4	8.07	14.3	14.3
SMD, microns (measured)	135	211	193	264
MMD, microns (measured)	269	272	235	327
Predicted SMD, microns Equation (25)	15.7	37.2	17.5	24.8
Predicted SMD, microns Equation (25) with corrected fuel and gas velocities	141.5	264	117	324

A second possibility for the discrepancy is that random sheet thickening due to drop formation on the impact plate could have resulted in excessive drop sizes at this test condition. No repeat tests were performed, and because of reasonable agreement between the predicted and experimental values for three out of four cases, no further modification to the analysis was undertaken.

Figure 30 shows the drop-size distribution for the pneumatic-impact injector test data. Also shown for comparison is the correlation for the air-assist atomizer reproduced from Figure 23. The two distributions are essentially identical.

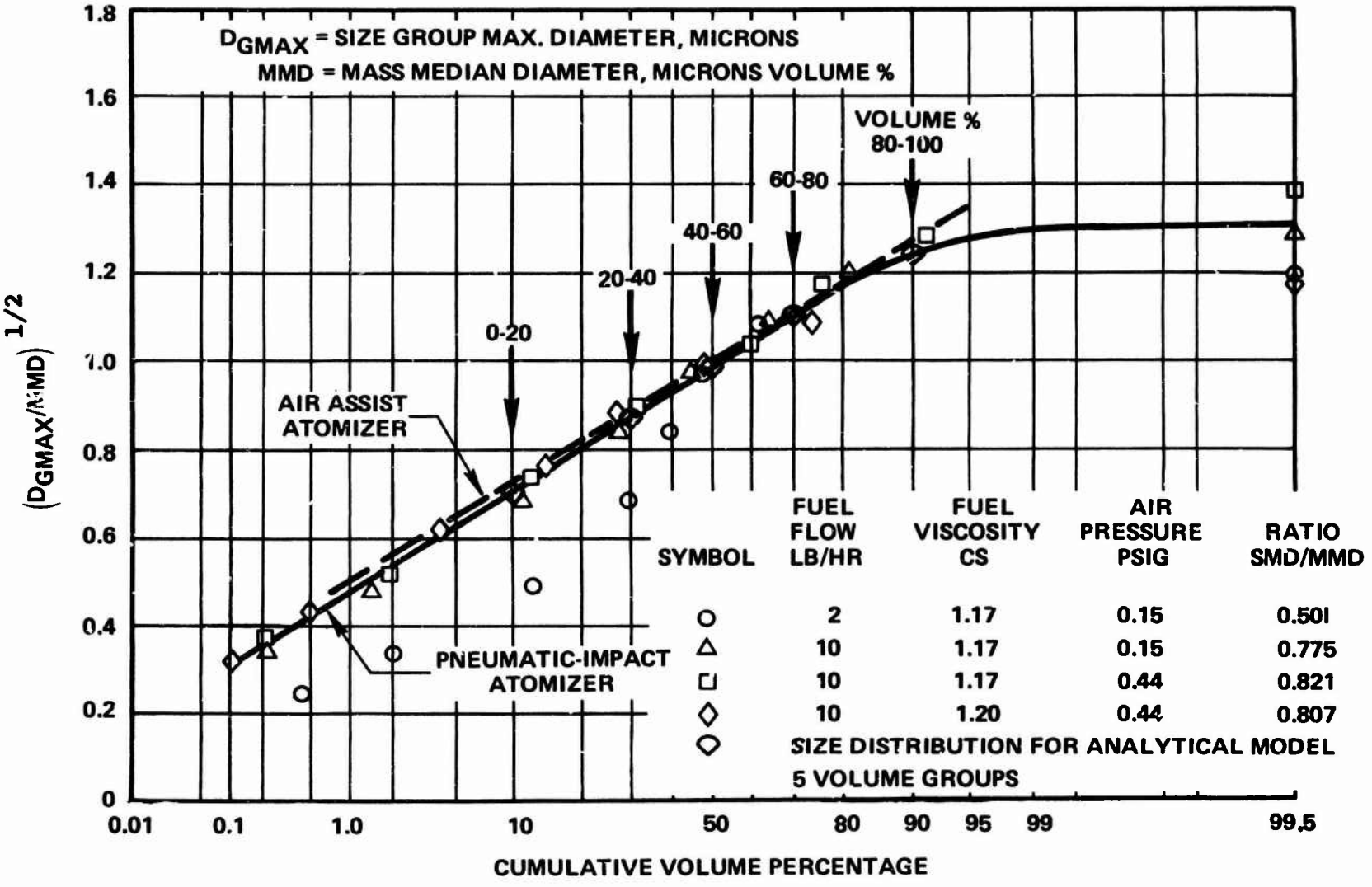


Figure 30. Drop-Size Distribution for Pneumatic-Impact Nozzle.

4.2.2.2 Circumferential Distribution

Circumferential distribution tests were attempted using the pneumatic-impact injector and the fuel distribution hardware shown in Figure 31. Quantitative data was found to be unobtainable due to the profile of the spray pattern. High velocity air through the venturi and the relatively large open area at the discharge forced the fuel air mist out of the collector.

However, visual observations did show a wake behind each strut holding the target plate to the venturi body, and large droplets being formed due to surface tension effects at the edge of the target plate. As a result of these observations the number of struts was reduced from four to two, and the lip of the impact plate was ground to a sharp edge. Retesting produced fewer large droplets and a more uniform distribution between the two struts.

4.2.2.3 Spray Envelope

The pneumatic-impact nozzle was tested in the fuel-injection rig, shown earlier in Figure 24, to determine the spray envelope characteristics in a manner similar to that described in Section 4.1.2.2. Data was obtained with duct air at approximately 200°F, over a velocity range from 8 to 200 feet per second and at pressures of 1, 8, and 16 atmospheres. Results were plotted in a manner similar to those described previously for the air-assist nozzle. Curves typical of these results in Figure 32 show a much greater radial trajectory spread for the pneumatic-impact nozzle than did the air-assist nozzle at equivalent test conditions. Some nonsymmetry of the profiles was initially believed to be due to gravity effects, but upon rotating the rig 180° and rerunning two points, the nonsymmetry was found to be due to uneven distribution from the nozzle. This nonsymmetry was particularly noticeable at the lower fuel flow rates.

Trajectory calculations were performed with the assumption that the droplet velocity leaving the plate was equal to the sheet velocity. These calculations resulted in predictions which showed lower droplet penetration than was observed experimentally. Similar calculations based on the assumption that the droplet velocity was equal to the velocity of the air passing through the discharge gap (between the venturi and the impact plate) resulted in overpenetration.

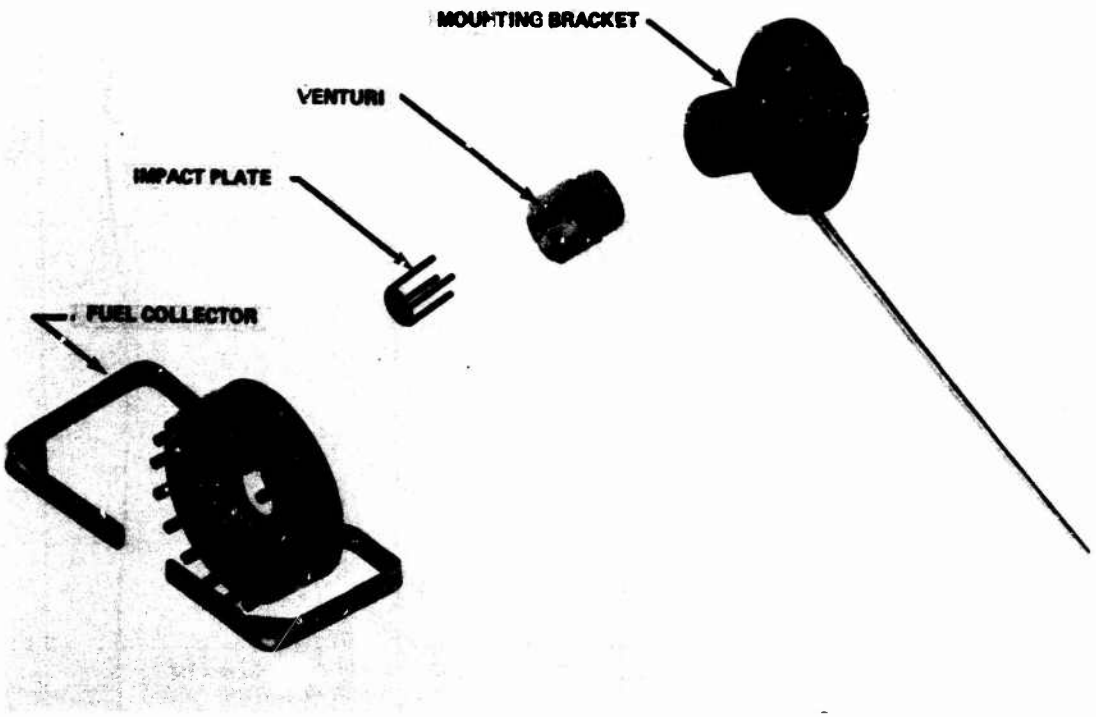


Figure 31. Pneumatic-Impact Injector Fuel Distribution Test Hardware.

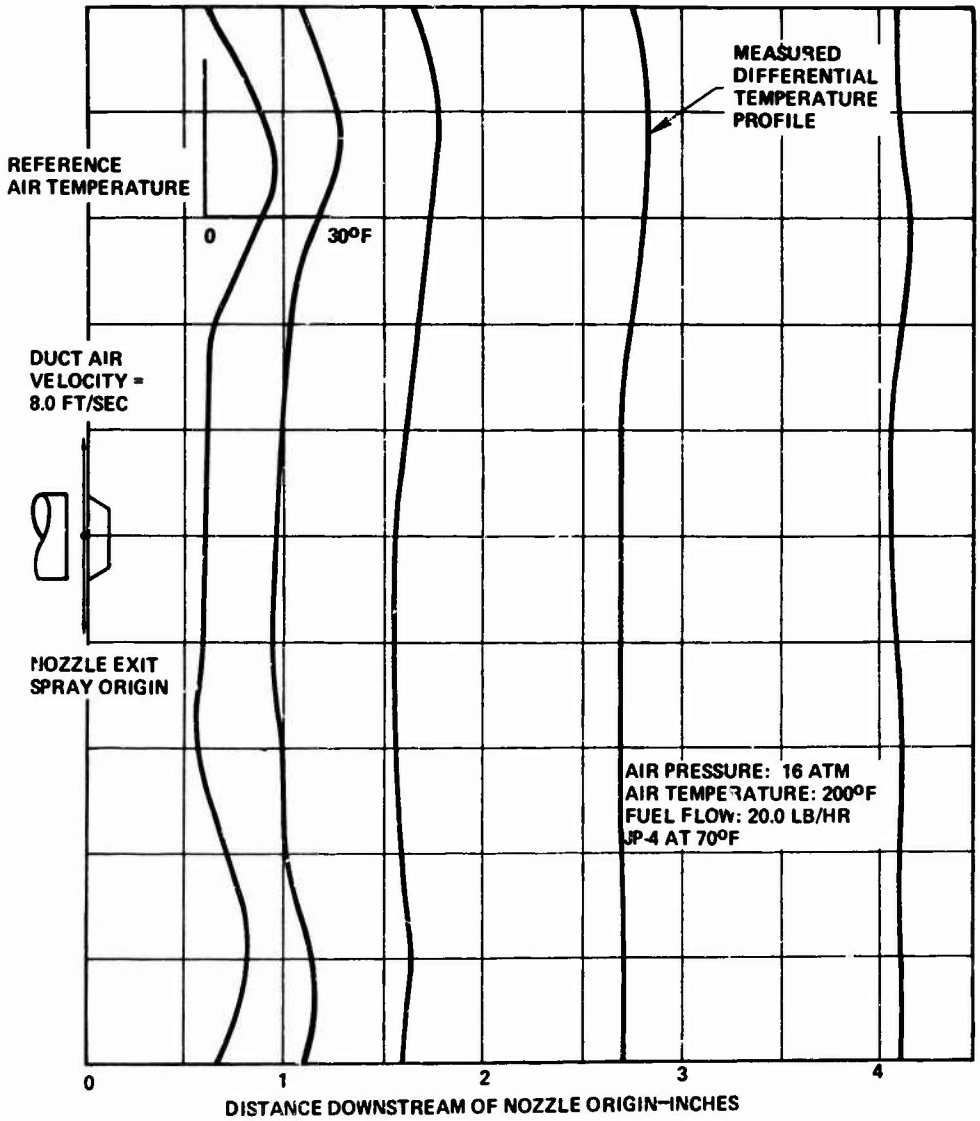


Figure 32. Pneumatic-Impact Injector Test Temperature Profiles.

The following empirical relationship was used to obtain the best correlation:

$$V_{droplet} = C\, V_{air} + V_{sheet} \qquad (27)$$

where $V_{droplet}$, V_{air} and V_{sheet} are droplet velocity, gap air velocity, and fuel sheet velocity, respectively. The empirical constant, C, was calculated by

$$C = 0.05\, P \qquad (28)$$

where P is chamber pressure in atmospheres. Experimental and predicted data using the above updated correlation are compared in Figure 33.

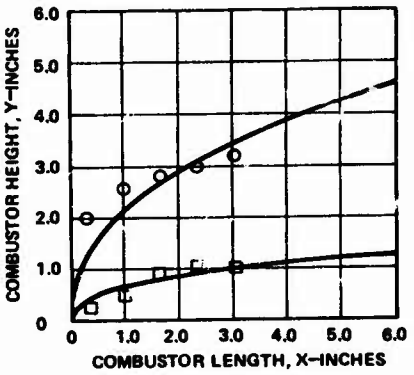
4.2.3 Conclusions

Based on analysis of the data and the correlations, the following conclusions were established:

- For a given chamber pressure and approach velocity the SMD and penetration both increase with increasing fuel flow rate.
- For a given fuel flow rate and approach air velocity, penetration depth increases with decreasing chamber pressure.
- The nozzle air field has an appreciable influence on the spray distribution from the impact plate.
- Nonsymmetry of the spray envelope could not be eliminated with the use of two or four supporting posts for the target plate.
- Droplet breakup calculations for the jet/venturi region do not appear to be realistic; however, the influence of this region on final distribution and SMD is minimal.

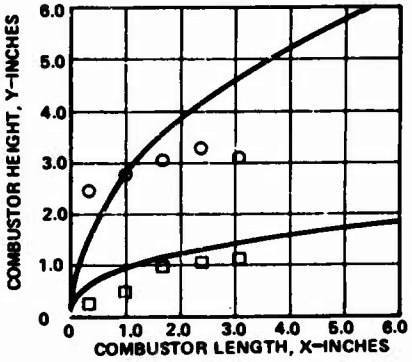
The pneumatic-impact nozzle is insensitive to fuel contamination problems but requires combustor pressure drop to drive and atomize the fuel. This causes atomization to deteriorate with decreasing pressure drop which can cause light-off problems.

Fuel impingement on liner walls can cause overheating problems with combustors of small dome height.



FUEL FLOW RATE = 20 LB/HR
APPROACH AIR VELOCITY = 40.6 FT/SEC
CHANNEL PRESSURE = 6 ATM
CALCULATED SMD = 38.3 MICRONS

FUEL FLOW RATE = 20 LB/HR
APPROACH AIR VELOCITY = 31.2 FT/SEC
CHANNEL PRESSURE = 16 ATM
CALCULATED SMD = 24 MICRONS



ANALYTICAL RESULTS ——————

○ OUTER SPRAY DROPLET BOUNDARIES FOR EXPERIMENTAL RESULTS

□ INNER SPRAY DROPLET BOUNDARIES FOR EXPERIMENTAL RESULTS

FUEL FLOW RATE = 35 LB/HR
APPROACH AIR VELOCITY = 31.2 FT/SEC
CHANNEL PRESSURE = 16 ATM
CALCULATED SMD = 29 MICRONS

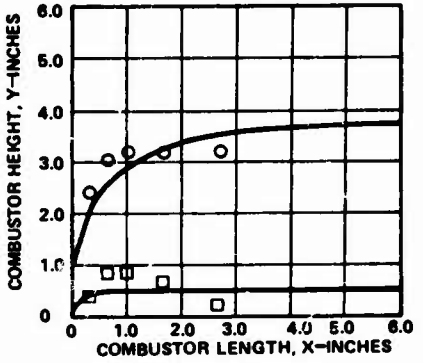


Figure 33. Comparison of Experimental and Analytical Spray Trajectories From Pneumatic-Impact Atomizer.

Distribution of the spray is influenced by target plate design and support system and by the primary-zone airflow patterns, which makes optimum design difficult.

Recommended limitations for the use of the pneumatic-impact injector systems are:

- In short combustors with many injection points to overcome possible contamination problems and to promote mixing
- In annular combustor systems with small channel heights to avoid impingement of fuel on the walls

4.3 L-PIPE INJECTOR

An L-pipe fuel injector is a low fuel pressure system which places a liquid fuel film on the combustor dome. The film is then evaporated from the dome and combustor walls by the hot recirculating combustion products. The device (primary pipe) by which the film is placed on the dome can be of several configurations, including J-pipe, T-pipe, L-pipe, or a "mushroom" shape.

Combustors using these injector types are generally considered to have several characteristic advantages over the typical fuel-pressure atomizing systems, such as:

- Low smoke
- High efficiency at part power
- Nonluminous (blue) flame which reduces radiation and, thus, wall cooling requirements
- Low fuel-pressure requirements
- Low fabrication costs

Typical disadvantages of these systems include:

- Ignition (light-off) difficulties, particularly with low combustor inlet temperatures
- Primary pipe durability due to the requirement of suspending the sheet metal tube in the hot recirculating combustion products
- Nonuniform fuel distribution and backup in the tube, particularly with low combustor pressure-drop systems

4.3.1 Model Definitions

The L-pipe injector (shown schematically in Figure 34) was the primary configuration examined in this program; however, the analysis is also applicable to the other configurations. The computer program derived for analysis of the L-pipe (vaporizer) fuel system is described in Appendix III.

The analysis is similar to that of the pneumatic-impact fuel nozzle. The air and relatively large fuel droplets enter the combustor through the L-pipe (analogous to the venturi in the pneumatic-impact system). The air (combustor pressure drop) accelerates the fuel to impinge first on the L-pipe elbow and then again on the combustor dome. The analysis of the flow in the L-pipe differs from that of the pneumatic-impact system because:

- The air and most of the fuel separate after leaving the primary pipe.
- The fuel evaporates as a film rather than as droplets.
- There is heat transfer to the fuel-air mixture through the L-pipe walls from the hot primary-zone gases.

External and internal heat-transfer coefficients are used to determine the heat input through the L-pipe. Calculations (and observations) indicate, however, that a very small fraction of the fuel is vaporized in the primary pipe.

Most of the fuel (those droplets larger than 10 microns) is placed on the dome and flows radially in a thin film. The calculations for fuel film evaporation from the dome are based on radial wall-jet analyses described by Gordon[33] and Watz[34]; i.e.,

$$Nu_x = h_x \frac{x}{k} = 0.368\ Rn_x^{0.566}\ Pr^{0.36}/(x/d)^{0.434} \qquad (29)$$

where x = radial distance from center of jet

d = jet diameter

Kinney[30] showed that the heat-transfer rate on the dome is significantly higher as a result of the fuel film; i.e.,

$$\dot{q}_{liquid}/\dot{q} = (0.0134 + 0.238\ W_f/L)\ Rn^{0.324} \qquad (30)$$

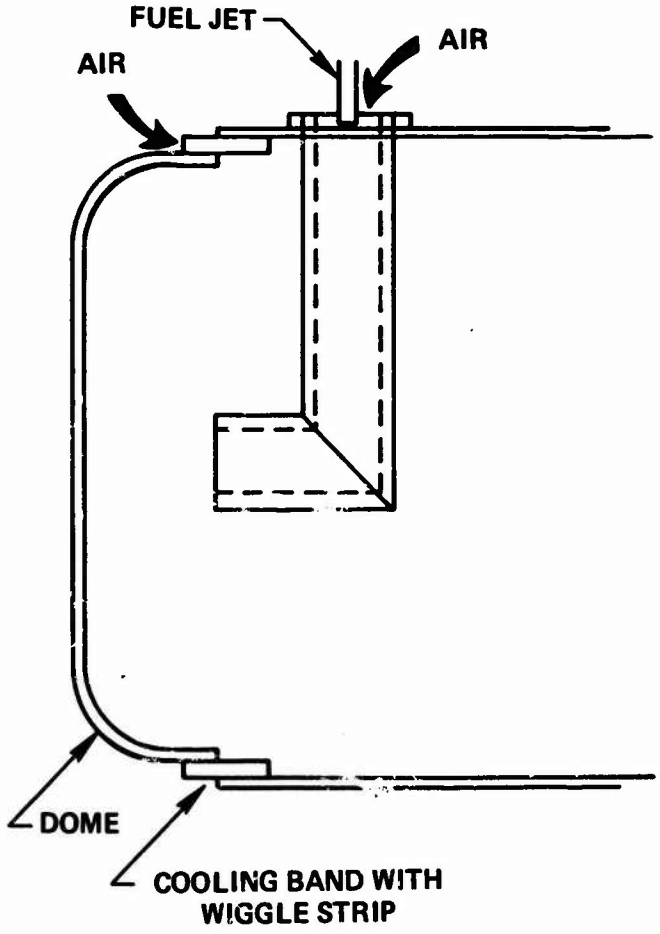


Figure 34. L-Pipe Vaporizer Fuel Injector.

where $\dot{q}_{liquid}$ = heat-transfer rate with film

$\dot{q}$ = heat-transfer rate without film

W_f/L = fuel flow rate per unit length

The calculations of fuel film thickness and velocity are also based on work by Kinney where these parameters are calculated from the fuel flow rate (W_f) and the surface friction coefficient (C_f). C_f is obtained from the von Karman analogy with:

$$\text{Stanton number} = C_f/2.0$$

$$\text{Friction factor} = 4.0\ C_f$$

The procedure for determining the primary-zone velocities and temperatures that produce the fuel evaporation is discussed in Section 5.0.

The fuel evaporation characteristics are determined from the work by Priem[6] discussed in Section 4.1.1.

Typical results from calculations of fuel film parameters in a 16-atmosphere environment are shown in Figure 35 as a function of radius along the combustor dome from the stagnation point of air-blast pipe impact. The most significant fact derived from these calculations is the relatively constant film thickness. The film velocity drops rapidly because of the combined effect of increasing radius and decreasing wall jet air velocity. The combined effect of reduced velocity and friction factor apparently balances to produce a relatively constant film thickness.

The evaporation rate is approximately linear and extends well beyond the 0.685-inch half width of the preliminary annular combustor design (Section 2.2.4). This indicates that the fuel film extends beyond the dome and evaporates along the side wall.

The L-pipe temperature calculation routines indicated metal temperatures on the order of 1200°F. Attempts to verify these calculations by tests were unsuccessful.

4.3.2 L-Pipe Injector Tests

The L-pipe test rigs were designed to provide quantitative data for fuel film thickness and distribution.

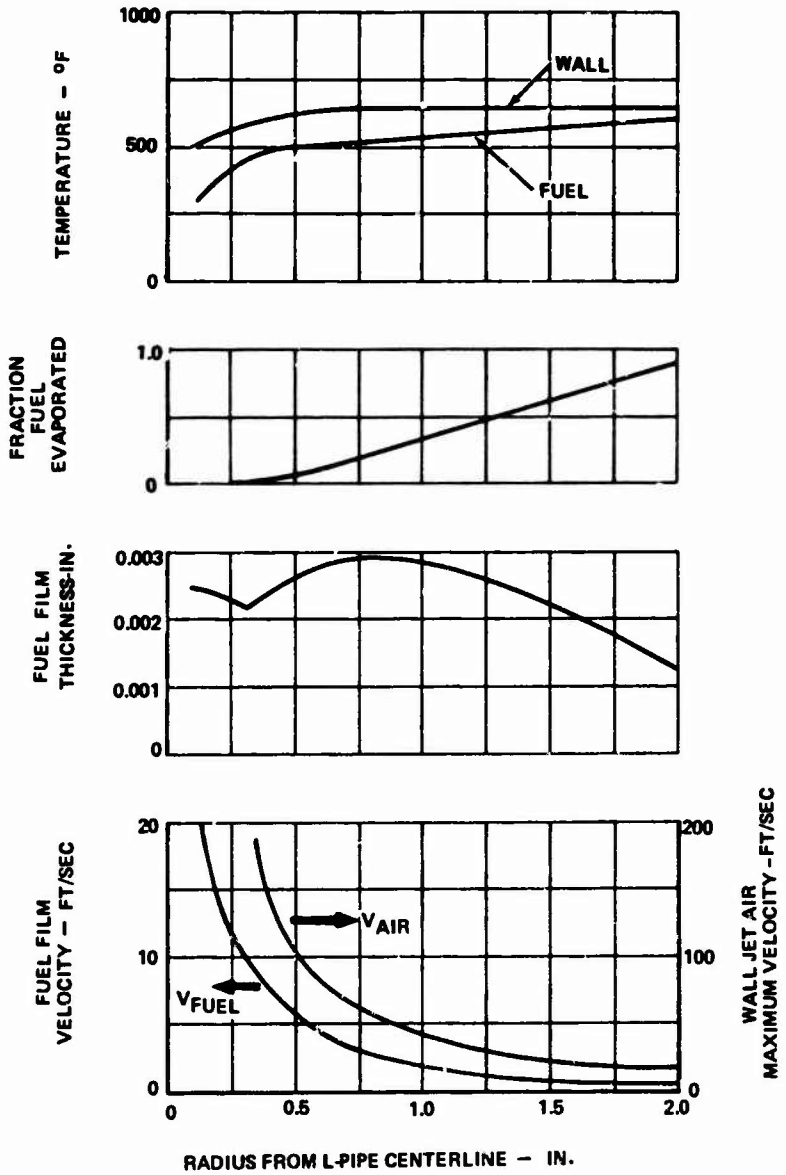


Figure 35. Fuel-Film Parameters for L-Pipe Injector at 16 Atmospheres.

Four primary-pipe configurations were tested:

(a) A standard L-pipe [Figure 36(a)], fabricated from stainless steel and Plexiglas (the Plexiglas model permitted flow visualization of the fuel within the L-pipe)

(b) A modified L-pipe [Figure 36(b)], which incorporated an insert at the exit to reduce fuel dribbling

(c) A rectangular-exit L-pipe [Figure 36(c)], which was expected to provide a circumferential distribution that is compatible with an annular combustor

(d) A straight fuel tube (not shown) to assess L-pipe elbow effects

4.3.2.1 Fuel Flow Distribution

Figure 37 illustrates the fuel flow circumferential distribution rig. For the tests, the target plate (simulated combustor dome) was horizontal. The L-pipe exit was positioned at the center of the target plate, and the distance from the L-pipe exit to the target plate was varied from 0.5 inch to 2.0 inches.

Air and fuel flow rates were varied to simulate those encountered in typical combustors. Fuel flow rates were varied from 2.0 to 30.0 pounds per hour, with air pressure drops from 4.0 to 6.0 inches of water. JP-4 fuel was used throughout the tests.

Figure 38 shows typical data that was obtained with the 18 fuel collection beakers. The ordinates on this figure (flow ratio) are the ratio of the fuel captured in each beaker to the average obtained in all beakers. Table VIII summarizes the range of flows (maximum to minimum) encountered for each nozzle type.

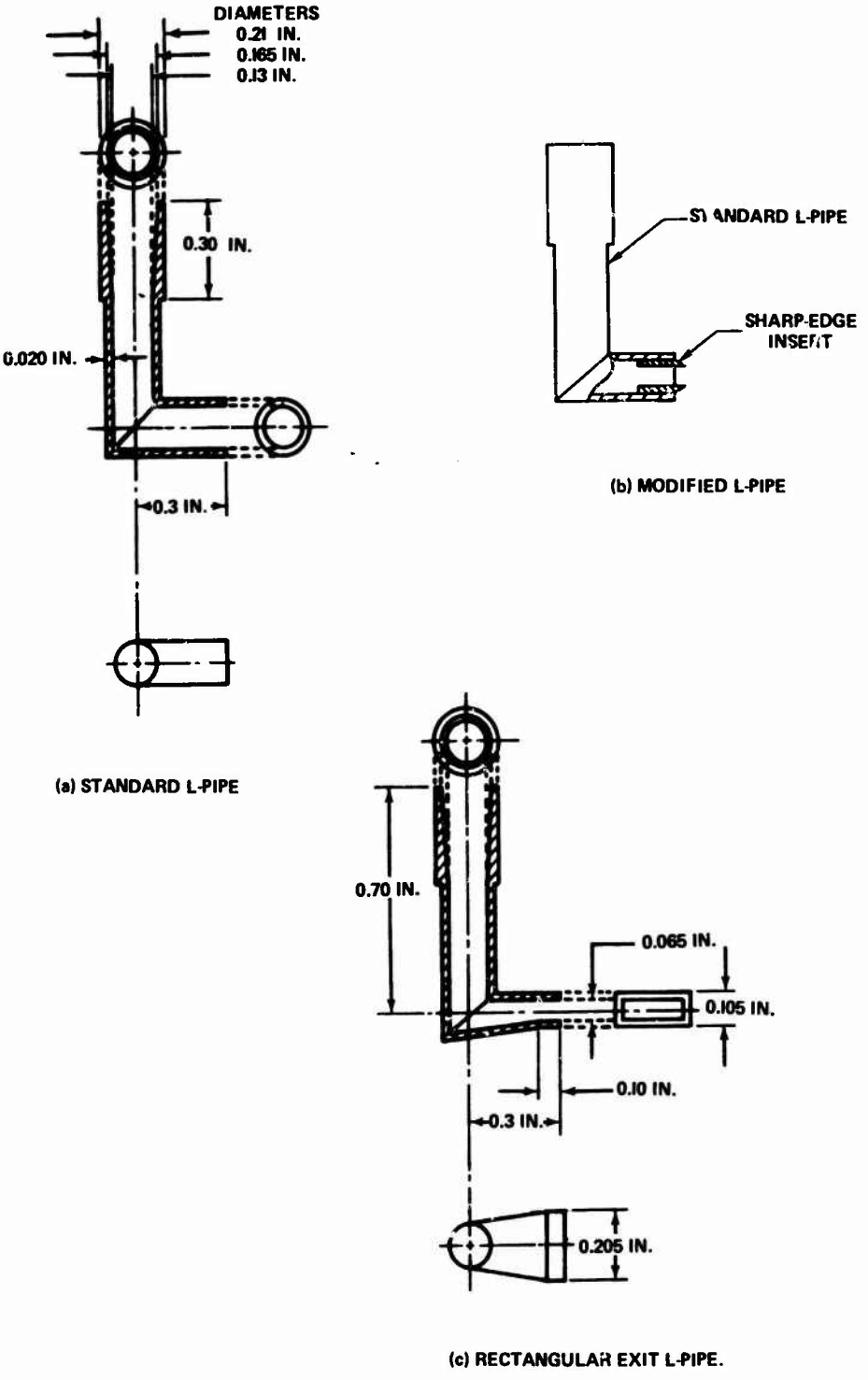
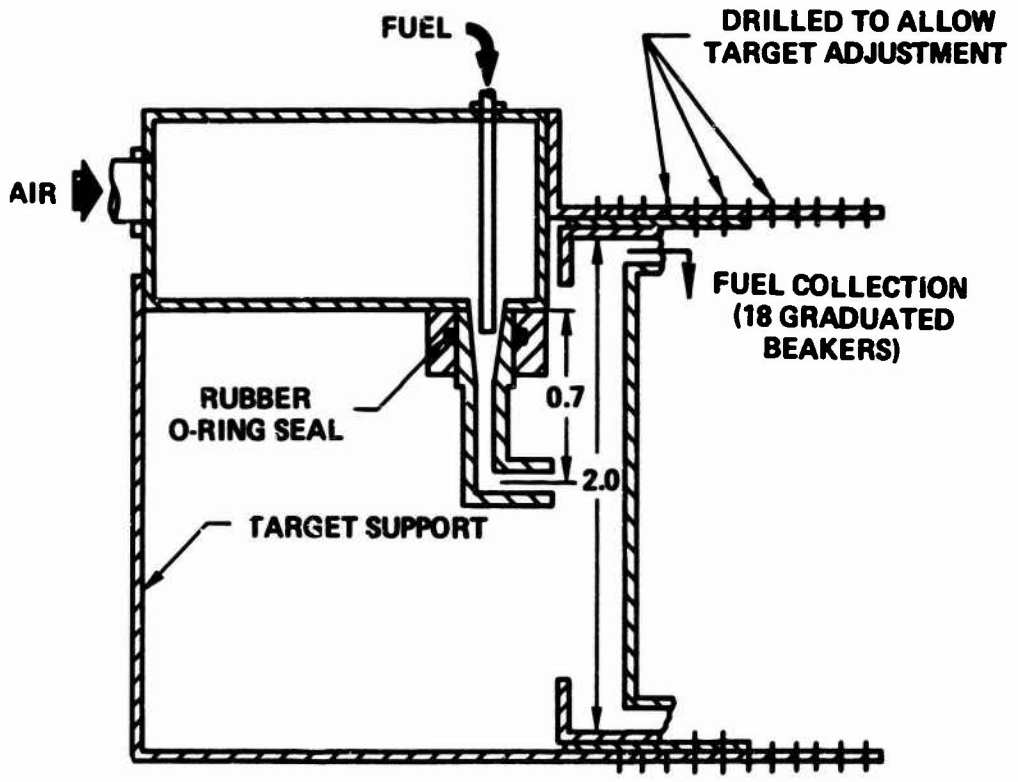
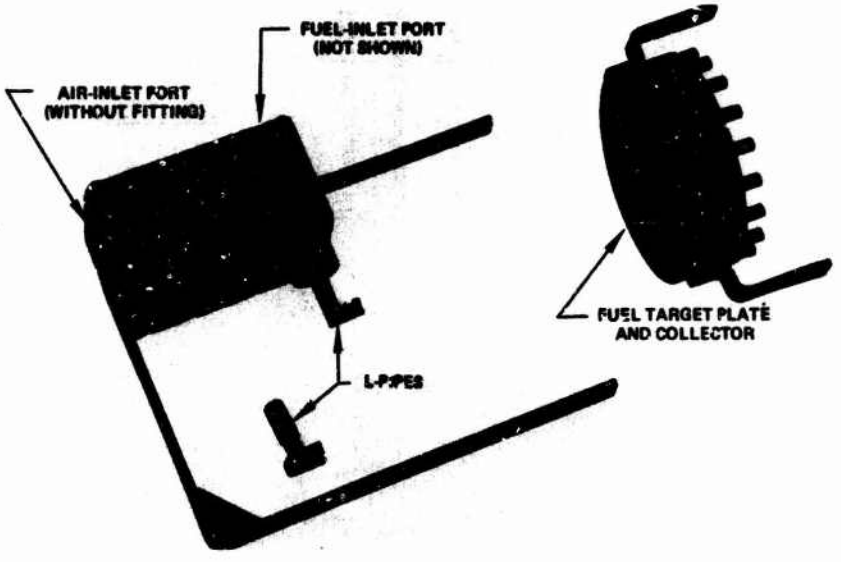


Figure 36. L-Pipe Configurations Tested.

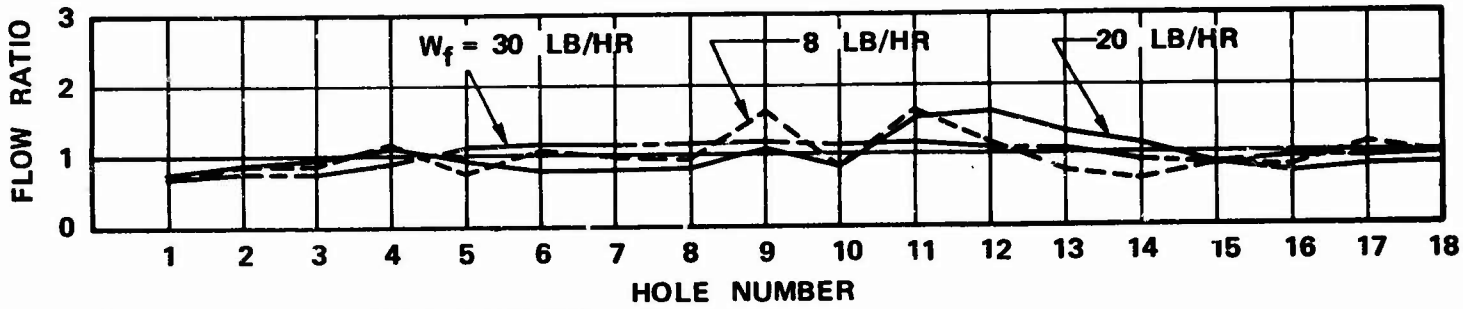


(a) RIG DESIGN SCHEMATIC

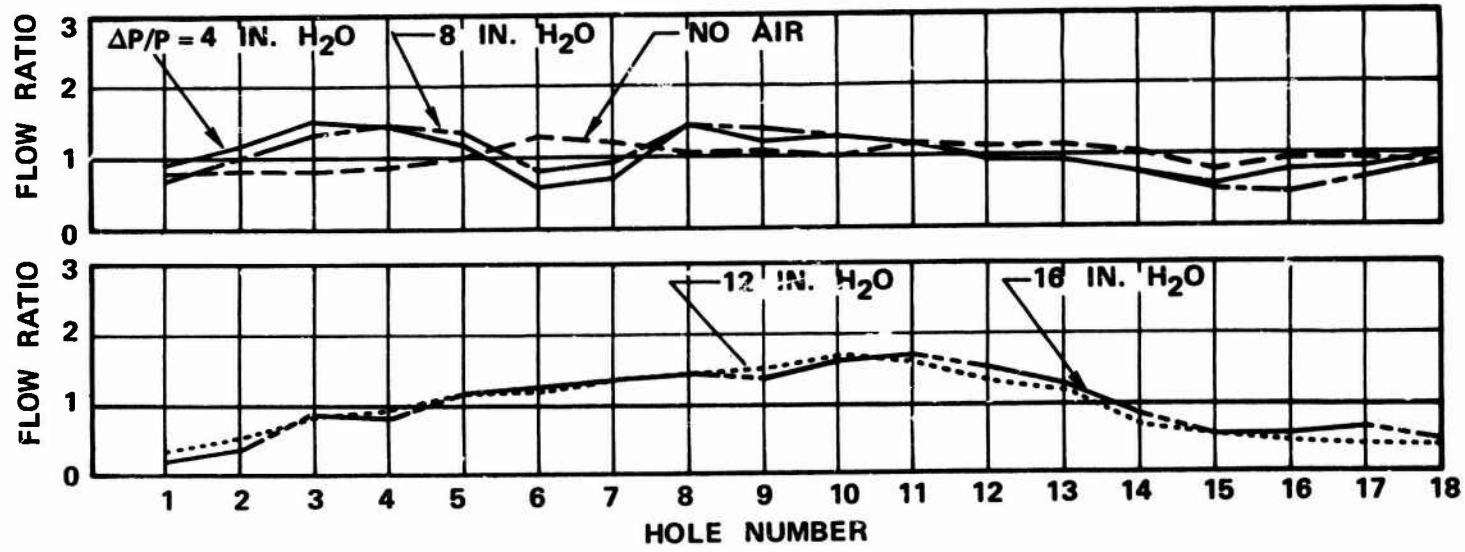


(b) RIG HARDWARE

Figure 37. L-Pipe Flow Distribution Rig.



VARYING FUEL FLOW WITHOUT AIRFLOW



FUEL FLOW OF 30 LB/HR WITH VARYING AIRFLOW

Figure 38. Circumferential Distribution of Fuel From Standard L-Pipe With Varying Fuel and Airflow Rates.

TABLE VIII. SPREAD IN FLOW RATIOS			
Flow Variation (Maximum to Minimum)			
Fuel Flow (lb /hr)	Standard (Circular) L-Pipe	Modified L-Pipe	Rectangular L-Pipe
2	4.2	4.7	-
8	1.5	1.4	1.5
20	1.7	1.1	2.5
30	1.4	2.0	2.9

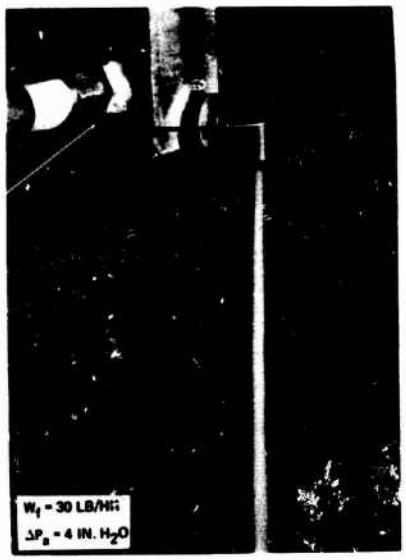
The standard and modified L-pipe configurations provided a more even distribution than the rectangular-exit L-pipe configuration. The distance from the L-pipe exit to the target plate did not have a significant effect. The rectangular discharge L-pipe appeared to produce a flatter spray pattern, but in other respects it produced results similar to the circular L-pipe. The distribution was not as uniform as for the circular L-pipe, as indicated by the spread in data as shown in Table VIII.

Figures 39 through 42 show the standard L-pipe and the rectangular-exit L-pipe without the collector target plate in position. These show the visual characteristics of various fuel flows and airflows. Surface tension effects caused the fuel to cling to the outside of the discharge end of the L-pipe. In an effort to reduce this effect, a sharp edge was provided at the end of the tube for the modified L-pipe. However, this modification did not overcome the problem.

Observation of flow utilizing the Plexiglas (transparent) L-pipe showed that at low fuel-flow rates with no airflow, the fuel ran down the outlet wall and dribbled onto the collection plate in a random direction. With airflow, the fuel was predominantly blown to one section of the collector. As the fuel flow was increased, this maldistribution was reduced.

The fact that the L-pipe systems in various attitudes have been shown to work satisfactorily in operating combustors indicates that fuel distribution may be significantly affected by the overall combustor flow pattern. For comparison purposes, a straight tube equal in size to the L-pipe was run to establish the distribution. These tests indicated that the





Reproduced from best available copy.

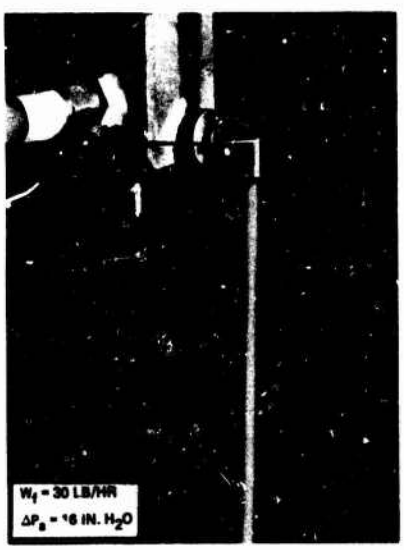


Figure 39. Fuel Flow From Standard Discharge L-Pipe.







Figure 40. Fuel Flow From Standard Discharge L-Pipe.

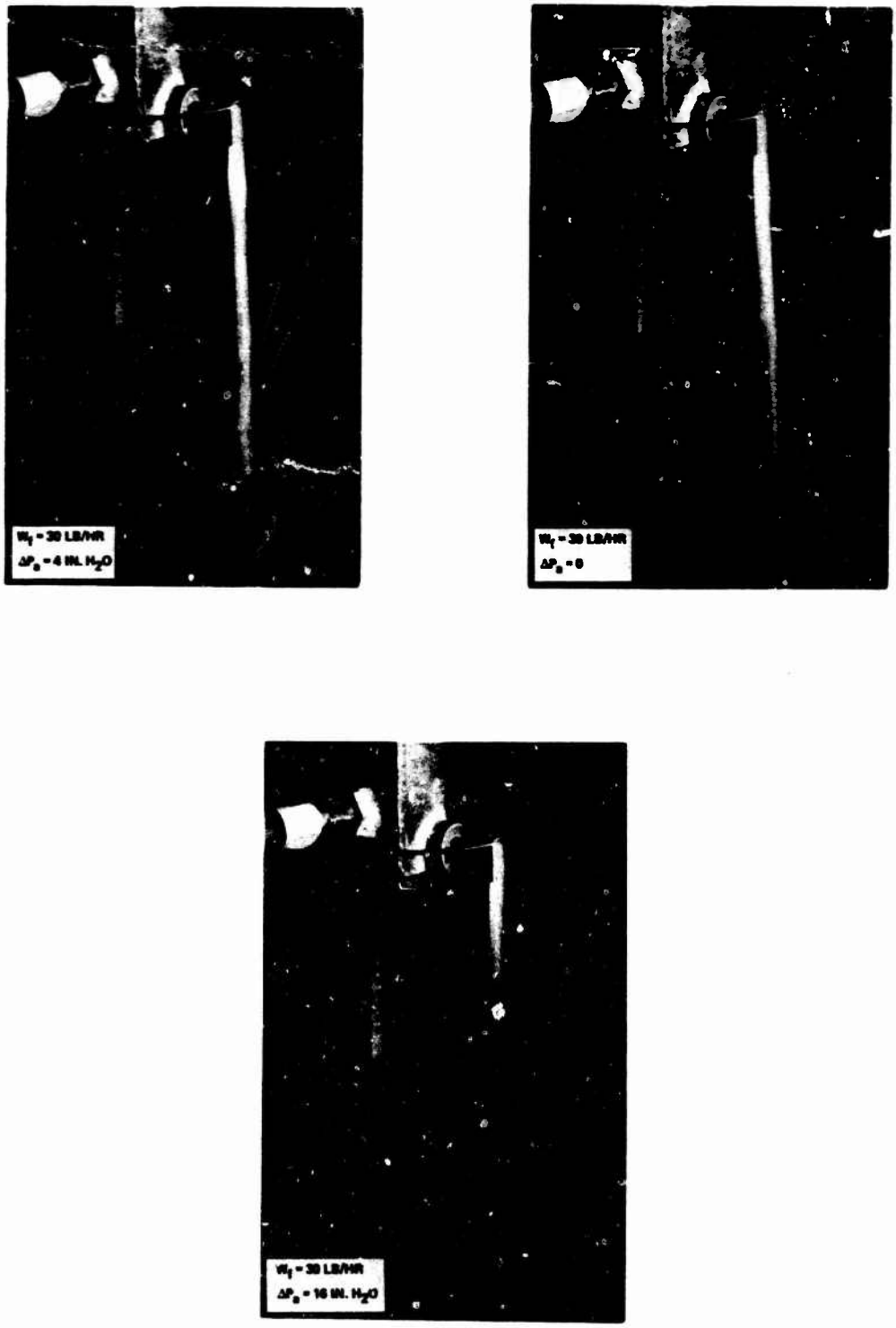
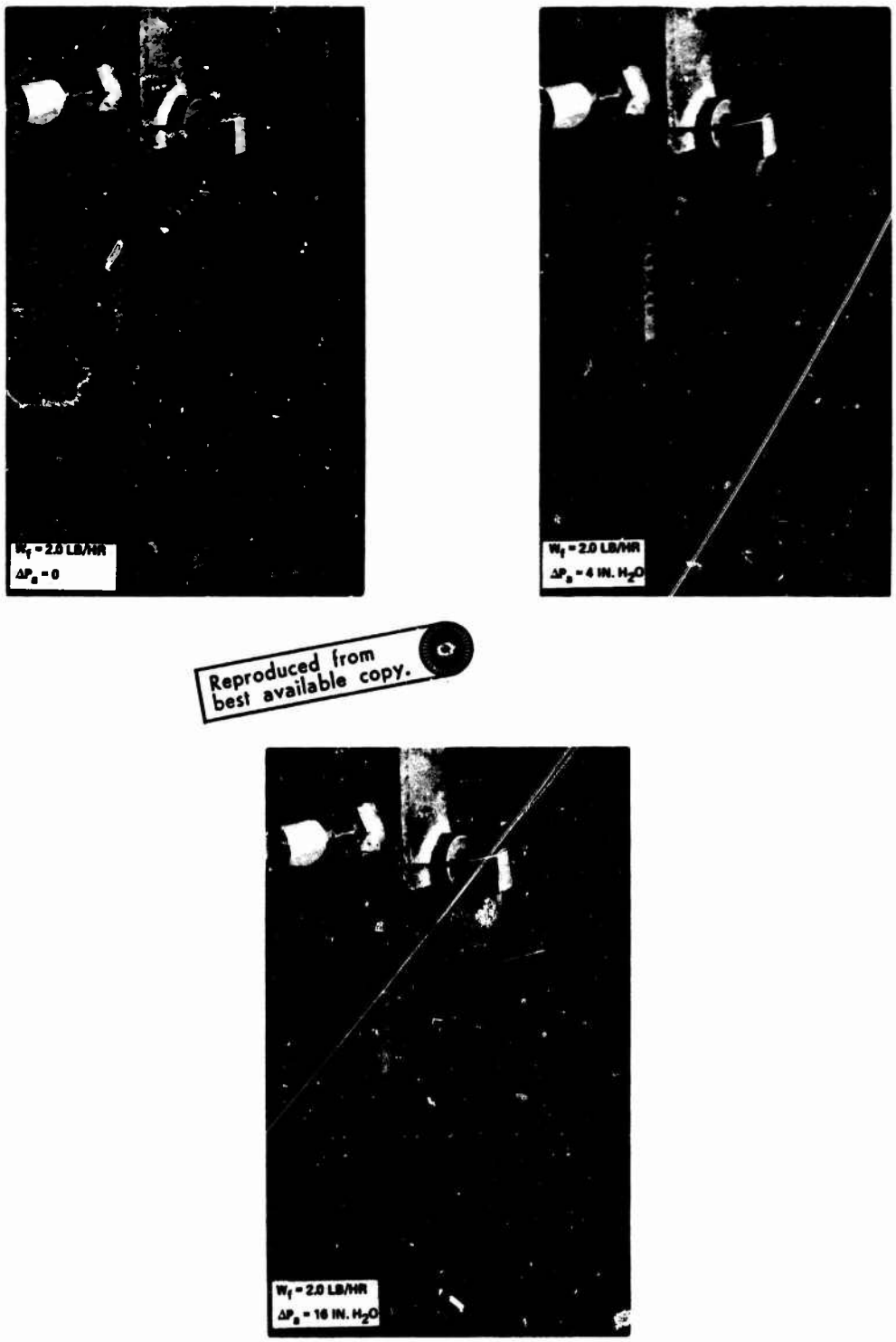


Figure 41. Fuel Flow From Rectangular Discharge L-Pipe.



Reproduced from best available copy.

Figure 42. Fuel Flow From Rectangular Discharge L-Pipe.

spread in the straight tube was similar to the L-pipe configuration, and that the elbow is not detrimental to performance. The fuel maldistribution probably results from aerodynamic instability of the fuel and air rather than from secondary flow effects due to the elbow. Observations of a hydraulic jump phenomena during the straight-tube tests showed that the diameter and shape of the jump would vary as a function of inlet test conditions. Only qualitative data could be obtained showing the dependence of jump characteristics on the height of the tube above the target plate, the amount of air through the tube, or the fuel flow rate. The following general observations were made:

- Increase of fuel flow causes an increase in the diameter of the jump with no airflow.
- High airflow (ΔP_{air}) causes the diameter of the jump to vary, even with the steady inlet conditions.
- Increase of the height of the tube above the target plate does not alter the average diameter of the jump but does tend to make it vary in shape.

Conclusions from these tests are that the L-pipe method of fuel injection can lead to gross nonuniformities in fuel distribution. No practical method for resolving this in the L-pipe itself has been found. This suggests that L-pipe system development may best be conducted in the actual combustor where the higher air velocities and high turbulence levels can serve to mix the vaporized fuel, resulting in a much better vapor-air distribution than would appear to be possible from liquid distribution tests at quiescent ambient conditions. Of the L-pipe configurations tested, the circular pipe gave the most consistent distribution. The increase in maldistribution with increased L-pipe airflow suggests that L-pipe airflow should be kept as low as possible, since its only purpose then, is to ensure that fuel is propelled to the combustor dome.

4.3.2.2 Film Thickness Measurement

Film thickness measurements were made with a Microderm "nondestructive coating thickness gauge," leased from Unit Process Assemblies, Inc., Woodside, New York. The instrument uses the principle of β-ray absorption and backscatter by the sample to determine its thickness. A β-ray source (strontium) is placed above a receiving plate, and the fuel sample is then placed between the source and the receiver. The number of rays transmitted through the sample to the receiver in a period of

time is a function of the atomic number and thickness of the sample.

A calibration of the gauge (JP-5 fuel) was obtained by fabricating a rectangular reservoir (1.0-inch by 0.080-inch). A known volume of fuel was placed in the reservoir by means of a drop-calibrated hypodermic needle. From the known values and wetted area, the thickness was calculated for each volume and the microderm scale was calibrated against these known thicknesses. At low volumes--i.e., low film thickness--some error was introduced due to uneven plate wetting. Several measurements were made where error was suspected, and in each case readings were taken at more than one location above the plate and film.

Figure 43 shows a schematic of the fuel-film test apparatus. The L-pipe was replaced by a straight tube with a circular cross section equal to that of the standard L-pipe. The test conditions are listed in Table IX.

TABLE IX. TEST CONDITIONS FOR FILM THICKNESS MEASUREMENT

Fuel flow, lb/hr	4, 10, 20,
Air ΔP, in. of H_2O	0, 5, 10, 15
h, in.	0.25, 0.50, 0.75
x, in.	0.50, 0.75, 1.0, 1.25, 150

For h and x dimensions, refer to Figure 43.

The test data obtained indicated the presence of the previously mentioned hydraulic jump and nonuniform distribution on the target plate. Figures 44 and 45 show the hydraulic jump and film thickness data for air ΔP = 15 inches of water, and air ΔP = 0 inch of water, respectively, with fuel flows of 4, 10, and 20 pounds per hour, and tube-to-target distance equal to 0.25 inch (all data is downstream of the jump).

Conclusions drawn from the film-thickness data are that with no airflow through the tube, and low fuel flows, the film will tend to have a uniform thickness after the initial jump. The addition of air with the fuel in the pipe caused peaks, valleys and splashing of the fuel, and an undefinable jump boundary.

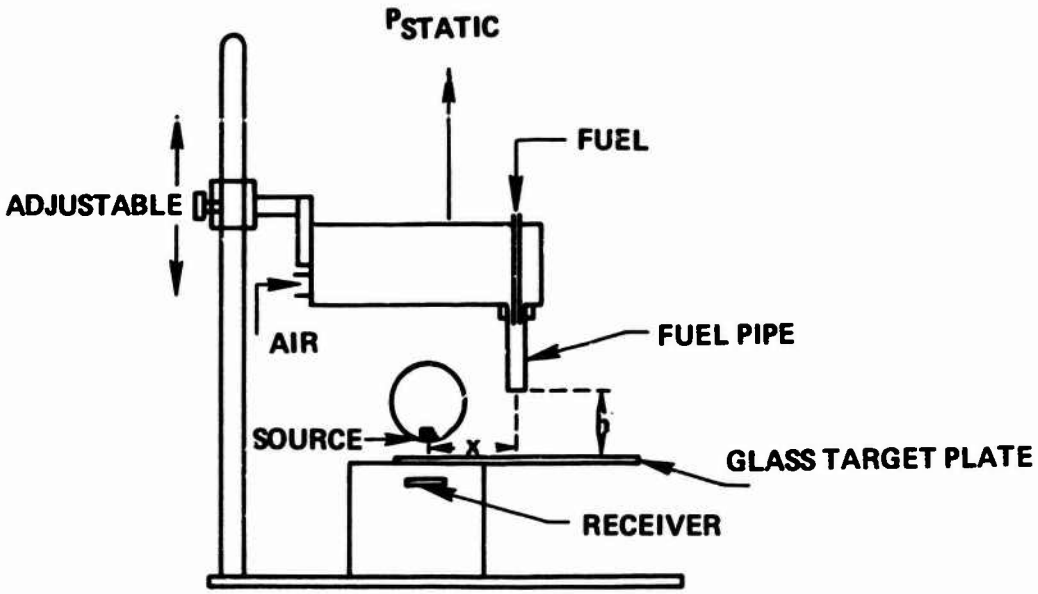


Figure 43. Film Thickness Measurement Apparatus.

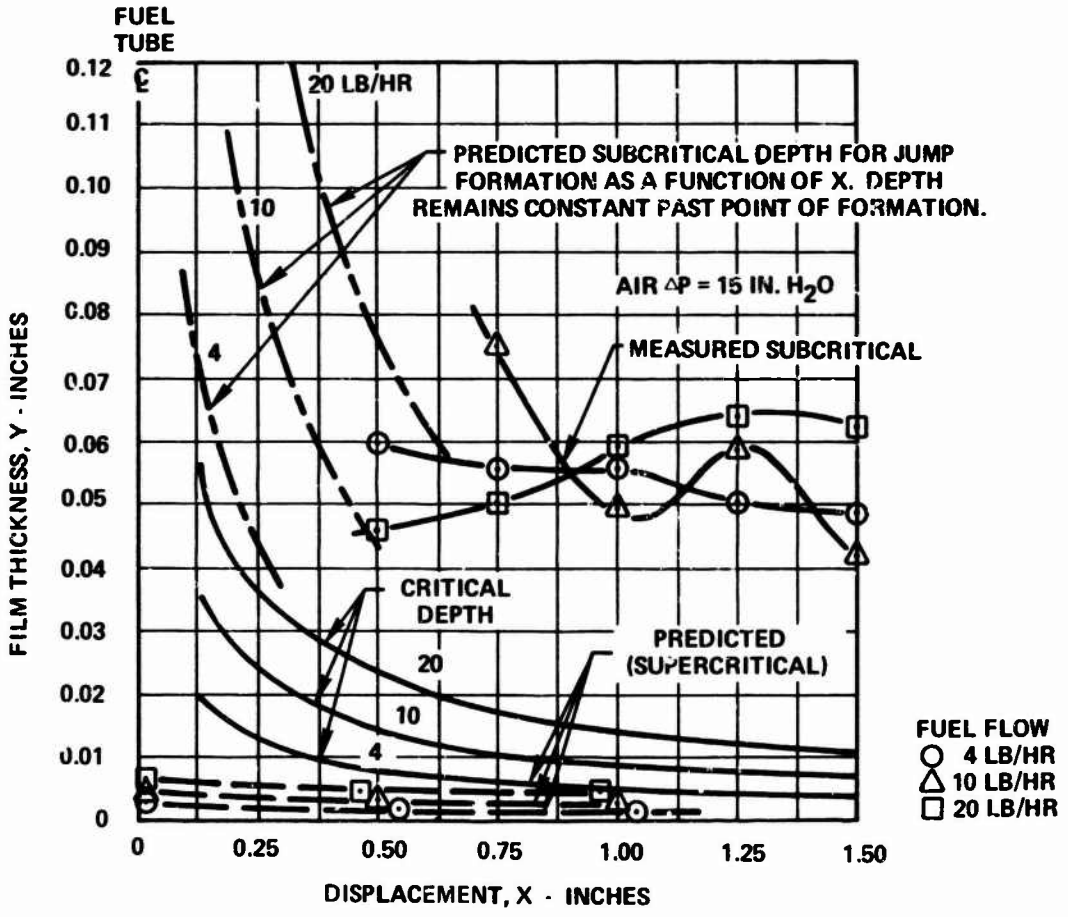


Figure 44. Straight Fuel Tube Film Thickness Measurements, Air ΔP = 15 Inches of H_2O.

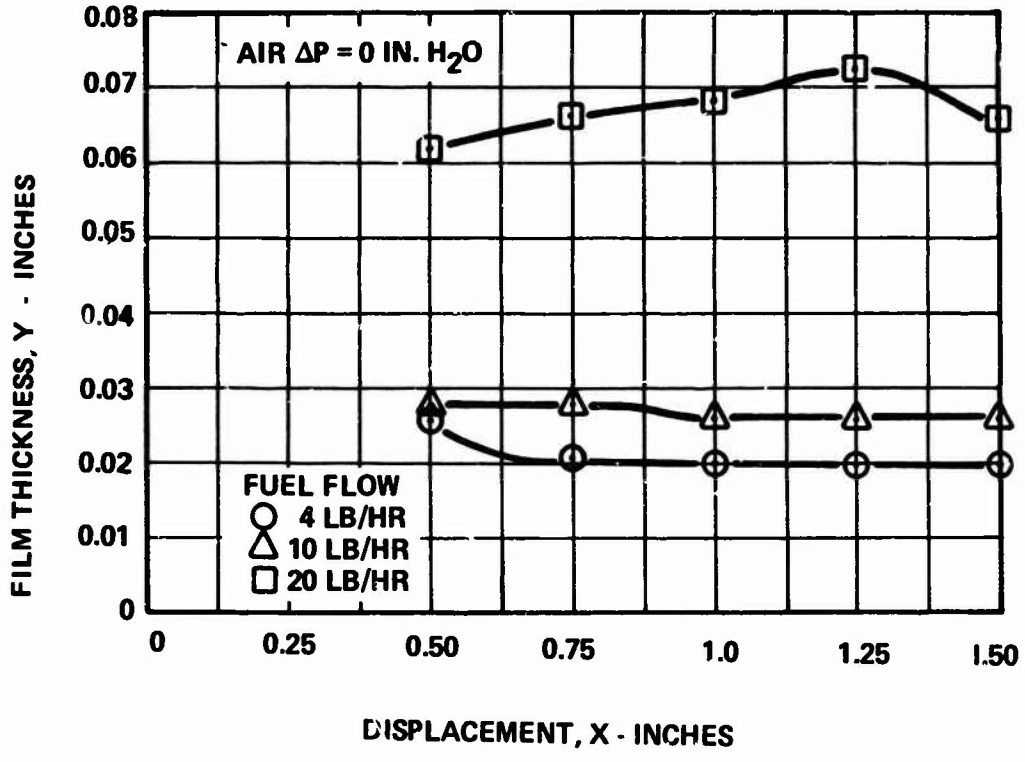


Figure 45. Straight Fuel Tube Film Thickness Measurement, Air ΔP = 0 Inch of H_2O.

4.3.3 Analytical Model Update

Analytical predictions of fuel film thickness are shown in Figure 44. Measured thicknesses are greater by a factor of 10 as the result of hydraulic jump formation. The size of the thickness-measurement instrument precluded measurements inside the jump ring. Classical open-channel flow theory relates the hydraulic jump to gravity forces in a sloping channel. Gravity, together with the degree of channel slope, causes the flow to be either subcritical or supercritical and has an analogy to subsonic and supersonic compressible flow.

The flow of a film on a level flat plate will be subcritical (low velocity and large thickness) unless there is sufficient air velocity over the film to force supercritical flow. In the case of the isolated L-pipe tests, air from the L-pipe alone is not sufficient to maintain supercritical flow beyond a radius of approximately 0.40 inch.

Hydraulic jump theory is discussed in most fluid mechanics texts--for example, Vennard.[35] A critical depth occurs at which the flow passes from supercritical to subcritical and is related to the flow per unit width (or unit circumference for radial flow).

$$Y_c = 12\left(\frac{w^2}{g}\right)^{1/3} = 0.001924\,\frac{W_f}{X}^{2/3} \qquad (31)$$

where Y_c = critical depth, inches

w = volume flow per unit width, cu ft per sec per ft

Critical depths calculated for the test points at 15 inches of water are also shown in Figure 44. Application of the impulse-momentum principle across a hydraulic jump leads to the following ratio of downstream to upstream film depth:

$$\frac{Y_2}{Y_1} = \frac{1}{2}\left[-1 + \sqrt{1 + \frac{8\,w^2}{g\,y_1^3}}\right] \qquad (32)$$

where y_2 = subcritical downstream depth

y_1 = supercritical upstream depth

For the tested conditions, the depth ratio is on the order of

$$\frac{y_2}{y_1} = \frac{8}{x}$$

where x = radial displacement from L-pipe centerline, inches.

Figure 44 shows the predicted subcritical depths that would occur as a function of jump radius, x. These predicted depths are consistent with the measured depths for a hydraulic jump radius of the order of 0.10 to 0.40 inch. Prediction of the location of the jump could be attempted by analyzing the friction drag on the liquid film and making a determination of the minimum air velocity required to maintain supercritical flow. Such an analysis would have to be strongly dependent on the overall configuration and is not deemed of sufficient benefit for pursuit at this time. The main point is to be cognizant of hydraulic jump phenomena and attempt to avoid its occurrence in film vaporizing designs by ensuring that the fuel film is continually scrubbed with high-velocity air.

4.3.4 Conclusions

Based on an analysis of the data and correlations, the following conclusions were drawn.

- The L-pipe method of fuel insertion can lead to gross nonuniformities in fuel distribution. This indicates that the flow field in the primary zone is of prime importance in the operation of this type of combustor.
- Only a small amount of fuel is actually vaporized within the fuel pipe.
- Fuel film thickness is not constant and a hydraulic jump may occur.
- Data obtained from tests not including the total combustion environment are not directly applicable to combustor design and must be viewed only qualitatively.

L-pipes provide a simple, inexpensive method of fuel insertion, but limi ations to their use may be imposed by the following:

- Fuel backup - The pressure drop across the combustion system is the means by which the fuel is driven through the L-pipe. At low combustor pressure drops, particularly at altitude start conditions, fuel can back up in the L-pipe and be discharged over the outer liner. This problem may be particularly severe when the L-pipes are in the inverted position with the pressure drops of the order of 1 percent.

- Fuel distribution - Fuel distribution within the combustor is highly sensitive to the primary zone flow field and dome design. Successful use therefore depends upon careful matching of the primary zone geometry with the L-pipe distribution.

- L-pipe integrity - The L-pipe is located within the combustor primary zone, thus making it more susceptible to overheating and mechanical failure.

Recommended limitations for the use of L-pipes are:

- Short life engines

- High pressure drop combustors

- Well developed primary-zone flow fields with a start nozzle, possibly required for cold inlet starts

5.0 PRIMARY ZONE

5.1 PRIMARY-ZONE RECIRCULATION

A two-dimensional fluid mechanics model with mixing-limited combustion was developed to predict flow field properties (velocities, temperatures, species concentrations, etc.) and resultant recirculation patterns within the primary zone. Fuel evaporation and droplet trajectory calculation routines (from the fuel insertion model) were also included. Several rig tests were conducted to obtain data for validation of the model.

5.1.1 Model Definition

Prediction of the fluid properties and recirculation patterns within the primary zone was first attempted by means of a numerical analysis technique (called SMAC*) developed at the Los Alamos Scientific Laboratory.[36] This method considered the problem as a time-dependent, incompressible, viscous fluid in two space dimensions.

The basic general differential equations used were:

$$\frac{\partial U}{\partial t} + \frac{1}{r^{\alpha}} \frac{\partial r^{\alpha} U^2}{\partial r} + \frac{\partial UV}{\partial Z} = - \frac{\partial \phi}{\partial r} + \nu \frac{\partial}{\partial Z} \left(\frac{\partial U}{\partial Z} - \frac{\partial V}{\partial r} \right) \qquad (33)$$

$$\frac{\partial V}{\partial t} + \frac{1}{r^{\alpha}} \frac{\partial r^{\alpha} UV}{\partial r} + \frac{\partial V^2}{\partial Z} = - \frac{\partial \phi}{\partial Z} - \frac{\nu}{r^{\alpha}} \frac{\partial}{\partial r} \left[r^{\alpha} \left(\frac{\partial U}{\partial Z} - \frac{\partial V}{\partial r} \right) \right] \qquad (34)$$

$$D = \frac{1}{r^{\alpha}} \frac{\partial r^{\alpha} U}{\partial r} + \frac{\partial V}{\partial Z} = 0 \qquad (35)$$

where $\phi = P/\rho$

Equations (33) and (34) establish a momentum balance in the "X" and "Y" directions, respectively, and Equation (35) establishes continuity.

Problems in the form of excessive computer time and program modification existed with this program. It became apparent that the development of the time-dependent solution for obtaining a steady-state solution and the inclusion of fuel

*Simplified marker and cell

evaporation, ignition lag, chemical kinetics, etc., would not be possible within the time available.

Several alternate flow-field computation techniques were examined in an attempt to circumvent the SMAC difficulties.

These included:

(a) A program by Gosman, et al,[37] which uses a very general finite-difference approach for solving the pertinent elliptic partial-differential equations for both two-dimensional and axisymmetric viscous, time-averaged flow fields, including turbulent flow with combustion

(b) An AiResearch-developed program which also uses a finite-difference approach for solving elliptic partial-differential equations, but is inviscid thus requiring an arbitrary loss distribution as input

(c) An empirical approach with the use of published data to predict spreading and entrainment of radial- and axial-wall jets

The Gosman et al program was shown to be the most readily adaptable to the combustor-type flow field and, thus, was selected for computation of both primary-zone and dilution-zone flow-field properties. The computer program prepared for the primary-zone analysis is described in Appendix IV.

5.1.1.1 Gosman Program Solution Technique

This general program scheme is capable of solving the pertinent elliptic partial-differential equations for a wide variety of two-dimensional and axisymmetric fluid mechanics problems, including turbulent flow with combustion. Arbitrary boundary conditions can be specified, along with variable grid spacing, curved boundaries, and swirling flow with recirculation. The analysis allows for recirculation and is not limited to a predominant flow direction.

The method is developed with the classic assumption that steady turbulent flow can be approximated by a laminar-flow solution in which molecular viscosity, conductivity, and diffusivity are replaced by effective viscosity and exchange coefficients varying with location, to characterize the transport properties of momentum, energy, and species concentration. The analysis starts from a generalized curvilinear orthogonal coordinate system that is primarily two-dimensional but allows for axial symmetry and rotational swirl. The coordinate system is shown

in Figure 46. By properly defining "metric" coefficients ℓ_i (i = 1, 2 etc.), a variety of coordinate types can be utilized, without changing the basic differential equations. These include Cartesian, cylindrical, cylindrical-polar, and spherical coordinates.

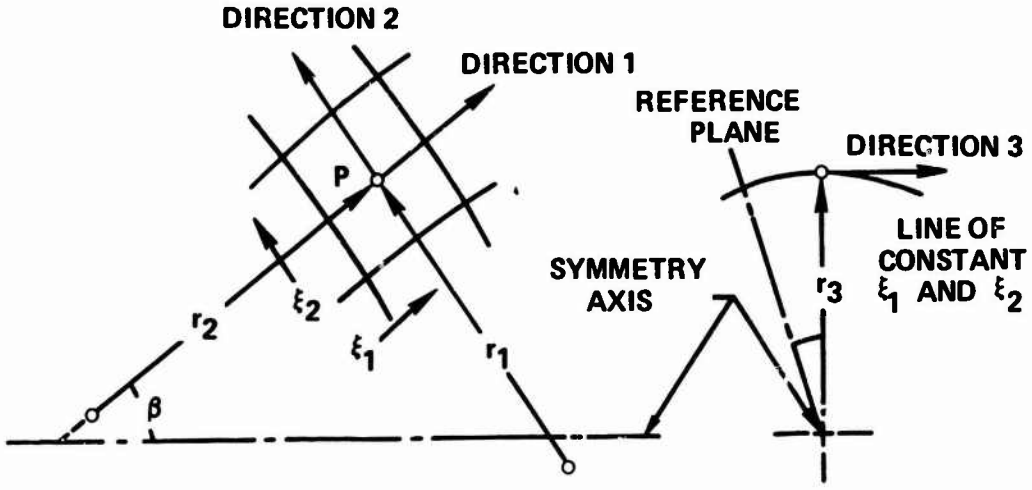


Figure 46. Gosman Coordinate System.

The dependent variables that characterize the flow field are:

m_j = mass of species j in unit mass of mixture (mass fraction)

p = fluid pressure

ρ = mixture density

t = mixture temperature

$\tilde{h}$ = mixture stagnation enthalpy

h_j = negative of j species heat of formation

C_{pj} = species j specific heat at constant pressure

$V^2/2$ = kinetic energy of mean motion

k = kinetic energy of turbulent motion

ℓ = turbulent length scale

The conservation equations of mass, momentum and energy involving pressure and velocity terms are transformed to those involving stream functions (whereby the overall mass conservation equation is automatically satisfied) and vorticity, which eliminates explicit dependence of pressure on the flow field. The resulting equations for all of the dependent variables are shown to be of identical form. A generalized equation is formulated and written as follows:

$$a_\phi \left\{\frac{\partial}{\partial \xi_1}\left(\phi\frac{\partial\psi}{\partial\xi_2}\right) - \frac{\partial}{\partial\xi_2}\left(\phi\frac{\partial\psi}{\partial\xi_1}\right)\right\} - \frac{\partial}{\partial\xi_1}\left\{b_\phi \frac{\ell_2 r}{\ell_1}\frac{\partial(C_\phi\phi)}{\partial\xi_1}\right\} \quad (36)$$

$$- \frac{\partial}{\partial\xi_2}\left\{b_\phi\frac{\ell_1 r}{\ell_2}\frac{\partial(C_\phi\phi)}{\partial\xi_2}\right\} + \ell_1\ell_2 r d_\phi = 0$$

In the above, ϕ represents any one of the dependent variables described in Table X, and ℓ_1 and ℓ_2 represent metric coefficients that are multiplying coefficients on the ξ coordinates. Table X lists the dependent variables, along with the forms of the a, b, c, and d terms. The first bracketed term multiplied by a_ϕ represents convection by fluid flow. The second and third bracketed terms account for diffusion, and the last term is the generation or source term.

The general equation is expressed in finite-difference form with "upwind" differencing. Boundary conditions for every independent variable must be specified in one of the following forms at each boundary node:

(a) The value of the variable

(b) The gradient at and normal to the boundary

(c) A relationship that connects the variable to values of the normal component of the velocity

For flows with combustion, a simplified procedure is developed to eliminate the need for solving separate equations for the species of fuel vapor, air, and combustion products. Because of stoichiometry, fuel and air disappear and products appear at proportional rates. It is also assumed that combustion is instantaneous (mixing limited). A fictitious dependent variable, ϕ_{fc}, is defined as

$$\phi_{fo} = W_f - W_a/i \quad (37)$$

where i = pounds of air required to burn 1 pound of fuel

TABLE X. TERMS OF THE GENERAL ELLIPTIC EQUATION

Dependent Variable	ϕ	a_ϕ	b_ϕ	c_ϕ	d_ϕ
Species	m_j	1	$\Gamma_{j,eff}$	1	$-R_j$
Enthalpy	$\tilde{h}$	1	$\Gamma_{h,eff}$	1	$-\frac{1}{\ell_1\ell_2 r}\frac{\partial}{\partial\xi_1}\left[\mu_{eff}\frac{\ell_2 r}{\ell_1}\left\{\left(1-\frac{1}{\sigma_h}\right)\frac{\partial V^2/2}{\partial\xi_1}+\left(\frac{1}{\sigma_k}-\frac{1}{\sigma_h}\right)\frac{\partial k}{\partial\xi_1}+\sum_j\left(\frac{1}{\sigma_j}-\frac{1}{\sigma_h}\right)h_j\frac{\partial m_j}{\partial\xi_1}\right\}\right] - \frac{1}{\ell_1\ell_2 r}\frac{\partial}{\partial\xi_2}\left[\mu_{eff}\frac{\ell_1 r}{\ell_2}\left\{\left(1-\frac{1}{\sigma_h}\right)\frac{\partial V^2/2}{\partial\xi_2}+\left(\frac{1}{\sigma_k}-\frac{1}{\sigma_h}\right)\frac{\partial k}{\partial\xi_2}+\sum_j\left(\frac{1}{\sigma_j}-\frac{1}{\sigma_h}\right)h_j\frac{\partial m_j}{\partial\xi_2}\right\}\right]$
Swirl velocity	rV_3	1	$\mu_{eff}r^2$	$\frac{1}{r^2}$	$\frac{\partial P}{\partial\xi_3}$
Vorticity	$\frac{w}{r}$	r^2	r^2	μ_{eff}	$-\frac{\partial}{\partial z}(\rho V_3^2)-\frac{r}{\ell_1\ell_2}\left[\frac{\partial}{\partial\xi_1}\left(\frac{V_1^2+V_2^2}{2}\right)\frac{\partial P}{\partial\xi_2}-\frac{\partial}{\partial\xi_2}\left(\frac{V_1^2+V_2^2}{2}\right)\frac{\partial P}{\partial\xi_1}\right]-r^2S_w$
Stream function	ψ	0	$\frac{1}{\rho r^2}$	1	$-\frac{w}{r}$
Turbulence kinetic energy	k	1	$\Gamma_{k,eff}$	1	$-S_k$
Turbulence scale	ℓ	1	$\Gamma_{\ell,eff}$	1	$-S_\ell$
Temperature	t	1	$\Gamma_{h,eff}$	1	0
Mixture fraction	ϕ_{fo}	1	Γ_{fo}	1	0

A corollary parameter for products is

$$\phi_{fp} = W_f + W_p/(1.0 + i) \tag{38}$$

where W_p = flow rate of products

It is further assumed that the turbulence exchange coefficients are equal for fuel, air, and products. These simplifications eliminate the source terms in the differential equation. A similar development is made for stagnation enthalpy; and with the assumption of constant specific heats, the temperature is expressed as a function of mixture ratio. If chemical kinetics is considered, this simplification would not be possible for all species conservation equations. The source terms are computed from standard Arrhenius-type rate equations.

The Gosman text presents two computer codings that apply the method described. The program given in Gosman, Chapter 6, termed "The Combustion Program," was initially employed to analyze a two-dimensional single slot entry configuration. This configuration was 1.37 inches high with an air jet 0.050 inch high entering at the lower wall. The eddy viscosity expression given in the text was used.

A series of computer runs was conducted with this configuration to evaluate the program capability in its original form. Conclusions drawn from these runs were:

(a) Nonuniform grid size using solid-wall lower boundary caused nonconvergence. Various vorticity boundary conditions discussed in the Gosman text provided no improvement. Use of underrelaxation, laminar instead of turbulent viscosity, and restriction of the exit width all failed to produce convergence.

(b) Convergence could be obtained only when using a uniform grid or an axisymmetric case with a nonuniform grid.

Computer time per node per equation per iteration was about 7 milliseconds (subsequent modification to the program and use of an optimum computer compilation option reduced this value to about 3 milliseconds) on a CDC 6400 machine.

The flow pattern produced was dependent on the exit boundary condition, which specifies that gradients at the exit in the flow direction be zero so that the streamlines are parallel. The result is that the edge of a recirculation zone cannot

exist at the exit. It is therefore necessary to correctly select the location of the exit to preclude influence on the recirculation zone.

5.1.1.2 Modifications to the Cosman Program

Inclusion of two-phase flow effects of droplet and film evaporation in the Gosman primary-zone model was undertaken. The evaporating fuel produces a positive source of CH_x in the same manner as the global-rate expression produces a negative source (disappearance) of fuel. The rate of fuel evaporation computed from the fuel-insertion models is converted to a volumetric creation rate for each grid node. This value is then added to the source term for the fuel for a resultant net creation of fuel.

The program was also revised to allow mass addition at other points on the boundary to provide for fuel evaporation off the walls and account for recirculating flow from air-blast pipes or impinging secondary or dilution air jets. Fuel vaporization rates are specified by assuming a flow velocity at the boundary that produces the desired mass flow. For impinging side-wall air jets, the recirculating flow input to the program is calculated from a method by Verduzio and Companaro[38] discussed later in this section (paragraph 5.1.1.4).

An extension of the computation to include combustion rate kinetics was required for combustion efficiency predictions. A simple two-step global kinetic scheme was preferred to an extensive chain mechanism scheme due to computer time limitations and intractability of the model.

The global reaction rate expressions reported by Williams et al[39] for the methane oxidation mechanism as given by

$$CH_4 + \frac{3}{2} O_2 \longrightarrow CO + 2H_2O \qquad (39)$$

$$CO + \frac{1}{2} O_2 \longrightarrow CO_2 \qquad (40)$$

were converted to the English System [foot-pound-second (FPS)] used in the Gosman program, and are given by

$$R_{CH_4} = -3.5 \times 10^5 \rho^2 \exp[-51629/T] m_{CH_4} \sqrt{m_{O_2} \cdot m_{H_2O}} \qquad (41)$$

and for carbon monoxide

$$R_{CO} = -1.2 \times 10^{10} \rho^2 \exp[-22647/T] m_{CO} \sqrt{m_{O_2} \cdot m_{H_2O}} \qquad (42)$$

where R = rate of species creation, lb per sec per cu ft

ρ = mixture density, lb per cu ft

m = species mass fraction

Species conservation must be applied to the species CH_4, CO, O_2, N_2, and H_2O. From Equation (39) on a mass basis,

$$R_{CH_4} = \frac{1}{3} R_{O_2} = -\frac{4}{9} R_{H_2O} = -\frac{4}{7} R_{CO} \qquad (43)$$

and from Equation (40),

$$R_{CO} = \frac{7}{4} R_{O_2} = -\frac{7}{11} R_{CO_2} \qquad (44)$$

The net creation of CO is

$$R_{CO_{net}} = -\frac{7}{4} R_{CH_4} - \frac{7}{11} R_{CO_2} \qquad (45)$$

The equality of reaction rates allows the combination of species conservation equations to eliminate source terms for three of the species conservation equations. Selecting CH_4 and CO_2 as the species for which rates will be used, the following transformed variables of H_2O, O_2 and CO generalized for CH_x fuel instead of methane are defined.

$$\phi_{H_2O} = m_{H_2O} + B\, m_{CH_x} \qquad (46)$$

$$\phi_{O_2} = m_{O_2} - A\, m_{CH_x} + \frac{4}{11} m_{CO_2} \qquad (47)$$

$$\phi_{CO_2} = m_{CO} + C\, m_{CH_x} + \frac{7}{11} m_{CO_2} \qquad (48)$$

where $A = \frac{32}{N}\left(\frac{1}{2} + \frac{X}{4}\right)$

$B = \frac{18.016X}{N}$

$C = \frac{28.01}{N}$

$N = 12.01 + 1.008X$

This results in three identical species conservation equations which have no source term and have to satisfy identical boundary conditions. Therefore, only one of them needs to be solved.

For a premixed fuel-air mixture, however, the solution of these equations is ϕ = constant.

Equation (41) for methane fuel was inserted in the Gosman program. Initial computations with a two-dimensional primary-zone subelement model with stoichiometric premixed mixture did not result in any appreciable reaction at inlet temperatures of 538° and 1260°R. At 538°R, $R_{CH_4}/\rho^2 m_{CH_4}\sqrt{m_{O_2} \cdot m_{H_2O}}$ rate is of the order of 10^{-26} seconds $^{-1}$, because of the high activation energy. It was found necessary to, in effect, light off the reaction by allowing the computation to iterate until the recirculation zone was formed and then impose an increased temperature, usually 4000°R, to initiate the reaction over a few iteration cycles. When this condition was removed, the computation then converged to a sustained combustion condition. Following this work, equations for both reactions were successfully implemented.

5.1.1.3 Comparison With Well-Stirred Reactor

A series of program computations was conducted with a two-dimensional primary-zone model with the use of an 8 x 8 non-uniform grid as a preliminary assessment of the effect of various loading conditions on the computed combustion efficiency.

Computations were performed for inlet temperatures of 538°, 900°, and 1260°R and pressures of 1.0 atmosphere and 0.37 atmosphere (which is combustor inlet pressure during the engine start cycle at 25,000 ft altitude), and inlet velocity was adjusted to cover a range of loading parameters. A premixed stoichiometric mixture was used and calculations were performed with adiabatic wall temperature boundary conditions.

A temperature rise of 4000°R was imposed during the 11th through the 14th iteration. This was sufficient to produce complete reaction of fuel and CO. After this temperature superposition was dropped, the iteration proceeded either to converge on a stable burning solution or to die out toward the original inlet temperature for loadings beyond blowout.

With increased loading the efficiency dropped gradually, then experienced sharp reductions when the cold inlet flow penetrated to the exit. Blowout finally occurs when the recirculation zone no longer provides sufficient energy to ignite the incoming mixture before it reaches the exit. These results were compared with stirred-reactor computations by Herbert[40] and with actual combustor data.

Figure 47 shows the results plotted as a function of Herbert's loading parameter, most commonly used for stirred reactors. Herbert's stirred reactor computations are also shown. At low loadings the primary-zone subelement model shows a faster rate of efficiency decrease, and blowout occurs at much lower loadings than for the stirred reactor. Q_1 is defined by

$$Q_1 = \frac{W}{VP^2} = K \exp(-E/RT_r) f(\text{composition, efficiency}) \quad (49)$$

T_r = reaction temperature

K = constant

V = reaction volume

Figure 48 shows the results versus Q_2, where Q_2 is defined by

$$Q_2 = \frac{W}{VP^2 \exp(T_1/n)} \quad (50)$$

where n = f (fuel-air ratio)

The gradual decay portions of the efficiency curves are brought together to a single line, but the drop-off is not correlated.

Data plotted as a function of the empirical loading parameter

$$Q_3 = \frac{W}{VP^2 \sqrt{T}} \quad (51)$$

is shown in Figure 49, together with two typical combustor empirical curves. The primary-zone subelement data falls

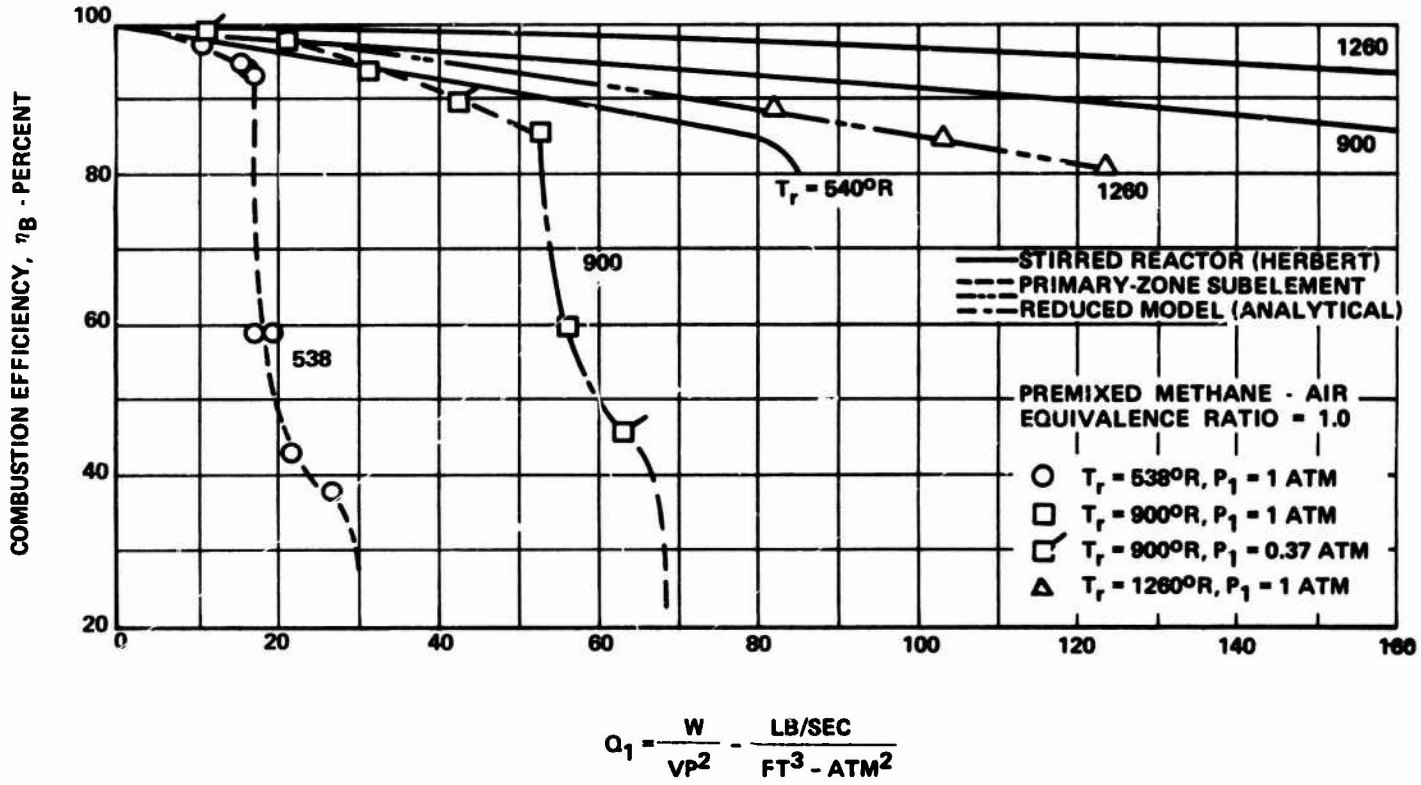


Figure 47. Primary-Zone Subelement Reduced Model Efficiency Versus Herbert's Loading Parameter.

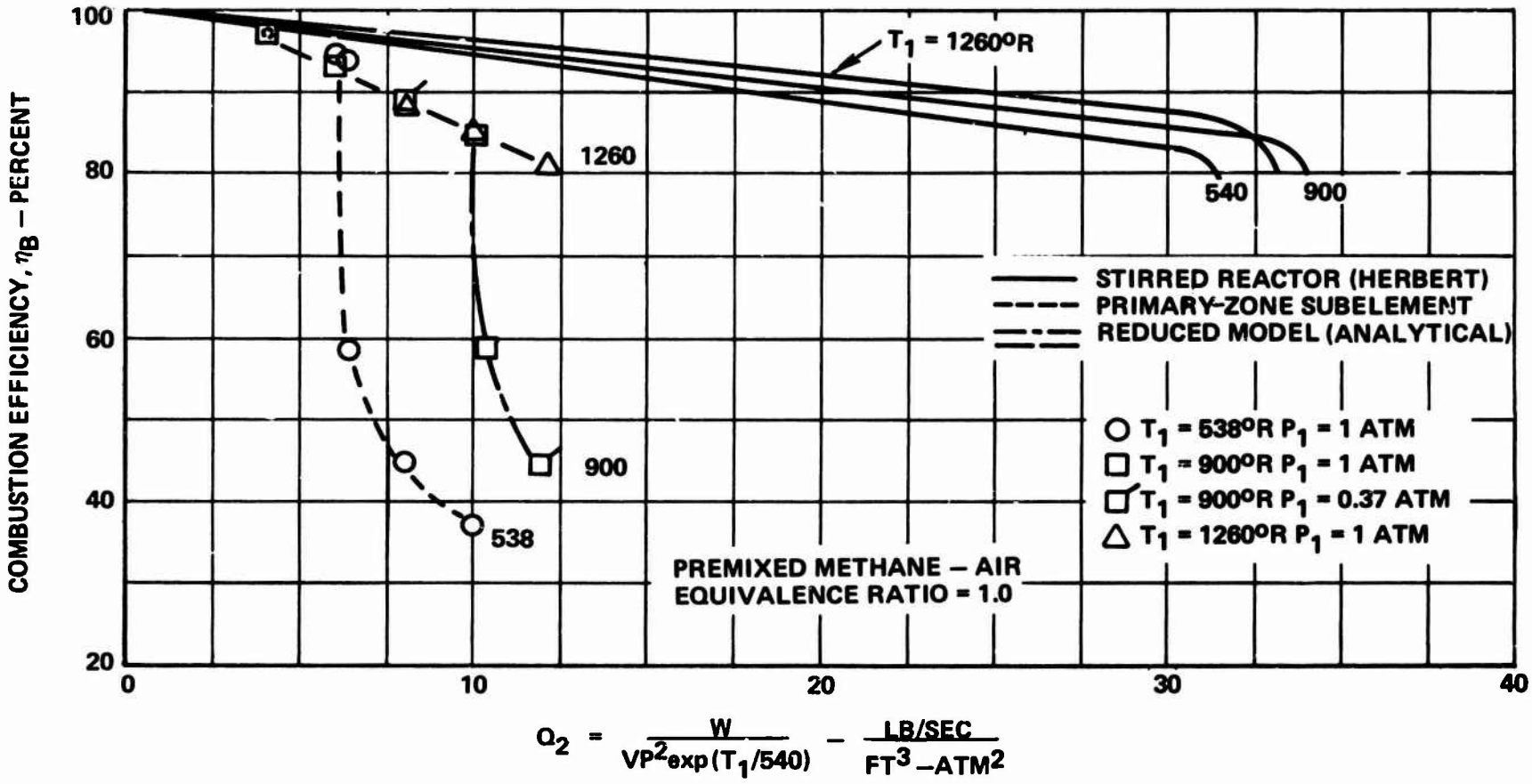


Figure 48. Primary-Zone Subelement Reduced Model Efficiency Versus Herbert's Loading Parameter.

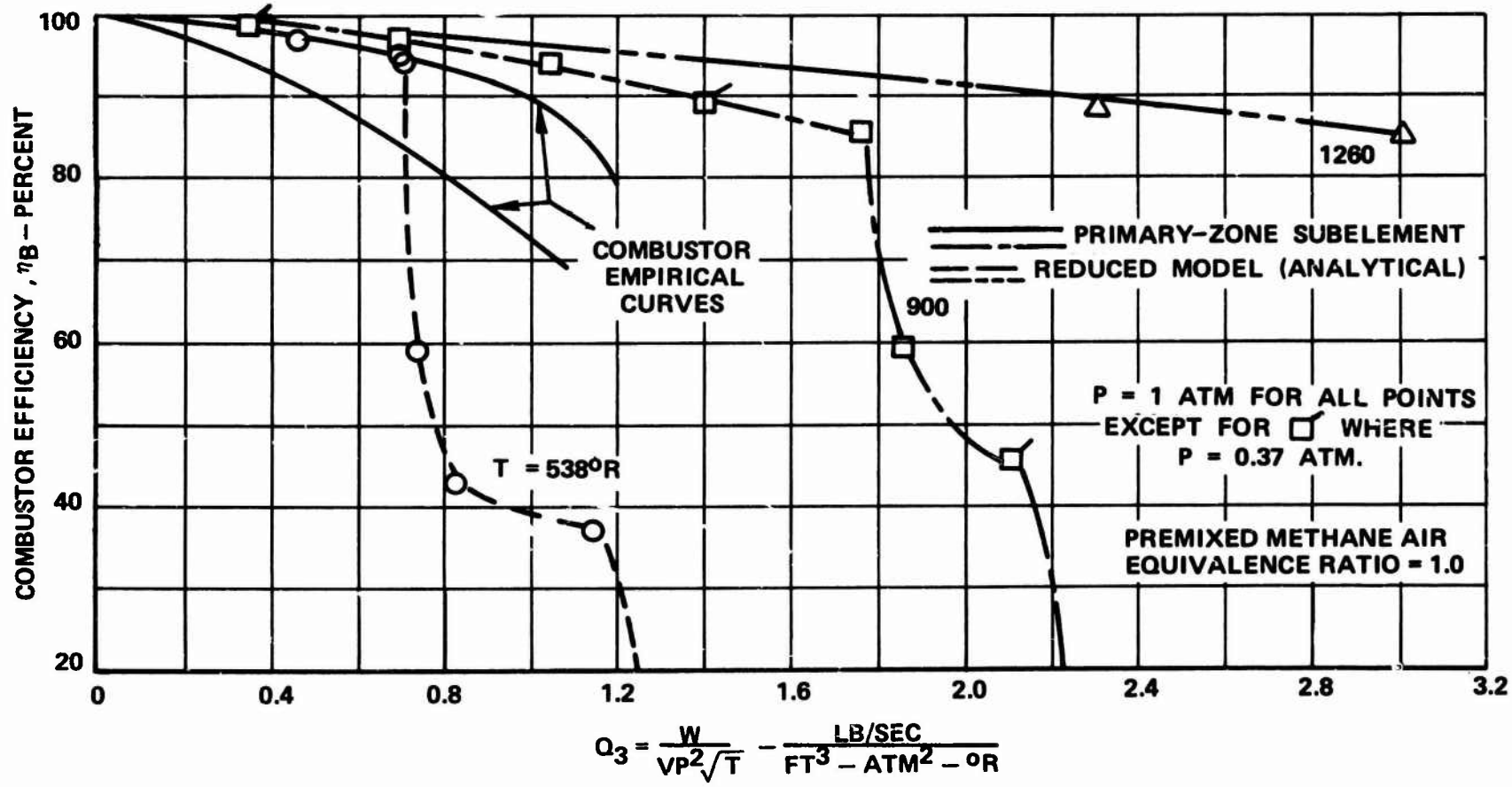


Figure 49. Primary-Zone Subelement Reduced Model Efficiency Versus Empirical Loading Parameter.

above the combustor experimental data and does not appear to be correlated as well as with parameter Q_2. Q_2 has been employed to correlate combustor data, and frequently the pressure is raised to the 1.75 or 1.8 power instead of 2.0. This difference is attributed to the effects of mixing and overall reaction order being less than 2. The primary-zone subelement reduced-model data correlated directly with P^2 since the global rates include the square of the density. It is concluded that the combustion efficiency calculation is reasonable and, within the framework of a very simple flow model, consistent with both stirred reactors as an upper-limit extreme and with practical combustors.

5.1.1.4 Impinging Jet Recirculation

The Gosman program cannot handle the inherently three-dimensional problem of multiple-jet injection and recirculation that results from jet impingement as depicted in Figure 50. A method presented by Verduzio and Campanaro[38] was used to provide information on recirculation ratios. As this reference is not generally available, a complete derivation is given in the following paragraphs. The results of this analysis provide a means for calculating recirculating flow and for optimizing the primary orifices to obtain maximum recirculation. The computer program prepared for this analysis is presented in Appendix V.

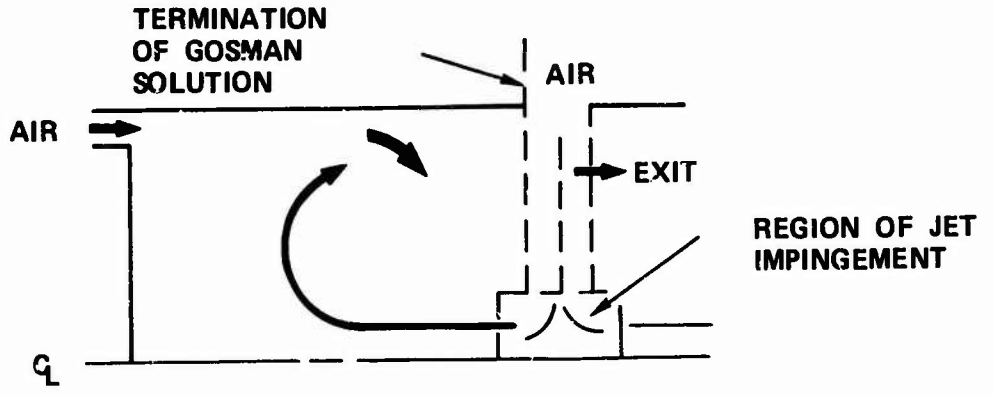


Figure 50. Jet Impingement Schematic.

The model used by Verduzio and Campanaro is depicted in Figure 51, showing the primary zone of a tubular combustor. The region of jet impingement at the centerline is considered as a control volume.

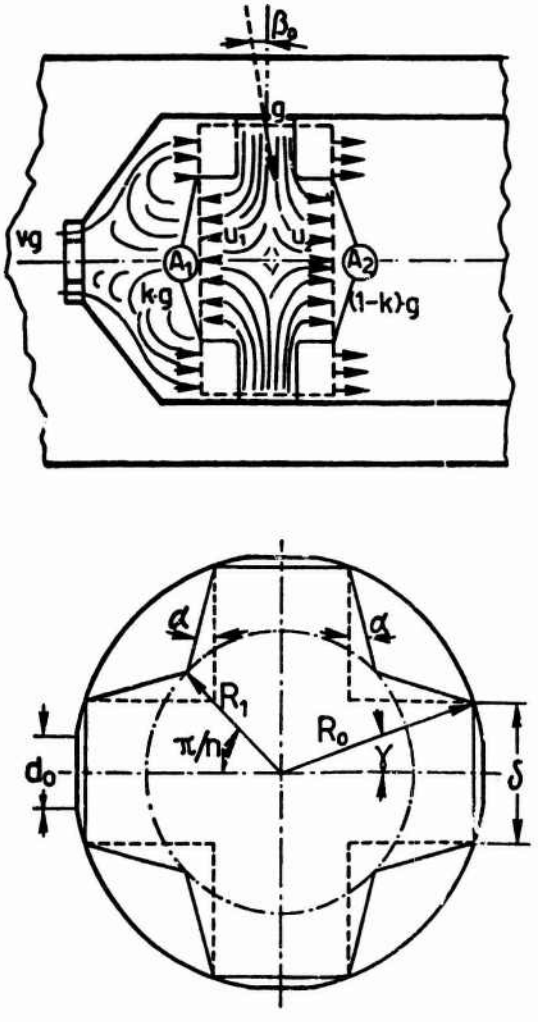


Figure 51. Recirculation Model.

A momentum balance equates the flow momentum to the pressure differential resulting from jet blockage.

$$-kgU_1 + (1-k)gU_2 - gU_F \sin \beta_o = g_c (P_1-P_2)A_o \qquad (52)$$

where g = mass flow through injection-jet holes

U_1 = velocity of upstream flow

U_2 = velocity of downstream flow

U_F = velocity of injection jets

k = fraction of g that flows upstream (recirculation ratio)

β_o = initial jet efflux angle

$P_1 - P_2$ = upstream to downstream pressure drop due to jet blockage

A_o = flame tube area

g_c = gravitational constant

This equation is applied over areas A_1 and A_2 equally and is defined as the circular area of total jet impingement shown inside radius R_1. From the model, the flow velocities can be expressed in terms of geometry by continuity relations

$$U_1 = \frac{kg}{\rho_o A_1} \qquad U_2 = \frac{(1-k)g}{\rho_o A_2} \qquad U_F = \frac{4g}{\rho_o n\pi d_o^2 \cos\beta_o}$$

The momentum equation can be solved for k with the use of these continuity relations:

$$k = \frac{1}{2}\left[1 - \frac{4A_1 \tan\beta_o}{n\pi d_o^2} - \frac{g_c \rho_o A_o A_1}{g^2} (P_1-P_2)\right] \qquad (53)$$

where d_o = injection orifice diameter

ρ_o = injected air density

n = number of holes

This relation can be solved if A_1 and P_1-P_2 are known. From the geometry, the circular A_1 is expressed in terms of parameter $B_i = R_1/R_0$.

$$B_i = \frac{\frac{\delta}{2R_o} + \tan\alpha \cos\gamma}{\sin\frac{\pi}{n} + \tan\alpha \cos\gamma} \tag{54}$$

where δ = effective jet width at the orifice greater than d_o due to jet distortion

α = angle of jet spreading

γ = angle defined by geometry = arc sin $\frac{\delta}{2R_0}$

$$\cos\gamma = \sqrt{1 - \left(\frac{\delta}{2R_0}\right)^2} \tag{55}$$

The factor α can be taken as 0.1 for most cases of jet spreading. Verduzio and Campanaro derive an approximate expression for δ given as

$$\delta = d_o \left[1 + \frac{F}{n^2} \cos^2\beta_o\right] \tag{56}$$

The factor $F \cos^2\beta_o$ is given as a function of β_o that can be approximated by a linear relationship

$$F \cos^2\beta_o = 16 - 0.4\ \beta_o \tag{57}$$

where $\beta_o = 0$ (normal injection)

$n = 4$

$\delta = 2\ d_o$

This is similar to the value of initial jet distortion developed in the dilution-zone analysis where $\delta = h$. From the above relationships, values of B_i can be calculated to obtain the value of A_1 required in the equation for k.

The pressure drop is calculated by assuming that the primary-zone exit flow experiences a sudden expansion loss when flowing past the injection jets. The conventional expression for expansion loss is

$$P_1 - P_2 = \frac{\rho_r}{2g_c} (U_R - U_3)^2 \tag{58}$$

where ρ_r = hot gas density

U_R = hot gas velocity between jets

U_3 = hot gas velocity downstream of the jets in the annular area between A_0 and A_2

Introducing continuity relations for the velocities

$$U_R = \frac{g_r}{\rho_r A_r} \qquad U_3 = \frac{g_r}{\rho_r A_3} \tag{59}$$

the pressure drop becomes

$$P_1 - P_2 = \frac{g_r^2}{2g_c \rho_r A_3^2} \left(\frac{A_3}{A_r} - 1 \right)^2 \tag{60}$$

where $A_3 = A_o - A_1 = A_o (1 - B_i^2)$

$A_r = A_o - A_1 - nA_j = A_o (1 - B_i^2) - nA_i$

A_i = blockage area of a jet

The hot gas flow rate, g_r, is the total primary-zone exit flow

$$g_r = (k + V)(1 + f_p)g \tag{61}$$

where V = ratio of flow through dome to flow, g, through holes

f_p = primary-zone fuel-air mass ratio

The pressure drop becomes

$$P_1 - P_2 = \frac{(k+V)^2(1+f)^2 g^2}{2g_c \rho_r A_o^2 (1-B_i^2)^2} \left(\frac{A_3}{A_r} - 1 \right)^2 \tag{62}$$

An expression for A_3/A_r is required to solve this equation. Verduzio and Campanaro[r] give, without derivation, the following relation apparently obtained from the geometry:

$$\frac{A_3}{A_r} = \frac{1}{\left[1 - \frac{nA_i}{A_o(1-B_i^2)}\right]} = \frac{1 - B_i^2}{1 - \frac{n}{\pi}\left[\arcsin \frac{\delta}{2R_o} + B_i \sin \left(\frac{\pi}{n} - \gamma\right)\right]} \tag{63}$$

This completes all the information required to solve for k.

Inserting the pressure-drop equation into the momentum balance equation for k,

$$k = \frac{1}{2}\left[1 - \frac{4A_o B_i^2 \tan\beta_o}{n\pi d_o^2} - \frac{\rho_o}{\rho_r} \cdot \frac{(k+V)^2(1-f)^2 B_i}{2(1-B_i^2)^2}\left(\frac{A_3}{A_r} - 1\right)^2\right]$$

Expanding the $(k + V)^2$ term and letting $\tau = \frac{\rho_o}{\rho_r}$

$$C_1 = \frac{1}{2}\left[1 - \frac{4A_o B_i^2 \tan\beta_o}{2\pi d_o^2}\right]$$

$$C_2 = \tau \frac{(1+f)^2 B_i^2}{4(1-B_i^2)^2}\left(\frac{A_3}{A_r} - 1\right)^2$$

the following is obtained

$$k = C_1 - C_2 (k^2 + 2kV + V^2)$$

Rearranging as a quadratic equation,

$$k^2 + 2\left(V + \frac{1}{2C_2}\right)k + \left(V^2 - \frac{C_1}{C_2}\right) = 0$$

with the solution

$$k = -\left(V + \frac{1}{2C_2}\right) \pm \sqrt{\left(V + \frac{1}{2C_2}\right)^2 - \left(V^2 - \frac{C_1}{C_2}\right)} \qquad (64)$$

For the normal injection ($\tan \beta_c = 0$), no dome flow ($V = 0$), and no blockage ($P_1 - P_2 = 0$), a value for $k = C_1 = 0.5$ is obtained, verifying an equal upstream-to-downstream flow split of the impinging jets. Figure 52 shows results from Verduzio and Campanaro indicating the effect of B_i, V, and τ on recirculation ratio k. The effect of β_o on k is shown in Figure 53, illustrating the reduction in recirculation with increasing initial efflux angle.

For fixed values of combustor pressure drop, combustor diameter, and number of holes, the mass flow that is recirculated, g_r, is a function of orifice diameter, d_o:

$$g_r = kg$$

The factor k will decrease with d_o, but g will increase. This suggests that g_r will be a maximum for some given orifice diameter. Substituting into the above equation the continuity relation for jet flow,

$$g = \rho_o U_F A_n = \rho_o \sqrt{2g_c \frac{\Delta P_c}{\rho_o}} \left(\frac{n\pi d_o^2}{4}\right) \qquad (65)$$

where ΔP_c = combustor pressure drop,

then $g_r = k\sqrt{2g_c\rho_o\Delta P_c}\left(\frac{n\pi d_o^2}{4}\right)$

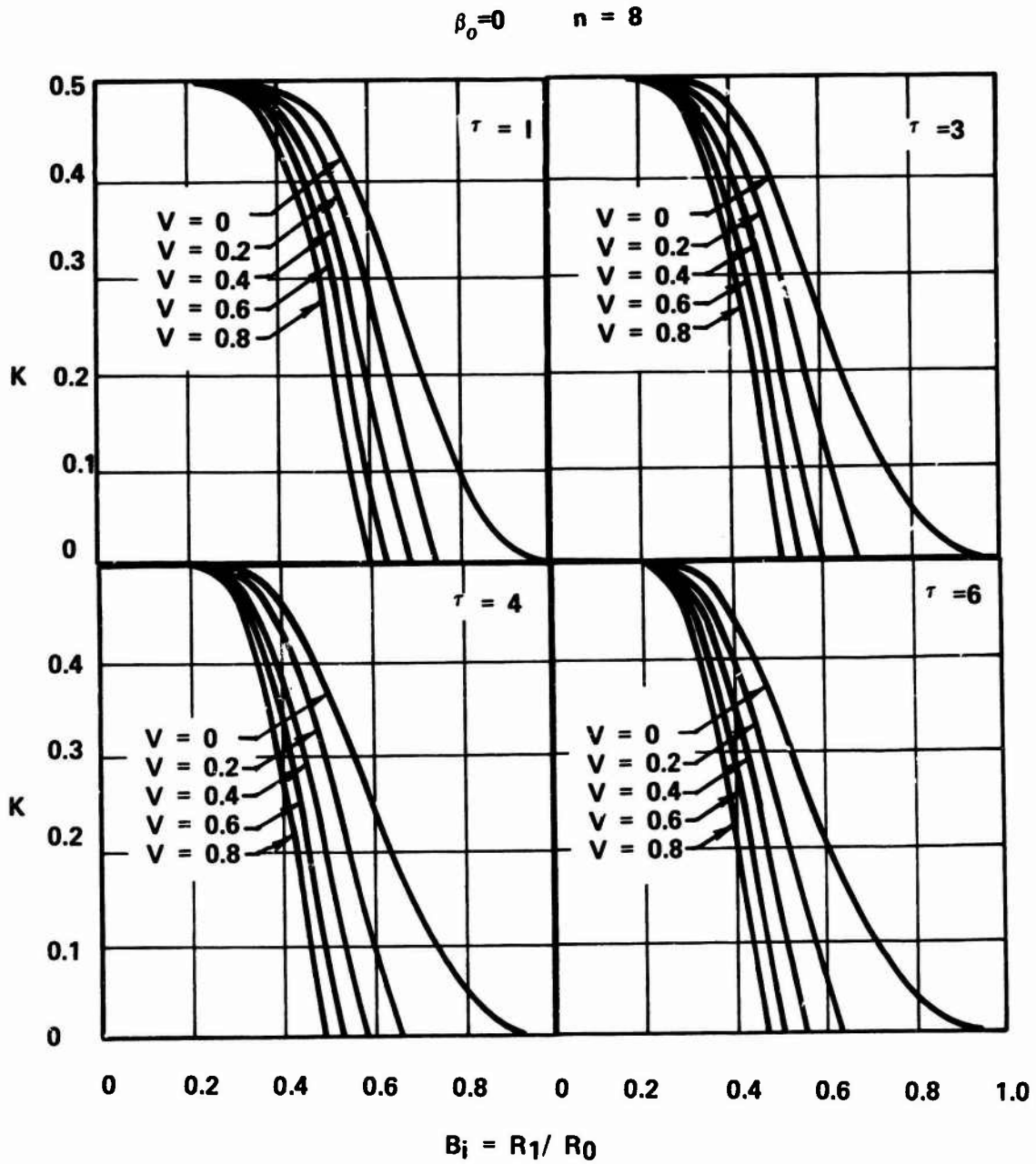


Figure 52. Recirculation Ratio as a Function of Radius Ratio, Temperature Rise, and Dome Flow for Normal Injection and Eight Holes.

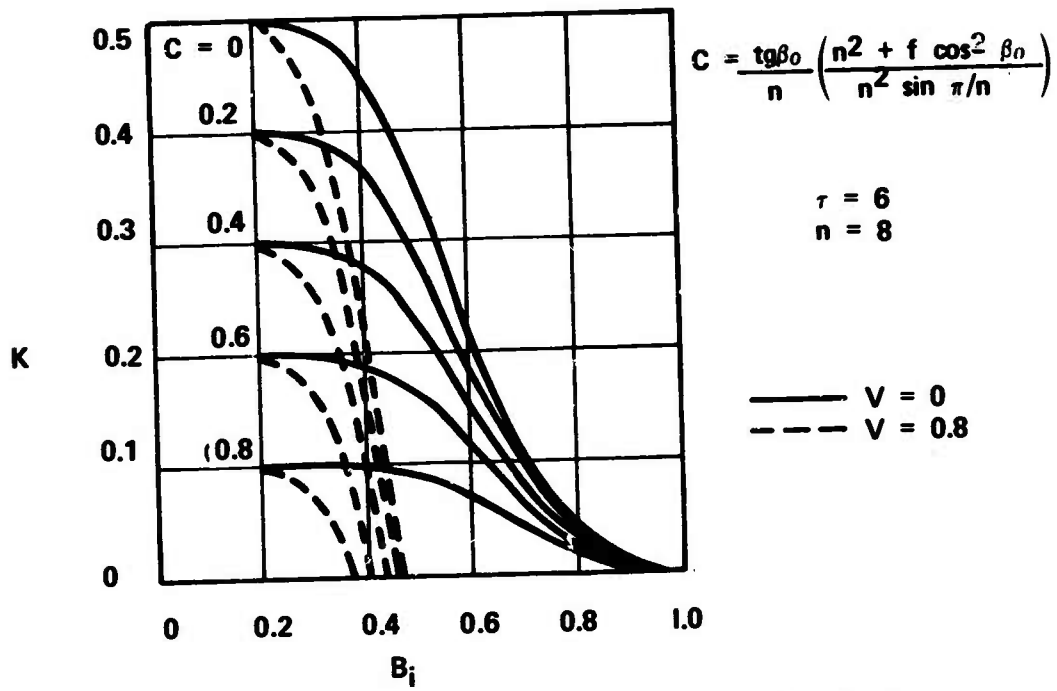


Figure 53. Effect of Jet Efflux Angle on Recirculation Ratio.

Inserting R_0^2 (combustor radius) and rearranging,

$$g_r = kn\pi \left(\frac{d_o}{2R_0}\right)^2 R_0^2 \sqrt{2g_c\rho_o\Delta P_c} \tag{66}$$

Let

$$E = \frac{g_r}{R_0^2\sqrt{2g_c\rho_o\Delta P_c}} = kn\pi\left(\frac{d_o}{2R_0}\right)^2 \tag{67}$$

This relation expresses g_r for fixed pressure drop and combustor diameter in terms of k, n, and $d_o/2R_0$.

Figure 54 shows this relationship and indicates that maximum recirculation is obtained with six holes at $d_o/2R_0 = 0.17$.

$$E = \frac{q_R}{C_e R_o \sqrt{2\rho\Delta p}}$$

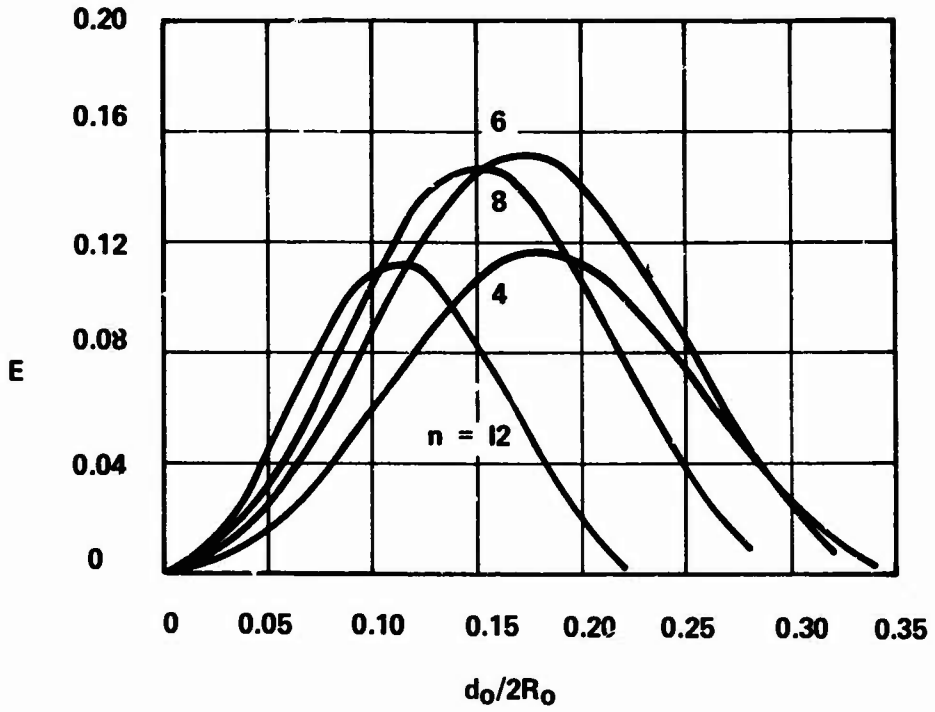


Figure 54. Recirculation Flow as a Function of Hole Diameter and Number of Holes.

Verduzio and Campanaro presented extensive test data that showed excellent agreement with their analysis for tubular combustors.

The preceding analysis was derived for tubular combustors. Application to annular combustors can be obtained by setting the radius R_0 equal to one-half the annular combustor width, equating the number of holes, n, to 2, and deriving a relationship for blockage area A_r in terms of the circumferential spacing between orifices.

5.1.2 Element Tests

Experimental validation of the two-dimensional primary-zone model was obtained by means of

- Plexiglas two-dimensional primary-zone water rig
- Plexiglas two-dimensional primary-zone airflow rig
- Two-dimensional primary-zone combustion rig
- Three-nozzle sector primary-zone combustion rig

5.1.2.1 Primary-Zone Element Water Rig Description

Five Plexiglas primary-zone models were tested in the water flow rig to provide visual (photographic) observation of flow patterns and velocity information for comparison with analytical flow-field calculations. A flow schematic of the water rig installation is shown in Figure 55. Figure 56 shows a typical test section and inlet and outlet transition sections.

To obtain the necessary visibility, the test sections were double the size of the two-dimensional hot section and mounted vertically in the rig. Since the models have wall boundaries, similarity considerations are limited to the local Reynolds numbers, with a 26:1 reduction in velocity required for water replacing air. Reynolds numbers greater than 10^4 were maintained, so that combustion effect considerations and the strict Reynolds numbers similarity requirement could be relaxed.

Polystyrene spheres of 0.C02-inch diameter and a density approximately the same as water were used for flow visualization.

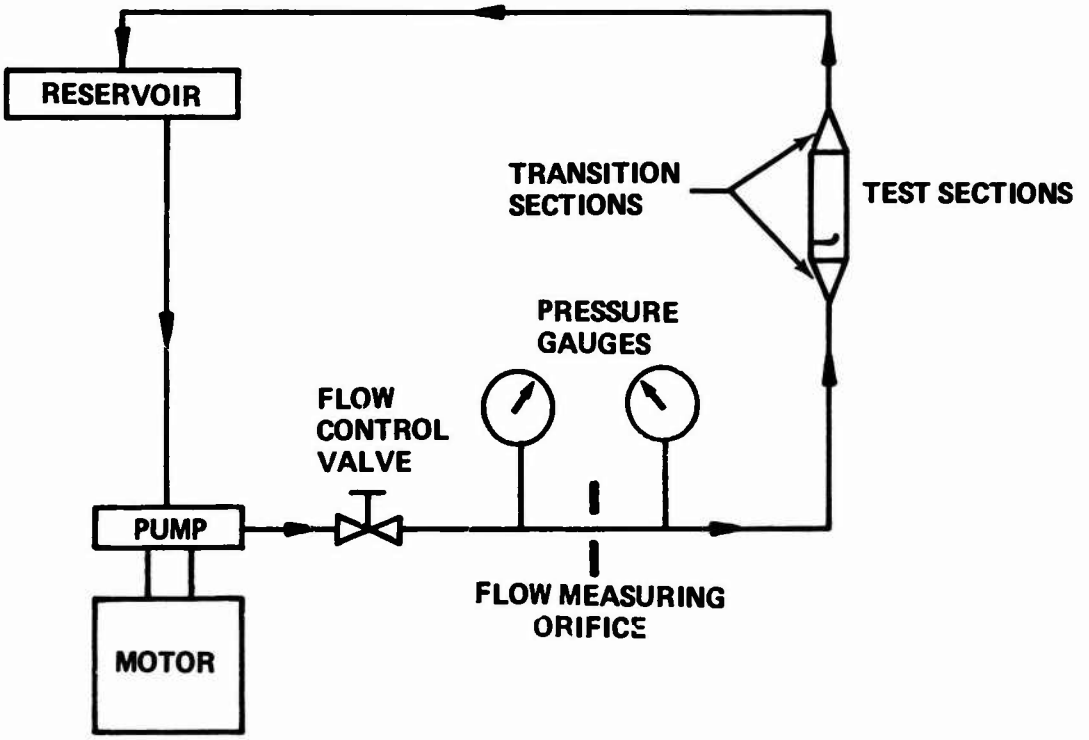


Figure 55. Primary-Zone Water Flow Rig Schematic.

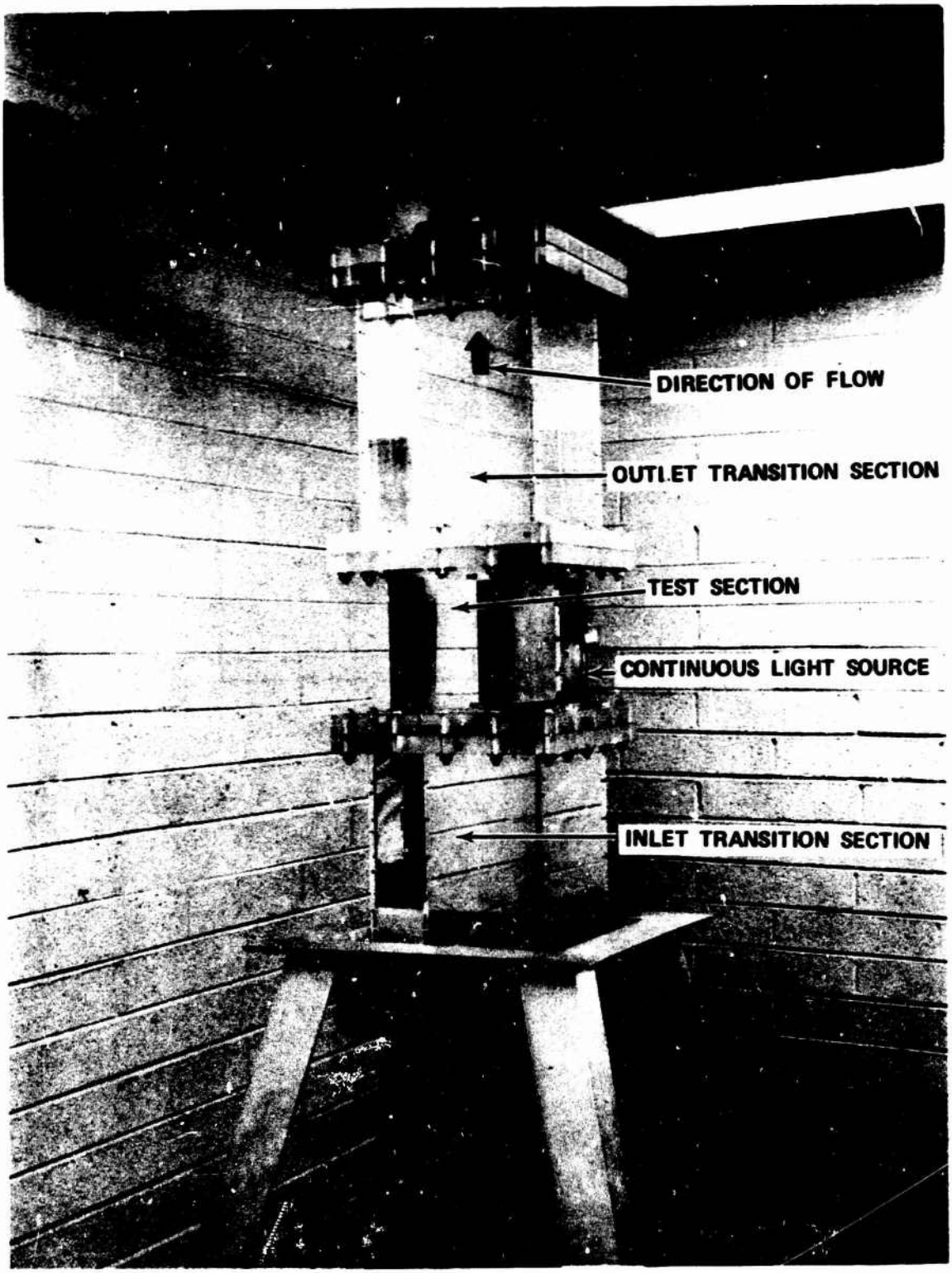


Figure 56. General View of Water Analog Test Section.

Other test hardware included:

- o Orifice plates and pressure gauges for flow measurement
- o A mesh screen in the inlet delivery plenum
- o A 1000-watt quartz lamp continuous light source
- o A double-slit lamp housing
- o A synchronized strobe light (2.5 milliseconds duration)
- o Moving and still picture cameras
- o Five test sections

5.1.2.1.1 Test Procedure

The five primary-zone configurations tested were:

- o Two-dimensional, single-entry subelement
- o Two-dimensional, three-nozzle, double-entry, air-assist injector system
- o Two-dimensional, three-nozzle, double-entry, L-pipe injector system
- o Two-dimensional, three-nozzle, double-entry, pneumatic-impact injector system
- o Two-dimensional, three-swirler, double-entry system

A cross section of the single-entry test section is illustrated in Figure 57. Tests showed that both the continuous light source and the synchronized strobe light were required to provide quantitative data for flow-field velocity evaluation. The continuous source and slit system were placed at one end of the test section, and the strobe light with a slit in the same plane as the continuous source was placed at the other side of the test section. The strobe flash was connected to the camera shutter, and this resulted in a bright streak of light showing the distance covered by the particles in the first 2.5 milliseconds of exposure time, followed by a less-intense light streak caused by the continuous source for the remainder of the time the shutter is open. This technique enabled the direction and velocity of the particles to be determined even in the case of slow-moving particles. Air

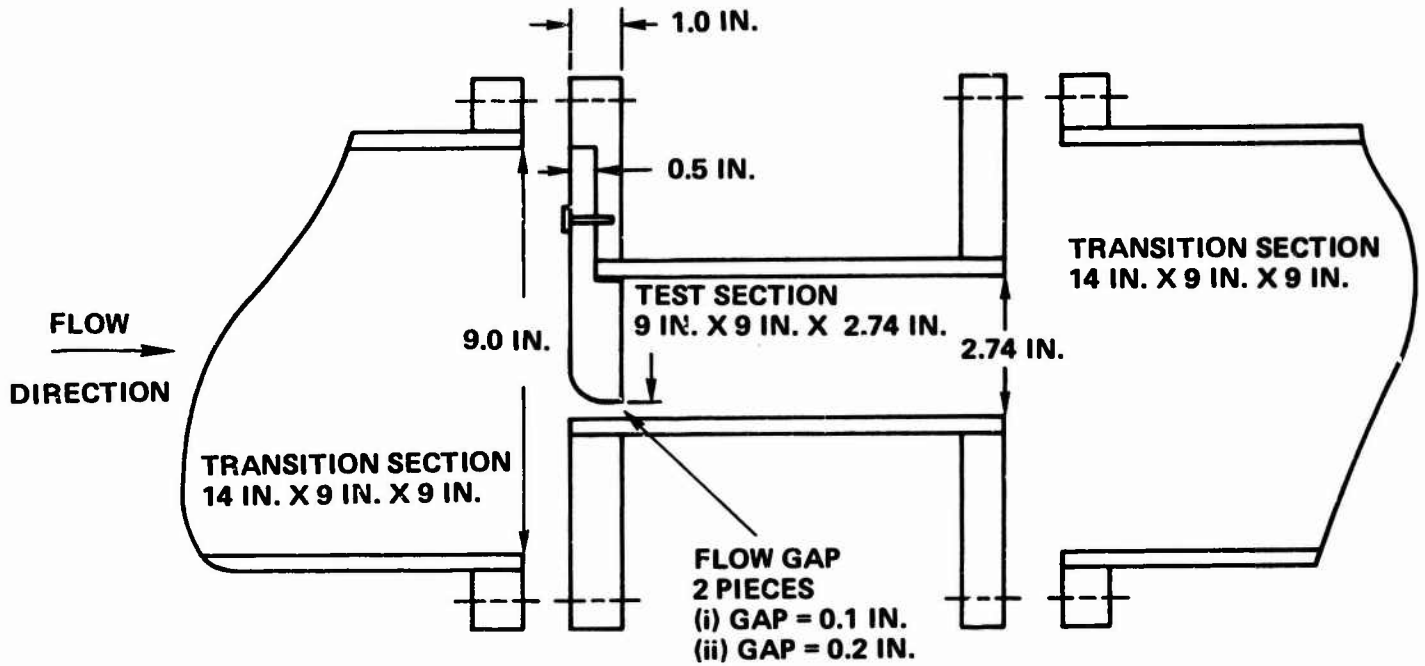


Figure 57. Two-Dimensional Primary-Zone Subelement Model.

velocities at the flow gap were simulated over the range of 100 to 400 feet per second. The tests indicated unstable flow in the primary zone, and as a result the primary-zone recirculation pattern would frequently be disrupted by interactions with the outlet transition section. For this reason longer test sections were fabricated for the other four configurations.

5.1.2.1.2 Eddy Viscosity Correlation

The primary-zone model was applied to the water model to study the effect of using different numerical values for eddy viscosity with a water inlet velocity of 10 feet per second. With a turbulent eddy viscosity of 1.096 pound per second per foot, which is 2500 times the molecular viscosity of water, the calculation produced a small recirculation zone with very rapid spreading of the jet. Reduction by a factor of 10 in the viscosity to 0.1096 caused the jet to no longer expand to the full width of the duct, and a large recirculation zone was formed with some reverse flow at the exit. A further reduction to 0.01096 brought the jet down near to the lower wall, and a small secondary recirculation zone was observed in the upper left-hand corner. This calculation agreed qualitatively with the flow pattern observed in the water model, as shown in Figure 58.

The necessity for arbitrary adjustment of the turbulent eddy viscosity to obtain satisfactory correlation with the experimental data indicated that a more universal procedure was required. Work by Spalding[41] and others has shown that the Prandtl-Komolgorov hypothesis would provide such a solution. This hypothesis states that the eddy viscosity is related to the kinetic energy of turbulent fluctuations by the relation

$$\mu_{eff} = 0.22\, k^{1/2}\, \rho \ell \qquad (67)$$

where μ_{eff} = turbulent eddy viscosity

k = turbulent kinetic energy

ℓ = length scale of turbulence

The implication of Equation (67) is that the turbulent Reynolds number asymptotically approaches a constant value. That is,

$$Rn = \frac{Vd\rho}{\mu} \rightarrow \frac{k^{1/2}\ell\rho}{\mu_{eff}} = \text{constant} \qquad (68)$$



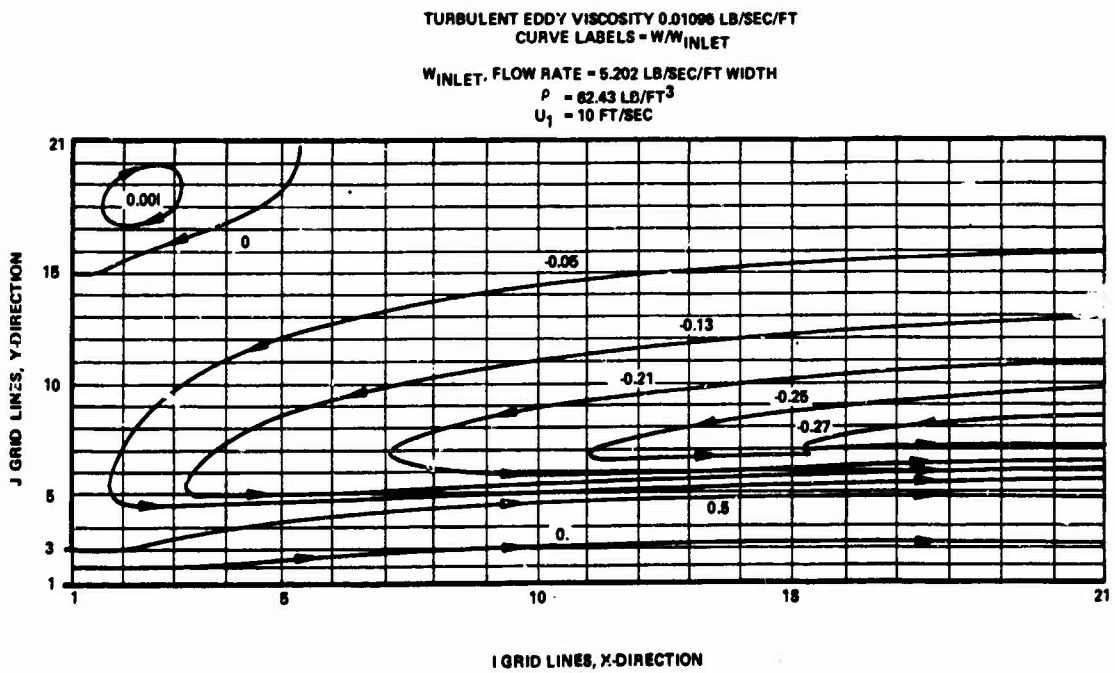


Figure 58. Water Model Flow Patterns.

To employ this concept fully, knowledge of the distribution of k and ℓ through the field is required. Transport equations for k and ℓ should be solved, but this would increase computation time and complexity beyond funding and schedule for this program. Wolfstein[42] employed the following relationship for turbulent kinetic energy from a jet with exit velocity (V).

$$k = 0.04\ V^2 \tag{69}$$

The length scale is generally expressed as 0.2 times the width of the mixing zone of a free jet. However, in the Gosman text, studies of mixing in film cooling flows indicated a length scale of 0.045 times slot width, outside the cooling film. Empirical relations, producing a decreasing length scale near the slot, were used within the film.

For the water model, the slot width was 0.1 inch, with a velocity at the slot of 10 feet per second. The turbulent eddy viscosity was calculated as

$$\mu_{eff} = 0.22\ k^{1/2}\ \rho\ell \tag{70}$$

$$= 0.22\ (0.2V)\,(62.43)\,(0.045s/12)$$

$$= 0.0103 \text{ lb per ft per sec}$$

This is within 6 percent of the value 0.01096 found by arbitrary adjustment. It was therefore decided that the above empirical relationship could be used for the turbulent kinetic energy formulation.

5.1.2.1.3 Double-Entry Rig Experiments

The four double-entry, two-dimensional test pieces were designed to use the same basic test section, with the separate fuel nozzle configurations being interchangeable in the section.

A sketch of the basic test section is shown in Figure 59. This section, with no additional hardware, was also used to simulate the air-assist system, as it was not anticipated that the relatively low flow of air-assist nozzles would have any effect on the mainstream flow field. Figure 60 shows the L-pipe and pneumatic-impact test pieces. The L-pipes were arranged such that a separate manifold could be used to deliver a measured flow directly to the injectors. Polystyrene tracer particles were also introduced into this flow. The effect of swirl was determined by replacing the inlet flow gap section with one containing three axial swirlers.

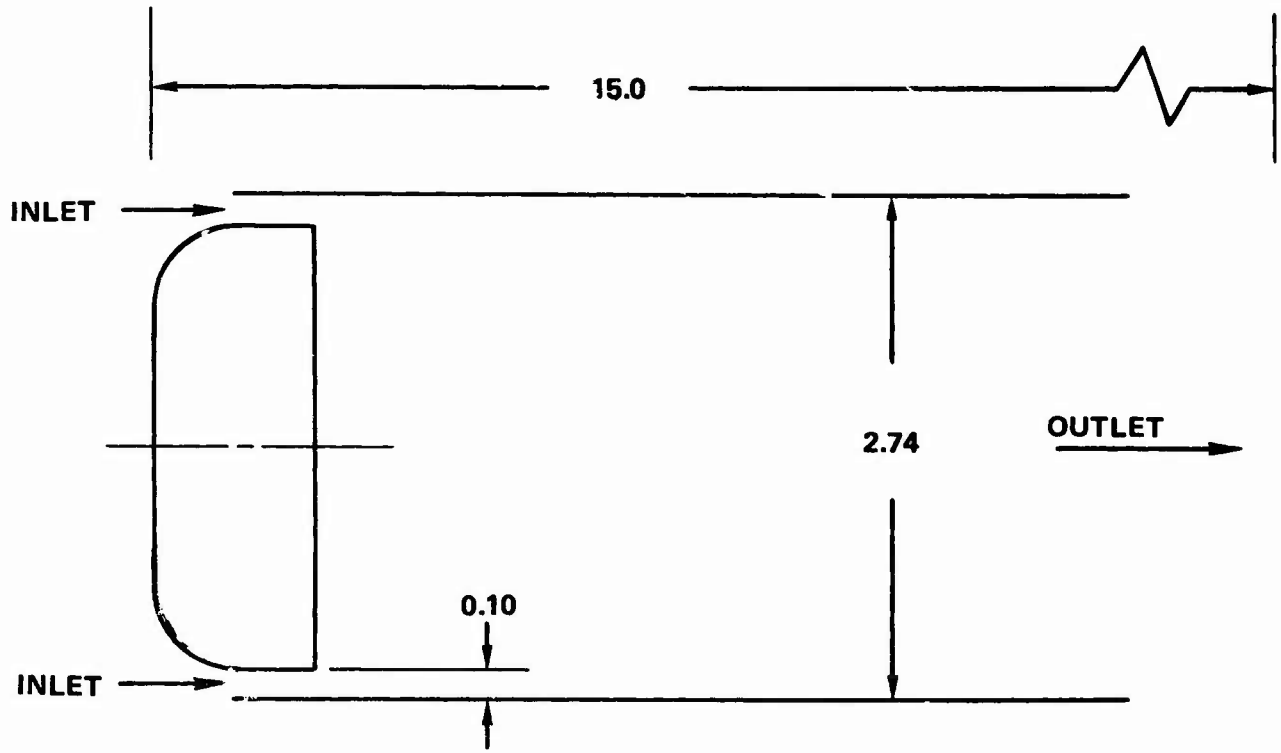
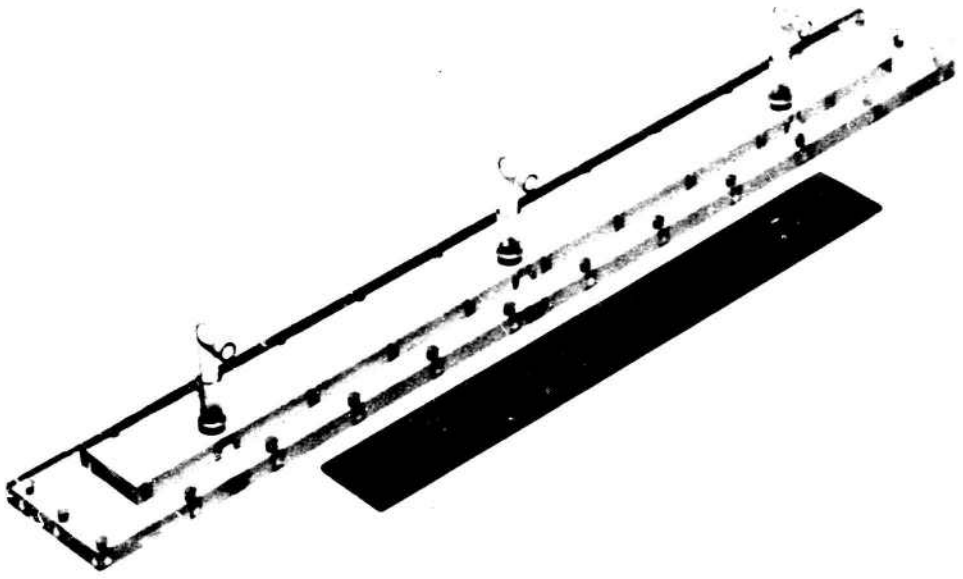
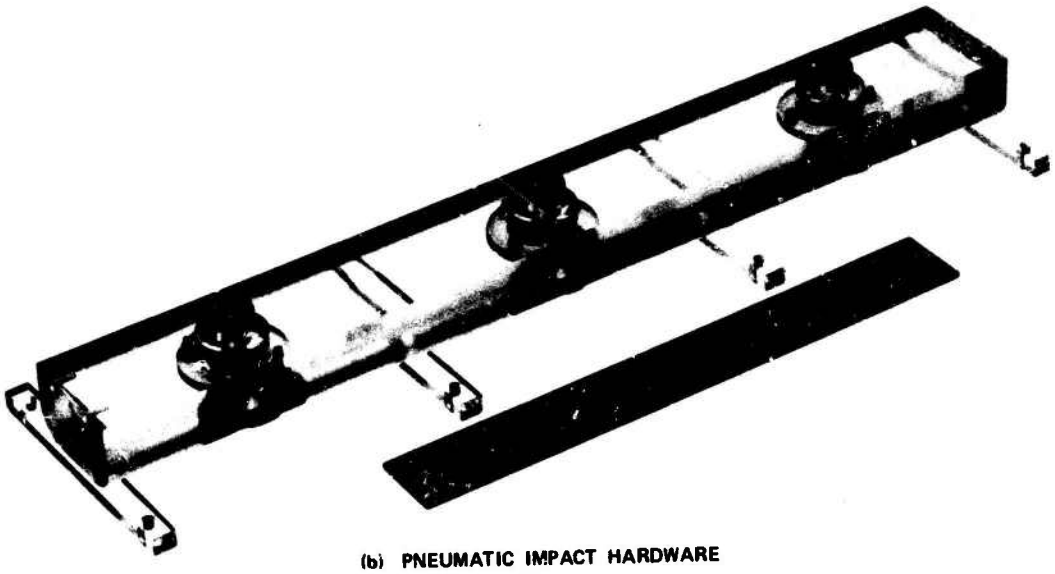


Figure 59. Water Model Basic Test Section, Double Entry.



(a) AIR BLAST (L-PIPE) INJECTOR HARDWARE



(b) PNEUMATIC IMPACT HARDWARE

Figure 60. Hardware for Water Model Rig.

Flow field data was recorded by means of both still and motion pictures. Velocities were determined from the movie film by tracing single-particle movement from frame to frame projected onto a white sheet. A series of particles was selected at random from the first frame, and the resultant paths were followed and drawn on the paper for each of the following frames until a trace of reasonable length was obtained, or until the particle moved out of the light beam. Figures 61 and 62 show typical flow field and velocity vector plots.

Some instability in the system was observed in all cases, but the flow patterns did not change significantly for the three types of fuel-insertion systems. A slight reduction in recirculation length was apparent, however, when the flow section containing the swirlers was used.

Recirculation length (h) was typically 60 times the flow gap height--i.e., approximately 6 inches for simulated air-gap velocities of 300 feet per second. A reduction of simulated inlet velocity to 150 feet per second appeared to reduce this length to approximately 5 inches.

One peculiarity of the flow was the tendency in many cases for the flow from one wall slot to traverse the full length of the model while the flow from another inlet jet stopped at the end of the recirculation zone, separated, and was entrained into the recirculation zone. A schematic of this single-sided recirculation and the double-sided recirculation is shown in Figure 63.

5.1.2.1.4 Analytical Prediction

A 21-by-21 nonuniform grid was used to cover the 2.74-inch-wide by 15-inch-long test section. Because of the nonsymmetry in the observed flow patterns, the entire flow section was calculated rather than a symmetric solution on one half of the last section. A nonuniform grid was necessary in order to accurately model the critical regions near the inlets. It was found that convergence could be obtained with nonuniform grid spacing when the eddy viscosity relations developed for turbulent flow were used.

The length scale previously used was 0.045 times the film slot width. The work of Kacker and Whitelaw[43] solving for turbulence kinetic energy with an empirical length scale distribution gave some insight into the required distribution. The basic results from Kacker and Whitelaw were that the mixing length increases with the distance from the inlet slot in the



Figure 61. Typical Water-Model Flow Pattern.

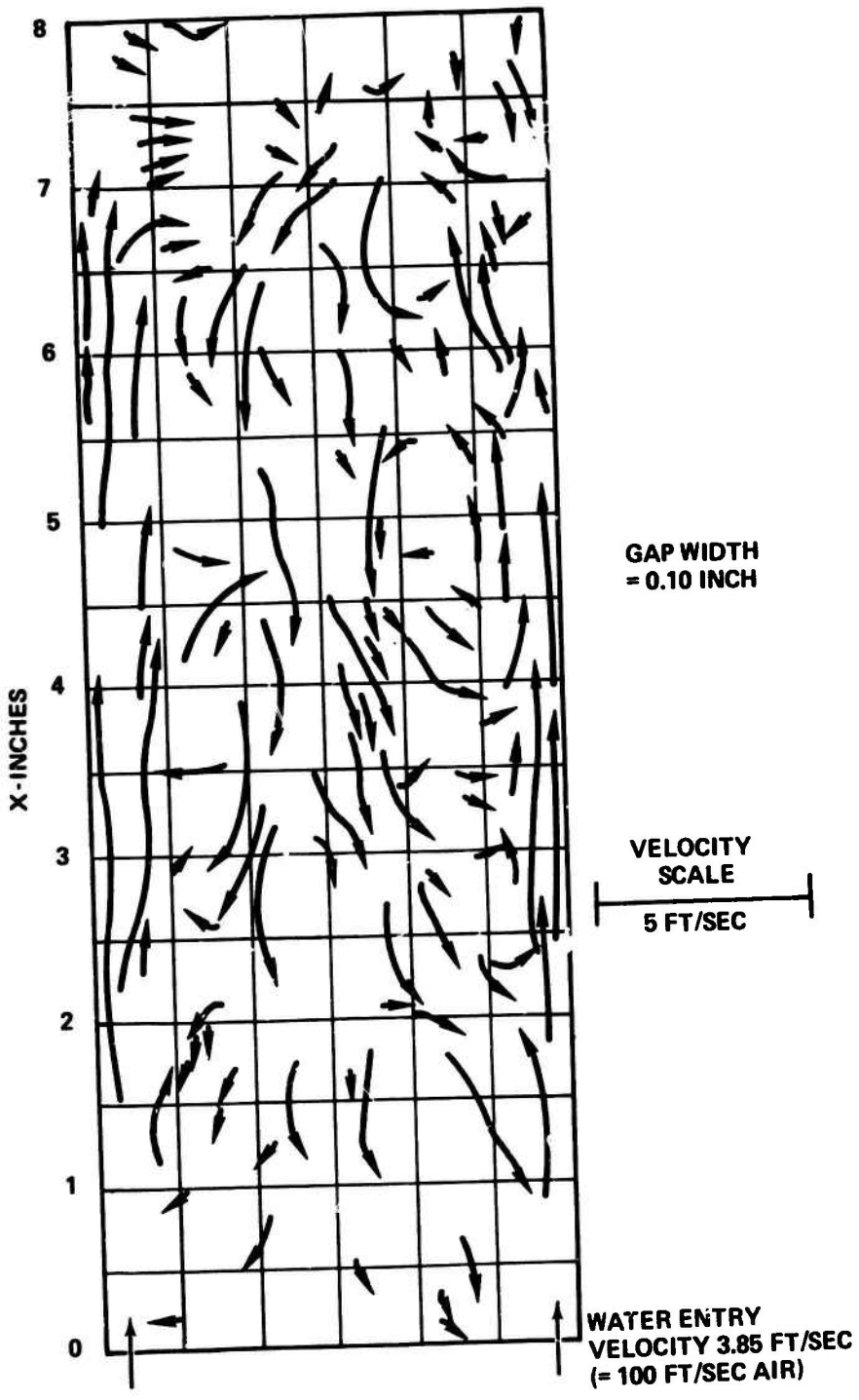


Figure 62. Velocity Vector Plot for Air-Assist Nozzle Primary Zone.

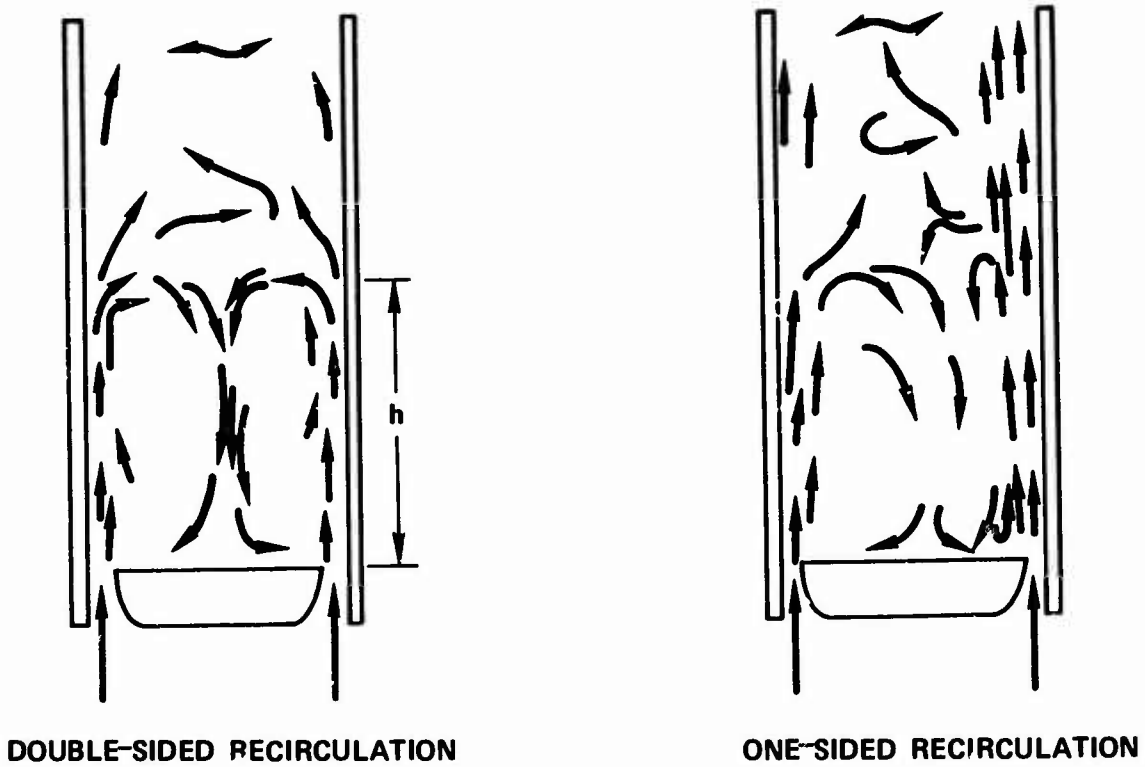


Figure 63. Typical Water-Model Flow Pattern.

downstream direction and with cross-stream distance away from the wall. Accordingly, the following relation was included for mixing length in the computations:

$$\ell = a(b + x/s)y \qquad (71)$$

where a = constant = 0.005 to 0.01

b = constant = 10 to 15

x = downstream distance from slot

s = slot width

y = cross-stream distance from wall

The ratio, x/s, is limited to a maximum between 10 and 20, and the constants, a and b, are functions of slot lip-width to slot-flow-width ratio and account for separated regions at the slot lip. The above assumptions cause the eddy viscosity to be low near the walls and higher in the free turbulent flow regions. Computations conducted to simulate 100 feet per second and 300 feet per second air inlet velocity at the slot (i.e., 3.84 and 10 feet per second water slot velocity) predicted recirculation zone lengths of 4.0 and 6.5 inches, respectively, with the main recirculation zone consisting of two unsymmetrical vortices. This is shown in Figure 64. Figure 65 shows the predicted axial velocity profiles in the cross-stream planes for a slot inlet velocity of 3.8 feet per second for water. These results agree well with those observed in the actual physical water model.

5.1.2.2 Two-Dimensional Cold-Flow Air Rig

Objectives of testing with the two-dimensional cold-flow Plexiglas air rig shown in Figure 66 were to

- Obtain cold-flow velocity profiles and recirculation data
- Determine the accuracy of a six-hole velocity vector probe in a recirculating flow region
- Develop a two-dimensional fuel manifold design for a two-dimensional hot flow rig
- Investigate the fuel and airflow distribution as affected by the addition of a "wiggle strip" in the flow gap

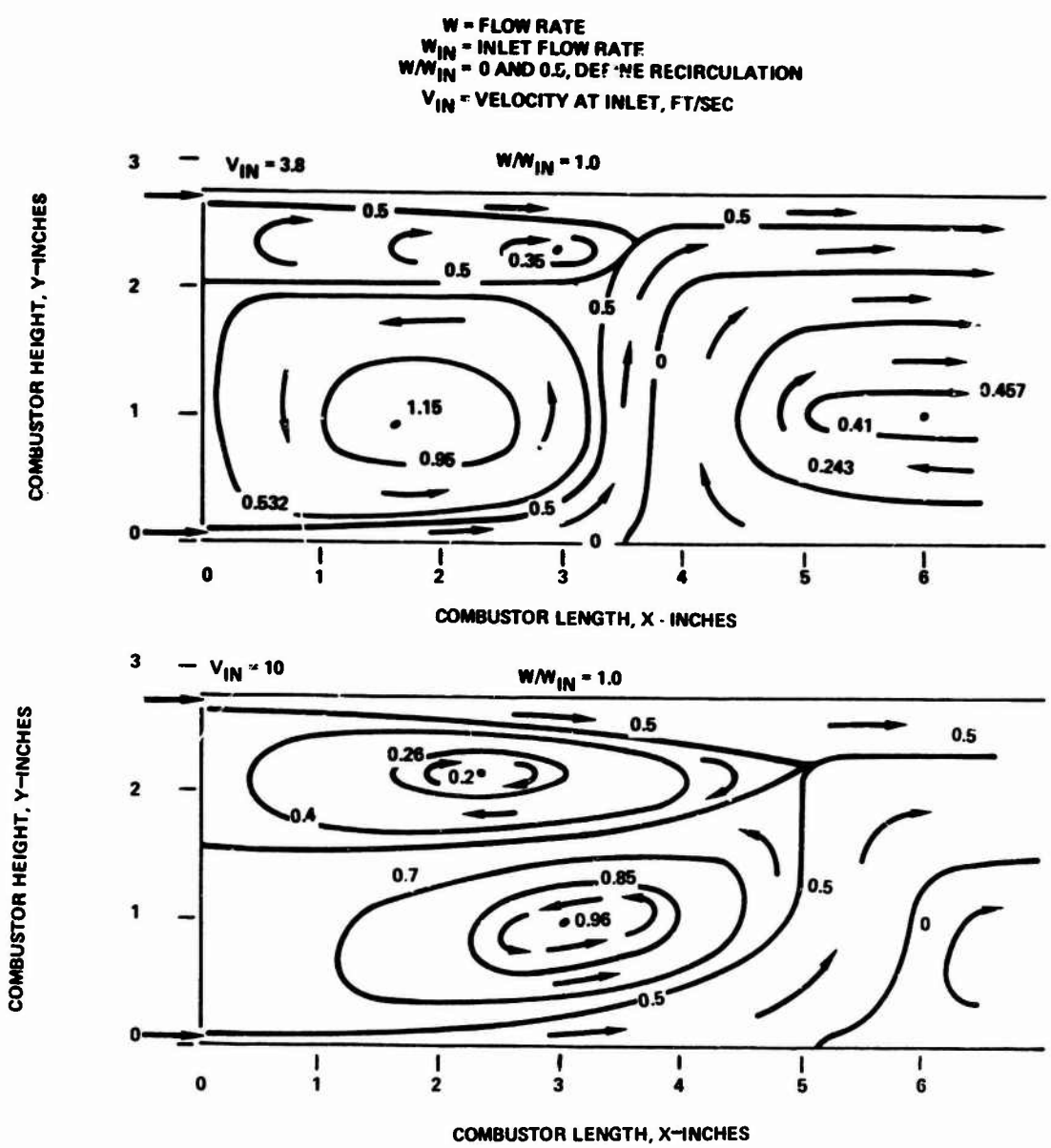


Figure 64. Double-Entry Water-Model Predicted Flow Patterns.

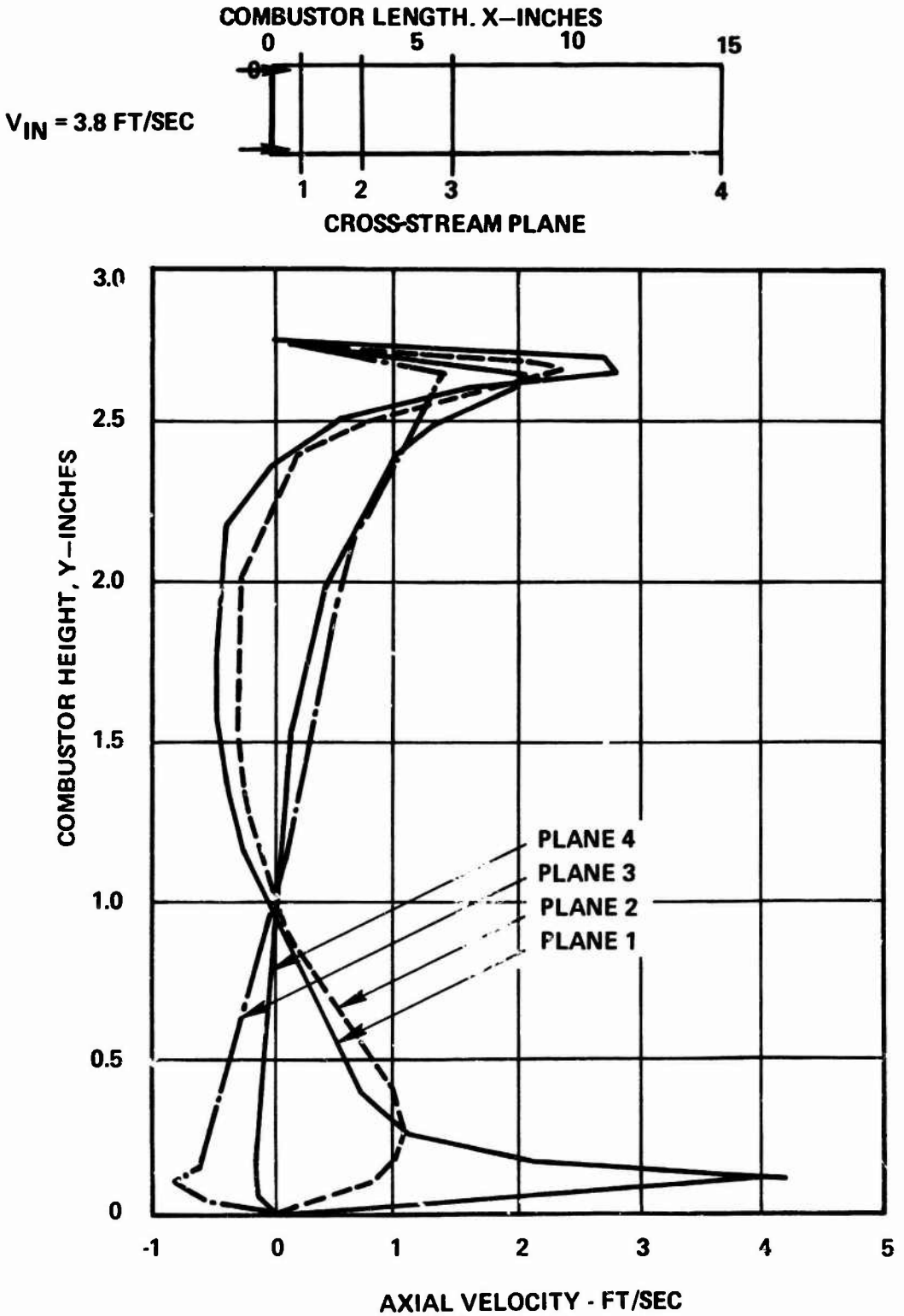
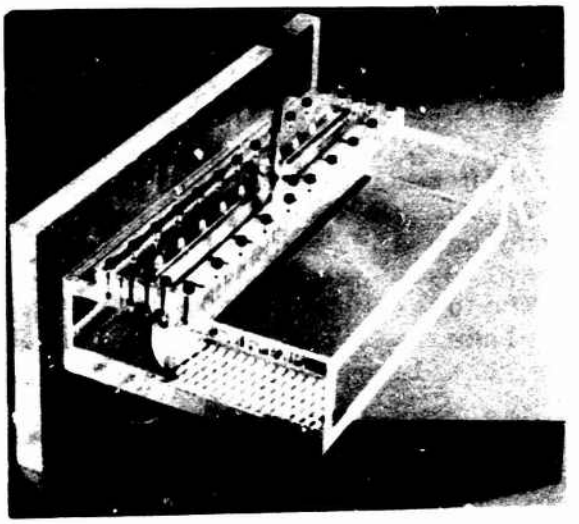


Figure 65. Double-Entry Water-Model Predicted Axial Velocity in Cross-Stream Planes.



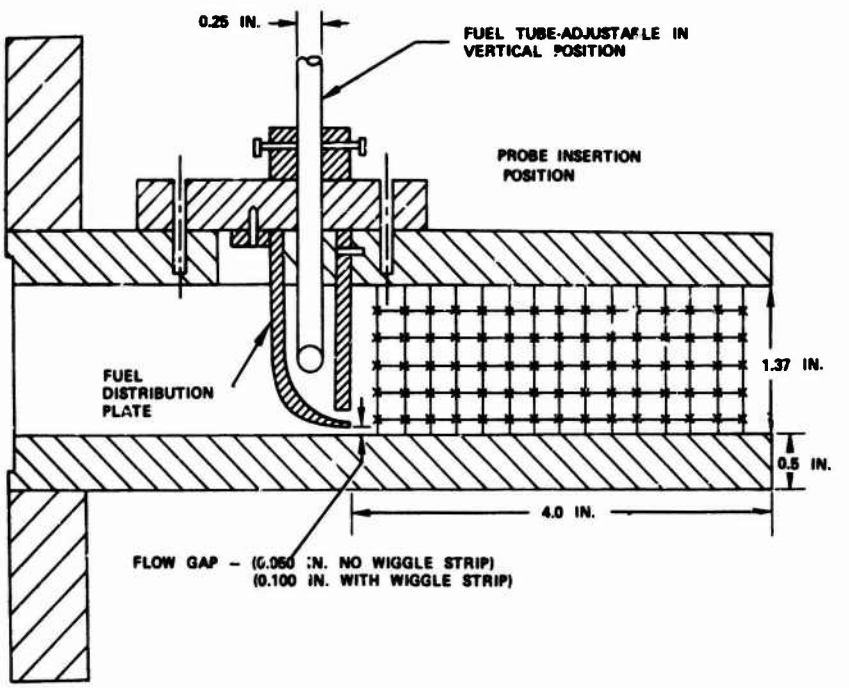


Figure 66. Two-Dimensional Cold-Flow Rig.

Velocity mapping with the rig was conducted with the use of cold airflow and the following probes:

- o Cobra probe, 1/8-inch diameter
- o Wedge probe, 1/4-inch diameter
- o Six-hole vector probe, 1/4-inch diameter

Flow gaps used were 0.05 inch and 0.100 inch, with air velocities ranging from 100 feet per second to 350 feet per second.

Most of the mapping was limited to the center vertical plane, with some additional data taken in planes 2.5 inches on each side of center. The data taken indicated some nonuniformity of flow from one plane to the other, even though uniform flow was measured along the length of the 0.05- and 0.10-inch flow discharge gaps.

5.1.2.2.1 Test Results

A schematic of the flow field typically obtained is given in Figure 67, showing a high-velocity region close to the lower wall and a recirculating region filling the bulk of the model. The initial point of recirculation fell outside the model discharge opening (confirming results obtained from the water model of the same configuration) and extended back into the model for about three-quarters of its length. An almost stagnant region was found to exist between the limits of the recirculating region and the wall shielding the fuel-distribution plate. Oscillating flow and high turbulence were observed at the interface region of the high-velocity downstream flow.

Of primary interest was the data obtained with the use of the 1/4-inch-diameter, six-hole vector probe, since a probe of this basic design was later used to map the flow fields in the hot rigs (with combustion). The results obtained indicated that velocity vectors could be obtained with a fair degree of accuracy by observing the maximum measured pressure and the pressure on either side of this maximum pressure. A curve was then faired through the points taken such that it was symmetrical over 120 degrees and passed through the maximum measured pressure and the pressures measured 60 degrees on either side. The peak of this faired curve then gives the direction of flow and total pressure at this point. The air velocity at this point (measured previously by means of the wedge probe) was then used to calculate the static pressure at the point. It was found that for the probe design used, static pressures were approximately 40 degrees on either side

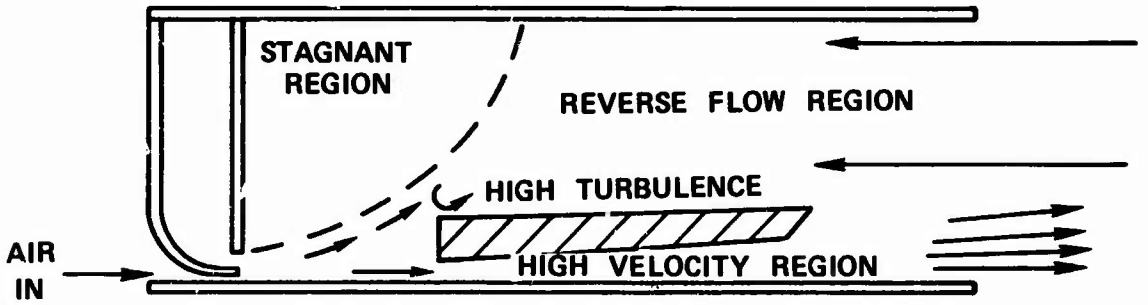


Figure 67. Primary-Zone Flow-Field Schematic.

of the true total on the faired curve. These results indicated that although the method is somewhat tedious and relies on some curve fairing, a probe of this design could be used with some degree of confidence for velocity vector measurements in a flow field of known density.

This rig was used for development of a fuel manifold design for the two-dimensional hot-flow rig. The fuel manifold had 0.0135-inch-diameter fuel discharge orifices drilled on 1.0-inch centers.

This manifold (tested without airflow), in conjunction with the fuel distribution plate, provided uniform fuel distribution in the test section for fuel-flow rates tested from 3 pounds per hour up to 15 pounds per hour. The uniformity of the fuel distribution was primarily the result of the surface tension at the end of the stainless steel fuel-distribution plate.

With the addition of airflow through the flow gap, no satisfactory method could be devised to ensure that this film was transferred from the distribution plate across the flow gap to the rig wall. Some improvement was observed when air was introduced into the fuel distribution section, but a significant amount of the fuel was still atomized by the flow gap air as it left the lip of the distribution plate.

A wiggle strip (0.01 inch thick, 0.5 inch wide, with a 1.0-inch wavelength) was inserted into the flow gap in an attempt to provide a "path" for the fuel across the air gap to the bottom wall. This wiggle strip did not significantly alter the results. It was noted, however, that when fuel was deposited on the bottom wall, the discrete fuel streams were created where the wiggle strip made contact with the bottom wall. The results suggested that for the typical L-pipe with dome cooling band configuration much of the fuel is atomized at the flow gap rather than transferred to and evaporated from the combustor wall as originally theorized.

5.1.2.2.2 Comparison of Analytical and Experimental Velocity Profiles

Figure 68 shows a comparison of experimental velocity measurements and those predicted by the analytical model for several inlet air velocities and different axial locations. It is apparent from the data that more measurements should have been taken for the region close to the wall, and ideally a smaller probe should have been used. (The probe used represented 18 percent of the total flow height, and undoubtedly this created errors in the measurements.) In spite of the above

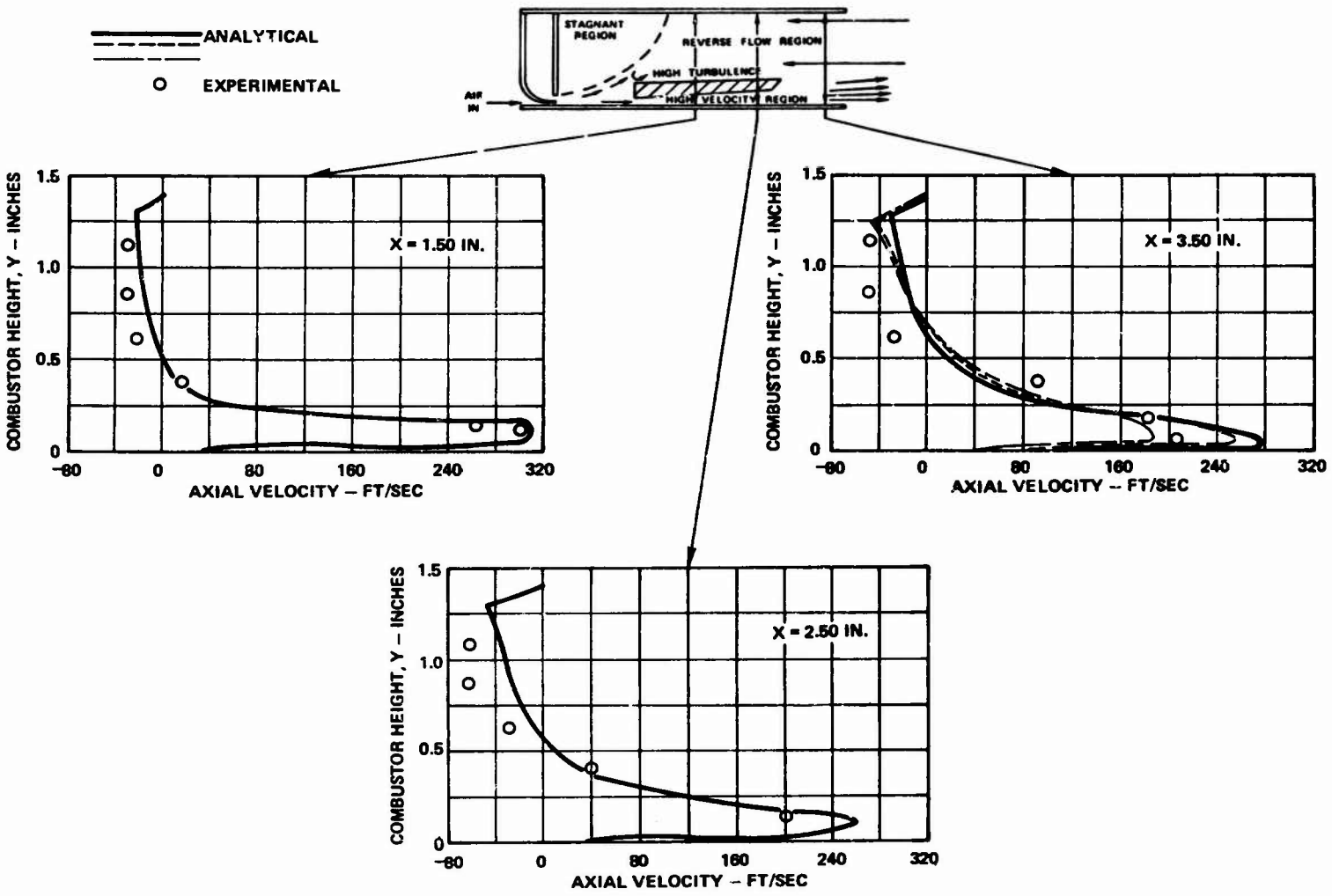


Figure 68. Two-Dimensional Cold-Flow Subelement Velocity Profiles, Analytical and Experimental.

limitations in the test procedure, the analytical and experimental results agreed reasonably well, and the recirculation region is accurately defined by the analytical model. In Figure 68 the constant $Z_{\mu k}$ is from the turbulent kinetic energy relationship:

$$k = Z_{\mu k} V^2 \qquad (72)$$

Attempts were made to correlate the data more accurately by varying the value of the constant $Z_{\mu k}$; the effect of this variation is also shown in Figure 68. Without more extensive experimental mapping, however, no definite conclusions can be drawn, but it is strongly indicated that a more realistic viscosity model could help in the overall model credibility.

5.1.2.3 Two-Dimensional Hot-Flow Rig

The hot-flow rig (Figure 69) consisted of a two-dimensional test section with the same physical dimensions as the cold-flow rig discussed previously.

The purposes of the tests conducted with this rig were to:

- Measure velocity and temperature profiles, gaseous emissions and flame radiation in a two-dimensional flow field with combustion for comparison with analytical solutions
- Measure fuel film evaporation characteristics in a combustor environment
- Establish design feasibility of instrumentation for measuring velocity and temperature prior to pressure rig tests

Rig instrumentation included the following:

- Gas Temperature Measurement - A platinum/platinum 10 percent rhodium aspirated water-cooled thermocouple (shown in Figure 70) was used to map temperature profiles within the primary zone. Because gas temperatures in subsequent primary-zone pressure rig tests were anticipated to be approximately 3500°F (above the temperature range of Pt/Pt10%Rh thermocouples), a double sonic temperature probe was also fabricated (Figure 71). The probe was tested in this rig to obtain a calibration against the Pt/Pt10%Rh thermocouple.

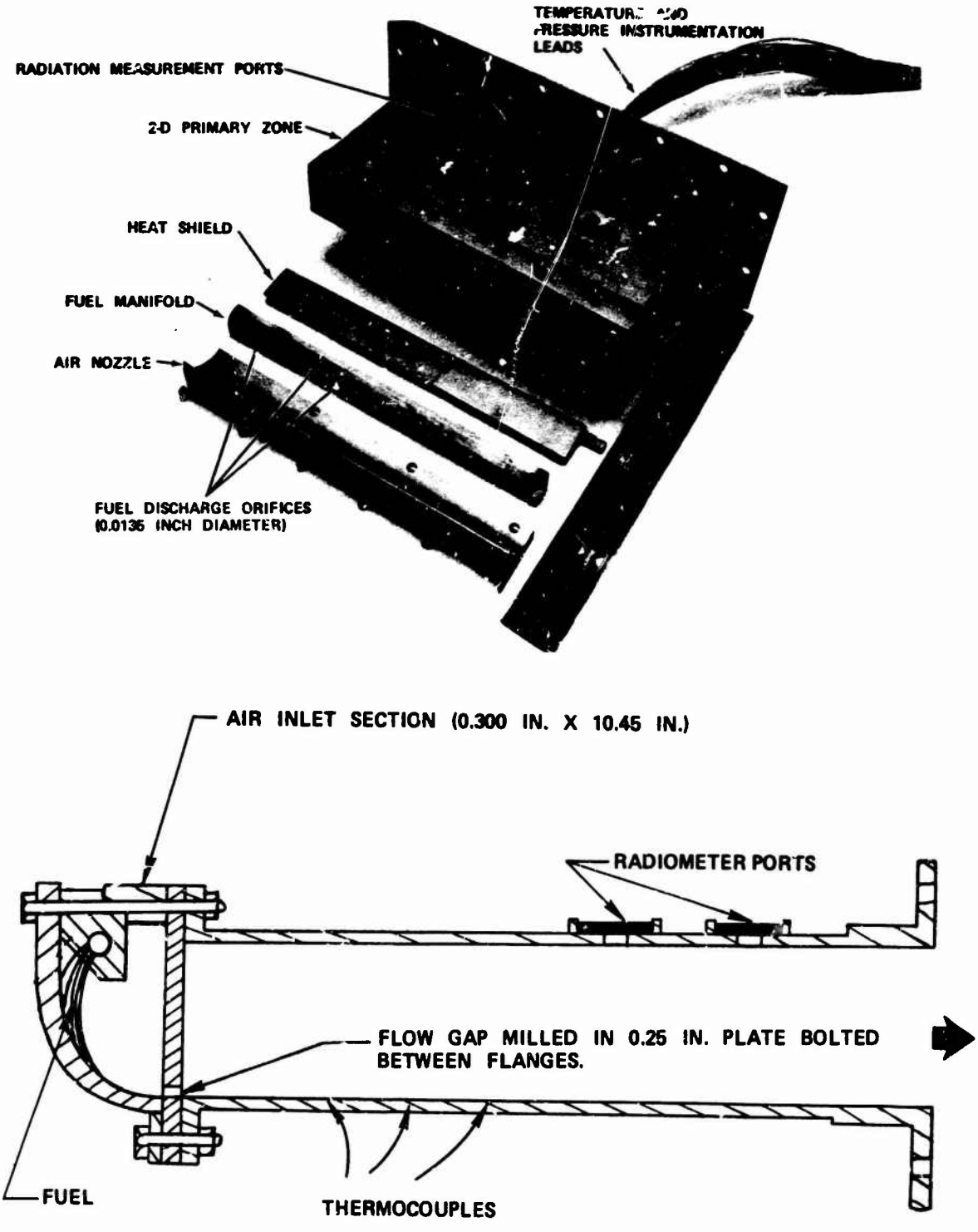


Figure 69. Hardware for Atmospheric Primary-Zone Rig.

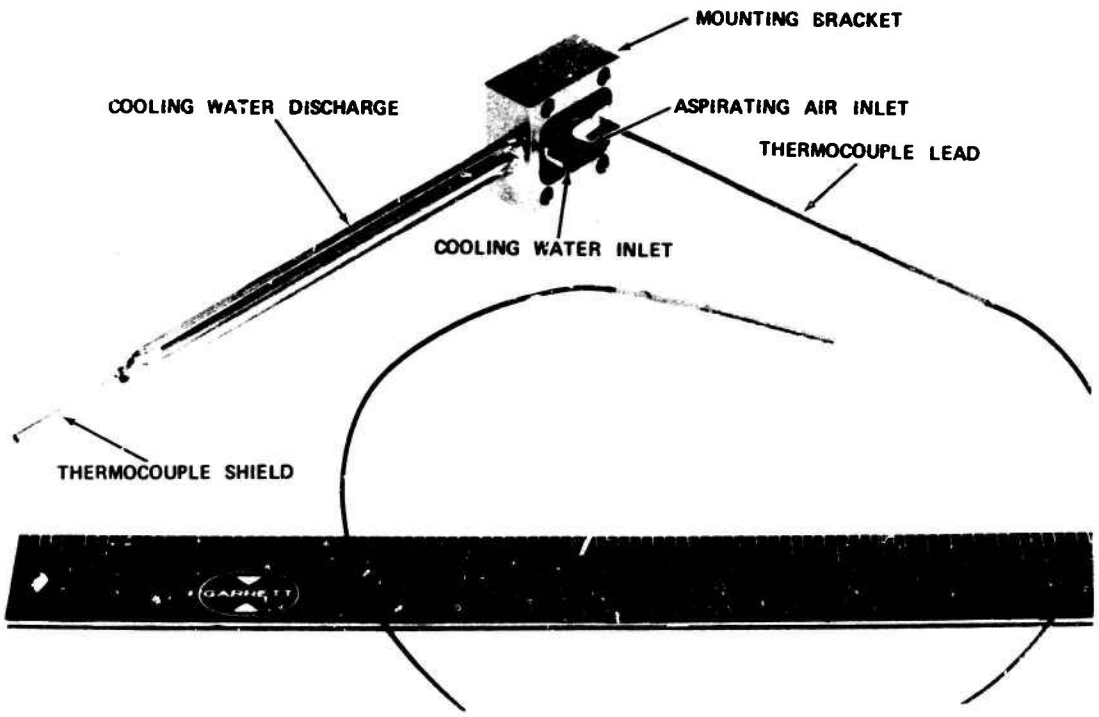


Figure 70. Water-Cooled, Shielded, Platinum/Platinum 10-Percent Rhodium Thermocouple.

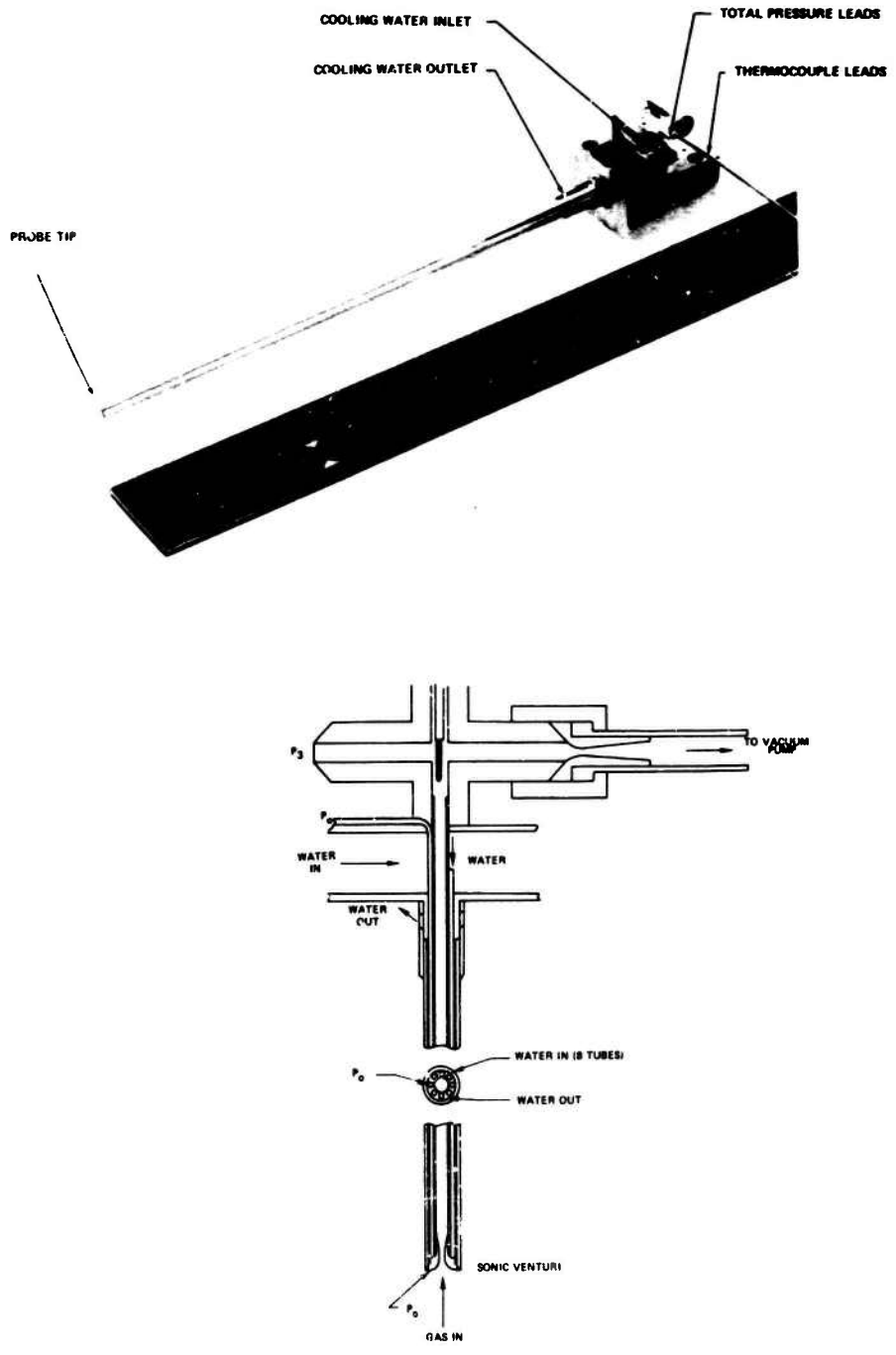


Figure 71. Double Sonic Venturi Temperature Probe.

- Velocity Measurement - A six-hole U-tube vector probe, water cooled as shown in Figure 72, was used to measure velocity vectors. The U-tube design was necessary to provide a sufficient cooling water flow rate.

- Radiation Measurement - Leeds and Northrup double-mirror Rayotubes (shown in Figure 73) were used to obtain flame radiation.

- Emission Measurement - The water-cooled probe shown in Figure 74 was used to obtain continuous gaseous emission samples. The sample analysis equipment included two nondispersive infrared analyzers for measurement of carbon monoxide and carbon dioxide, a heated flame ionization detector to measure total unburned hydrocarbons, and a chemiluminescent analyzer to measure oxides of nitrogen.

5.1.2.3.1 Test Results

Results of the Pt/Pt10%Rh thermocouple survey are shown in Figures 75 and 76 for two fuel flows and three vertical planes. These fuel flows were selected such that at the higher flow (64 pounds per hour) the fuel film could be observed at the burner discharge plane, and at the lower fuel flow (36 pounds per hour) the fuel film had evaporated before reaching the burner discharge plane as indicated by the centerline lower-wall thermocouple. This was also checked visually, and a stable flame could be seen in the burner. Combustion stability was a problem in this primary-zone rig. Even at the lower fuel flow, burner fuel-air ratio was extremely high (f/a=0.343). Reducing the fuel flow to less than 25 pounds per hour resulted in flame instability and partial blowout across the channel. As shown by Figures 75 and 76, the flame was not uniformly two-dimensional but, in the three planes surveyed, exhibited the same basic profile. The flame region began close to the lower wall and moved upward down the length of the burner. In the case of the center surveys, the flame appeared to originate at the flow gap; whereas in the case of the off-center planes, the flame appeared to originate farther downstream.

Calibration of the double-sonic probe against the Pt/Pt10%Rh probe was complicated by the inherent instability of the flame and by some mechanical failures due to differential thermal expansion of the separate tubes comprising the probe.

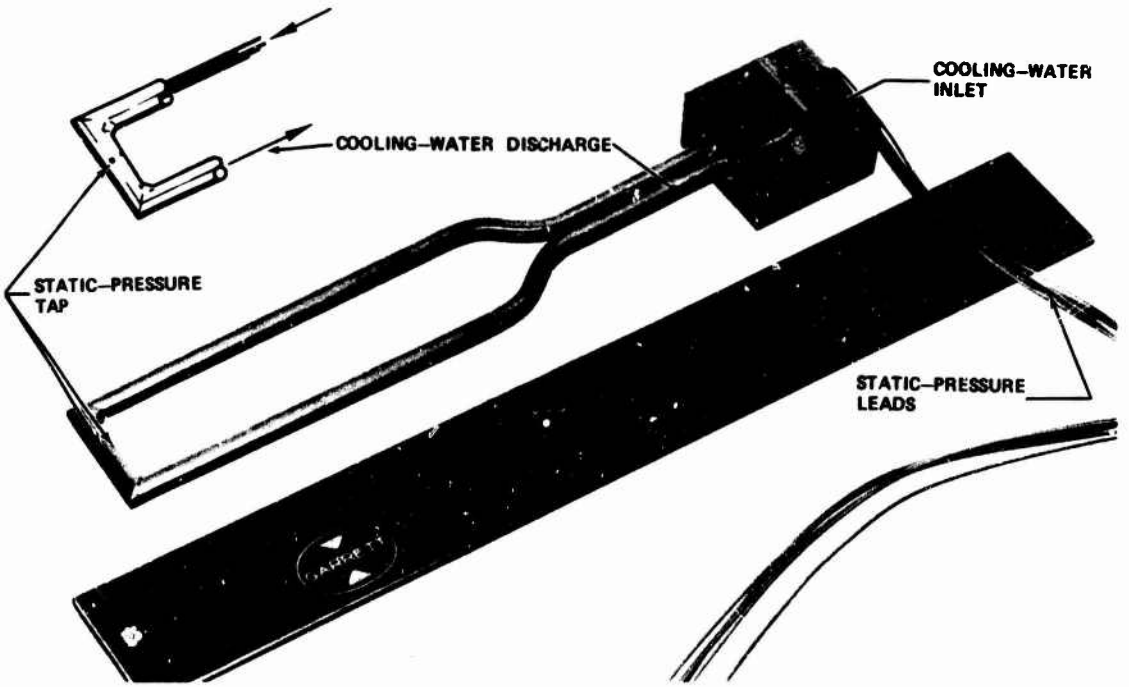


Figure 72. Water-Cooled, U-Tube Velocity Vector Probe.

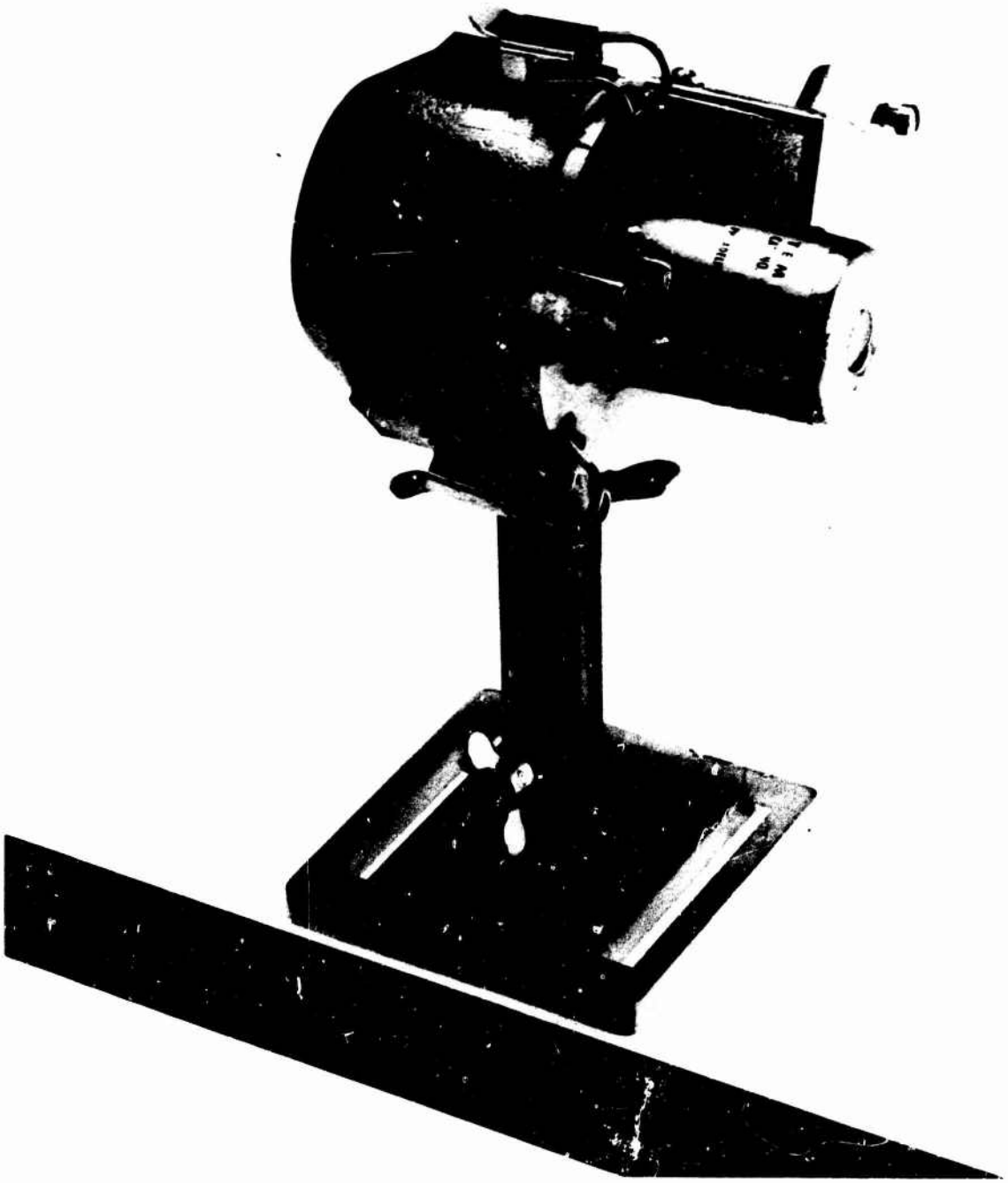


Figure 73. Leeds and Northrup Double Mirror Type Rayotube.

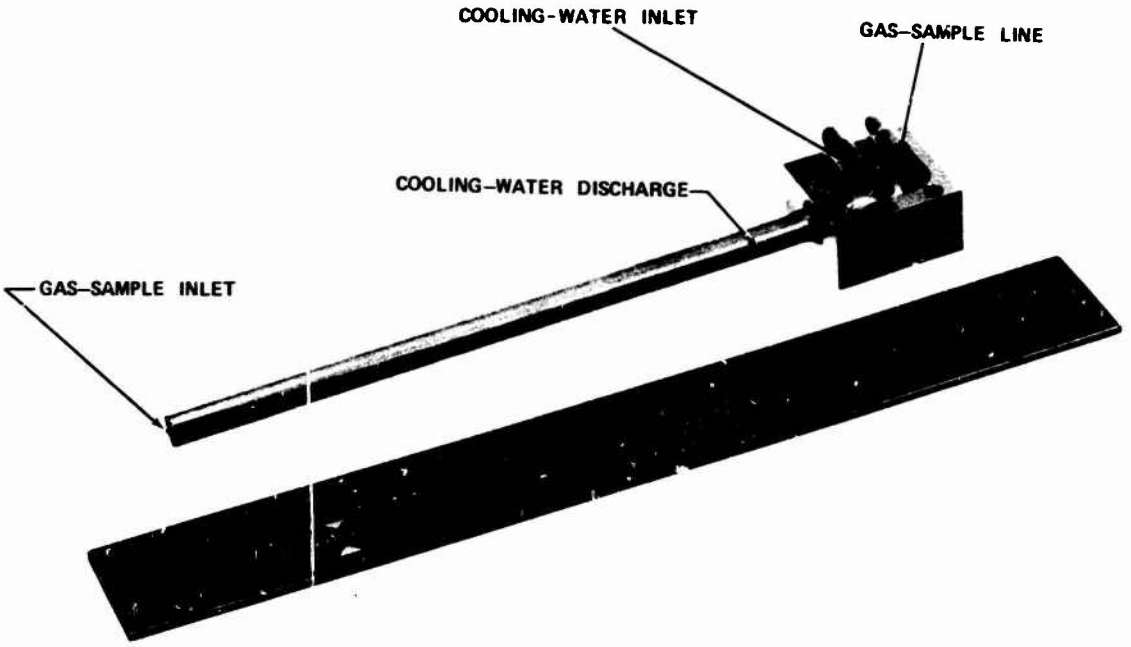
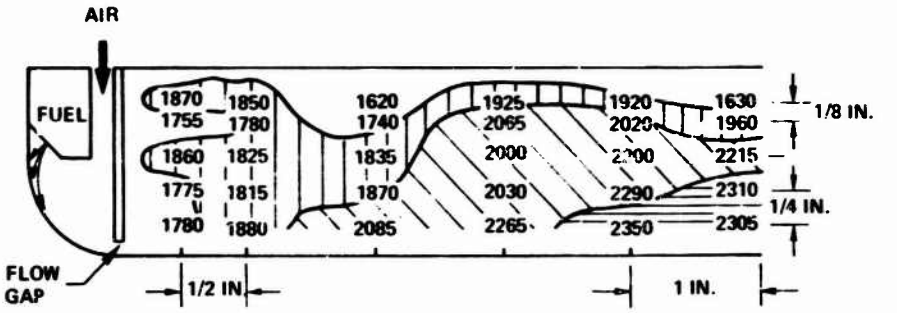
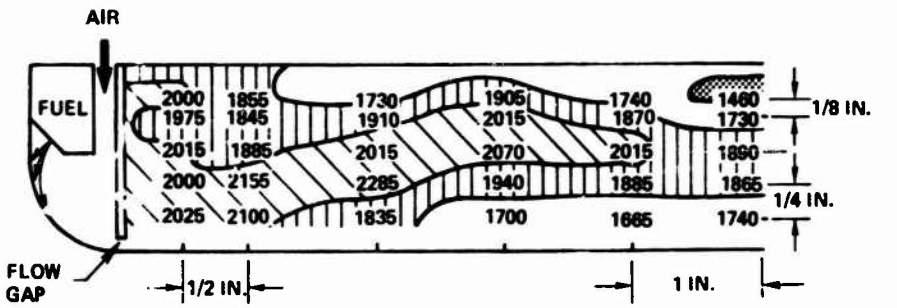


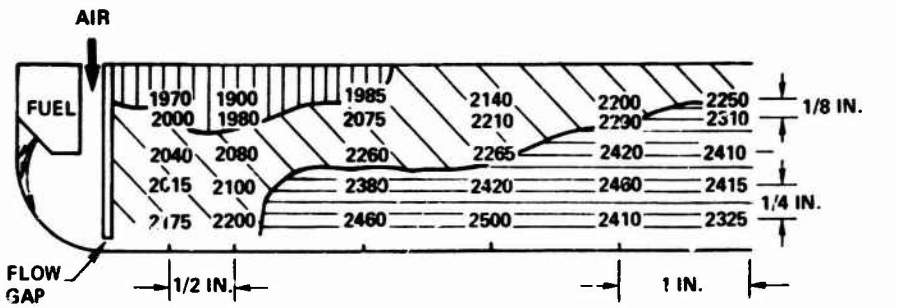
Figure 74. Water-Cooled Emission Measurement Probe.



(a) 2-1/2 INCHES LEFT OF CENTER LOOKING FROM DISCHARGE END



(b) VERTICAL PLANE AT CENTER LINE



(c) 2-1/2 INCHES RIGHT OF CENTER LOOKING FROM DISCHARGE END

LESS THAN 1600°F
1600 TO 1800°F
1800 TO 2000°F
2000 TO 2300°F
>2300°F

INLET CONDITIONS (SET)

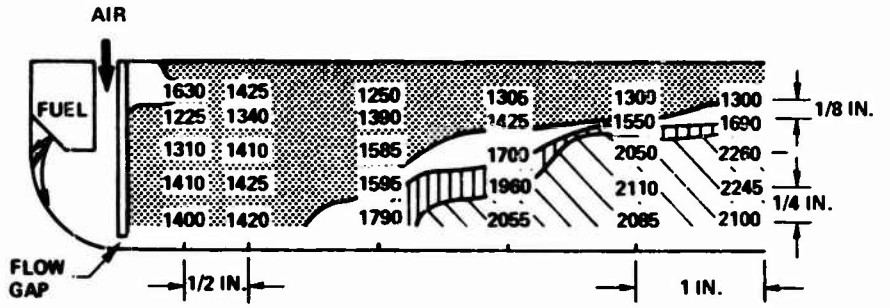
W_a = 105 LB/HR

V_{gap} = 300 FT/SEC

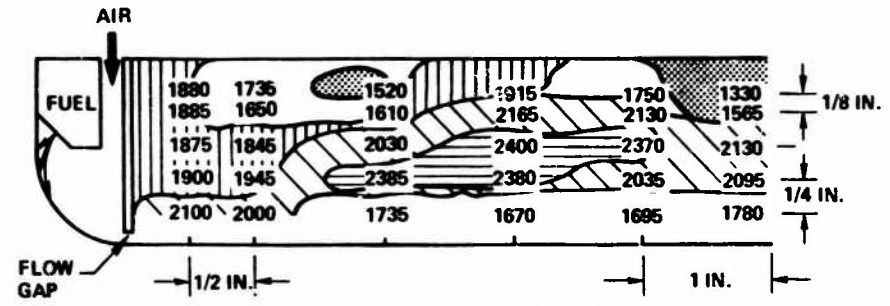
T_a = 795/810°F

W_f = 64 LB/HR

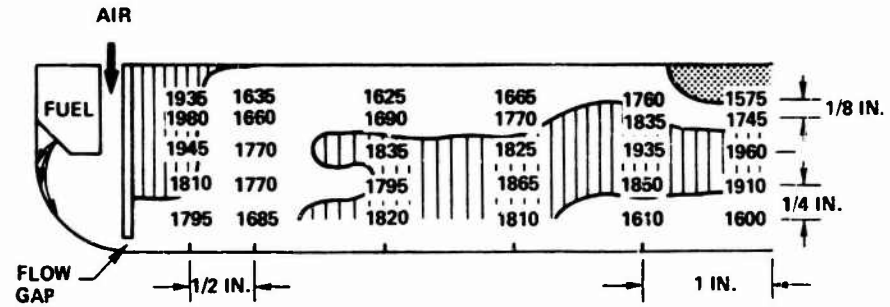
Figure 75. Two-Dimensional Atmospheric Rig Temperature Distribution.



(a) 2-1/2 INCHES LEFT OF CENTER LOOKING FROM DISCHARGE END



(b) VERTICAL PLANE AT CENTER LINE



(c) 2-1/2 INCHES RIGHT OF CENTER LOOKING FROM DISCHARGE END

LESS THAN 1600°F
1600 TO 1800°F
1800 TO 2000°F
2000 TO 2300°F
GREATER THAN 2300°F

INLET CONDITIONS (SET)

W_a = 105 LB/HR

V_{slot} = 300 FT/SEC

T_a = 792°F

W_f = 36 LB/HR

Figure 76. Two-Dimensional Atmospheric Rig Temperature Distribution.

Double-sonic temperatures were calculated by first applying a geometric calibration factor:

$$T_1 = \left[\left(\frac{A_1^2}{A_2^2}\right)\left(\frac{P_1^2}{P_2^2}\right)\right] T_2 \qquad (73)$$

where

T_1 = geometric calibrated gas temperature

A_1 = upstream nozzle throat area

A_2 = downstream nozzle throat area

P_1 = gas total pressure

P_2 = downstream total pressure

T_2 = downstream measured temperature

This calibrated temperature was then divided into the temperature measured by the Pt/Pt10%Rh probe at the same location, and the values obtained were averaged to obtain the true calibration factor and error.

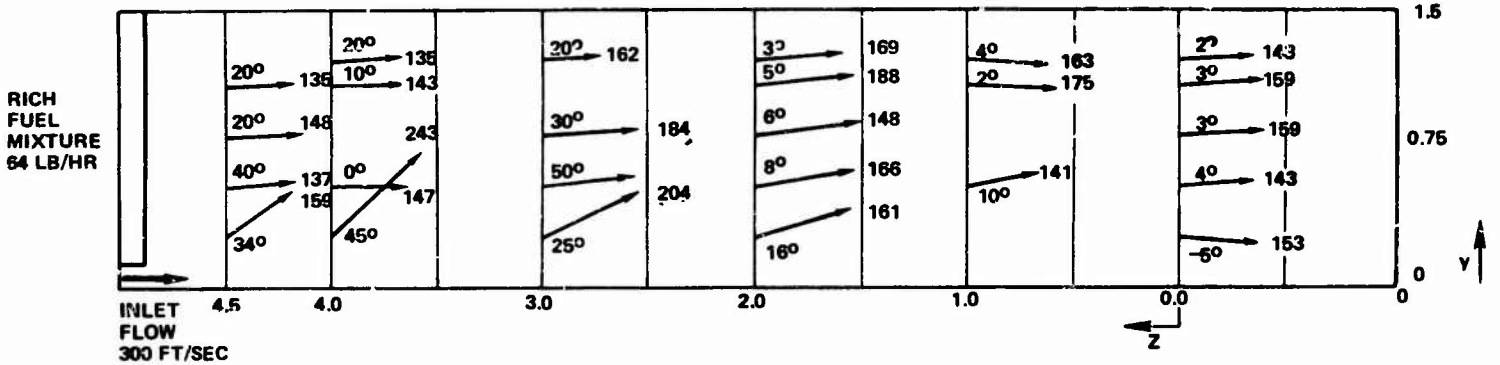
The final calibration used to calculate the gas temperature was

$$T_{gas} = 0.93 \left(\frac{P_1}{P_2}\right)^2 T_2 \qquad (74)$$

Velocity maps were obtained using the six-hole vector probe. Test conditions and probe location points were set to be the same as those set for the Pt/Pt10%Rh thermocouple, thus providing temperature data for density calculations. From the pressures obtained from the velocity vector probe, and the calculated density values, local velocities and directions were calculated.

Figure 77 shows center plane velocity vectors for fuel flows of 64 pounds per hour and 36 pounds per hour with slot inlet velocity of approximately 300 feet per second. The high fuel-flow condition indicates no recirculation region, whereas the lower flow shows recirculation in the upper half of the combustor.

Emission data was recorded for an inlet slot velocity of 300 feet per second, at fuel flows of 36 and 64 pounds per hour. Probe surveys were taken at the burner exit in three planes



PRESSURE TAP SPACING = 60°

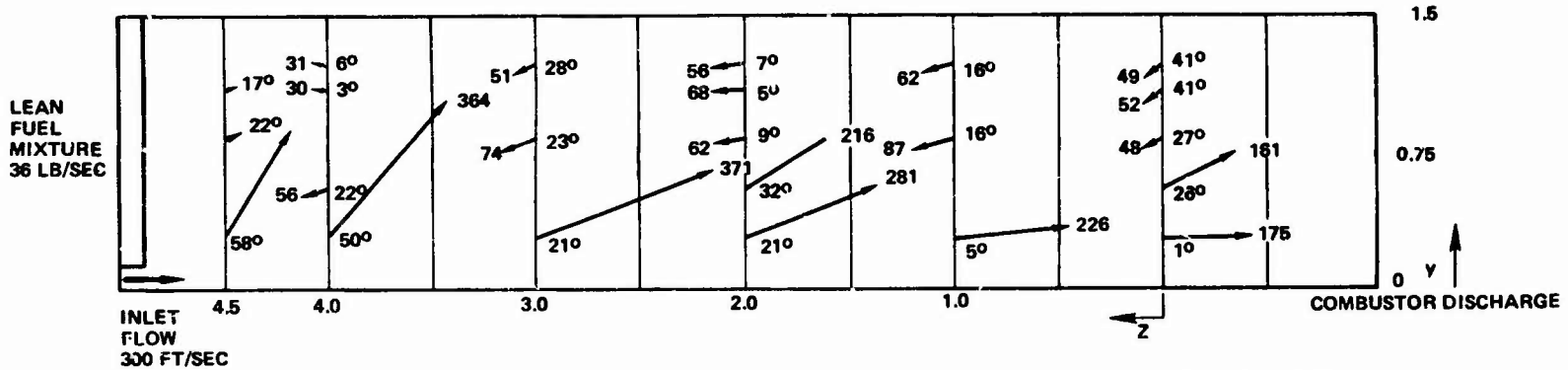


Figure 77. Velocity Vectors, Two-Dimensional Atmospheric Rig.

with five positions each. The combustor inlet air was vitiated and the temperature was equal to 800°F, and background emission data was taken.

Typical emission data is shown in Table XI. Unburned hydrocarbons are seen to increase substantially toward the bottom of the rig, where the fuel was evaporating. At all points the

TABLE XI. PRIMARY-ZONE SUBELEMENT RIG EMISSION DATA IN THE CENTRAL PLANE

Probe Height from Bottom (inches)	CO_2 (percent)	HC (ppm)	NO (ppm)	NO_X (ppm)
Fuel Flow = 36 lb/hr				
1.125	3.12	1,750	2.5	3.8
0.875	2.49	1,900	3.0	4.0
0.625	1.784	3,500	3.0	4.5
0.375	2.14	7,000	6.5	6.5
0.125	5.08	13,500	14.0	7.0
Fuel Flow = 64 lb/hr				
1.125	5.8	5,600	9.0	6.0
0.875	4.9	7,000	8.0	9.5
0.625	5.7	10,500	17.0	10.5
0.375	5.7	13,000	14.0	10.0
0.125	4.4	15,000	12.0	10.0

Combustor inlet air emissions:
CO_2 = 2.23%, CO = 12.8%, NO_x = 20 ppm
HC = 30 ppm
Inlet air temperature = 800°F
Inlet slot velocity = 300 ft/sec
CO greater than 2500 ppm at all points

NO_x level was less than the combustor inlet level, and in some cases less than the NO alone. These abnormalities were attributed to the excessively high hydrocarbon levels, resulting in partial NO decomposition.

The fuel evaporation data shown in Figures 78 and 79 were obtained in the two-dimensional hot-flow rig using lower-wall thermocouples. Fuel flows were varied from 25 pounds per hour to 64 pounds per hour, with air inlet velocity and temperature equal to approximately 300 feet per second and 800°F, respectively. Center plane readings show that for fuel flows of 45 pounds per hour and 65 pounds per hour, the fuel film extends the length of the combustor (verified visually), whereas when the fuel flow was reduced to 35 pounds per hour, fuel film evaporation was essentially complete at about 2.75 inches downstream of the inlet slot. This was also found to be the case for 25 pounds per hour fuel flow. Fuel flows below 25 pounds per hour were not possible due to lean blowout occurring below this value. Readings at a plane 2.5 inches off center did not clearly show evaporation length, which indicated nonuniformity of the film.

To supplement the film evaporation data obtained from this rig a film evaporation plate (shown in Figure 80) was tested in the fuel injector rig under more controllable conditions. Fuel film length was also determined by thermocouples mounted flush with the surface and located at 0.25-inch intervals along its centerline. Test conditions are listed in Table XII.

TABLE XII. FUEL EVAPORATION PLATE TEST CONDITIONS, FUEL-INSERTION RIG

Air Velocity (ft/sec)	Pressure (atm)	Temperature (°F)
50	1	300, 400, 650
	4	650
	8	650
100	1	300, 400, 650
	4	650
200	1	300, 400, 650
	4	650

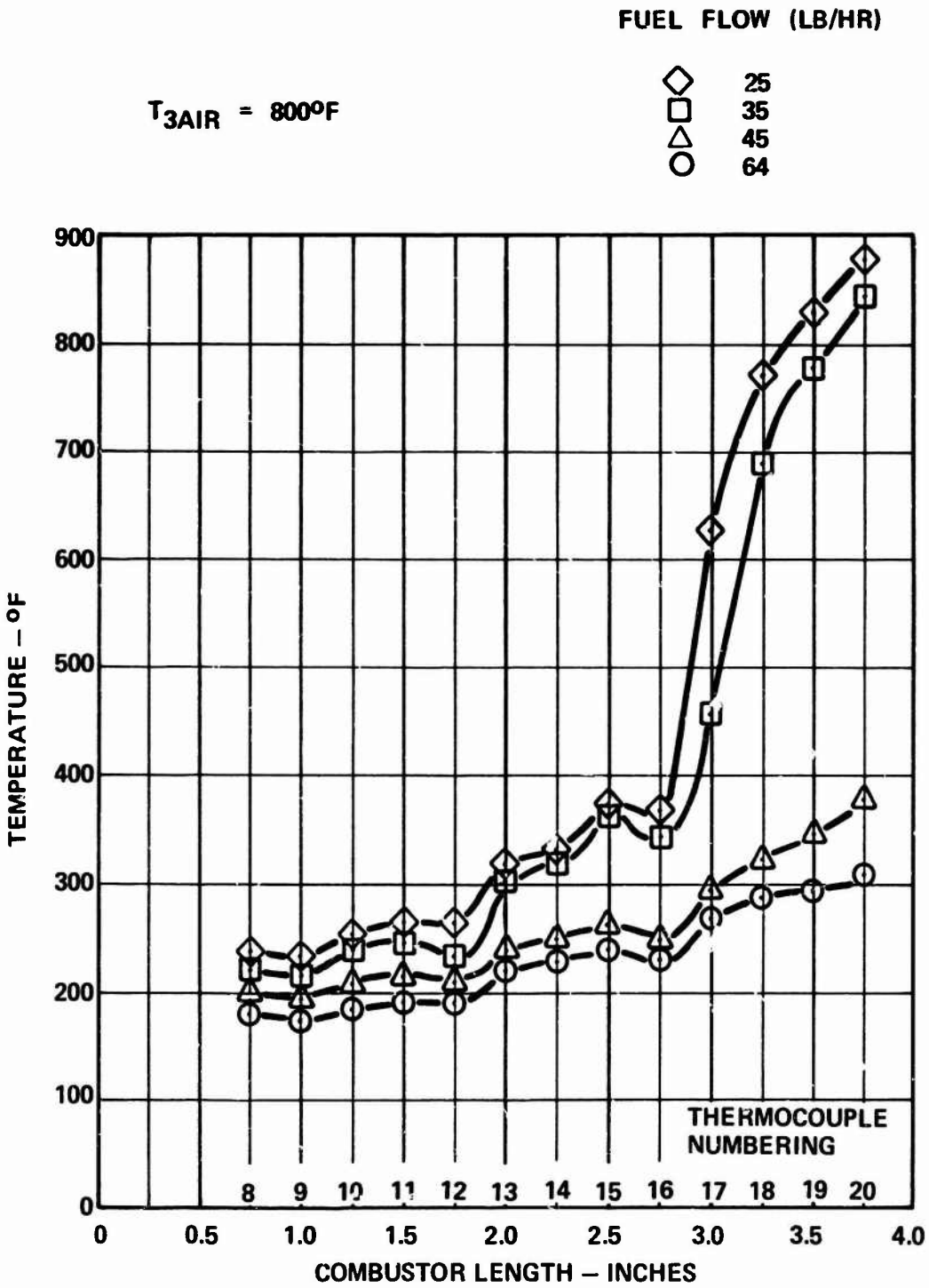


Figure 78. Two-Dimensional Atmospheric Rig - Fuel Evaporation, Centerline Thermocouples Only.

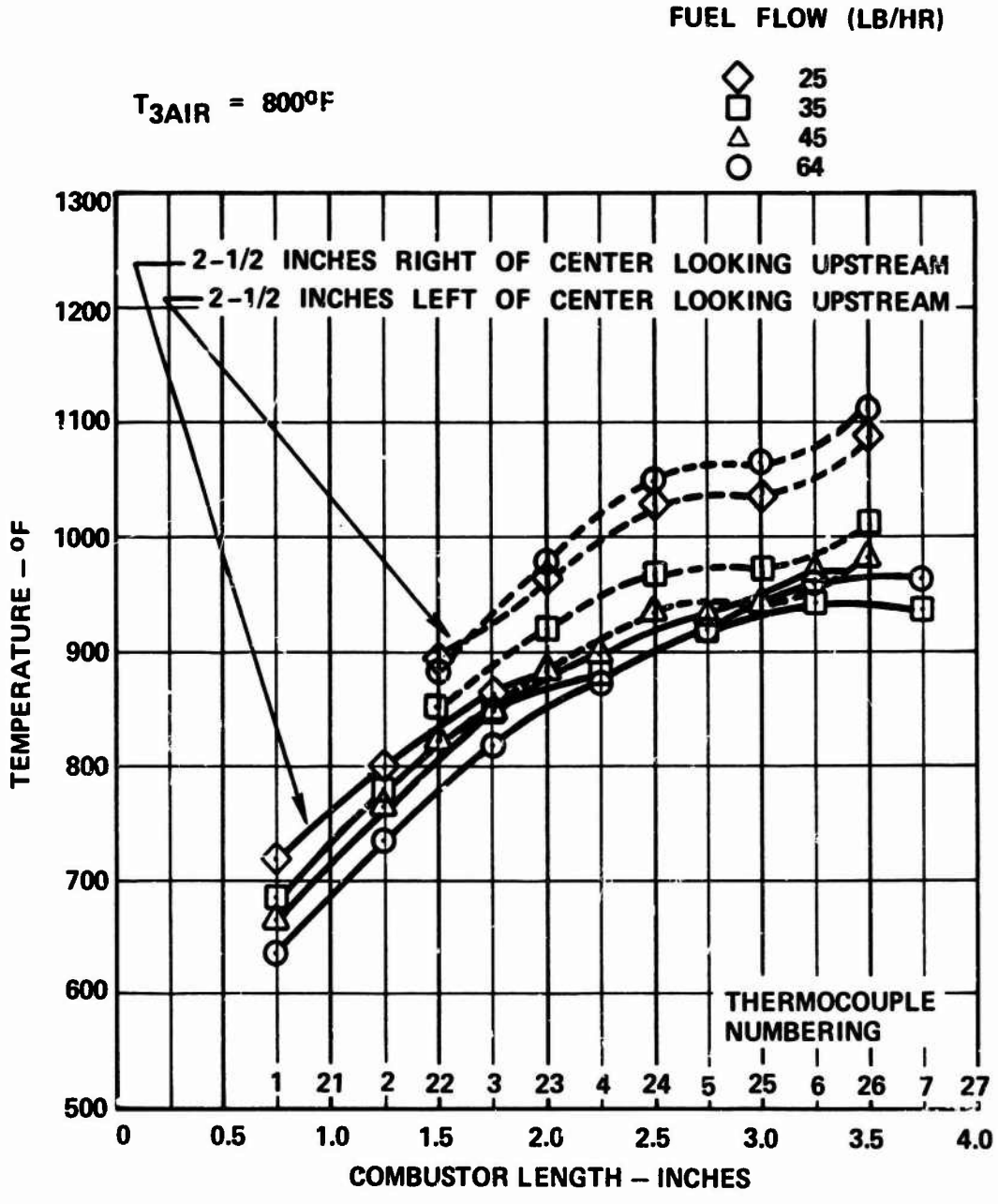


Figure 79. Two-Dimensional Atmospheric Rig - Fuel Evaporation, Thermocouples 2.5 Inches Left and Right of Centerline.

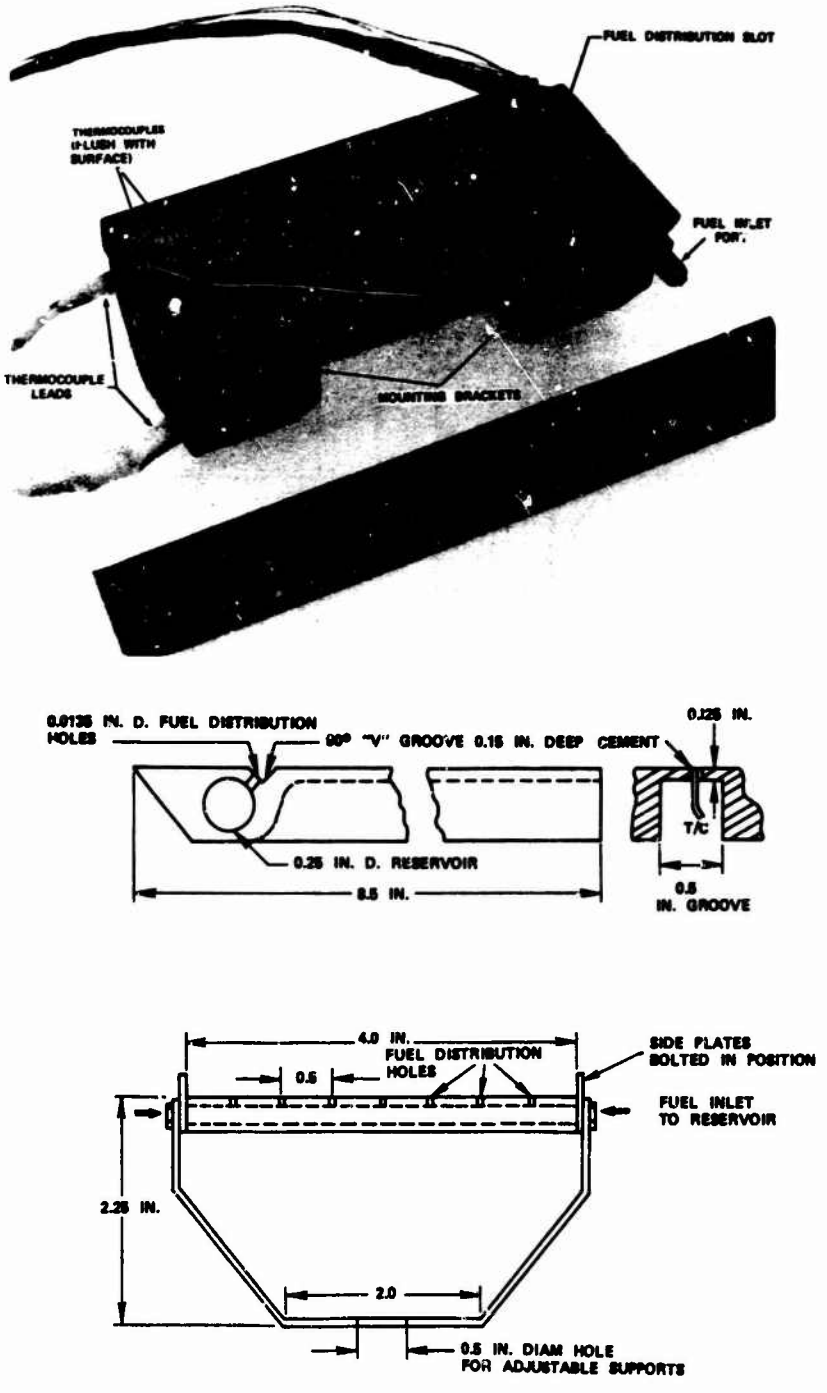


Figure 80. Fuel Evaporation Plate.

The experimental data obtained was limited to pressures not exceeding 8 atmospheres and temperatures not exceeding 650°F to avoid detonation at higher pressure and temperatures. The point of significant temperature increase was defined as the end of the film. The effect of varying the temperature from 300°F to 400°F could not be accurately determined, as the final point of fuel evaporation could not be readily located. At the higher air temperature condition (650°F), evaporation lengths could clearly be determined.

5.1.2.3.2 Comparison of Analytical and Experimental Evaporation Rates

Figures 81, 82, and 83 show the measured film-evaporation rates, the initial predictions (Section 4.3.1), and predictions with updated heat-transfer coefficients for 1, 4, and 8 atmospheres' pressure. The initial predictions were essentially linear with fuel flow. The measured rates show good agreement with predictions at low fuel flows, but show shorter evaporation lengths at high fuel flows. This effect, reported by Kinney and Abramson,[30] is the result of the fuel film thickness entering the turbulent portion of the wall boundary layer producing film rippling, which approximately doubles the heat-transfer rate. This occurs when the following wall-distance parameter exceeds a value of 21:

$$y^+ = \frac{\sqrt{\tau_o/\rho_o}}{\mu_o/\rho_o} \qquad (75)$$

where

Y^+ = wall-distance parameter

τ_o = wall shear stress

ρ_o = fluid density at wall

μ_o = fluid viscosity at wall

The above parameter is directly related through integration of the universal turbulent velocity profile to a flow-rate parameter defined as

$$w^+ = \frac{W_f/Z}{\rho\nu} \qquad (76)$$

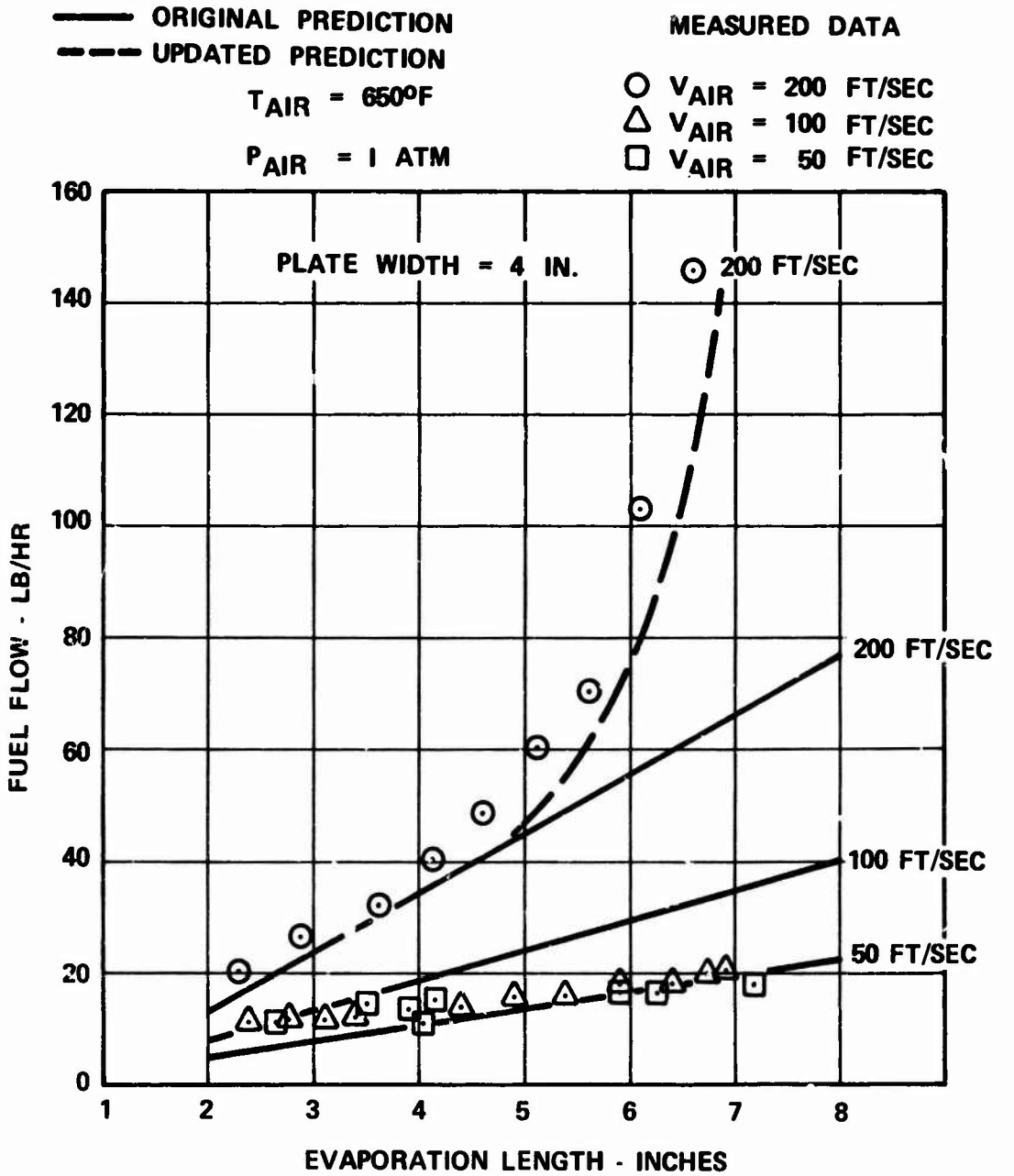


Figure 81. Film Evaporation Lengths at 1 Atmosphere.

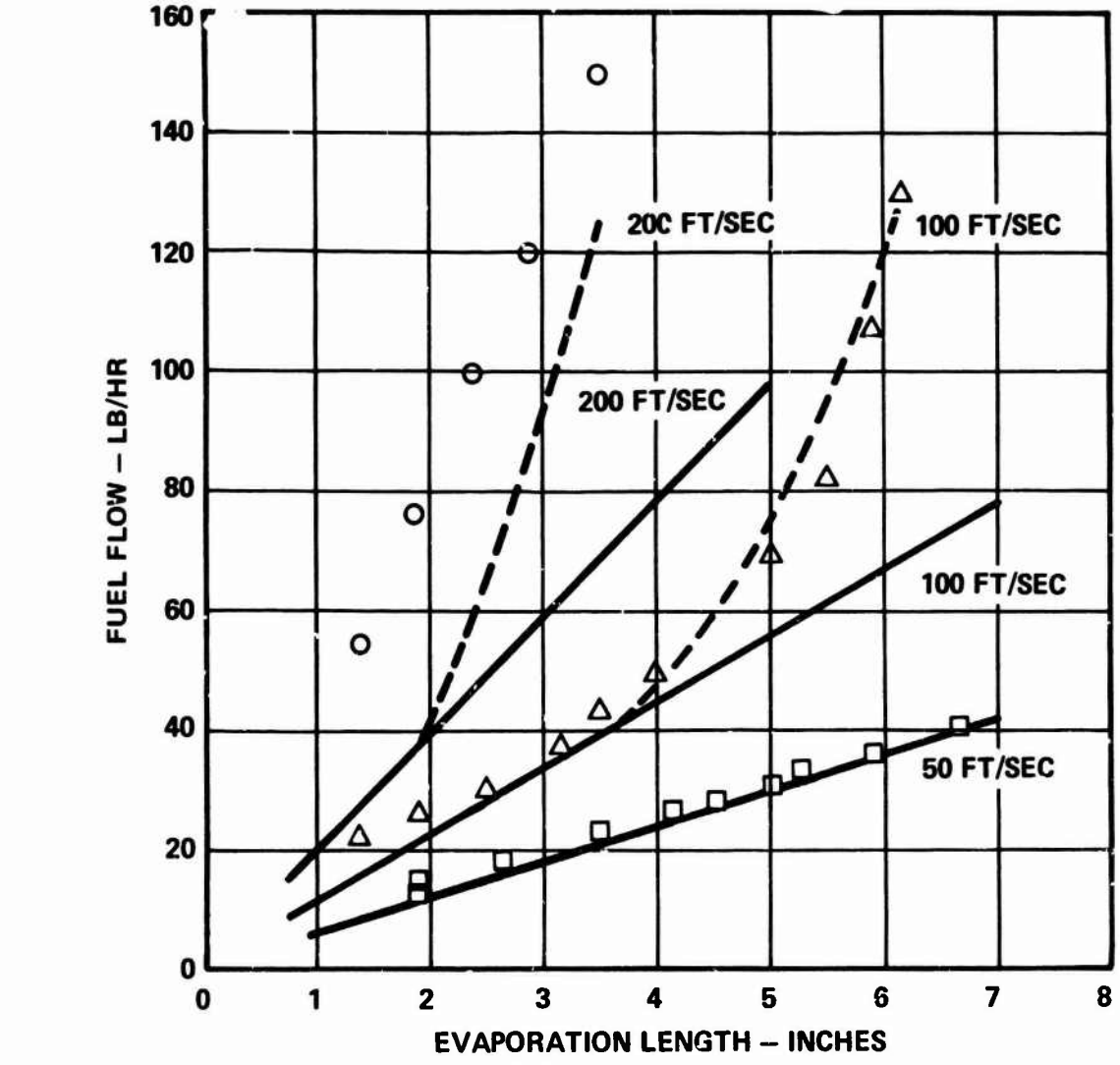


Figure 82. Film Evaporation Lengths at a Pressure of 4 Atmospheres.

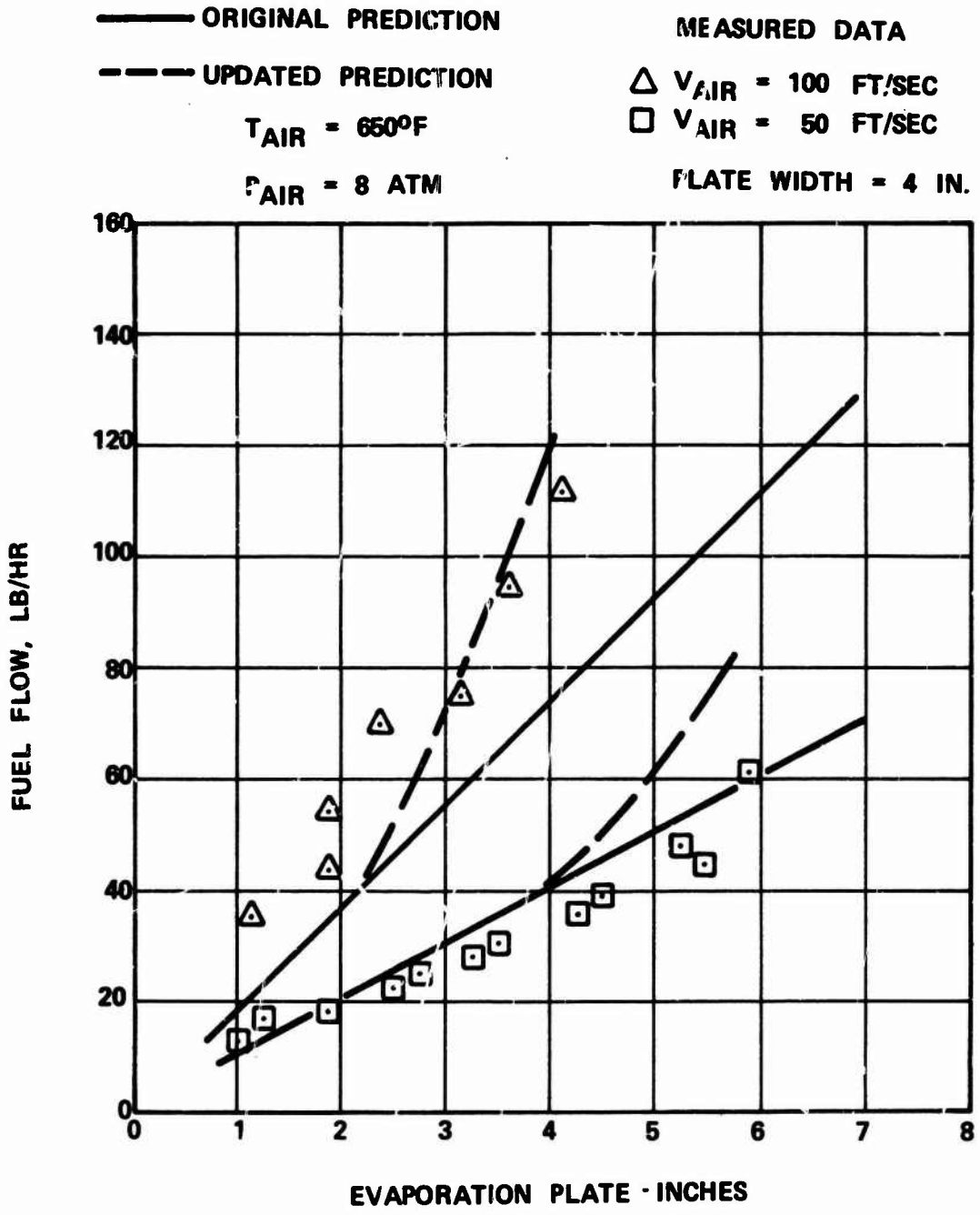


Figure 83. Film Evaporation Lengths at 4 Atmospheres.

where Z = wall width, ft

ρ = fuel density, lb per cu ft

ν = fuel kinematic viscosity, sq ft per sec

The w^+ parameter is more convenient than y^+ and has a value of 163 when y^+ is 21. For the conditions of the 4-inch-wide flat-plate tests, this value of w^+ occurs at a fuel flow rate of about 40 pounds per hour. This is the level of flow at which the measured length data begins to deviate from linearity. Based on correlation of the data, the following relation for heat-transfer coefficient was obtained:

$$\frac{h_x^*}{h_x} = 1.0 + 0.011\, w \qquad (77)$$

where w = fuel flow per unit width, lb per hr per ft

h_x^* = rippled film heat-transfer coefficient

h_x = normal film heat-transfer coefficient

The value of h_x is given by Equation (29), Section 4.3.1, for radial flow. For a flat plate or cylindrical wall, a more appropriate h_x is given by Kays.[44]

$$Nu_x = 0.0295\, Pr^{0.6} Rn_x^{0.8} \qquad (78)$$

where Nu_x = local Nusselt number ($h_x x/k$)

Pr = gas Prandtl number

Rn_x = length Reynolds number

This relation was used for the flat-plate predictions. Updated predictions give good agreement with the data in most cases. During testing at 1 atmosphere, it was observed that in some cases the film did not spread uniformly across the plate. This represents the major uncertainty in the data.

Figure 84 shows the typical variation of fuel-film temperature as a function of fuel flow at 4 atmospheres. Predicted temperatures agree well with measured values over the initial lengths but are lower at the end point. This is attributed to axial conduction effects in the 0.5-inch-thick test plate which are

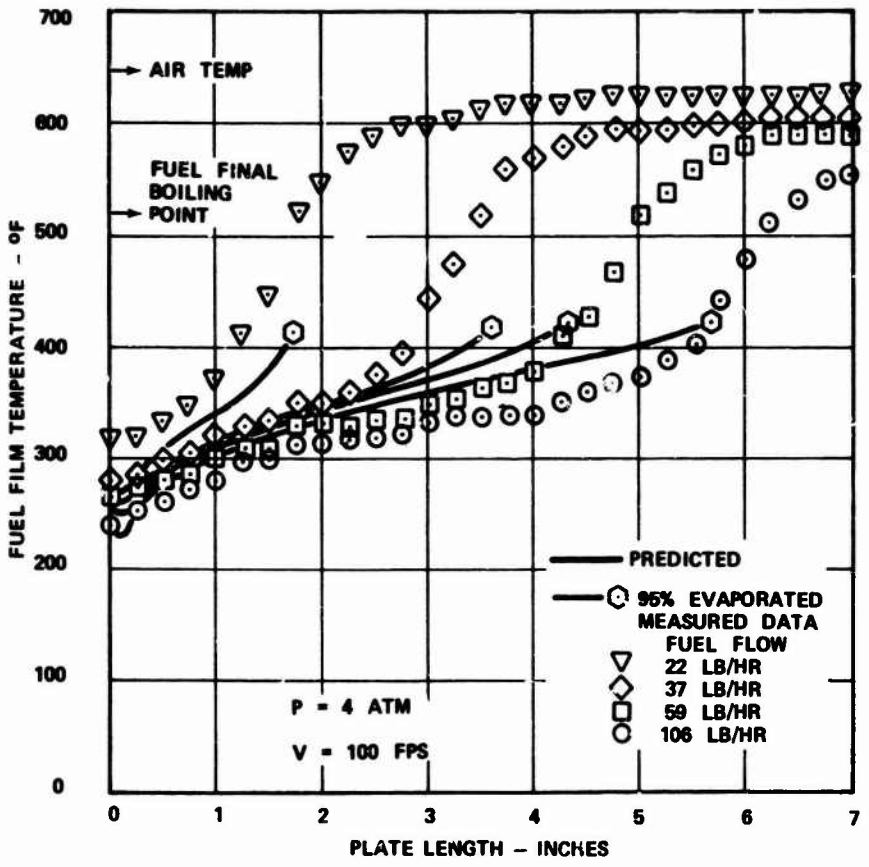


Figure 84. Fuel Film Predicted and Measured Temperature.

neglected in the analysis. Conduction effects in an actual thin-wall combustor should be negligible.

In all cases, the predicted 95-percent end-point falls within the region of steep rise in measured temperatures that defines the region of final boiling.

Based on these results it was concluded that this model could be successfully used to define evaporation lengths for guidance in fuel nozzle spacing and as an input to the primary-zone model.

5.1.2.3.3 Comparisons of Analytical and Experimental Profiles for the Two-Dimensional Hot-Flow Model

Figure 85 presents a comparison between the experimentally obtained and analytically calculated temperature profiles for the 36-pound-per-hour fuel flow as a function of passage height at different axial distances downstream of the inlet slot. These profiles are typical of those obtained at each of the four axial data positions in the primary zone, with the following expected trends observed as a function of increasing axial distance:

- The temperature peak at the point of maximum axial velocity becomes less pronounced.
- The maximum temperature along the duct passage height is reduced.

The same qualitative trends are seen in both experimental and analytical profiles; however, the quantitative agreement is limited. Several simplifications in the method of analysis and physical hardware limitations may account for this lack of quantitative agreement:

- Perhaps most significant is the strong indication that a more rigorous method of predicting turbulent flow conditions is needed. The concept that there is a close relationship of Reynolds stress to turbulent energy should be employed, and it is evident that the energy values used should be derived by solution of the transport equation.
- The fact that the effect of the unvaporized residual fuel in the gas stream was not accounted for is another source of analytical inaccuracy. There is no real quantitative evidence of what portion of the total fuel flow is represented, or of the variation of fuel distribution along the width of the vaporizing

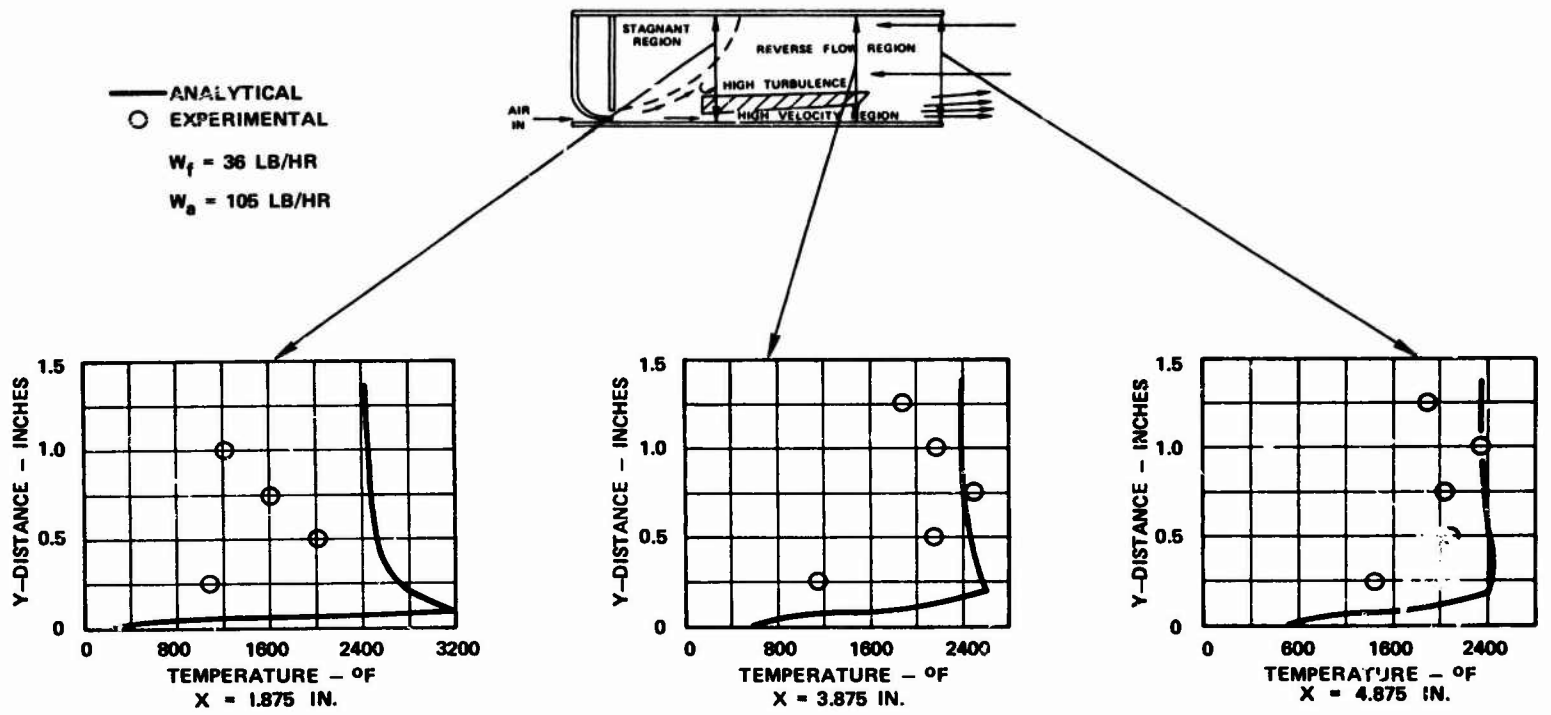


Figure 85. Comparison of Experimental and Analytical Temperature Profiles at Different Axial Distances Downstream From Inlet Slot.

surface, and therefore no quantitative evidence of local fuel-air ratios.

- The flow field is assumed to be strictly two-dimensional when in fact it is subject to three-dimensional effects.

- The flow field is assumed to have adiabatic boundaries when, actually, there is some heat transfer through the duct walls.

Figure 86 is a similar plot of axial velocity profiles as a function of duct height for the discharge plane of the duct at different axial distances downstream of the inlet slot. Again the qualitative agreement between measured and calculated data is consistent, but quantitatively the correlation is lacking due to the limitations outlined above.

5.1.2.4 Three-Nozzle-Sector Primary-Zone Rig

The pressure rig was designed for testing primary-zone annular segments at pressures up to 16 atmospheres. The annular segments represented primary zones for each of the three fuel-injection systems (air-assist, pneumatic-impact, and L-pipe).

The instrumentation develcped in the two-dimensional primary-zone rig was utilized with a traverse system having three degrees of freedom. The purpose of testing with this rig was to evaluate:

- Burning-zone location

- Velocity and temperature profiles

- Ignition energy requirements

- Flame radiation

5.1.2.4.1 Test Section Description

The following rig and hardware were used in the test program:

- Basic rig assembled on the support cart, shown in Figure 87(a).

- Primary test section plenum, shown in Figure 87(b).

- L-pipe primary-zone sector, shown in Figure 88.

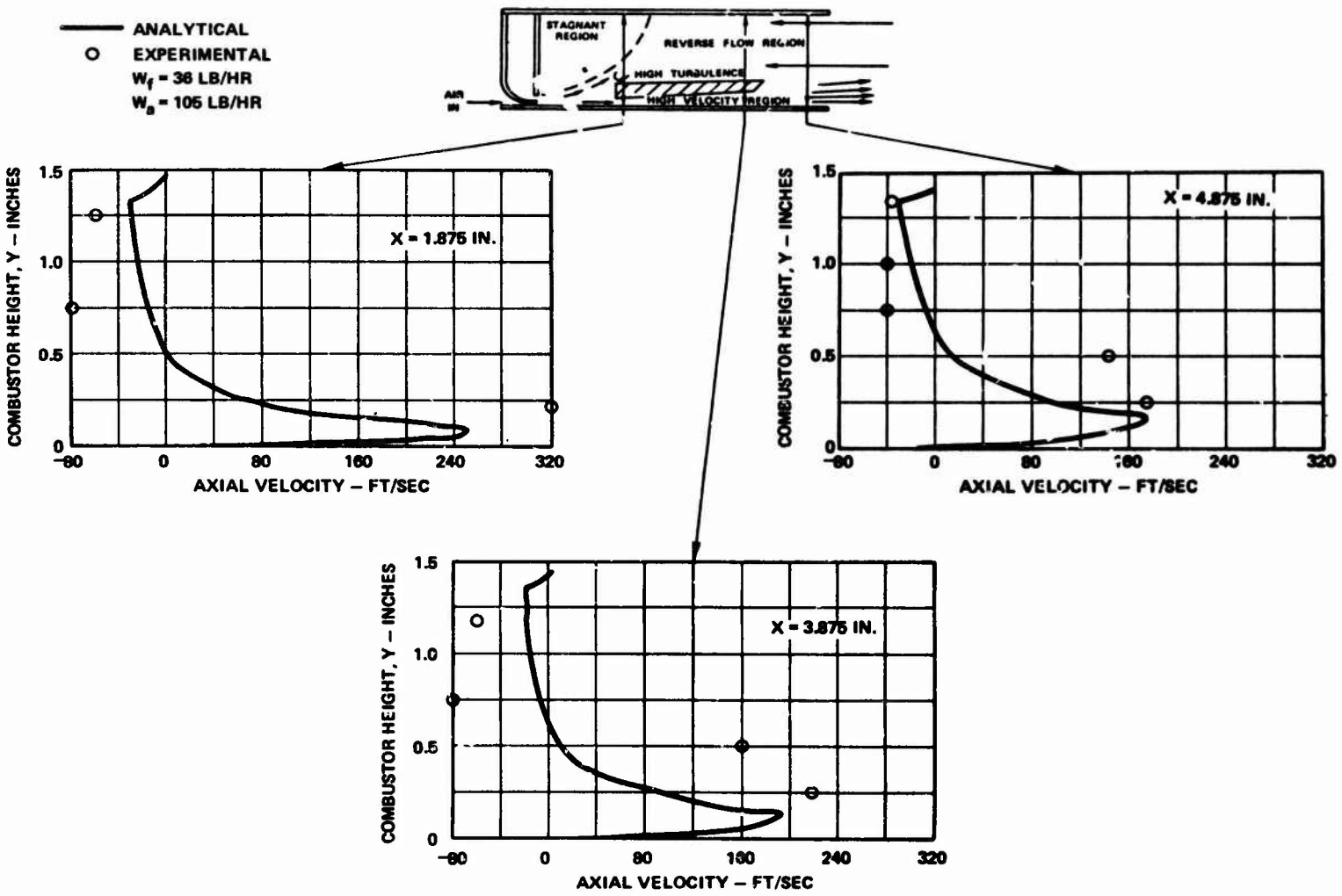


Figure 86. Comparison of Analytical and Experimental Velocity Profiles at Various Axial Distances Downstream From Inlet Slot.

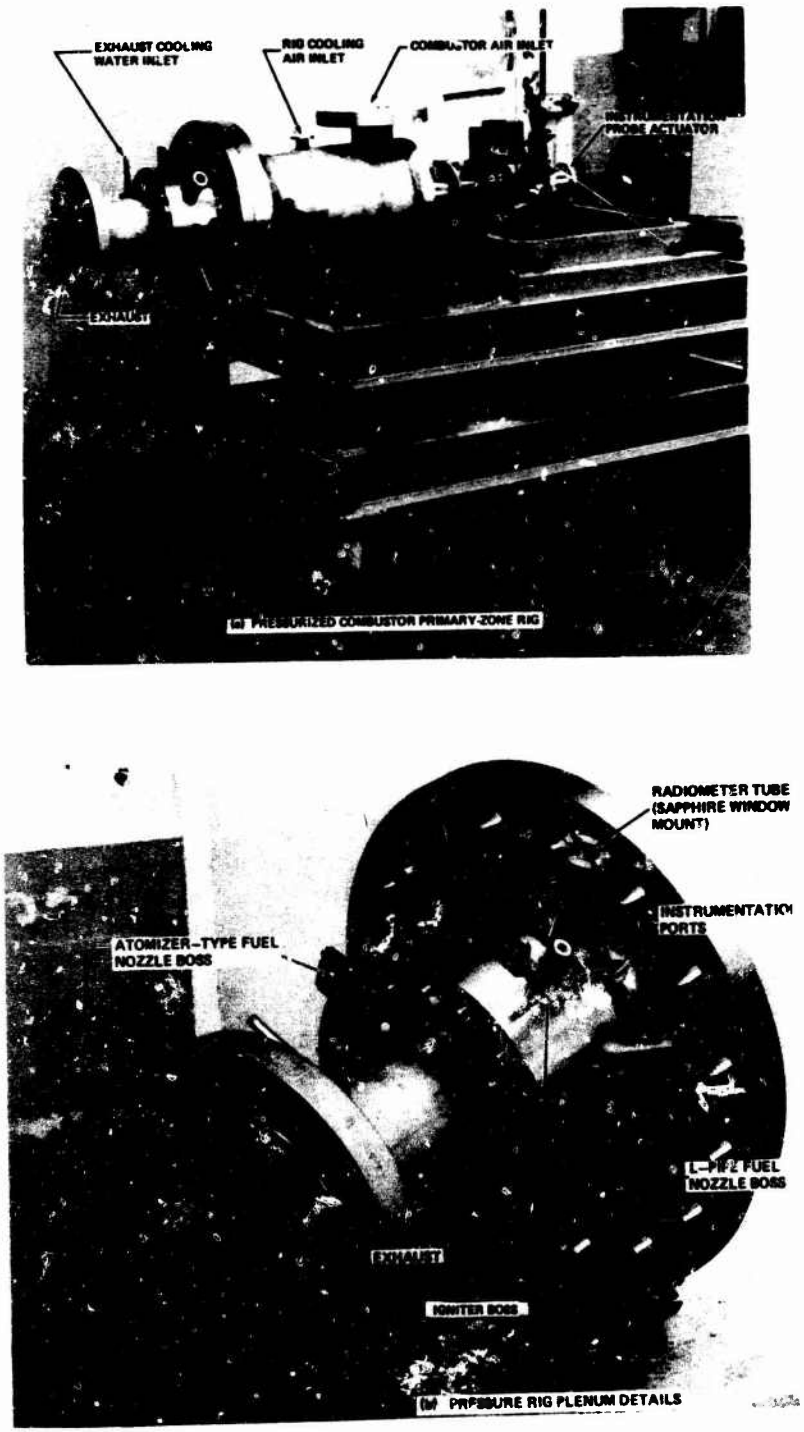


Figure 87. Pressurized Combustor Primary-Zone Rig Hardware.

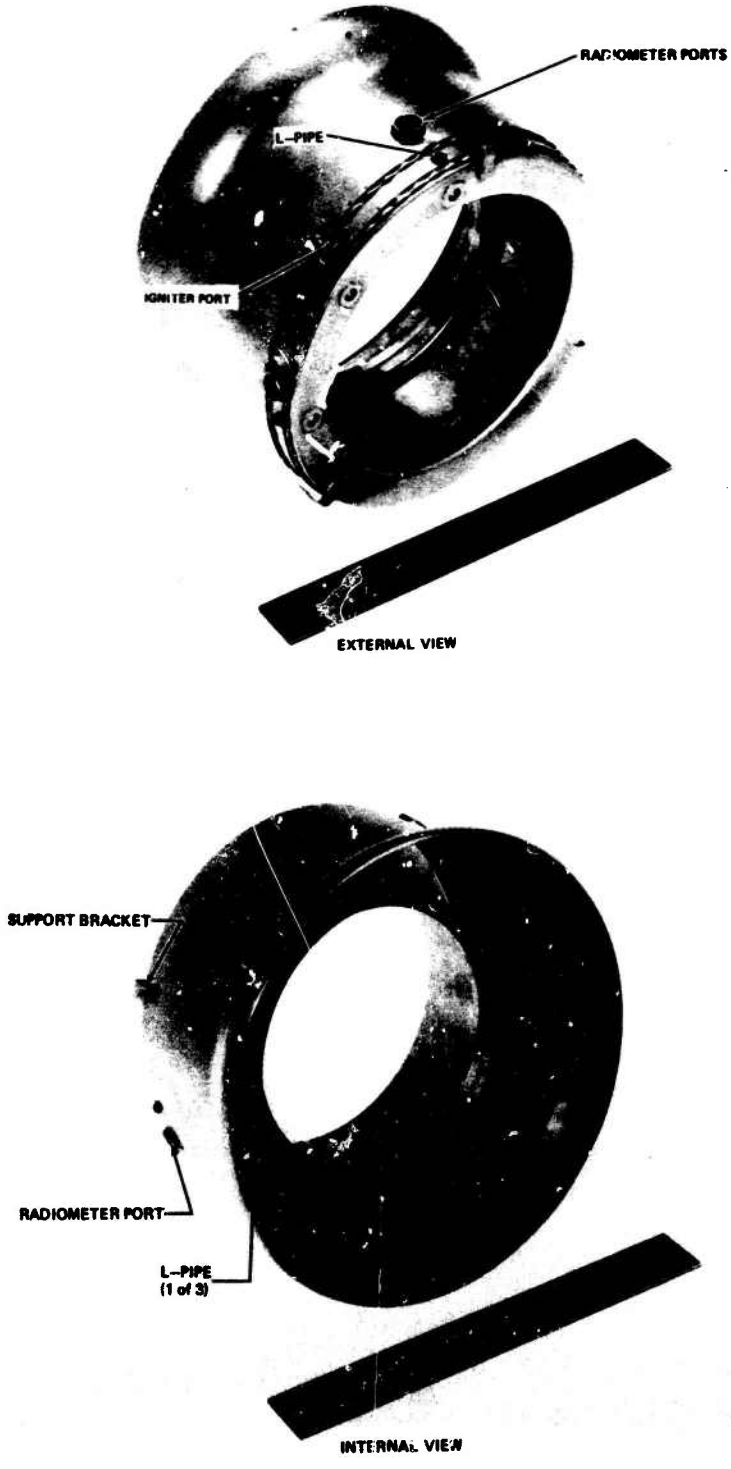


Figure 88. L-Pipe Combustor Primary-Zone Sector.

- o Air-assist and pneumatic-impact primary-zone sector, shown in Figure 89. (The same primary-zone sector was used for both fuel nozzle types.)

- o Air-assist fuel nozzle assembly, shown in Figure 90.

- o Pneumatic-impact fuel nozzle assembly, shown in Figure 91.

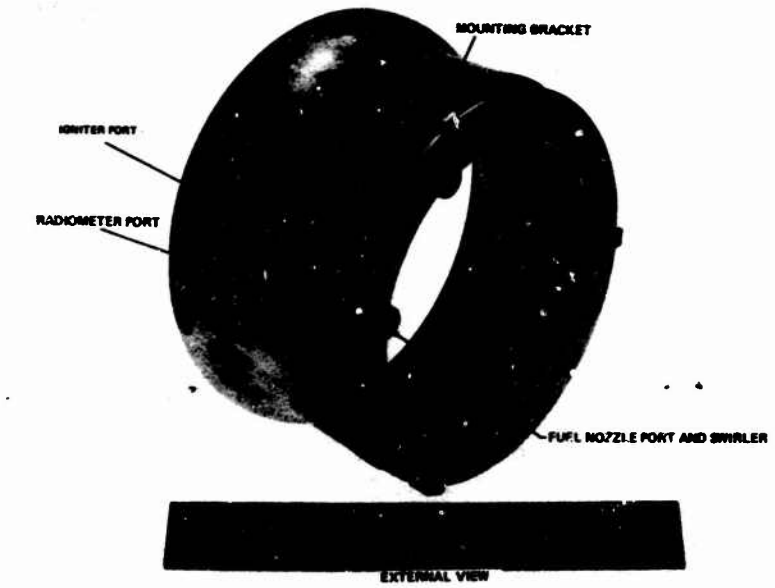
5.1.2.4.2 Test Results

Initial testing was conducted with each section in an atmospheric rig to visually observe flame location and quality. The L-pipe primary-zone sector was subsequently tested in the pressure rig.

Atmospheric testing of the air-assist atomizer primary zone was conducted with air-assist pressure varying from 0 to 30 psi. A value of 10 psi was considered optimum and was used for the major part of the tests. Results showed a lack of stability, and high fuel-air ratios were required to distribute the flame completely throughout the sector (indicating the possible need for reduced fuel nozzle spacing). Testing with thermal paint indicated liner wall local temperatures in excess of 1700°F. Similar overheating problems were encountered with the pneumatic-impact nozzle tests. It was suspected that the liner overheating in both cases was due to fuel droplets reaching the liner wall and burning at this location.

With the pneumatic-impact nozzle, tests showed good stability and flame quality without air preheat. With the addition of preheat, however, pulsing and instability resulted. This could be caused by some fuel evaporating in the nozzle fuel tube prior to discharge into the venturi. The fuel tubes were insulated and retested, but no improvement was observed.

An attempt to reduce droplet impingement on the walls and to increase recirculation and stability within the pneumatic-impact/air-assist sector was made by including a 10-vane radial swirler system, shown in Figure 92. Results obtained with these radial swirlers, using JP-4 and JP-5 fuel, indicated improved (and almost identical) light-off and stability performance for both the pneumatic-impact and air-assist systems. Flame quality was improved, particularly in the case of the air-assist system, which exhibited a well-formed, nonluminous flame. The pneumatic-impact system produced a slightly poorer formed and more luminous flame. In neither case were wall temperatures reduced to an acceptable level.



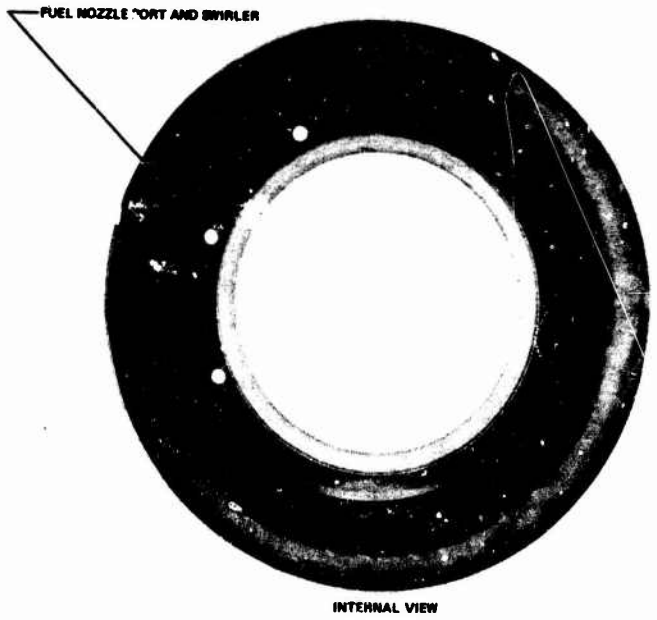


Figure 89. Annular Combustor Primary-Zone Segment for Air-Assist and Pneumatic-Impact Fuel Nozzles.

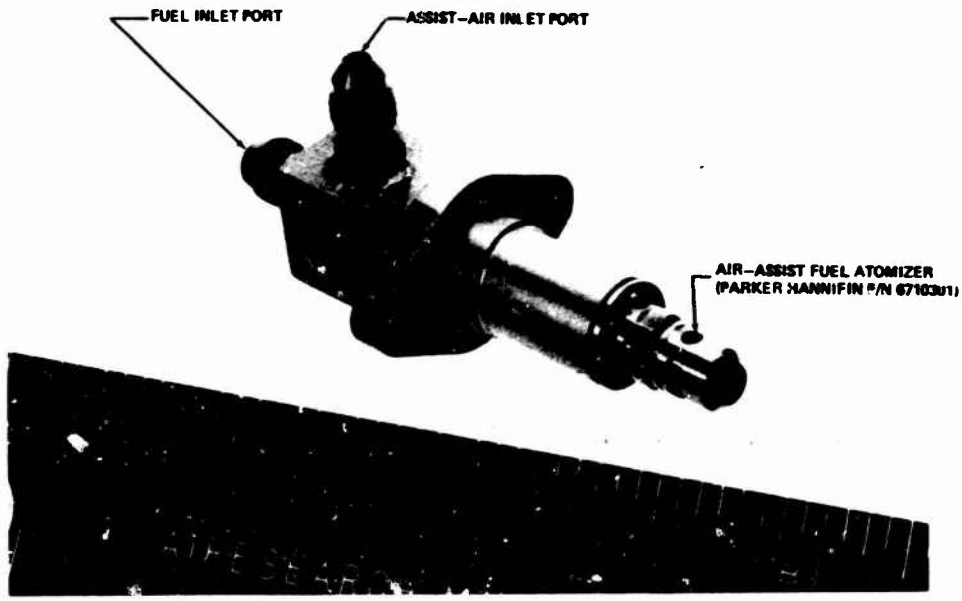


Figure 90. Air-Assist Fuel Nozzle Assembly.

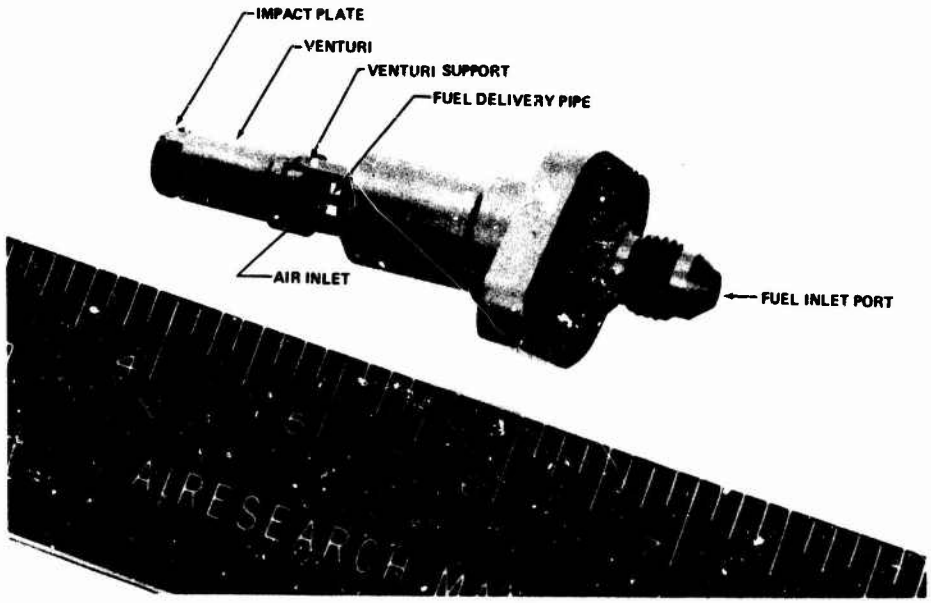


Figure 91. Pneumatic-Impact Fuel Nozzle.

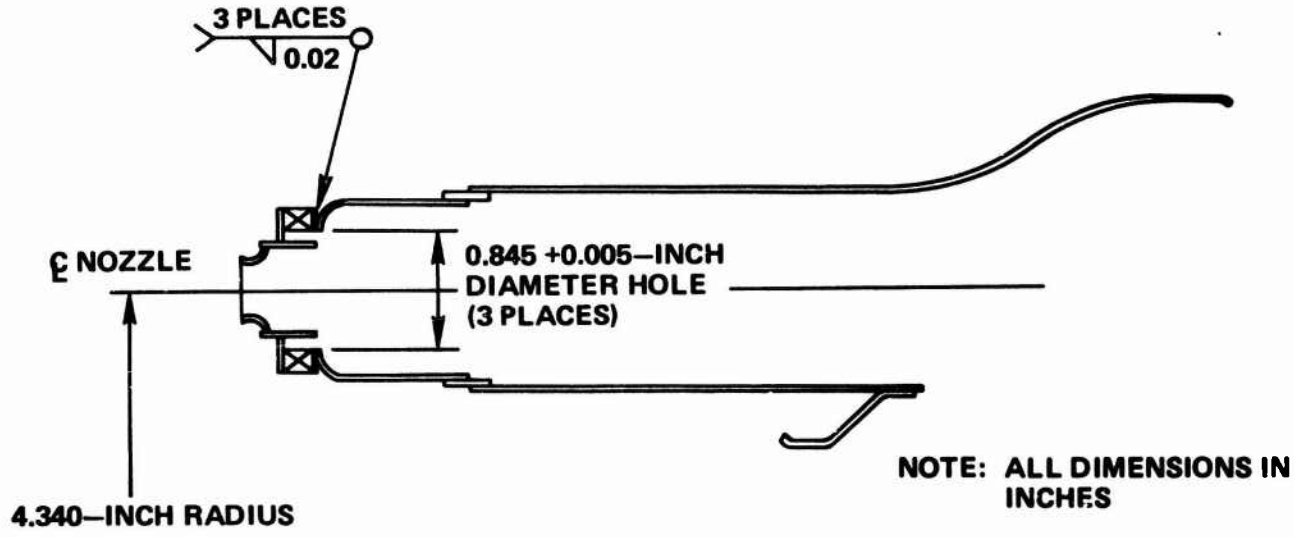


Figure 92. Radial Swirler System on Modified Pneumatic-Impact/Air-Assist Nozzle Section.

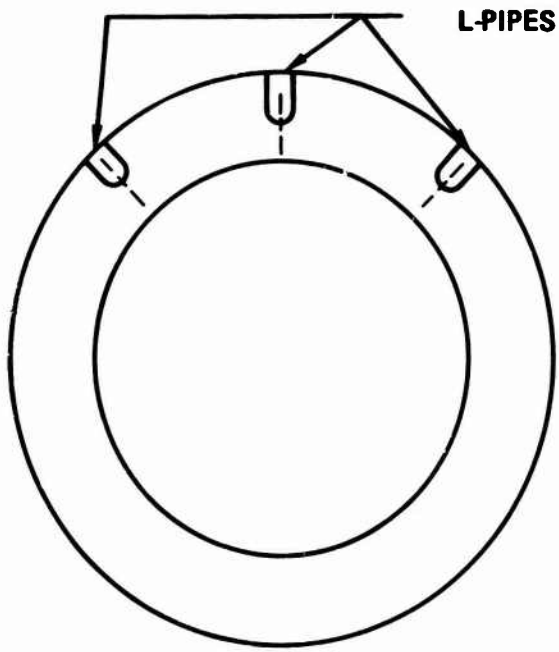
Fuel distribution observations using the L-pipe sector indicated that significant gravity effects were present in both the L-pipes and on the back wall of the dome. Fuel could be seen dripping from the L-pipe discharge, and the fuel that reached the dome from the L-pipes (situated at the top of the annulus, Figure 93) spread downward until it completely covered the rear wall of the dome.

Tests with combustion resulted in problems at low fuel flows. These were due to the lack of flame propagation to the three nozzles. At high fuel flows, however, the combustor burned as a full annular system, with the flame propagating throughout the annulus and not being contained, as intended, in the vicinity of the three injectors.

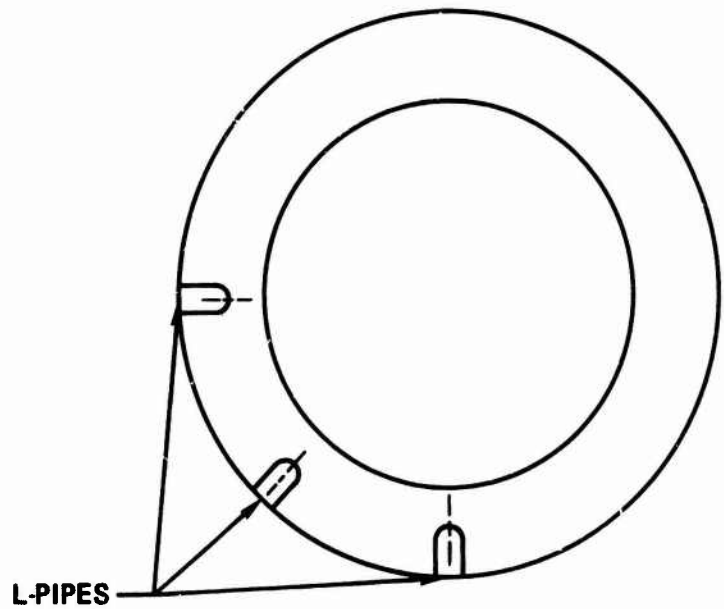
Air preheat of 550°F did not provide sufficient evaporation of the film to limit this spreading. Lean-blowout tests showed a lack of stability in the system and indicated the necessity for a design change.

The modification made was to insert axial swirlers in the dome back wall in line with each L-pipe, as shown in Figure 94. This modification was designed to create a low-pressure region at the center of the swirlers and, thus, provide some increased recirculation and stability. This also resulted in an effectively increased pressure drop across the L-pipe to assist in overcoming the gravity effects on the fuel at the L-pipe discharge. Atmospheric testing of this configuration showed that stability and flame quality were significantly improved and that the flame was within the boundaries of the sector as intended. Further testing with this combustor was therefore conducted in the pressure rig.

Initial temperature profile mapping was conducted with the L-pipe segment at a pressure of 1 atmosphere using the water-cooled Pt/Pt10%Rh thermocouple. The primary purpose of this test was to provide data for the calibration of the modified double-sonic probe. The results obtained showed an acceptable circumferential temperature distribution and an almost flat radial profile. However, fuel flow requirements for stable combustion were found to be more than twice those measured previously in the atmospheric rig. Possible causes for this difference were noted, and each was individually checked. Results from this series of checks indicated that when cooling water was added to the probe and rig cooling air was used to back-pressure the discharge blast shield, a reduction in lean stability was experienced. However, this lean stability reduction was not sufficient to fully explain the large fuel flow required. The only remaining possibility was that the orientation of the fuel delivery tubes relative to gravitational effects was the cause.



(a) ORIENTATION DURING ATMOSPHERIC RIG TESTS



(b) ORIENTATION DURING INITIAL PRESSURE RIG TESTS

Figure 93. L-Pipe Orientation During Atmospheric Rig and Pressure Rig Test.

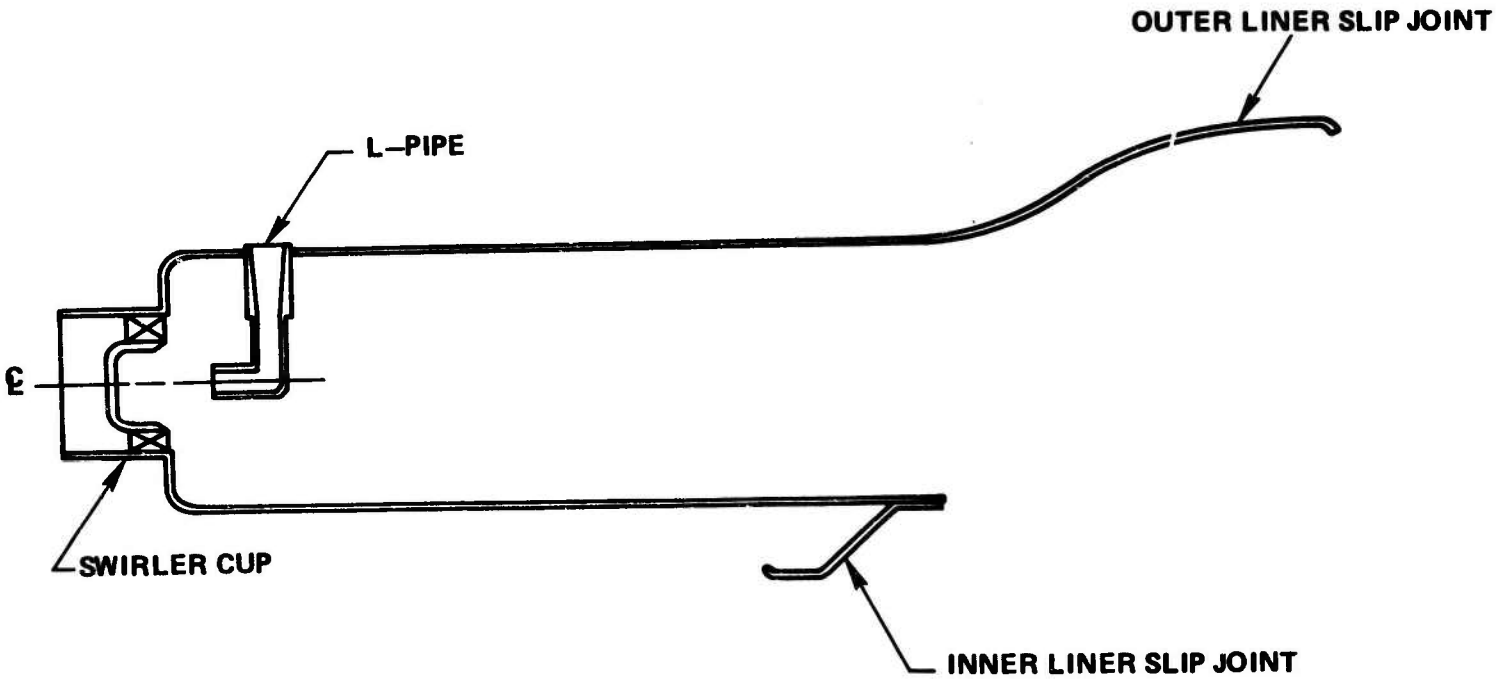


Figure 94. L-Pipe Combustor Modified With Air Swirlers.

Testing in the atmospheric rig had been undertaken with the center L-pipe in the vertical position and the other two fuel pipes positioned at 45 degrees to the right and left of this vertical fuel pipe, as depicted schematically in Figure 93. In this configuration, all the fuel tubes had some gravity assistance in transporting the fuel through the L-pipe. Testing in the pressure rig had been undertaken with the sector turned through 135 degrees (Figure 93--i.e., with one fuel tube "upside down," one fuel tube horizontal, and the center fuel tube between these two, at 45 degrees to the vertical and horizontal). With the lack of gravity assistance, the possibility existed that the fuel was backing up in the L-pipe and running around the outside of the combustor. Disassembly of the rig and inspection of the combustor revealed fuel stains at the lower swirler location and around the cooling slots. In addition, the swirler and a small portion of the cooling band were melted.

The damaged swirler was replaced, the cooling slot repaired, and the rig reassembled with the sector positioned with the center fuel tube vertical, as in Figure 93. A further precaution was taken by extending the length of the fuel delivery tubes such that the tube discharge location within the L-pipe was almost at the L-pipe 90-degree bend. Stability testing repeated the results previously obtained in the atmospheric rig, indicating no fuel backup.

Ignition and blowout tests conducted with the inverted and noninverted tubes indicated that even with the longer fuel tube some fuel backup still occurred with the inverted L-pipes at pressure drops of about 1 percent.

5.1.3 Combustor Evaluation Tests

Subsequent combustor evaluation tests were conducted at inlet air pressures of 6 to 12 and 16 atmospheres and inlet air temperatures of up to 820°F. The objectives of the tests were:

- To obtain additional primary-zone temperature data
- To obtain velocity profile data to validate the flow-field model
- To measure flame radiation
- To determine ignition characteristics

Problems experienced throughout the testing included:

- Instrumentation failures due mainly to differential thermal expansions and cooling difficulties
- Combustor warpage due to only three-eighths of the combustor containing the burning zone.
- Difficulty in determining true sector fuel-air ratio
- Final failure of the combustor due to wall damage. This damage was due to the fact that only a sector of the combustor contained flame, thus causing high thermal gradients, uneven growth and eventually buckling of the liner.

5.1.3.1 Temperature Profiles

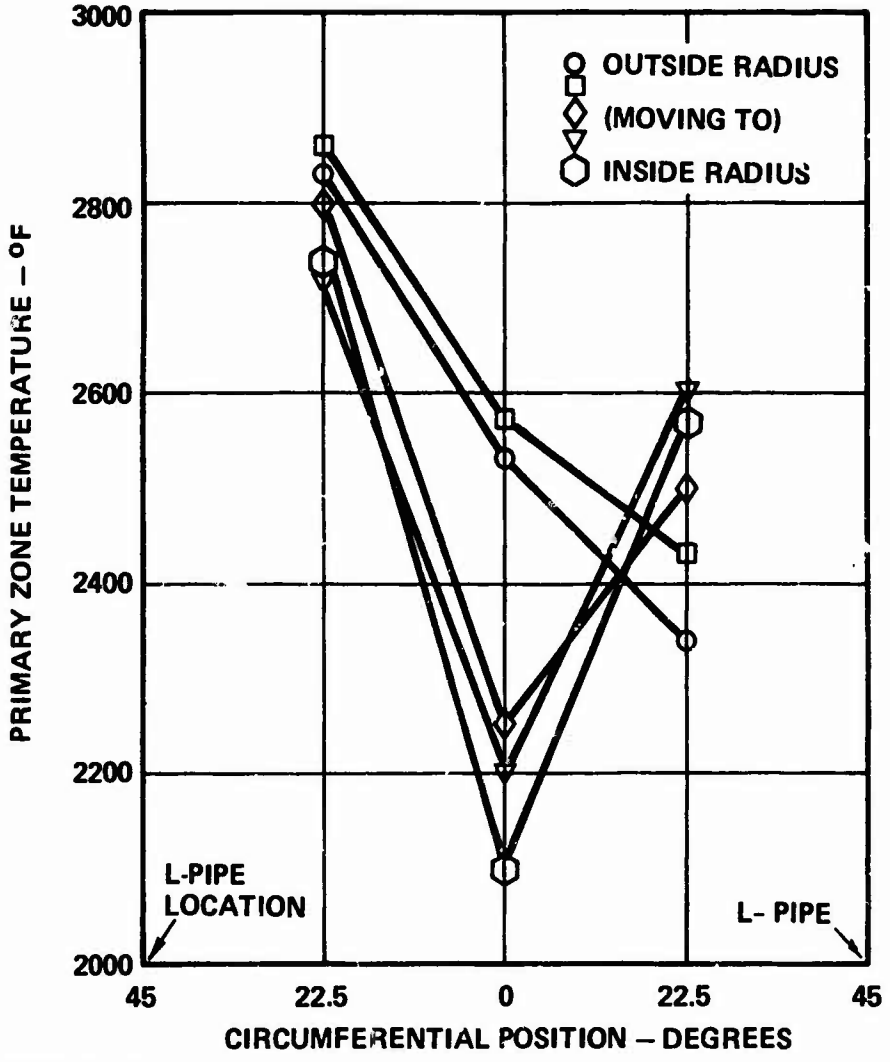
Temperature mapping was conducted using both the platinum/platinum 10 percent rhodium and the double-sonic probes. Readings were taken at the primary-zone exit plane and at three planes within the primary zone. The center L-pipe was mapped at positions in line with the L-pipe at 22.5 degrees on either side of the L-pipe. At each of these locations, five equally spaced probe positions were set across the height of the combustor. Typical data obtained are presented in Figures 95 and 96.

5.1.3.2 Velocity Profiles

Velocity mapping using the six-hole vector probe was conducted at locations corresponding to those mapped with the temperature probe, to facilitate local density calculations. Typical profile data obtained are presented in Figures 97 and 98. At 1 atmosphere a strong recirculation zone extends from beyond the primary-zone discharge plane to the dome. Data obtained at 6 atmospheres showed a strong recirculation zone at the discharge plane (4 inches down from the dome rear wall) but no recirculation at a plane 1 inch down from the dome wall.

5.1.3.3 Analytical Predictions

Initial predictions for the primary-zone flow failed to converge, and for this reason it was necessary to introduce a blockage into the flow field. This blockage effectively simulates impinging dilution-zone jets with some of the dilution air then recirculating into the primary zone, as shown schematically in Figures 99 and 100.



W_a = 12.4 LB/MIN ($\Delta P/P$ = 0.03)

W_f = 16.8 LB/HR (JP-4)

T_3 = 510°F

Figure 95. Temperature Traverse Data for L-Pipe Plus Swirler Primary Zone (Axial Position Is at the Exit Plane).

W_a = 12.4 LB/MIN ($\Delta P/P = 0.03$)

W_f = 16.8 LB/HR (JP–4)

T_3 = 510°F

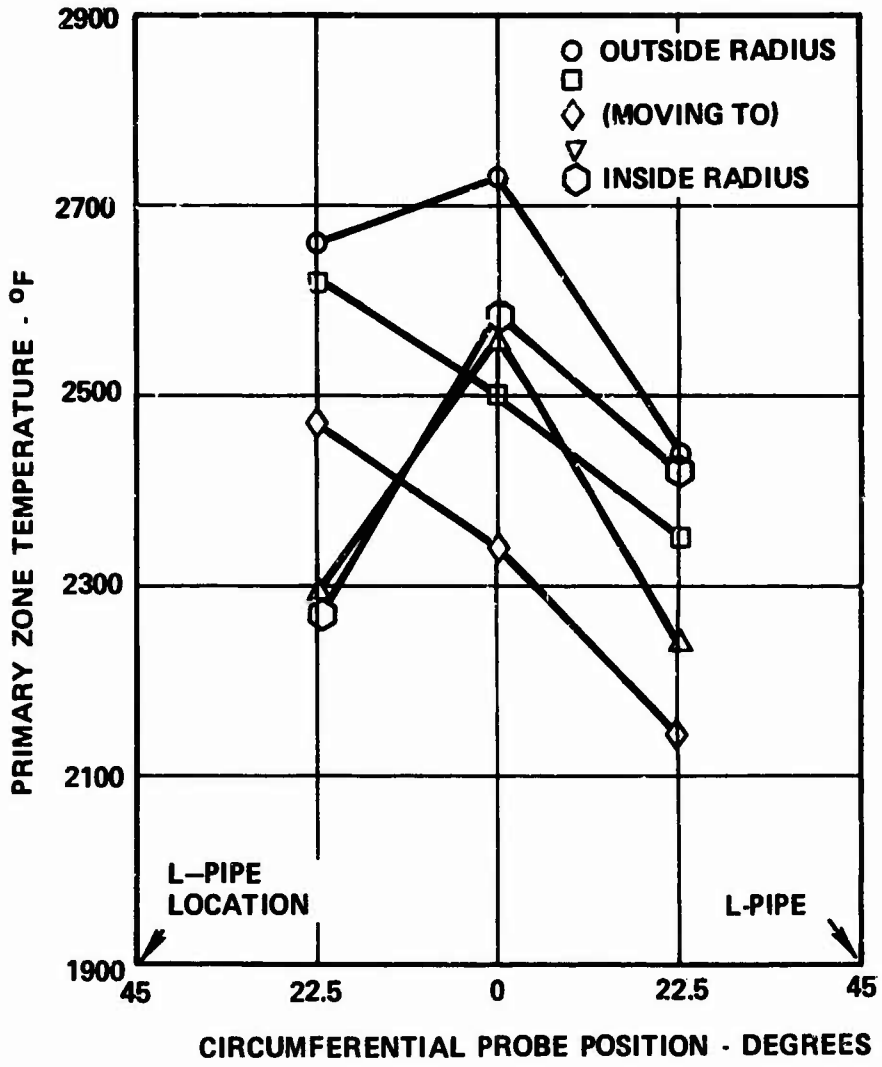


Figure 96. Temperature Traverse Data for L-Pipe Plus Swirler Primary Zone (Axial Position Is 3.0 Inches in From Exit Plane).

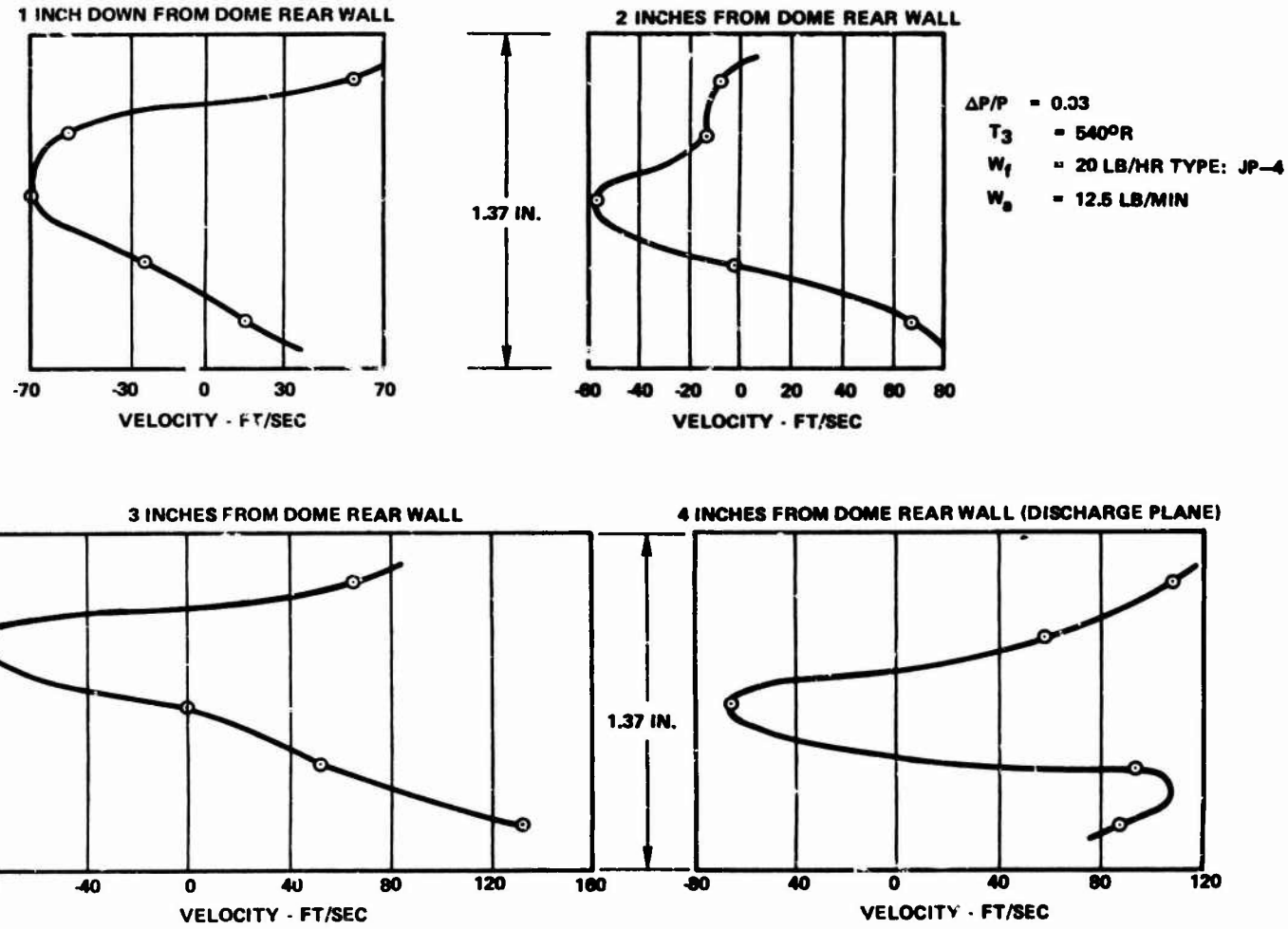


Figure 97. L-Pipe Primary-Zone Axial Velocity Profiles at 1 Atmosphere (In Line With Swirler).

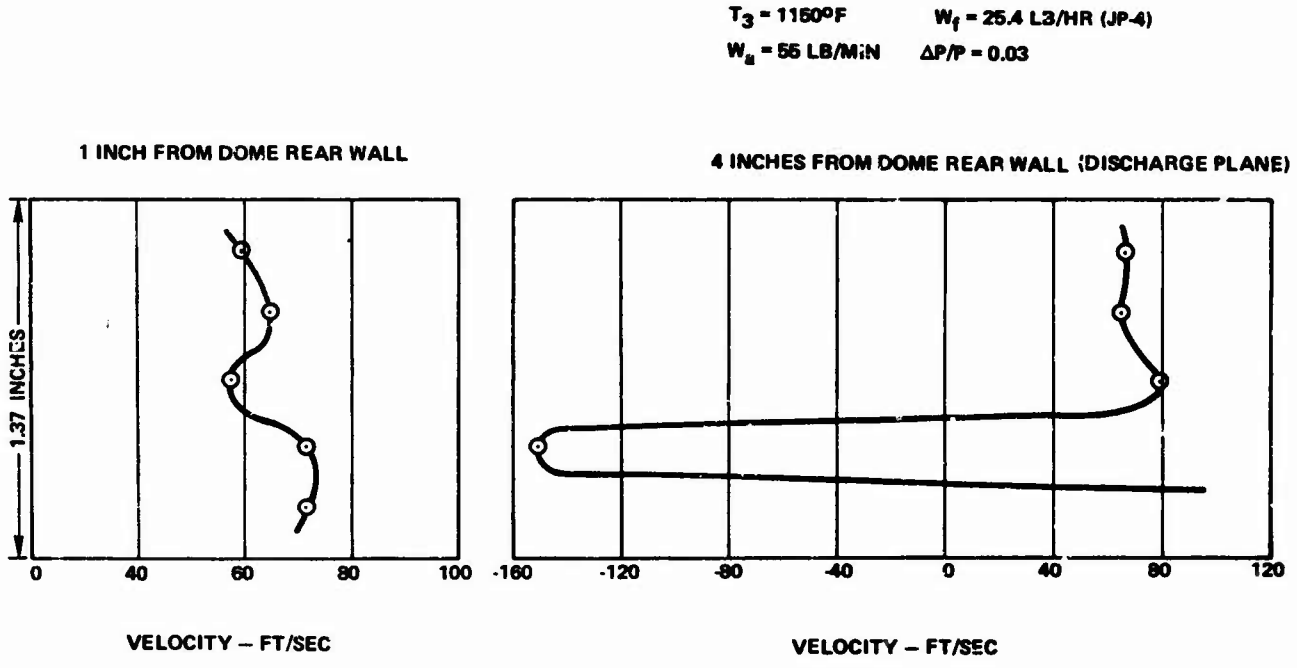


Figure 98. L-Pipe Primary-Zone Axial Velocity Profiles at 6 Atmospheres (In Line With Swirler).

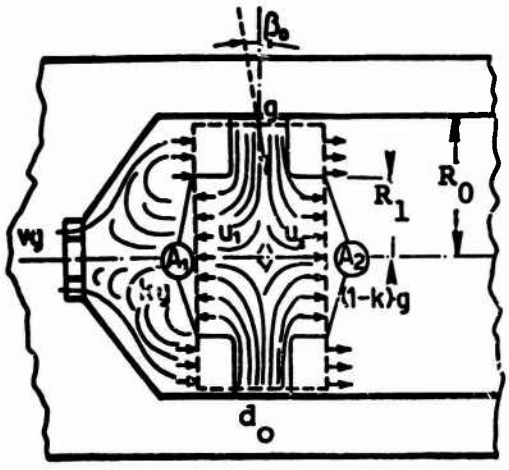


Figure 99. Impingement Jet Profiles.

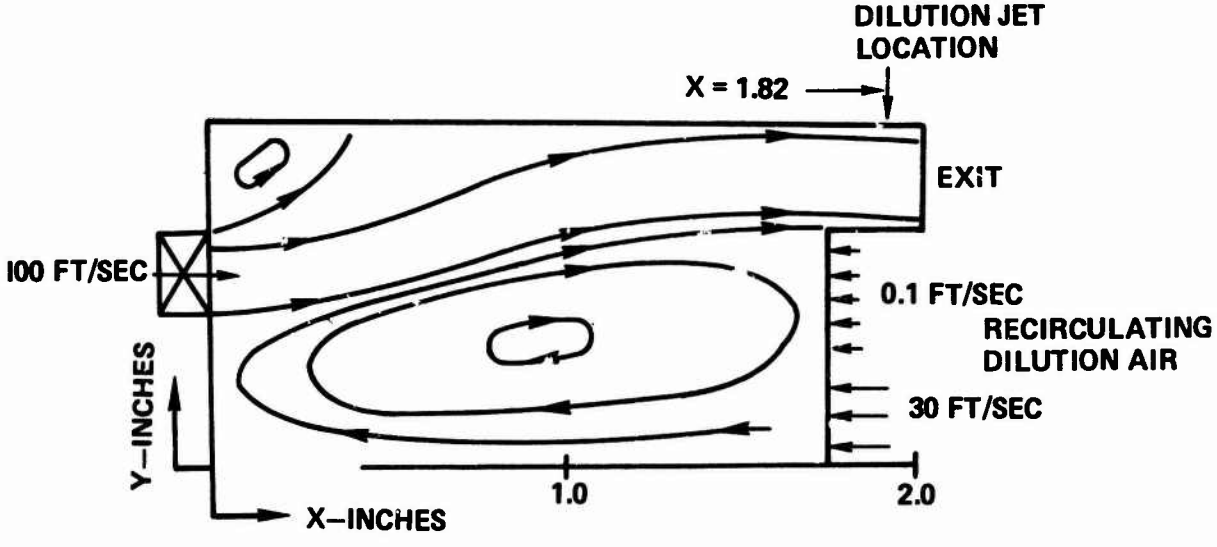


Figure 100. Primary-Zone "Blockage".

Figures 101 and 102 show typical analytical velocity and temperature profiles predicted at planes located 0.3 inch and 1.58 inches down from the back wall of the dome. The profiles show axial components for both cold flow and flow with combustion of a premixed fuel-air mixture (fuel-air ratio = 0.062). The velocity profiles obtained in this manner compare qualitatively with those obtained experimentally at 1 atmosphere in the L-pipe primary zone shown in Figure 97.

The analytical temperature profiles predicted are not directly comparable with the experimentally obtained profiles, since the solution does not account for hot gas entrainment into the dilution air and the experimental system was neither premixed nor at the same fuel-air ratio.

5.1.4 Conclusions

The following conclusions were drawn from the primary-zone testing and analytical modeling:

(a) With water model testing, good agreement can be obtained between analytical predictions and physical flows using the two-dimensional finite-difference technique.

(b) Instrumentation for internal mapping of combustors is a problem because of the high thermal gradients and cooling problems encountered.

(c) True two-dimensionality in a combustor is extremely difficult to attain.

(d) Fuel atomization systems for low-dome-height combustors must be designed to prevent atomized fuel from impinging on liner surfaces.

(e) L-pipe fuel-injection systems in low-airflow, low-pressure-drop combustors present the problem of fuel backing up in the pipe.

(f) Modeling of an uncontained primary zone is not practical, since it is not a realistic system for testing. An effective downstream blockage simulating the dilution zone is required to obtain convergence.

(g) The primary-zone analytical model is sensitive to grid size and spacing.

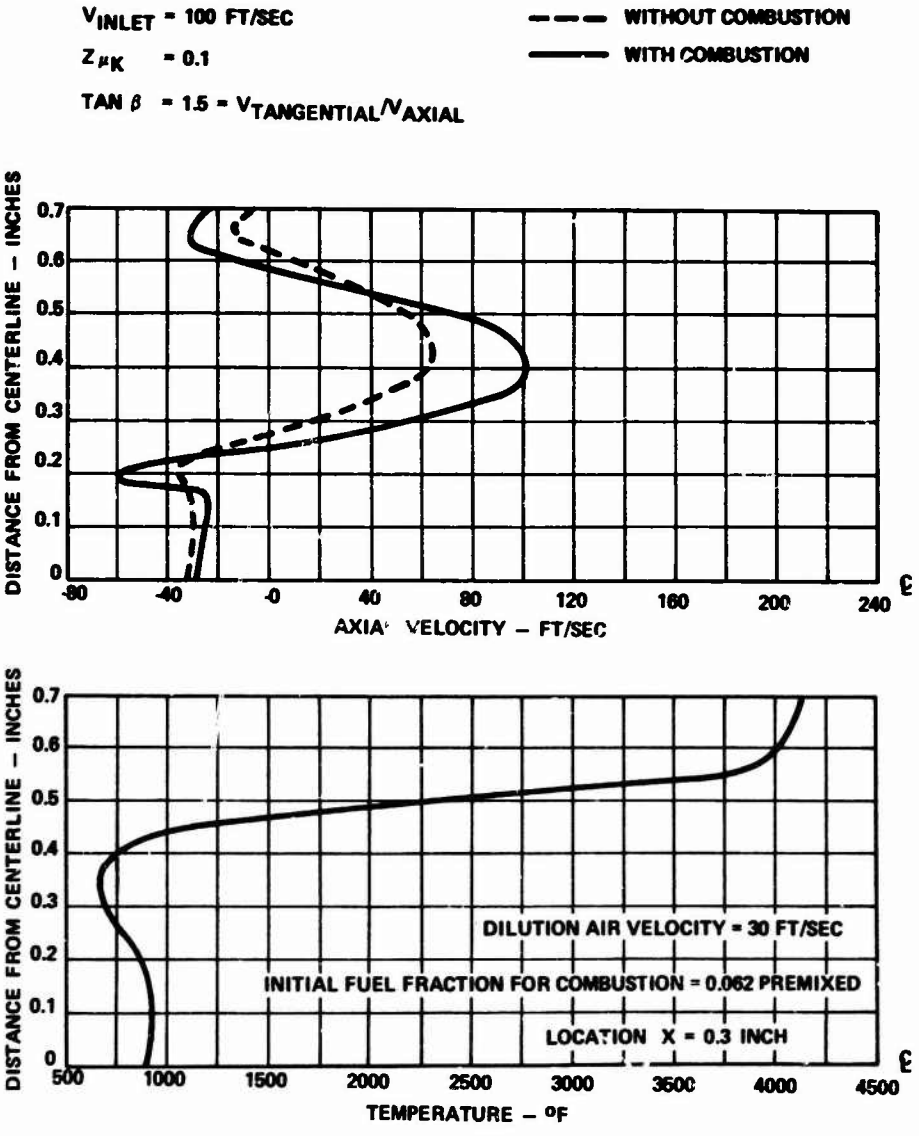


Figure 101. Primary-Zone Velocity and Temperature Profiles (Predicted).

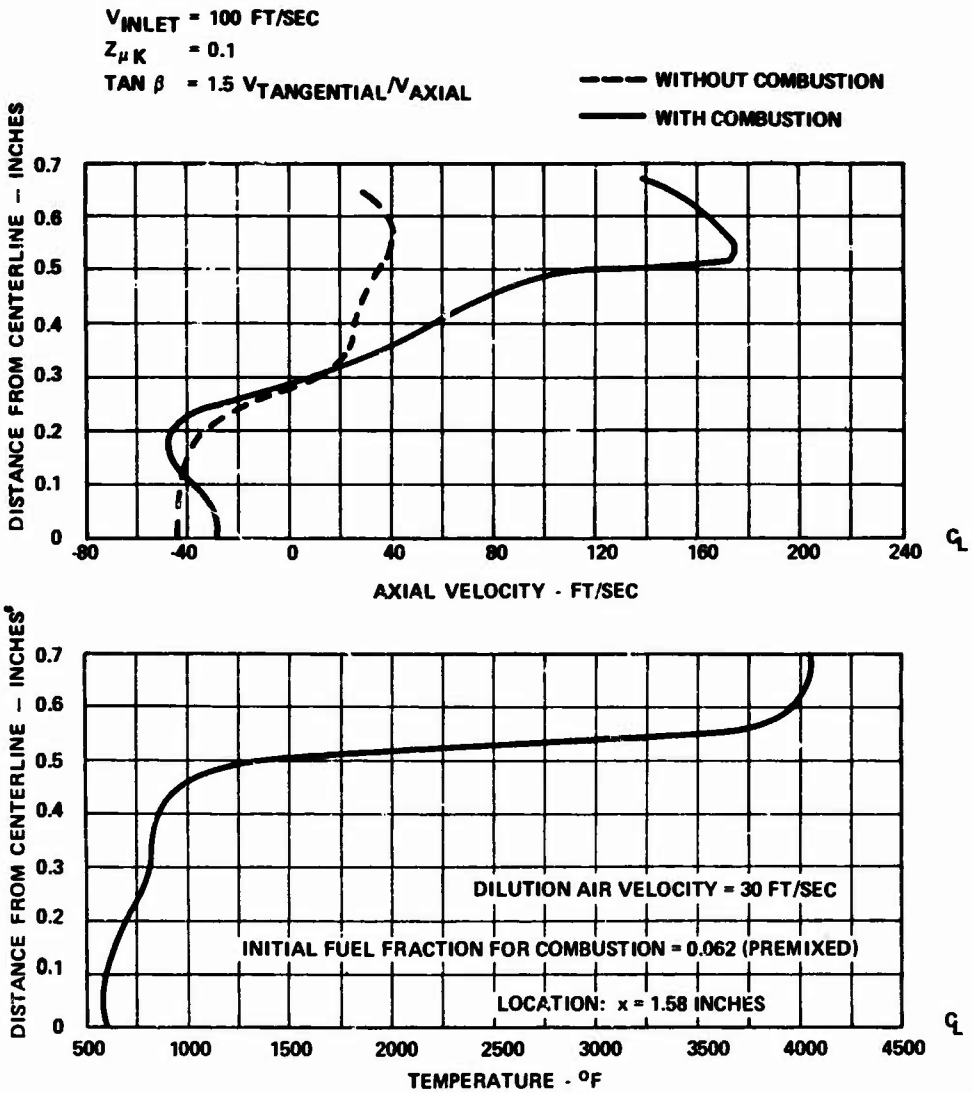


Figure 102. Primary-Zone Velocity and Temperature Profiles (Predicted).

(h) A more realistic viscosity model is required to more exactly model the primary zone analytically.

5.2 PRIMARY-ZONE IGNITION ENERGY REQUIREMENTS

The majority of gas turbine engines use spark ignition systems of the high-tension capacitance-discharge type. Low-tension exciters in conjunction with shunted surface gap igniters may become more desirable as igniter durability is improved. These low-voltage systems offer significant reductions in condenser size, cost, and EMI output; unlike the air-gap igniters, they are not subject to spark suppression as a result of increased operating pressures.

Generally, 20 to 30 percent of the exciter-stored energy can be delivered to the igniter. Here, the energy is further dissipated into noise and electromagnetic radiation; the remainder is finally delivered as thermal energy. For this analysis, the assumption was made (based on work by Watson)[45] that 2 percent of the ignition system stored energy is delivered in the form of thermal energy.

5.2.1 Ignition Model Equation

The development of the ignition model followed the analysis of Lefebvre[46] in which a spark-ignited spherical volume (kernel) of a critical size was defined, based on the heat release from the flame surface of the kernel and the heat loss. The critical size kernel of diameter d, ft, can be defined by

$$d = 32400\ Tu^{1.67}\ U^{0.67} / P_3^{0.85}\ T_3^{0.93} \qquad (79)$$

where Tu = turbulence intensity at the flame surface
U = mixture velocity, ft/sec
P_3 = inlet pressure, lb/ft^2
T_3 = inlet temperature, °R

The diameter can then be related to the minimum ignition energy, E_{min}, required by assuming that this energy equals the heat necessary to bring the kernel up to spontaneous ignition temperature, T_{sp},

$$E_{min} = \frac{\pi d^3}{6} \rho_{sp}\ C_p\ (T_{sp} - T_3) \qquad (80)$$

where

$$\rho_{sp} = P_3 / R\ T_{sp}$$

Then,

$$E_{min} = \frac{\pi d^3}{6}\left(\frac{P_3 C_p}{R}\right)\left(1 - \frac{T_3}{T_{sp}}\right) \quad (81)$$

Neglecting T_3 / T_{sp},

$$d = [6RE/\pi C_p P_3]^{1/3} \quad (82)$$

Combining Equations (79) and (82) and solving for E,

$$E_{min} = 146 \times 10^{12}\ Tu^5\ U^2/P_3^{\ 1.55}\ T_3^{\ 2.79} \text{ joules} \quad (83)$$

The flammability limits of uniform mixtures of vaporized JP fuel and air are as follows: fuel to air mixture ratios of approximately 0.035 and 0.27 by weight,[47] as indicated in Figure 103. Overall mixture ratios greater than 0.27 are combustible when the fuel is present in liquid droplets (or the vapor is not mixed uniformly with the air, not considered in this analysis). The fuel carried by the airflow to the igniter will normally consist of both liquid and vapor; however, at low temperatures very little vapor will be present and the fuel will be in the form of droplets. Ignition of such mixtures requires that the energy input be sufficient to vaporize enough fuel to reach the flammability limit near the igniter. Figure 104 shows the strong dependence of vapor formation rate on the droplet size, thus indicating the critical requirement of including droplet size in the analysis. However, as can also be seen from Figure 104, droplets larger than approximately 50 microns will contribute very little vapor for combustion in the initial ignition process. For this reason only those droplets less than 50 microns can be considered significant in supplying vapor for ignition. In spray atomizers typical of use in gas turbines, 70 percent of the spray volume exists in droplets larger than the SMD. Hence, 30 percent of the total liquid fuel-air ratio at the igniter is used as a parameter multiplied by the factor $(50/SMD)^2$ to give the fuel-air ratio due to vaporization at the igniter. The factor $(50/SMD)^2$ varies with the droplet surface area, with the 50-micron size droplet being chosen as the maximum size that would completely vaporize in the spark and ensure combustion.

Inlet air and fuel temperatures will greatly affect the degree of vaporization of the liquid droplets injected by the nozzle ahead of the igniter. The fuel temperature influences the vapor fuel-air ratio at the igniter primarily through its effect on the liquid fuel viscosity and the resulting droplet size and distribution. The fuel and air temperature together affect the initial stage vaporization prior to arrival at the igniter location. An arithmetic average of the fuel and air

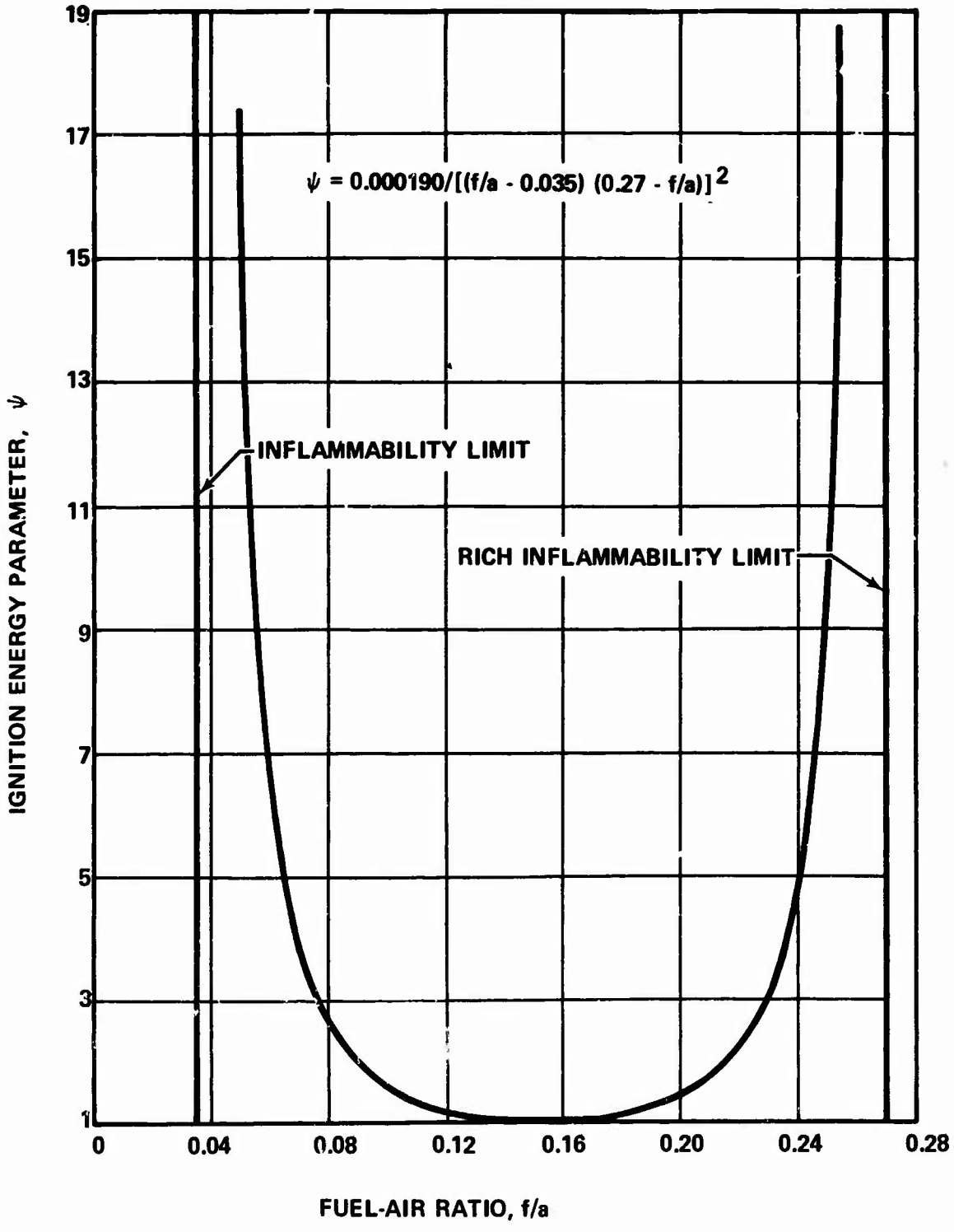


Figure 103. Ignition Energy Versus Fuel-Air Ratio for Jet Fuels.

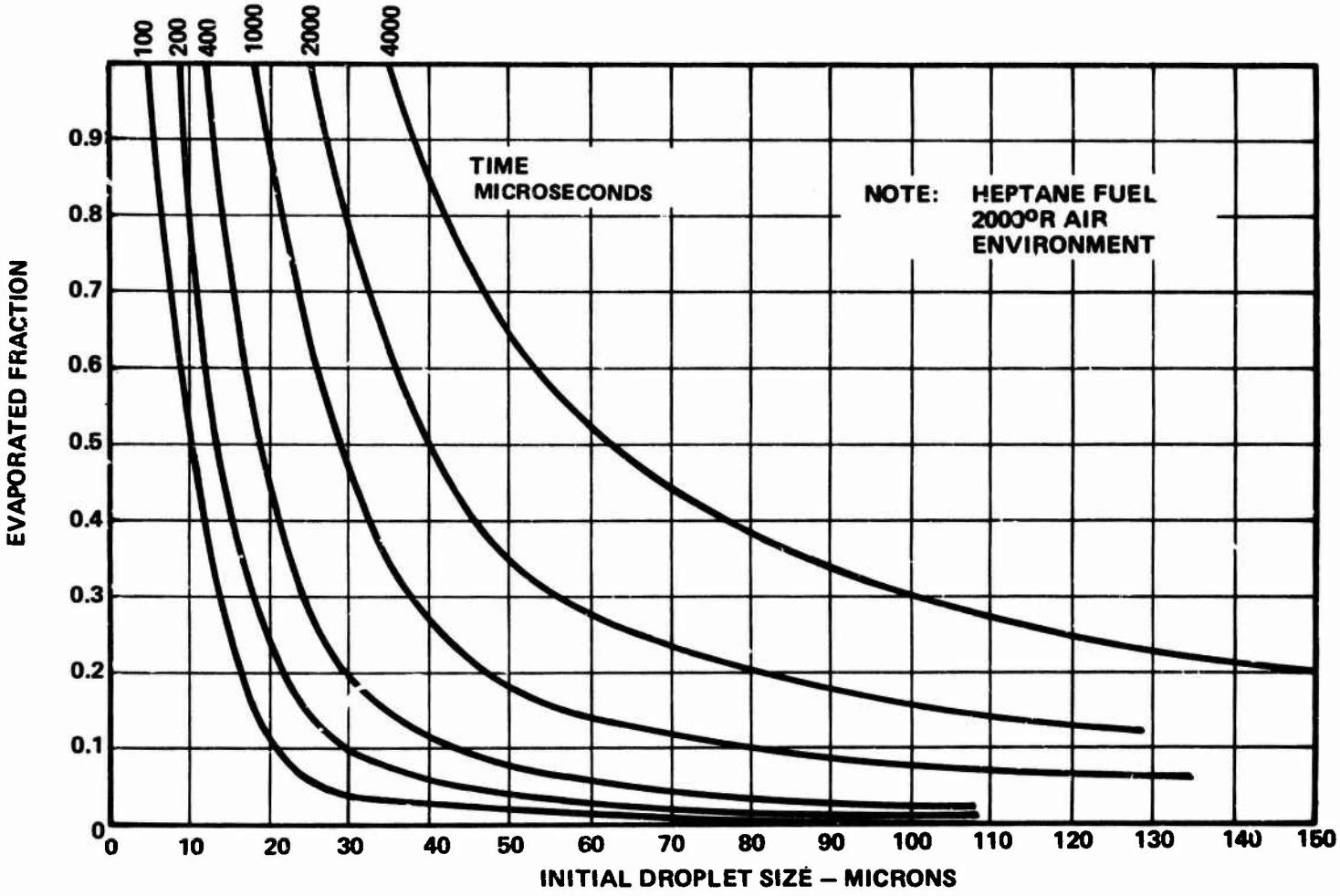


Figure 104. Evaporation Fraction of Fuel Droplets as a Function of Size and Time.

temperature is used to obtain the fuel vapor pressure prior to the igniter spark.

Based on the above considerations the initial vaporized fuel, F_{VAP}, including the effect of droplet size can be determined by

$$F_{VAP} = M_V P_V / M_a P_a + 0.3\, F_{liq} (50/SMD)^2 \qquad (84)$$

where M_V = molecular weight of the vaporized fuel

M_a = molecular weight of air

P_v = partial pressure of the vaporized fuel

P_{ap} = partial pressure of air

F_{VAP} = fuel-air ratio near the igniter

F_{liq} = primary zone fuel-air ratio

and by the general ignition energy equation wherein Equation (67) is used. The ignition energy parameter can be written as

$$E_{min} = 2.78 \times 10^{10}\, Tu^5 U^2 / P_3^{1.55} T_3^{2.79} \left[(F_{VAP} - 0.035)(0.27 - F_{VAP}) \right]^2 \qquad (85)$$

where Tu = turbulence fraction

Figures 105, 106, and 107 are typical of the curves obtained using the above equation. Figure 107 shows the effect of turbulence level on ignition energy requirements. The true fraction turbulence of the airflow at the igniter is not known but it is believed to be in the range of 0.02 to 0.04, when the spark and flame-generated turbulence is considered in addition to the basic airflow turbulence. A fraction turbulence value of 0.03 was used in obtaining Figures 105 and 106 in which stored ignition energy is plotted against liquid fuel-air ratio.

The shape of these curves can be compared directly with the combustion stability curve (Figure 103) for vaporized fuel-air ratio. The curves show that higher ignition energy is required as the mixture velocity increases. As droplet size decreases, approaching the rich limit, the greater number of small droplets for a fixed fuel volume results in an effective increase in the fuel-air ratio due to more evaporation. This then requires an increase in ignition energy. However, when approaching the lean limit the reverse is true and a lower ignition energy is required. An optimum liquid fuel-air ratio falls at

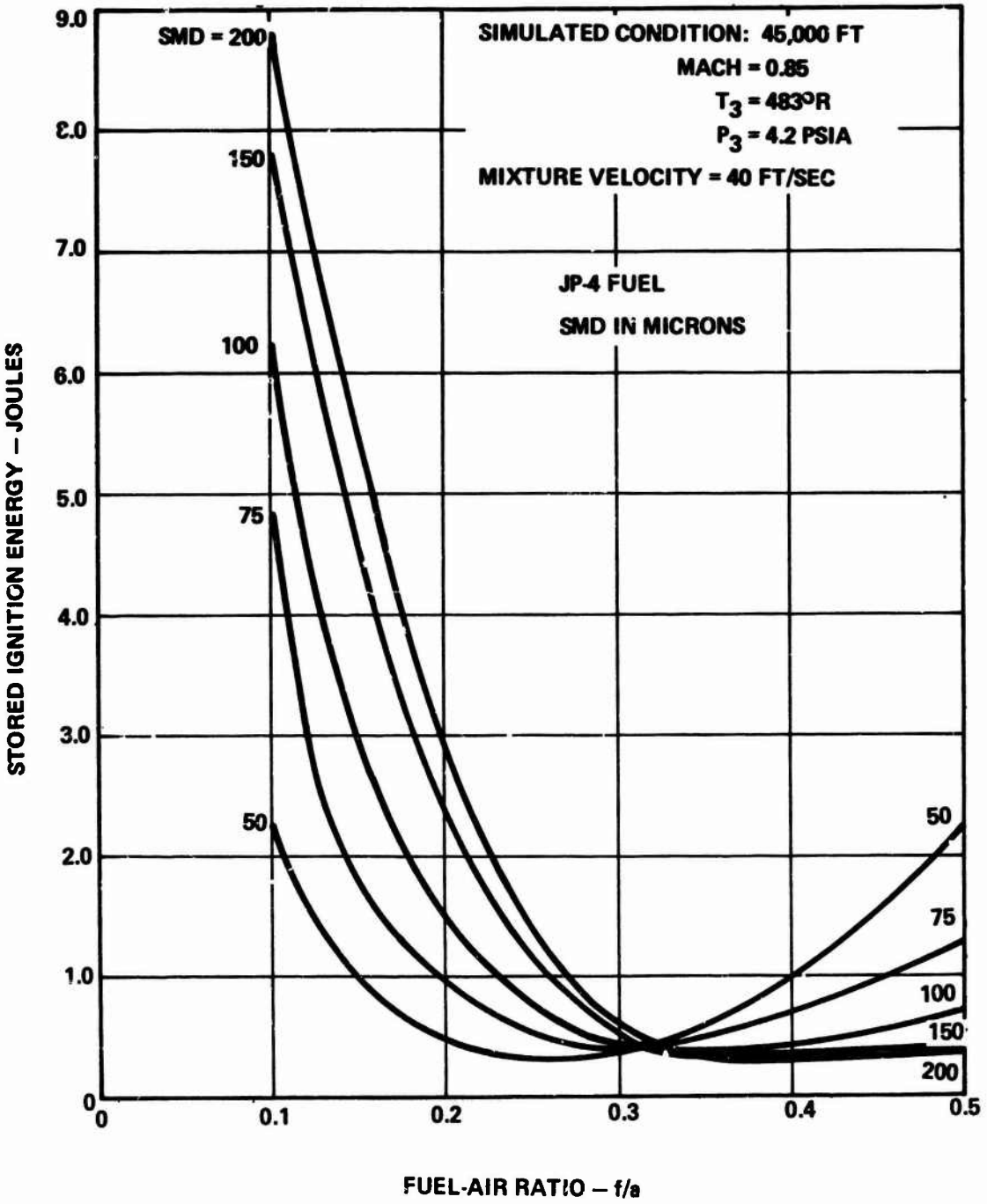


Figure 105. Predicted Minimum Ignition Energy Requirements for Primary Zone (Mixture Velocity is 40 ft/sec).

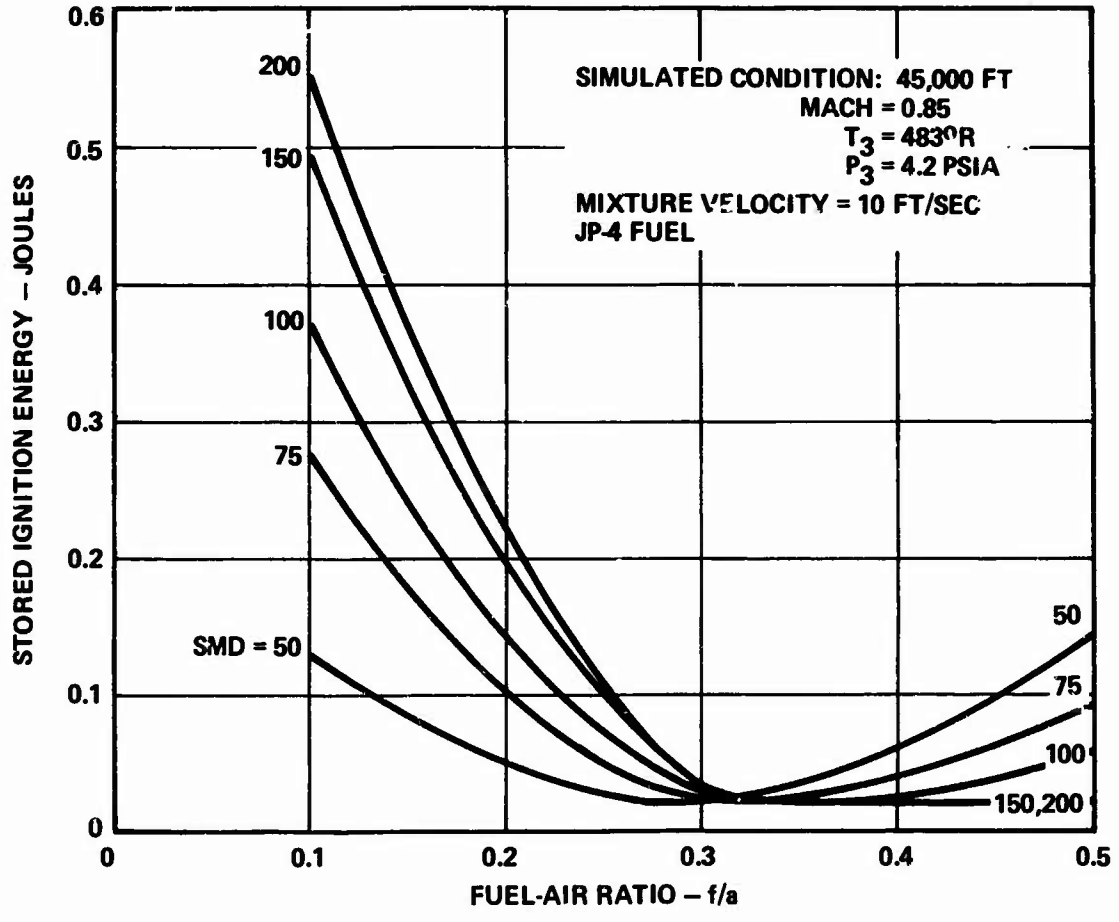


Figure 106. Predicted Minimum Ignition Energy Requirements for Primary Zone (Mixture Velocity Is 10 ft/sec).

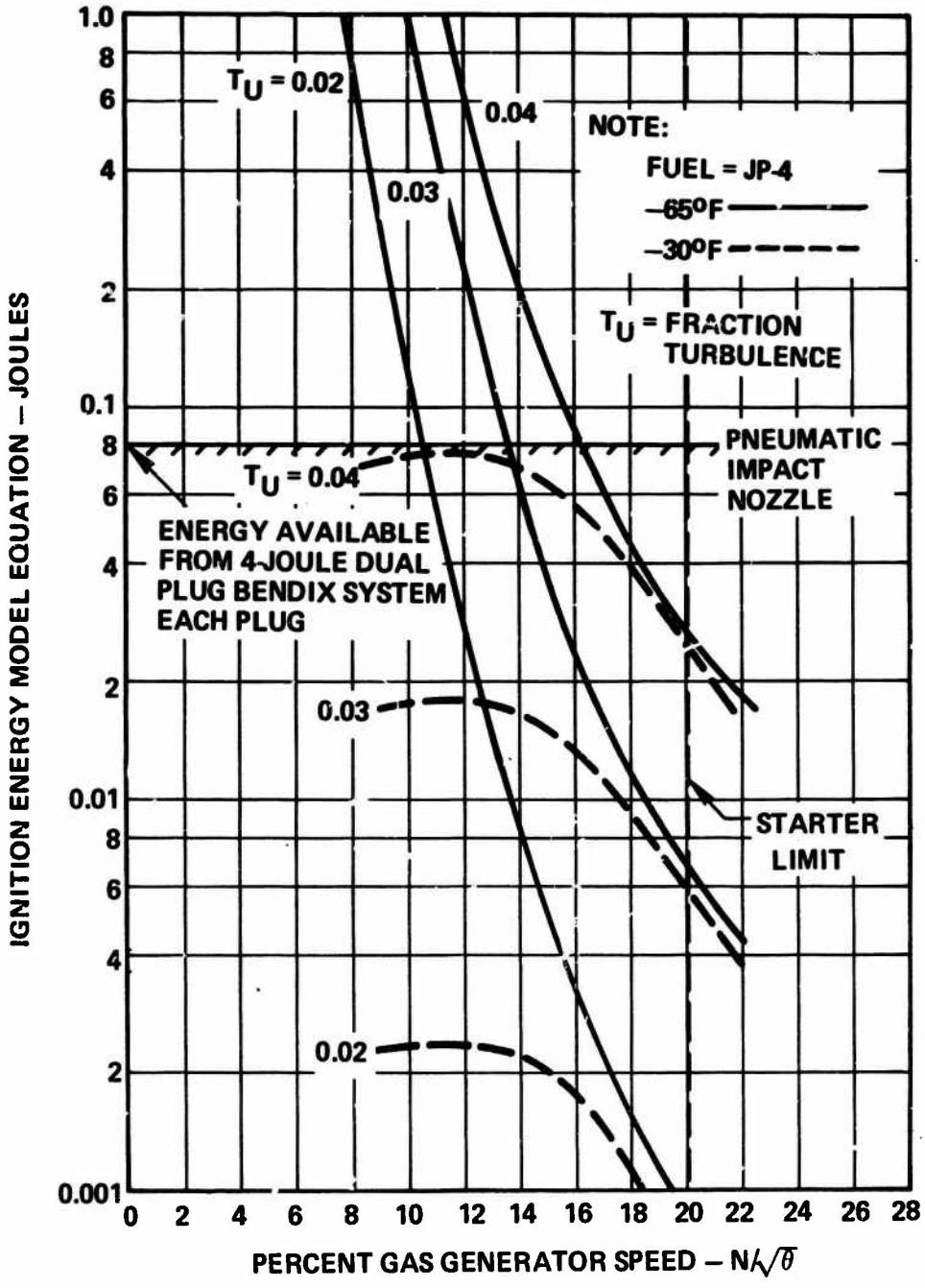


Figure 107. Combustor Ignition Energy Requirements.

approximately 0.32. Analytical results obtained for JP-5 and JP-8 fuels indicated that significantly higher ignition energies would be required for these fuels at the conditions given, and the SMD values should be below 150 microns.

5.2.2 Experimental Ignition Energy Requirements

Ignition data was obtained with the L-pipe plus swirler configuration described earlier in Section 5.1. The results, shown in Table XIII, were obtained by increasing the fuel flow rate with the igniter on until ignition was obtained.

The fuel flow required for this ignition was then preset and two more ignition checks were made with this preset fuel flow.

A maximum fuel flow for ignition was set at 60 pounds per hour and the maximum sparking duration was limited to 7 seconds.

The fuel flows listed are for three L-pipes only, whereas the airflows are total airflow to the full annulus (see discussion in Section 5.1.2). A rough overall test segment liquid fuel-air ratio can be determined by using a value of 47 percent of the total airflow quoted. This percentage represents the percentage of the total full annulus area located in the section, and includes swirlers and cooling band open area.

As shown, attempts to obtain ignition using JP-5 fuel were unsuccessful at the three airflow settings. Since the characteristics of JP-5 and JP-8 are similar, no tests were conducted for the latter fuel.

A parametric study was conducted to compare the experimental results with the analytical predictions. A direct comparison was not possible due to the lack of available input data, i.e., mixture velocity, SMD, local fuel-air ratio at the igniter and turbulence intensity. Assumed values for the parameters were:

Turbulence intensity fraction	0.03
Initial liquid fuel-air ratio	0.1, 0.3, 0.5
Mixture velocity (ft/sec)	10, 40
SMD (microns)	50, 150, 300

These values were selected to cover the range expected to exist in the configuration tested. The analytical results obtained, shown in Table XIV, predicted ignition capability with JP-4 fuel, and stored ignition energies of less than 12.5 joules were confirmed by experimental results. The single no-light experimental point (45,000 feet, Mach = 0.85, 4.26 joules stored energy) is predicted for 40 feet per second mixture velocity

TABLE XIII. IGNITION AND LEAN-LIMIT BLOWOUT DATA FROM L-PIPE PLUS SWIRLER PRIMARY ZONE

Test Conditions*	Stored Ignition Energy (Joules)	Ignition Fuel Flow (lb/hr)		Lean-Limit Blowout Fuel Flow (lb/hr)	
		JP-4	JP-5	JP-4	JP-5
1. Sea level static (Simulated)	4.26	29.0	No-light**	9.9	--
W_a = 24 lb/min	6.45	22.5	No-light		
T_3 = 170°F	10.31	25.0	No-light		
P_3 = 20.6 psia	12.49	19.5	No-light		
$\Delta P/P$ = 2.2%					
2. 25,000 feet, M = 0.0 (Simulated)	4.26	32.0	No-light	7.0	--
W_a = 8.4 lb/min	6.45	22.2	No-light		
T_3 = 76°F	10.31	24.2	No-light		
P_3 = 7.9 psia	12.49	17.0	No-light		
$\Delta P/P$ = 1.6%					
3. 45,000 feet, M = 0.85 (Simulated)	4.26	No-light	No-light	9.5	--
W_a = 6.6 lb/min	6.45	28.7	No-light		
T_3 = 72°F	10.31	29.8	No-light		
P_3 = 4.2 psia	12.49	29.6	No-light		
$\Delta P/P$ = 1.6%					

*Spark rate = 3 sparks/second
**"No-light" was concluded after unsuccessful ignition attempts at fuel flows up to 60 lb/hr.

TABLE XIV. IGNITION MODEL PREDICTIONS

SMD (microns)	Mixture Velocity (ft/sec)	Flight Condition Altitude (ft)	Mach Number	f/a = 0.1		f/a = 0.3		f/a = 0.5	
				JP-4	JP-5	JP-4	JP-5	JP-4	JP-5
50	10	0	0	L	L	L	L	L	L
50	10	25,000	0	L	L	L	L	L	L
50	10	45,000	0.85	L	L	L	L	L	L
50	40	0	0	L	L	L	L	L	L
50	40	25,000	0	L	X	L	L	L	L
50	40	45,000	0.85	L	X	L	L	L	L
150	10	0	0	L	X	L	L	L	L
150	10	25,000	0	L	X	L	X	L	L
150	10	45,000	0.85	L	X	L	X	L	L
150	40	0	0	L	X	L	L	L	L
150	40	25,000	0	L	X	L	X	L	X
150	40	45,000	0.85	L	X	L	X	L	X
300	10	0	0	L	X	L	X	L	L
300	10	25,000	0	L	X	L	X	L	X
300	10	45,000	0.85	L	X	L	X	L	X
300	40	0	0	L	X	L	X	L	L
300	40	25,000	0	L	X	L	X	L	X
300	40	45,000	0.85	L	X	L	X	L	X

L - Light Off
X - No Light
Stored Ignition Energy Limit = 12.5 Joules

and SMD values greater than 75 microns. Comparison with JP-5 analytical data was not possible, since no successful light-offs were obtained experimentally. The predicted light-off points for JP-5 do indicate that this will be the case unless the SMD values are below 150 microns.

5.2.3 Conclusions

The ignition model equation may only be used as a guide in determining the minimum ignition energy required for a particular system, due to the assumptions necessary in the input data. Mixture velocity and SMD can be calculated with some confidence, but the initial liquid fuel-air ratio in the region of the igniter, and particularly the turbulent intensity fraction, may be subject to considerable error.

6.0 DILUTION ZONE

The functions performed by the dilution zone are:

- Force containment of primary zone
- Reduce the bulk temperature of the gases from the primary zone to the required average turbine inlet temperature
- Mix with the primary products, reduce the temperature gradients, and trim the temperature profile and pattern factor (PF) to that required at the turbine inlet. However, the dilution zone cannot correct gross temperature gradients that can be produced by a poorly functioning primary zone.

The dilution-zone performance is dependent on the distribution and properties of the flow in the annulus surrounding the combustor and by the trajectories and mixing characteristics of the flow which enters the combustor through the dilution orifices. The dilution-zone analysis is comprised of the following models:

- An orifice discharge coefficient (C_D) and jet efflux angle model
- An annulus loss model
- A dilution jet trajectory and mixing model

The derivation of these models and dilution-zone element tests which were conducted to update and validate these models are presented in the following paragraphs. The computer program prepared for this analysis is presented in Appendix VI.

6.1 MODEL DEFINITION

6.1.1 Discharge Coefficient and Efflux Angle Model

The port (orifice) configurations used in a combustor design can be arranged into three basic categories:

- Flush port, with some flow bypassing the port
- Plunged port which is similar to the flush port but with a relatively large radius orifice

- o Scooped port which uses the airflow dynamic head to ram air into the orifice

Primary-zone components such as swirlers, primary pipes, and venturi sections are handled separately because the flow through these orifices is controlled more by geometry rather than by approach conditions.

Considering first the flush port configuration, Gurevich[48] gives analytical equations based on a potential flow solution.

A schematic of the basic model is shown in Figure 108 and is based on an infinite, two-dimensional slot of width b.

The following parameters are defined for this analysis:

a/L = annulus width change/upstream width
b/L = slot width/upstream annulus width
n = annulus upstream flow rate/slot flow rate, W_{a1}/W_j
c = upstream annulus velocity/slot velocity, V_{a1}/V_j
β = jet efflux angle
C_D = discharge coefficient

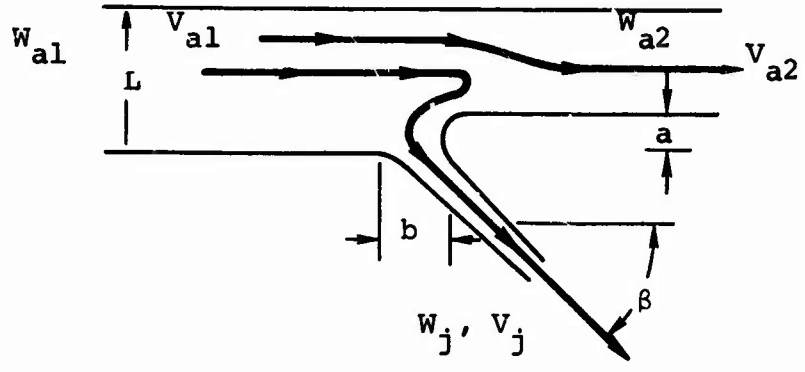


Figure 108. Dilution Port Model Schematic.

From the Gurevich analysis the following relations are obtained:

$$c = \cos\beta/\left(1-\frac{1}{2n}\right) \tag{86}$$

$$\frac{b}{L} = \frac{1}{\pi}\left[\frac{\pi\sin\beta}{n} - \frac{\cos\beta}{n}\ln\left(\frac{1+\cos\beta}{1-\cos\beta}\right)\right.$$

$$+ \frac{\left(1-\frac{1}{2n}\right)^2 + \cos^2\beta}{\left(1-\frac{1}{2n}\right)\cos\beta}\ln\left\{\frac{\left(1-\frac{1}{2n}\right)+\cos\beta}{\left(1-\frac{1}{2n}\right)-\cos\beta}\right\} \tag{87}$$

$$\left. - \frac{\left(1-\frac{1}{2n}\right)^2 + \left(1-\frac{1}{n}\right)^2\cos^2\beta}{\left(1-\frac{1}{2n}\right)\cos\beta}\ln\left\{\frac{\left(1-\frac{1}{2n}\right)+\left(1-\frac{1}{n}\right)\cos\beta}{\left(1-\frac{1}{2n}\right)-\left(1-\frac{1}{n}\right)\cos\beta}\right\}\right]\frac{\cos\beta}{\left(1-\frac{1}{2n}\right)}$$

$$C_D = \frac{L}{b}\left(\frac{2\cos\beta}{2n-1}\right) \tag{88}$$

These equations are applied to three-dimensional orifices by maintaining area similarity through the following relationships:

$$b/_L = A_H/A_{ea} \tag{89}$$

where A_H = orifice area = $\frac{\pi}{4}D^2$ for circular hole

A_{ea} = effective annulus area with boundary-layer blockage effects

For a given application, the annulus upstream conditions and the static pressure inside the combustor must be specified. With the above equations, an orifice can be sized to pass a specified flow rate, or the flow through a specified orifice can be calculated. The procedure for each is outlined as follows.

For given values of annulus and orifice flow rates and velocities, c can be calculated and then the efflux angle can be found from Equation (86). For the special case where all annulus flow passes through the orifice, n = 1 and

$$\cos\beta = c/2$$

If the orifice flow is a negligible portion of the annulus flow, n approaches infinity,

$$\cos\beta = c$$

This latter equation is used as an approximation in many references, even where n does not approach infinity.

After the value of β is obtained, Equation (87) can be used to calculate b/L and A_H/A_{ea} from Equation (89); then from Equation (88), C_D can be calculated.

For the alternate problem, with the orifice specified, the above procedure is used in an iterative solution starting with an estimated flow rate (value of n). The iteration is continued until n converges to a small difference between iterations.

Figures 109 and 110 show discharge coefficient and efflux angle as functions of the pressure drop parameter, $\alpha = (P_s)_{al} - (P_s)_j / (P_t)_{al} - (P_s)_j$, and flow ratio, 1/n.

where P_{al} = annulus static pressure

P_{tl} = annulus total pressure

P_{sj} = static pressure within the jet

Figure 111 shows the variation of orifice area relative to annulus effective area.

6.1.2 Annulus Loss Model

The annulus loss model is used to calculate pressure losses and airflow distribution around the combustor liner.

Annulus losses and flow distribution are computed from the generalized influence coefficient method given by Shapiro.[29] This method leads to the following equation for loss in total pressure for a small finite length of duct:

$$\frac{dP_t}{P_t} = \frac{KM^2}{2}\left[\frac{dT_t}{T_t} + \frac{4fdx}{D} + C_D\left(\frac{dA_B}{A}\right) + 2(1-y)\frac{dW}{W}\right] \qquad (90)$$

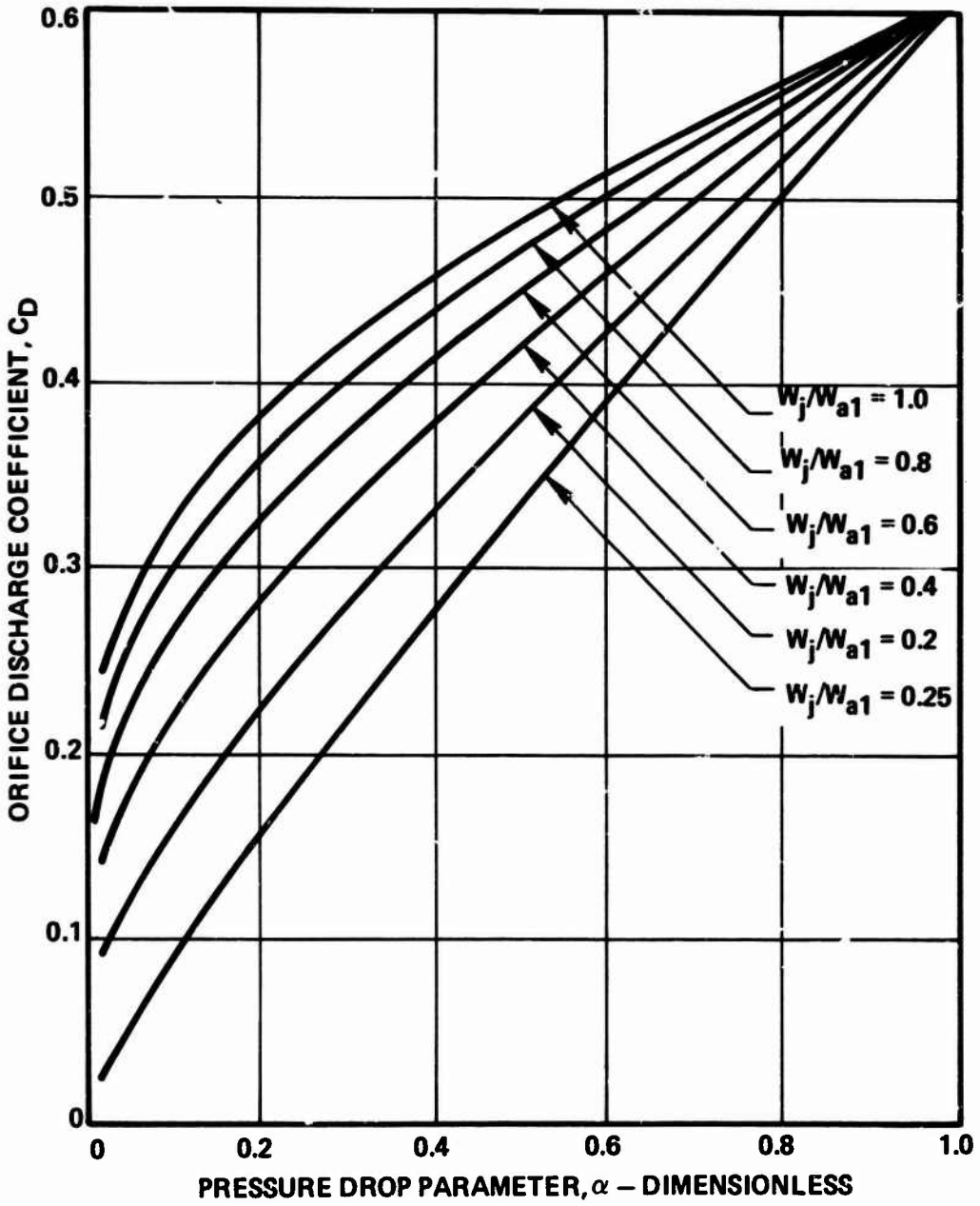


Figure 109. Discharge Coefficient Versus Pressure Drop Parameter, α, and Flow Ratio.

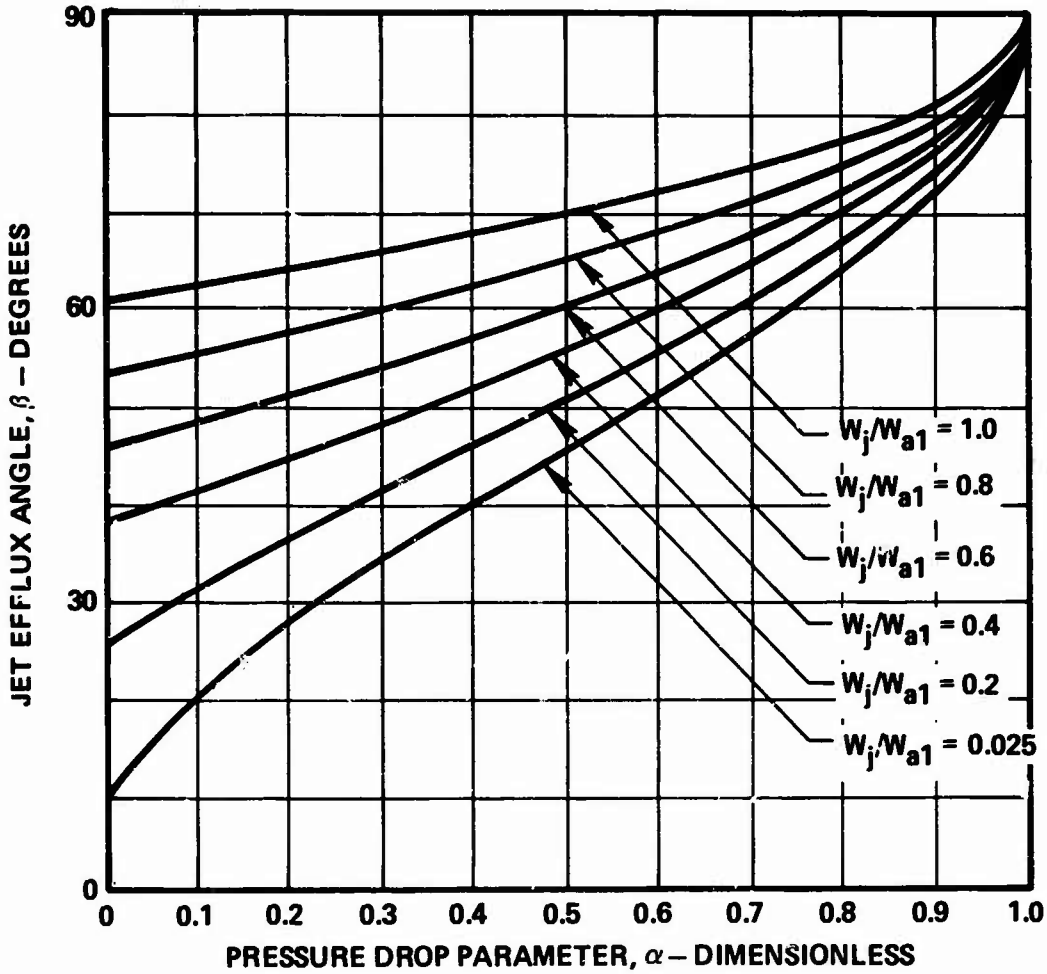


Figure 110. Jet Efflux Angle Versus Pressure Drop Parameter, α, and Flow Ratio.

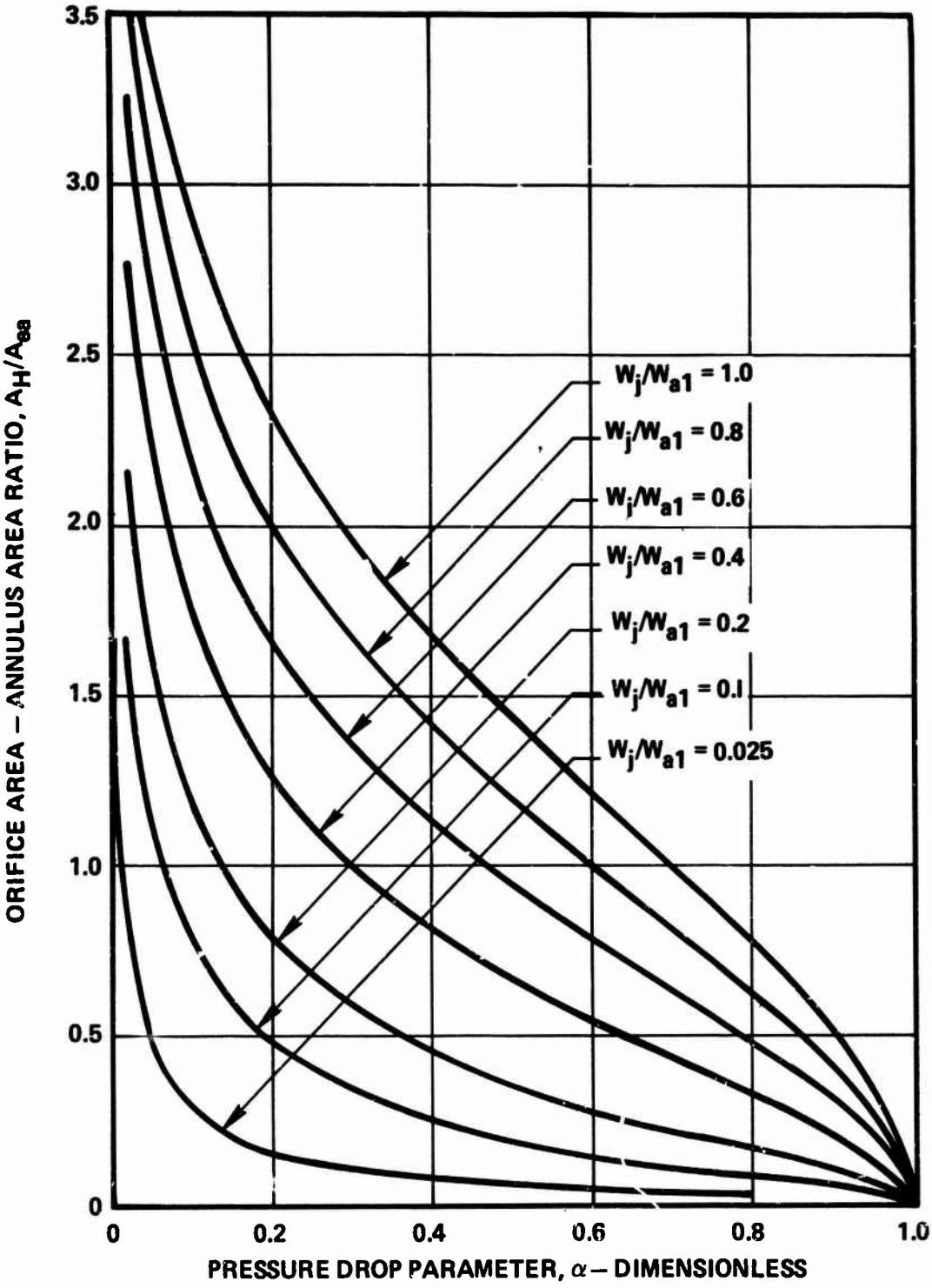


Figure 111. Orifice Area - Annulus Area Ratio Versus Pressure Drop Parameter, α, and Flow Ratio.

where P_t = total pressure

M = average Mach number in element

T_t = total temperature

f = wall friction factor

dx = element length

D = duct hydraulic diameter

C_D = drag coefficient of inserted bodies

A_B = frontal area of inserted body

A = duct area

y = velocity of injected mass/duct velocity

dW = injected mass flow

W = duct mass flow

The Mach number is obtained from a similar influence coefficient equation given by Shapiro. The above analysis includes the effect of area change, heat transfer, friction, drag, and mass addition.

Swirl effects are accounted for by solving the above equations in the direction of actual flow, together with an equation for angular momentum with friction losses. The computer program for this model generates a pictorial representation of the combustor and tabulates the flow parameters at specified stations. A typical computer plot is shown in Figure 112. The program can calculate pressure drop from an assigned fixed-orifice geometry, or can size orifices for a desired pressure drop and an assigned flow distribution.

The flow discharge coefficients and efflux angles for the orifices along the annulus are determined by the previous model.

The compressor exit flow profiles and circumferential variations usually have an effect on combustor performance, particularly on exit temperature distribution. Experience has demonstrated that the combustor pressure drop must be maintained at a minimum of twice the compressor exit dynamic head. The combustor liner itself thus serves as a screen

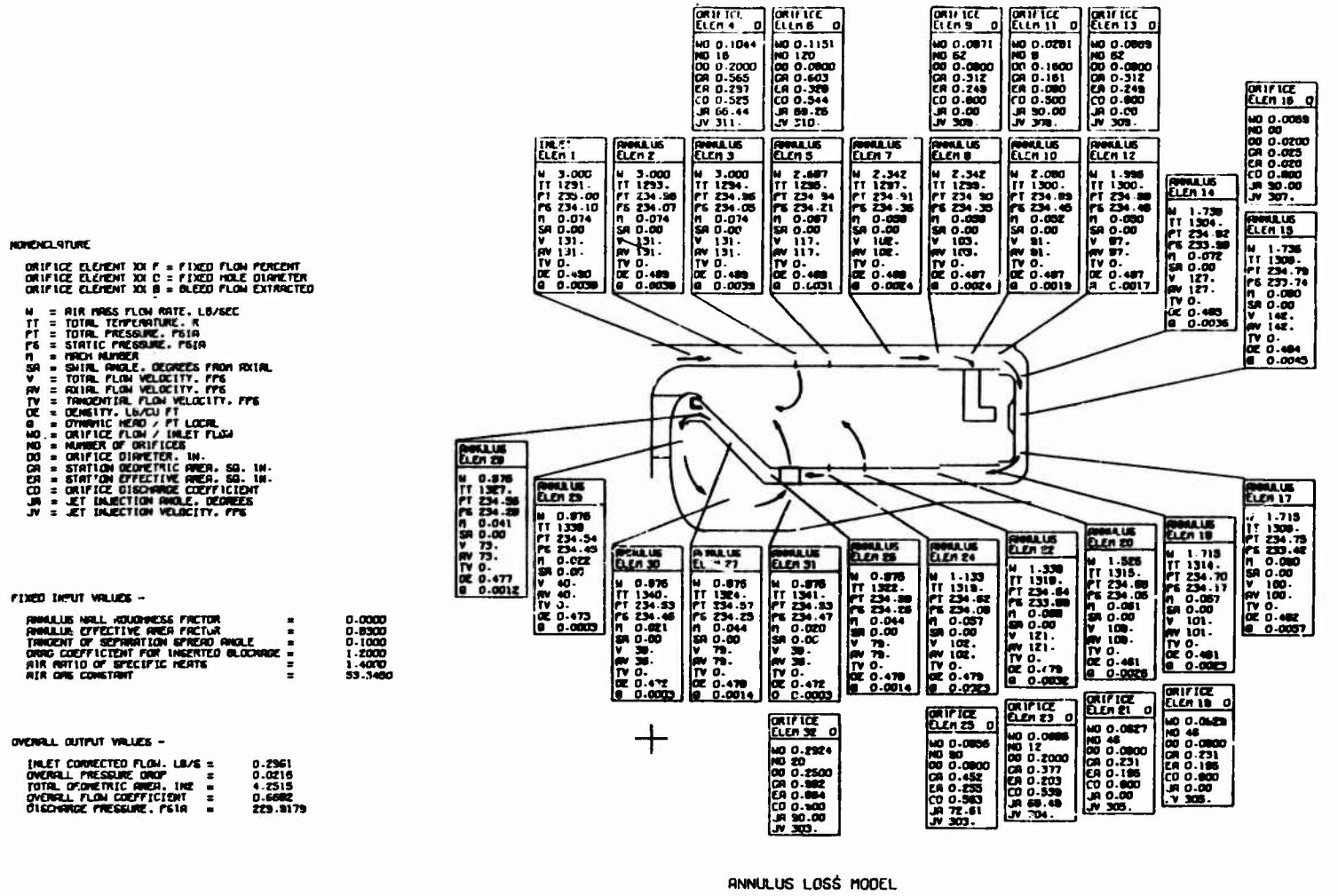


Figure 112. Computer Plot for Annulus Loss Program Output.

to back-pressure the flow and even out minor variations in compressor exit profiles. If means can be developed for predicting the effects of distortion on combustor performance, operation at lower pressure drops may be possible.

The analytical method for this model employs several of the other models in combination. The analytical procedure followed includes the use of the primary-zone program, together with the annulus loss model, to predict combustor flow distributions for various assumed compressor exit conditions. The illustrative annulus loss model was run for various swirl angles. Figure 113 shows the effect of swirl angle on pressure drop and the relative flow split between the inner and outer combustor walls for both constant mass flow and constant absolute velocity.

At low swirl angles with constant mass flow, the increase in pressure drop is slight, with a sharp increase occurring beyond 30 degrees. For a reverse-flow combustor, the inlet swirl angle is magnified substantially at the inner radius. As swirl increases, this produces a shift in flow distribution, with flow decreasing through the inner wall of the combustor and increasing through the outer wall.

The two-dimensional primary-zone program can be employed to predict decay of compressor profiles in either the radial or the circumferential direction. The program can be used in predicting combustor inlet diffuser performance. These flow distributions are then input to the models that apply to the inner combustor flow to predict effects on exit profiles.

6.1.3 Jet Trajectory and Mixing Models

Dilution jet modeling must consider

(a) A jet trajectory analysis

(b) A mixing analysis, based on mass entrainment to determine velocity and temperature decay and jet spreading

(c) A profile decay analysis to predict profile changes after jet mixing

Both empirical and analytical jet trajectory models were considered. Although an analytical model was selected, the derivations of both models are presented for reference.

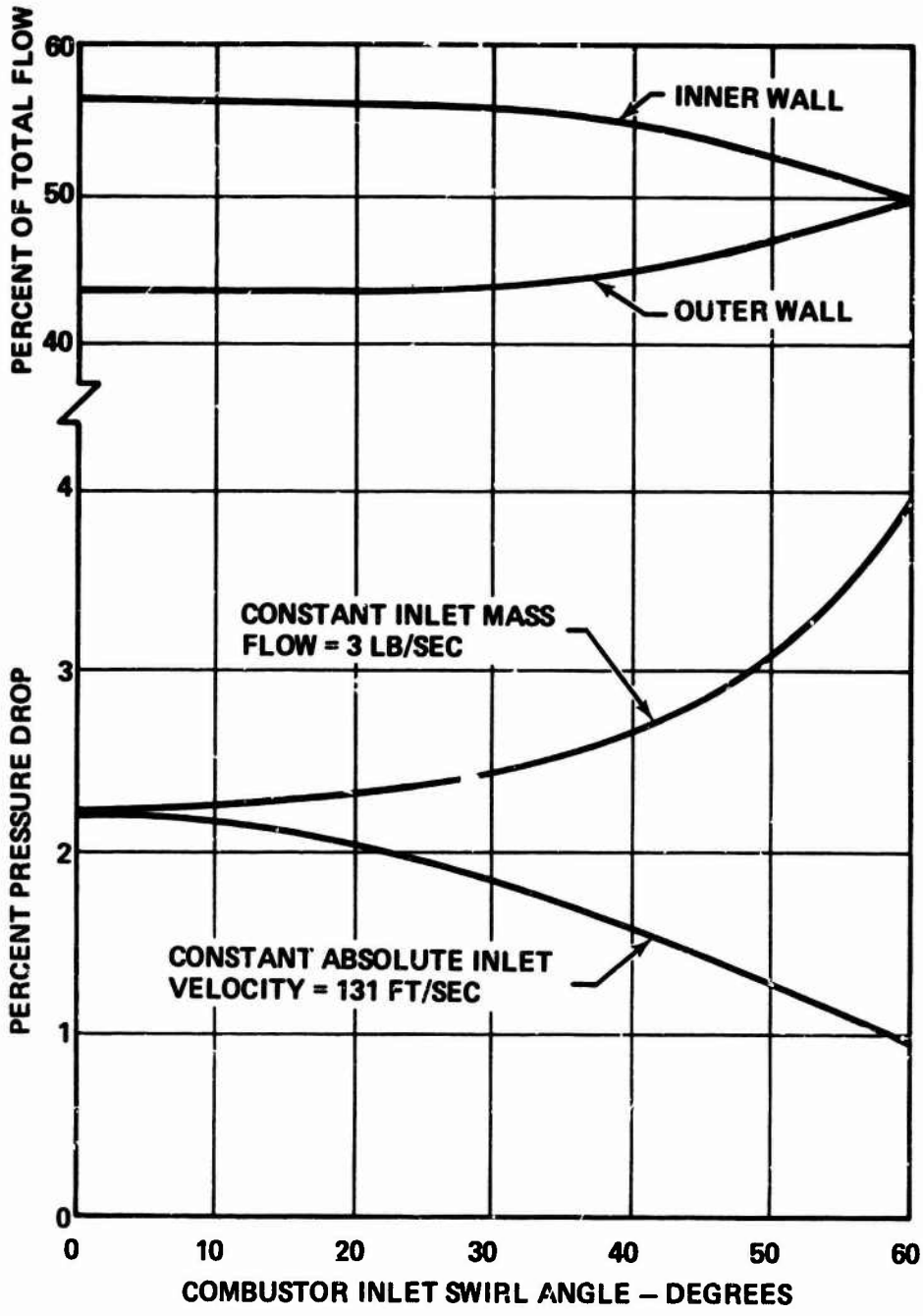


Figure 113. Effect of Compressor Exit Flow Swirl on Combustor Pressure Loss and Flow Distribution.

6.1.3.1 Empirical Trajectory Method

The initial step in analysis of dilution-zone mixing is the prediction of the mixing jet centerline trajectory. The path is influenced by the relative jet-to-mainstream momentum flux and by the configuration of the duct. Extensive work is reported in the literature on single jets in a relatively large duct. This work is well summarized by R. J. Margason[49]. C. W. Carlson et al[50] and E. R. Norster[51,52] have presented alternate relationships.

The trajectory equation given by Margason is an empirical power law equation, with the centerline defined as the maximum jet mass concentration as visually observed from photographs of water-misted jets. The equation is

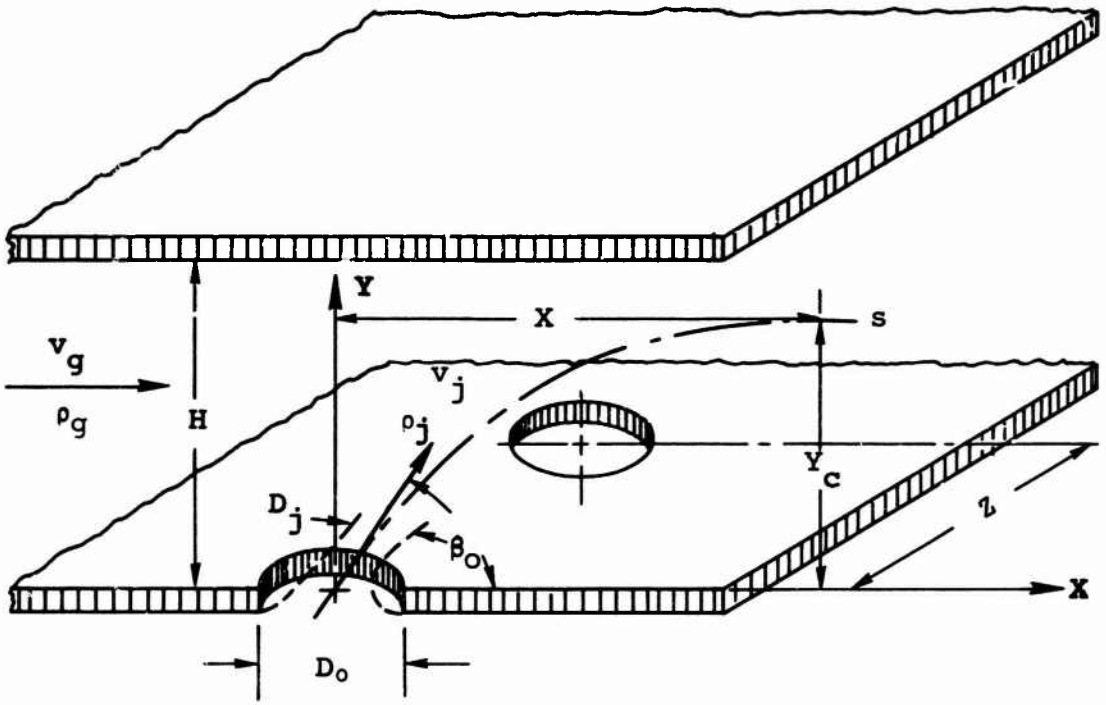
$$\frac{X}{D_{jo}} = \frac{R^2}{4 \sin \beta} \left(\frac{Y_c}{D_{jo}}\right)^3 - \left(\frac{Y_c}{D_{jo}}\right) \cot \beta \qquad (91)$$

The parameters are defined in Figure 114.

Carlson correlated data from several references for normal jet injection and defined the centerline as the point of maximum jet mass concentration. Centerline data is plotted empirically versus the following parameters:

$$Y' = \frac{Y_c/D_{jo}}{G^{1.2}\, e^{(1.07 - 60\, D_{jo}^2/ZH)}} \qquad (92)$$

$$X' = \frac{X/D_{jo}}{G^{1.2}\, e^{(2.80 - 60\, D_{jo}^2/ZH)}} \qquad (93)$$



V_g = mainstream velocity, ft per sec

V_j = jet velocity, ft per sec

ρ_g = mainstream density, lb_m per cu ft

ρ_j = jet density, lb_m per cu ft

β_o = angle of initial jet injection relative to mainstream direction = 0° or efflux angle

D_{jo} = jet initial dia, ft = $\sqrt{C_d}\, D_o$

D_o = orifice diameter, ft

X = length in mainstream flow direction from centerline of orifice, ft

Y_c = depth of jet centerline penetration, ft

H = duct height, ft

Z = duct width per orifice, ft

$V_e = \sqrt{\rho_g/\rho_{jo}}\; V_g/V_{jo}$

$G = \rho_j V_j/\rho_g V_g$

$R^2 = \rho_j V_j^{\,2}/\rho_g V_g^{\,2}$

C_D = orifice discharge coefficient

s = jet path length from orifice, ft

Figure 114. Jet Trajectory Parameter Definition.

Maximum penetration is achieved at Y' = 1.0 and

$$\frac{Y_{cmax}}{D_{jo}} = G^{1.2} \exp\ (1.07 - 60\ D_{jo}/\ ZH) \tag{94}$$

At this point, X' is also equal to 1.0 and

$$\frac{X_{max}}{D_{jo}} = G^{1.2} \exp\ (2.80 - 60\ D_{jo}/ZH) \tag{95}$$

Norster developed the following trajectory equation by considering conservation of momentum, including entrainment effects. The jet centerline is defined as the point of minimum temperature.

$$\frac{Y_c}{Y_{cmax}} = 1 - C_1 \exp\ (C_2\ X/Y_{max}) \tag{96}$$

Constant C_1 is a function of injection angle (efflux angle), β_o, and is equal to 0.7 for 90 degrees injection and 0.9 for 71 degrees injection. Constant C_2 is given as

$$C_2 = -\left(\frac{W_{jo}}{W_{je}}\right) \cdot \left(\frac{V_j}{V_g}\right) \tag{97}$$

where W_{jo} = injected jet weight flow rate, lb per sec

W_{je} = weight flow entrained in jet, lb per sec

Norster presents empirical data for the ratio W_{jo}/W_{je} as a function of velocity ratio and injection angle. From this data an empirical expression has been developed by AiResearch for entrainment ratio to give C_2 as

$$C_2 = -\frac{\rho_j V_j}{\rho_g V_g} \left(\frac{0.3\ (\beta_o/90.)}{1 - \exp(-0.59\ V_j/V_g)}\right) \tag{98}$$

To complete this trajectory equation, a relationship for Y_{cmax} is required. Norster gives the following empirical equation as a function of duct diameter (tests were in a tubular duct) and jet to mainstream momentum ratio:

$$\frac{Y_{cmax}}{D_{duct}} = C_3 \sin \beta_j \left(\frac{W_j V_j}{W_g V_g} \right)^{0.5} \qquad (99)$$

where W_g = mainstream weight flow rate, lb per sec

D_{duct} = duct diameter, in.

Introducing continuity relations, this becomes

$$\frac{Y_{cmax}}{D_j} = C_3 \sin \beta_o \left(\frac{\rho_j V_j^2}{\rho_g V_g^2} \right)^{0.5} = C_3 \sin \beta_o R \qquad (100)$$

C_3 is given as 1.224 by Norster for 90-degree injection only and revised to 1.15 to include the injection angles.

6.1.3.2 Analytical Trajectory Methods

Trajectory analytical methods can be grouped into two types. The first treats the jet as a solid body and uses discharge coefficients for cylinders or ellipses, together with a pressure differential across the jet in the mainstream direction, to compute the deflection. The second method deals with mass and momentum entrained from the mainstream into the jet and is generally concluded in the literature to be more reasonable.

The second method was selected for use in this program. Braun and McAllister[53] describe this method and list most of the pertinent references. All of these analyses deal with jets in a uniform stream integrating the momentum equation to obtain an analytical expression for the jet axis trajectory. To extend the method to the case of variable mainstream velocity and temperature, the basic equations derived were utilized but the mainstream was subdivided into segments. Each finite segment was assumed to have constant temperature and velocity, and the change in jet axis angle passing through that segment

was calculated. Mass entrained into the jet was computed for each segment, based on empirical spreading rates. Spreading of the jet was computed, based again on empirical data. With use of nondimensional jet velocity profiles as presented by Keffer,[54] a similar nondimensional temperature profile, and integrating mass flux continuity equation, local velocity and temperature profiles were computed.

The analysis is based on the assumption that mass flux entrained into the jet carries in the full cross-flow velocity. McAllister shows that this is reasonable, in spite of the fact that most of the mass is entrained by back flow in the jet wake. Any deceleration of fluid before its subsequent entrainment results in pressure gradients in the vicinity of the jet, with resultant changes in momentum flux.

The analysis is initiated by considering the momentum flux balance for the control volume depicted in Figure 115. This control volume differs from that of McAllister, being limited to a thin plane through the jet, parallel to the wall from which the jet exists.

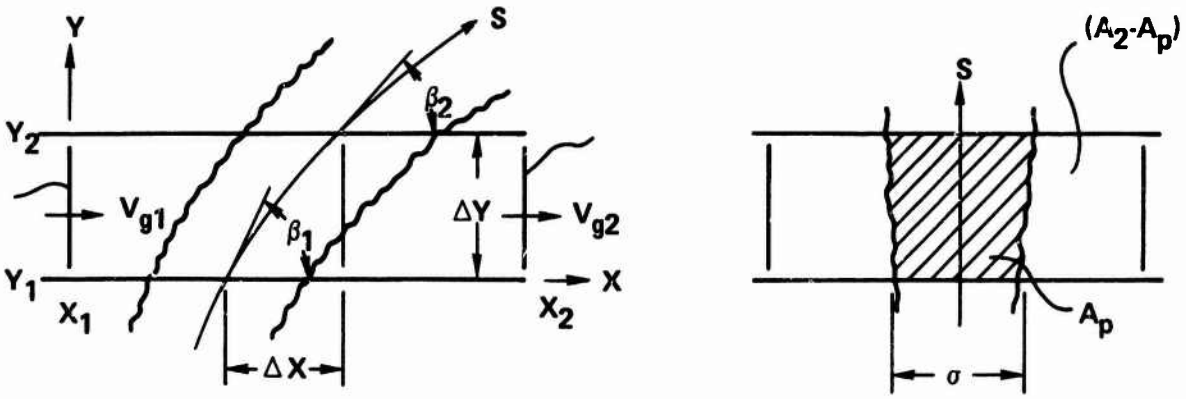


Figure 115. Jet Trajectory Momentum Flux Control Volume.

The analysis was established with the following assumptions:

(a) The velocity vectors in each jet cross section are parallel to the jet trajectory axis.

(b) Average pressure differences between corresponding surfaces of the control volume are neglected in comparison to the momentum terms.

(c) The jet trajectory is, therefore, given by the resultant momentum vector.

The flow through plane X_2 (Area A_2) is divided into two parts:

(a) An exterior region, A_2-A_p, having the free-stream velocity, V_{g2}.

(b) A wake region, A_p, which is the projection of the jet shadow onto area A_2 with zero velocity.

With these assumptions, the momentum balance in the Y direction is formed on the basis that the jet momentum normal to the mainstream is a constant and equal to the jet momentum at the orifice exit, $M_{jo} \times \sin \beta_o$.

$$\int_{A_{j1}} \rho_{j1} V_{j1}^2 \sin \beta_1 \, dA_{j1} = \int_{A_{j2}} \rho_{j2} V_{j2}^2 \sin \beta_2 \, dA_{j2} \qquad (101)$$

By assumption (a), $\sin \beta$ is constant over A_j; therefore,

$$M_{j1} \sin \beta_1 = \sin \beta_1 \int \rho_{j1} V_{j1}^2 \, dA_{j1} \qquad (102)$$

$$M_{j2} \sin \beta_2 = \sin \beta_2 \int \rho_{j2} V_{j2}^2 \, dA_{j2} \qquad (103)$$

$$M_{j1} \sin \beta_1 = M_{j2} \sin \beta_2 = M_{jo} \sin \beta_o \qquad (104)$$

$$M_{j1} = \frac{M_{jo} \sin \beta_o}{\sin \beta_1} \qquad M_{j2} = \frac{M_{jo} \sin \beta_o}{\sin \beta_2}$$

The X-momentum equation is written with constant mainstream properties over the element length ΔY:

$$\rho_{g1} V_{g1}^2 A_1 = M_{j1} \cos \beta_1 = \rho_{g2} V_{g2}^2 (A_1 - A_p) + M_{j2} \cos \beta_2 \quad (105)$$

The jet momentum terms, M_{j1} and M_{j2}, are eliminated with the Y-momentum equations

$$M_{j1} \cos \beta_1 = \frac{M_{jo} \sin \beta_o}{\sin \beta_1}, \quad \cos \beta_1 = M_{jo} \sin \beta_o \cot \beta_1 \quad (106)$$

$$M_{j2} \cos \beta_2 = \frac{M_{jo} \sin \beta_o}{\sin \beta_2} \quad (107)$$

The X-momentum equation with rearrangement can be written

$$\cot \beta_2 = \cot \beta_1 + \frac{\left(\rho_{g2} V_{g2}^2 - \rho_{g1} V_{g1}^2\right) A_1 + \rho_{g2} V_{g2}^2 A_p}{M_{jo} \sin \beta_o} \quad (108)$$

Note that this equation gives the inverse of the trajectory slope

$$\cot \beta = \frac{dx}{dy} \quad (109)$$

This equation can be further simplified by assuming that in the neighborhood of the jet element ΔY, the gas properties are constant over the length ΔX of the layer.

$$\rho_{g2} = \rho_{g1} = \rho_g \quad (110)$$

$$V_{g2} = V_{g1} = V_g \quad (111)$$

This assumption does not limit the variability of ρ_g and V_g with both X and Y when integration is performed over the entire jet. The X-momentum equation can then be simplified to

$$\cot \beta_2 = \cot \beta_1 + \frac{\rho_g V_g^2 A_p}{M_{jo} \sin \beta_o} \quad (112)$$

We now introduce the parameter defined as effective gas velocity (V_e) or momentum flux ratio R^2.

$$\frac{1}{R^2} = V_e^2 = \frac{\rho_g V_g^2}{M_{jo}/A_o} = \frac{\rho_g V_g^2}{\rho_{jo} V_{jo}^2} \quad (113)$$

Introducing R into the momentum equation,

$$\cot \beta_2 = \cot \beta_1 + \frac{V_e^2}{\sin \beta_o} \times \frac{A_p}{A_o} \qquad (114)$$

The effective jet width is now expressed as a linear function of path length, s, and is, in reality an expression for the lateral spreading of the jet, σ. McAllister gives the following relation for σ:

$$\sigma = \sigma_o + Ks \qquad (115)$$

where σ_o is the effective width at the jet orifice accounting for an apparent origin of zero jet width located "a" diameters upstream of the orifice.

$$\sigma = K\ (2\ a\ D_{jo} + s) \qquad (116)$$

giving

$$A_p = \int_y \sigma\ dy \qquad (117)$$

The factor K is an empirical spreading rate parameter. McAllister examined experimental data and applied his analysis to the data. He adjusted the K factor until predicted trajectories matched the measured data. This resulted in the relationship between K and the parameter R that is given in Figure 116. A fixed value of 0.8 for "a" was used in the matching process.

For the small element ΔY, σ is assumed constant at the value for s at that element, and then

$$\Delta A_p = K(2\ a\ D_{jo} + s)\ \Delta Y \qquad (118)$$

Noting that

$$A_o = \frac{\pi\ D_{jo}^2}{4} = \frac{\pi}{4}\ C_D\ D_o^2 \qquad (119)$$

where C_D is the orifice discharge coefficient

Equation (114) now becomes

$$\cot \beta_2 = \cot \beta_1 + \frac{4\ K\ V_e^2}{\pi \sin \beta_o} \left(2\ a + \frac{s}{D_{jo}}\right) \frac{\Delta Y}{D_{jo}} \qquad (120)$$

The trajectory analysis is now completed. Computation of the trajectory path is accomplished in steps of $\Delta Y/D_{jo}$. The initial input required includes

- Initial jet angle, β_o
- Spreading rate factor, $K = f(V_e)$
- Momentum ratio parameter, $V_e = f(X, Y)$

6.1.3.2.1 Predicted Trajectories

The derived equation for local jet angle (Equation 105) was used, together with initial conditions, a relationship between K_i and V_e, a virtual source "a" of 0.8, and V_e specified as a function of Y, to predict trajectories in uniform streams for comparison with the data available in the literature. A typical comparison is shown in Figure 117 which indicates that good agreement exists with perhaps a slight tendency to predict underpenetration. No data was available in the literature for jets in a varying mainstream. However, results obtained by the above method with the use of three inlet profiles are shown in Figures 118 and 119.

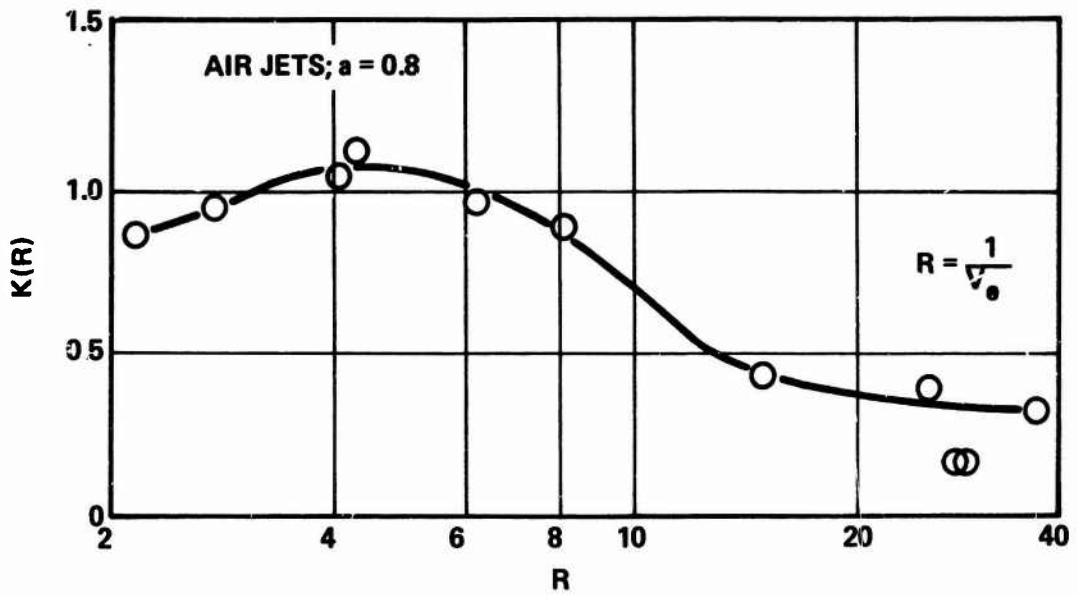


Figure 116. Spreading Rate Parameter for Published Air Jets.

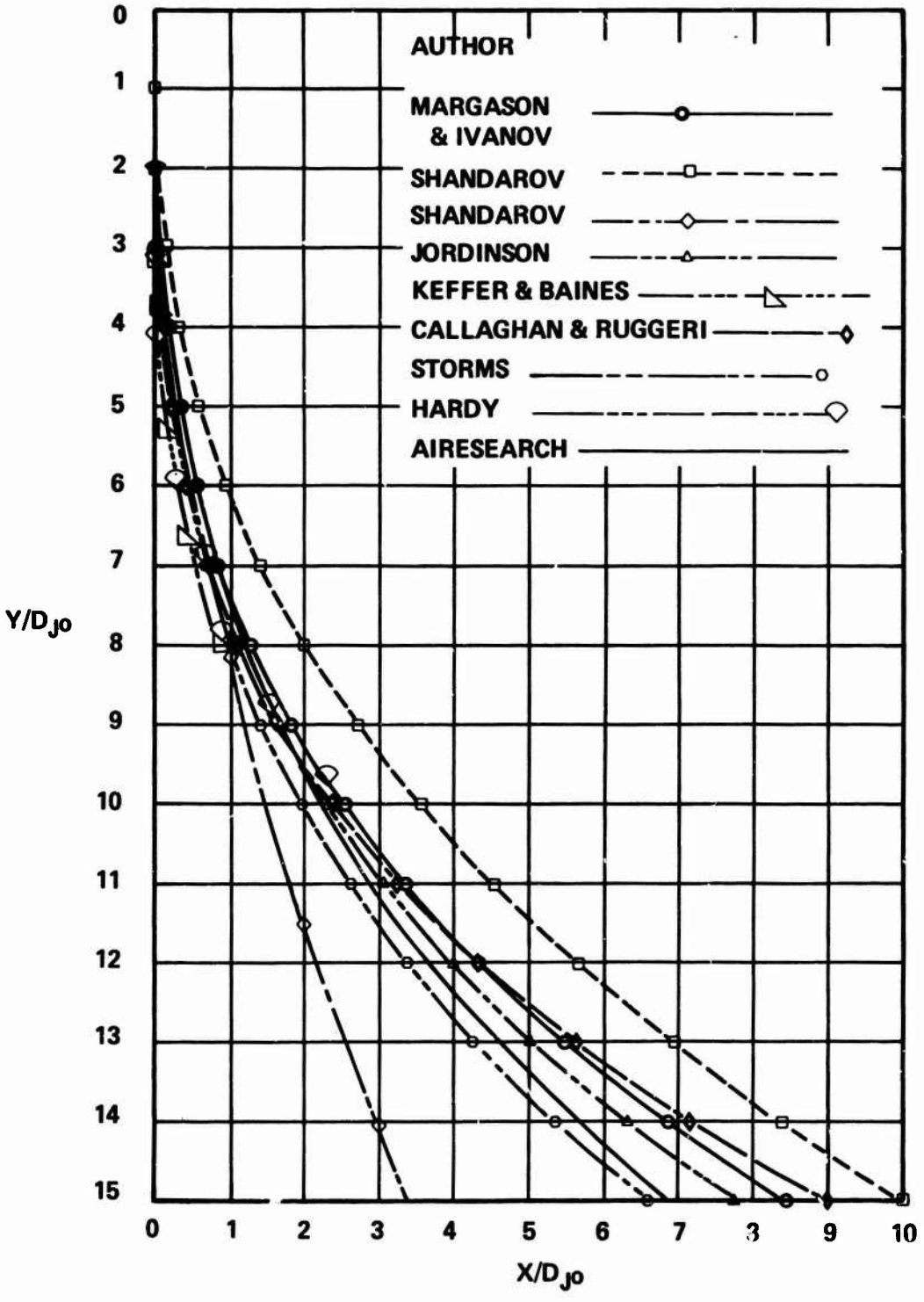


Figure 117. Jet Trajectories From Several References.

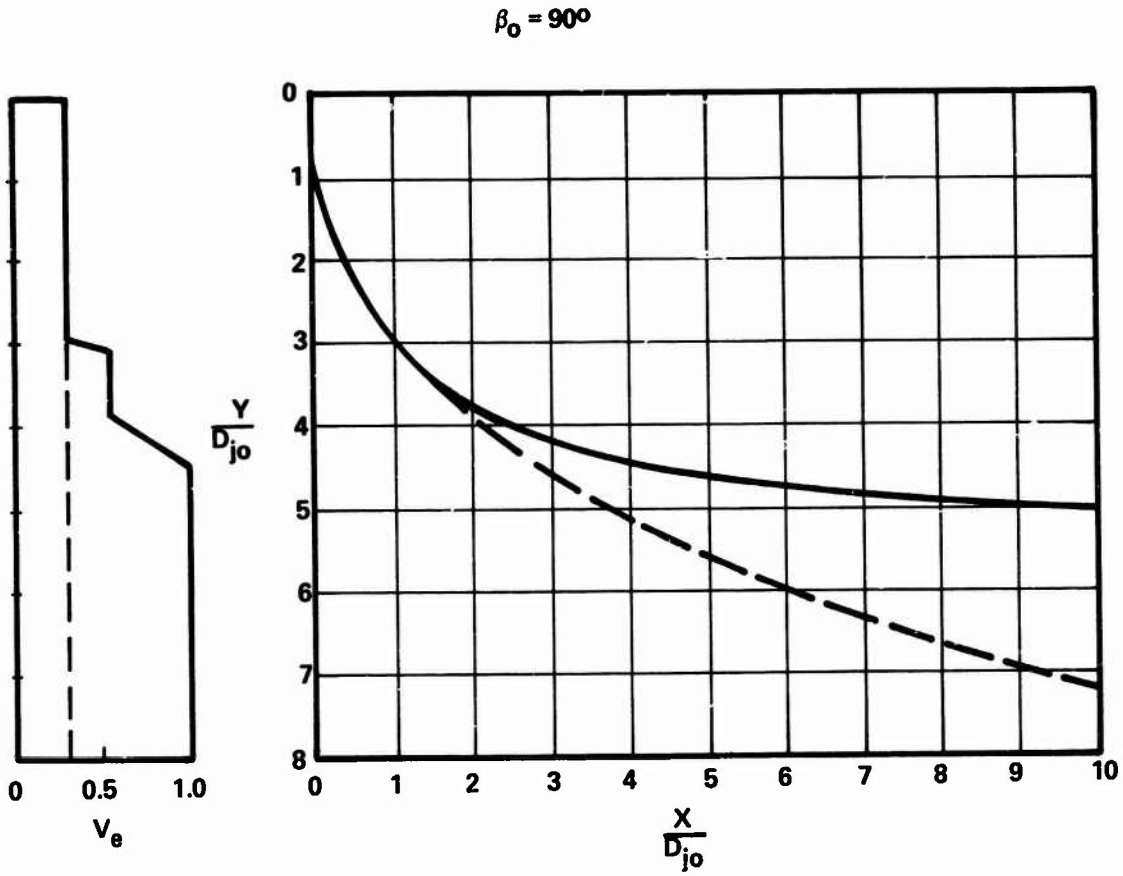


Figure 118. Effect of Mainstream Profile on Jet Trajectory.

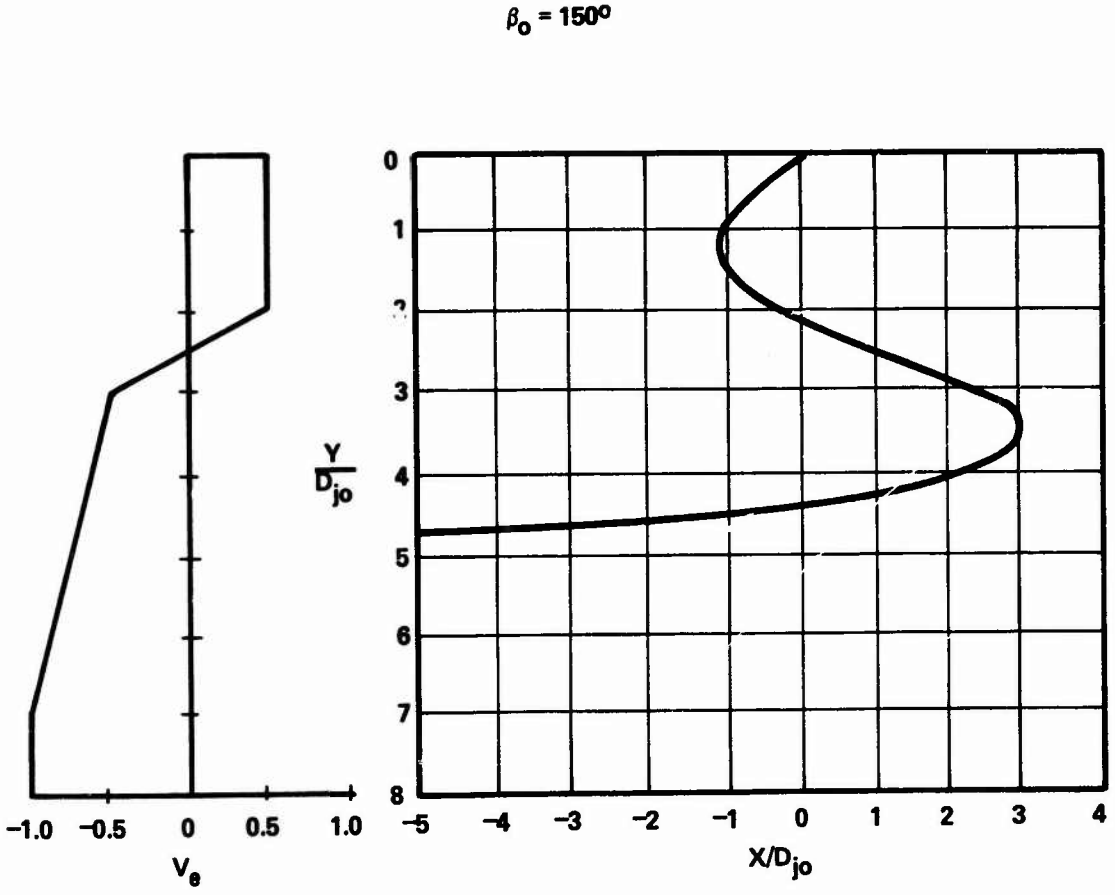


Figure 119. Effect of Mainstream Profile Reversal on Jet Trajectory.

Lateral jet spreading is of importance in spacing dilution holes. Figure 120 shows results from the trajectory analysis. The trajectory, spreading, and decay relationships provide the information necessary to size the dilution orifices so that the jets can be projected into the region of maximum primary-zone exit temperature for optimum dilution effectiveness when opposed jets impinge at the centerline. The recirculation analysis of Verduzio and Companaro[38] was modified for annular combustion systems and employed to calculate the resultant mixed flow.

6.1.3.2.2 Velocity and Temperature Decay

After the trajectory is obtained, information regarding the decay of velocity and temperature along the trajectory is required to assess the mixing rates. McAllister developed the necessary relations to perform these calculations. Measured jet profiles of both velocity and temperature can be represented by the following profile parameter equation:

$$f(\eta) = \frac{V-V_g}{V_c-V_g} = \frac{T-T_g}{T_c-T_g} = \frac{1}{[1 + (\sqrt{2}-1)\eta^2]^2} \qquad (121)$$

The factor η is the lateral radius divided by the radius at which the profile parameter equals 0.5. The rate of spreading of the half-radius for velocity is empirically expressed as

$$r_{1/2} = c\, s' \sqrt{1-K^2\cos^2\phi} \qquad (122)$$

where s' = path length from apparent origin, a.

Based on the assumption that the jet is an ellipse with an aspect ratio of 1:5,

$$K^2 = 1-(1/5)^2 = 0.96$$

The constant c has a value of 0.215 for cross-wind jets and 0.09 for axisymmetric jets, and ϕ is the rotational angle around the circumference of the ellipse. The following equation for velocity decay was obtained by use of the above relations in continuity analysis, integrating over angle ϕ and out to a radius where the profile parameter is 0.1, and including density effects in McAllister's derivation:

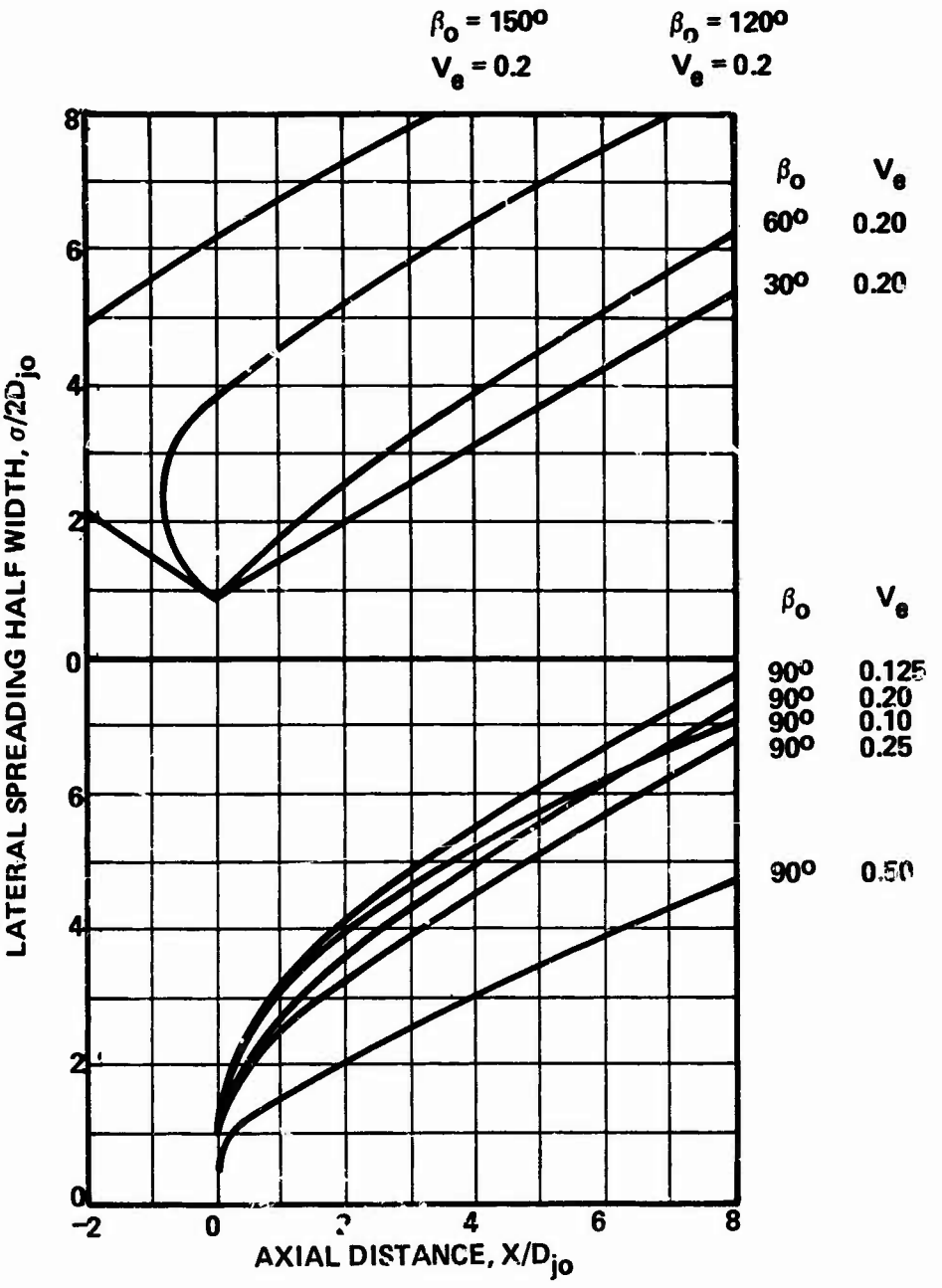


Figure 120. Jet Lateral Spreading for Various Injection Angles and Effective Velocity Ratios.

$$\frac{V_c - V_g}{V_{jo} - V_g} = \left(\frac{W/W_{jo}}{(2c)^2 (2-K^2) (s'/D_{jo})^2} - \frac{\eta_1^2}{2} V_e \sqrt{\frac{\rho_g}{\rho_o}} \right) \qquad (123)$$

$$\times \frac{1}{\frac{\rho_g}{\rho_o} \left(1 - V_e \sqrt{\frac{\rho_o}{\rho_g}}\right) \left(\frac{1-\sqrt{f(0.1)}}{2\sqrt{2-1}}\right)}$$

where η is obtained from the jet similarity profile given by Keffer and Baines[54] and shown in Figure 121.

A similar relation was derived for temperature. However, it is deemed sufficiently accurate to use the velocity decay times the Prandtl number.

6.2 RIG TESTS AND MODEL UPDATE

Rig tests that were conducted to provide data to update the model included discharge coefficient and efflux angle measurements, and jet trajectory and mixing mapping. These tests and the resulting model update are presented below.

6.2.1 Discharge Coefficient Tests and Model Update

6.2.1.1 Rig Tests

The discharge coefficient rig, Figure 122, was designed to be capable of determining the discharge coefficient of an orifice in a flat plate, a combustor or any part of a combustor. Included in the design was the capability to be used as either open-to-plenum or with air passing across the test orifice at any required velocity. Airflow to the test piece could be regulated, and airflow through the test piece was set by means of a vacuum system and the use of up to nine calibrated orifices. The effective open area and discharge coefficient of the test piece could then be calculated. The effect of varying the passage height and/or air velocity above the test piece could also be determined. Nine 0.75-inch-diameter plunged orifices and three 0.5-inch-diameter plunged orifices were calibrated.

Rig instrumentation included two static taps on each side of the orifices, total and static taps at the test piece location, and total taps at the variable passage-height discharge location. The instrumentation was used to measure differential pressure, ΔP, and flow rate, W_a, across the calibrated orifices,

$$\frac{J - J_g}{J_c - J_g} = \frac{1}{[1 + (\sqrt{2} - 1)\,\eta^2]^2}$$

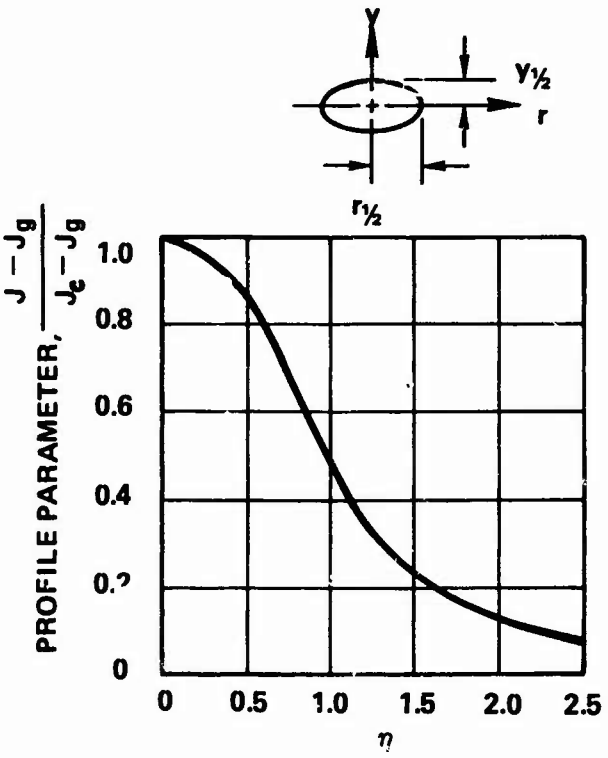
J = LOCAL TEMPERATURE OR VELOCITY

J_c = CENTERLINE TEMP. OR VEL.

J_g = MAINSTREAM TEMP. OR VEL.

r = LATERAL RADIUS

y = TRANSVERSE RADIUS



$r_{1/2}$, $y_{1/2}$ = RADIUS AT 0.5 PROFILE PARAMETER

$y_{1/2}$ = $1/5\, r_{1/2}$

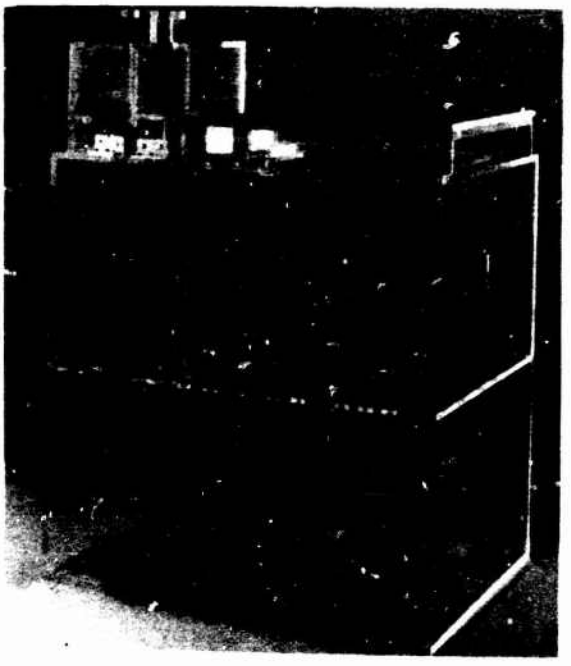
$r_{1/2}$ TEMP. = $1/P_r\, r_{1/2}$ VEL.

$\eta = r/r_{1/2}$ or $y/y_{1/2}$

$r_{1/2}$ VEL = 0.215 S'

S' = JET TRAJECTORY PATH FROM APPARENT ORIGIN

Figure 121. Jet Profile Parameter for Velocity and Temperatures.



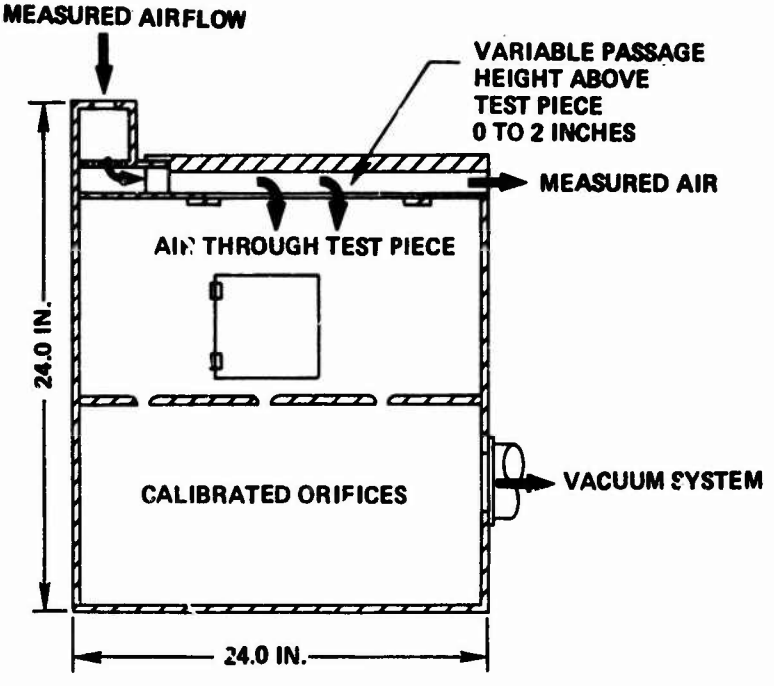


Figure 122. Discharge Coefficient Rig.

ΔP and W_a across the test piece, and directional velocity across the test piece. A comparison of ΔP across the test piece and ΔP across the calibrated orifices for the measured airflow rate was then used to calculate the effective open area and discharge coefficient of the test piece.

Testing was completed for the following configurations:

- Single circular orifice--thick wall
- Single circular orifice--thin wall
- Single circular orifice--thin wall plunged
- Multiple circular orifices--thick wall
- Single rectangular orifice--thick wall
- Single crescent-shaped orifice--thick wall
- 4X-size cooling-slot configuration

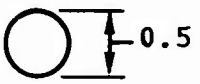
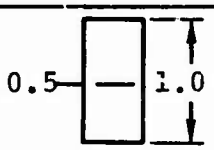
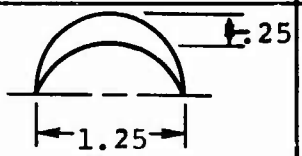
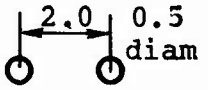
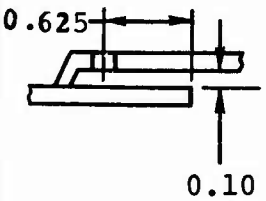
Test configurations are described in Table XV. Test conditions established are listed in Table XVI. For each of the above, the effect of passage flow on both C_D and the efflux angle was determined. Additional tests were conducted to determine the effective open area of the L-pipes, pneumatic-impact nozzles, swirlers, and cooling bands on the primary-zone configurations. Values were obtained for open-to-plenum conditions only; this was repeated for each combustor modification prior to testing.

6.2.1.2 Test Results and Model Update

Figure 123 shows the discharge coefficient data for the single 0.5-inch-diameter flush orifice. Also shown on the figure is the predicted discharge coefficient function based on the theoretical relation for a flush circular hole as discussed previously. Predicted values agree well with the data for the single flush orifice test.

The open annulus data at a pressure drop parameter, α, of 1.0 agrees exactly with the predicted value. With annulus flow (annulus height of 0.7 inch), discharge coefficients at α near 1.0 are slightly higher than predicted. This may be an influence of the wall thickness. It was concluded that the analytical prediction for single flush orifices is verified and that the relatively thick walls used in small combustors should not have a substantial influence.

TABLE XV. DISCHARGE COEFFICIENT TEST CONFIGURATION

Configuration Name	Configuration	Orifice Total Area (sq in.)	Equivalent Circular Diameter (in.)	Ratio of Max. Width to Wall Thickness
Single 1/2-inch circular hole		0.196	0.5	4.0-thick wall >10.0-thin wall and plunged
Rectangle		0.500	0.747	8.0
Crescent		0.27	0.586	2.0
Five 1/2-inch circular holes		0.98	0.5	4.0
4-times-size cooling slot 10 holes with 0.2-in. diameter		0.314	0.2	1.66

NOTE: Walls are 0.125 inch thick except for circular thin wall and circular plunged orifices.

TABLE XVI. DISCHARGE COEFFICIENT TEST CONDITIONS

Annulus Airflow (lb/sec)	Orifice ΔP (in. of H_2O)	Annulus Velocity (ft/sec)	Nominal Jet Velocity (ft/sec)	Pressure Drop Parameter (α)	C_D Data Curve Plot Symbol
0.25	0.5	45	90	0.76	□
0.25	1.0	45	120	0.86	
0.25	2.0	45	150	0.91	
0.25	4.0	45	205	0.95	
0.25	6.0	45	245	0.97	
0.49	0.5	90	145	0.61	○
0.49	1.0	90	160	0.68	
0.49	2.0	90	190	0.79	
0.49	4.0	90	235	0.85	
0.49	6.0	90	270	0.89	
0.99	0.5	180	230	0.41	△
0.99	1.0	180	240	0.46	
0.99	2.0	180	265	0.57	
0.99	4.0	180	300	0.66	
0.99	6.0	180	330	0.72	
1.22	0.5	220	265	0.37	◇
1.22	1.0	220	280	0.40	
1.22	2.0	220	300	0.49	
1.22	4.0	220	330	0.59	
1.22	6.0	220	365	0.66	

SEE TABLE XVI FOR SYMBOL DEFINITION

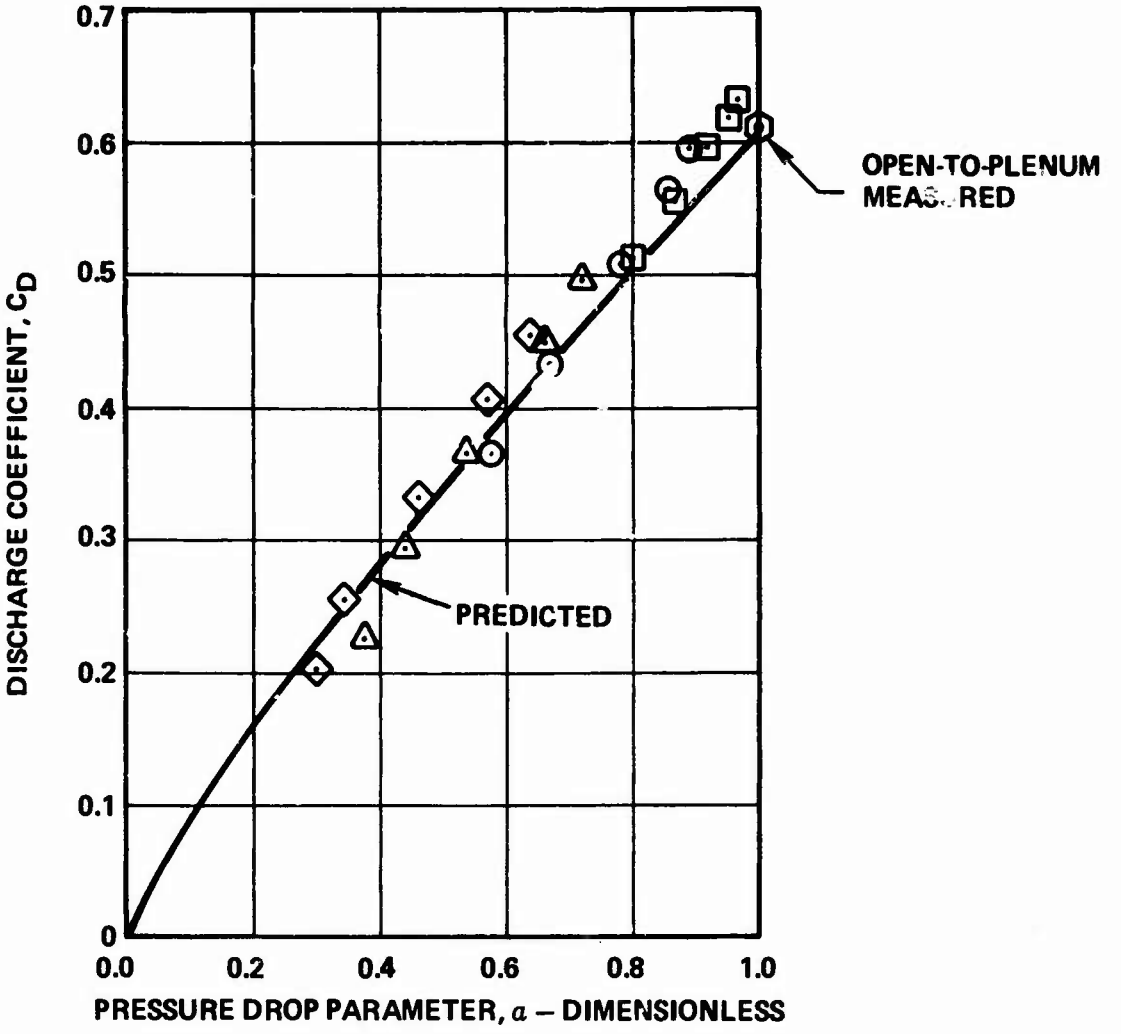


Figure 123. Discharge Coefficient Data for the Circular Orifice.

Figure 124(a) shows discharge coefficient data for the single rectangular orifice. The open annulus data point is 4 percent higher than the prediction for a flush circular hole, and closed annulus data generally is higher by about 10 percent than the circular-orifice prediction. There is also a noticeable trend in the data at a given annulus airflow for the discharge coefficient to drop off at a greater rate than the predicted curve. This trend, to a slighter extent, is also observed with the circular orifice. This is attributed to wall-thickness effects but, considering the accuracy of the data, does not appear to warrant inclusion in analytical correlations, since it is not good practice to use low α values in a combustor design. A second curve is shown based on a 10-percent upward adjustment of the flush orifice predicted curve. By applying this correction, the analytical prediction can be used for designs with rectangular orifices.

Figure 124(b) presents data for the crescent-shaped orifice. In spite of its substantially different shape, the discharge coefficient characteristic is quite similar to that of the circular orifice. Deviation from the predicted curve occurs at α greater than 0.9 with an open annulus value of 0.678.

For design purposes it can be concluded that a flush orifice of any shape can be represented by an equivalent circular orifice. The effect of α on discharge coefficient is adequately described by the analytical procedure. For the case of the rectangle, a 10-percent incremental correction, constant at all values of α, improves the prediction.

The effect of multiple holes is shown in Figure 124(c). Data is consistently higher than the predicted values and higher than the data for the single orifice. The predicted discharge coefficients are slightly higher for this configuration because of the higher ratio of jet flow to annulus flow, but the predicted increase is only on the order of 1 percent, while the measured values are generally about 10 percent higher. It is possible that the higher jet flow rates resulted in a shift in annulus duct velocity profile upstream of the orifice row or resulted in local reductions of static pressure at the discharge side.

Figure 125 presents discharge coefficient characteristics for a 4-times-size slot-cooling device typical of that tested later in this program (see Section 7.2.2). Even though the air is metered through flush orifices, the discharge coefficient curve is about 40 percent greater than that for the single orifice. This is attributed to the effect of the inner deflection skirt that spreads and diffuses the jet air. For analytical prediction purposes, the computed coefficient for

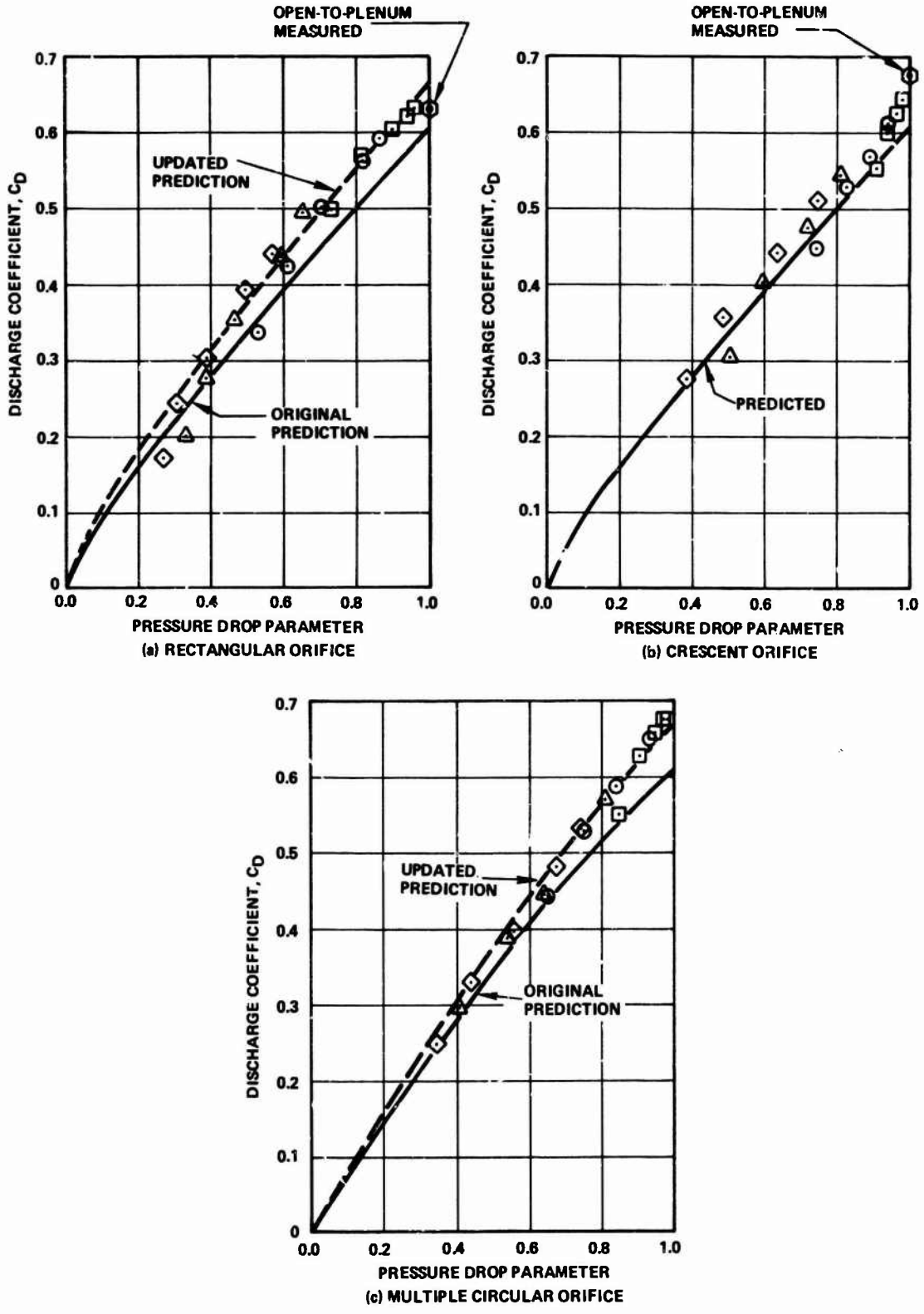


Figure 124. Discharge Coefficient Data Versus Pressure Drop Parameter for Different Orifices.

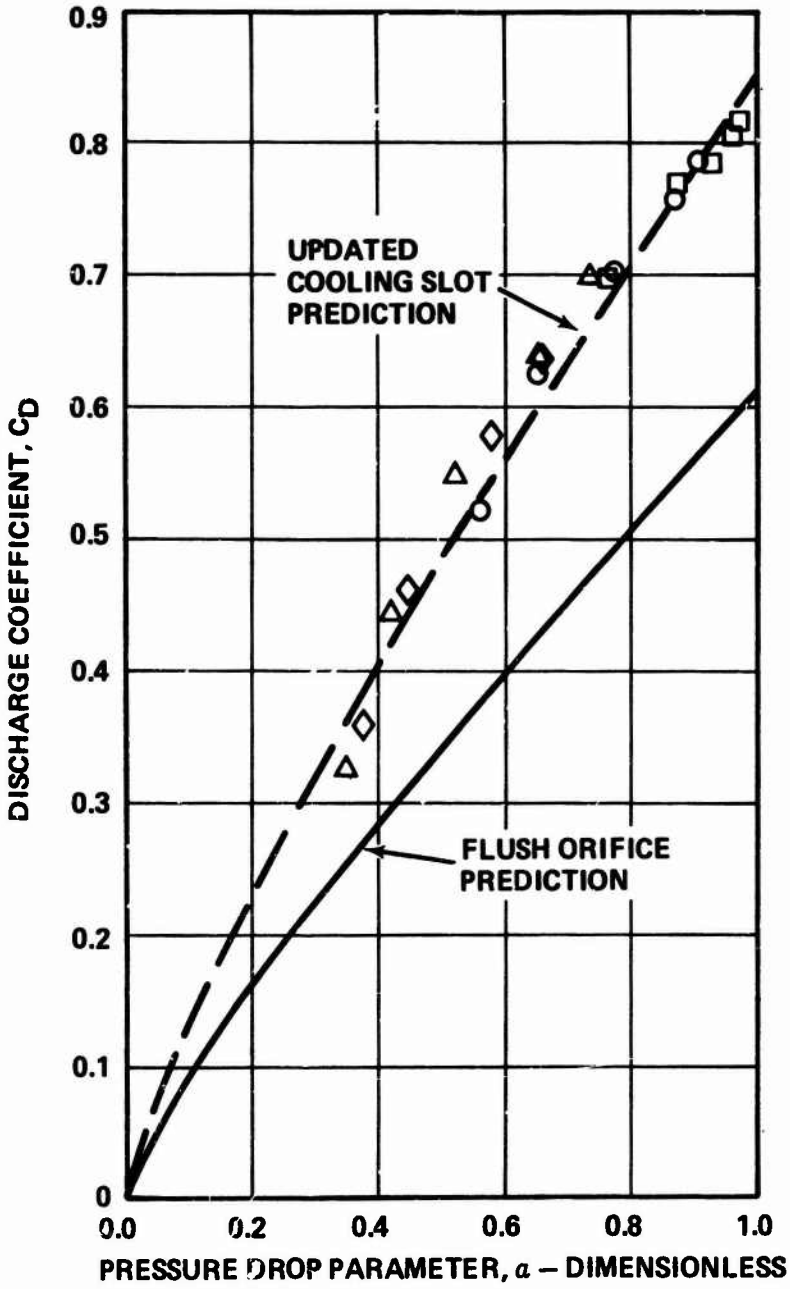


Figure 125. Discharge Coefficient Data for Cooling Slot.

a single orifice can be multiplied by 1.4 to obtain the coefficient for a cooling skirt.

Jet efflux angle data is shown in Figure 126 for all test configurations. The method of measurement was limited to a resolution of ±5 degrees. Observed angles were substantially higher (closer to the jet axis) than those predicted and showed little variations with the α parameter. This is attributed to the thick walls. It can be concluded that for small combustors with low ratios of orifice diameter to wall thickness, penetration of orifice jets will not be as sensitive to annulus flow conditions as it is in larger combustors.

In general, it can be concluded that there is little difference in the discharge coefficients for large or small combustors but that jet efflux angles are more nearly constant for smaller combustors.

As a result of the low variation in jet efflux angle observed for the thick-walled configurations, two additional tests were conducted with a thin-walled flush orifice and a plunged (thick-walled) orifice, both with a 0.5-inch open diameter. Figure 127 shows the discharge coefficient of the thin-walled orifice and the thick-walled orifice. Figure 128 shows the jet efflux angle for the thin-walled orifice with a variation that more nearly follows the analytical prediction. One discrepancy is that the measured angle for a given annulus velocity does not appear to change with a change in the pressure drop parameter, α. The wide variation in angle is clearly undesirable, as it increases combustor sensitivity where variation in inlet conditions is of concern. It is therefore concluded that any form of thin-walled orifice should be avoided. If the size of the orifice is such that the ratio of the minimum width to wall thickness is greather than 4.0, the orifice should be plunged.

Figure 129 shows the discharge coefficient for the plunged orifice. The open-to-plenum ($\alpha = 1.0$) discharge coefficient is 0.9. The measured data is seen to be well represented by the updated prediction obtained by multiplying the flush orifice prediction by a constant of 1.475.

Jet efflux angle data for the plunged orifice is also shown in Figure 129. Except for one point the angle is constant at 80°. This is similar to the characteristics of the thick-walled, square-edged orifice.

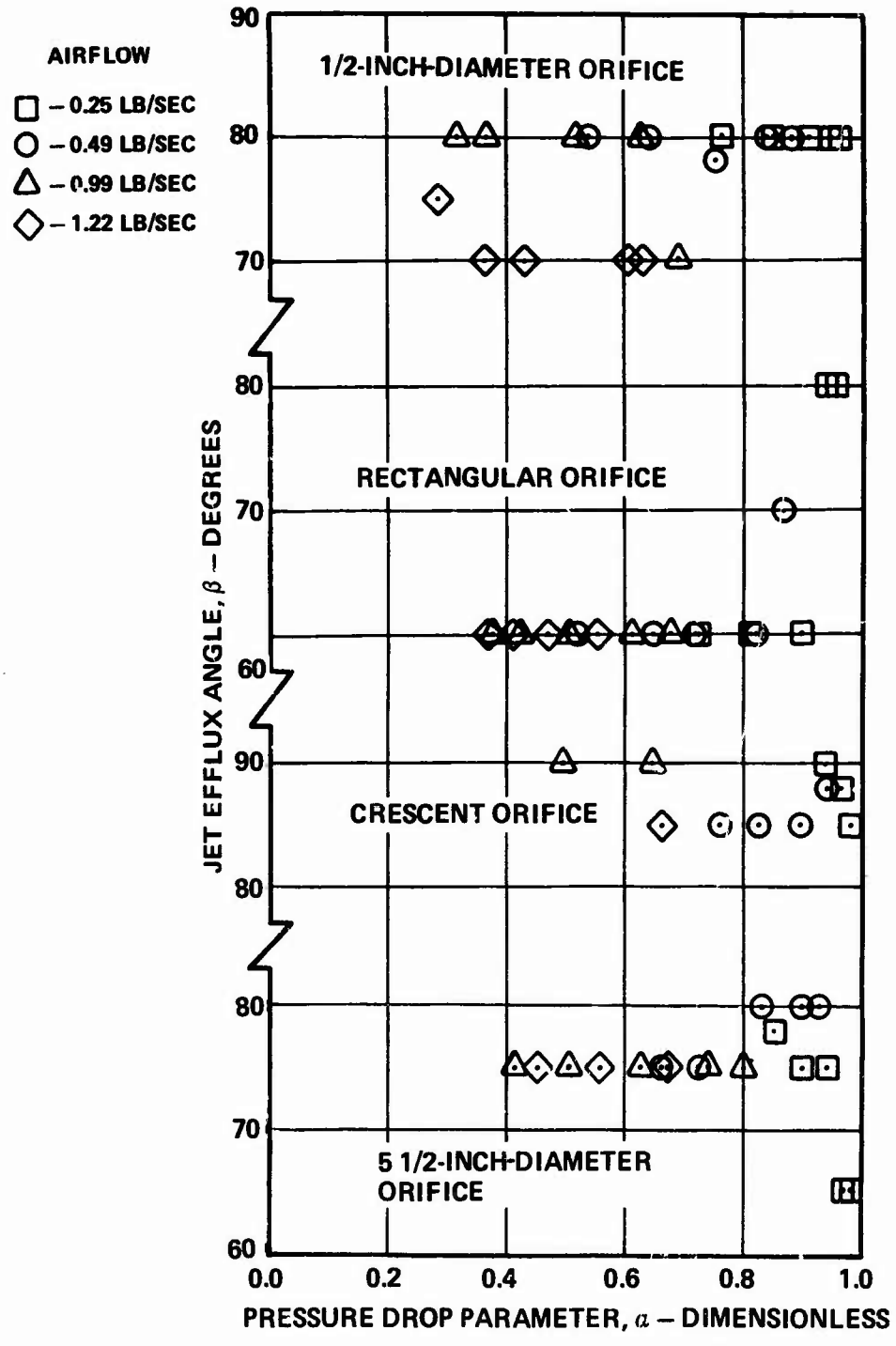


Figure 126. Comparison of Jet Efflux Angle Data.

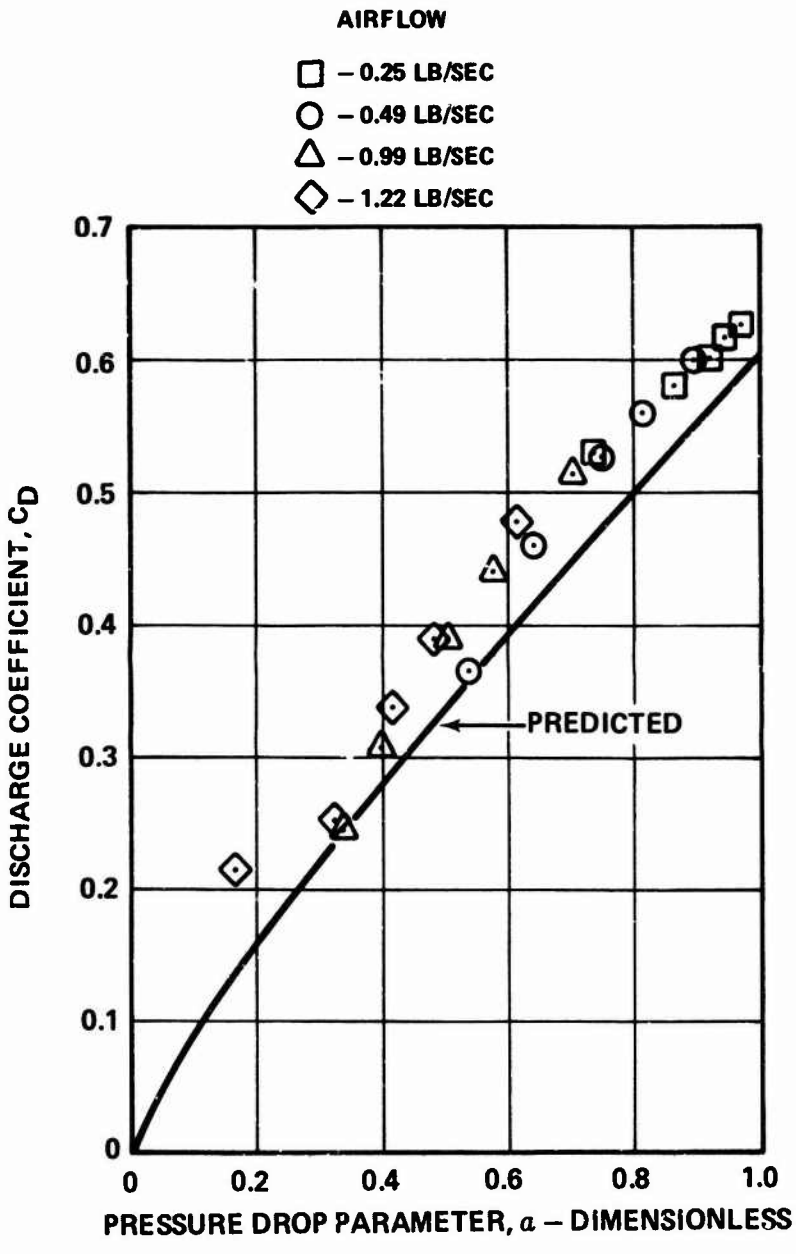


Figure 127. Discharge Coefficient Data for the Thin-Walled Circular Orifice.

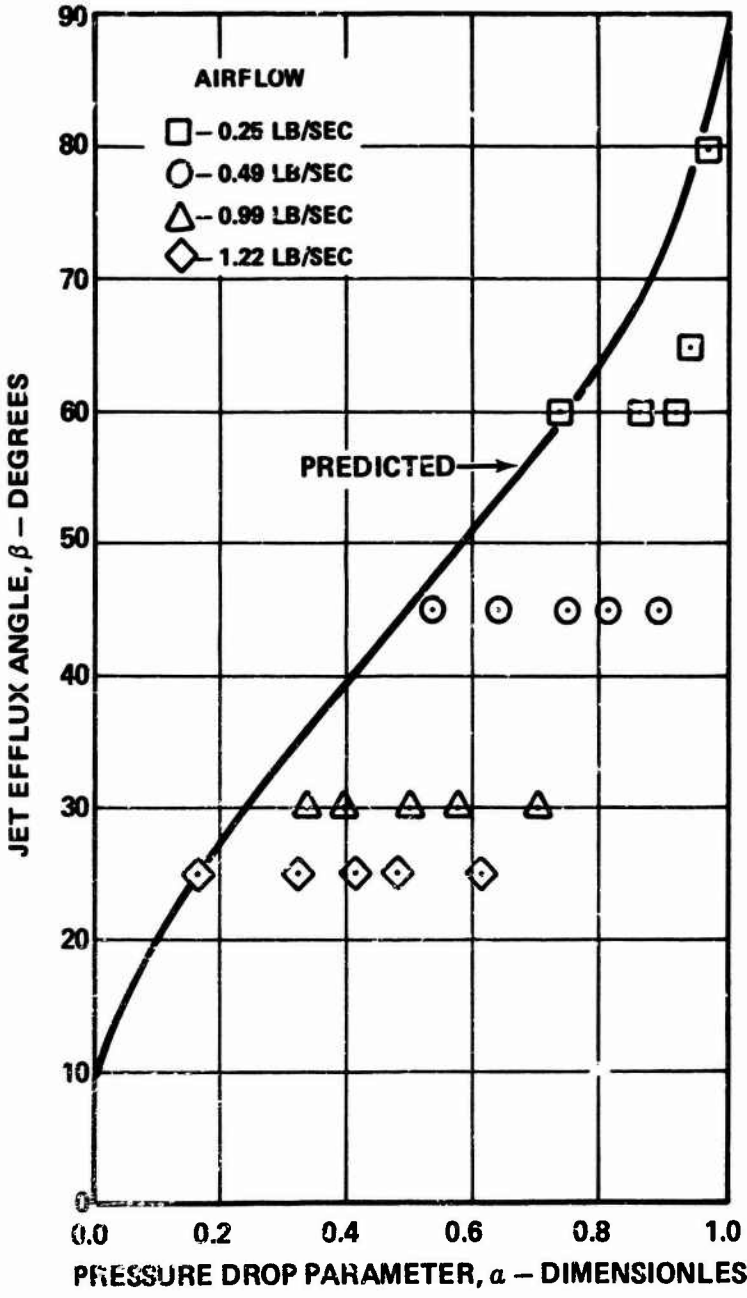


Figure 128. Jet Efflux Angle Data for Thin-Walled Circular Orifice of 0.5-Inch Diameter.

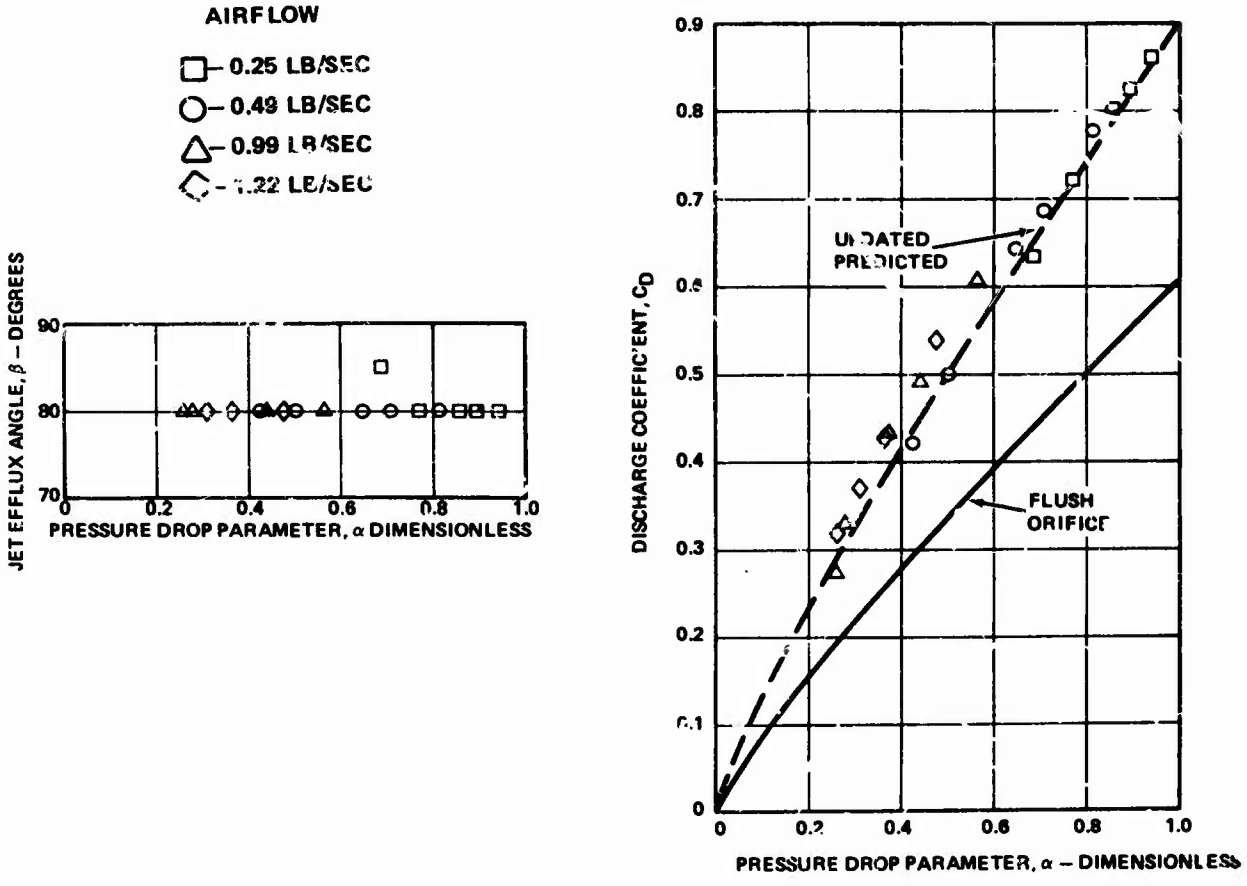


Figure 129. Jet Efflux Angle Data and Discharge Coefficient Data for Plunged Circular Orifice.

6.2.2 Dilution-Zone Tests and Model Update

6.2.2.1 Rig Tests

A dilution-zone rig was designed to permit tests with various dilution-zone orifice configurations to verify the jet trajectory analysis. The rig was capable of producing (a) a temperature profile, (b) a jet angle, and (c) jet penetration. It was also capable of being used to indicate cooling-film effectiveness and show the effect on cooling-film air due to entrainment by dilution jets. The cooling-film effectiveness tests are described in Section 7.2.2.

Figure 130 shows a schematic of the dilution-zone test rig. Inlet air temperature was limited to a maximum of approximately 800°F, with dilution air and profile generator air being ambient. Test Section B incorporates the profile generator (two designs available) that was set to provide a modified radial profile or removed when a uniform profile was required.

The dilution zone and test piece (Section C) had removable sides so that either Plexiglas or mild steel could be used as required. One side was drilled to allow probes to be inserted to measure temperature profile, jet angle, and jet penetration for the various test pieces.

A cobra or wedge probe with thermocouple attached was used to map the dilution-zone temperature and velocity profiles, and visual observations were made with the use of tracers and Plexiglas sides of the test section.

Section D was a straight section, as shown for initial tests. Curved sections were also made to measure the effect on temperature profile due to duct curvature.

Figure 131 shows different views of the dilution-zone rig. Figures (a) and (b) show external views of the rig. Figure (c) shows an internal view of the test section, looking upstream toward the inlet screen and profile generators.

The rig had provisions for data measurement in a 7x12x27 point data matrix. The duct was 4 inches high by 12 inches wide. Probe holes were located in the 4-inch side spaced 1/2 inch apart in a square matrix with seven stations across the height and 12 stations in the axial direction. The 27 stations for each hole were defined to cover the 12-inch duct width. Depth increments are 0.25 inch over the center 4 inches and 0.5 inch at the extremes. The test orifice is located on the 12-inch side at the duct center.

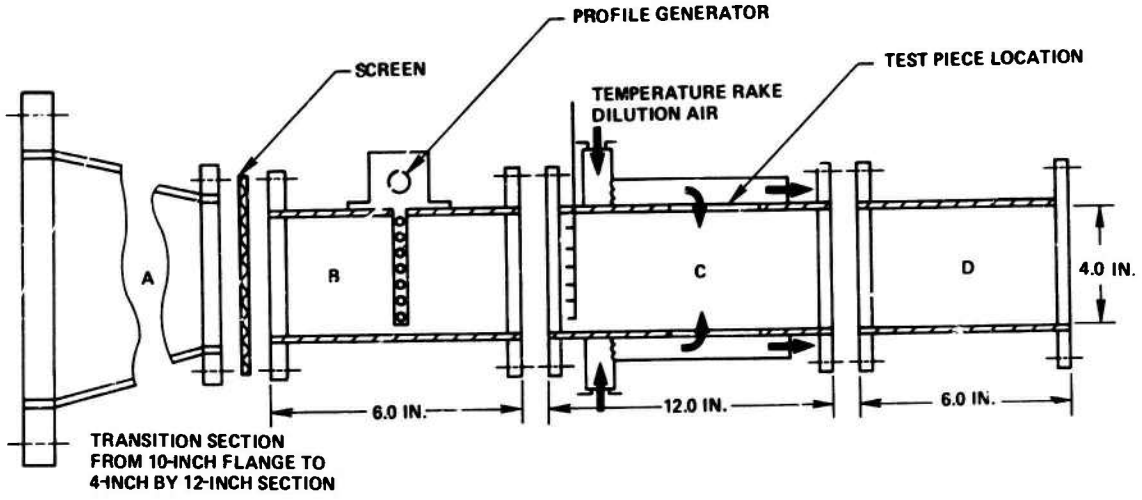


Figure 130. Dilution-Zone Element Test Rig Schematic.

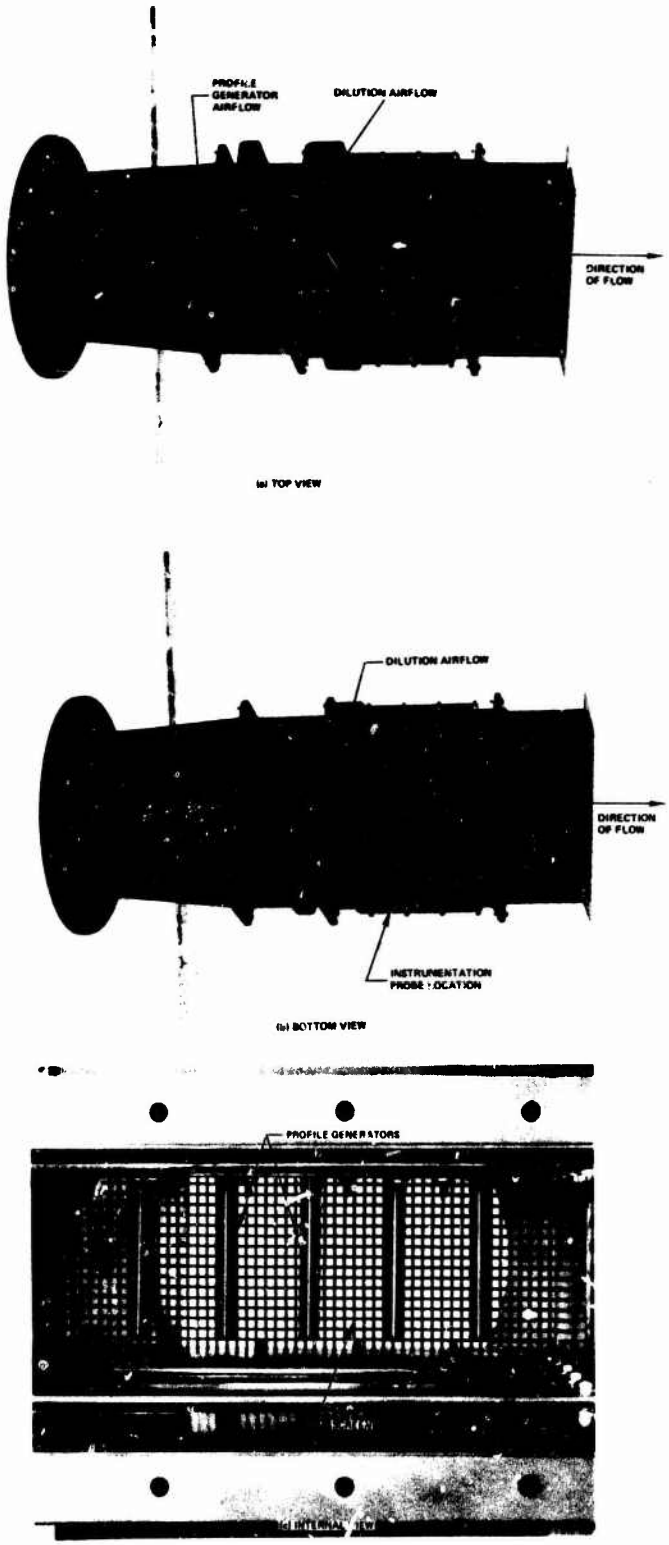


Figure 131. Dilution-Zone Test Rig.

Test hardware included:

- o Orifice and cooling slot configurations which were described in Table XV
- o Multiple- and opposed-port orifice plates--two identical plates with a single row of 0.50-inch-diameter ports spaced 4 diameters apart
- o Staggered-port orifice plates--a plate with a single row of 0.50-inch-diameter ports spaced 4 diameters apart and staggered laterally 2 diameters from the orifices of the multiple-port plates
- o A 4-times-size liner cooling slot
- o Constant-area turning duct--a rig adapter to examine mixing at 90-degree and 180-degree increments of duct wall turning on a partially diluted profile
- o Reduced-area turning duct--similar to the above except a 0.5 area reduction with the 180° turn (Figure 132)

6.2.2.2 Test Results and Model Update

The purpose of the initial tests was to examine the effect of gas-stream velocity and orifice configuration on the trajectory of a single jet in a uniform-profile mainstream.

The spreading-rate parameter, K, is related to the width of the jet by the following relation:

$$K = \frac{A_p/A_{jo}}{\left(2a + \frac{s}{D_{jo}}\right)\frac{\Delta y}{D_{jo}}} \qquad (124)$$

where A_p = area of jet projected on a plane normal to the cross-flow direction

A_{jo} = jet initial area at the orifice

For a given value of V_e, it was expected that the effect of a noncircular jet would be to influence the ratio A_p/A_{jo}. This ratio is approximately proportional to the width of the orifice, divided by the orifice area. Three basic orifices were tested--one circular, one rectangular, and one crescent-shaped.

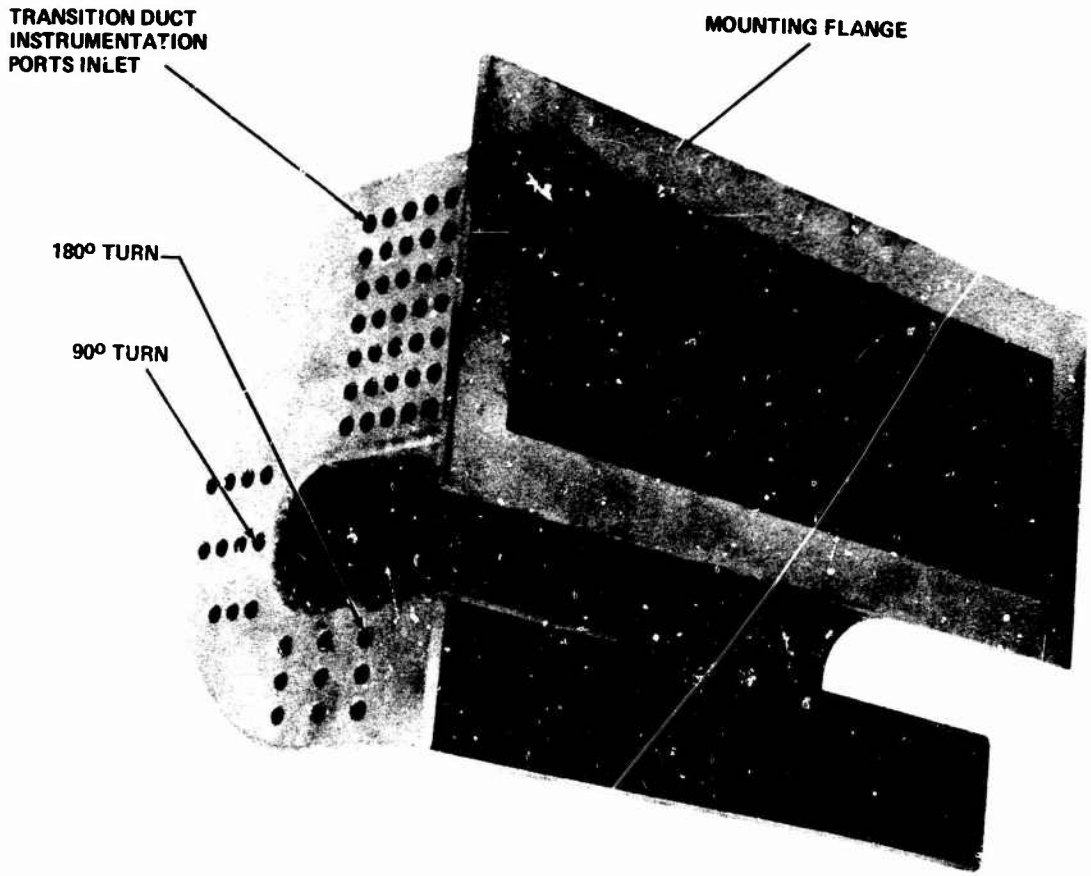


Figure 132. Reduced-Area Transition Duct.

The rectangular orifice has the lowest width-to-area ratio and was therefore expected to penetrate farthest, with less rapid mixing. The crescent shape has the highest width-to-area ratio and should penetrate the least, but mix rapidly. The crescent shape was selected on the fact that the first three to four diameters of jet length are taken up in deforming a circular jet into a crescent shape, with a width-to-length ratio of about 5. Therefore, the crescent shape should accelerate mixing rates by providing a jet already formed in the crescent shape.

The configuration for the initial tests consisted of a uniform primary-air temperature profile with dilution air admitted through a single 0.500-inch-diameter sharp-edged orifice located on the transverse centerline of the mixing duct upper wall. The dilution supply duct from which this air was supplied was closed off at its exhaust end, so that all the dilution flow passed through the orifice.

The entire dilution-air profile was mapped utilizing a wedge-type yaw probe, indexed to points in a 0.50 x 0.50 x 0.25 rectangular cubic matrix--this probe giving flow vector angle, P_{total}, P_{static}, and T_{total} for the gas at each point. Table XVII shows conditions that were mapped.

TABLE XVII. DILUTION-ZONE TEST CONDITIONS

V_e	$V_{primary}$ (ft/sec)	$V_{secondary}$ (ft/sec)	$T_{primary}$ (°F)	$T_{secondary}$ (°F)	ΔT (°F)
0.25	72	250	260	60-70	≈200
0.50	145	250	260	60-70	≈200
0.75	223	250	260	60-70	≈200
0.50	176	250	600	65	535

A computer program reduces the data to provide profile plots of temperature in two mutually perpendicular planes, parallel to the mainstream. In addition, velocity vectors are drawn in the x-y plane to show the direction and magnitude of local velocity. Data in the horizontal plane depicts the spreading of the jet across the duct. Data in the vertical plane depicts penetration, deflection of the jet from the axis of entry, and spreading such as would occur across a combustor annulus.

Data from the center plane is compared with the predicted jet centerline trajectories in Figure 133. Agreement is good for the 0.5 and 0.75 effective velocity ratios (V_e), while 0.25 condition shows greater penetration than predicted. Predicted penetration is dependent on spreading rate parameter K, and a lower value of K increases penetration. The relationship given for K showed a peak at a V_e of 0.25. Based on the data, it appeared that this peak was not as sharp as previously anticipated. The trajectory prediction procedure was adjusted to provide a revised relationship for K to match the measured trajectories. The two test points of V_e = 0.5 compared the effect of mainstream temperature. The nearly exact coincidence of the data confirmed the V_e parameter as the proper correlating relation.

Lateral spreading data was obtained for the test conditions given in Table XVII. Temperature plots showed that for all test points, spreading was approximately 2 diameters on either side of the orifice.

Due to the good agreement with the theoretical profiles indicated by the circular orifice mapping, mapping of the remaining configurations was limited to a single V_e value of 0.5 and profile configuration at only three data planes normal to the primary flow direction in the downstream direction.

Data obtained for the various configurations tested was used to determine the spreading rate parameters (K). A plot of the experimental data as a function of effective velocity ratio (V_e) is compared with original predictions in Figure 134.

Typical comparisons of predicted jet trajectories, using this updated spreading parameter curve and those obtained experimentally, are shown in Figure 135. Good agreement was obtained for all configurations. In the case of the multiple opposed and nonopposed orifices [Figure 135(d)], a blockage factor was included equal to the orifice diameter times half the duct depth.

The x-z plane temperature profiles for the five unopposed holes indicated that for successful interaction and mixing of these jets within a realistic axial length, orifice spacing must be reduced to less than 4 diameters.

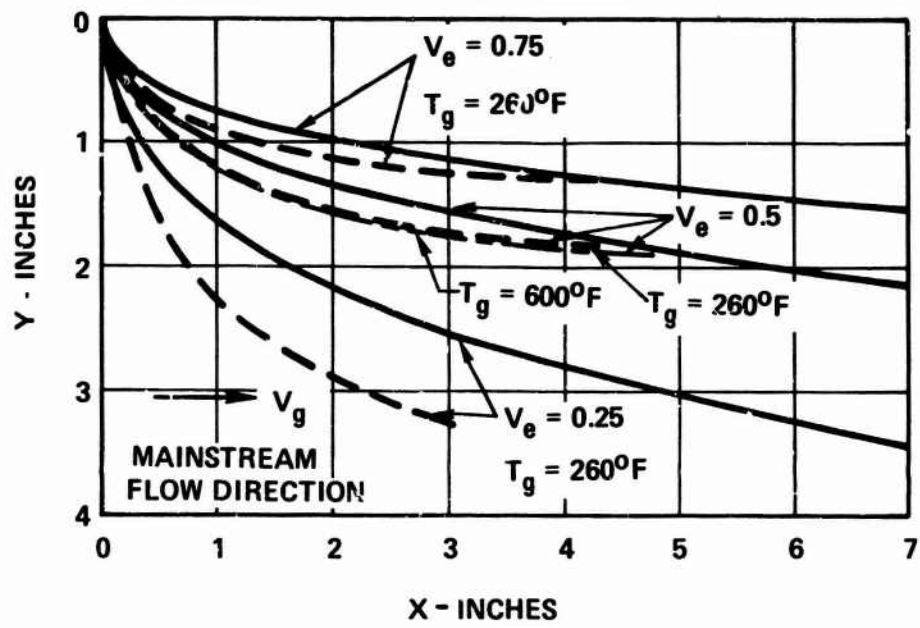


Figure 133. Dilution-Zone Measured and Predicted Jet Centerline Trajectories.

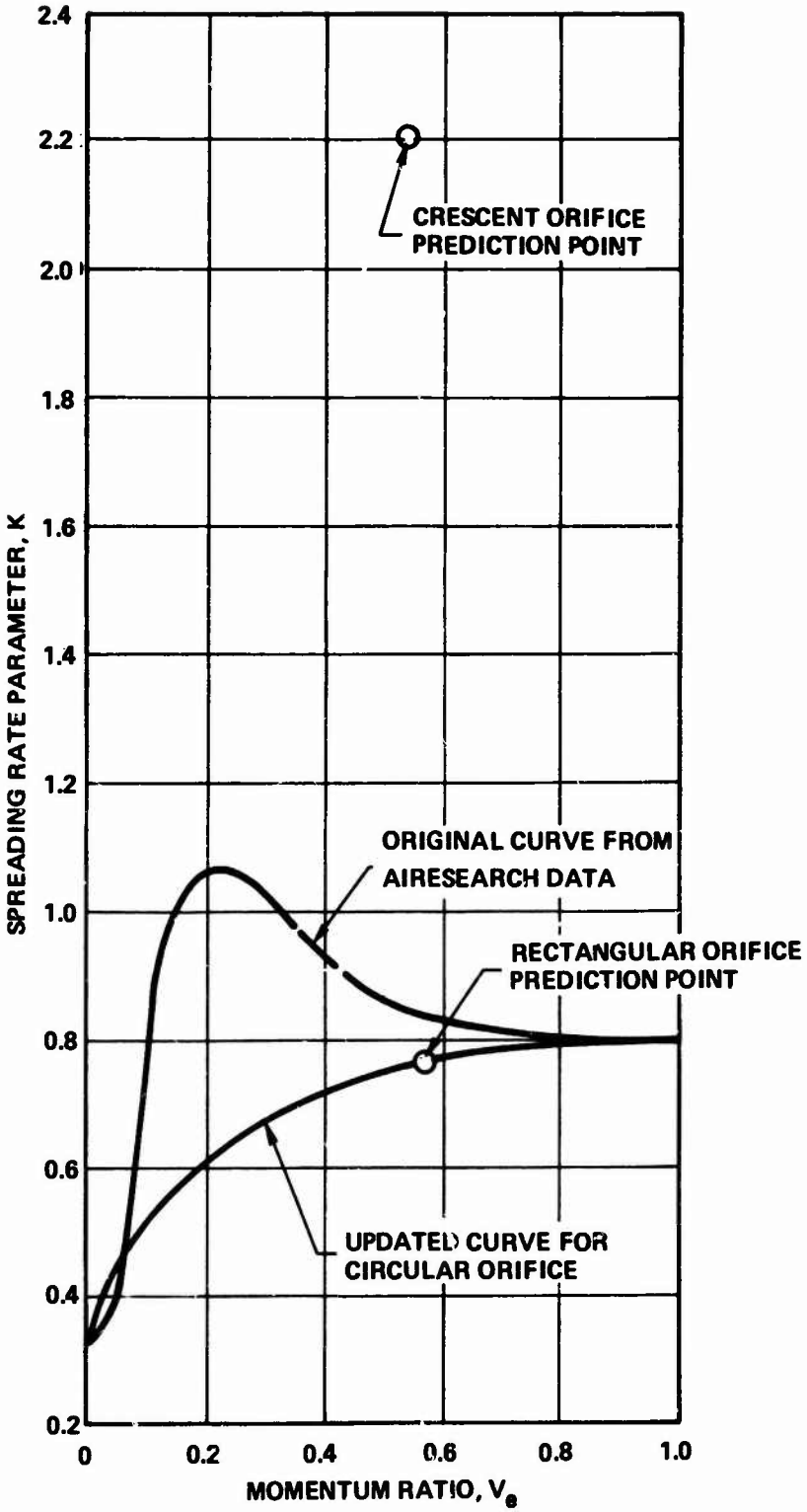


Figure 134. Spreading Rate Parameter.

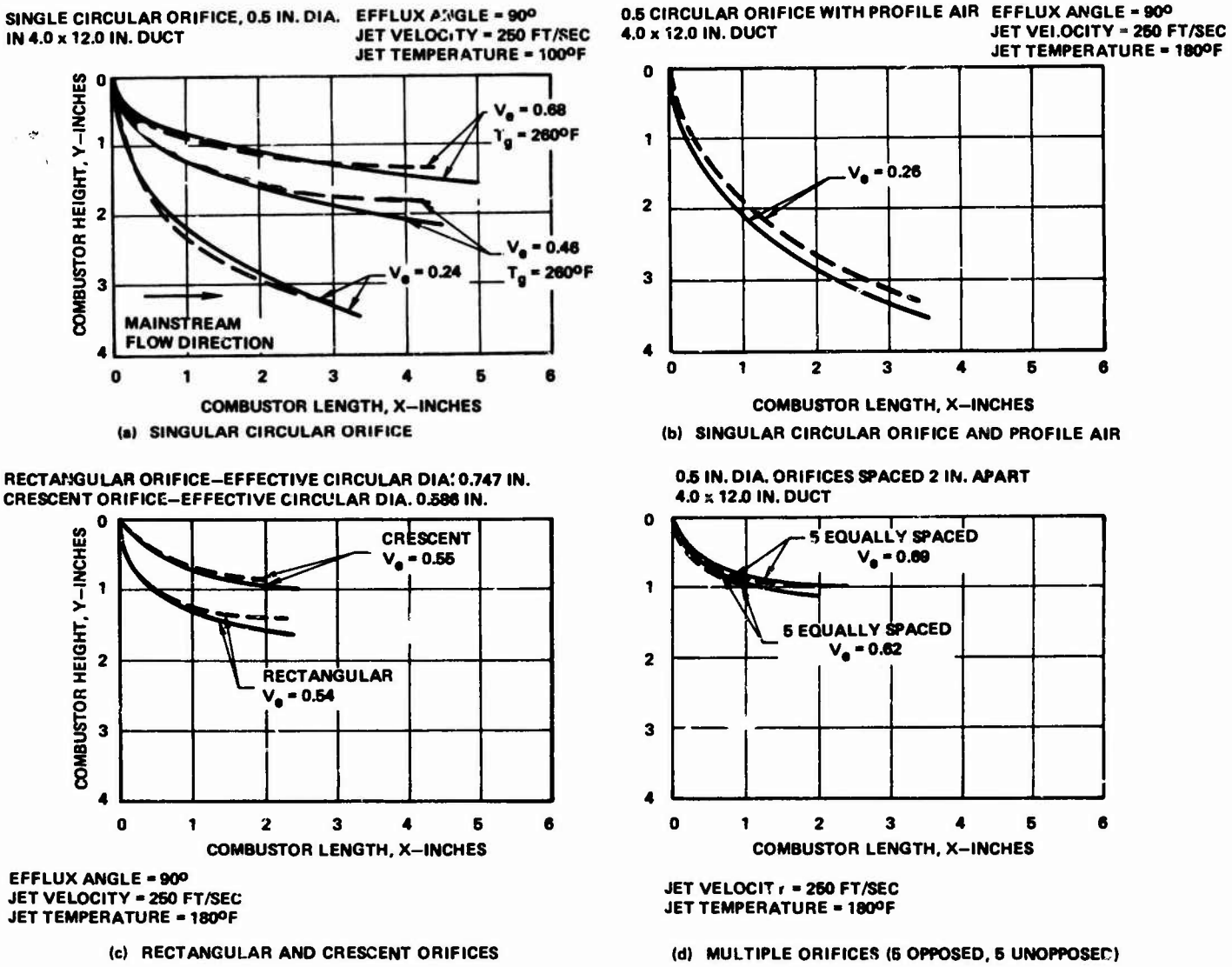


Figure 135. Updated Measured and Predicted Jet Centerline Trajectories.

An experimental investigation of pattern-factor improvement as a function of mixing-duct length and geometry is summarized in Figure 136. The results presented show a gradual decrease in pattern factor with increasing axial length followed by a more rapid decrease as the flow passes through the 180-degree turning duct. Tests were also conducted in a constant area duct to determine whether area reduction or turning exerts the predominant effect on pattern factor. Results of the test indicated that the flow separated in the constant-area turn, and a valid comparison could not be made. It is therefore concluded that constant-area ducts are not practical.

6.3 CONCLUSIONS

Reviewing the discharge coefficient testing and analyses, the following conclusions were drawn:

- The effect of annulus velocity can be predicted provided that the open-to-plenum discharge coefficient data is available.
- The use of plunged or thick-walled orifices has a beneficial effect on maintaining large, constant jet efflux angles.
- Thin-walled orifices result in small efflux angles that vary as a function of annulus velocity.
- Cooling skirt orifice discharge coefficients are 1.4 times those of single orifices due to the effect of the deflection skirt.
- The annulus loss model presented needs no further updating and can be used to check flow distribution following the design of the combustor system derived in Phase III.

After reviewing the dilution-zone testing and analyses, the following conclusions were drawn:

- The effective velocity ratio, V_e, is a successful correlating parameter for predicting the trajectory of the dilution air into the dilution zone.
- The predicted peak of the spreading-rate parameter curve at a value of $V_j = 0.25$ does not appear to exist.

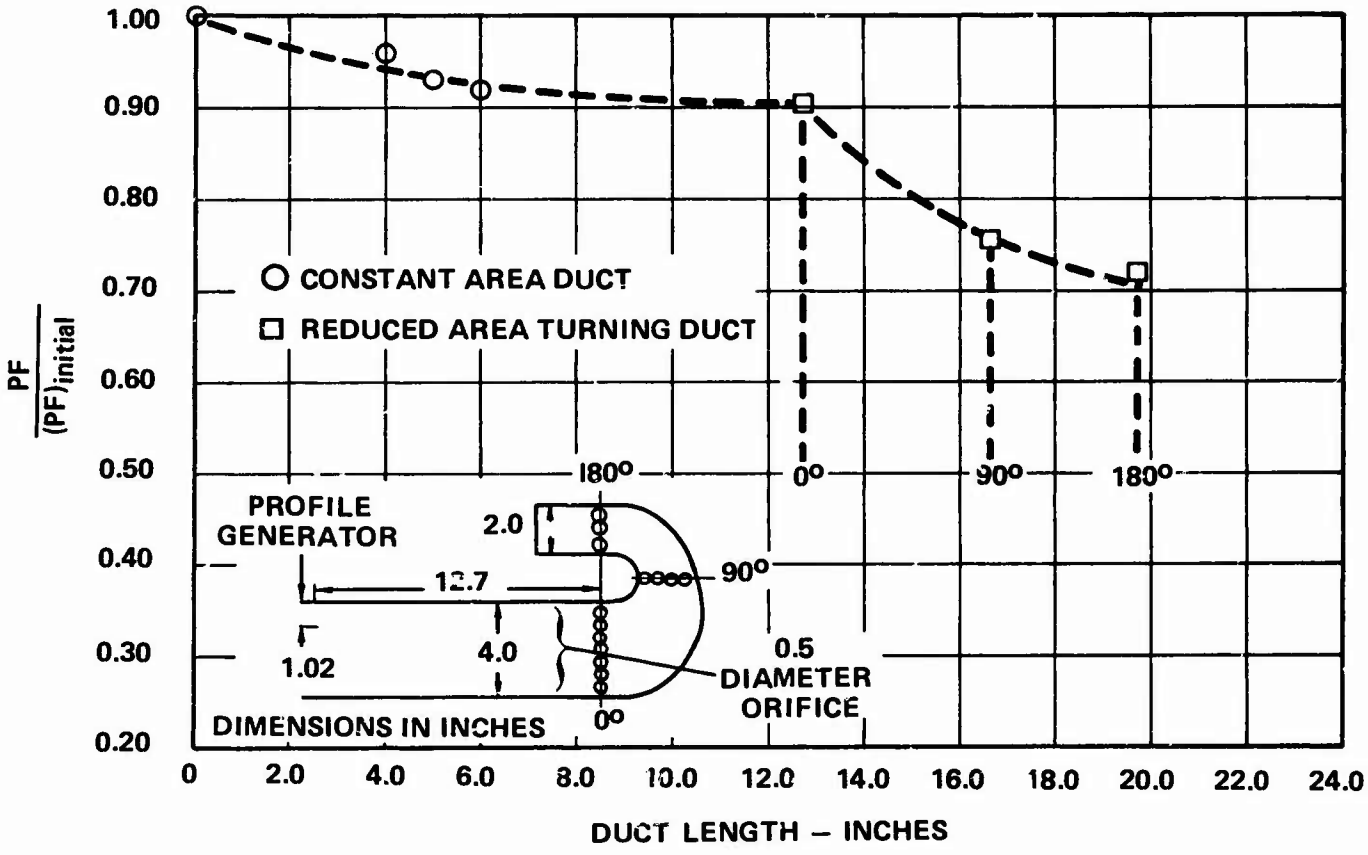


Figure 136. Pattern Factor.

- Circular orifice spreading extends to two diameters on either side of the orifice.

- Rectangular orifice penetration was less than anticipated and approximately equal to that of the circular orifice with a diameter equal to the rectangular width.

- Minimum penetration with maximum mixing was obtained with the crescent-shaped orifice.

- Pattern factor shows a gradual decrease with the mixing-duct length, and a more rapid decrease as the flow turns 180 degrees in a reducing-area duct.

Limitations imposed on the design of liner orifice configurations are total allowable pressure drop and combustor air available. In general, only limited air is available for pattern-factor trimming in the dilution zone; this necessitates careful design of the primary zone and efficient use of the air in this region to minimize the air required in the dilution zone. Pressure drop, combustor height, primary-zone temperature velocity profile, required pattern factor, and average T_4 directly influence orifice size and spacing. Current design techniques are, in general, limited to obtaining the desired overall combustor pressure drop and the overall fuel-air ratio as a function of axial location. Preliminary combustion tests to determine temperature profiles are necessary before the orifice configurations can be optimized. This limitation will be eliminated as the combustor flow-field prediction techniques are further developed to more accurately predict primary-zone flow-field characteristics.

Compressor discharge variations (swirl, distortion, strut separation, etc.) may impose some severe limitations on orifice design. Additionally, extreme difficulty exists in compensating for these variations in the design of cooling-skirt geometry.

7.0 LINER COOLING

The discussions of liner cooling and the stress analyses are combined in this section because the structural integrity (or life) of a combustor depends on the material properties and the effect of the accumulated thermal and stress histories on these properties. In order to achieve a long-life, lightweight combustor, the design analysis must consider (a) low-cycle fatigue due to thermal gradients and pressure loading, (b) creep distortion and plastic instability due to compressive hoop-pressure loading and exposure to high temperatures, and temperature cycling, and (c) effects of vibration. The stress, temperatures, and temperature gradients imposed on a combustor must be maintained at levels commensurate with the properties of the selected material.

Existing analytical techniques were adapted to assess the stress imposed on thin elastic shells of revolution with axisymmetric loading and the effect of temperature gradients on low-cycle-fatigue life. Analytical models were derived to assess film-cooling effectiveness and heat-transfer rates, and radiant heat loading. Combustor-element rig tests were conducted to provide data to update and validate these models. Finally, the detailed film-cooling models and simplified expressions for several of the candidate liner cooling concepts were used to quantitatively compare the following:

- Influence of various flow parameters, such as mass-injection rate, mainstream to cold-stream mass-flow-rate ratio, turbulence, temperature and velocity profiles in the mainstream, and injection angle
- Influence of hole characteristics, such as hole diameter, hole spacing, and types of holes and their arrangement
- Influence of pressure drop and other cycle requirements
- Structural integrity of the flame tube

7.1 STRESS ANALYSIS

A stress-analysis model was adapted to evaluate the stress distribution in a combustor shell. The model consists of a computer program that analyzes thin elastic shells of revolution with axisymmetric loading. The program computes axial, radial, and hoop forces, axial and hoop moments, axial and radial displacements, meridional rotation, meridional hoop and shear stresses, and equivalent stresses in a thin shell.

The computer program was used to conduct a stress analysis of a typical combustor configuration and to predict combustor life based on a hot-spot analysis described in Section 7.1.3. The results of these analyses, as well as a description of the analytical model, are presented in the following paragraphs.

7.1.1 Method of Solution

The original analysis is attributed to Love[55] and was reduced to two simultaneous second-order differential equations by Reissner[56] without the thermal-expansion terms. These result from the eight equations for equilibrium, compatibility, and stress-strain relations of Love's first approximate thin-shell theory.

The finite-difference forms of the basic equations are used to solve for the coefficients at the initial edge and again to determine elastic rotation of the meridional tangent and the internal radial force per unit circumferential arc-length at the terminal edge.

The assumptions inherent in the thin-shell theory are that (a) the shell thickness is everywhere less than 1/10 of the radius of curvature; (b) everywhere in the shell, the displacements are small in relation to the dimensions of the shell; and (c) the normal to the middle surface of the unstrained shell remains normal and unextended when the shell is strained. In effect, the latter indicates that transverse strain is neglected.

Geometry input for the shell analyzed is, for convenience, made up of a number of parts, each being either a cylinder, conical section, or toroidal section, and each having thickness, temperature, and pressure input as linear functions of arc length.

The shell may be subjected to local or distributed loads, as long as they are axisymmetric. Local axial forces may be applied at any point in the shell, but radial forces and moments can be applied only at the shell edges.

7.1.2 Combustor-Shell Analysis

The computer program was used to conduct a brief analysis of a typical annular combustor configuration. A schematic of the combustor and the results of the analysis are shown in Figure 137. The stress levels were acceptable except in the vicinity of the cooling bands. A more detailed design analysis would undoubtedly show that flexibility introduced by the drilled holes behind the cooling band reduces these stresses.

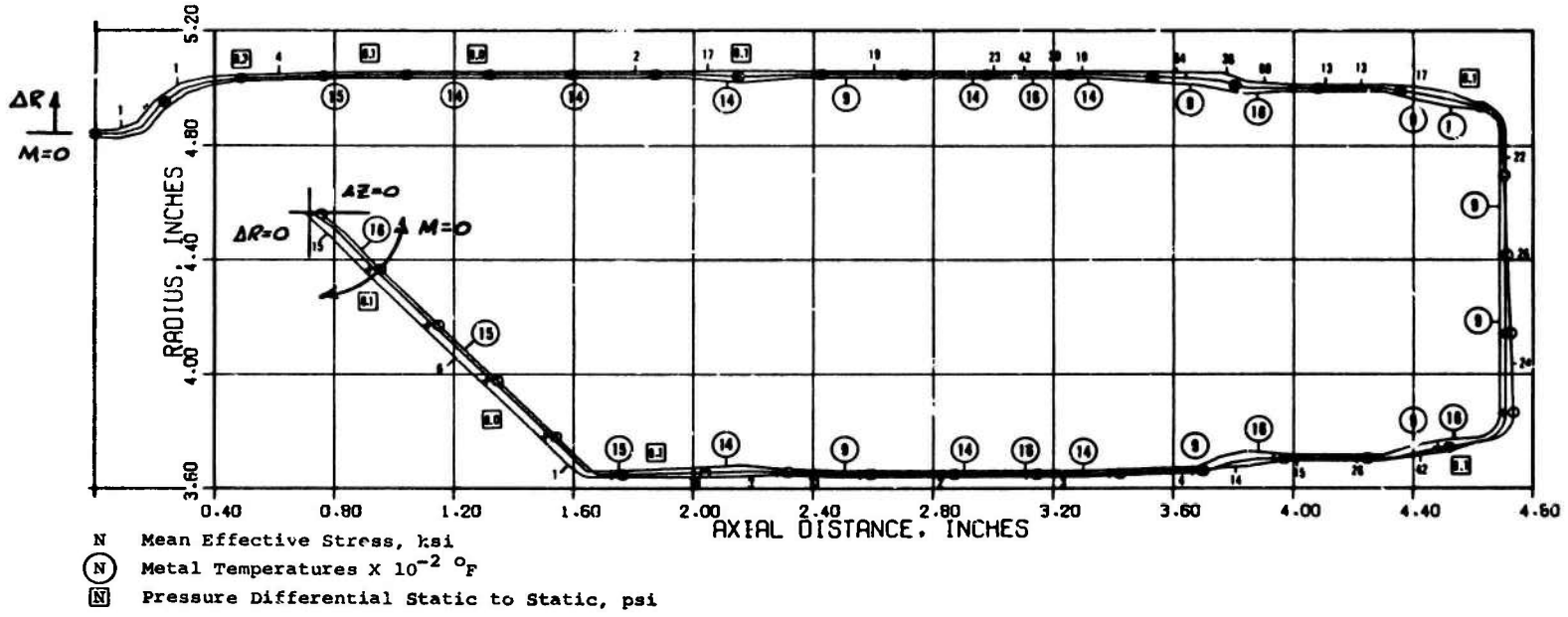


Figure 137. Combustor Stress Analysis (Including Temperature and Pressure Distribution).

7.1.3 Combustor Wall Temperature Gradient

To analyze the importance of the effect of temperature gradients on the low-cycle-fatigue life of combustors, a stress model of a typical combustor hot spot was established. The "hot-spot" model that was used is shown in Figure 138. The model consisted of a circular hot spot with a uniform maximum temperature, T_{max}, over the center 0.25-inch diameter, linearly varying down to the minimum temperature, T_{min}, in the remainder of the 1-inch-diameter hot spot. Because of the symmetrical nature of this model, the stress computations were independent of the metal thickness.

The model was utilized to predict elastic stress ranges in the hot-spot region for temperature gradients of 200°, 400°, 800°, 1200°, and 1600°F per inch, with maximum temperatures of 1200°, 1600°, and 1800°F. The calculated IN-586 elastic stress ranges for the above temperature gradients are presented in Figure 139. The results indicate that the stress range is a linear function of temperature gradient, $\Delta T/L$, as was expected for an elastic stress analysis.

With use of the calculated elastic stress and the low-cycle-fatigue data given in Section 3.0, the calculated combustor life was determined. A comparison of the predicted combustor life as a function of the hot-spot temperature gradient is plotted in Figure 140, as well as the trend observed in previous actual combustor testing. The comparison between the calculated low-cycle-fatigue life and the actual test data is quite good, in view of the simplicity of the combustor hot-spot model as compared with the complexity of this program. This indicates that the simplified combustor hot-spot model is a reasonable approximation of actual combustor hot spots. However, it must be realized that this curve is somewhat optimistic, and consideration should also be given to vibration, thermal cycle gradients, and combustion stability.

7.2 COMBUSTOR COOLING ANALYSIS

Cooling requirements are one of the primary constraints imposed on small, advanced combustors. For small engines with high turbine inlet temperatures, cooling-flow air is a significant percentage of the total inlet air, thus reducing the quantity available for the dilution zone. Cooling flow requirements are high because (a) the surface-to-volume ratio of combustors increases rapidly as the engine size and core airflow is reduced, and (b) advanced engine cycles continue to increase cycle pressure ratios, which raises the temperature of the compressor discharge air, and therefore lowers the attendant cooling capacity.

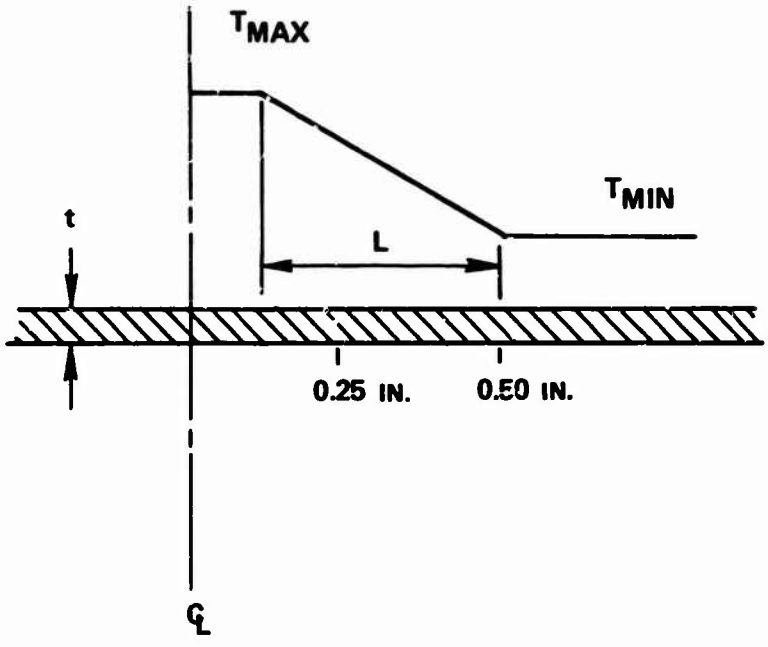


Figure 138. Hot-Spot Model Schematic.

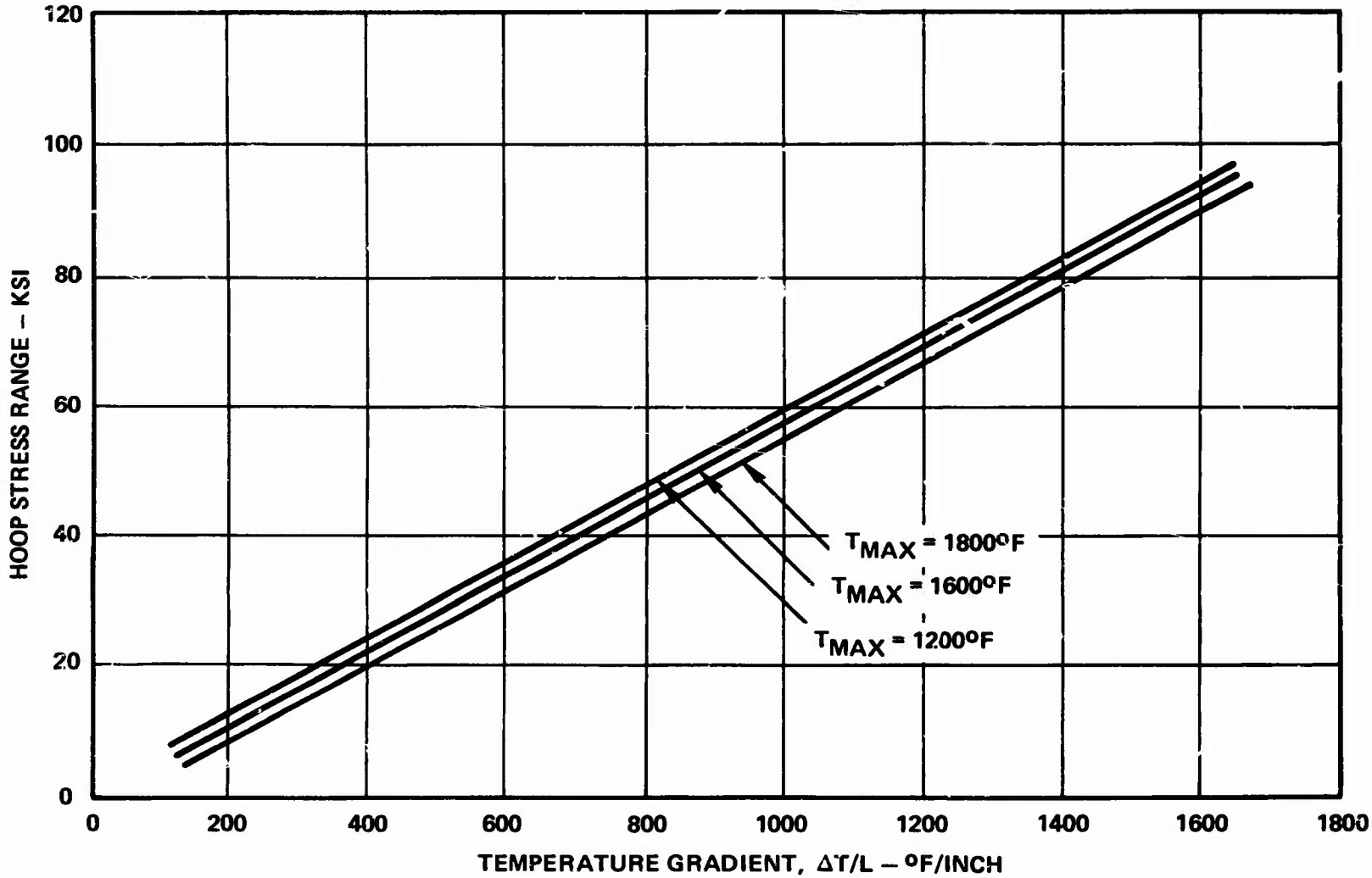


Figure 139. Stress Range Versus Temperature Gradient for IN-586.

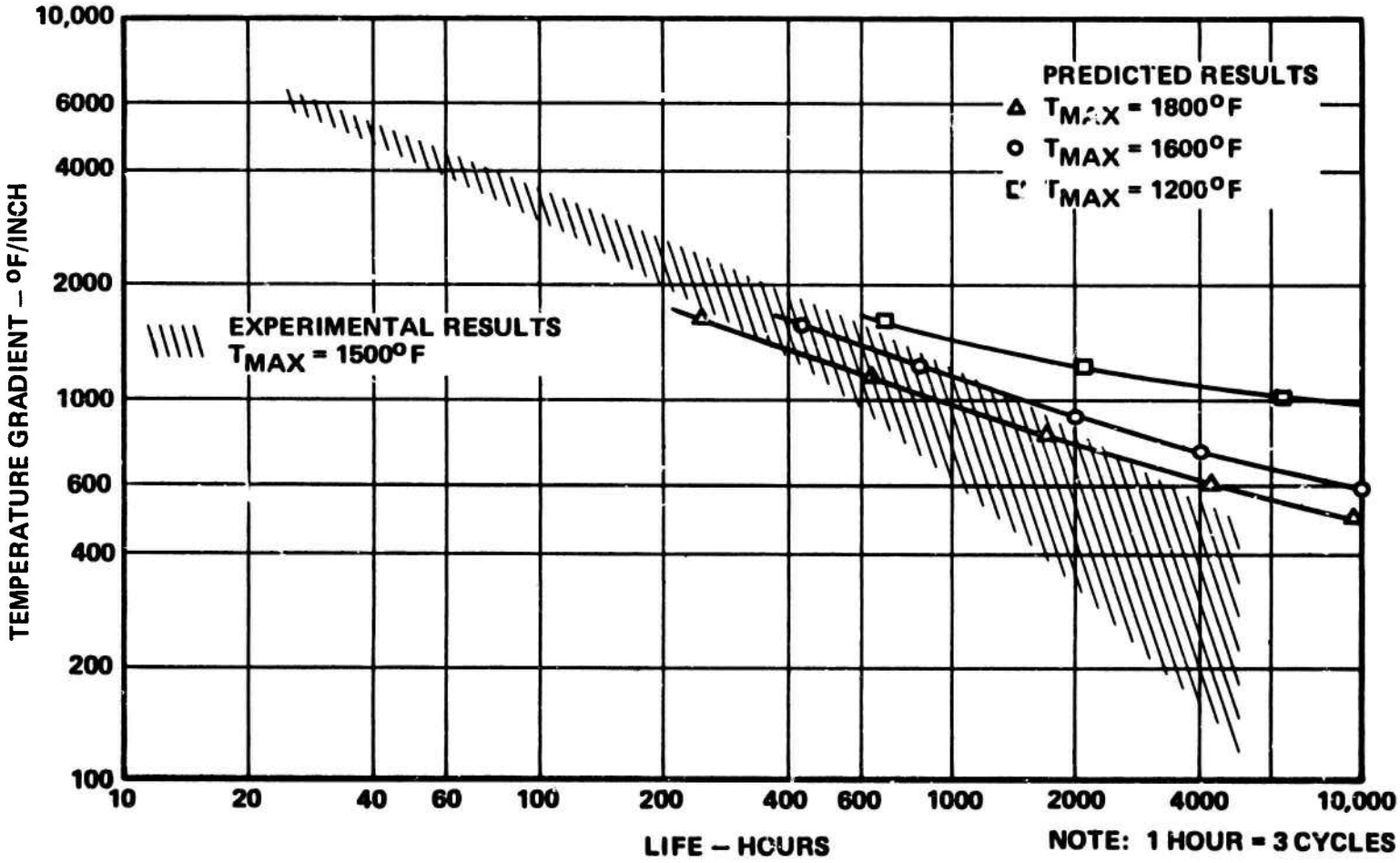


Figure 140. Combustor Life Versus Temperature Gradient for IN-586.

Alternate design approaches could consider the use of a high-temperature ceramic or refractory material for the liner and thereby preclude the requirement for cooling. The candidate ceramic materials, however, were considered inadequately developed at this time to be used for combustor test hardware in the program.

The most widely used combustion-liner cooling method is film cooling through approximately two-dimensional slots located at several axial positions along the combustor wall. Other cooling methods are known to be more effective but either are not sufficiently developed or impose unacceptable penalties such as pressure drop, fabricability cost, and particle contamination.

Transpiration cooling is the most effective known means of combustor wall cooling but was not pursued because the fabrication technology was not sufficiently developed and because of low tolerance to dust contamination. Impingement cooling is also an effective cooling scheme but requires a higher combustor pressure drop than the 3 percent specified for this program.

Convection cooling was briefly considered, but the fabrication cost and complexity associated with the surface extensions (fins) are prohibitive for consideration as a small engine production-combustor application. Recent work with roughened exterior surfaces (i.e., a rough metal spray or a chemical etching process) may result in an effective application of this cooling concept.

It was concluded after some preliminary analysis that (a) film cooling is adequate (though marginal) for the specified cycle parameters of this program, and (b) parametric design equations to optimize film-cooling effectiveness would contribute to the overall program objectives. The combustor cooling analysis consisted of three separate analytical models and supporting rig tests:

(a) With the use of existing data, empirical correlations were prepared to predict the performance of four classes of film-cooling configurations. A series of rig tests was conducted at Arizona State University to obtain effectiveness and heat-transfer coefficient data for parametric variations of each of the four configurations, and this data was used for updating the initial analytical model.

(b) A 4-times-size film-cooling slot was tested to determine mixing rates between the cooling film and the combustor mainstream flow. The data was used to confirm a numerical solution of mixing.

(c) An analytical model for flame (or gaseous) radiation was prepared. Data obtained during the high-pressure primary-zone rig tests was used to assess the validity of the analytical model.

These efforts are described in the following paragraphs.

7.2.1 Film-Cooling Analysis

One of the major variables in film-cooling performance is the injection geometry. The cooling film can be injected through lines of arrays of individual openings in the surface, or through slots that attempt to place the film onto the surface in a continuous, unbroken sheet. The shape and spacing of the openings, together with the angle of the film flow through the openings, result in innumerable configurations that could be used. Of course, the best protection for a downstream surface for a given coolant flow rate will be provided by an injection configuration that places a continuous coolant layer onto the surface in a manner that minimizes mixing between the coolant and primary streams.

For small combustors, cooling-film injection through continuous flush slots is precluded by manufacturing techniques, cost, and/or flow-metering considerations. Yet, if spaces are left between the coolant openings, the mainstream can flow onto the protected surface unimpeded. Moreover, the individual dilution jets penetrating into the mainstream allow the hot mainstream to mix in downstream of the jet, reducing the attendant effectiveness in cooling the surface. If the average cooled surface temperature is tolerable, the large local surface temperature variations present with these configurations may render the cooling scheme unacceptable. These problems have been overcome somewhat in most combustor liners by metering the coolant flow through a row of holes and then directing it onto a cover or splash plate to spread it out into a more or less continuous sheet at the injection point. Figure 141 schematically illustrates this type of configuration.

This section presents the results of an extensive experimental study of the performance characteristics of four classes of injection configurations thought to be suitable for gas-turbine combustion/chamber-liner cooling. These

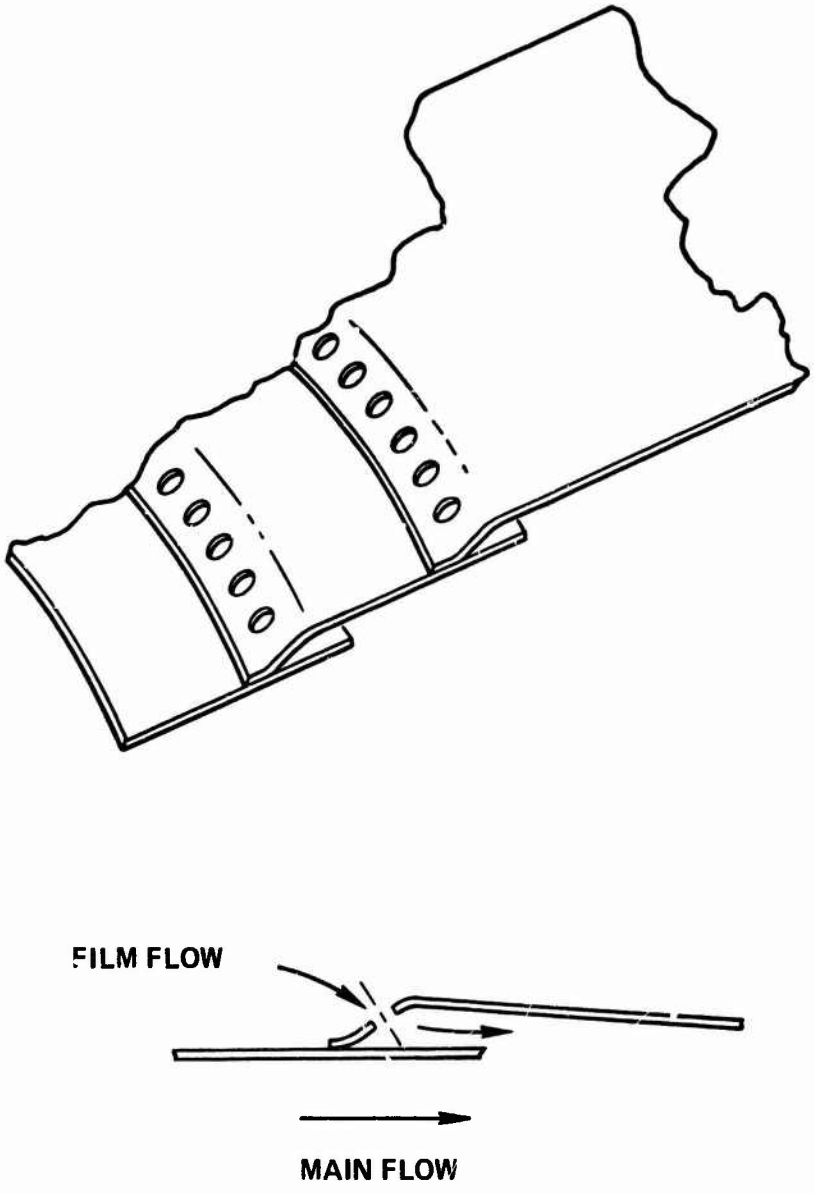


Figure 141. Combustor Film-Cooling Schematic.

results were published in an ASME report[57]. These four configurations are termed impingement film (IF), pinched impingement film (PIF), impingement film with wiggle strip (IF/WS), and hole-step (HS). They are shown schematically in Figure 142.

In the PIF configuration, a larger volume is provided in the impingement zone, as compared with the IF configuration, in anticipation that this will promote better spreading of the jets in the spanwise direction before injection onto the protected surface.

It was anticipated that better jet spreading and, thus, improved film-cooling coverage will accompany longer cover-plate lengths, L, for fixed values of the other geometrical and flow variables. However, long cover-plate lengths will be prone to deformation in actual engine operating conditions, and some type of restraint such as a wiggle-strip will undoubtedly be necessary. The hole-step configuration was included because it is simple to manufacture (a machined ring with drilled holes); and since the cover plate is eliminated, this configuration is not susceptible to deformation.

The initial correlations of film cooling performance for the four classes of cooling configurations were based on data for similar but less complex geometries. These correlations, detailed descriptions of the test procedures, and test results are presented by Love[55]. A summary of the test procedures, apparatus, and final correlations is presented in the following paragraphs.

7.2.1 1 Procedure and Apparatus

The film-cooling effectiveness, η_{Film}, is defined as

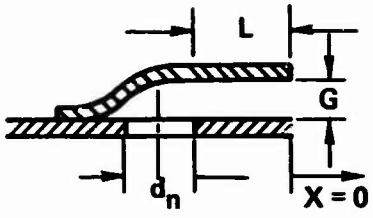
$$\eta_{Film} = (T_m - T_{aw})/(T_m - T_f) \qquad (15)$$

where T_m = mainstream temperature

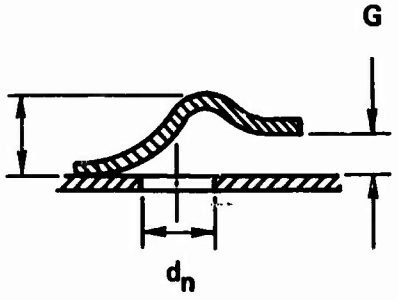
T_w = wall temperature

T_{aw} = adiabatic wall temperature

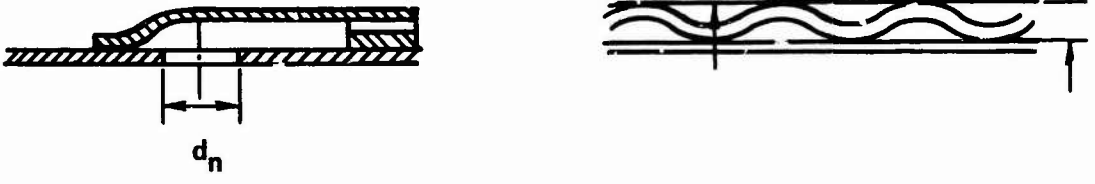
T_f = coolant film temperature



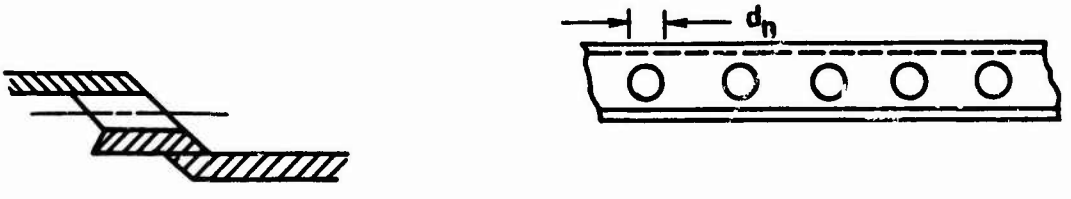
IMPINGEMENT FILM (IF)



PINCHED-IMPINGEMENT FILM (PIF)



IMPINGEMENT FILM WITH WIGGLE STRIP (IF/WS)



HOLE-STEP (HS)

Figure 142. Cooling Slot Geometry Schematics.

In design practice, correlations of η_{Film} are used to obtain T_{aw} for use in conjunction with a convective heat-transfer coefficient, h, to predict the local heat flux ($\dot{q}/A$) for a given surface temperature:

$$\dot{q}/A = h(T_{aw}-T_w) \tag{126}$$

If correlations for T_{aw} with film cooling are available, then a common procedure is to use the heat-transfer coefficient that is associated with the primary flow alone. Unfortunately, this procedure is generally inadequate for predicting heat-transfer rates in the important region immediately downstream of the injection site. In this near region, the injection of the secondary fluid, even if two-dimensional, can significantly alter the flow pattern from that of the primary flow alone, and the effective heat-transfer coefficients may be either increased or decreased, depending on the amount and nature of the injection.

In this program, heat-transfer rates were measured directly; in effect, both h and T_{aw} were determined at the same time. Average surface heat-transfer rates were measured over finite chordwise distances, ℓ, downstream of the injection point. These rates were compared to the heat-transfer rate measured with the same surface and mainstream conditions without injection. The ratio of average surface heat transfer with injection to that without injection, ϕ, is presented nondimensionally as

$$\phi = \phi\ (\overline{W},\overline{T},\ \ell/s) \tag{127}$$

where

$$\overline{T} = (T_m-T_f)/(T_m-T_w) \tag{128}$$

and s is the actual width of a two-dimensional injection slot.* $\overline{W}$ is the ratio of the coolant mass velocity to the mainstream mass velocity. Alternatively, $\overline{W}'$ may be used, which employs the film mass flow per unit area of slot gap.

The functional relationship implied in Equation (127) was obtained from a nondimensionalization of the governing boundary-layer momentum and energy equations and appropriate boundary conditions for two-dimensional slot injection, uniform surface temperature, and small temperature differences.

---

*s_{eq} as used later is the width of an equivalent slot of equal discharge area for the case of hole injection.

The assumption of small temperature differences is consistent with a linear formulation of the energy problem where film cooling ($T_m > T_f$) and film heating ($T_m < T_f$) are similar problems governed by the same equations and boundary conditions.

When $\bar{T} = 0$, $T_f = T_m$ and the value of ϕ at this point indicates the hydrodynamic effect of the film on the downstream surface heat transfer. Previous work has shown that this effect, averaged over a surface length of 35 slot widths, is quite small for $0.25 \leq \bar{W} \leq 0.78$.

When $\phi = 0$, the average surface heat-transfer rate is zero, although in general the local rates on the surface will not be zero. If the value of $\bar{T}$, when $\phi = 0$, is denoted by $\bar{T}_{ad}$, then

$$\bar{T}_{ad} = (T_m - T_f)/(T_m - T_{aw}) \qquad (129)$$

Here T_{aw} must be interpreted as the surface temperature corresponding to zero average surface heat flux. The inverse of $\bar{T}_{ad}$ has the form of film-cooling effectiveness, although the actual surface condition is not in general locally adiabatic.

Thus, the value of $\bar{T}_{ad} = 0$ essentially conveys effectiveness information, whereas the value of ϕ at $\bar{T} = 0$ indicates the effects of injection on heat transfer that are not available from adiabatic wall temperature distribution alone. A value of ϕ at $\bar{T} = 0$, ϕ_o, equal to unity, indicates that the average surface heat flux can be predicted by Equation (126) with the primary flow heat-transfer coefficient. The percent increase or decrease in ϕ_o from unity is directly proportional to the error incurred in predicting surface heat flux from Equation (126) with the primary flow heat-transfer coefficient and measured adiabatic wall temperatures.

It should be emphasized that the information conveyed with the ϕ parameter is heat-transfer-rate information, which is obtainable only with heat-transfer test surfaces that are nonadiabatic. With injection configurations such as the present, where the probability that $\phi_o = 1.0$ is very high, the present test method possesses considerable advantages over conventional adiabatic surface measurements.

The film-cooling facility used for these tests consisted of an open-cycle wind tunnel, shown schematically in Figure 140. Mainstream air at up to 150 feet per second was supplied from ambient laboratory conditions with an upstream blower. The heated secondary, or film, air was supplied from the laboratory compressed-air supply. Both flows were orifice-metered in accordance with ASME standards. The injection section consisted of a plenum chamber with baffles and screens topped by removable test pieces (fabricated from acrylic plastic) that provided the different injection configurations.

A close-up of the test section showing the relationship between the test piece and the heat-transfer surface is shown in Figure 144. During a transient test with secondary injection, all the flow variables, including T_f and T_m, were maintained constant; so, at any given time during the transient, the value of T_w (measured) and the value of q [calculated from Equation (126)] correspond to a single value of $\overline{T}$. This calculated heat-transfer rate was normalized with the rate observed for the same mainstream conditions and surface temperature in the absence of injection.

A total of 33 different test pieces was fabricated. Six typical impingement film test pieces are shown in Figure 145. The geometry of the four basic configurations is shown in Figures 146 through 149. Dimensional variations of each of the configurations are presented in tabular form in each figure.

7.2.1.2 Summary of Results and Conclusions

The impingement film, pinched-impingement film, and wiggle-strip configurations that were studied can all be classified as hole injection onto a cover or splash plate, which directs the flow onto the downstream surface. The most significant geometric parameters governing the film-cooling performance for these configurations are the open-area ratio, s_{eq}/G, and the relative cover-plate length, L/G. The other geometric effects explored in the pinched-impingement film configurations and in the wiggle-strip configurations appear to have much smaller effects on film-cooling performance.

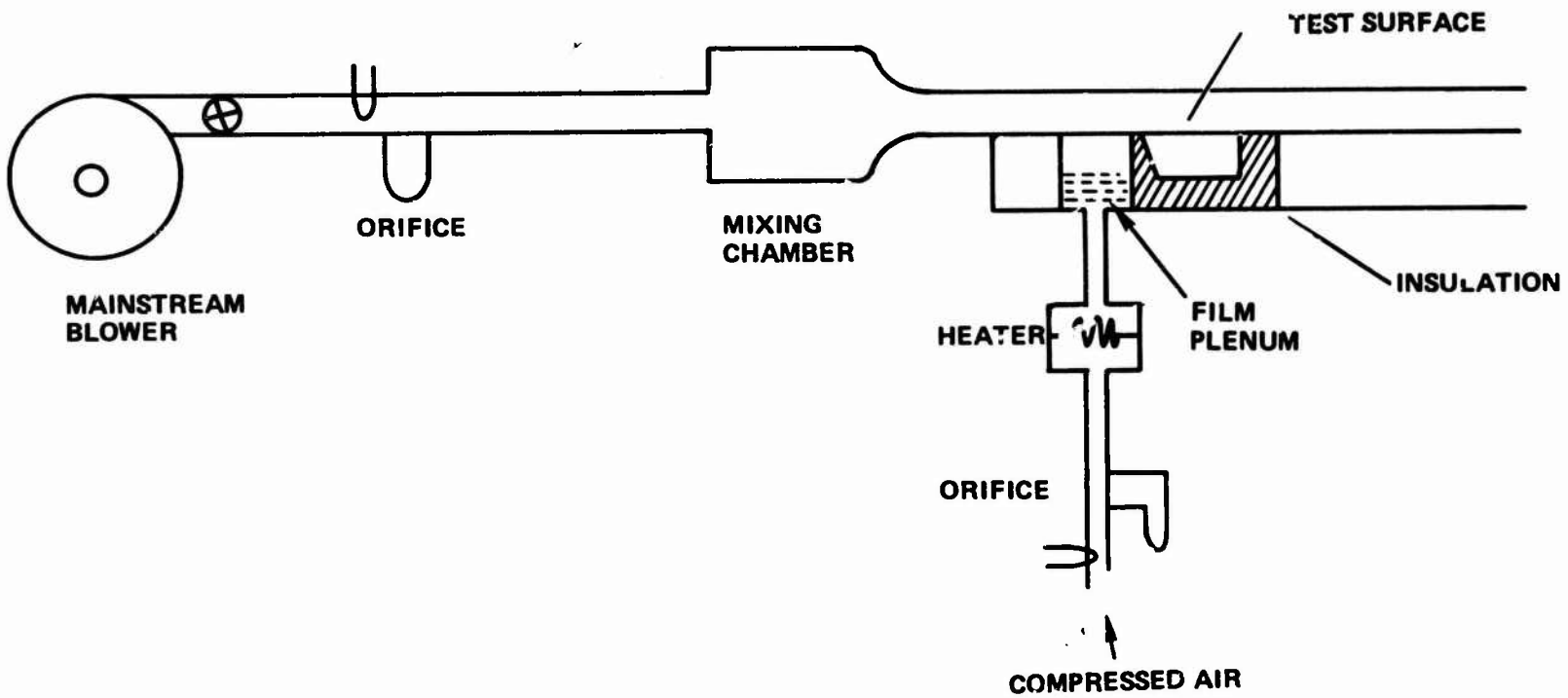


Figure 143. Film-Cooling Test Facility Schematic.

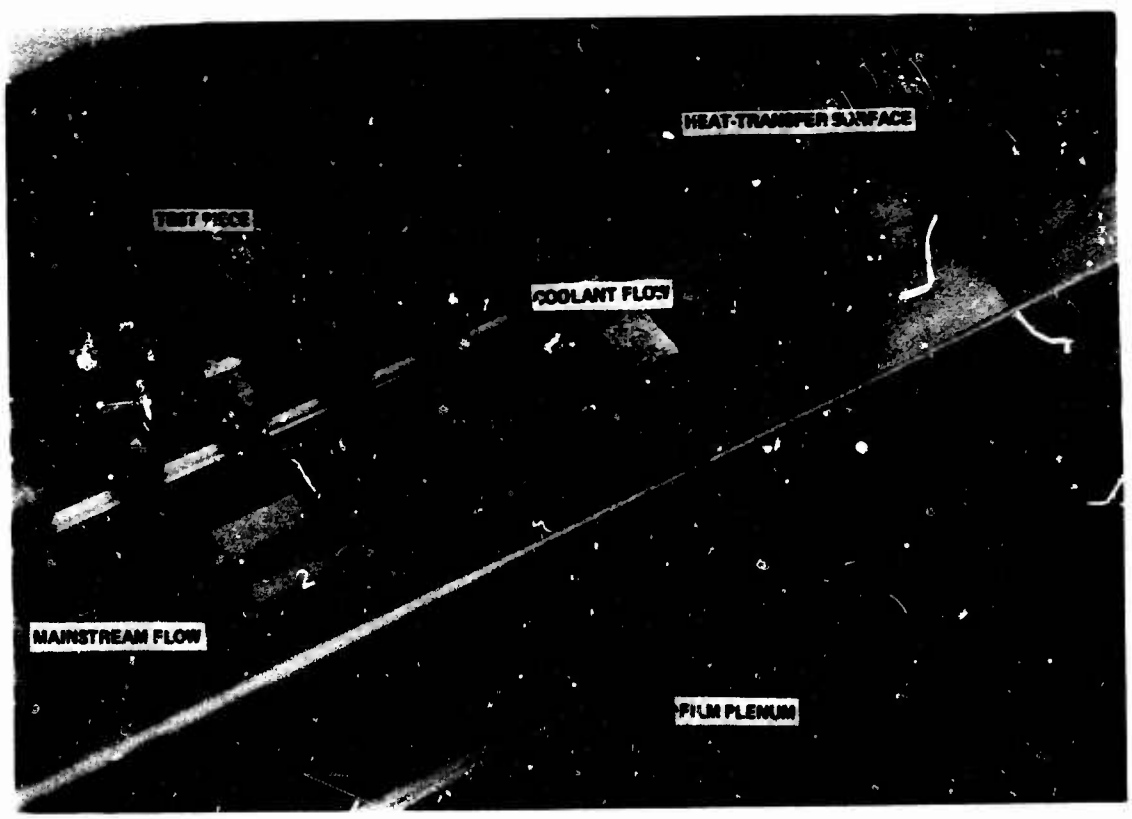


Figure 144. Film-Cooling Test Section.

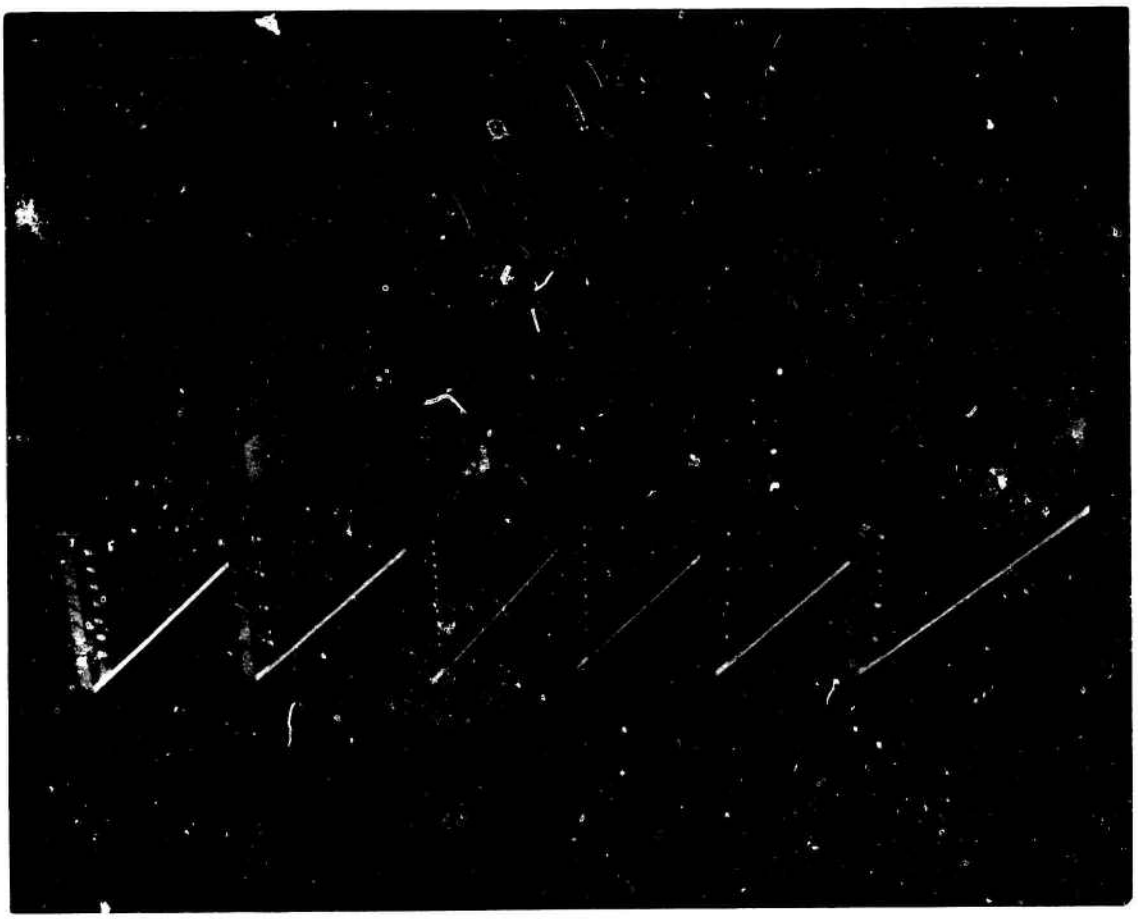


Figure 145. Typical IF Test Pieces.

Configuration	Hole Diameter (d_n)	Lip Length (L)	Gap (G)	Lip Thickness (t)	Number of Holes (n)
IF-1	0.050	0.050	0.025	0.020	7
IF-2	0.100	0.100	0.050	0.040	4
IF-3	0.100	0.250	0.050	0.040	4
IF-4	0.100	0.100	0.050	0.020	4
IF-5	0.100	0.100	0.050	0.040	7
IF-6	0.100	0.100	0.050	0.040	10
IF-7	0.050	0.150	0.050	0.040	7
IF-8	0.100	0.175	0.050	0.040	4
IF-9	0.100	0.100	0.100	0.040	7
IF-10	0.100	0.175	0.050	0.040	5
IF-11	0.100	0.100	0.030	0.040	7

ALL DIMENSIONS IN INCHES

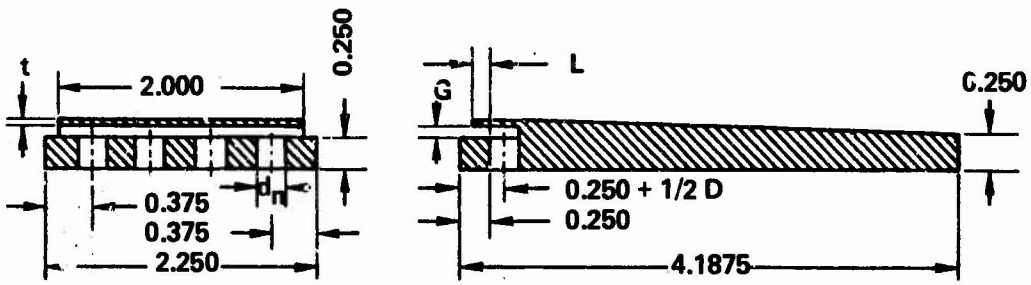


Figure 146. Impingement Film Configurations.

Configuration	Hole Diameter (d_n)	Lip Length (L)	Gap (G)	Lip Thickness (t)	Number of Holes (n)
PIF-1 (u)	0.050	0.250	0.050	0.062	7
PIF-2 (d)	0.050	0.250	0.050	0.062	7
PIF-3 (u)	0.050	0.250	0.050	0.062	13
PIF-4 (d)	0.050	0.250	0.050	0.062	13
PIF-5 (u)	0.050	0.050	0.050	0.062	7
PIF-6 (d)	0.050	0.050	0.050	0.062	7
PIF-7 (u)	0.050	0	0.050	0.062	7
PIF-8 (d)	0.050	0	0.050	0.062	7
PIF-9 (m)	0.050	0.250	0.050	0.062	7
PIF-10 (m)	0.050	0.250	0.050	0.062	13

ALL DIMENSIONS IN INCHES

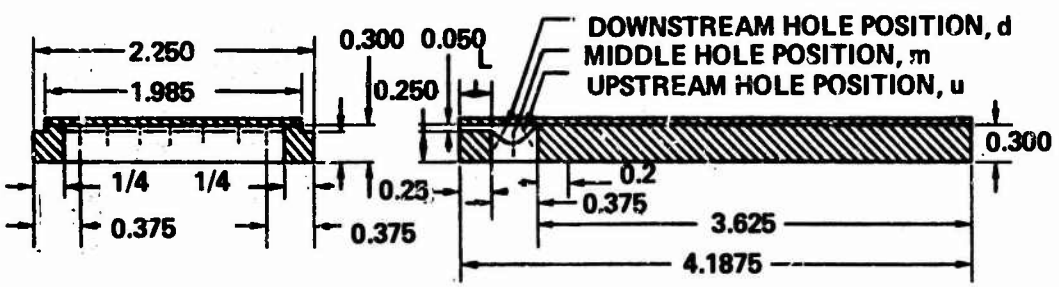
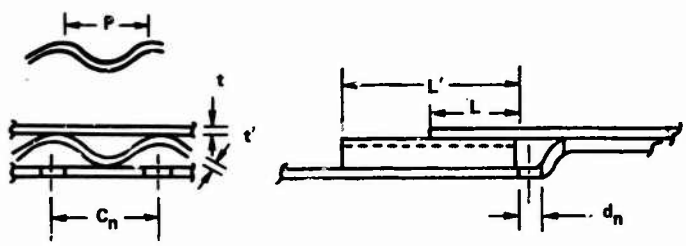


Figure 147. Pinched-Impingement Film Configurations.

Configuration	Hole Diameter (d_n)	Lip Length (L)	Gap (G)	Lip Thickness (t)	Number of Holes (n)	Wiggle-Strip Thickness (n)	Wiggle-Strip Length (L')	Wiggle-Strip Pitch (P)
IF/WS-1 (u)	0.100	0.100	0.050	0.040	4	0.010	0.250	0.500
IF/WS-2 (d)	0.100	0.100	0.050	0.040	4	0.010	0.250	0.500
IF/WS-3 (u)	0.100	0.250	0.050	0.040	4	0.010	0.250	0.500
IF/WS-4 (d)	0.100	0.250	0.050	0.040	4	0.010	0.250	0.500
IF/WS-5 (u)	0.100	0.250	0.050	0.040	4	0.010	0.125	0.500
IF/WS-6 (d)	0.100	0.250	0.050	0.040	4	0.010	0.125	0.500
IF/WS-7 (u)	0.100	0.175	0.050	0.040	4	0.010	0.125	0.500
IF/WS-8 (d)	0.100	0.175	0.050	0.040	4	0.010	0.125	0.500

ALL DIMENSIONS IN INCHES



(a) WIGGLE-STRIP GEOMETRY



(b) WIGGLE-STRIP ORIENTATION

Figure 148. Impingement Film With Wiggle-Strip Configurations.

Configuration	Hole Diameter (d_n)	STEP Height (S)	STEP Angle (α)	Number of Holes (n)
HS-1	0.050	0.125	45°	20
HS-2	0.075	0.187	45°	15
HS-3	0.100	0.125	45°	10
HS-4	0.050	0.125	60°	20

ALL DIMENSIONS IN INCHES

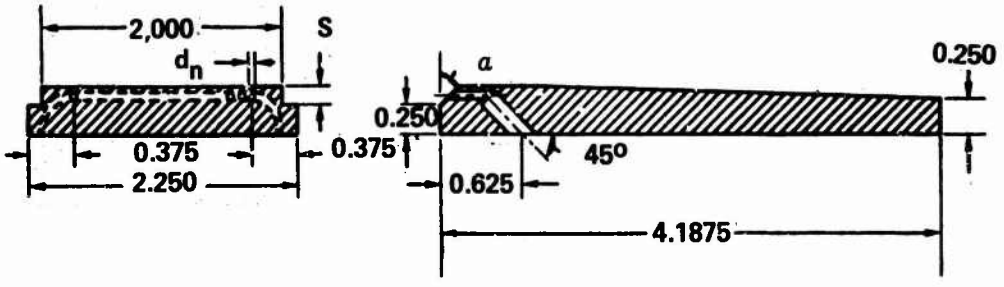


Figure 149. Hole-Step Configurations.

7.2.1.2.1 Impingement Film Configuration

In general, for the impingement film configuration, cooling performance tends to increase with increasing $\bar{W}$ but is relatively insensitive to $\bar{W}' > 0.6$. Figure 150 presents the data for the IF configurations with $0.60 \leq \bar{W} \leq 2.46$. The vertical bars on the figure represent the range of ordinate values calculated from the test results. In some cases, the bars have been displaced slightly from their actual ℓ/G value for clarity. For values of $\bar{W}$ less than 0.6 ($0.154 \leq \bar{W}' \leq 0.45$), the data indicated that performance decreases as a function of downstream distance.

The data can be represented by the following equations:

For $\bar{W}' > 0.6$,

$$\frac{\bar{T}_{ad}}{[1.0 + 0.614\ (G/s_{eq} - 1.0)][1.0 + 0.083\ (5.0 - L/G)]} = 0.81 + 0.0093\ (\ell/G)\ (\pm 10\%) \qquad (130)$$

For $0.154 \leq \bar{W}' \leq 0.45$,

$$\frac{\bar{T}_{ad}\ (\bar{W}')^{0.02}\ (\ell/G)}{[1.0 + 0.0614\ (G/s_{eq} - 1.0)][1.0 + 0.083\ (5.0 - L/G)]} = 0.72 + 0.00512\ (\ell/G)\ (\pm 15\%) \qquad (131)$$

The individual effects of the geometrical parameters L/G, G/d_n, etc., are not nearly as evident in the ϕ-values as in the values of $\bar{T}_{ad}$. The parameter that displays the most consistent influence on ϕ is the injection rate, $\bar{W}'$. In general, as $\bar{W}'$ is increased from a small value, say $\bar{W}' = 0.2$, the value of ϕ also tends to increase, but the effect is not very consistent between $\bar{W}' = 0.2$ and $\bar{W}' = 0.45$. Here ϕ should be interpreted as a magnification factor on the average heat-transfer coefficient that would be used over the cooled-panel length in the absence of the film-cooling slot. This magnification is probably caused by many factors, including the high turbulence levels generated in the jets before and during their turning by the cover plate, and by the probable mainflow separation at the cooling lip and reattachment.

Figure 151(a) shows data for the IF configurations for $0.154 \leq \bar{W}' \leq 0.45$. This data is represented by the following equation:

$$\phi = 1.3 \pm 25\% \qquad (132)$$

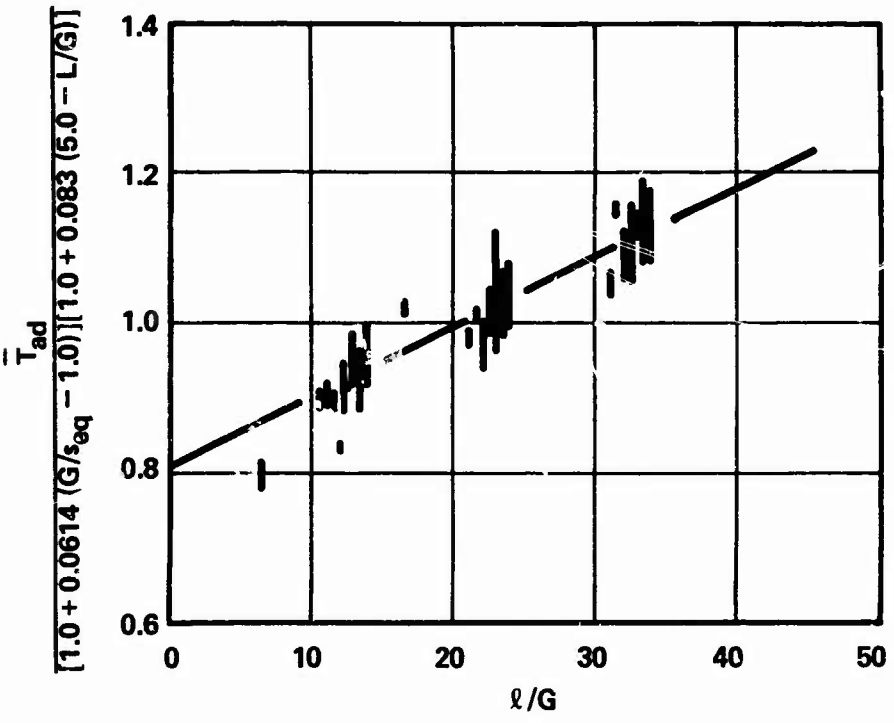


Figure 150. $\bar{T}_{ad}$ Correlation Versus ℓ/G for $\bar{W}'$ Greater Than 0.6.

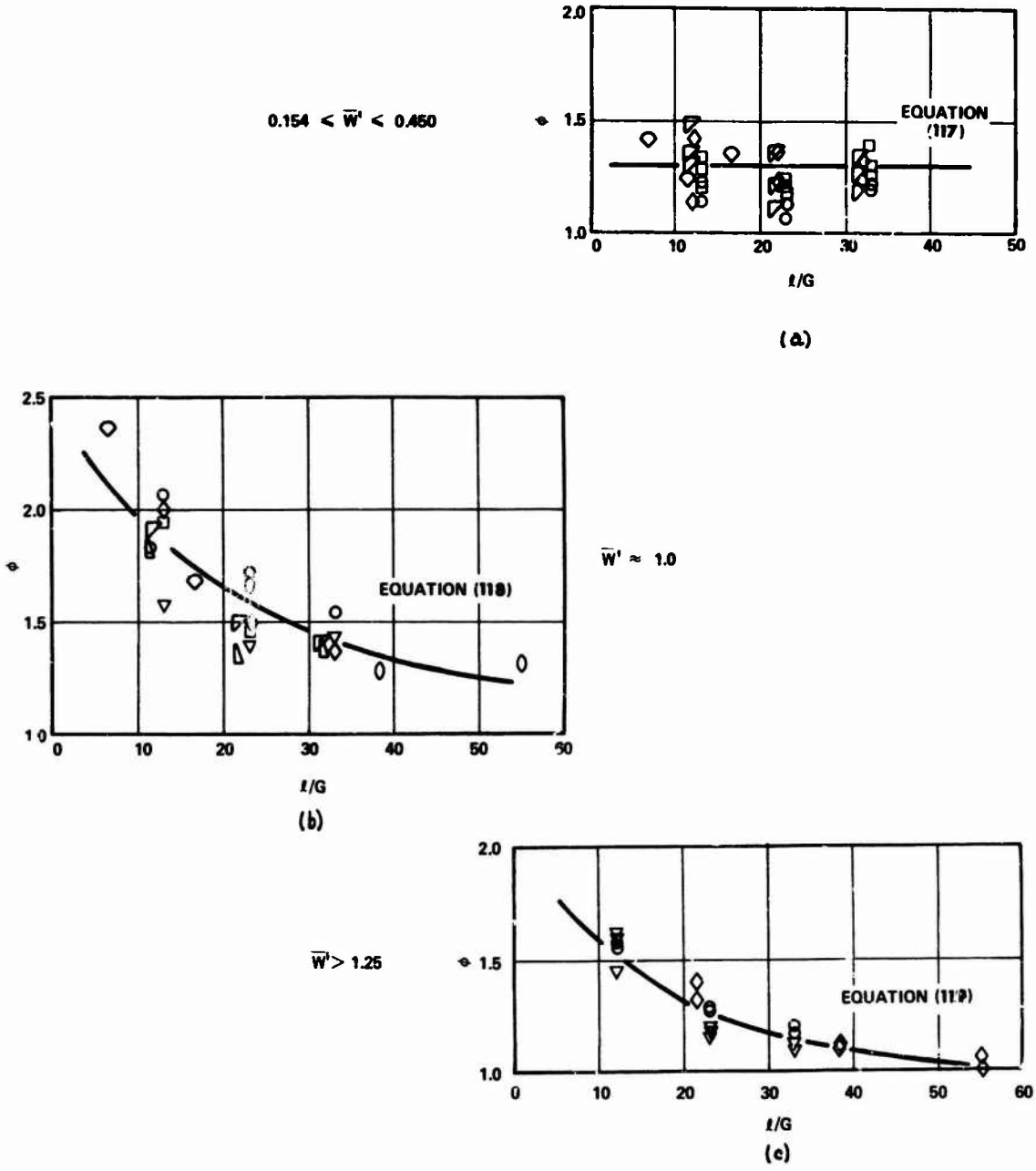


Figure 151. ϕ Versus ℓ/G Correlation.

There is a gap in the data between $\bar{W}' = 0.45$ and $\bar{W}' = 0.6$, but at $\bar{W}' = 0.6$, the data begins to exhibit a stronger dependence on the downstream distance, ℓ. This is also illustrated in Figure 151(b), which presents data for $\bar{W}' = 1.0$. Again, in this range, the influence of $\bar{W}'$ is somewhat inconsistent, but the variation of ϕ is relatively small. Consequently, the data of Figure 151(b) represents the range $0.6 \leq \bar{W}' \leq 1.25$. It is correlated by the equation

$$\phi = 3.45\ (\ell/G)^{-0.25},\ \pm 20\% \qquad (132)$$

$$\text{for } 0.6 \leq W' \leq 1.25$$

For $\bar{W}'$ values greater than 1.25, increasing $\bar{W}'$ consistently increases ϕ, and this is illustrated in Figure 151(c). The data is correlated by the equation

$$\phi(\bar{W}')^{-0.72} = 2.42(\ell/G)^{-0.2},\ \pm 15\% \qquad (133)$$

$$\text{for } \bar{W}' > 1.25$$

7.2.1.2.2 Impingement Film With Wiggle-Strip Configuration

Analysis of the IF and IF/WS data showed that both $\bar{T}_{ad}$ and ϕ are essentially unaffected by the addition of a wiggle strip.

It should be noted that the configurations explored represent only a small portion of possible wiggle-strip sizes, shapes, and lengths. The main variations studied were the length of the wiggle strip, L', relative to the cover-plate length, L ($0.5 \leq L'/L \leq 2.5$), and the strip orientation. Despite these limitations, the results should be representative of a fairly large class of wiggle-strip designs.

Thus, a very important conclusion of this study is that if a wiggle strip is necessary in a film-cooling slot to maintain the slot dimensions, it can be added without sacrificing the film-cooling performance, provided that strips similar to those tested are employed.

7.2.1.2.3 Pinched-Impingement Film Configuration

The objectives of the PIF tests were (a) to discern the effect of a small plenum upstream of the film gap, and (b) to see if the orientation of the film orifices (see Figure 152) in the plenum has any effect on performance. During each test, only one row of holes was used.

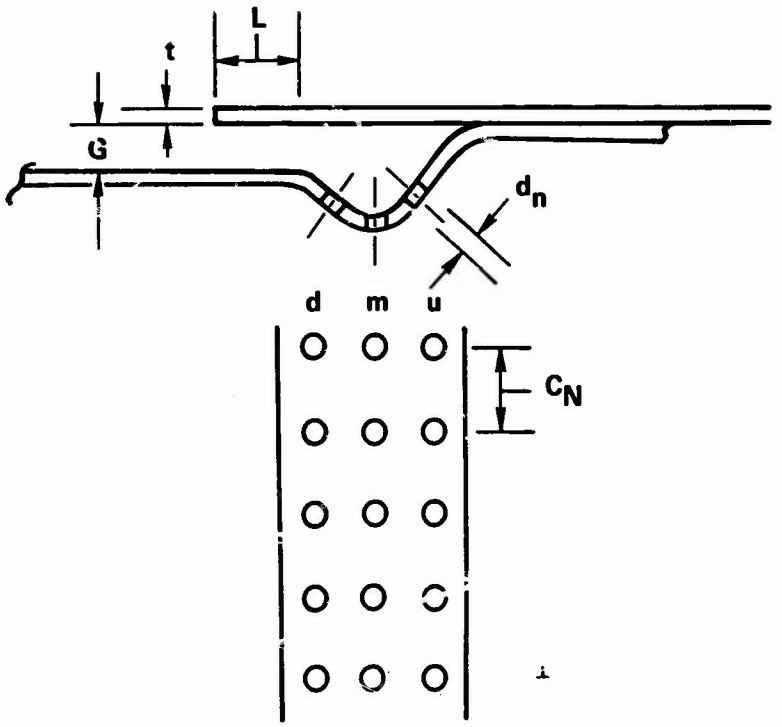


Figure 152. Pinched-Impingement Film Geometry.

From an analysis of the data, it was concluded that the performance is similar to that achieved with the impingement-film configurations, and performance is not significantly affected by the location of the injection holes. Typical results are presented in Figure 153. The solid line on Figure 153 represents the correlating equation previously derived for the impingement-film results (Equation 129).

It should be noted that while the pinched-impingement-film configuration may add to the fabrication cost, the design concept adds rigidity to the typically thin combustor walls. Although additional surface area is exposed to the hot combustion gas, metal temperatures are maintained at a low level by the impinging cooling flow on the inside (admittedly at the expense of increased cooling air film temperature).

7.2.1.2.4 Hole-Step Configuration

Data for the HS configuration showed somewhat poorer performance than IF configurations having the same $\bar{W}$. As expected, the best results were obtained with a large number of holes, since this tends to approach a nearly continuous cooling film.

7.2.1.2.5 Correlating Equations

The design equations derived for the four classes of film-cooling configurations of the present study can best be summarized by those derived for the impingement-film configuration, since the equations are directly applicable to three of the four geometries tested. The minor differences noted for the hole-step configuration should be considered prior to use of the hole-step design.

The correlated adiabatic wall temperatures (in terms of $\bar{T}_{ad}$) are given by

$$\bar{T}_{ad}\ (\bar{W}')^{B}/A = C + D(\ell/G) \qquad (134)$$

where $A = [1.0 + 0.0614(G/s_{eq} - 1.0)][1.0 + 0.083(5.0 - L/G)]$

and

$$\begin{aligned} B &= 0.02(\ell/G) && ;\ 0.154 \leq \bar{W} \leq 0.45 \\ &= 0 && ;\ \bar{W} > 0.6 \\ C &= 0.72 && ;\ 0.154 \leq \bar{W}' \leq 0.45 \\ &= 0.81 && ;\ \bar{W}' > 0.6 \\ D &= 0.00512 && ;\ 0.154 \leq \bar{W}' \leq 0.45 \\ &= 0.0093 && ;\ \bar{W}' > 0.6 \end{aligned}$$

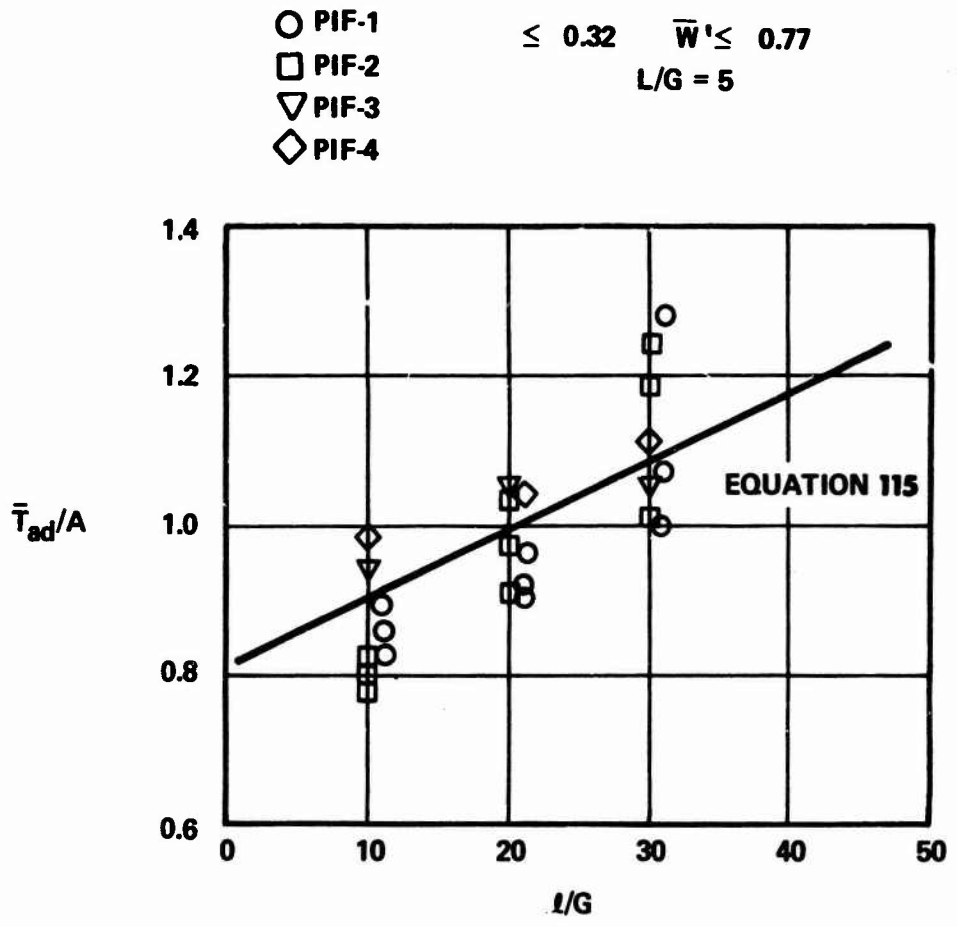


Figure 153. Pinched-Impingement Film Geometry Test Results.

Also, for the heat-transfer rates

$$\phi(\bar{W}')^{E} = F\ (\ell/G)^{H} \qquad (135)$$

where $E = 0$; $0.154 \leq \bar{W}' \leq 1.25$

$= -0.72$; $\bar{W}' > 1.25$

$F = 1.3$; $0.154 \leq \bar{W}' \leq 0.45$

$= 3.45$; $0.6 \leq \bar{W}' \leq 1.25$

$= 2.42$; $\bar{W}' > 1.25$

$H = 0$; $0.154 \leq \bar{W}' \leq 0.45$

$= -0.25$; $0.6 \leq \bar{W}'$

7.2.2 Cooling Film Mixing

Experimental and analytical studies were conducted to study mixing rate between cooling air and hot (main) stream. The impingement-film cooling-slot configuration (shown as 4-times-size cooling slot in Table XV) was used to study velocity and temperature profiles in line with and between cooling-slot delivery holes. A two-dimensional parabolic program based upon the Patanker-Spalding method was also used to predict the flow field.

7.2.2.1 Experimental Results

The dilution-zone rig was used to study cooling-air/mainstream mixing from a 4-times-size cooling band. Test conditions were as defined in Table XVIII. Values of total pressure and temperature were taken at radial increments of 0.020 inch for a depth of 0.5 inch across and beyond the slot discharge. These traverses were taken in line with and between cooling-slot delivery holes at six equally spaced axial positions from 0.1 inch downstream of the slot to 3.6 inches down from the slot. Typical velocity and temperature profiles are shown in Figures 154 and 155. The predicted results shown by dashed lines will be discussed later in this section. Note the non-similarity between velocity and temperature profiles, especially at axial stations near the cooling slot. This occurs because of the lip finite thickness inducing a low-pressure region,

TABLE XVIII. COOLING FILM MIXING TEST CONDITIONS

Slot Flow			Mainstream Flow			$\bar{W}$
Airflow (lb/min)	Temp (°F)	Velocity (ft/sec)	Airflow (lb/min)	Temp (°F)	Velocity (ft/sec)	$\frac{(\rho V)_{Slot}}{(\rho V)_{Mainstream}}$
2.21	Approx 320	Approx 135	181	730	283	0.71
2.21	Approx 320	Approx 135	109	730	170	1.19
2.21	Approx 320	Approx 135	64	730	100	2.03
2.21	Approx 320	Approx 135	46.5	730	73	2.79

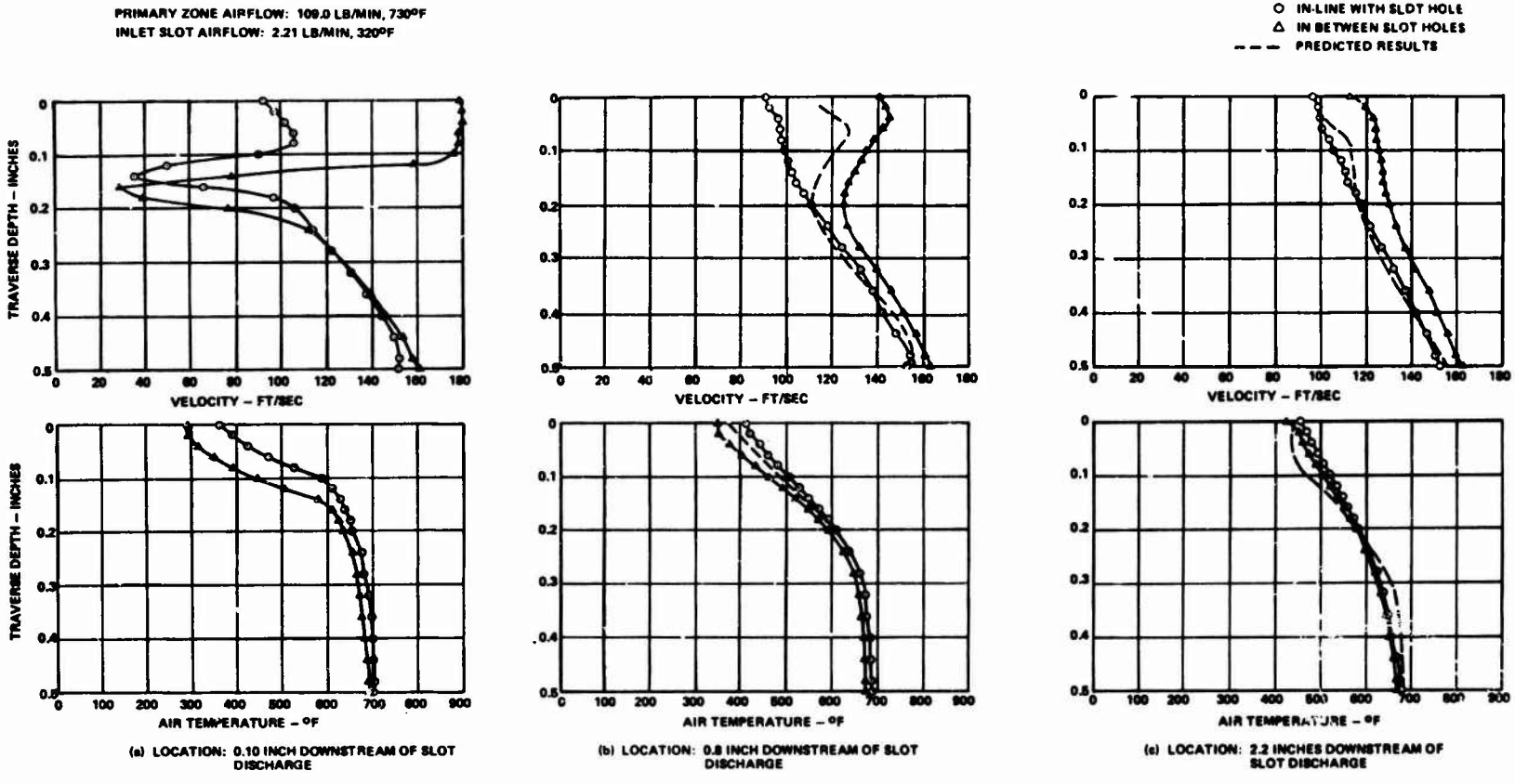


Figure 154. Cooling Film Mixing Results ($\bar{W}$ = 1.19).

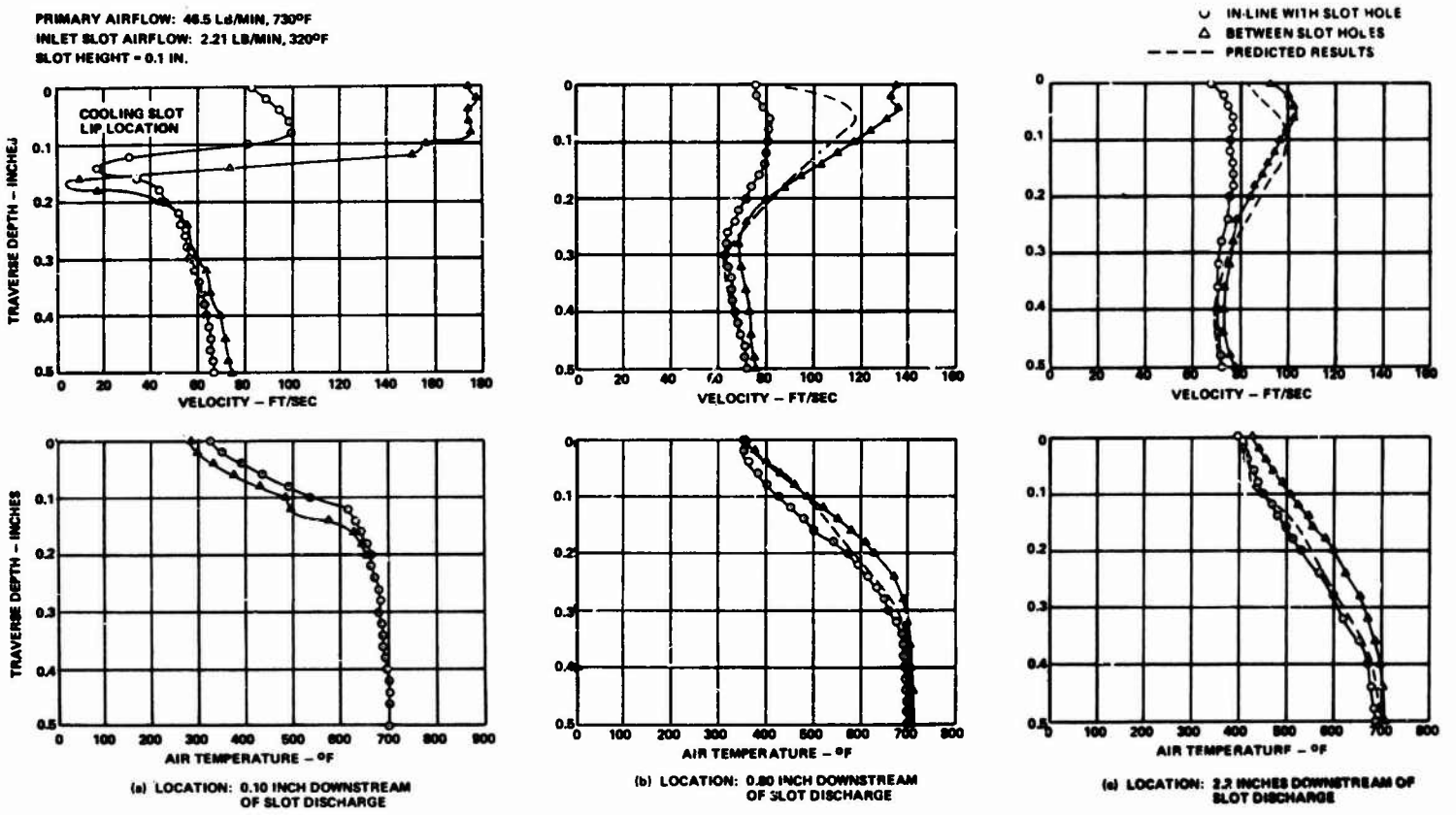


Figure 155. Cooling Film Mixing Results ($\bar{W}$ = 2.79).

resulting in lower axial velocity near the lip region. The flow field in line with the cooling slot entry holes is remarkably different from that between cooling slot delivery holes, in spite of using a continuous splash plate. The velocity decay rates and temperature-rise rates, as shown in Figures 156 and 157 for two depths (0.02 and 0.06 inch), for in-line and between the entry holes are also different, thus indicating the 3-D flow effects even at axial stations beyond 20 times the slot height.

The mixing characteristics of the cooling airstream with the mainstream can be studied by noticing isothermal lines. The mixing depth, y (defined as the transverse location for each axial station where temperature was 600°F), variation with x for different $\overline{W}$ values is shown in Figure 158. Both y and x have been normalized by slot height, s. Note that the mixing is reduced with decreasing $\overline{W}$, that the mixing rates are rapid for the first eight slot heights downstream, followed by a slower rate for up to 22 slot heights.

Beyond 30 slot heights the mixing is very rapid, indicating uneffectiveness of the cooling-film protection. It can also be concluded tentatively that mixing is minimized (i.e., η_{FILM} is maximized) by matching mainstream and cooling-film velocities and not mass velocities for the case studied. This may not be true for cooling in an actual gas turbine combustor because of higher turbulence level and radiant heat loading.

7.2.2.2 Analytical Predictions

A two-dimensional parabolic computer program was used to predict velocity and temperature profiles downstream of the cooling slot. The numerical scheme involves simultaneous solution of the parabolic, two-dimensional partial differential momentum and energy equations with temperature-dependent properties.

In the present work, the measured velocity and temperature profiles obtained nearest the cooling band (0.10 inch downstream of the lip) are averaged in the spanwise direction and used as initial, or starting, values for the numerical computations. Corresponding spanwise averaged or two-dimensional equivalent downstream values of velocity and temperature are predicted numerically for the panel surface temperature distribution that was present when the profiles were obtained. The predicted and measured downstream profiles are compared, and the reasonably good agreement obtained establishes confidence in the numerical solution. Next, the same measured initial profiles are used, together

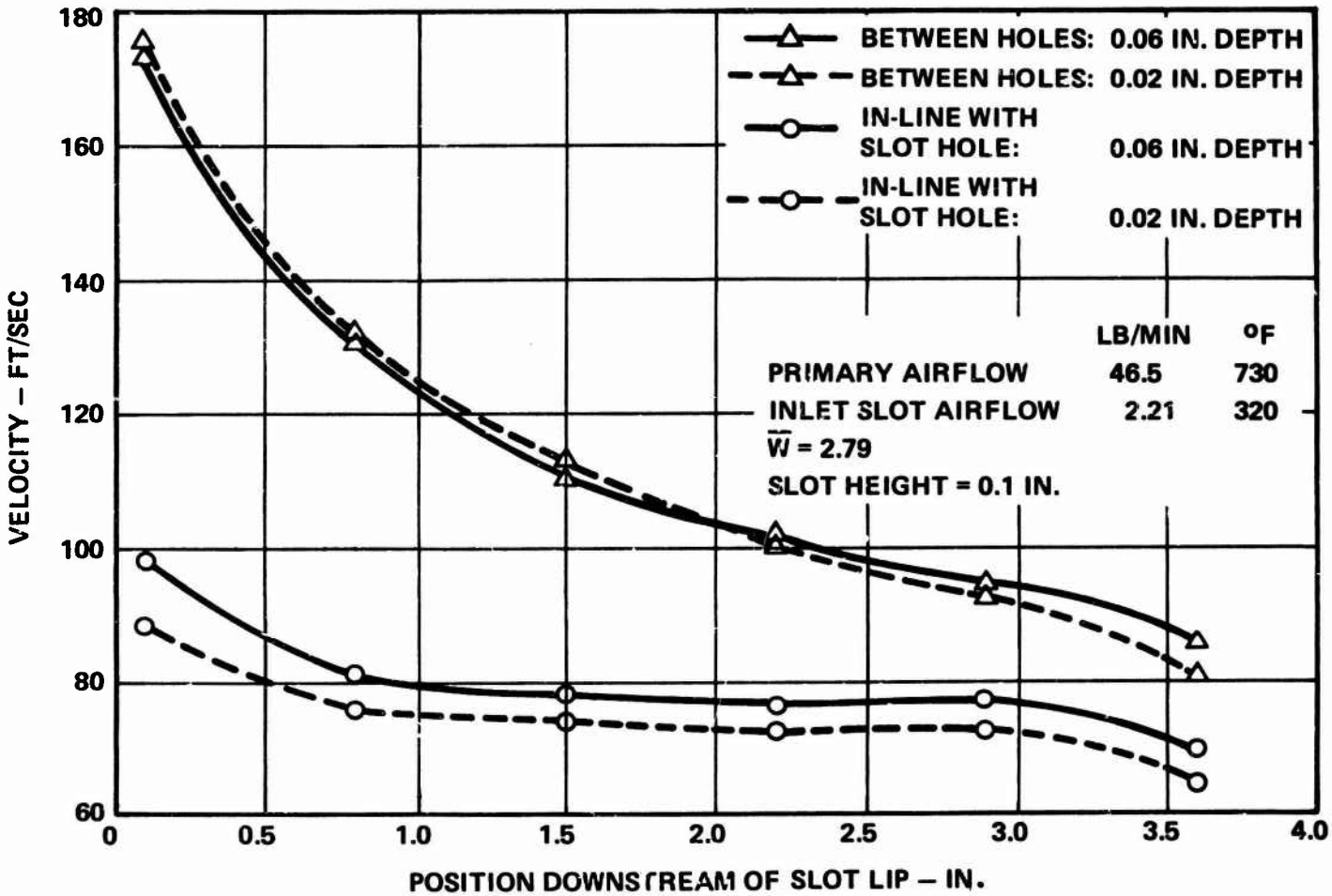


Figure 156. Velocity Decay Curves.

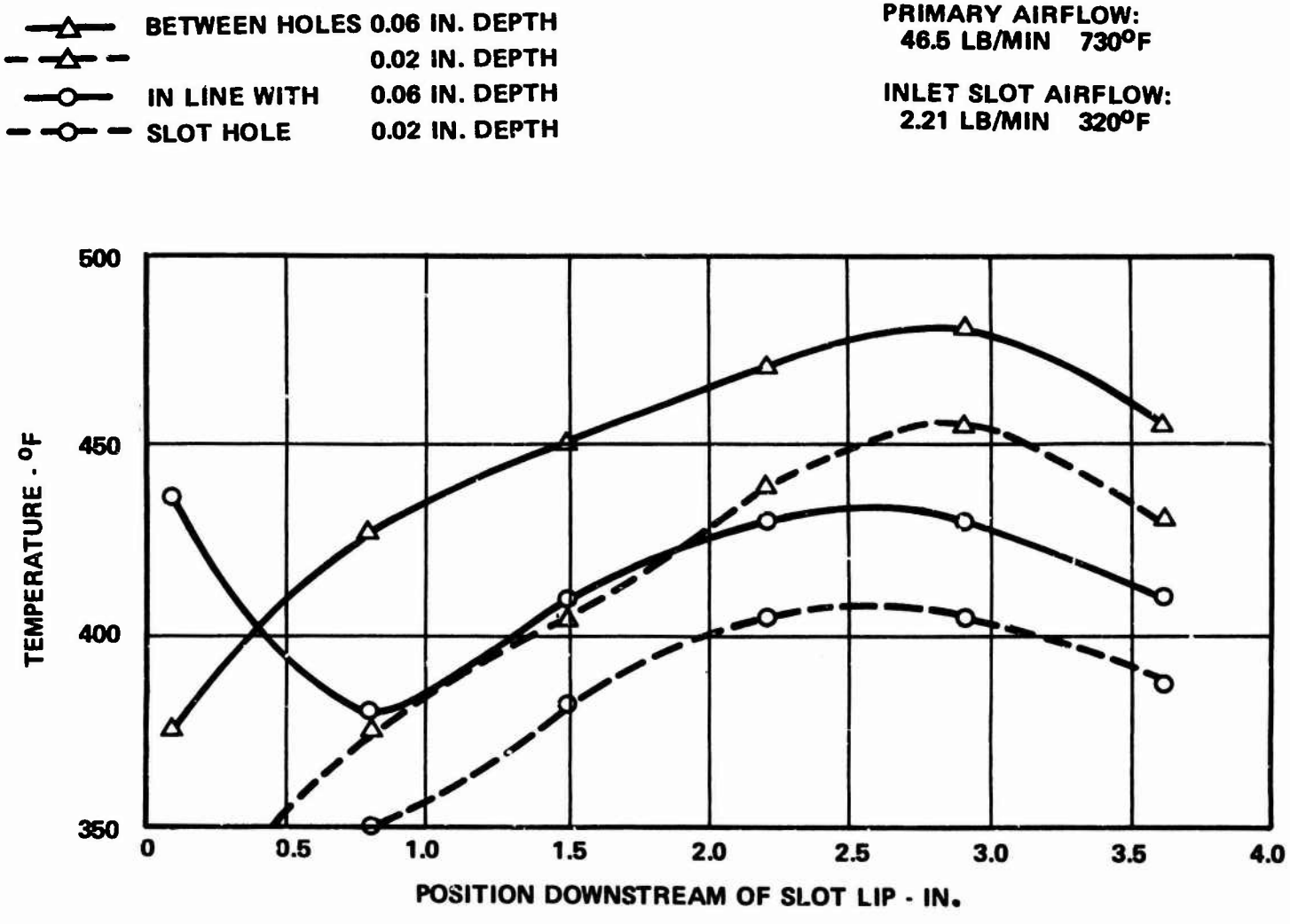


Figure 157. Temperature Decay Curves.

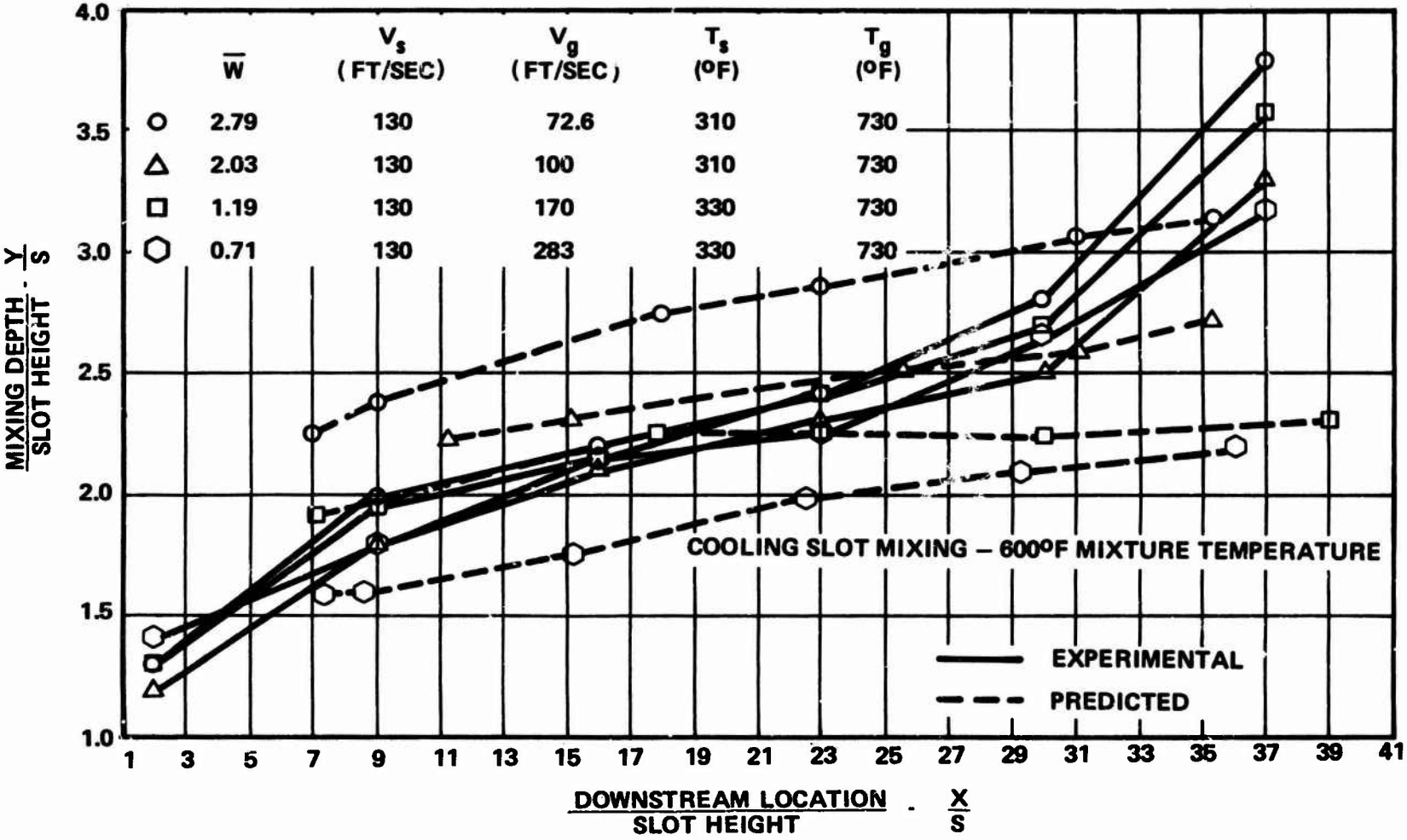


Figure 158. Cooling Film Mixing Rates.

with an adiabatic surface boundary condition, to numerically predict the adiabatic wall temperature distribution for the injection conditions.

The initial velocity and temperature profiles (0.100 inch downstream of the slot) are presented in Figures 154(a) and 155(a) for values of $\overline{W}$ = 2.79 and 1.19, respectively. Of particular interest is the spanwise variation in velocity and temperature apparent from the surveys taken in line with the supply holes and between the slot holes. The spanwise variation in velocity is significant and, taken alone, seems to indicate that three-dimensional effects introduced by the supply holes still dominate the flow despite the long (6.25) lip-to-gap spacing ratio. From a film-cooling standpoint, however, the small variation in spanwise temperature profiles is more significant and indicates that full spanwise coverage of the film has been achieved.

For the numerical predictions of the equivalent two-dimensional downstream fields, the measured in-line and between-line values of Figures 154(a) and 155(a) were arithmetically averaged and used as starting values for the downstream computations.

Figures 154(b) and 154(c) show results of the numerical computations for the $\overline{W}$ = 2.79 test at two locations, 0.80 inch and 2.20 inches downstream of the lip. Figures 155(b) and 155(c) show similar results for the $\overline{W}$ = 1.19 tests. Although considerable spanwise velocity difference still exists at these downstream locations, the good agreement noted for the predicted and measured temperature profiles lends confidence to the use of the equivalent two-dimensional numerical procedure for predicting the film-cooling performance. Figure 159 shows downstream surface temperatures predicted for the four cases with an adiabatic boundary condition. Predicted mixing depths shown in Figures 154 and 155 are similar to those measured, indicating again that mixing is minimized as cooling-film velocity approaches mainstream velocity.

7.3 RADIANT HEAT-TRANSFER ANALYSIS

7.3.1 Model Definition

An analysis to determine the net radiant heat flux to a combustor surface element must include flame radiation, gas radiation, gas attenuation, and wall-to-wall exchange considerations. In-depth studies of the above exchange mechanisms can be obtained from the literature. For this reason, only a brief review of the basic concepts is given.

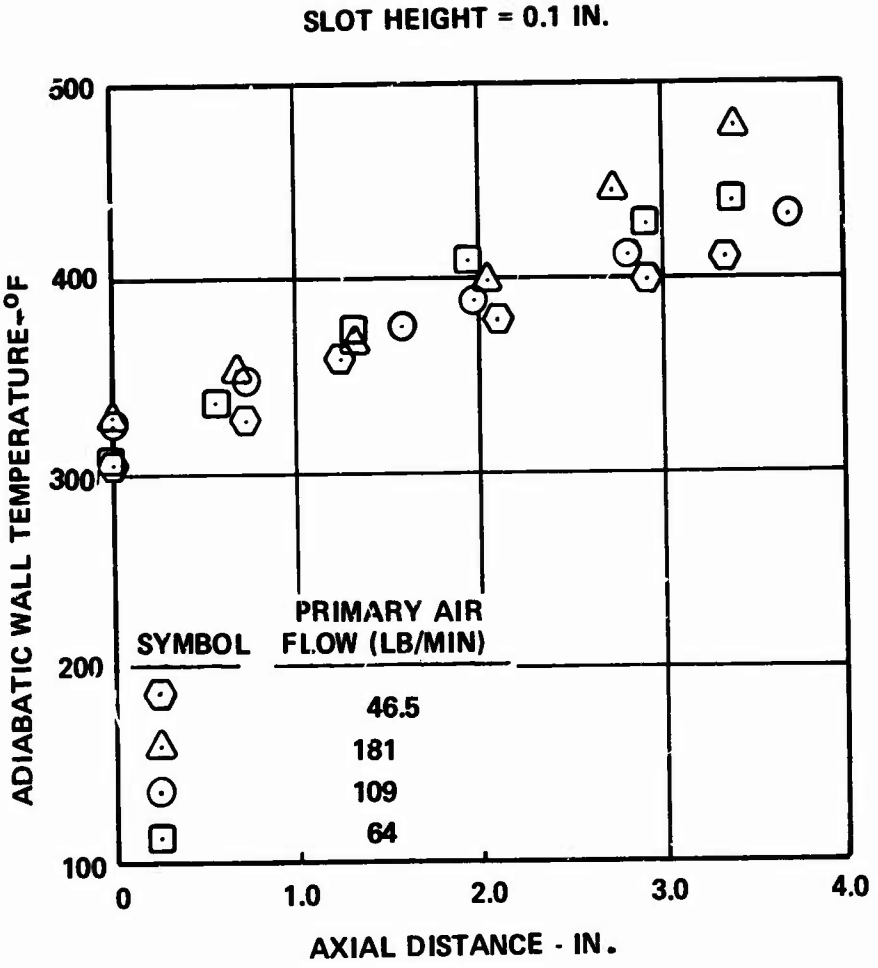


Figure 159. Predicted Adiabatic Wall Temperature Versus Axial Distance.

The monochromatic radiation intensity of a blackbody (or perfect radiator) in a direction normal to the surface is defined by Planck's law:

$$I_{\lambda bn} = \frac{2C_{1\lambda}}{\lambda^5 \left(e^{C_2/\lambda T} - 1\right)} \qquad (135)$$

where $I_{\lambda bn}$ = monochromatic radiation intensity, Btu/hr/ft^2/μ

$C_1 = 1.889 \times 10^7$, Btu μ^4/hr/ft^2

$C_2 = 25896$ μ°R

λ = wavelength, μ

T = temperature, °R

Total emission, E, is obtained by integrating this equation over all wavelengths. The resulting relation, $E = \sigma T^4$, is known as the Stefan-Boltzmann law, in which

E = emission, Btu/hr/ft^2

σ = Stefan-Boltzmann constant

$= 0.173 \times 10^{-8}$ Btu/hr/ft^2/°R^4

T = temperature, °R

The true emission from a real surface, however, is not equal to that from a perfect radiator. The ratio of the emissive power of any body to that of a blackbody is known as the emissivity (ε). In general, the emissivity of a surface is a function of surface temperature, surface finish, material, and direction. Thermodynamic equilibrium dictates that the energy absorbed by a body must be equal to that emitted--i.e., absorptivity α = emissivity ε.

Gas radiation can be characterized as either nonluminous or luminous. Nonluminous radiation is a banded (discrete wavelength) type of emission, whereas luminous radiation is a continuous type of emission, similar to, but not identical with, that produced by a blackbody. A plot of intensity versus wavelength is shown in Figure 160 to illustrate this point. The important nonluminous bands in a gas turbine combustor are those due to carbon dioxide and water vapor. The continuous luminous radiation is due to carbon particle emission.

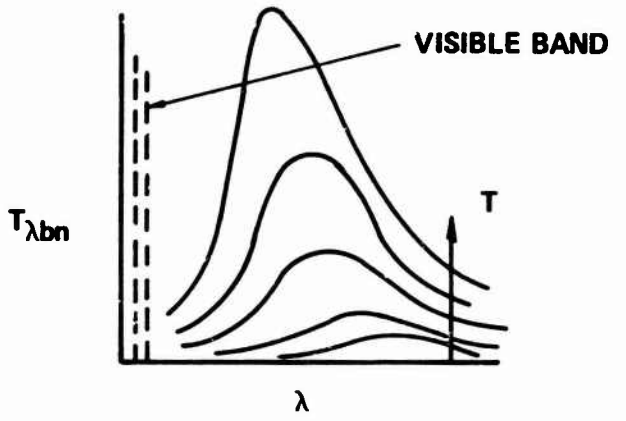


Figure 160. Monochromatic Radiation Intensity Versus Wavelength.

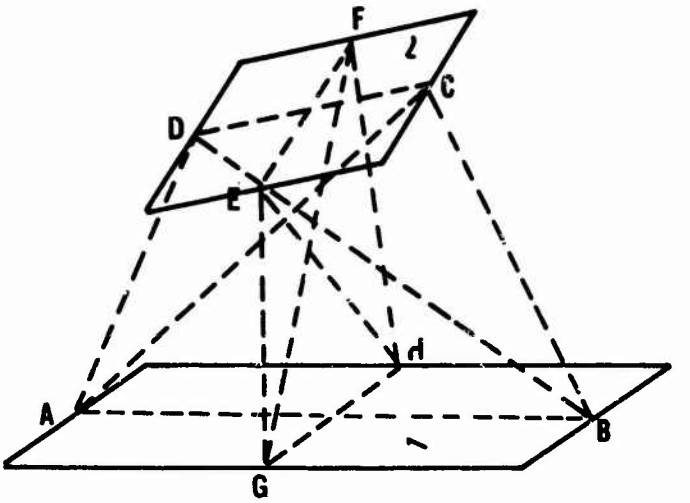


Figure 161. Three-Dimensional Geometry.

7.3.1.1 Radiant Interchange With Transparent Media

For a multizoned enclosure, consideration should be given to surface reflections and the fraction of the emission from that radiating surface which reaches and is absorbed by the surface under consideration. This is known as the view (or form) factor.

The view factor for energy leaving Surface 1 (Area A_1) being received on Surface 2 (Area A_2) is defined as

$$F_{12} = \frac{1}{A_1} \int_{A_1} \int_{A_2} \frac{\cos\theta_1 \cos\theta_2}{\pi r^2} \, dA_2 dA_1 \qquad (136)$$

where r = distance between surfaces

θ_1 = angle between the normal to A_1 and a line forming the center of A_1 to A_2

θ_2 = angle between the normal to A_2 and the line joining the center of A_2 to A_1

Evaluation of the view factors is, in general, extremely complex, but a relatively simple three-dimensional factor can be defined by an extension of Hottel's[63] two-dimensional "string method." The general geometry considered is shown in Figure 161, and the resulting view factor, F_{12}, is

$$F_{12} = \frac{\overline{AC} + \overline{BD} - (\overline{AD} + \overline{BC})}{2AB} \qquad \frac{(\overline{FG} + \overline{EH}) - (\overline{EG} + \overline{FH})}{2GH} \qquad (137)$$

i.e., the three-dimensional factor is defined as the product of the two two-dimensional factors.

Comparison with a number of analytical solutions showed no error for two-dimensional view factors and maximum of 15 percent error in three-dimensional factors for typical combustor type geometries. It is anticipated that all combustor walls will have a surface emissivity of 0.8 or greater so that any additional complications necessary to account for reflections can be ignored without introducing significant error.

7.3.1.2 Radiant Interchange in Participating Media

Gas radiation has been correlated by Hottel[58] with use of a mean-beam-length concept. Hottel defined the mean beam length

as the radius of a gas hemisphere that will radiate to the unit area at the center of its base the same as the average radiation over the area from the actual gas mass. An approximate mean-beam-length formula was suggested by Hottel:

$$MBL = 4\ V/A \tag{138}$$

where MBL = mean beam length, ft

V = volume of gas, ft^3

A = total surface area enclosing volume, ft^2

A comparison of values obtained with use of this simple formula with values obtained by path-length integration showed only small percentage differences for parallelepiped gas shapes. It was therefore concluded that the approximate beam-length formula should be used.

Numerous methods are available in the literature for estimating gas emissivities.[59,60,61] Most are based on data taken at less than 5 atmospheres' pressure. Of the methods available, that recommended by Reeves[61] is the most convenient to use. He recommends that nonluminous emissivity be given as

$$\bar{\varepsilon}_g = 1 - \exp\left(-3.86 \times 10^4\ P(f/a)^{0.5}(MBL)^{0.5}\ T_g^{-1.5}\right) \tag{139}$$

where P is in atmospheres, MBL in feet, and T_g in °R.

Equation (138) was compared with emissivity obtained from charts prepared by Hottel for fuel of the type C_nH_{2n} at stoichiometric and fuel lean conditions. The results obtained showed that Reeves' correlation underestimates the emissivity from 6 to 17 percent through the range 1 to 5 atmospheres, with less error between 6 and 10 atmospheres. It was necessary to extrapolate Hottel's water-vapor emissivity data to obtain values beyond 2.4 atmospheres.

Radiation from a surface element through the gas to another surface element is partially absorbed by the gas. A simple formulation was derived based on Hottel's charts for carbon dioxide and water vapor.

$$\text{Absorptivity } \bar{\alpha}_g = \bar{\varepsilon}_g\ (T_g/T_s)^{0.55} \tag{140}$$

This equation gives values that are generally 2 percent less than those obtained with use of Hottel's charts when the gas

temperature in Reeves' equation is replaced by the assumed surface temperature. For the range of values selected for the comparisons, the absorptivity was typically 14 percent greater than the emissivity.

7.3.1.3 Luminous Radiation

Luminous radiation from a flame appears to the eye as a yellow-orange-red flame and is caused by carbon particles in the flame that emit over a nearly continuous spectrum. Determination of the carbon particle concentration would facilitate the calculation of luminosity, but no successful method is available for concentration predictions.

A luminosity factor (L_f) as evaluated by Thring and Holliday[62] can be included in Reeves' equation to account for the luminous radiation

$$L_f \; 7.53 \; (C/H - 5.5)^{0.84} \qquad (141)$$

(for a typical jet fuel of C_nH_{2n} composition, the luminosity factor, $L_f = 4.2$).

The luminous flame emissivity can now be predicted from Reeves' equation by replacing P by the product of the pressure in atmospheres and the luminosity factor.

The separate radiation factors outlined above provide the necessary inputs for the radiation interchange equations.

7.3.1.4 Radiation Interchange Equation

The radiation interchange equations are developed for a typical surface and gas-element geometry as shown in Figure 162.

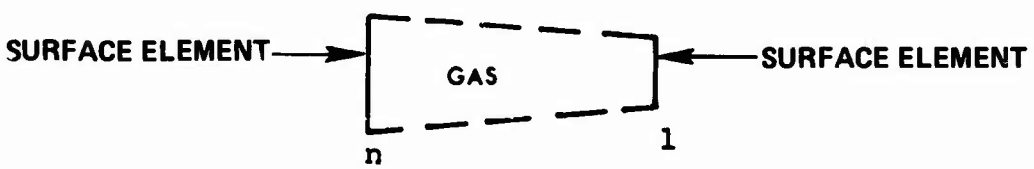


Figure 162. Typical Surface and Gas Element.

The heat transfer from Surface n to Surface 1 (q_{n-1}) is the emission from Surface n, $\bar{\epsilon}_n A_n F_{n1} E_n$, less the fraction of this emission absorbed by the gas, $\bar{\alpha}_g$. Thus, the incident radiation on 1 from n is

$$\dot{q}_{n-1}(\text{incident}) = \bar{\varepsilon}_n A_n F_{n1} E_n - \bar{\alpha}_g \bar{\varepsilon}_n A_n F_{n1} E_n$$

$$= \tau_g \bar{\varepsilon}_n A_n F_{n1} E_n \quad (\text{since } \tau_g = 1 - \bar{\alpha}_g) \tag{142}$$

The fraction of this radiation that is absorbed by Surface 1 is the absorptivity, $\bar{\alpha}_1$. For thermodynamic equilibrium, the absorptivity and emissivity are equal, with a gray surface assumed, and the heat transfer from Surface n absorbed by Surface 1 is

$$\dot{q}_{n-1}\ (\text{absorbed}) = \tau_g \bar{\varepsilon}_1 \bar{\varepsilon}_n A_n F_{n1} E_n \tag{143}$$

$$= \tau_g \bar{\varepsilon}_1 \bar{\varepsilon}_n A_1 F_{1n} E_n \quad (\text{since } A_n F_{n1} = A_1 F_{1n})$$

Similarly, the heat transfer from Surface 1 that is absorbed by Surface n is

$$\dot{q}_{n-1}\ (\text{absorbed}) = \tau_g \bar{\varepsilon}_n \bar{\varepsilon}_1 A_1 F_{1n} E_1 \tag{144}$$

All three equations [(142), (143), and (144)] include only the direct interchange. The effect of surface reflections is assumed negligible in view of the anticipated surface emissivities.

The heat transfer from the gas element shown in Figure 162 to Surface 1 is

$$\dot{q}_{g-1} = \bar{\varepsilon}_g A_1 E_g \tag{145}$$

and the amount of this radiation absorbed by Surface 1 is

$$\dot{q}_{g-1} = \bar{\varepsilon}_1 \bar{\varepsilon}_g A_1 E_g \tag{146}$$

The heat transfer from Surface 1 absorbed by the gas element is

$$\dot{q}_{1-g} = \bar{\alpha}_g \bar{\varepsilon}_1 A_1 E_1 \tag{147}$$

The net radiant heat transfer at Surface 1 is therefore equal to the sum of the radiation from Surface n to Surface 1 and the radiation from the gas to Surface 1, less the sum of the radiation from Surface 1 to Surface n and the radiation from Surface 1 to the gas.

That is, $Q = q_{n-1} + q_{g-1} - q_{1-n} - q_{1-g}$ (148)

$$= \bar{\epsilon}_g \bar{\epsilon}_n \bar{\epsilon}_1 A_1 F_{1n} (E_n - E_1) + \bar{\epsilon}_1 \bar{\epsilon}_g A_1 (E_g - E_1)$$

where the gas is assumed gray (i.e., $\bar{\alpha}_g = \bar{\epsilon}_g$).

7.3.2 Element Tests

Thermal radiation of the gas and flame was measured at three locations within the L-pipe combustor primary zone. Measurement was by means of three Leeds and Northrup Rayotubes, each having a focal length of 12 inches and a target diameter of 0.25 inch. The three instruments were calibrated by Leeds and Northrup with the use of a blackbody source viewed through a sapphire window. Calibration output was in the form of Rayotube output signal in millivolts versus radiant heat flux in Btu per hour per square foot.

The Rayotubes were focused into the combustor through sapphire windows, as shown in Figure 163. Figures 164 and 165 show the orientation of the viewport on the combustor. Each viewing port was surrounded by a well and was supplied with external air, both to cool the window and to keep it clean. The optics of the 12.0-inch focal length Rayotubes were such that the instrument viewed the radiation within the truncated cone shown previously in Figure 163--i.e., for the combustor 1.37 inches in depth, the back-wall diameter was 0.35 inch. The mean beam length for this truncated cone was 0.3 inch. This value of mean beam length was used in the emissivity correlation to predict emission from this truncated cone as a function of pressure level, temperature, luminosity, and fuel-air ratio. The predictions for both luminous and nonluminous radiation as functions of gas temperature and pressure are shown in Figures 166 and 167. For nonluminous emission, L_f = 1, the fuel-air ratio was assumed to be 0.04, since this is a representative value of nonluminous emission. As shown, the predicted radiant heat flux increases significantly with both temperature and pressure. For luminous emission, the luminosity factor was taken as 4.2, and the fuel-air ratio was assumed to be 0.06, as a representative value for luminous emission. Again the significant effect of temperature and pressure is shown.

Figure 168 shows the influence of fuel-air ratio as an isolated parameter with the luminosity factor as a constant. Fuel-air ratio as such is of secondary importance in comparison to the effect of luminosity, pressure level,and temperature. This is,

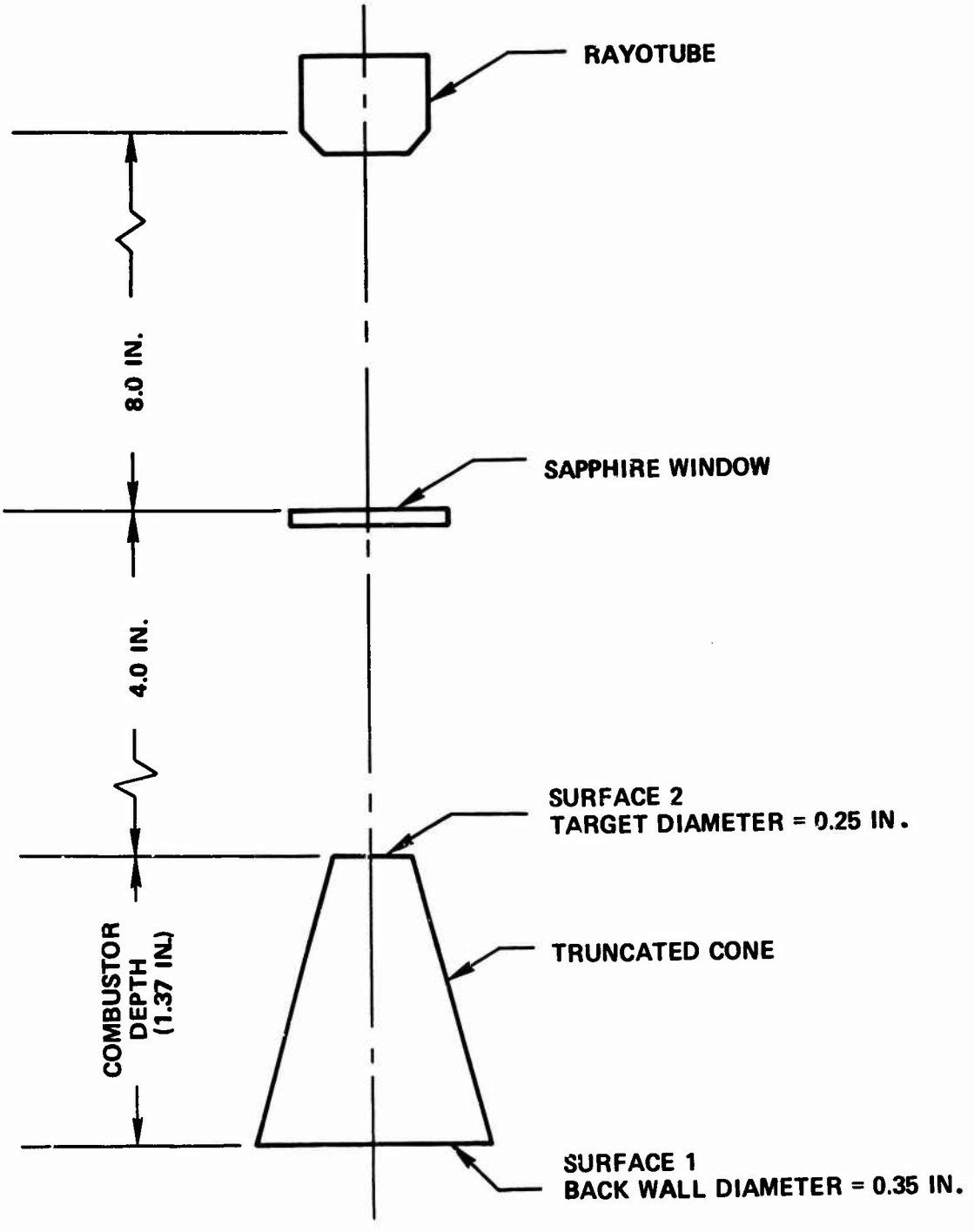


Figure 163. Test Configuration Schematic for Flame Radiation Measurement (Not to Scale).

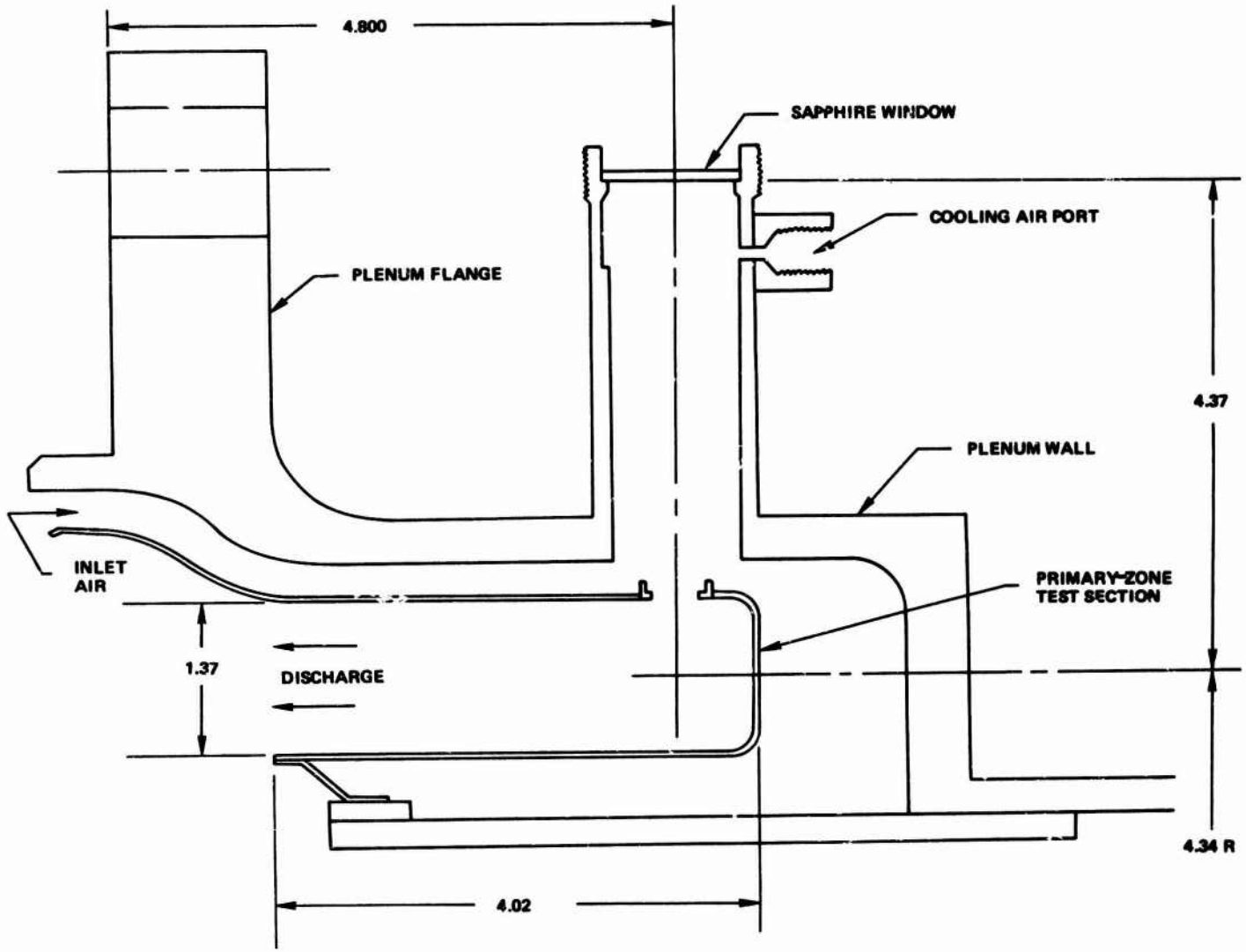


Figure 164. Combustor/Radiation Port Orientation (Port Number 1).

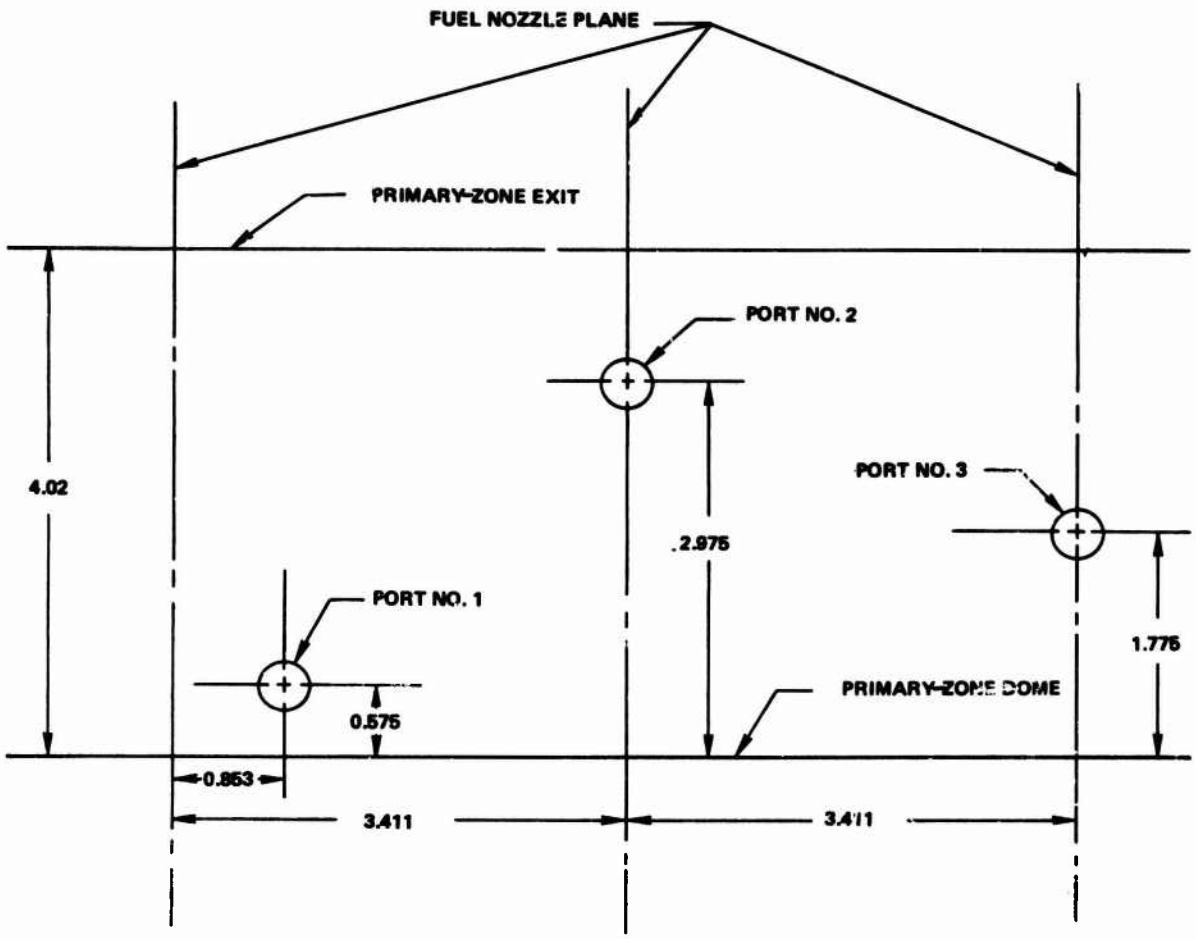


Figure 165. Schematic of Unfolded Primary Zone (Top View) Showing Axial and Circumferential Orientation of Radiation Measurement Ports Relative to Fuel Nozzles.

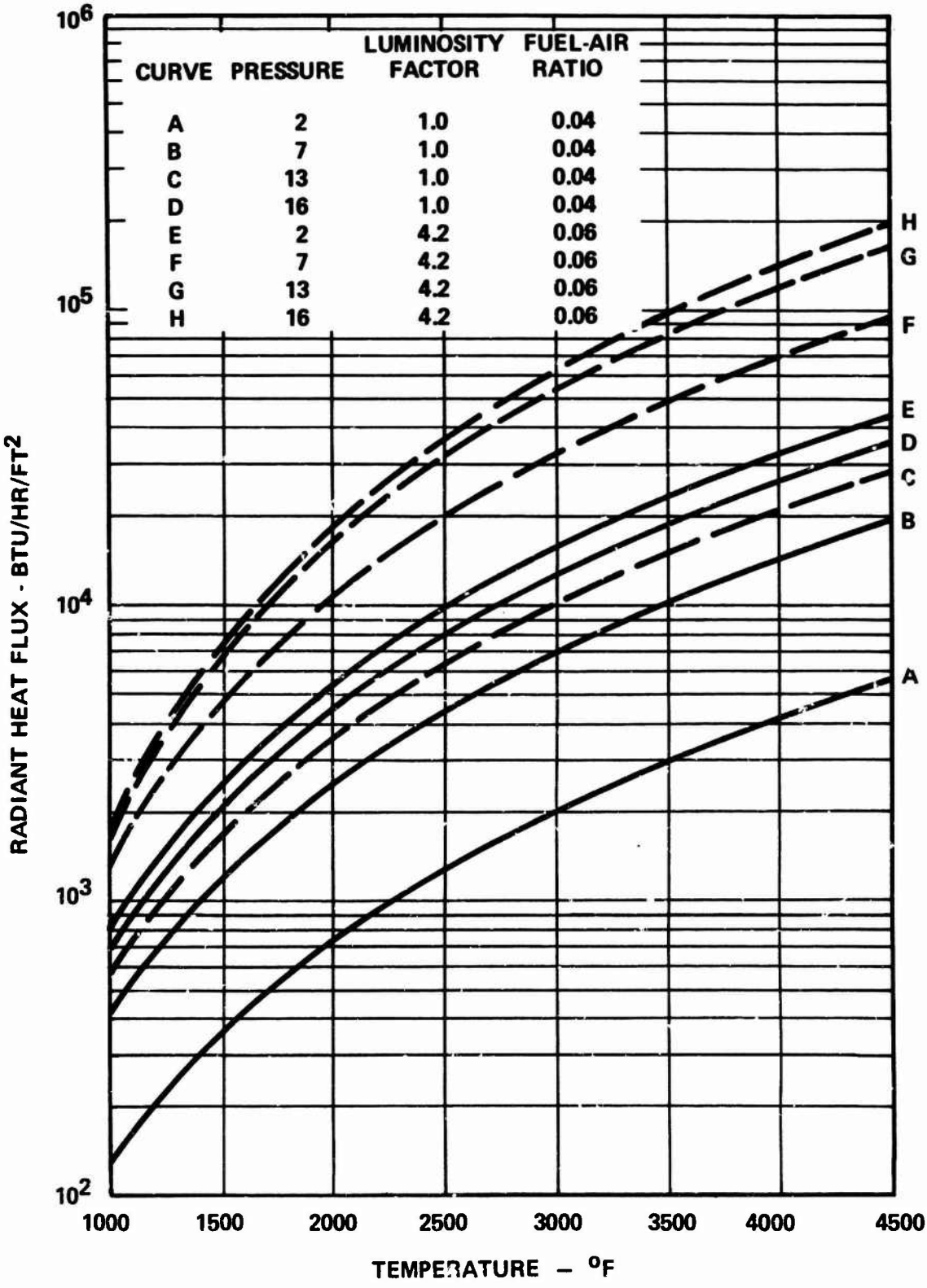


Figure 166. Measured and Predicted Heat Flux.

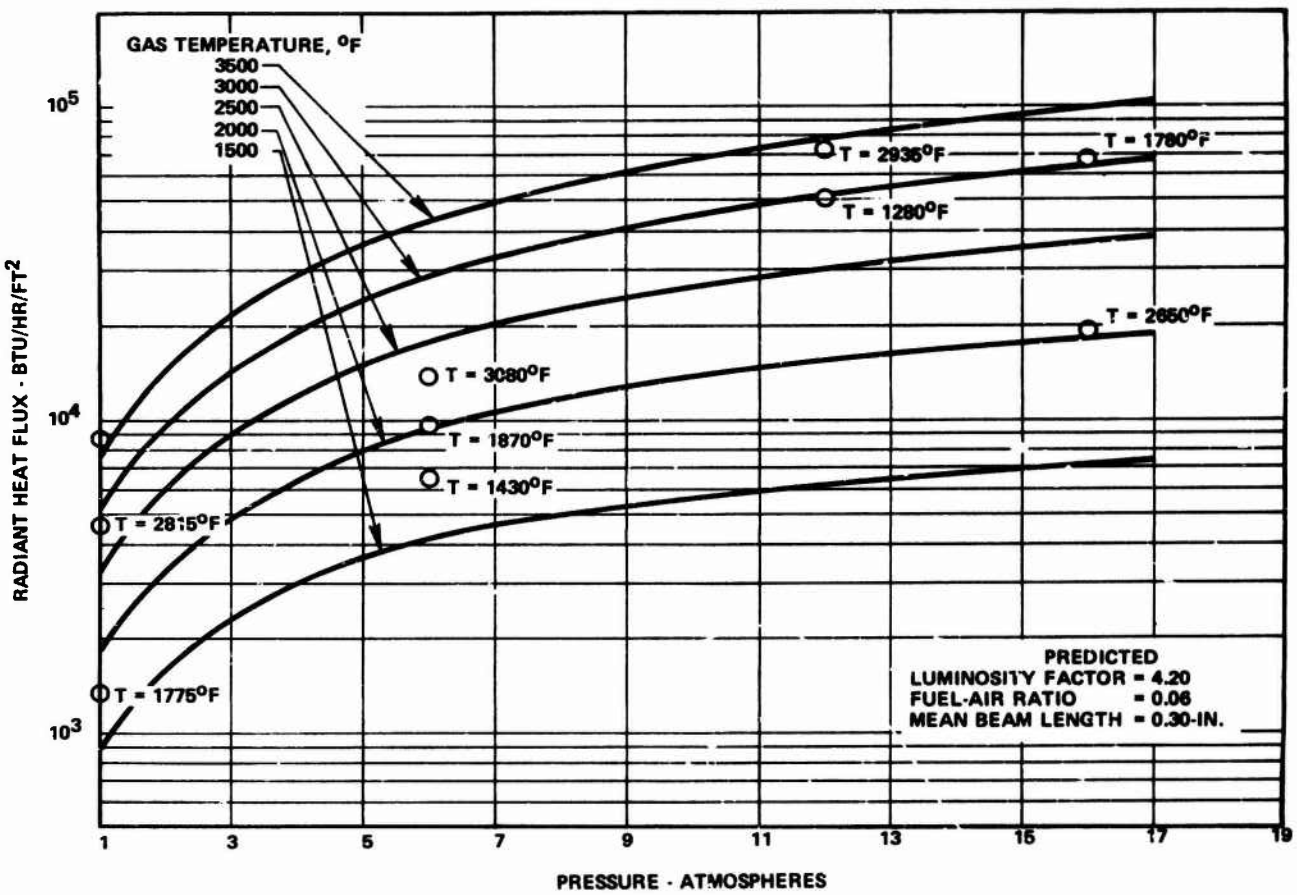


Figure 167. Measured and Predicted Heat Flux.

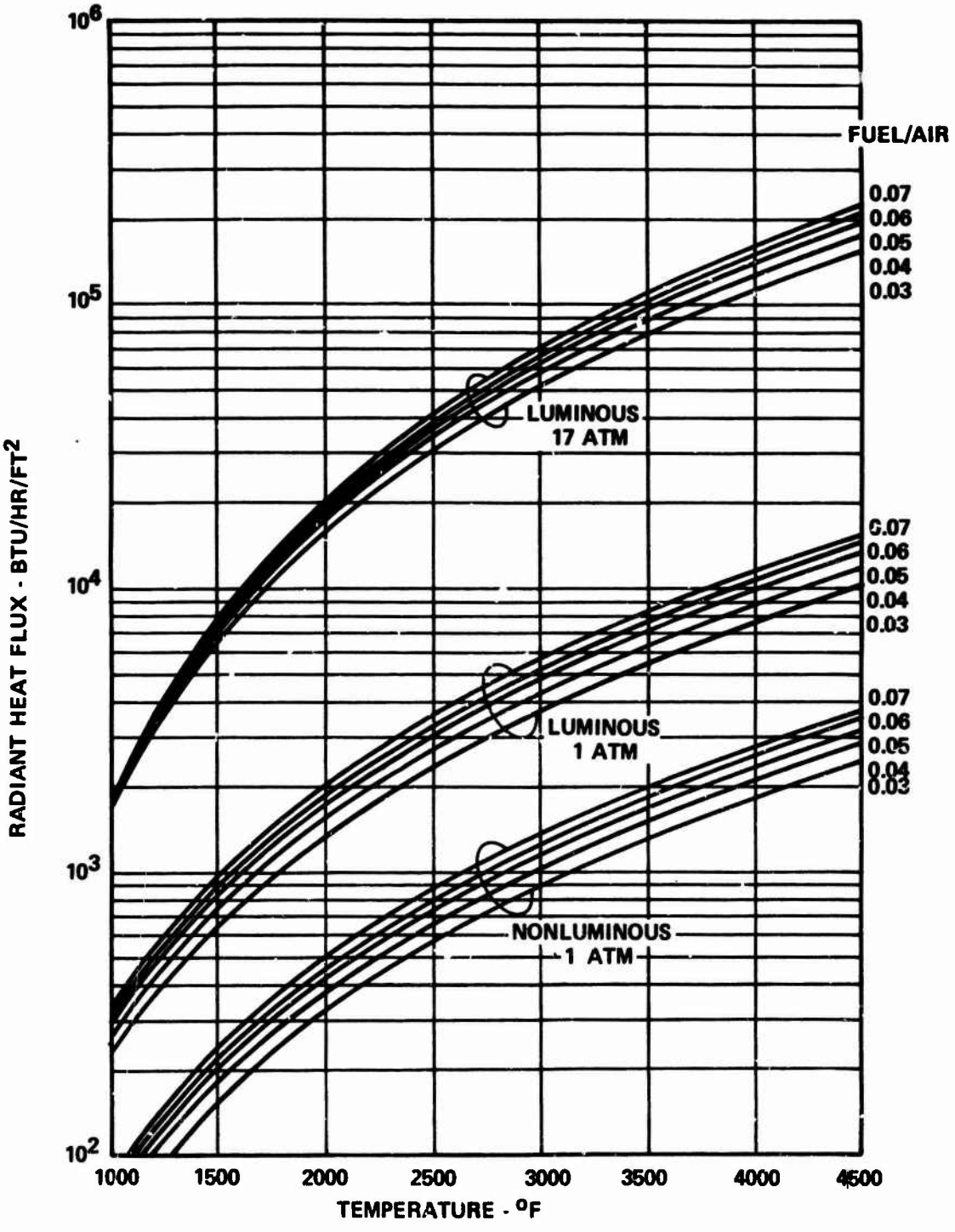


Figure 168. Radiant Heat Flux Variation With Fuel-Air Ratio.

of course, eliminating the effect of fuel-air ratio on the luminosity factor.

Radiant flux experimental data was obtained for viewing ports 1 through 3, as shown in Figure 165. Each Rayotube was aligned to be normal to the viewing port in the combustor wall and at 12 inches focal length. The wall temperatures cited in the results of Table XIX are the values directly opposite the viewing port and are used to correct the radiant flux data. Gas temperatures were taken at three radial positions in line with each viewing port. The Rayotube signal levels were not constant for some conditions, but visual observation through the viewing ports confirmed that the flame itself was "flickering" and that it was not caused by instrumentation instability.

Determination of local fuel-air ratios was not possible, but because this ratio is a second-order variable in the emissivity prediction equation, the predicted and the measured data were compared.

The portion of the radiant energy attributable to emission and reflection for the combustor back wall was calculated from

$$\dot{q}_r = F_{12} \sigma \bar{\varepsilon}_r T_r^4 \qquad (149)$$

where $\dot{q}$ = back-wall emission

F_{12} = view factor

σ = Stefan-Boltzmann constant

$\bar{\varepsilon}_r$ = back-wall emissivity

T_r = back-wall temperature

All the above quantities are known, assumed, or measured, except for the view factor. For the geometry (truncated cone) considered, the view factor calculated from Equation (135) is equal to 0.0886. Assumed back-wall emissivities of 0.9 and 0.9 were used in conjunction with the back-wall temperature measurements and the view factor to determine the flux attributable to the back wall. The correct flame and gas flux is the total radiation less this back-wall radiation.

Figure 167 is a plot of predicted radiant heat flux for both luminous and nonluminous radiation at pressure levels of 2, 7, 13, and 16 atmospheres. For both emission levels, typical fuel-air ratios were assumed--0.04 for the nonluminous case and

TABLE XIX. RADIATION TEST CONDITIONS, DATA, AND RESULTS

Combustor Operating Conditions					Radiant Heat Flux Data						Radiant Heat Flux		
Airflow (lb/min)	Inlet Temperature (°F)	Inlet Pressure (atm)	ΔP/P (%)	Fuel Flow (lb/hr)	View Port Number	Wall Temperature (°F)	Gas Temperature (°F) Inner	Center	Outer	Rayotube Signal (millivolts)	Observed (Btu/hr/ft X 10^4)	Correction Term (Btu/hr/ft X 10^4)	Corrected (Btu/hr/ft X 10^4)
12.4	500	1.0	3.0	16.8	1	1090	2575	2540	2440	0.094	0.95	0.07 to 0.08	0.87 to 0.88
12.4	500	1.0	3.0	16.8	2	1340	-	1840	1710	0.186	2.46	0.13 to 0.14	2.32 to 2.33
12.4	500	1.0	3.0	16.8	3	1115	2630	2840	2980	0.075	0.55	0.08 to 0.09	0.46 to 0.47
55	690	6.0	3.98	25.5	1	890	3500	2250	3500	0.123 to 0.131	1.42 to 1.52	0.04 to 0.05	1.37 to 1.48
55	690	6.0	3.98	25.5	2	1155	22	1800	1600	0.080 to 0.089	1.00 to 1.15	0.08 to 0.09	0.91 to 1.07
55	690	6.0	3.98	25.5	3	850	1000	1750	1540	0.086 to 0.089	0.66 to 0.70	0.03 to 0.04	0.62 to 0.67
135	700	12.0	3.96	94.5	1	1475	2385	3500	2924	0.655 to 0.751	7.0 to 7.9	0.14 to 0.16	6.84 to 7.76
135	700	12.0	3.86	94.5	2	1280	1094	1408	1340	0.410 to 0.426	5.1 to 5.3	0.11 to 0.13	4.97 to 5.19
156	810	16.0	3.31	69.7	1	1230	1750	1991	1591	0.594 to 0.669	6.8 to 7.2	0.10 to 0.11	6.29 to 7.10
156	810	16.0	3.31	69.7	2	1280	3071	2174	2218	0.149 to 0.159	2.0 to 2.1	0.11 to 0.13	1.87 to 1.98

0.06 for the luminous case. Data points of Table XIX are plotted on Figure 167, and these show qualitative agreement with the predicted lines.

7.3.3 Conclusions

A review of the data and analysis was made, and the following conclusions were drawn:

- The prediction technique provides data of the correct order of magnitude.
- The assumptions made in the analysis do not invalidate the technique.
- Experimental data is difficult to obtain, and more controllable conditions will be required for improved quantitative analysis.

Either luminous or nonluminous radiation to the walls of a combustor necessitates the use of a percentage of the total available combustor airflow for cooling purposes. As inlet temperature, inlet pressure, and discharge temperature increase, so does the percentage of total air required for cooling. With low-airflow, high-turbine-inlet-temperature combustors, this cooling air can be greater than 50 percent of the total airflow.

Minimizing the liner surface area to minimize the amount of cooling air required reduces the inner and outer radii with an even greater effect on combustor volume. This decrease in volume adversely affects altitude relight capabilities and increases the heat loading of the liner. If dome height is reduced to limit outer liner radius and thus surface area, fuel impingement on the liner walls and quenching must be considered. Fuel impingement is a major cause of liner hot spots; and if partial quenching and carbon formation take place, luminous radiation from the carbon particles significantly increases the radiation flux, thus requiring a further increase in cooling. Other undesirable effects include reduced combustion efficiency, increased carbon monoxide, and unburned hydrocarbon emission levels.

Cooling requirements with the use of conventional film cooling techniques are one of the most severely limiting factors in the design of low-airflow, high-pressure, high-temperature-rise combustors. When recuperation is used with the cycle that was utilized for this program, calculations show that as much as 60 percent of the total airflow would be required for cooling, indicating that alternate cooling techniques are necessary.

Alternate techniques could include impingement cooling and convective cooling, possibly combined with film cooling. An ideal solution would be an uncooled ceramic-type liner, but at the present time this does not appear feasible for production application.

8.0 CONCLUSIONS AND RECOMMENDATIONS

8.1 CONCLUSIONS

The following conclusions were derived from the activities of Phases I and II of the program:

(a) The fuel-injector models successfully correlated experimental and analytical data for three fuel-injection systems. The major problem identified for small combustors concerns excessive or uncontrolled impingement of fuel on the combustor wall. Air-assist and pneumatic-impact injectors provide excellent atomization, but this advantage is largly negated in small, narrow-annulus combustors by wall impingement. L-pipe injectors attempt to capitalize on the wall impingement problem by purposely depositing fuel on the combustor dome to achieve controlled evaporation, but problems were experienced with poor distribution and durability. It was concluded that the emphasis should be placed on a system that achieves good atomization without wall impingement and with good contamination resistance.

(b) The primary-zone model based on the Spalding-Cosman two-dimensional elliptic program successfully predicted flow patterns for the two-dimensional water rig and the two-dimensional cold-flow rig. Some problems were experienced when hot flow with combustion was considered, but the results still showed that predictions for the gross flow-field characteristics are possible.

(c) At the present time, the method is not capable of successful emission predictions, but can be used for the preliminary design phase of combustion systems to minimize development time. It can also be used to determine the effects of minor hardware changes.

(d) Particularly for small combustors, primary-zone performance is highly dependent on the means by which the recirculation zone is terminated. Analysis and development can be most effective when the primary and dilution zones are considered together, rather than separately.

(e) The dilution-zone models can be successfully applied to the prediction of orifice discharge coefficients and outer annulus flow effects, including compressor exit distortion. Jet and cooling-flow penetration and spreading rates can be determined. The effects of duct length and duct turning on pattern factor can be estimated.

(f) The ignition energy model requires estimates of turbulence level, vapor fuel-air ratio at the igniter, and mixture velocity, all of which are difficult to determine. A parametric study showed that the model can be used as a guide to required energy levels for ignitions.

(g) Film-cooling models that successfully predict the film effectiveness and film mixing characteristics of impingement film-cooling slots can predict liner cooling performance with fair accuracy.

(h) The flame radiation model is capable of predicting the order of magnitude of the heat flux based on the assumption of either luminous or nonluminous emissivity. View factors can be included for most combustor shapes with errors not exceeding $\pm$15 percent.

(i) Material screening tests have shown that IN-586 is well suited for combustor application.

The individual models combine to form a successful tool in the initial stages of combustor design, and provide considerable assistance in rapidly estimating the effect of proposed hardware changes. The above capability therefore can be used to minimize development time and costs.

8.2 RECOMMENDATIONS FOR FUTURE ANALYTICAL STUDIES

It is recommended that the following analytical studies be undertaken to further develop analytical modeling of gas turbine combustors.

- Internal flow modeling with respect to turbulence modeling, faster computation scheme, and realistic kinetic scheme

- Prediction of air recirculation ratio from the primary holes of annular combustors

- Three-dimensional dilution-zone analysis

- Fuel-injection models, such as predicting SMD of any injector, matching of fuel injector with dome, and interaction between droplets

- Cooling-air requirement studies with respect to the effect of flow field, turbulence level, and radiant heat loading

- Application of different element models to predicting emission, combustion efficiency, etc., of any combustor

8.3 RECOMMENDATIONS FOR FUTURE EXPERIMENTAL AND DEVELOPMENT STUDIES

It is recommended that the following experimental and/or development studies be undertaken in conjunction with or independent of analytical studies:

- Experimental work to update fluid-dynamic models such as primary-zone model, three-dimensional dilution-zone model, etc.

- Effect of surface-to-volume ratio of combustors on performance and emission

- Effect of different wall-cooling schemes on combustion efficiency and emission

- Noise prediction and trade-off between noise, pollutant emissions, and combustor performance

- Detailed study of flow conditions at the igniter tip to improve input data for the ignition model

LITERATURE CITED

1. Hadley, J. R., MATERIALS RANKING FOR USAAMRDL ADVANCED, SMALL, HIGH-TEMPERATURE-RISE COMBUSTOR PROGRAM, PE-8349-MR, AiResearch Manufacturing Company of Arizona, June 16, 1972.

2. Hadley, J. R., USAAMRDL ADVANCED, SMALL, HIGH-TEMPERATURE-RISE COMBUSTOR PROGRAM MATERIAL DESIGN DATA, MP-5525-MR, AiResearch Manufacturing Company of Arizona, August 19, 1971.

3. International Nichel Brochure, SUMMARY OF EXPERIMENTAL DATA, ALLOY IN-586-X, August 1968.

4. Frazer, R. P., LIQUID FUEL ATOMIZATION, Sixth Symposium (International) on Combustion, Report 91, Reinhold Publishing Corporation, New York, New York, 1957, pp 687-701.

5. Igebo, R. D., ATOMIZATION ACCELERATION AND VAPORIZATION OF LIQUID FUELS, Sixth Symposium (International) on Combustion, Report 90, Reinhold Publishing Corporation, New York, New York, 1957, pp 684-687.

6. Priem, R.J., and Heidman, M. F., PROPELLANT VAPORIZATION AS A DESIGN CRITERION FOR ROCKET ENGINE COMUBSTION CHAMBERS, NASA TR R-67.

7. Nelson, W. L., PETROLEUM REFINERY ENGINEERING, McGraw-Hill Book Company, Inc., New York, 1949.

8. Wallmer, L. E., and Walna, H. J., GENERALIZATION OF TURBOJET AND TURBINE PROPELLER ENGINE PERFORMANCE IN WINDMILLING CONDITION, NACA Report RME51, J23, December 1961.

9. Gladden, J. K., Goglia, J. J., and Ward, H. C., PHYSICAL PROPERTIES OF JP-4 FUELS AND DEVELOPMENT OF EQUATIONS FOR PREDICTING FUEL SYSTEM PERFORMANCE UNDER TWO-PHASE FLOW CONDITIONS, WADS Technical Report 55-422, Part 2, November 1955.

10. Barnett, H. C., and Hibbard, R. R., PROPERTIES OF AIRCRAFT FUELS, NADA TN 3276, August 1956.

11. Roberts, J. K., HEAT AND THERMODYNAMICS, Blackie and Son, Ltd., 1945.

12. Maxwell, J. B., DATA BOOK ON HYDROCARBONS, D. Van Nostrand, 1950.

13. Nixon, A. C., et al, VAPORIZING AND ENDOTHERMIC FUELS FOR ADVANCED ENGINE APPLICATIONS, Technical Report AFAPL-TR-67-114 Air Force Aero Propulsion Laboratory, Part III, Volume II, February 1970.

14. Mellor, R., Chigier, N. A., and Beer, J. M., PRESSURE JET SPRAY IN AIR STREAM, ASME 70 GT 101, May 1970.

15. Fraser, R. P., Dombrowski, N., and Routley, J. H., ATOMIZATION OF A LIQUID FUEL SHEET BY AN IMPINGING AIR STREAM, Chemical Engineering Science, Volume 18, N6, June 1963, pp 33g-53.

16. Giffen, E., and Muraszew, A., THE ATOMIZATION OF LIQUID FUELS, Chapman and Hall, 1953.

17. Eisenklam, P., et al., EVAPORATION RATES AND DRAG RESISTANCE OF BURNING DROPS, Eleventh International Combustion Symposium, The Combustion Institute, 1967, pp 715-727.

18. Natrajan, R., and Brzustowski, T. A., SOME NEW OBSERVATIONS ON THE COMBUSTION OF HYDROCARBON DROPLETS AT ELEVATED PRESSURES, Combustion Science and Tech. 2, 1970, pp 259-269.

19. Streeter, V. L., ed, HANDBOOK OF FLUID DYNAMICS, McGraw-Hill Book Company, Inc., New York, pp 17-31.

20. Lane, W. R., and Green, H. L., SURVEYS IN MECHANICS, G. K. Batchelor and R. M. Davies, ed., Cambridge University Press, New York, 1956, pp 162-215.

21. Handon, A. R., et al, SHOCK TUBE INVESTIGATION OF THE BREAKUP OF DROPS BY AIR BLASTS, Physics of Fluids, 8, 1963, pp 1070-1080.

22. Taylor, G. J., PROCEEDINGS ROYAL SOCIETY, London, 226A, 34, 1954.

23. Valentas, K. J., et al, BREAKAGE AND COALESCENCE IN DISPERSED PHASE SYSTEMS, Ind. Eng. Chem. Fund 5 (4), 1966, pp 533-542.

24. Kazam, H. J., et al, DEFORMATION AND BREAKUP OF LIQUID DROPLETS IN A SIMPLE SHEAR FIELD, Ind. Eng. Chem. Fund 7 (4), 1962, pp 576-581.

25. Hinze, J. O., FUNDAMENTALS OF HYDRODYNAMICS MECHANISM OF SPLITTING IN DISPERSION PROCESS, Journal American Institute Chemical Engineers, 1955, p 289.

26. Eiseklam, P., ATOMIZATION OF LIQUID FUEL FOR COMBUSTION - I, Combustion 33(1), 1961, pp 22-29.

27. CONTAMINATED FUEL PROGRAM, BUWEPS CONTRACT NOW63-0790-C1, SUMMARY OF COMBUSTION SYSTEM DEVELOPMENT, AiResearch Report GT-7756-R, June 1966.

28. Putnam, et al, INJECTION AND COMBUSTION OF LIQUID FUELS, Aeronautical Research Lab, Contract AF33-(038) 13501, Technical Report 56-344, Document NO. AD 118KG.

29. Shapiro, A. H., COMPRESSIBLE FLUID FLOW, The Ronald Press Company, New York.

30. Kinney, G. R., Abramson, A. E., and Sloop, J. L., INTERNAL LIQUID FILM COOLING EXPERIMENTS WITH AIR STREAM TEMPERATURES TO 2000°F IN 2- AND 4-INCH DIAMETER HORIZONTAL TUBES, NACA Report 1087, 1952 for Lewis Propulsion Laboratory, Ohio.

31. Ricou, F. P., and Spalding, D. B., MEASUREMENT OF ENTRAINMENT BY AXISYMMETRICAL TURBULENT JETS, J. of Fluid Mechanics, November 1960.

32. Bakke, P., AN EXPERIMENTAL INVESTIGATION OF WALL JET, Journal of Fluid Mechanics, Volume 2, Part 5, July 1957, pp 467-472.

33. Gordon, R., and Cobonpue, J., HEAT TRANSFER BETWEEN A FLAT PLATE AND JETS OF AIR IMPINGING ON IT, International Developments in Heat Transfer, International Heat Transfer Conference, 1961.

34. Walz, D. R., SPOT COOLING AND HEATING OF SURFACES WITH HIGH VELOCITY IMPINGING AIR JETS, PART 2 - CIRCULAR JETS ON PLANE AND CURVED SURFACES, SLOT JETS ON CURVED SURFACES, T.R. No. 61, Office of Naval Research Contract NQNR 225 (23), Stanford University, California, 1964.

35. Vennard, J. K. ELEMENTARY FLUID MECHANICS, Third Edition, John Wiley and Sons, New York, 1957.

36. Amsden, A. A., and Harlow, F. H., THE SMAC METHOD: A NUMERICAL TECHNIQUE FOR CALCULATING IN-COMPRESSIBLE FLUID FLOWS, Los Alamos Scientific Laboratory Report No. LA-4370, May 1970.

37. Gosman, A. D., et al, HEAT AND MASS TRANSFER IN RECIRCULATING FLOWS, Academic Press, London and New York, 1969.

38. Verduzio and Companaro, THE AIR RECIRCULATION RATIO IN CAN-TYPE GAS TURBINE COMBUSTION CHAMBERS, Granfield International Propulsion Symposium, 1969, The College of Aeronautics, Granfield, Bedford, England.

39. Williams, G. C., Hattel, H. C., and Morgan, A. C., THE COMBUSTION OF METHANE IN A JET-MIXED REACTOR, Twelfth Symposium (International) on Combustion, Combustion Institute, 1968.

40. Herbert, M. V., A THEORETICAL ANALYSIS OF REACTION RATE CONTROLLED SYSTEMS, Combustion Researches and Reviews, 1957, Agard, Butterworths Publications, London, 1957.

41. Launder, B. C., and Spalding, D. B., TURBULENCE MODELS AND THEIR APPLICATION TO THE PREDICTION OF INTERNAL FLOWS, presented at a Symposium on Internal Flows, University of Salford, 20-22 April, 1971.

42. Wolfstein, M., CONVECTION PROCESSES IN TURBULENT IMPINGING JETS, Imperical College of Science and Technology, Department of Mechanical Engineering, SF/R/I/Z, November 1967.

43. Kacker, S. C., and Whitelow, J., PREDICTION OF WALL-JET AND WALL WAKE FLOWS, Journal of Mechanical and Engineering Sciences, Volume 12, No. 6, 1970, pp 404-420.

44. Kays, W. M., CONVECTIVE HEAT AND MASS TRANSFER, McGraw-Hill Book Company, Inc., New York, New York, 1966.

45. Watson, E. A., IGNITION RESEARCH WORK CARRIED OUT BY THE LUCAS ORGANIZATION WITH SPECIAL REFERENCE TO HIGH ALTITUDE PROBLEMS, Report No. L5988, November 1954.

46. Lefebre, A. H., IGNITION THEORY AND ITS APPLICATION TO THE ALTITUDE RELIGHTING PERFORMANCE OF GAS TURBINE COMBUSTORS, Granfield International Propulsion Symposium, Propulsion Department, the College of Aeronautics, Granfield, Bedford, England, 1969.

47. Burnett, Henry C., and Hibbard, Robert R., PROPERTIES OF AIRCRAFT FUELS, NACA TN 3276, 1956, p 34.

48. Gurevich, M. I., THEORY OF JETS IN AN IDEAL FLUID, Pergamon Press, pp 52-59.

49. Margason, R. J., THE PATH OF A JET DIRECTED AT LARGE ANGLES TO A SUBSONIC FREE STREAM, NASA TN D-4919, November 1968.

50. Carlson, C. W., Hsu, J. J., and Meyers, G. A., THE PENETRATION AND MIXING OF AIR JETS DIRECTED PERPENDICULAR TO A STREAM, ASME Report 68-WA-GT-8, 1968.

51. Norster, E. R., FIRST REPORT ON JET PENETRATION AND MIXING STUDIES (Rep. PD/JPI), College of Aeronautics, Cranfield, England, 1962.

52. Norster, E. R., SECOND REPORT ON JET PENETRATION AND MIXING STUDIES (Rep. PD/JP2), College of Aeronautics, Cranfield, England, 1964.

53. Braun, G. W., and McAllister, J. D., CROSSWIND EFFECTS ON TRAJECTORIES AND CROSS SECTIONS ON TURBULENT JETS, NASA SP-218, ANALYSIS OF A JET IN A SUBSONIC CROSSWIND, a Symposium at Langley Research Center, 1969.

54. Keffer, J. F., and Baines, W. D., THE ROUND TURBULENT JET IN A CROSSWIND, Jour. Fluid Mech., Volume 15, April 1963.

55. Live, A. E. H., A TREATISE ON THE MATHEMATICAL THEORY OF ELASTICITY, Cambridge University Press, Cambridge, England, 1927.

56. Reissner, E., ON THE THEORY OF THIN ELASTIC SHELLS, Reissner Anniversary Volume, J. W. Edwards, Ann Arbor, Michigan, 1949, p 231.

57. Metzyer, D. E., HEAT TRANSFER TO FILM-COOLED COMBUSTION CHAMBER LINERS, ASME Publication 72-WA/HT-32, 1972.

58. Hottel, H. C., and Sarofirn, A. F., RADIATIVE TRANSFER, McGraw-Hill Book Company, Inc., New York, 1967.

59. Eckert, E. R. G., and Drake, R. M., HEAT AND MASS TRANSFERS, McGraw-Hill Book Company, Inc., New York, 1959.

60. Hamilton, D. C., and Morgan, W. R., RADIANT INTERCHANGE CONFIGURATION FACTORS, NACA TN 2836, 1952.

61. Reeves, D., FLAME RADIATION IN AN INDUSTRIAL GAS TURBINE COMBUSTION CHAMBER, N.G.T.E. M285, October 1956.

62. Thring, M. W., and Holliday, D. K., THE RADIATION FROM FLAMES IN A SMALL SCALE OIL FIRED FURNACE, ARC Report 18237, Aeronautical Research Council, England, 1956.

APPENDIX I

AIR-ASSIST PRESSURE ATOMIZER COMPUTER PROGRAM 1527

1.0 INTRODUCTION

Computer Program 1527 analyzes a pressure atomizer to determine spray formation and evaporation. The atomizer can be a simplex or dual-orifice type and may have air assist. Spray trajectories and evaporation are computed for two optional ambient environments.

2.0 PROGRAM INPUT

Program input is shown in Figure 169. The first card is a title card. The second card defines the atomizer with the following data:

(a) Atomizer type: 1 = simplex, 2 = dual orifice

(b) Air-assist option: 1 = no assist, 2 = with assist

(c) Primary fuel flow number, $PPH/PSI^{0.5}$

(d) Secondary fuel flow number, $PPH/PSI^{0.5}$

(e) Spray cone angle, deg

(f) Effective area of the assist air shroud, sq in.

(g) Primary orifice diameter, in.

(h) Secondary orifice diameter, in.

The third and fourth data cards are entered only for a dual orifice type and contain the fuel flow versus pressure characteristic of the combined flow divider and secondary orifice. The first point is the flow-divider crack point, and the remaining four points are selected over the anticipated flow range.

The fifth card defines the atomizer flow conditions:

(a) Fuel type, 2 = JP-5, 4 = JP-4

(b) Airflow option: 1 = uniform stream, 2 = 2-D Gosman flow field input from TAPE1

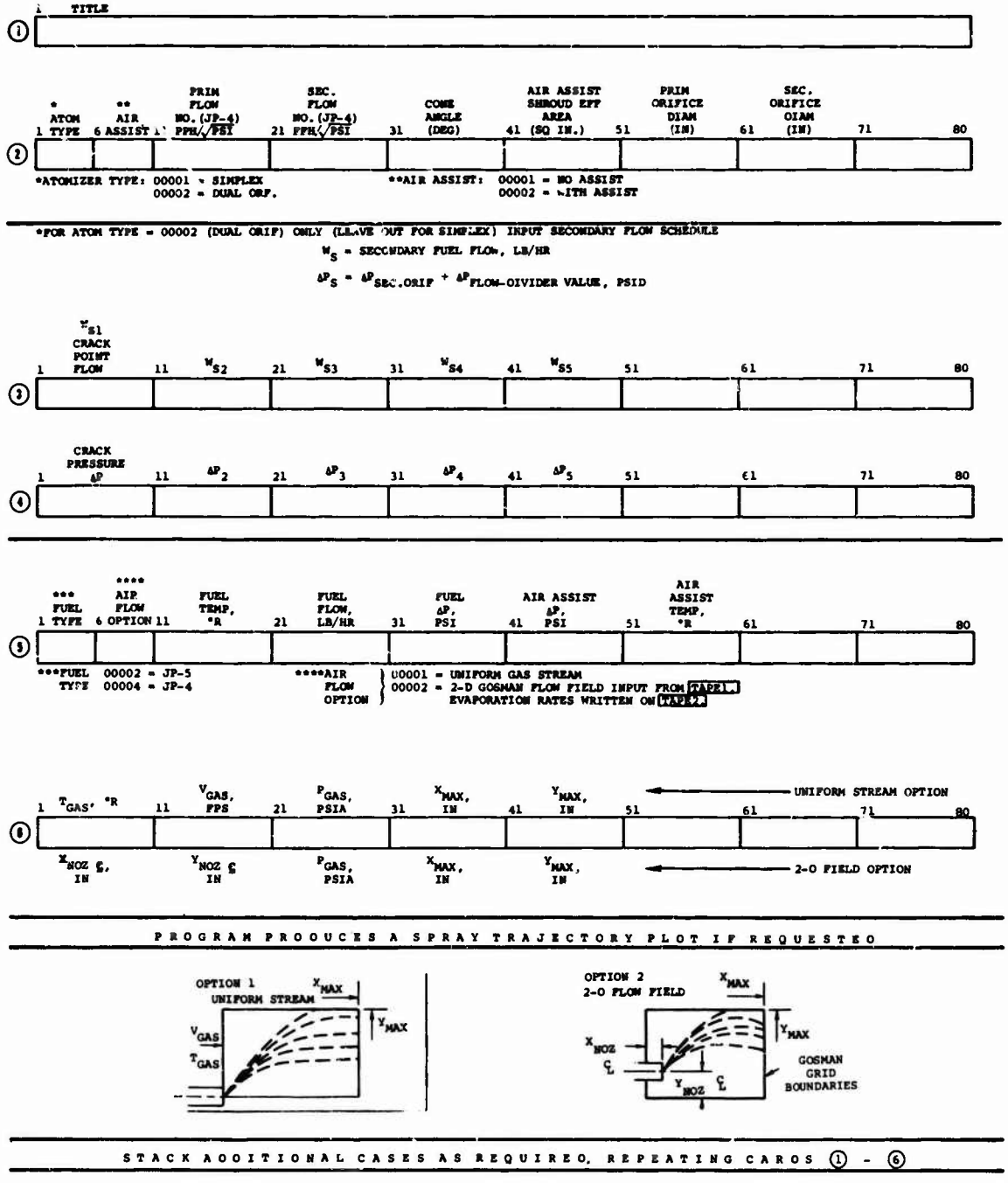


Figure 169. Air-Assist Pressure Atomizer Program No. 1527 Input Data.

(c) Fuel inlet temperature, °R

(d) Fuel flow rate, lb/hr

(e) Fuel differential pressure, psi (optional)

(f) Assist air differential pressure, psi

(g) Assist air temperature, °R

If (e) above (fuel differential pressure) is entered, the fuel flow is computed from the flow number, and the fuel flow entered (d) is ignored. If (e) is blank or zero, the entered fuel flow is used.

There are two airflow options to define the ambient environment for spray trajectory calculations. Option 1 defines an airstream with uniform velocity and temperature flowing parallel to the axis of the atomizer. A positive value for gas velocity denotes flow in the spray direction. Option 2 provides for the input of a disk file or tape, identified as TAPE1, containing a two-dimensional flow field as obtained with Gosman Program Number 1338. For this option, the fuel evaporation rates in lb/sec/ft^3/radian are written on TAPE2 for input into the Gosman program.

The sixth data card contains the following information required for the airflow options:

Option 1, Uniform Streams

(a) T_{gas}, airstream temperature, °R

(b) V_{gas}, airstream velocity, ft/sec

(c) P_{gas}, airstream pressure, psia

(d) X_{max}, flow field length limit, in.

(e) Y_{max}, flow field radial limit, in.

Option 2, 2-D Flow Field

(a) Y_{noz}, axial location of the spray origin relative to the flow-field origin

(b) Y_{noz}, radial location of the spray origin relative to the flow-field origin

(c) P_{gas}, flow-field gas pressure, psia

(d) X_{max}, flow-field length limit, in.

(e) Y_{max} flow-field radial limit, in.

3.0 PROGRAM COMPUTATIONS

A listing of the program is presented in Table XX. For a dual orifice nozzle, the drop size is computed from a combined sheet thickness from both orifices. Spray trajectories and evaporation are then computed for each five drop-size groups sized in ratios to the SMD.

4.0 PROGRAM OUTPUT

A copy of a program output for the two typical cases is shown in Table XXI. A plot tape is written to plot the trajectories for each of the five drop groups. When Option 2 is specified, an output tape, identified as TAPE2, is written containing the total evaporation rates at each grid node in the Gosman program solution that supplied the two-dimensional flow field.

This program can be run separately from the Gosman program with tapes saved between runs. The two programs can also be run together in a combined sequential run for repetitive iteration of the solutions.

5.0 PROGRAM USAGE

No attempt has been made to provide for the design of internal details of the atomizer. This type of atomizer is best made by fuel nozzle manufacturers who can provide the orifice diameters required for program input.

Injector performance can be computed at critical engine conditions such as light-off, maximum loading, idle, and maximum power design points.

SMD only, without spray trajectories, can be computed with OPTION1 by setting X_{max} and Y_{max}, Card 6 to zero. When fuel-flow and air-assist conditions are determined to provide satisfactory SMD levels, spray trajectories can then be computed to assess spray penetration. This provides guidance in fuel nozzle spacing and prevention of combustor wall impingement.

Finally, the program can be used in conjunction with a primary-zone flow field obtained from the Gosman program to provide information required for computing ignition energy and primary-zone performance.

TABLE XX. LISTING FOR PROGRAM NO. 1527

```
$$$
```

TABLE XX. (CONTD)

```
     /       4.7,2.15,1.43,1.23,1.04,.93,.79,.69,.61,.55,.49,.44  /
      DATA TS / 50.,100.,150.,200.,250.,300.,350.,400.,450.,500. /
      DATA SGTARS / .72,.76,.80,.84 /
      DATA NTARST,NTARSS,NTARF        / 10,4,7/
      DATA SRFTNS / 21.,18.2,15.5,13.,10.6,8.2,5.9,3.9,2.0,.2,
     1 23.1,20.5,18.0,15.6,13.4,11.1,9.0,7.0,5.1,3.3,
     2 23.9,21.8,19.6,17.5,15.4,13.4,11.4,9.5,7.7,6.,
     3 24.9,22.9,21.0,19.1,17.3,15.5,13.8,12.1,10.4,8.8  /
      CALL PLOTS (0,0,0)
C     INPUT DATA
    1 READ (60,1000) TITLE
      IF (EOF(60)) 999,2
  999 CALL PLOT(0.,0.,999)
      CALL EXIT
    2 WRITE (61,1010) TITLE
      DO 3  I=1,500
      X(I)=0.
    3 Y(I)=0.
      XMAX=10.
      YMAX=10.
      XSTART=0.
      YSTART=0.
CCCCCC
      READ(60,1020)KORIF,KAIRAS,FN1,FN2,CONEAN,AREASH,DORF1,DORF2
      IF(KORIF.EQ.1)WRITE(61,1021)FN1,CONEAN,DORF1
      IF(KORIF.EQ.2)WRITE(61,1022)FN1,FN2,CONEAN,DORF1,DORF2
      IF(KAIRAS.EQ.1)WRITE(61,1023)
      IF(KAIRAS.EQ.2) WRITE(61,1024) AREASH
      IF(KORIF.NE.2) GO TO 4
      READ(60,1040) FLOWS
      WRITE(61,1050)FLOWS
      READ(60,1040)DELPS
      WRITE(61,1051)DELPS
    4 CONTINUE
CCCCCC
      READ(60,1041)KFUEL,IOPT,TFUEL,PPH,DELP,DELPSH,TSH
      WRITE(61,1042)KFUEL,IOPT,TFUEL,PPH,DELP,DELPSH,TSH
      IF(IOPT.NE.1) GO TO 6
CCCCCC
      READ(60,1040)TAMB,VAIR,PS,XMAX,YMAX
      WRITE(61,1053) TAMB,VAIR,PS
      GO TO 7
    6 CONTINUE
C     XSTART, YSTART ARE INPUT IN INCHES
CCCCCC
      READ(60,1040)XSTART,YSTART,PS,XMAX,YMAX
      WRITE(61,1052)XSTART,YSTART,PS,XMAX,YMAX
      XSTART= XSTART / 12.
      YSTART= YSTART / 12.
      XMAX=XMAX/12.
      YMAX=YMAX/12.
    7 CONTINUE
      VAA= 0.
      WAIR= 0.
      IF (KAIRAS .EQ. 1) GO TO 11
      PR= (PS + DELPSH) / PS
      FMA2= 5. * (PR**.2857 - 1.)
      IF (FMA2 .GT. 1.) FMA2= 1.
      TSA= TSH / (1. + .2 * FMA2)
      VAA= 49.02 * SQRT(TSA * FMA2)
      RHOAIR= 2.6995 * PS / TSA
      PRP= (1. + .2 * FMA2) **3.5
      PSP= (PS + DELPSH) / PRP
      WAIR= AREASH * VAA * 2.6995 * PSP / TSA / 144. * 3600.
      WRITE (61,2110) WAIR, VAA
   11 TFUELR= TFUEL
```

TABLE XX. (CONTD)

```
      TFUEL=TFUEL-459.69
C     SPECIFIC GRAVITY (OMLS) FOR FUEL
      SGF=TAB (TFUEL,T2(1,KFUEL),SGFUEL(1,KFUEL),NTAB2)
      SG60F= TAB(60.,T2(1,KFUEL),SGFUEL(1,KFUEL),NTAB2)
      DO 12 I=1,NTAB5S
   12 DUMDUM(I)= TAB(TFUEL,T5,SHFTNS(1,1),NTAB5T)
      TAU= TAB(SG60F, SGTAB5,DUMDUM, NTAB5S)
C     DENSITY OF FUEL
      RHOFUL= 62.428 * SGF
C     VISCOSITY OF FUEL (CENTISTOKES)
      FMU= TAB (TFUEL,T3(1,KFUEL),VISFUL(1,KFUEL),NTAB3)
      WRITE (61,)140)SGF,FMU
      CONX= COS(CONEAN / 57.29578 * .5) * SQRT(RHOFUL)
      SLM1= 3.359 * FN1 / DORF1 / CONX
      SLM2= 0.
      IF (KORIF .NE. 1) SLM2= 3.359 * FN2 / DORF2 / CONX
      SLM= SLM1 + SLM2
      WRITE (61,2100) SLM1, SLM2
C     CONSTANTS FOR CALCULATIONS
      CON1= .764 /SGF
      CON2= PPH**.205
      CON3= (FMU) / 1.5)**.3
      CON4= 9266. / RHOFUL
CCCCCC
      ELIM= .96
      SI= .01
      S=S1/12.
      DX= S
      CON9= 39.37E-6 /12.
C
      IN=2
      JN=2
      VAIRH)=VA1R
      VAIRV1=0.
      TS1=TAMH
      VA1RH=VAIRH1
      VAIRV=VAIRV1
      TS=TS1
      X1(I)=0.
      X2(1)=0.
      X1(IN)=XMAX/12.
      X2(JN)=YMAX/12.
      IF(IOPT.EQ.1) GO TO 9
      REWIND 1
      READ(1) IN, JN, XI, X2, R
      READ (1)
      READ (1) G1
      READ (I) G2
      READ (1) R0
      READ (1)
      READ (I) T
      REWIND I
      REWIND 2
      DO 8 I=1,441
    8 FEVAP(I)= 0.
    9 CONTINUE
C     CALCULATIONS BEGIN * * * * * * * * *
      DELP1= (PPH* CON1/ FN1)**2
      IF (KORIF .EQ. 1) GO TO 5
      IF (DELP1 .GE. DELPS(1)) GO TO 20
      WRITE (61,1070)
      KORIF =1
      GO TO 10
    5 IF (DELP1 .NE. 0.) GO TO 10
      DELPI=DELP
      PPH= FN1*SQRT(DELP1)/CON1
```

```
      CONC= PPH**.205
   10 VFUEL= SQRT(CON4 * DELP1)
      IF (KAIRAS .EQ. 2) GO TO 18
      SMD=225. * CON2 * CON3 / DELP1**.354
      GO TO 19
   18 QMR= WAIR / PPH
      VR= VFUEL / VAA
      VEP= .438 * QMR **.1 * VAA * SQRT(.5 + VR **2 - VR)
      SMD= 196. * SQRT(TAU * SLM / RHOAIR) * FMU **.095 / VEP
   19 DELPEQ= DELPI
      DELP2=0.
      DELPVN=0.
      PPM1=PPH
      PPM2=0.
      GO TO 90
   20 KROSS=0
      KOUNT=0
      DO  70 I=1,5
      DELPVN= DELPS(I)
   30 PPM2= TAB (DELPVN,DELPS,FLOWS,5)
      DELP2= (PPM2 * CONI/ FN2)**2
      PPM1= PPH- PPM2
      DELP1= (PPM1 * CONI/ FN1))**2
      DELPVG= DELP1-DELP2
      ERRORN= DELPVN- DELPVG
      IF (ABS(ERRORN) .LE. .1) GO TO 80
      IF (I .EQ. 1) GO TO 60
      IF (ERRORN * ERRORO .LT. 0.) GO TO 40
      IF (KROSS .EQ. 0) GO TO 60
      DELPVO= DELPVN
      ERRORO= ERRORN
      GO TO 50
   40 IF (KROSS .NE. 0) GO TO 50
C     ROOT IS BETWEEN DELPS(I-1) AND DELPS(I)
      KROSS=1
      DELTA= DELPVN- DELPVO
   50 DELTA= DELTA * .5
      DELPVN= DELPVO + DELTA
      KOUNT= KOUNT +1
      IF (KOUNT .LT. 50) GO TO 30
      WRITE (61,1080) DELPVO,DELPVN
      CALL EXIT
   60 ERRORO= ERRORN
      DELPVO= DELPVN
   70 CONTINUE
      WRITE (61,1090)
      CALL EXIT
C     CONVERGENCE
   80 DELPEQ= (DELP1*PPM1 + DELP2 * PPM2 ) / PPH
      VFUEL= SQRT(CON4 * DELPEQ)
      IF (KAIRAS .EQ. 2) GO TO 84
      SMD= 330. * CON2 * (FMU / 1.5)**.3 / DELPEQ**.354
      GO TO 90
   84 QMR= WAIR / PPH
      VR= VFUEL / VAA
      VEP= .438 * QMR **.1 * VAA * SQRT(.5 + VR **2 - VR)
      SMD= 196. * SQRT(TAU * SLM / RHOAIR) * FMU **.095 / VEP
   90 CONTINUE
C     NOTE-- COORD. SYSTEM OF EVAP IS HORIZ. + TO RIGHT, VERTICAL + TO
C              BOTTOM.  THETA IS MEASURED FROM + HORIZ. TOWARDS  + VERTICAL
      THETA1=-CONEAN /57.2957R *.5
      SINT1=SIN(THETA1)
      COST1=COS(THETA1)
      OPTION= 1.
      IF(IOPT.EQ.2)CALL AIRPRP(XSTART,YSTART,VAIRH1,VAIRV1,TS1)
      MAXK=0
```

```
      WRITE(6I,1110) DELP1,PPH1,DELP2,PPH2,DELPVN,VFUEL,SMD
      WRITE (6I,2120) QM9, VEP
      DO 150 I=1,5
C     DIA IS IN MICRONS
      DIA(I)= DIASMD(I,KAIRAS) * SMD
C     D  IS IN FEET
      D(I)= DIA(I) * CON9
      E(I)= 0.
      EW(I)= 0.
      W(I)= D(I)**3*RHOFUL*3.14159265 / 6. / 1.5
      WST(I)= W(I)
      VF(I)= VFUEL
      TF(I)= TFUELR
      INTER= 1
      KKK=1
C **  THETA= THETAI
      SINI= SINT1
      COSI= COST1
      X(I,I)= XSTART
      Y(I,I)= YSTART
      K1= 0
      EW1= EW(I)
      IF (IOP1 .EQ. 2) CALL FEVAPC (XSTART,YSTART,K1,EW1,EW(I))
CCCCCC
      DRO(I,I)=D(I)/CON9
      EVP(I,I)=0.
      TTF(1,I)=TFUELR
      VEF(I,I)=VFUEL
CCCCCC
      VAIRH= VAIRH1
      VAIRV= VAIRV1
      TS= TS1
      KOVER=1
      KOUNT= 2
      XOLD= XSTART
      YOLD= YSTART
      KOLD= I
  100 IF (KOLD .LT. 6) GO TO 101
      KOLD= 1
      KOUNT= KOUNT +1
      IF (KOUNT .GT. 100) GO TO 110
CCCCCC
  101 IF (E(I) .LT. ELIM) CALL EVAP (INTER,I)
      IF (INTER .LT. 0) GO TO 120
      INTER= 2
C     X, Y IN FEET
      X(KOUNT,I)= XOLD   +S * COST
      Y(KOUNT,I)= YOLD   -S * SINT
      W(I)= W(I) - DELM(I)
      EW(I)= 1. - W(I) / WST(I)
      IF (IOPT .EQ. 2)
     1CALL FEVAPC (X(KOUNT,I), Y(KOUNT,I), K1, EW1,EW(I))
CCCCCC
      DRO(KOUNT,I)=D(I)/CON9
      EVP(KOUNT,I)=E(I)*100.
      IF(E(I).LT..001) EVP(KOUNT,I)=0.
      TTF(KOUNT,I)=TF(I)
      VEF(KOUNT,I)=VF(I)
CCCCCC
C     CHECK IF THIS INTERVAL CROSSED EVAP. STORE POINT
      K= KKK
CCCCCC
      DO 600 L=K,10
      KKK= L
      EP= FLOAT(L) * .1
      IF (L .EQ. 10) EP= .95
```

TABLE XX. (CONTD)

```
      IF (ESAVE(I) .GE. EP .OR. E(I) .LT. EP) GO TO 610
C     INTERPOLATE FOR (X1,X2) IN FEET
      DUM= 0.
      TEMP= E(I) - ESAVE(I)
      IF (TEMP .NE. 0.) DUM= (EP - ESAVE(I) ) / TEMP
      X1E(I,L)=        XOLO    + DUM * (X(KOUNT,I) - XOLO    )
      X2E(I,L)=        YOLO    + DUM * (Y(KOUNT,I) - YOLO    )
      XINCH=X1E(I,L)*12.
      YINCH=X2E(I,L)*12.
  600 WRITE(61,2010) I,EP,XINCH,YINCH
      GO TO 120
C     CHECK IF HAVE HIT A BNORY
  610 IF (X(KOUNT,I) .GE. X1(1) ) GO TO 620
      DUM= 4HLEFT
      GO TO 650
  620 IF (X(KOUNT,I) .LE. X1(IN)) GO TO 630
      DUM= 5HRIGHT
      GO TO 650
  630 IF (Y(KOUNT,I) .GE. X2(1) ) GO TO 640
      DUM= 6HBOTTOM
      GO TO 650
  640 IF (Y(KOUNT,I) .LE. X2(JN)) GO TO 105
      DUM= 3HTOP
  650 WRITE (61,2000) I,DUM
  655 DO 660 L= KKK,10
      X1E(I,L)= X(KOUNT,I)
  660 X2E(I,L)= Y(KOUNT,I)
      GO TO 120
  105 IF (INTER .LT. 0) GO TO 655
C **  THETA= ATAN2(DUM1,DUM2)
      SINT= DUM1 / VF(I)
      COST= DUM2 / VF(I)
      XOLO= X(KOUNT,I)
      YOLO= Y(KOUNT,I)
      KOLD= KOLD + 1
      IF(IOPT.EQ.2)CALL AIRPRP(X(KOUNT,I),Y(KOUNT,I),VAIRH,VAIRV,TS)
      GO TO 100
  110 KOVER=KOVER+1
      IF (KOVER .LT. 10) GO TO 111
      WRITE (61,1100) I
      KOUNT= KOUNT-1
      GO TO 655
C     COMPRESS 100 PTS INTO 50 AND CONTINUE
  111 DO 112 J=4,100,2
      K=J/2
CCCCCC
      ORD(K,I)=ORD(J,I)
      EVP(K,I)=EVP(J,I)
      TTF(K,I)=TTF(J,I)
      VEF(K,I)=VEF(J,I)
CCCCCC
      X(K,I)=X(J,I)
  112 Y(K,I)=Y(J,I)
      KOUNT=51
      GO TO 100
  118 WRITE (61,1170) I
  120 NNN(I)= KOUNT
      IF (MAXK .LT. KOUNT) MAXK=KOUNT
      K1= -1
      IF (IOPT .EQ. 2)
     1CALL FEVAPC (X(KOUNT,I),Y(KOUNT,I),K1,EW1,EW(I))
  150 CONTINUE
      IF (IOPT .EQ. 1) GO TO 151
      WRITE (61,1200) FEVAP
      WRITE (2) FEVAP
      REWIND 2
```

```
  151 WRITE (6,1180) (I,IF(I),VF(I),O(I),E(I),I=1,5)
      WRITE (6,1120) (LABELS(I),LABELS(6),I=1,5),(DIA(I),I=1,5)
      DO 158 I=1,5
      N= NNN(I) + 1
      IF (N .GT. MAXK) GO TO 158
      DO 156 J=N,MAXK
      DRD(J,I)= 0.
      TTF(J,I)= 0.
      VEF(J,I)= 0.
      EVP(J,I)= 0.
      X(J,I)=0.
  156 Y(J,I)= 0.
  158 CONTINUE
      DO 160 J=1,MAXK
C     CONVERT TO INCHES FOR PLOTTING AND PRINTING
      DO 169 I=1,5
      X(J,I)= X(J,I) * 12.
  169 Y(J,I)= Y(J,I) * 12.
CCCCCC
      WRITE(6,1130) (X(J,I),Y(J,I),I=1,5),(DRD(J,I),TTF(J,I),VEF(J,I),
     + EVP(J,I),I=1,5)
  160 CONTINUE
C     PLOTTING
      CALL PLOT(1.0,1.,-3)
CCCCCC
      Q=1.
CCCCCC
      IF(YMAX.GT.1.1.OR.XMAX.GT.1.4) Q=2
      IF(YMAX.GT.2.1.OR.XMAX.GT.2.8) Q=4
      IF(YMAX.GT.4.1.OR.XMAX.GT.5.8) Q=8
      IF(YMAX.GT.8.1.OR.XMAX.GT.11.5) Q=16
CCCCCC
      XL= 1.50*Q
      YL=1.25*Q
      DELX=XL/12.
      DELY=YL/10.
      CALL AXIS(0.,0.,1HX,-1,12.,0.,0.,DELX)
      CALL  AXIS (0.,0.,1HY,1,10.,90.,0.,DELY)
CCCCCC
      YL=8.5
      DO 180 I=1,5
      N=NNN(I)
      X(N+1,I)=0.
      Y(N+1,I)=0.
      X(N+2,I)=DELX
      Y(N+2,I)=DELY
      CALL LINE (X(1,I),Y(1,I),N,1,10,I)
CCCCCC
      XL=4.5
      CALL SYMBOL (XL,YL,.10,I,0.,-1)
      XL=XL+ .2
      CALL SYMBOL (XL,YL,.10,LABELS(I),0.,8)
      XL=XL+.80
      CALL SYMBOL (XL,YL,.10,46,0.,-1)
      XL=XL+.2
      CALL SYMBOL (XL,YL,.10,6HVOLUME,0.,6)
CCCCCC
      XL=XL+1.
      CALL NUMBER(XL,YL,.1,DIA(I),0.,2)
      XL=XL+.8
      CALL SYMBOL(XL,YL,.1,7HMICRONS,0.,7)
CCCCCC
      YL=YL+.2
  180 CONTINUE
      CALL PLOT (0.,-.5,-3)
      CALL SYMBOL (.5,10.5,.20,TITLE,0.,80)
```

```
      CALL SYMBOL (1.,10.,.10,21HINJECTOR TRAJECTORIES ,0.,21)
      IF (KORIF .EQ. 2) GO TO 190
      CALL SYMBOL (.5,9.8,.10,7HSIMPLEX ,0.,7)
      GO TO 200
  190 CALL SYMBOL (.5,9.8,.10,12HDUAL ORIFICE ,0.,12)
  200 IF (KAIRAS .EQ. 1) GO TO 210
      CALL SYMBOL (2.5,9.8,.10,4HWITH,0.,4)
      GO TO 220
  210 CALL SYMBOL (2.5,9.8,.10,7HWITHOUT,0.,7)
  220 CALL SYMBOL (3.2,9.8,.10,10HAIR ASSIST ,0.,10)
      CALL SYMBOL (.5,9.6,.10,11HCONE ANGLE=  ,0.,11)
      CALL NUMBER (1.7,9.6,.10,CONEAN,0.,1)
      CALL SYMBOL (.5,9.4,.10,5HFUEL= ,0.,5)
      CALL SYMBOL (1.1,9.4,.10,LABELF(KFUEL),0.,10)
      CALL SYMBOL (2.5,9.4,.10,7HFUEL T=  ,0.,7)
      CALL NUMBER (3.2,9.4,.10,TFUELR,0.,1)
CCCCCC
      CALL SYMBOL(.5,9.2,.1,4HSMD=,0.,4)
      CALL NUMBER(1.0,9.2,.1,SMD,0.,2)
      CALL SYMBOL(1.8,9.2,.1,7HMICRONS,0.,7)
CCCCCC
      CALL SYMBOL (.5,8.8,.10,28HFLOW NUMBER  PPH     DELTA P  ,0.,28)
      CALL NUMBER (.5,8.65,.10,FN1,0.,5)
      CALL NUMBER (1.7,8.6,.10,PPH1,0.,2)
      CALL NUMBER (2.3,8.65,.10,DELP1,0.,2)
      IF (KORIF .EQ. 1) GO TO 230
      CALL NUMBER (.5,8.5,.10,FN2,0.,5)
      CALL NUMBER (1.7,8.5,.10,PPH2,0.,2)
      CALL NUMBER (2.3,8.5,.10,DELP2,0.,2)
      CALL SYMBOL (.5,8.3,.10,12HFLOW DIVIDER ,0.,12)
      CALL SYMBOL (1.,8.15,.10,14HCRACK DELTA P=  ,0.,14)
      CALL NUMBER (2.4,8.15,.10,DELPS(1),0.,2)
      CALL SYMBOL (1.,8.0,.10,14HVALVE DELTA P=  ,0.,14)
      CALL NUMBER (2.4,8.0,.10,DELPVN,0.,2)
  230 IF (KPLOT .EQ. 0) GO TO 240
      KPLOT=0
CCCCCC
      CALL PLOT(16.,-12.5,-3)
      GO TO 1
  240 KPLOT=1
CCCCCC
      CALL PLOT(-1.,11.5,-3)
      GO TO 1
 1000 FORMAT (8A10)
 1010 FORMAT (1H1,8A10  /)
 1020 FORMAT(2I5,6F10.0)
 1021 FORMAT(1X,32HSIMPLEX ATOMIZER, FLOW NUMBER =  ,F10.5,14H CONE ANGL
     1E=  F10.5,10H ORIF DIA=   F6.3)
 1022 FORMAT(1X,38HDUAL ORIFICE ATOMIZER, PRIM FLOW NO = ,F10.5,15H SEC
     *FLOW NO =    F10.5,14H CONE ANGLE =   F10.5 / 15H PRIM ORIF DIA=
     2  F6.3,14H SEC ORIF DIA=   F6.3)
 1023 FORMAT(1X,18HWITHOUT AIR ASSIST  )
 1024 FORMAT(1X,32HWITH AIR ASSIST,  SHROUD AREA = ,F10.5,6H SQ IN  )
 1040 FORMAT (8F10.0)
 1041 FORMAT(2I5,5F10.0)
 1042 FORMAT(2X,39HKFUEL IOPT TFUEL PPH DELP DELPSH TSH = ,2I5,5F10.5)
 1050 FORMAT(1X,17HSEC FLOW SCHED =  ,5F10.5)
 1051 FORMAT(1X,17HSEC PRES SCHED =  ,5F10.5)
 1052 FORMAT(1X,62HARBITRARY FLOW OPTION, X START, Y START, P GAS, X MAX
     *, Y MAX = ,5F10.5)
 1053 FORMAT(1X,43HUNIFORM FLOW OPTION, T AMB, VAIR, P AMB = ,3F10.5)
 1070 FORMAT (43HDUAL ORIFICE IS ACTING AS SIMPLEX ATOMISER   )
 1080 FORMAT (22H0SOLUTIONS, OELPVO=  E12.4,5X, 7HOELPVN=  E12.4)
 1090 FORMAT (38H0NO SOLUTION WITHIN VALVE TABLE VALUES   )
 1100 FORMAT (42H0ITERATION REACHED MAX, OF 500 FOR DROPLET ,I5,
     121H, CALCULATION STOPPED  )
```

```
 1110 FORMAT(//13HODELTA P (1)=  ,F10.2, 5X, 8HPPH (1)=F10.2 /
     1 13H DELTA P (2)=  ,F10.2, 5X, 8HPPH (2)=  ,F10.2 /
     2 13H DELTA P (V)=  ,F10.2,7X,6HVFUEL=  F10.2/
     3 6H SMD= ,F10.2)
CCCCCC
 1120 FORMAT(1H0,5X,A8,A10,4(8X,A8,A10)/
     * 1H0,10X,FA.3,4(18X,FA.3),1X,7HMICRONS /
     * 1H0,8X,1HX,10X,1HY,4(14X,1HX,10X,1HY)/
     * 2X,5(5X,1H0,4X,2HTF,3X,2HVF,2X,5HE*100,2H /)//)
CCCCCC
 1130 FORMAT(2X,5(   F10.2,F11.2,5X)/2X,5(3X,F5.0,F6.0,F5.0,F5.0,2H / ))
 1140 FORMAT (4H0SG=  E12.4,7H (OMLS) ,4X,10HVISC FUEL=  E12.4,12H CENTI
     1STOKES  )
 1170 FORMAT (8H OROPLET    ,I3,15H HAS EVAPORATED        )
 1180 FORMAT  (26H0LAST DROPLET CONDITIONS--     /
     1  6X,4HDROP,5X,2HTF,13X,2HVF,14X,1H0,14X,1HE  /
     2    5 (5X,I5,4E15.5 /) /)
 1200 FORMAT (7H0FEVAP= / 21(1H0,7E12.4 / 2(1X,7E12.4/) ) )
 2000 FORMAT (13H0**** DROPLET  ,I3, 9H HAS HIT  ,A7, 8HBOUNDARY    )
 2010 FORMAT (8H0DROPLET   ,I3,3H E=  F4.2,5X,8H X1, X2=  2F9.5,3H IN)
 2100 FORMAT (26H0FUEL SHEET THICK., PRIM =  F9.1,7H, SEC =  F9.1,
     1 3H MICRONS       )
 2110 FORMAT (17H0ASSIST AIR FLOW=     F8.3, 6H LB/HR, 10H VELOCITY=
     1 F7.1,4H FPS)
 2120 FORMAT (21H0AIR/FUEL MASS RATIO=   F12.3,19H EFF. AIR VELOCITY=
     1 F10.1)
      END
      SUBROUTINE FEVAPC (X , Y , K1, EW1, EW)
      COMMON / KIMH / X1(21),X2(21),G1(21,21),G2(21,21),R0(21,21),T(21,
     1 21), IN, JN, R(21), FEVAP(21,21)
      COMMON / INPUT/ KFUEL, DEQ, GAP, PPH
C     CALC. AND STORE FUEL EVAPORATION RATE FOR GOSMAN PROGRAM
C
      IF (K1 .LT. 0) GO TO 50
C     DETERMINE WHICH ELEMENT VOLUME
      JN1= JN - 1
      DO 10 JJ= 2,JN1
      S1= (X2(JJ) + X2(JJ-1)) * .5
      S2= (X2(JJ) + X2(JJ+1)) * .5
      IF ( Y .LT. S1 .OR. Y .GE. S2) GO TO 10
      J= JJ
      GO TO 20
   10 CONTINUE
      GO TO 40
   20 IN1= IN - 1
      DO 30 II= 2,IN1
      S)= (X1(II) + X1(II-1)) * .5
      S2= (X1(II) + X1(II+1)) * .5
      IF (X .LT. S) .OR. X .GE. S2) GO TO 30
      I= II
      GO TO )00
   30 CONTINUE
C     NOT IN A VOLUME
   40 IF (K) .EQ. 0) RETURN
      IF (ISAVE .EQ. 0) RETURN
      I= 0
C     CALC. FEVAP(I,J) FOR ISAVE, JSAVE
   50 IF (ISAVE .EQ. 0 ) RETURN
      VOL= (X1(ISAVE+1) - X1(ISAVE-1)) * (X2(JSAVE+1)-X2(JSAVE-1)) * .25
     1 * R(JSAVE)
      IF (R(JSAVE) .NE. 1. .OR. R(JSAVE+1) .NE. 1.) VOL= VOL * 6.28318
      DEW= EW - EW1
      FEVAP(ISAVE,JSAVE)= FEVAP(ISAVE,JSAVE) + DEW * PPH / 18000. / VOL
      EW1= EW
      IF (I .NE. 0) GO TO 60
      ISAVE= 0
```

TABLE XX. (CONTD)

```
      K1= 0
      RETURN
   60 ISAVF= 1
      JSAVE= J
   70 RETURN
  100 IF (K1 .NE. 0) GO TO 110
      K1= 1
      GO TO 60
  110 IF (I .EQ. ISAVE .AND. J .EQ. JSAVE) GO TO 70
      GO TO 50
      END
      SUBROUTINE AIRPRP (X,Y,VAIRH,VAIRV,TS)
      COMMON / KIMH / X1(21),X2(21),G1(21,21),G2(21,21),RO(21,21),T(21,
     1 21), IN , JN
C     NOTE-- COORD. SYSTEM OF EVAP IS HORIZ. + TO RIGHT, VERTICAL + TO
C              BOTTOM
      DO 10 J=1,JN
      I=J
      IF (X2(J) - Y) 10,70,20
   10 CONTINUE
   20 IF (1 .EQ. 1) I=2
      KKK=1
   40 T1 = TAB(X,X1,T (1,I),IN)
      G11= TAB(X,X1,G1(1,1),IN)
      G21= TAB(X,X1,G2(1,I),IN)
      RO1= TAB(X,X1,RO(1,I),IN)
      IF (KKK) 60,80,50
   50 J=1
      I= I - 1
      KKK= -1
      T2= T)
      G12= G11
      G22= G21
      RO2= RO1
      GO TO 40
   60 DEL= (Y - X2(I) ) / (X2(J) - X2(I))
      TS   =      T1 + (T2  - T1 ) * DEL
      DUM  =     RO1 + (RO2 - RO1) * DEL
      VAIRH=    (G11 + (G12 - G11) * DEL ) / DUM
      VAIRV=  - (G21 + (G22 - G21) * DEL ) / DUM
   65 RETURN
   70 KKK=0
      GO TO 40
   80 TS= T1
      VAIRH= G11 / RO1
      VAIRV= - G21 / RO1
      GO TO 65
      END
      FUNCTION TAB (X,XX,YY,NTAB)
      DIMENSION XX(1), YY(1)
      F=1.
      IF (XX(1).GT.XX(2)) F=-F
      DO 10 J=1,NTAB
      I=J
      IF (F*(XX(1)-X)) 10,40,20
   10 CONTINUE
   20 IF (I.NE.1) GO TO 30
      I=2
   30 J=I-1
      DEL=XX(I)-XX(J)
      IF (DEL.EQ.0.) GO TO 50
      TAB=(YY(I)*(X-XX(J))-YY(J)*(X-XX(I)))/DEL
      RETURN
   40 TAB=YY(I)
      RETURN
   50 WRITE(61,60) X,I,J
```

TABLE XX. (CONTD)

```
      CALL EXIT
   60 FORMAT (24H0***ERROR IN ROUTINE TAB,E15.4,2I5)
      END
      SUBROUTINE EVAP (INTER,I)
C     DROPLET EVAPORATION.
C     PROGRAMMED 1-22-71 BY M. TANI.
C
CCCCC THIS ROUTINE IS THE SAME AS IN PROGRAM IMPACT EXCEPT
C           FOR THE CARD CHANGE MARKED C$$$
C
C     D,TF,VF,E       ARE INPUT FOR DROP NO. I
C**** NOTE-- FUEL PROPERTY EQUATIONS ARE ONLY FOR JP4 AND JP5/JP8 ***
C
      COMMON / INPUT / KFUEL,DEQ,GAP,PPH,TITLE(8)
      COMMON / DEVAP/ DUMMY(20),D(5),TF(5),VF(5),VREL(5),      RN(5),
     1 CD(5),DRAG(5),FN(5),      CP(5),DELQ(5),SG(5),FRMD(5),DELTF(5),
     2 TIMS(5),FMASS(5),ALPHA(5),DELV(5),E(5),DX,W(5),VFSAVE(5),TFSAVE(5
     3 ),DSAVE(5),ESAVE(5),DSTART(5),SGSG60(5),SG60(5),DELM(5)
     4,OPTION,VAIRM,VAIRV,SINT,COST,DUM1,DUM2
      COMMON / TRAJ / VFUEL,TFUEL,TFUELF,SGF,FMU,RHOF,PS,PT,TS,TT,
     1DUMMZQ(3),VAIR
      DIMENSION TAIRTB(7),AIRKTB(7),AIRMUT(7),AIRCPT(7)
      DATA TAIRTB / 400.,600.,1000.,1500.,2000.,2500.,3000. /
     1, AIRKTB / .0114,.0165,.0252,.0344,.0422,.0486,.054T /
     2,AIRMUT /1.E-5,1.3E-5,1.885E-5,2.5E-5,3.015E-5,3.48E-5,3.9E-5 /
     3, AIRCPT /.2404,.2409,.249,.2642,.2772,.2868,.293I /,NTARAR/7/
      DATA G,GAMMA,R,PI04,GOGM1,GM102,PI /32.174,1.4,1545.327,.7853982,
     1 3.5,.2, 3.1415927 /
C
      AIRM= 28.966
      CONSTI= G * GAMMA * R * TS / AIRM
C     CHECK FOR FIRST ENTRY TO ROUTINE (INTER=1)
      IF (INTER .NE. 1) GO TO 50
C     ESTIMATE NEXT STATION CONDITIONS
      VF2= VF(1)
      TF2= TF(I)
      D2=  D(I)
      E2=  E(I)
      DSTART(I)= D(I)
      GO TO 55
C     ESTIMATE NEXT STATION CONDITIONS
   50 VF2= 2. * VF(I) - VFSAVE(I)
      TF2= 2. * TF(I) - TFSAVE(I)
      D2= 2. * D(1) - DSAVE(I)
      IF (D2 .LT. 1.E-10) D2= 1.E-10
      E2= 2. * E(1) - ESAVE(I)
      IF (E2 .GT. .99) E2=  99
      IF (E2 .LT. 0.) E2= 0.
C     INITIALIZE FOR ITERATION ON D
   55 KOUNTC= 1
      SGRESD= SGRFCT (E(I))
      SG(1)= SGFCT (TF(I),SGRESD)
      SG60(I)= SGFCT (519.69,SGRESD)
      IF (INTER .EQ. 1) SGSG60(I)= SG(I) / SG60(I)
      W(1)= PI / 6. * D(I)**3 * SG(I) * 62.428
      DELDG= D2 - D(I)
      KOUNTD=0
   60 KOUNTB= 1
      DZ= (D(I) + D2) * .5
      CIRCUM= PI * DZ
      TEMPA= PI04 * DZ**2
      TEMPD= TEMPA * DZ / 1.5
C     INITIALIZE FOR ITERATION ON TF
      DELTFG= TF2 - TF(I)
      EZ= (E(I) + E2) * .5
      VAPM= VAPMF (EZ)
```

```
      SGRESD= SGRFCT (EZ)
C     AVERAGE TEMPERATURES, CALC. PROPERTIES
   70 TFZ= (TF(I) + TF2) * .5
      TMX= (TS + TFZ) * .5
      PAS= PASF(TFZ,EZ)
      IF (PAS .LT. PS-.01) GO TO 80
C     AT BOILING POINT.
      PAS= PS - .01
      KOUNTO=1
   80 VAPK= VAPKF(TMX,VAPM)
      VAPMU= VAPMUF(TMX)
      VAPLAM= VAPLMF(TFZ)
      CP(I)= CPFCT(TFZ,SGRESD)
      VAPCP= VAPCPF(TMX)
      SG(I)= SGFCT(TFZ,SGRESD)
      FRMO(I)= SG(I) * 62.428
      VAPD= VAPDF(TMX,PS)
      IF (VAPD .LT. .00005) VAPD= .00005
      ALP= PS / PAS * ALOG(PS / (PS - PAS) )
C     AIR PROPERTIES
      AIRK=TAB(TMX,TAIRTH,AIRKTH,NTABAR)
      AIRMU=TAB(TMX,TAIRTB,AIRMUT,NTABAR)
      AIRCP=TAB(TMX,TAIRTB,AIRCPT,NTABAR)
C     DIFFUSION ZONE PROPERTIES
      QK= PAS / PS * .5
      QJ= 1. - QK
      QKMX= QJ * AIRK + QK * VAPK
      QMUMX= QJ * AIRMU + QK * VAPMU
      QMMX= QJ * AIRM + QK * VAPM
      QCPMX= (QJ * AIRM * AIRCP + QK * VAPM * VAPCP) / QMMX
      QRHOMX= PS * QMMX * 144. / R / TMX
      SC= QMUMX / VAPD / QRHOMX
      PR= QCPMX * QMUMX / QKMX * 3600.
      TEMPE= DZ * QRHOMX / QMUMX
      QMASS= TEMPD * SG(I) * 62.428
      TEMPF= .6 * SC**.3333333333
CCCCCC
      TEMPG=CIRCUM*VAPD*VAPM*PAS*ALP/R/TMX*144.
      TEMPH= .6 * PR**.3333333333
      TEMPI= VAPCP / CIRCUM / QKMX
      TEMPJ= CIRCUM * QKMX * (TS - TFZ) / 3600.
      TEMPK = TEMPD * SG(I) * CP(I) * 62.428
C     INITIALIZE FOR ITERATION ON VF
      DELVG= VF2 - VF(I)
      KOUNTA= 1
C     CALCULATE DELTA V FOR DROP
  100 VFZ= (VF(I) + VF2) * .5
      IF (OPTION .EQ. 0.) GO TO 115
      VRV= VFZ   * SINT - VAIRV
      VRH= VFZ   * COST - VAIRH
      VREL(I)= SQRT(VRV**2 + VRH**2)
      SPHI= VRV / VREL(I)
      CPHI= VRH / VREL(I)
      VSIGN= 1.
      GO TO 120
  115 VREL(I)= VAIR - VFZ
      VSIGN= 1.
      IF (VREL(I) .GE. 0.) GO TO 120
      VREL(I)= - VREL(I)
      VSIGN= -VSIGN
  120 RN(I)= VREL(I) * TEMPE
CCCCCC
CCCCC CO(I)= 18.5 /RN(I)**.6
CCCCC CO(I)= 24. / RN(I) + 4.6674887 * RN(I) * (-.33660937 + RN(I) * (
CCCCC1 3.266239E-3 - 2.933821E-6 * RN(I) ))
      IF (RN(I) .GE. 10.) CO(I)= 24. / RN(I) + 3.09 / RN(I) **.314
```

```
      IF (RN(I) .LT. 10.) CD(I)= 24. / RN(I) + 3.54 / RN(I) **.345
      IF (RN(I) .LE. .5) CD(I)= 24. / RN(I) * (1. + .1875 * RN(I) )
      IF (CD(I) .LT. .4) CD(I)= .4
CCCCCC
      FMACH2= VREL(I)**2 / CONST1
      TEMPB= PS * ( (1. + GMI02 * FMACH2)**GOGMI - 1.)
      DRAG(I) = TEMPB * CD(I) * TEMPA * 144.
      ALPHA(I)= DRAG(I)  / QMASS * VSIGN * G
      IF (OPTION .EQ. 0.) GO TO 140
C     MODIFY FOR EFFECT OF G
C$$$  DUM1= G - ALPHA(I) * SPHI
      DUM1=   - ALPHA(I) * SPHI
      DUM2= -ALPHA(I) * CPHI
      ALPHA(I)= SQRT (DUM1**2 + DUM2**2)
      SINB= DUM1 / ALPHA(I)
      COSB= DUM2 / ALPHA(I)
  140 TIMS(I)= DX / VF(I)
      DUMMY1= VF(I)**2
      DUMMY2= 2. * DX * ALPHA(I)
C     CHECK IF ROUND/OFF ERROR I S A PROBLEM
      IF (ABS(DUMMY2 / DUMMY1)  .LT. 1.E-7) GO TO 180
      TIMS(I)= (SQRT(DUMMY1 + DUMMY2) - VF(I) ) / ALPHA(I)
  180 DELV(I)= ALPHA(I) * TIMS(I)
      IF (OPTION .EQ. 0.) GO TO 185
      VRV= VRV + DELV(I) * SINB
      VRH= VRH + DELV(I) * COSB
      DUM1= VRV + VAIRV
      DUM2= VRH + VAIRH
      VF2= SQRT(DUM1**2 + DUM2**2)
      GO TO 186
  185 VF2= VF(I) + DELV(I)
C     CHECK IF WITHIN TOLERANCE
  186 IF (ABS(1. - DELVG / DELV(I) ) .LE.  .01) GO TO 200
      DELVG= DELV(I)
      IF ( ABS(DELVG) .LT..01) GO TO 200
      KOUNTA= KOUNTA + 1
      IF (KOUNTA .LT. 25) GO TO 100
  190 WRITE (61,1000) KOUNTA, KOUNTB, KOUNTC, KOUNTD, I
      WRITE (61,1001) TF2,VF2,D2,E2
      INTER= -1
      IF (OPTION .NE. 0.) GO TO 300
      CALL EXIT
C     HAVE CONVERGED ON VF2.  NOW CALC. DELTA TF, WF
  200 TEMPC= SQRT(RN(I))
      QNUM= 2. + TEMPF * TEMPC
      DELW = QNUM * TEMPG
CCCCCC
      IF((DELW*TIMS(I)).GT.QMASS) DELW=QMASS/TIMS(I)
      QNUM= 2. + TEMPH * TEMPC
  210 Z= DELW / QNUM * TEMPI
      ZZ= Z / (EXP(Z) - 1.)
      QVZ= QNUM * ZZ * TEMPJ
      IF (KOUNTD .EQ. 0) GO TO 240
C     AT BOILING POINT.  ASSUME DELTF= 0.
      IF (VAPLAM .EQ. 0.) GO TO 190
      DELWN= QVZ / VAPLAM
CCCCCC
      IF((DELWN*TIMS(I)).GT.QMASS) DELWN=QMASS/TIMS(I)
      IF (ABS(DELWN  - DELW) .LE. .001 * ABS(DELW) ) GO TO 220
      DELW= DELWN
      KOUNTD= KOUNTD + 1
      IF (KOUNTD .LT. 25) GO TO 210
      GO TO 190
  220 IJK=1
      KOUNTD=1
C     AT BOILING POINT, CALC TF2 BASED ON PS AND E2
```

TABLE XX. (CONTD)

```
  230 TF2= PASF (PS, E2)
      DELTF(I)= TF2 - TF(I)
      GO TO 250
  240 DELTF(I)= (QVZ - DELW * VAPLAM) * TIMS(I) / TEMPK
      TF2= TF(I) + DELTF(I)
CCCCCC
      IF(KFUEL.EQ.4.AND.TF2.GT.1092.8) TF2=1092.8
CCCCCC
      IF(KFUEL.EQ.2.AND.TF2.GT.1210.4) TF2=1210.4
C     CHECK IF WITHIN TOLERANCE
  250 IF (ABS( DELTF(I) - DELTFG) .LE. .01*ABS(DELTF(I)) ) GO TO 260
      DELTFG= DELTF(I)
      IF ( ABS(DELTFG) .LT. 1.) GO TO 260
      KOUNTB= KOUNTB + 1
      IF (KOUNTB .LT. 25) GO TO 70
      GO TO 190
C     HAVE CONVERGED ON TF2.  NOW CALC. DELTA D
  260 IJK=0
  270 W2= W(I) - DELW * TIMS(I)
      IF (W2 .LT. 1.E-30) W2= 1.E-30
      SGRESD= SGFCT (E2)
      SG(I)= SGFCT(TF2,SGRESD)
      SG60(I)= SGFCT (519.69,SGRESD)
      D2= (6. * W2 / PI / SG(I) / 62.428)**.3333333333
      IF (D2 .LT. 1.E-10) D2= 1.E-10
      E2= 1. - (D2 / DSTART(I))**3 * SG(I) / SG60(I)/ SGSG60(I)
      IF (E2 .GT. .99) E2= .99
      IF (E2 .LT. 0.) E2= 0.
      DELD= D2 - D(I)
C     CHECK IF WITHIN TOLERANCE
      IF (ABS(1. - DELD3 / DELD) .LE. .01)GO TO 300
      DELDG= DELD
      IF (ABS(DELDG) .LT. 1.E-7) GO TO 300
      KOUNTC= KOUNTC + 1
      IF (KOUNTC .LT. 20) GO TO 50
      GO TO 190
C     HAVE CONVERGED ON ALL PARAMETERS FOR THIS INTERVAL
C     SAVE OLD CONDITIONS, SET NEW ONES
  300 VFSAVE(I)= VF(I)
      VF(I)= VF2
      TFSAVE(I)= TF(I)
      TF(I)= TF2
      DSAVE(I)= D(I)
      D(I)= D2
      ESAVE(I)= E(I)
      E(I)= E2
      DELQ(I)= QVZ * TIMS(I)
      DELM(I)= DELW * TIMS(I)
 1000 FORMAT(18H0**** T AP FAILURE     ,4I5,5X,7HDROPLET  I5)
 1001 FORMAT (4E15.5)
      RETURN
      END
      FUNCTION PASF (T,E)
C     T= TEMPER. (R), E= FRACTION EVAPORATED
C     PASF= FUEL VAPOR PRESSURE (PSIA) FOR JP4, JP5/JP8
      COMMON / INPUT / KFUEL,DEQ,GAP,PPM,TABLE(8)
      DIMENSION CK1(7,4), CK2(7,4), ETAB(7)
      DATA ETAB / 0.,.1, .3, .5, .7, .9 ,1.0 /
     1, CK1 / 0., 0., 0., 0., 0., 0., 0.,
     2 155810.,386390.,585230.,817550.,1321200.,3175400.,10497000.,
     3 0., 0., 0., 0., 0., 0., 0.,
     4       40497.,136750.,286430.,604200.,1399600.,7044100.,77680000./
     5, CK2 / 0., 0., 0., 0., 0., 0., 0.,
     6 7414.8,8548.4,9066.7,9484.0,10083.,11178.,12670.,
     7 0., 0., 0., 0., 0., 0., 0.,
     8        4816.,6269.,7151.,8042.,9045.,10974.,13839. /
```

TABLE XX. (CONTD)

```
C
      IF (KFUEL .NE. 2 .AND. KFUEL .NE. 4) GO TO 150
C     IF (T .LT. 0 , ARGUMENT IS (-PS).  FIND AND RETURN CORRES. TEMPERATURE
      PSTAT=-T
      DO 50 J=1,7
      I=J
      IF (E - ETAB(J)) 60,90,50
   50 CONTINUE
      GO TO 70
   60 IF (I .EQ. 1) I=2
   70 K=1
   80 IF (PSTAT .LT. 0.) GO TO 83
      PASF= CK2(I,KFUEL) /  ALOG(CK1(I,KFUEL) / PSTAT )
      GO TO 84
   83 PASF=CK1(I,KFUEL) * EXP( -CK2(I,KFUEL) / T )
   84 IF (K) 110,100,85
   85 PSAVE= PASF
      J=I
      I= I - 1
      K= -1
      GO TO 80
   90 K=0
      GO TO 80
  100 RETURN
  110 PASF= PASF + (PSAVE - PASF) / (ETAB(J) - ETAB(I)) * (E - ETAB(I))
      GO TO 100
  150 WRITE (61,1000) KFUEL
 1000 FORMAT (25H0PASF CANNOT HANDLE FUEL=     I5)
      CALL EXIT
      END
      FUNCTION VAPCPF (T)
C     T= TEMPER. (R), VAPCPF= CP FOR JP4, JP5/JP8 FUEL VAPOR
      COMMON / INPUT / KFUEL,DEQ,GAP,PPH,TITLE(8)
      IF (KFUEL .EQ. 2) GO TO 50
      VAPCPF= .180 + .000565 * T
      GO TO 100
   50 VAPCPF= .069 + .000530 * T
  100 RETURN
      END
      FUNCTION VAPMUF (T)
C     T= TEMPER. (R), VAPMUF= MU FOR JP4, JP5/JP8 FUEL VAPOR
      COMMON / INPUT / KFUEL,DEQ,GAP,PPH,TITLE(8)
      IF (KFUEL .EQ. 2) GO TO 50
      VAPMUF=  808.E-9 + 7.64E-9 * T
      GO TO 100
   50 VAPMUF= 248.E-9 + 6.31E-9 * T
  100 RETURN
      END
      FUNCTION VAPKF(T,W)
C     T= TEMPER. (R), VAPKF= K FOR FUEL VAPOR
C     W= MOLECULAR WEIGHT
      DIMENSION WTAB(4),ATAB(4),BTAB(4),TABK(4)
      DATA WTAB/50., 100., 150., 300. /, NTAB /4/,
     1 ATAB / -.006362,-.006358,-.006284,-.006010 /,
     2 BTAB / .0000297,.0000273,.0000259,.0000235 /
C
      DO 10 I=1,NTAB
   10 TABK(I)= ATAB(I) + BTAB(I) * T
      VAPKF= TAB (W,WTAB,TABK,NTAB)
      RETURN
      END
      FUNCTION SGFCT (T,SG60R)
C     SG60R =  SG RESIDUE AT 60 DEG F
C     T= TEMPER. (R), SGFCT= SG FOR JP4 AND JP5 LIQUID FUEL
      SGFCT= SG60R + .208 - .0004* T
      RETURN
```

TABLE XX. (CONTD)

```
      END
      FUNCTION SGRFCT (E)
C     E= FRACTION EVAPORATED, SG60= SG AT 60 DEG F
C     SGRFCT= SG RESIDUE AT 60 DEG F FOR JP4, JP5/JP8 LIQUID FUEL
      COMMON / INPUT / KFUEL,DEQ,GAP,PPH,TITLE(8)
      DATA SG604/ .775 / , SG6058 / .806 /
      SG60= SG604
      IF (KFUEL .NE. 4) SG60= SG6058
      SGRFCT= 1.076 / ( (1.076 / SG60 - 1.) * (1. - .67 * E) + 1. )
      RETURN
      END
      FUNCTION VAPDF (T,P)
C     T= TEMPER. (R) , P= STATIC PRESSURE
C     VAPDF= DIFFUSIVITY FOR HEPTANE-OXYGEN
      VAPDF= 2.083 / P  * (T * (T * 1.1319E-9 + 1.973E-6) - 9.815E-4)
      RETURN
      END
      FUNCTION VAPMF (E)
C     E= FRACTION EVAPORATED, VAPMF= MOLECULAR WEIGHT OF JP4, JP5/JP8
C                   FUEL VAPOR
      COMMON / INPUT / KFUEL,DEQ,GAP,PPH,TITLE(8)
      DIMENSION ETAB(7), TABMV(7,4)
      DATA ETAB / 0., . , .3, .5, .7, .9, 1.0 /, NTAB /7/,
     1 TABMV / 0., 0., 0., 0., 0., 0., 0.,
     2 148.12,163.29,169.88,175.04,182.25,194.86,211.07,
     3         0., 0., 0., 0., 0., 0., 0.,
     4         93.25, 114.60, 126.61, 138.16, 150.59, 173.21, 204.76 /
C
      VAPMF= TAB(E, ETAB, TABMV(1,KFUEL), NTAB)
      RETURN
      END
      FUNCTION VAPLMF(T)
C     T= TEMPER (R), VAPLMF= LATENT HEAT OF VAPORISATION FOR JP4,BTU/LB
C                ALSO, JP5/JP8
      COMMON / INPUT / KFUEL,DEQ,GAP,PPH,TITLE(8)
      IF (KFUEL .EQ. 2) GO TO 50
      VAPLMF= 0.
      IF (T .LT. 1092.88) VAPLMF= 13.20 * (1092.88 - T) **.39
      GO TO 100
   50 VAPLMF= 0.
      IF (T .LT. 1210.45) VAPLMF= 10.75 * (1210.45 - T) **.41
  100 RETURN
      END
      FUNCTION CPFCT (T,SGR60)
C     T= TEMPER (R), CPFCT, CP FOR LIQUID JP4, JP5/JP8
C     SGR60= SG RESIDUE AT 60 DEG F FOR JP4
      CPFCT= ( .181 + .00045 * T) / SQRT(SGR60)
      RETURN
      END
```

TABLE XXI. PROGRAM NO. 1527 OUTPUT

```
UPDATED AIR ASSIST NOZZLE TEST CASE 4-1

SIMPLEX ATOMIZER, FLOW NUMBER =    2.24000 CONE ANGLE=    85.00000 ORIF DIA=  .025
WITH AIR ASSIST,  SHROUD AREA =     .00025 SQ IN
 KFUEL ICRT TFUEL PPH DELP DELPSH TSH =     4     1 530.00000  10.00000  -0.00000  10.00000 530.00000
UNIFORM FLOW OPTION, T AMB, VAIR, P AMB = .1290.00000 100.00000  14.70000

ASSIST AIR FLOW=    .500 LB/HR VELOCITY=  936.7 FPS

SG=   .7684E+00 (OMLS)    VISC FUEL=   .1132E+01 CENTISTOKES

FUEL SHEET THICK., PRIM =     58.9, SEC =      0.0 MICRONS


DELTA P (1)=     19.70     PPH (1)=     10.00
DELTA P (2)=      0.00     PPH (2)=      0.00
DELTA P (V)=      0.00       VFUEL=     61.69
SMD=     121.35 MICRONS

AIR/FUEL MASS RATIO=         .050 EFF. AIR VELOCITY=     201.4 FPS

DROPLET  1 E= .10      X1, X2=   .32514   .26455 IN

DROPLET  1 E= .20      X1, X2=   .73138   .52521 IN

**** DROPLET  1 HAS HIT TOP    BOUNDARY

DROPLET  2 E= .10      X1, X2=   .63091   .51167 IN

**** DROPLET  2 HAS HIT TOP    BOUNDARY

**** DROPLET  3 HAS HIT TOP    BOUNDARY

**** DROPLET  4 HAS HIT TOP    BOUNDARY

**** DROPLET  5 HAS HIT TOP    BOUNDARY

LAST DROPLET CONDITIONS--
     DROP     TF              VF              D              E
       1     .64038E+03      .72261E+02     .22622E-03     .28213E+00
       2     .59126E+03      .66615E+02     .35825E-03     .12771E+00
       3     .57091E 03      .64809E+02     .45774E-03     .94078E-01
       4     .55855E+03      .63792E+02     .56581E-03     .72033E-01
       5     .54810E+03      .62972E+02     .74624E-03     .48721E-01

0 - 20 / VOLUME        20 - 40 / VOLUME        40 - 60 / VOLUME        60 - 80 / VOLUME        80 - 100 / VOLUME

      75.098                  113.094                 143.187                 175.951                 230.856 MICRONS

      X       Y               X       Y               X       Y               X       Y               X       Y
D     TF   VF E*100 /     D     TF   VF E*100 /     D     TF   VF E*100 /     D     TF   VF E*100 /     D     TF   VF E*100 /

 0.00      0.00           0.00      0.00           0.00      0.00           0.00      0.00           0.00      0.00
76.  530.  62.  0. /     113.  530.  62.  0. /     143.  530.  62.  0. /     176.  530.  62.  0. /     231.  530.  62.  0. /
  .04       .03            .04       .03            .04       .03            .04       .03            .04       .03
75.  535.  62.  1. /     113.  533.  62.  1. /     143.  532.  62.  1. /     176.  531.  62.  0. /     230.  531.  62.  0. /
  .07       .07            .07       .07            .07       .07            .07       .07            .07       .07
75.  541.  62.  3. /     113.  535.  62.  2. /     143.  534.  62.  1. /     176.  533.  62.  1. /     230.  532.  62.  0. /
  .11       .10            .11       .10            .11       .10            .11       .10            .11       .10
```

INPUT DATA

FUEL VELOCITY, FPS

SPRAY TRAJECTORY

TABLE XXI. (CONTD)

75. 546. 63. 4. / .15 .13	112. 538. 62. 2. / .15 .13	143. 536. 62. 2. / .15 .13	175. 534. 62. 1. / .15 .13	230. 533. 62. 1. / .15 .13
74. 551. 63. 6. / .19 .16	112. 541. 62. 3. / .19 .17	142. 537. 62. 2. / .19 .17	175. 535. 62. 1. / .19 .17	230. 533. 62. 1. / .19 .17
74. 556. 64. 7. / .23 .19	112. 544. 63. 4. / .23 .20	142. 539. 62. 3. / .22 .20	175. 537. 62. 2. / .22 .20	230. 534. 62. 1. / .22 .20
74. 562. 64. 8. / .27 .22	112. 546. 63. 4. / .26 .23	142. 541. 62. 3. / .26 .23	175. 538. 62. 2. / .26 .23	230. 535. 62. 1. / .26 .23
74. 567. 64. 9. / .31 .25	111. 549. 63. 5. / .30 .26	142. 543. 63. 4. / .30 .26	175. 539. 62. 3. / .30 .27	229. 536. 62. 2. / .30 .27
74. 573. 65. 10. / .35 .28	111. 552. 63. 6. / .34 .29	142. 545. 63. 4. / .34 .30	175. 541. 62. 3. / .34 .30	229. 537. 62. 2. / .34 .30
73. 578. 65. 10. / .39 .31	111. 555. 63. 6. / .38 .32	141. 547. 63. 5. / .38 .33	174. 542. 63. 3. / .37 .33	229. 538. 62. 2. / .37 .33
73. 584. 66. 11. / .43 .34	111. 557. 64. 7. / .42 .35	141. 549. 63. 5. / .42 .36	174. 543. 63. 4. / .41 .36	229. 539. 62. 2. / .41 .37
73. 589. 66. 12. / .47 .37	111. 560. 64. 8. / .46 .38	141. 550. 63. 5. / .45 .39	174. 545. 63. 4. / .45 .40	229. 539. 62. 3. / .45 .40
73. 594. 67. 13. / .52 .39	111. 563. 64. 8. / .50 .42	141. 552. 63. 6. / .49 .42	174. 546. 63. 4. / .49 .43	229. 540. 62. 3. / .49 .43
73. 598. 67. 14. / .56 .42	110. 566. 64. 9. / .54 .45	141. 554. 63. 6. / .53 .45	174. 547. 63. 5. / .53 .46	229. 541. 62. 3. / .52 .46
72. 603. 69. 15. / .60 .45	110. 569. 65. 9. / .58 .47	141. 556. 64. 7. / .57 .48	174. 549. 63. 5. / .57 .49	228. 542. 63. 3. / .56 .50
72. 607. 68. 16. / .64 .47	110. 571. 65. 9. / .62 .50	140. 558. 64. 7. / .61 .52	173. 550. 63. 5. / .61 .52	228. 543. 63. 4. / .60 .53
72. 611. 69. 18. / .69 .50	110. 574. 65. 10. / .66 .53	140. 560. 64. 7. / .65 .55	173. 551. 63. 6. / .64 .55	228. 544. 63. 4. / .64 .56
72. 615. 69. 19. / .73 .52	110. 577. 65. 10. / .70 .56	140. 562. 64. 8. / .69 .58	173. 553. 63. 6. / .68 .59	228. 545. 63. 4. / .68 .59
71. 618. 69. 20. / .77 .55	110. 580. 66. 11. / .74 .59	140. 564. 64. 8. / .73 .61	173. 554. 63. 6. / .72 .62	228. 546. 63. 4. / .72 .63
71. 622. 70. 21. / .82 .57	110. 583. 66. 11. / .78 .62	140. 566. 64. 9. / .77 .64	173. 555. 64. 7. / .76 .65	228. 546. 63. 4. / .75 .66
71. 625. 70. 22. / .86 .60	110. 585. 66. 12. / .83 .65	140. 567. 65. 9. / .81 .67	173. 557. 64. 7. / .80 .68	228. 547. 63. 5. / .79 .69
70. 629. 71. 24. / .90 .62	109. 588. 66. 12. / .87 .67	140. 569. 65. 9. / .84 .69	173. 558. 64. 7. / .82 .69	227. 548. 63. 5. / 0.00 0.00
70. 632. 71. 25. / .95 .64	109. 590. 67. 13. / .88 .69	140. 571. 65. 9. / 0.00 0.00	172. 559. 64. 7. / 0.00 0.00	0. 0. 0. 0. / 0.00 0.00
70. 635. 72. 26. / .99 .67	109. 591. 67. 13. / 0.00 0.00	0. 0. 0. 0. / 0.00 0.00	0. 0. 0. 0. / 0.00 0.00	0. 0. 0. 0. / 0.00 0.00
69. 638. 72. 27. / 1.03 .69	0. 0. 0. 0. / 0.00 0.00	0. 0. 0. 0. / 0.00 0.00	0. 0. 0. 0. / 0.00 0.00	0. 0. 0. 0. / 0.00 0.00
69. 640. 72. 28. /	0. 0. 0. 0. /	0. 0. 0. 0. /	0. 0. 0. 0. /	0. 0. 0. 0. /

TABLE XXI. (CONTD)

```
UPDATED AIR ASSIST NOZZLE TEST CASE 4-2

DUAL ORIFICE ATOMIZER. PRIM FLOW NO =    2.24000 SEC FLOW NO =    8.96000 CONE ANGLE =   85.00000
PRIM ORIF DIA=  .025 SEC ORIF DIA=  .050
WITH AIR ASSIST.  SHROUD AREA =     .00025 SQ IN
SEC FLOW SCHED =    0.00000  10.00000  20.00000  30.00000  40.00000
SEC PRES SCHED =  100.00000 125.00000 150.00000 200.00000 250.00000
 KFUEL ICPT TFUEL PPH DELP DELPSH ISH =     4    1 530.00000  35.00000  -0.00000  10.00000 530.00000
UNIFORM FLOW OPTION. T AMB. WAIR, P AMB = .1290.00000 100.00000  14.70000

ASSIST AIR FLOW=    .500 LB/HR VELOCITY=  936.7 FPS

SG=   .7684E+00 (OMLS)    VISC FUEL=   .1132E+01 CENTISTOKES

FUEL SHEET THICK.. PRIM =     58.9. SEC =    117.9 MICRONS


DELTA P (1)=    125.56     PPH (1)=     25.24
DELTA P (2)=      1.17     PPH (2)=      9.76
DELTA P (V)=    124.39       VFUEL=    132.50
SMD=    256.39

AIR/FUEL MASS RATIO=        .014 EFF. AIR VELOCITY=     165.1

**** DROPLET  1 HAS HIT TOP    BOUNDARY

**** DROPLET  2 HAS HIT TOP    BOUNDARY

**** DROPLET  3 HAS HIT TOP    BOUNDARY

**** DROPLET  4 HAS HIT TOP    BOUNDARY

**** DROPLET  5 HAS HIT TOP    BOUNDARY

LAST DROPLET CONDITIONS--
     DROP      TF              VF              D               E
        1    .54696E+03      .12744E+03      .51740E-03      .45923E-01
        2    .53084E+03      .12980E+03      .77862E-03      .24758E-01
        3    .53602E+03      .13065E+03      .98795E-03      .16980E-01
        4    .53435E+03      .13117E+03      .12156E-02      .12310E-01
        5    .53285E+03      .13151E+03      .15947E-02      .80779E-02


     0 -  20 / VOLUME          20 -  40 / VOLUME          40 -  60 / VOLUME          60 -  80 / VOLUME          80 - 100 / VOLUME

          159.730                    238.953                    302.530                    371.762                    487.137 MICRONS

        X                          X                          X                          X                          X
     D     TF    VF     Y E+100 /     D     TF    VF     Y E+100 /     D     TF    VF     Y E+100 /     D     TF    VF     Y E+100 /     D     TF    VF     Y E+100 /
   0.00        0.00                     0.00        0.00                     0.00        0.00                     0.00        0.00                     0.00        0.00
 160.  530.  132.    0. /           239.  530.  132.    0. /           303.  530.  132.    0. /           372.  530.  132.    0. /           487.  530.  132.    0. /
   .04         .03                      .04         .03                      .04         .03                      .04         .03                      .04         .03
 160.  531.  132.    0. /           239.  530.  132.    0. /           302.  530.  132.    0. /           372.  530.  132.    0. /           487.  530.  132.    0. /
   .07         .07                      .07         .07                      .07         .07                      .07         .07                      .07         .07
 160.  532.  132.    0. /           239.  531.  132.    0. /           302.  531.  132.    0. /           372.  530.  132.    0. /           487.  530.  132.    0. /
   .11         .10                      .11         .10                      .11         .10                      .11         .10                      .11         .10
 159.  532.  132.    1. /           239.  531.  132.    0. /           302.  531.  132.    0. /           372.  531.  132.    0. /           487.  530.  132.    0. /
   .15         .13                      .15         .13                      .15         .14                      .15         .14                      .15         .14
 159.  533.  132.    1. /           239.  532.  132.    0. /           302.  531.  132.    0. /           372.  531.  132.    0. /           487.  531.  132.    0. /
```

TABLE XXI. (CONTD)

.18 .17 159. 534. 131. 1. /	.18 .17 239. 532. 132. 1. /	.18 .17 302. 531. 132. 0. /	.18 .17 371. 531. 132. 0. /	.18 .17 487. 531. 132. 0. /
.22 .20 159. 535. 131. 1. /	.22 .20 239. 533. 132. 1. /	.22 .20 302. 532. 132. 0. /	.22 .20 371. 531. 132. 0. /	.22 .20 487. 531. 132. 0. /
.26 .24 159. 536. 131. 2. /	.26 .24 238. 533. 132. 1. /	.24 .24 302. 532. 132. 1. /	.26 .24 371. 531. 132. 0. /	.26 .24 487. 531. 132. 0. /
.30 .27 159. 537. 131. 2. /	.30 .27 238. 533. 131. 1. /	.30 .27 302. 532. 132. 1. /	.30 .27 371. 532. 132. 0. /	.30 .27 487. 531. 132. 0. /
.33 .30 159. 537. 130. 2. /	.33 .30 238. 534. 131. 1. /	.33 .30 302. 533. 132. 1. /	.33 .30 371. 532. 132. 1. /	.33 .30 487. 531. 132. 0. /
.37 .34 159. 538. 130. 2. /	.37 .34 238. 534. 131. 1. /	.37 .34 302. 533. 132. 1. /	.37 .34 371. 532. 132. 1. /	.37 .34 487. 531. 132. 0. /
.41 .37 159. 539. 130. 3. /	.41 .37 238. 535. 131. 1. /	.41 .37 302. 533. 132. 1. /	.41 .37 371. 532. 132. 1. /	.41 .37 487. 532. 132. 0. /
.45 .40 159. 540. 130. 3. /	.44 .40 238. 535. 131. 1. /	.44 .40 302. 534. 131. 1. /	.44 .40 371. 533. 132. 1. /	.44 .40 487. 532. 132. 0. /
.48 .44 158. 541. 129. 3. /	.48 .44 238. 536. 131. 2. /	.48 .44 302. 534. 131. 1. /	.48 .44 371. 533. 132. 1. /	.48 .44 486. 532. 132. 1. /
.52 .47 158. 541. 129. 3. /	.52 .47 239. 536. 131. 2. /	.52 .47 302. 534. 131. 1. /	.52 .47 371. 533. 132. 1. /	.52 .47 486. 532. 132. 1. /
.56 .50 158. 542. 129. 3. /	.56 .50 238. 536. 131. 2. /	.55 .51 301. 534. 131. 1. /	.55 .51 371. 533. 132. 1. /	.55 .51 486. 532. 132. 1. /
.59 .54 158. 543. 129. 4. /	.59 .54 238. 537. 130. 2. /	.59 .54 301. 535. 131. 1. /	.59 .54 371. 533. 131. 1. /	.59 .54 486. 532. 132. 1. /
.63 .57 158. 544. 128. 4. /	.63 .57 238. 537. 130. 2. /	.63 .57 301. 535. 131. 1. /	.63 .57 371. 534. 131. 1. /	.63 .57 486. 532. 132. 1. /
.67 .60 158. 545. 128. 4. /	.67 .60 238. 538. 130. 2. /	.67 .61 301. 535. 131. 1. /	.67 .61 371. 534. 131. 1. /	.66 .61 486. 533. 132. 1. /
.71 .63 158. 546. 128. 4. /	.70 .64 237. 538. 130. 2. /	.70 .64 301. 536. 131. 2. /	.70 .64 371. 534. 131. 1. /	.70 .64 486. 533. 132. 1. /
.74 .67 158. 546. 128. 4. /	.74 .67 237. 539. 130. 2. /	.74 .67 301. 536. 131. 2. /	.74 .67 371. 534. 131. 1. /	.74 .67 486. 533. 132. 1. /
.77 .69 158. 547. 127. 5. /	.76 .69 237. 539. 130. 2. /	.75 .69 301. 536. 131. 2. /	.75 .69 371. 534. 131. 1. /	.75 .69 486. 533. 132. 1. /

APPENDIX II

PNEUMATIC-IMPACT FUEL INJECTOR COMPUTER PROGRAM 1528

1.0 INTRODUCTION

Computer Program 1528 analyzes pneumatic-impact type fuel injectors to determine airflow conditions and fuel spray drop size. Spray trajectories and evaporation are computed for three optional ambient environments. This appendix describes the program imput preparation and usage. The program can also be used for an L-pipe spraying into a swirler cup.

2.0 PROGRAM INPUT

Program input is shown in Figure 170. The first card is a title card; the desired ambient environment indicator, a 1, 2, or 3, is entered in Column 1. The three ambient conditions, depicted on the data sheet, are:

Option 1: A uniform temperature and velocity stream flowing past the nozzle in a direction parallel to the nozzle axis. This option is used for basic spray trajectory and evaporation studies.

Option 2: Spray test stand option with gravity effect. Airflow is from the nozzle only with a quiescent environment. Gravity acts in a direction along the nozzle axis.

Option 3: A two-dimensional flow field for temperature and velocity as generated by the two-dimensional Gosman Program 1338. The flow field is obtained from a disk file or magnetic tape written by the Gosman program. This input source must be identified as TAPE1.

The second data input card contains the following information:

(a) $V_{air\ guess}$, Initial guess of air velocity at D_1, may be left blank. This is used to shorten iteration time if approximate velocity is known.

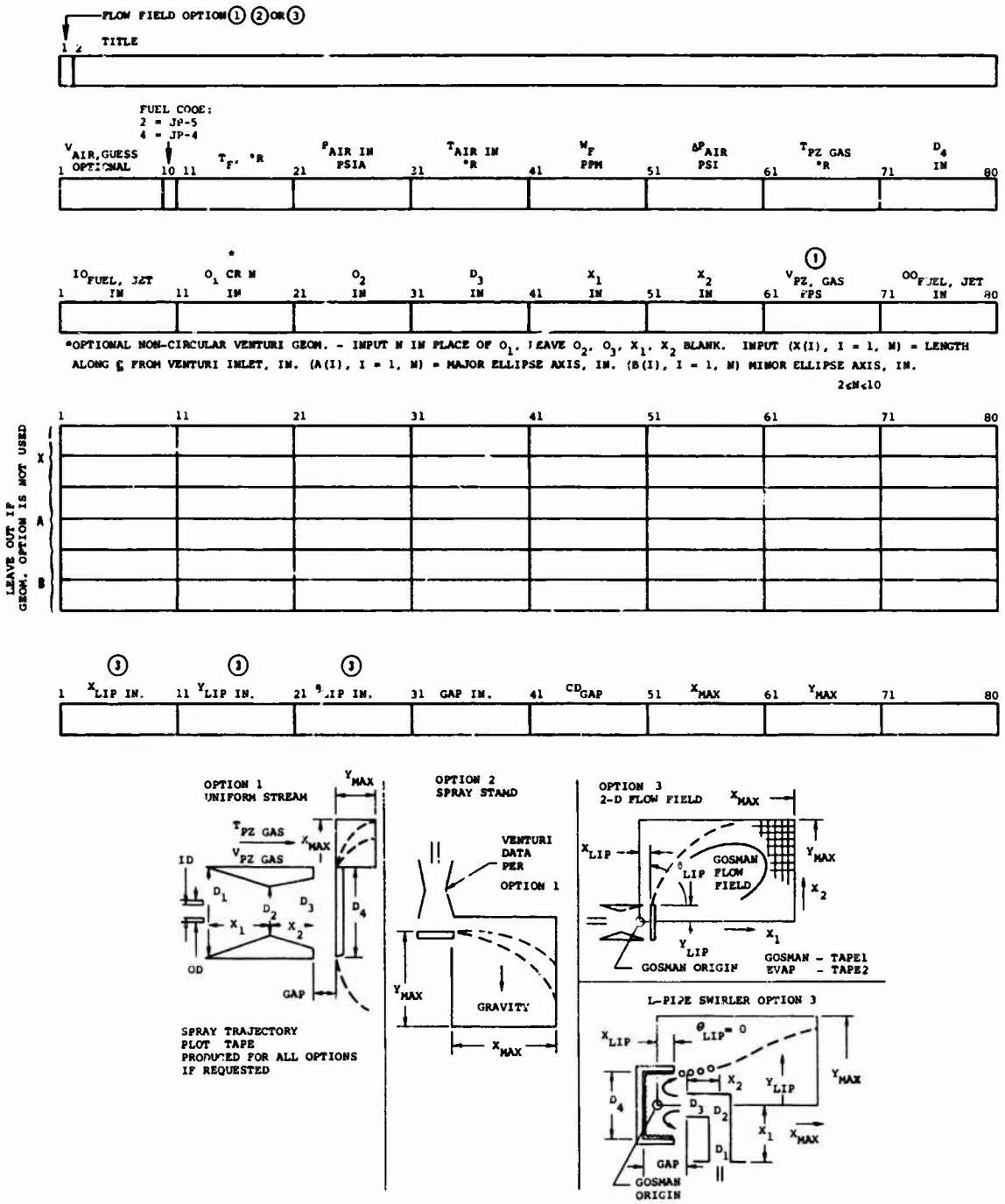


Figure 170. Pneumatic-Impact Injector Program No. 1528 Input Data.

(b) Fuel code: enter 2 for JP-5 or 4 for JP-4

(c) T_F, fuel temperature, °R

(d) $P_{air\ in}$, total air pressure at venturi inlet, psia

(e) $T_{air\ in}$, air temperature at venturi inlet, °R

(f) W_F, fuel flow, lb/hr/injector

(g) ΔP_{air}, injector differential air pressure, psi

(h) $T_{PZ\ gas}$: Option 1 only, enter temperature, °R, of uniform stream. Options 2 and 3, blank.

(i) D_4, diameter of impact plate, in.

The third data card requires the following information:

(a) $ID_{fuel\ jet}$, inside diamter of fuel tube, in.

(b) D_1 or N, venturi inlet diameter if venturi is circular. If noncircular, enter number of sets of X, A, and B in ellipse table.

(c) D_2, venturi minimum diameter, in. (May be less, equal, or greater than D_1.) Leave blank if noncircular.

(e) X_1, length from venturi inlet to D_2, in.

(f) X_2, length from D_2 to venturi exit, in.

(g) $V_{PZ\ gas}$: Option 1 only, enter velocity, fps, of uniform stream. Options 2 and 3, blank.

(h) $OD_{fuel\ jet}$, outside diameter of fuel jet, in. D_1 and OD determine venturi inlet area.

If the noncircular option is desired, leave D_2, D_3, X_1 and X_2 blank.

Specify ellipse major diameters, A, and minor diameters, B, as functions of the distance, X, along the axis from the venturi inlet at up to 10 points. Enter the number of points in place of D_1 on the second data card. Cards with X, A, and B are entered after the third card.

The last card contains the following information:

(a) X_{lip}, Option 3 only, locates axial position of the lip relative to the origin of the Gosman 2-D flow field. Options 1 and 2, blank.

(b) Y_{lip}, Option 3 only, locates radial position of the lip relative to the origin of the Gosman 2-D flow field. Options 1 and 2, blank.

(c) θ_{lip}, angle of initial spray direction relative to horizontal, deg.

(d) GAP, gap between venturi exit and impact plate, in.

(e) $C_{D\ gap}$, gap discharge coefficient (recommend 0.6).

(f) X_{max}, limits spray trajectory distance. See data sheet. For Option 3, X_{max} should be set at the Gosman grid boundary.

(g) Y_{max}, limits spray trajectory distance. See data sheet. For Option 3, Y_{max} should be set at the Gosman grid boundary.

3.0 PROGRAM COMPUTATIONS

A listing of the computer program is presented in Table XXII. Airflow through the venturi and exit gap is computed, including area change, drop evaporation and drag, and friction loss. Inlet velocity is iterated until the pressure drop matches that input. If the exit-gap effective area is less than the venturi exit, air velocity at the gap is increased by the area ratio. If the gap effective area is greater than the venturi exit area, the velocity at the gap remains the same as that at the venturi exit. Drop size is computed at the gap from a computed fuel-sheet thickness and effective air velocity corrected for radial-flow-velocity decay.

Spray trajectories are computed for the three options by a drag coefficient and the relative velocity between the drops and the air. The spray is divided into five drop-size groups, sized in ratios to the SMD.

TABLE XXII. LISTING OF PROGRAM NO. 1528

```
$$$
```

TABLE XXII. (CONTD)

```
      DATA T5 / 50.,100.,150.,200.,250.,300.,350.,400.,450.,500.
      DATA SGTAB5 / .72,.76,.80,.84 /
      DATA NTAB5T,NTAB5S,NTABRF        / 10,4,7/
      DATA SRFTNS / 21.,18.2,15.5,13.,10.6,8.2,5.9,3.9,2.0,.2,
     1 23.1,20.5,18.0,15.6,13.4,11.1,9.0,7.0,5.1,3.3,
     2 23.9,21.8,19.6,17.5,15.4,13.4,11.4,9.5,7.7,6.,
     3 24.9,22.9,21.0,19.1,17.3,15.5,13.8,12.1,10.4,8.8  /
      DATA RNTAB / 3.E3,1.E4,3.E4,1.E5,3.E5,1.E6,1.E7  /,
     1 FTAB /.011,.008,.00625,.005,.00445,.0041,.0040  /
      DATA T9R /500.,600.,700.,800.,900.,1000.,1100.,1200.,1400.,1600./,
     1 CPTAB /.2405,.2410,.2422,.2440,.2462,.2490,.2519,.2550,.2613,
     2 .2670/
      DATA NTAB9 / 10 /
      CALL PLOTS (0,0,0)
    1 READ (60,1000) TITLE
      IF (EOF(60)) 999,2
  999 CALL PLOT (0.,0.,999)
      CALL EXIT
C     MASK OFF FIRST CHARACTER IN TITLE
    2 IWORD=ANO (TITLE(1),MASK1)
C     FILL REST OF WORD WITH BLANKS
      IWORD= IWORD + IZRBKS
      DO 10 I=1,NLABEL
      KOVRLY= 1
      IF (LABELS(I) .EQ. IWORD) GO TO 50
   10 CONTINUE
      WRITE (61,3000)
      CALL EXIT
   50 CALL OVERLAY (KFILE,KOVRLY,0)
      GO TO 1
 1000 FORMAT (8A10)
 3000 FORMAT (43H0FIRST CHARACTER IN TITLE DETERMINES OPTION      )
      END
      FUNCTION DIAMTR (X)
      COMMON XL1,XL2,DIA1,DIA2,SLOPE1,SLOPE2
      COMMON NXXXX,AXISMJ(10),AXISMN(10),XXXX(10)
      IF (NXXXX .NE. 0) GO TO 100
      IF (X .GT. XL1) GO TO 20
      DIAMTR= DIA1 + SLOPE1 * X
   10 RETURN
   20 DIAMTR= DIA2 + SLOPE2 *(X- XL1)
      GO TO 10
  100 DIAMTR= TAB(X,XXXX,AXISMJ,NXXXX)
      GO TO 10
      END
      FUNCTION SMDF (TAU,ETAR,RHOG,QMR,SL,VT,VR)
      SMDF= 6. *1.4E4 *SQRT(TAU/RHOG)*ETAR**.21 *(1.+ .065/QMR/SQRT(QMR)
     1  )*
     1SQRT( SL/ (VT**2 *( VR *(.5 *VR -1.) +1.) )  )
      RETURN
      END
      FUNCTION TAB (X,XX,YY,NTAB)
      DIMENSION XX(1), YY(1)
      F=1.
      IF (XX(1).GT.XX(2)) F=-F
      DO 10 J=1,NTAB
      I=J
      IF (F*(XX(I)-X)) 10,40,20
   10 CONTINUE
   20 IF (1.NE.1) GO TO 30
      I=2
   30 J=I-1
      DEL=XX(I)-XX(J)
      IF (DEL.EQ.0.) GO TO 50
      TAB=(YY(I)*(X-XX(J))-YY(J)*(X-XX(I)))/DEL
      RETURN
```

TABLE XXII. (CONTD)

```
   40 TAB=YY(I)
      RETURN
   50 WRITE(61,60) X,I,J
      CALL EXIT
   60 FORMAT (24H0***ERROR IN ROUTINE TAB,E15.4,2I5)
      END
*DECK E
      SUBROUTINE EVAP (INTER,I)
C     DROPLET EVAPORATION.
C     PROGRAMMED 1-22-71 BY M. TANI.
C
C     D,TF,VF,E       ARE INPUT FOR DROP NO. I
C**** NOTE-- FUEL PROPERTY EQUATIONS ARE ONLY FOR JP4 AND JP5/JP8 ***
C
      COMMON / INPUT / KFUEL,DEQ,GAP,PPH,TITLE(8)
      COMMON / QEVAP/ DUMMY(20),D(5),TF(5),VF(5),VREL(5),      RN(5),
     1 CD(5),DRAG(5),FN(5),      CP(5),QELQ(5),SG(5),FRMO(5),QELTF(5),
     2 TIMS(5),FMASS(5),ALPHA(5),DELV(5),E(5),QX,W(5),VFSAVE(5),TFSAVE(5
     3 ),DSAVE(5),ESAVE(5),DSTART(5),SGSG60(5),SG60(5),QELM(5)
     4,QPTION,VAIRH,VAIRV,SINT,COST,DUM1,DUM2
CCCCCC
     * ,WST(5),EW(5)
      COMMON / TRAJ / VFUEL,TFUEL,TFUELF,SGF,FMU,RHOF,PS,PT,TS,TT,
     1DUMMZQ(3),VAIR
      COMMON / OVRLY / KOVRLY
      DIMENSION TAIRTB(7),AIRKTB(7),AIRMUT(7),AIRCPT(7)
      DATA TAIRTB / 400.,600.,1000.,1500.,2000.,2500.,3000. /
     1, AIRKTB / .0114,.0165,.0252,.0344,.0422,.0486,.0547 /
     2,AIRMUT /1.E-5,1.3E-5,1.885E-5,2.5E-5,3.015E-5,3.48E-5,3.9E-5 /
     3, AIRCPT /.2404,.2409,.249,.2642,.2772,.2868,.2931 /,NTABAR/7/
      DATA G,GAMMA,R,PI04,GOGMI,GMI02,PI /32.174,1.4,1545.327,.7853682,
     1 3.5,.2, 3.1415927 /
C
      AIRM= 28.966
      CONST1= G * GAMMA * R * TS / AIRM
C     CHECK FOR FIRST ENTRY TO ROUTINE (INTER=I)
      IF (INTER .NE. I) GO TO 50
C     ESTIMATE NEXT STATION CONDITIONS
      VF2= VF(I)
      TF2= TF(I)
      D2=  D(I)
      E2=  E(I)
      DSTART(I)= D(I)
      GO TO 55
C     ESTIMATE NEXT STATION CONDITIONS
CCCC
   50 CONTINUE
      VF2=VF(I)
      TF2=TF(I)
      D2=D(I)
      E2=E(I)
CCCCCC
      IF (D2 .LT. 1.E-10) D2= 1.E-10
      IF (E2 .GT. .99) E2= .99
      IF (E2 .LT. 0.) E2= 0.
C     INITIALIZE FOR ITERATION ON D
   55 KOUNTC= 1
      SGRESD= SGFCT (E(I))
      SG(I)= SGFCT (TF(I),SGRESD)
      SG60(I)= SGFCT (519.69,SGRESD)
      IF (INTER .EQ. I) SGSG60(I)= SG(I) / SG60(I)
CCCCCC
      DELDG= D2 - D(I)
      KOUNTD=0
   60 KOUNTB= 1
      DZ= D(I)
```

TABLE XXII. (CONTD)

```
      CIRCUM= PI * DZ
      TEMPA= PI04 * DZ**2
      TEMPD= TEMPA * DZ / I.5
C     INITIALIZE FOR ITERATION ON TF
      DELTFG= TF2 - TF(I)
      EZ= E(I)
      VAPM= VAPMF (EZ)
      SGRESD= SGRFCT (EZ)
C     AVERAGE TEMPERATURES, CALC. PROPERTIES
   70 TFZ= TF(I)
      TMX= (TS + TFZ) * .5
      PAS= PASF(TFZ,EZ)
      IF (PAS .LT. PS-.01) GO TO 80
C     AT BOILING POINT.
      PAS= PS - .01
      KOUNTO=1
   80 VAPK= VAPKF(TMX,VAPM)
      VAPMU= VAPMUF(TMX)
      VAPLAM= VAPLMF(TFZ)
      CP(I)= CPFCT(TFZ,SGRESD)
      VAPCP= VAPCPF(TMX)
      SG(I)= SGFCT(TFZ,SGRESD)
      FRHO(I)= SG(I) *62.428
      VAPD= VAPDF(TMX,PS)
      IF (VAPD .LT. .00005) VAPD= .00005
      ALP= PS / PAS * ALOG(PS / (PS - PAS) )
C     AIR PROPERTIES
      AIRK=TAB(TMX,AIRTB,AIRKTB,NTABAR)
      AIRMU=TAB      TAIRTB,AIRMUT,NTABAR)
      AIRCP=TAB(     .TAIRTB,AIRCPT,NTABAR)
C     DIFFUSION ZONE PROPERTIES
      QK= PAS / PS * .5
      QJ= 1. - QK
      QKMX= QJ * AIRK + QK * VAPK
      QMUMX= QJ * AIRMU + QK * VAPMU
      QMMX= QJ * AIRM + QK * VAPM
      QCPMX= (QJ * AIRM * AIRCP + QK * VAPM * VAPCP) / QMMX
      QRHOMX= PS * QMMX * 144. / R / TMX
      SC= QMUMX / VAPD / QRHOMX
      PR= QCPMX * QMUMX / QKMX * 3600.
      TEMPE= DZ * QRHOMX / QMUMX
      QMASS= TEMPD * SG(I) * 62.428
      TEMPF= .5 * SC**.3333333333
CCCCCC
      TEMPG= CIRCUM * VAPD * VAPM * PAS * ALP / R / TMX * 144.
      TEMPH= .6 * PR**.3333333333
      TEMPI= VAPCP / CIRCUM / QKMX
      TEMPJ= CIRCUM * QKMX * (TS - TFZ) / 3600.
      TEMPK = TEMPD * SG(I) * CP(I) * 62.428
C     INITIALIZE FOR ITERATION ON VF
      DELVG= VF2 - VF(I)
      KOUNTA= 1
C     CALCULATE DELTA V FOR DROP
  100 VFZ= VF(I)
      IF (OPTION .EQ. 0.) GO TO 115
      VRV= VFZ    * SINT - VAIRV
      VRH= VFZ    * COST - VAIRH
      VREL(I)= SQRT(VRV**2 + VRH**2)
      SPHI= VRV / VREL(I)
      CPHI= VRH / VREL(I)
      VSIGN= 1.
      GO TO 120
  115 VREL(I)= VAIR - VFZ
      VSIGN= 1.
      IF (VREL(I) .GE. 0.) GO TO 120
      VREL(I)= - VREL(I)
```

TABLE XXII. (CONTD)

```
      VSIGN= -VSIGN
CCCCCC
  120 CONTINUE
CCCCCC
      IF(VREL(I).LT.1.) VREL(I)=1.
CCCCCC
      RN(I)=VREL(I)*TEMPE
      CD(I)= 27. / RN(I)**.84
      FMACH2= VREL(I)**2 / CONST1
      TEMPB= PS * ( (1. + GM1O2 * FMACH2)**GOGM1 - 1.)
CCCCCC
      IF(TEMPB.LE.0.) TEMPB=1.E-20
      DRAG(I) = TEMPB * CD(I) * TEMPA * 144.
      ALPHA(I)= DRAG(I)  / QMASS * VSIGN * G
      IF (OPTION .EQ. 0.) GO TO 146
C **
C **  NOTE SPECIAL CASE FOR SPRAY STAND OPTION
      DUM1= - ALPHA(I) * SPH1
      IF (KOVRLY .EQ. 2) DUM1= G + DUM1
C **
      DUM2= -ALPHA(I) * CPHI
      ALPHA(I)= SQRT (DUM)**2 + DUM2**2)
      SINB= DUM1 / ALPHA(I)
      COSB= DUM2 / ALPHA(I)
  140 TIMS(I)= DX / VF(I)
      DUMMY1= VF(I)**2
      DUMMY2= 2. * DX * ALPHA(I)
C     CHECK IF ROUND/OFF ERROR I S A PROBLEM
      IF (ABS(DUMMY2 / DUMMY1)  .LT. 1.E-7) GO TO 180
      TIMS(I)= (SQRT(DUMMY1 + DUMMY2) - VF(I) ) / ALPHA(I)
  180 DELV(I)= ALPHA(I) * TIMS(I)
CCCCCC
      IF(ABS(DELV(I)).GT.VREL(I)) DELV(I)=VSIGN*(VREL(I)-1.)
      IF (OPTION .EQ. 0.) GO TO 185
 2000 FORMAT(1X,10E11.3)
      VRV= VRV + DELV(I) * SINB
      VRH= VRH + DELV(I) * COSB
      DUM1= VRV + VAIRV
      DUM2= VRH + VAIRH
      VF2= SQRT(DUM1**2 + DUM2**2)
      GO TO 186
  185 VF2= VF(I) + DELV(I)
C     CHECK IF WITHIN TOLERANCE
CCCCCC
  186 IF(ABS(DELV(I)-DELVG).LE. .01*ABS(DELV(I))) GO TO 200
      DELVG= DELV(I)
      IF ( ABS(DELVG) .LT..01) GO TO 200
      KOUNTA= KOUNTA + 1
      IF (KOUNTA .LT. 25) GO TO 100
  190 WRITE (61,1000) KOUNTA, KOUNTB, KOUNTC, KOUNTD, I
 1000 FORMAT(1RH0**** EVAP FAILURE     ,4I5,5X,7HDROPLET  I5)
      WRITE (61,)001) TF2,VF2,D2,E2
 1001 FORMAT (4E15.5)
      INTER= -1
      IF (OPTION .NE. 0.) GO TO 300
      CALL EXIT
C     HAVE CONVERGED ON VF2.  NOW CALC. DELTA TF, WF
  200 TEMPC= SQRT(RN(I))
      QNUM= 2. + TEMPF * TEMPC
      DELW = QNUM * TEMPG
CCCCCC
      IF((DELW*TIMS(I)).GT.QMASS) DELW=QMASS/TIMS(I)
      QNUM= 2. + TEMPH * TEMPC
  210 Z= DELW / QNUM * TEMPI
      ZZ= Z / (EXP(Z) - 1.)
      QVZ= QNUM * ZZ * TEMPJ
```

TABLE XXII. (CONTD)

```
      IF (KOUNTD .EQ. 0) GO TO 260
C     AT BOILING POINT.  ASSUME DELTF= 0.
      IF (VAPLAM .EQ. 0.) GO TO 190
      DELWN= QVZ / VAPLAM
CCCCCC
      IF((DELWN*TIMS(I)).GT.QMASS) DELWN=QMASS/TIMS(I)
      IF (ABS(DELWN  - DELW) .LE. .001 * ABS(DELW) ) GO TO 220
      DELW= DELWN
      KOUNTD= KOUNTD + 1
      IF (KOUNTD .LT. 25) GO TO 210
      GO TO 190
  220 IJK=1
      KOUNTD=1
C     AT BOILING POINT. CALC TF2 BASED ON PS AND E2
  230 TF2= PASF (-PS, E2)
      DELTF(I)= TF2 - TF(I)
      GO TO 250
  240 DELTF(I)= (QVZ - DELW * VAPLAM) * TIMS(I) / TEMPK
      TF2= TF(I) + DELTF(I)
CCCCCC
      IF(KFUEL.EQ.4.AND.TF2.GT.1092.8) TF2=1092.8
      IF(KFUEL.EQ.2.AND.TF2.GT.1210.4) TF2=1210.4
CCCCCC
CCCCCC
      DELTF(I)=TF2-TF(I)
C     CHECK IF WITHIN TOLERANCE
  250 IF (ABS( DELTF(I) - DELTFG) .LE.  .01*ABS(DELTF(I)) ) GO TO 260
      DELTFG= DELTF(I)
      IF ( ABS(DELTFG) .LT. 1.) GO TO 260
      KOUNTB= KOUNTB + 1
      IF (KOUNTB .LT. 25) GO TO 70
      GO TO 190
C     HAVE CONVERGED ON TF2.  NOW CALC. DELTA D
  260 IJK=0
  270 W2= W(I) - DELW * TIMS(I)
      IF (W2 .LT. 1.E-30) W2= 1.E-30
      SGRESD= SGPFCT (E2)
      SG(I)= SGFCT(TF2,SGRESD)
      SG60(I)= SGFCT (519.69,SGRESD)
      D2= (6. * W2 / PI / SG(I) / 62.428)**.3333333333
      IF (D2 .LT. 1.E-10) D2= 1.E-10
      E2= 1. - (D2 / DSTART(I))**3 * SG(I) / SG60(I)/ SGSG60(I)
      IF (E2 .GT. .99) E2= .99
      IF (E2 .LT. 0.) E2= 0.
      DELD= D2 - D(I)
C     CHECK IF WITHIN TOLERANCE
CCCCCC
      IF(ABS(DELD-DELDG).LE. .01*ABS(DELD)) GO TO 300
      DELDG= DELD
      IF (ABS(DELDG) .LT. 1.E-7) GO TO 300
      KOUNTC= KOUNTC + 1
      IF (KOUNTC .LT. 20) GO TO 60
      GO TO 190
C     HAVE CONVERGED ON ALL PARAMETERS FOR THIS INTERVAL
C     SAVE OLD CONDITIONS, SET NEW ONES
  300 VFSAVE(I)= VF(I)
      VF(I)= VF2
      TFSAVE(I)= TF(I)
      TF(I)= TF2
      DSAVE(I)= D(I)
      D(I)= D2
      ESAVE(I)= E(I)
      E(I)= E2
      DELQ(I)= QVZ * TIMS(I)
      DELM(I)= DELW * TIMS(I)
      RETURN
```

TABLE XXII. (CONTD)

```
      END
*DECK P
      FUNCTION PASF (T,E)
C     T= TEMPER. (R), E= FRACTION EVAPORATED
C     PASF= FUEL VAPOR PRESSURE (PSIA) FOR JP4, JP5/JP8
      COMMON / INPUT / KFUEL,NEQ,GAP,PPH,TITLE(8)
      DIMENSION CK1(7,4), CK2(7,4), ETAB(7)
      DATA ETAB / 0.,.1, .3, .5, .7, .9 ,1.0 /
     1, CK1 / 0., 0., 0., 0., 0., 0., 0.,
     2 155810.,386390.,585230.,817550.,1321200.,3175400.,10497000.,
     3 0., 0., 0., 0., 0., 0., 0.,
     4       40497.,136750.,286430.,604200.,1399600.,7044100.,77680000./
     5, CK2 / 0., 0., 0., 0., 0., 0., 0.,
     6 7414.8,8548.4,9060.7,9484.0,10083.,11178.,12670.,
     7 0., 0., 0., 0., 0., 0., 0.,
     8        4816.,6269.,7151.,8042.,9045.,10974.,13839. /
C
      IF (KFUEL .NE. 2 .AND. KFUEL .NE. 4) GO TO 150
C     IF (T .LT. 0 , ARGUMENT IS (-PS).  FIND AND RETURN CORRES. TEMPERATURE
      PSTAT=-T
      DO 50 J=1,7
      I=J
      IF (E - ETAB(J)) 60,80,50
   50 CONTINUE
      GO TO 70
   60 IF (I .EQ. 1) I=2
   70 K=I
   80 IF (PSTAT .LT. 0.) GO TO 83
      PASF= CK2(I,KFUEL) /  ALOG(CK1(I,KFUEL) / PSTAT )
      GO TO 84
   83 PASF=CK1(I,KFUEL) * EXP( -CK2(I,KFUEL) / T )
   84 IF (K) 110,100,85
   85 PSAVE= PASF
      J=I
      I= I - 1
      K= -1
      GO TO 80
   90 K=0
      GO TO 80
  100 RETURN
  110 PASF= PASF + (PSAVE - PASF) / (ETAB(J) - ETAB(I)) * (E - ETAB(I))
      GO TO 100
  150 WRITE (61,1000) KFUEL
 1000 FORMAT (25H0PASF CANNOT HANDLE FUEL=     15)
      CALL EXIT
      END
      FUNCTION VAPCPF (T)
C     T= TEMPER. (R), VAPCPF= CP FOR JP4, JP5/JP8 FUEL VAPOR
      COMMON / INPUT / KFUEL,NEQ,GAP,PPH,TITLE(8)
      IF (KFUEL .EQ. 2) GO TO 50
      VAPCPF= .180 + .000565 * T
      GO TO 100
   50 VAPCPF= .069 + .000530 * T
  100 RETURN
      END
      FUNCTION VAPMUF (T)
C     T= TEMPER. (R), VAPMUF= MU FOR JP4, JP5/JP8 FUEL VAPOR
      COMMON / INPUT / KFUEL,NEQ,GAP,PPH,TITLE(8)
      IF (KFUEL .EQ. 2) GO TO 50
      VAPMUF=   808.E-9 + 7.64E-9 * T
      GO TO 100
   50 VAPMUF= 248.E-9 + 6.31E-9 * T
  100 RETURN
      END
      FUNCTION VAPKF(T,W)
C     T= TEMPER. (R), VAPKF= K FOR FUEL VAPOR
```

TABLE XXII. (CONTD)

```
C     W= MOLECULAR WEIGHT
      DIMENSION WTAB(4),ATAB(4),BTAB(4),TABK(4)
      DATA WTAB/50., 100., 150., 300. /, NTAB /4/,
     1 ATAB / -.006362,-.006358,-.006284,-.006010 /,
     2 BTAB / .0000297,.0000273,.0000259,.0000235 /
C
      DO 10 I=1,NTAB
   10 TABK(I)= ATAB(I) + BTAB(I) * T
      VAPKF= TAB (W,WTAB,TABK,NTAB)
      RETURN
      END
      FUNCTION SGFCT (T,SG60R)
C     SG60R =  SG RESIDUE AT 60 DEG F
C     T= TEMPER. (R), SGFCT= SG FOR JP4 AND JP5 LIQUID FUEL
      SGFCT= SG60R + .208 - .0004* T
      RETURN
      END
      FUNCTION SGRFCT (E)
C     E= FRACTION EVAPORATED, SG60= SG AT 60 DEG F
C     SGRFCT= SG RESIDUE AT 60 DEG F FOR JP4, JP5/JP8 LIQUID FUEL
      COMMON / INPUT / KFUEL,DEQ,GAP,PPH,TITLE(8)
      DATA SG604/ .775 / , SG6058 / .806 /
      SG60= SG604
      IF (KFUEL .NE. 4) SG60= SG6058
      SGRFCT= 1.076 / ( (1.076 / SG60 - 1.) * (1. - .67 * E) + 1. )
      RETURN
      END
      FUNCTION VAPDF (T,P)
C     T= TEMPER. (R) , P= STATIC PRESSURE
C     VAPDF= DIFFUSIVITY FOR HEPTANE-OXYGEN
      VAPDF= 2.083 / P  * (T * (T * 1.1319E-9 + 1.973E-6) - 9.815E-4)
      RETURN
      END
      FUNCTION VAPMF (E)
C     E= FRACTION EVAPORATED, VAPMF= MOLECULAR WEIGHT OF JP4, JP5/JP8
C                    FUEL VAPOR
      COMMON / INPUT / KFUEL,DEQ,GAP,PPH,TITLE(8)
      DIMENSION ETAB(7), TABMV(7,4)
      DATA ETAB / 0., .1, .3, .5, .7, .9, 1.0 /, NTAB /7/,
     1 TABMV / 0., 0., 0., 0., 0., 0., 0.,
     2 148.12,163.29,.69.88,175.04,182.25,194.86,211.07,
     3         0., 0., 0., 0., 0., 0., 0.,
     4         93.26, 114.60, 126.61, 138.16, 150.59, 173.21, 204.76 /
C
      VAPMF= TAB(E, ETAB, TABMV(1,KFUEL), NTAB)
      RETURN
      END
      FUNCTION VAPLMF(T)
C     T= TEMPER (R), VAPLMF= LATENT HEAT OF VAPORISATION FOR JP4,BTU/LB
C                ALSO, JP5/JP8
      COMMON / INPUT / KFUEL,DEQ,GAP,PPH,TITLE(8)
      IF (KFUEL .EQ. 2) GO TO 50
      VAPLMF= 0.
      IF (T .LT. 1092.88) VAPLMF= 13.20 * (1092.88 - T) **.39
      GO TO 100
   50 VAPLMF= 0.
      IF (T .LT. 1210.45) VAPLMF= 10.75 * (1210.45 - T) **.41
  100 RETURN
      END
      FUNCTION CPFCT (T,SGR60)
C     T= TEMPER (R), CPFCT, CP FOR LIQUID JP4, JP5/JP8
C     SGR60= SG RESIDUE AT 60 DEG F FOR JP4
      CPFCT= ( .181 + .00045 * T) / SQRT(SGR60)
      RETURN
      END
*DECK D1
```

TABLE XXII. (CONTD)

```
      OVERLAY (IMPACT,1,0)
      PROGRAM TSTRIG
C
C     PROGRAM TO CALCULATE TRAJECTORIES FOR PNEUMATIC IMPACT ATOMIZER
C     WITH UNIFORM V AND T FIELD.  FUEL SPRAY PERPENDICULAR TO AIR
C     STREAM.  ********** TEST RIG **********
C
C
      COMMON / TRAJ / VFUEL,TFUEL,TFUELF,SGF,FMU,RHOF,PS,PT,TS,TT,
     I RHOAIR,AIRMU,G,VAIR,SM01
CCCCCC
     * ,XMAX,YMAX
      COMMON / INPUT / KFUEL,DEQ,GAP,PPH,TITLE(8),VGAS,TGAS
C
      COMMON/ TABLES / T1(7),VISAIR(7),T2(2,4),SGFUEL(2,4),T3(12,4),
     IVISFUL(12,4),NTAB1,NTAB2,NTAB3,NFUELS
      COMMON / TABLES / T5(10),SGTAB5(4),SRFTNS(10,4),NTAB5T,NTAB5S,
     I DIASMO(5),NDIASM,RNTAB(7),FTAB(7),NTABRF,T4R(11),PRATAB(11),NTAB4
      COMMON/TABLES/ T8R(8),TKTAB(8),NTAB8,T9R(10),CPTAB(10),NTAB9
      DIMENSION DIA(5)
      COMMON XL1,XL2,DIA1,DIA2,SLOPE1,SLOPE2
      COMMON NXXXX,AXISMJ(10),AXISMN(10),XXXX(10)
      COMMON / QEVAP/ DUMMY(20),D(5),TS(5),VF(5),VREL(5),      RN(5),
     1 CD(5),DRAG(5),FN(5),      CP(5),DELQ(5),SG(5),FRMD(5),DELTF(5),
     2 TIMS(5),FMASS(5),ALPHA(5),DELV(5),E(5),DX,W(5),VFSAVE(5),TFSAVE(5
     3 ),DSAVE(5),ESAVE(5),DSTART(5),SGSG60(5),SG60(5),DELM(5)
     4,OPTION,SPACE(6)
CCCCCC
     * ,WST(5),EW(5)
C
C
C     INPUT DATA
C
C     KFUEL= FUEL TYPE (1,2,3,4)
C     TFUELR= FUEL TEMPERATURE (R)
C     P3= AIR PRESSURE (PSIA)
C     T3R= AIR TEMPERATURE (R)
C     PPH= FUEL FLOW RATE (LB/HR)
C     DELP= DELTA PRESSURE (PSIA)
C
C
    2 TITLE(8)= 10H(TEST RIG)
      WRITE (61,1010) TITLE
      OPTION=0.
CCCCCC
      READ(60,1201) VAG,KFUEL,TFUELR,P3,T3R,PPH,DELP,TGAS,DIA4
 1201 FORMAT(F9.0,I1,7F10.2)
CCCCCC
      WRITE(61,1202) VAG,KFUEL,TFUELR,P3,T3R,PPH,DELP,TGAS,DIA4
 1202 FORMAT (11H0  VA GUESS , 5H FUEL,4X,6HTFUELP ,8X,2HP3 ,7X,3HT3R ,
     I 7X, 3HPPH , 6X,4HDELP ,6X,4HTGAS ,6X,4HDIA4 / 1X,F10.4,I5,7F10.4)
C     GEOMETRY PARAMETERS (IN)
      READ (60,1210)FJETID,DIA1,DIA2,DIA3,XL1,XL2,VGAS,FJETDO
      WRITE(61,1290)FJETID,DIA1,DIA2,DIA3,XL1,XL2,VGAS,FJETDO
      NXXXX= 0
      IF (DIA2 .NE. 0.) GO TO 190
C     READ TABLE OF X VS. MAJOR AXIS AND MINOR AXIS
      NXXXX= DIA1
      READ (60,1210) (XXXX(I),I=1,NXXXX)
      WRITE(61,1370) (XXXX(I),I=1,NXXXX)
 1370 FORMAT (1H0,10F10.3)
      READ (60,1210) (AXISMJ(I),I=1,NXXXX)
      WRITE(61,1370) (AXISMJ(I),I=1,NXXXX)
      READ (60,1210) (AXISMN(I),I=1,NXXXX)
      WRITE(61,1370) (AXISMN(I),I=1,NXXXX)
      DUMMY(1)= 3600.
```

TABLE XXII. (CONTD)

```
      DO 140 I=1,NXXXX
      IF (AXISMN(1) .EQ. 0.) AXISMN(I)= AXISMJ(I)
      DUMMY(2)= AXISMN(I) * AXISMJ(I)
      IF (DUMMY(2) .GT. DUMMY(1)) GO TO 140
      DUMMY(1)= DUMMY(2)
      J=I
  140 AXISMJ(I)= SQRT(DUMMY(2))
      DIA1= AXISMJ(1)
      DIA2= AXISMJ(J)
      DIA3= AXISMJ(NXXXX)
      XL1= XXXX(J)
      XL2= XXXX(NXXXX) - XL1
      DO 150 I=1,NXXXX
      XXXX(I)= XXXX(I) / 12.
  150 AXISMJ(I)= AXISMJ(I) / 12.
  190 CONTINUE
CCCCCC
      READ(60,1210)X1STRT,X2STRT,THETST,GAP,CDGAP,XMAX,YMAX
      WRITE(61,1400) X1STRT,X2STRT,THETST,GAP,CDGAP,XMAX,YMAX
 1400 FORMAT (1H0,6X,4HXLIP,6X,4HYLIP,2X,8HTHET LIP,7X,3HGAP,5X,5HCDGAP,
     1 6X,4HXMAX,6X,4HYMAX / 1X, 8F10.4 )
      DEQ= DIA3
C     RATBUP= CONSTANT FOR BREAK-UP LENGTH
      RATBUP= 2.40
      PI= 3.14159
      PI04= PI*.25
      PI0576= PI04/ 144.
      Z8=PI04*(DIA1**2-FJETOD**2)
C     CONVERT  DIAMETERS, LENGTHS TO FEET
      DIA1= DIA1 /12.
      DIA2= DIA2 /12.
      DIA3= DIA3 /12.
      DIA4= DIA4 /12.
      AGAP= CDGAP * PI * DIA4 * GAP / 12.
      XL1= XL1 /12.
      XL2= XL2 /12.
      TFUELF= TFUELR- 459.69
      T3F= T3R- 459.69
C     FUEL SPECIFIC GRAVITY (OMLS)
      SGF= TAB(TFUELF,T2(1,KFUEL),SGFUEL(1,KFUEL),NTAB2)
      SG60F  =TAB(60.,T2(1,KFUEL),SGFUEL(1,KFUEL),NTAB2)
C     FUEL VISCOSITY (CENTISTOKES)
      FMU= TAB(TFUELF,T3(1,KFUEL),VISFUL(1,KFUEL),NTAB3)
C     AIR VISCOSITY (LB/SEC/FT)
      AMU= TAB(T3F,T1,VISAIR,NTAB1)
      WRITE (61,1140) SGF,FMU,AMU
      RHOA= 2.69917 * (P3 -DELP) / T3R
      RHOF= 62.428 * SGF
C     CALCULATE GUESS FOR V (AIR).
CCCCCC
      VAIRG=VAG
CCCCCC
      IF(VAG.EQ.0.) VAIRG=SQRT(9266.*DELP/RHOA)
      KNTVA=0
      GAMMA=1.4
      C4= GAMMA-1.
      C1= C4*.5
      C2= GAMMA/ C4
      C3= GAMMA *.5
      C15= (GAMMA + 1.) / C4
      C5= C15 * .5
      C16= C15 - 1.
      Z1= 453.59/ 1728. / 2.54**3
      Z2= PI0576*FJET10 **2 *3600.
      Z3= Z8 * 3600. / 144.
      Z4= 2.54 *12.
```

TABLE XXII. (CONTD)

```
      SL= .5 *FJETID * 2.54
      Z5= 39.37E-6 /12.
      DX= .02 /12.
      XEND=  XL1 +XL2
      SLOPE1= (DIA2 - DIA1) / XL1
      SLOPE2= (DIA3 - DIA2) / XL2
      Z7= .2*PPH/3600.
      Z9=RHOF*PI04/I.5
      G=32.174
      Z10=G*GAMMA*53.35
      Z11= FJETID*.5
      VFUEL= PPH / Z2 / RHOF
C     SURFACE TENSION (DYNE/CM)
      DO 310 I=1,NTAB5S
  310 DUMMY(I)= TAB(TFUELF,T5,SRFTNS(I,I),NTAB5T)
      TAU= TAB(SG60F   ,SGTAB5,DUMMY,NTAB5S)
      ETAR= FMU * SGF
      RHOG= Z1 * RHOA
      VT= Z4 * VFUEL
      KPHINT=0
C
C
C
C     BEGIN CALC. WITH GUESSED VALUE FOR V (AIR)
C
  300 KNTVA= KNTVA+1
      QMA= RHOA * Z3 * VAIRG
      QMR= QMA /PPH
      VR= VAIRG / VFUEL
      SMD1= SMDF (TAU,ETAR,RHOG,QMR,SL,VT,VR)
C
C                                   2714=D NT ASAN ,2 .ON LEDOM NOITASIMOTA      C
C
C                                                        )UAT(TRQS =)1(YMMUD
C       / RV / 276000. * FGS * UMF * )1(YMMUD( TRQS * DITEJF * 6E05. =IDMS
C                                                              ) RMQ  1
C
C
      WRITE (61,1110) VAIRG, KNTVA ,SMD1
C     INITIALIZE FOR CALCULATIONS THROUGH THE FUEL TUBE
      DO 320 I=1,5
      DIA(I)= DIASMD(I)* SMD1
      D(I)= DIA(I) * Z5
C     DROPLET MASS.  CONSTANT THROUGHOUT FUEL TUBE.
      FMASS(I)=D(I)**3*Z9
CCCCCC
      W(I)=FMASS(I)
CCCCCC
      WST(I)=FMASS(I)
      E(I)=0.
      FN(I)=Z7/FMASS(I)
      TF(I)= TFUELR
  320 VF(I)= VFUEL
      BRUPL=RATBUP* SMD1
      XN= BRUPL * Z5
      XSTART= XN
      XFRACT= XSTART + Z11
      FRACTN= 0.
      TT=T3R
      PT=P3
      VAIR= VAIRG
      DUMMY= VAIR**2 / TT
      FMACH2= DUMMY / (Z10 - DUMMY * C1)
      C7= 1. + C1 * FMACH2
      TS= T3 / C7
      PS= PT / C7 **C2
```

TABLE XXII. (CONTD)

```
      RHOA= 2.69917 * PS / TS
      WAIR= RHOA * Z8 / 144. * VAIR
CCCCCC
      WTOT=WAIR
      KK=0
      RHOAIR= RHOA
      DDUCT= DIAMTR (XN)
      AIRMU= AMU
      ADUCT= PI04 * DDUCT**2
      INTER=1
CCCCCC
      FDW=0.
CCCCCC
      DELT0=0.
CCCCCC
      DP00P0=0.
CCCCCC
      FFM=0.
CCCCCC
      C11=(ADUCT-Z8/144.)/(Z8/144.)
C
C     BEGIN CALCULATIONS OVER INTERVAL DX
C
CCCCCC
  330 CONTINUE
  331 C7= 1. + C1*FMACH2
CCCCCC
      IF(KPRINT.NE.0) WRITE(61,2500)
CCCCCC
 2500 FORMAT(1H0)
CCCCCC
      BIGK=C7/(1.-FMACH2)
CCCCCC
      FMACH2=FMACH2*(1.+BIGK*(-2.*C11+2.*FFM/WTOT+DELT0/TT-2.*DP00P0))
  335 FMACH= SQRT(FMACH2)
  336 KK=1
      TS= TT/C7
      PS= PT/ C7**C2
      VAIR= FMACH* SQRT(Z10 * TS)
      RHOAIR= 2.69917*PS/TS
      IF (KPRINT .EQ. 0) GO TO 337
      DUMMY(1)= XN * 12.
      WRITE (61,1250) TS,PS,TT,PT,FMACH ,VAIR,DUMMY(1)
 337  IF (XN .GE. XEND) GO TO 500
      TEMPB= RHOAIR/AIRMU
      RNAIR= VAIR *DDUCT * TEMPB
C     FRICTION FACTOR F
      IF (RNAIR .LT. RNTAB (1)) GO TO 340
      F= TAB(RNAIR,RNTAB ,FTAB  ,NTABRF)
      GO TO 350
  340 F= 16./ RNAIR
  350 TEMPA= RHOAIR / 9266.
      CPAIR= TAB(TT,T9R,CPTAB,NTAB9)
      DQ=0.
      TOTDRG=0.
      FL=0.
CCCCCC
      FDW=0.
CCCCCC
      FFM=0.
CCCCCC
      NOCLAS=0
      DO 360 I=1,5
CCCCCC
      IF(E(I).GT..989999) GO TO 360
      CALL EVAP (INTER,I)
```

TABLE XXII. (CONTD)

```
      DIA(I)=D(I)/12.
CCCCCC
      DQ=DQ+ FN(I)*DELQ(I)
      TOTDRG=TOTDRG +FN(I)*DRAG(I) * TIMS(I)
      FL = FL + VRFL(I) * TIMS(I)
CCCCCC
      FDW=FDW+2.*(1.-VF(I)/VAIR)*DELM(I)*FN(I)/WTOT
CCCCCC
      FFM=FFM+DELM(I)*FN(I)
  360 CONTINUE
      INTER=2
C     ADJUST DRAG AND HEAT FOR FRACTION OF FUEL INVOLVED
      TOTDRG= TOTDRG * FRACTN
      DQ= DQ * FRACTN
CCCCCC
CCCCCC
      FDW=FDW*FRACTN
CCCCCC
      FFM=FFM*FRACTN
CCCCCC
      IF(NDCLAS.GT.0) FL=FL/NDCLAS
CCCCCC
      WTOT=WTOT+FFM
      WAIRST= ADUCT * RHOAIR * FL
      XNP1= XN + DX
      IF (XNP1 .LE. XEND) GO TO 380
      XNP1= XEND
  380 DDUCTP= DIAMTR (XNP1)
      ADUCTP= PI04 * DDUCTP**2
      DAREA= ADUCTP- ADUCT
      C6= FMACH2
      C11= DAREA / ADUCT
      C12= 4. * F * DX / DDUCT
      C13= TOTDRG /(C3* PS    * ADUCT *C6) / 144. *C12
CCCCCC
      DELTO=-DQ/WTOT/CPAIR
CCCCCC
      DPODP0=-C3*C6*(DELTO/TT+C13+FDW)
C     SET AIR PARAMETERS AT END OF INTERVAL
      PT= PT *(1.+ DP0DP0)
CCCCCC
      TT=TT+DELTO
C     ADJUST FUEL PARAMETERS FOR FRACTION INVOLVED
CCCCCC
      FRACT1= 1.
      IF (XNP1 .LT. XFRACT) FRACT1= 1. - (1. -(XNP1-ASTART)/Z11)**2
      TEMP1= FRACT1 - FRACTN
CCCCCC
      DO 401 I=1,5
CCCCCC
      IF(E(I).GT..989999) GO TO 401
      TF(I)= (FRACTN*TF(I) + TEMP1*TFUELR )/ FRACT1
      SGRESD= SGRFCT (ESAVE(I))
      SG(I)= SGFCT (TF(I), SGRESD)
      SG60(I)= SGFCT (519.69,SGRESD)
CCCCCC
      W2= W(I) - DELM(I) * FRACTN
CCCCCC
      IF(W2.LT.1.E-30) W2=1.E-30
      D(I)=(6.* W2 / PI / SG(I) / 62.428)**.3333333333
CCCCCC
      IF(D(I).LT.1.E-10) D(I)=1.E-10
      E(I)= 1. - ( D(I) / DSTART(I) )**3 * SG(I) / SG60(I)/ SGSG60(I)
CCCCCC
      IF(E(I).GT..99) E(I)=.99
      IF (E(I) .LT. 0.) E(I)=0.
```

TABLE XXII. (CONTD)

```
  400 VF(I)= (FRACTN*VF(I) + TEMP1*VFUEL )/ FRACT1
CCCCCC
      W(I)=W2
CCCCCC
      EW(I)=1.-W(I)/WST(1)
CCCCCC
  401 CONTINUE
  405 IF (KPRINT .EQ. 0) GO TO 410
      WRITE (61,1260) TF
      WRITE (61,1270) VF
CCCCCC
      WRITE(61,1350) E
 1350 FORMAT(4H E = 5F15.5)
      WRITE(61,2402) EW
 2402 FORMAT(4H EW= 5F15.5)
      WRITE(61,2401) DIA
 2401 FORMAT(4H D = 5F15.5)
      WRITE(61,2403) W
 2403 FORMAT(4H W = 5F15.5)
CCCCCC
  410 XN= XNP1
      AIRMU= TAB (TT  -459.69,T1,VISAIR,NTAB1)
      DDUCT= DDUCTP
      ADUCT= ADUCTP
      FRACTN= FRACT1
      GO TO 330
C
C     FUEL TUBE CALC. COMPLETE
C
C     CALC. EFFECT OF GAP
CCCCCC
  500 CONTINUE
      AGAPVC=PI*DIA3*GAP/)2.*CDGAP
      AGAPE=PI*DIA4*GAP/·2.
      FMGAP=FMACH
      IF(AGAPVC.GE.ADUCTP) AGAPVC=ADUCTP
      IF(AGAPVC.GE.ADUCTP) GO TO 502
      AGAP=AGAPVC
CCCCCC
      FMGAP= FMACH * ADUCTP / AGAP
      IF (FMGAP .LT. 1.) GO TO 501
      WRITE (61,1410) FMGAP
      CALL EXIT
  501 FMAVE2= (FMACH + FMGAP) **2 * .25
      DUMMY(1)=  (1. + C1 * FMAVE2) / (1. - FMAVE2)
      FMGAP= EXP (DUMMY(1) * ALOG(ADUCTP/AGAP) ) * FMACH
      C7= 1. + C1 * FMGAP**2
      TS= TT / C7
      PS= PT / C7**C2
CCCCCC
      VAIR= FMGAP * SQRT(Z10 * TS)
  502 CONTINUE
      PRINT 1250,TS,PS,TT,PT,FMGAP,VAIR
      IF(DIA4.LE.DIA3+6.*GAP/12.) GO TO 503
      QGAP=RHOAIR*VAIR*VAIR/9266.
      CPID=(1.-1./(AGAPE/AGAPVC)**2.)
      ETAD=.5
      DPT=CPID*(1.-ETAD)*QGAP
      PT=PT-DPT
      PS=PS+CPID*ETAD*QGAP
      VAIR=VAIR*AGAPVC/AGAPE
      FMGAP=VAIR/SQRT(Z10*TS)
  503 CONTINUE
      PRINT 1250,TS,PS,TT,PT,FMGAP,VAIR
CCCCCC
C     CHECK IF GUESSED V(AIR) WAS O.K.
```

TABLE XXII. (CONTD)

```
      DELPC= P3 - PS
      WRITE (61,1220) DELP,DELPC,KNTVA
      IF (ABS(DELPC- DELP) .LE.  .020* DELP) GO TO 520
C     NOT WITHIN TOLERANCE
  510 VAIRG= VAIRG *SQRT(DELP/DELPC)
      IF (KNTVA .LT. 10) GO TO 300
      WRITE (61,1100) KNTVA
      CALL EXIT
  520 IF (KPRINT .NE. 0) GO TO 550
      KPRINT=1
      GO TO 510
C
C     CALC. AVERAGE FUEL VELOCITY AND TEMPERATURE
C
  530 VFUEL=(VF(1)+VF(2)+VF(3)+VF(4)+VF(5) )*.2
      TFUEL=(TF(1)+TF(2)+TF(3)+TF(4)+TF(5) )*.2
      WRITE (61,1300) E
      WRITE (61,1250) TS,PS,TT,PT,FMGAP,VAIR
      QMR= WAIR / PPH  * 3600.
      QCO= .00632294* WAIR   /P3/ AOUCTP * SQRT( T3R / DELP * PS)
      WRITE (61,1515)      WAIR,QCO,QMR
      IF (E(1) .GT. .01) GO TO 580
  570 TFUELF=TFUEL-459.69
      SGF=TAB(TFUELF,T2(1,KFUEL),SGFUEL(1,KFUEL),NTAB2)
      FMU= TAB(TFUELF,T3(1,KFUEL),VISFUL(1,KFUEL),NTAB3)
      RHOF=62.428*SGF
      DO 560 I=1,NTAB5S
  560 DUMMY(I)= TAB(TFUELF,TS,SRFTNS(1,I),NTAB5T)
      TAU= TAB(SG60F   ,SGTAB5,DUMMY,NTAB5S)
      ETAR= FMU * SGF
      RHOG= Z1 * RHOAIR
      VT= Z4 * VFUEL
      VR= VAIR  / VFUEL
CCCCCC
      PPH=PPH*(1.-(EW(1)+EW(2)+EW(3)+EW(4)+EW(5))*.2)
      SL= PPH / (3600. * RHOF * VFUEL * PI * DIA4) * Z4
      SLM=SL/Z4/3.281E-6
      SMD1= SMDF (TAU,ETAR,RHOG,QMR,SL,VT,VR)
      FUELP=RHOF*VFUEL**2/9264.
CCCCCC
      WRITE(61,1230)VFUEL,TFUEL,VAIR,TT,FUELP,SMD1,PPH,SLM
C     CALCULATE TRAJECTORIES
      IF(XMAX.GT.0.) CALL TRAJ1(DIASMD)
      GO TO 1
  580 SUM= 0.
      SUM1= 0.
      DO 590 I=1,5
      SUM= SUM + W(I)
  590 SUM1= SUM1 + (TF(I) - TF(3)) * W(I) * (CP(I) + CP(3))
      TFUEL= SUM1 * .5 / SUM / CP(3)  + TF(3)
      GO TO 570
  700 WRITE (61,1240)
      CALL EXIT
    1 CONTINUE
C
 1010 FORMAT (1H1,8A10  /)
 1100 FORMAT (21HONO CONVERGENCE AFTER  ,I5,10HITERATIONS    )
 1110 FORMAT ( 8H0V(AIR)= F12.3,I10,5X,6HSMD=  F6.2)
 1140 FORMAT (4H0SG=  E12.4,7H (OMLS) ,4X,10HVISC FUEL=  E12.4,12H CENTI
     1STOKES  ,4X,10HVISC AIR =  E12.4,10H LB/SEC/FT        )
 1200 FORMAT (I10,7F10.2)
 1210 FORMAT (8F10.3)
 1220 FORMAT ( 6H0DELP= F10.4,4X, 6H0ELPC= F10.4,4X, 6HCOUNT=  I5)
CCCCCC
 1230 FORMAT(7H0VFUEL= F6.2,2X,6HTFUEL= F6.2,2X,5HVAIR= F6.2,2X,3HTT=
CCCCCC
```

TABLE XXII. (CONTD)

```
     *F6.1 ,2X,6HFUELP= F6.2,2X,6HSMD= F8.2,2X,6HPPH= F10.6,2X,
     * 4HSLM= F7.3 )
 1240 FORMAT (26H0MACH NO ITERATION FAILURE      )
 1250 FORMAT (4H TS= F8.2,3X,3HPS= F8.4,3X,3HTT= F8.2,3X,3HPT= F8.4,3X,
     1 2HM= F8.5,3X,5HVAIN= F8.2,3X,4HXIN=  F8.5)
 12 ) FORMAT (4H TF= 5F15.2)
 1270 FORMAT (4H VF= 5F15.2)
 1280 FORMAT (5H0FUEL ,4X,6HTFUELR ,8X,2HP3 ,7X,3HT3R ,7X,3HPPM,6X,4HDEL
     1P ,6X,4HTGAS,6X,4HDIA4   /  I5,7F10.4)
 1290 FORMAT (1H0,4X,5HJETID ,6X,4HDIAI ,6X,4HDIA2,6X,4HDIA3,7X,3HXL1,7X
     1 ,3HXL2,6X,4HVGAS,5X, 5HJETDD      / 8F10.4)
 1300 FORMAT (3H0E=  5F15.5)
 1410 FORMAT (13H0GAP MACH NO=      F10.5)
 1515 FORMAT (15H0AIR FLOW RATE=  F11.5,4H PPS,5X,17HDISCHARGE COEFF.=
     1 F8.4 ,5X,15HAIR-FUEL RATIO=    F10.4)
      END
*DECK T
      SUBROUTINE TRAJ1(DIA5MD)
C
C     PROGRAM TO CALCULATE TRAJECTORIES FOR IMPACT INJECTORS
C     WITH CONSTANT V AND T FIELD.  FUEL SPRAY PERPENDICULAR TO AIR FLOW
C          ***** ***** TEST RIG ***** *****
C
      COMMON / TRAJ / VFUEL,TFUELR,TFUELF,SQ,FMU,RHOFUL,P5,P1,TS,TT,
CCCCCC
     1RHOAIR,AMU,G,VAIRST,SMD,XMAX,YMAX
      COMMON / INPUT / KFUEL,DEQ,GAP,PPH,TITLE(8),VGAS,TGAS
      COMMON / QEVAP/ DUMMY(20),D(5),TF(5),VF(5),VREL(5),      RN(5),
     1 CD(5),DRAG(5),FN(5),      CP(5),DELQ(5),SG(5),FRMO(5),DELTF(5),
     2 TIMS(5),FMASS(5),ALPHA(5),DELV(5),E(5),DX,W(5),VFSAVE(5),TFSAVE(5
     3 ),USAVE(5),ESAVE(5),DSTART(5),SG566V(5),SG60(5),DELM(3)
     4,OPTION,VAIRH,VAIRV,SINT,COST,DUM1,DUM2
CCCCCC
     * ,WST(5),EW(5)
      COMMON /PLOTHG / KPLOT
C
      DIMENSION X(102,5),Y(102,5),NNN(5),LABELS(6),DIA5MD(5),DIA(5)
      DIMENSION LABELF(4)
CCCCCC
      DIMENSION DRD(102,5),EVP(102,5),TTF(102,5),VEF(102,5)
C
      DATA LABELF/ 10H5MELLDYN M ,10HJP5---JP8  ,10HJET A-1    ,3HJP4/
      DATA LABELS/ 8H 0 -  20,8H20 -  40, 8H40 -  60, 8H60 -  80,
     1 8H80 - 100, 10H / VOLUME  /
C
      OPTION=1.
      DO 3  I=1,5I0
      X(I)=0.
    3 Y(I)=0.
C     CONSTANTS FOR CALCULATIONS
      SI= .01
      ELIM= .96
      S=SI/12.
      DX=5
      CON9= 39.37E-6 /12.
C     CALCULATIONS BEGIN * * * * * * * * *
C     DEFINE INITIAL (XX,YY) AND VAIR   (DISTANCE IN INCHES)
      XX= 5. * SMD * CON9 * 12.
      YY= 0.
      VAIRH1= 0.
      VAIRV1= VGAS
      TT= TGAS
      VAIRST= VGAS
C     PS IS OK.  CALC. PT, TS
      DUMM= VGAS**2 / TT
      FMACH2= DUMM / (2403.076 - DUMM * .2)
```

TABLE XXII. (CONTD)

```
      C7= 1. + .2 * FMACH2
      TS= TT / C7
      PT= PS * C7**3.5
      THETAI= 0.
      ANGLIM= 1.56
      VELLIM= 1.0
      XLIMIT=8.
CCCCCC
      XLIMIT=YMAX
CCCCCC
      YLIMIT=XMAX
      SINTI=SIN(THETAI)
      COSTI=COS(THETAI)
      MAXK=0
      DO 150 I=1,5
C     DIA IS IN MICRONS
      DIA(I)= DIASMO(I) * SMO
C     D  IS IN FEET
      D(I)= DIA(I) * CON9
      E(I)= 0.
CCCCCC
      EW(I)=0.
CCCCCC
      W(I)=D(I)**3*RHOFUL*3.14159265/4./1.5
CCCCCC
      WST(I)=W(I)
      VF(I)= VFUEL
      TF(I)= TFUELR
      INTER=1
      THETA= THETAI
      VAIRH= VAIRHI
      VAIRV= VAIRVI
      SINT=SINTI
      COST=COSTI
      X(1,I)=XX
      Y(1,I)=YY
CCCCCC
      DRD(1,I)=D(I)/CON9
      EVP(1,I)=0.
      TTF(1,I)=TFUELR
      VEF(1,I)=VFUEL
CCCCCC
      KOVER=I
      KOUNT= 1
      NO=0
  100 KOUNT= KOUNT +1
      IF (KOUNT .GT. 100) GO TO 110
CCCCCC
  101 IF (E(I) .LT. ELIM) CALL EVAP (INTER,I)
      IF (INTER .LT. 0) GO TO 120
      INTER=2
      J= KOUNT
      IF (NO .EQ. 0) J= KOUNT - 1
      X(KOUNT,I)= X(J,I) +SI* COST
      Y(KOUNT,I)= Y(J,I) +SI* SINT
CCCCCC
      W(I)=W(I)-DELM(I)
CCCCCC
      EW(I)=1.-W(I)/WST(I)
CCCCCC
      DRD(KOUNT,I)= D(I)/CON9
      EVP(KOUNT,I)= E(I)*100.
CCCCCC
      EVP(KOUNT,I)=EW(I)*100.
      IF(E(I).LT. .001) EVP(KOUNT,I)=0.
      TTF(KOUNT,I)=TF(I)
```

TABLE XXII. (CONTD)

```
      VEF(KOUNT,I)=VF(I)
CCCCCC
      IF (E(I) .GE. ELIM) GO TO 118
      IF (X(KOUNT,I) .GT. XLIMIT) GO TO 119
CCCCCC
      IF(Y(KOUNT,I).GT.YLIMIT) GO TO 117
      IF (Y(KOUNT,I) .GE. 0.) GO TO 105
      WRITE (61,1150) I
      Y(KOUNT,I)=0.
  105 THETA= ATAN (DUM1/DUM2)
      SINT= DUM1 / VF(I)
      COST= DUM2 / VF(I)
CCCCCC
  108 NO= NO +1
      IF (NO .GT. 3) NO=0
      IF (NO .NE. 0) GO TO 101
      GO TO 100
  110 KOVER=KOVER+1
      IF (KOVER .LT. 10) GO TO 111
      WRITE (61,1100) I
      KOUNT= KOUNT-1
      GO TO 120
C     COMPRESS 100 PTS INTO 50 AND CONTINUE
  111 DO 112 J=4,100,2
      K=J/2
CCCCCC
      ORD(K,I)=ORD(J,I)
      EVP(K,I)=EVP(J,I)
      TTF(K,I)=TTF(J,I)
      VEF(K,I)=VEF(J,I)
CCCCCC
      X(K,I)=X(J,I)
  112 Y(K,I)=Y(J,I)
      KOUNT=50
      GO TO 100
CCCCCC
  117 WRITE(61,1151) I
 1151 FORMAT(8H DROPLET  13,19H HAS HIT LOWER WALL  )
CCCCCC
      GO TO 120
  118 WRITE (61,1170) I
      GO TO 120
  119 WRITE (61,1160) I
  120 NNN(I)= KOUNT
      IF (MAXK .LT. KOUNT) MAXK=KOUNT
  150 CONTINUE
      WRITE (61,1180) (I,TF(I),VF(I),D(I),E(I),I=1,5)
      WRITE (61,1120) (LABELS(1),LABELS(6),I=1,5),(DIA(I),I=1,5)
      DO 158 I=1,5
      N= NNN(I) + 1
      IF (N .GT. MAXK) GO TO 158
      DO 156 J=N,MAXK
      ORD(J,I)= 0.
      TTF(J,I)= 0.
      VEF(J,I)= 0.
      EVP(J,I)= 0.
      X(J,I)=0.
  156 Y(J,I)= 0.
  158 CONTINUE
      DO 160 J=1,MAXK
CCCCCC
      WRITE(61,1130) (X(J,I),Y(J,I),I=1,5),(ORD(J,I),TTF(J,I),VEF(J,I)
     + ,EVP(J,I),I=1,5)
  160 CONTINUE
C     PLOTTING
CCCCCC
```

TABLE XXII. (CONTD)

```
      CALL PLOT(1.,1.,-3)
  170 CONTINUE
      Q=1.
CCCCCC
      IF(YMAX.GT.1.1.OR.XMAX.GT.1.4) Q=2
      IF(YMAX.GT.2.1.OR.XMAX.GT.2.8) Q=4
      IF(YMAX.GT.4.1.OR.XMAX.GT.5.8) Q=8
      IF(YMAX.GT.8.1.OR.XMAX.GT.11.5) Q=16
CCCCCC
      XL= 1.50*Q
      YL=1.25*Q
CCCCCC
      DELX=XL/12.
      DELY=YL/10.
      CALL AXIS(0.,0.,1HX,-1,12.,0.,0.,DELX)
      CALL  AXIS (0.,0.,1HY,1,10.,90.,0.,DELY)
CCCCCC
      YL=0.5
      DO 180 I=1,5
      N=NNN(I)
      X(N+1,I)=0.
      Y(N+1,I)=0.
      X(N+2,I)=DELX
      Y(N+2,I)=DELY
      CALL LINE (X(1,I),Y(1,I),N,1,10,I)
CCCCCC
      XL=4.5
      CALL SYMBOL (XL,YL,.10,7,0.,-1)
      XL=XL+ .2
      CALL SYMBOL (XL,YL,.10,LABELS(I),0.,8)
      XL=XL+.80
      CALL SYMBOL (XL,YL,.10,66,0.,-1)
      XL=XL+.2
      CALL SYMBOL (XL,YL,.10,6HVOLUME,0.,6)
CCCCCC
      XL=XL+1.
      CALL NUMBER(XL,YL,.1,DIA(I),0.,2)
      XL=XL+.8
      CALL SYMBOL(XL,YL,.1,7HMICRONS,0.,7)
CCCCCC
      YL=YL+.2
  180 CONTINUE
      CALL PLOT (0.,-.5,-3)
      CALL SYMBOL (.5,10.5,.20,TITLE,0.,80)
      CALL SYMBOL (1.,10.,.10,21HINJECTOR TRAJECTORIES ,0.,21)
      CALL SYMBOL (.5,9.4,.10,5HFUEL= ,0.,5)
      CALL SYMBOL (1.1,9.4,.10,LABELF(KFUEL),0.,10)
      CALL SYMBOL (2.5,9.4,.10,7HFUEL T=  ,0.,7)
      DUM1=TFUELR
      CALL NUMBER (3.2,9.4,.10,DUM1,0.,1)
      CALL SYMBOL (.5,9.2,.10,10HSTATIC  P=  ,0.,10)
      CALL NUMBER (1.7,9.2,.10,PS  ,0.,1)
      CALL SYMBOL (2.5,9.2,.10,4H, T=  ,0.,4)
      CALL NUMBER (3.1,9.2,.10,TT  ,0.,1)
      CALL SYMBOL (.5,9.0,.10,13HAIR VELOCITY=  ,0.,13)
      CALL NUMBER (1.8,9.0,.10,VAIRST,0.,1)
CCCCCC
      CALL SYMBOL(.5,8.8,.1,4HSMD=,0.,4)
      CALL NUMBER(1.0,8.8,.1,SMD,0.,2)
      CALL SYMBOL(1.8,8.8,.1,7HMICRONS,0.,7)
CCCCCC
  230 IF (KPLOT .EQ. 0) GO TO 240
      KPLOT=0
CCCCCC
      CALL PLOT(16.,-12.5,-3)
      GO TO 250
```

TABLE XXII. (CONTD)

```
  240 KPLOT=I
CCCCCC
      CALL PLOT(-1.,11.5,-3)
  250 RETURN
 1100 FORMAT (42H01TERATION REACHED MAX. OF 500 FOR DROPLET ,I5,
     *  12IH, CALCULATION STOPPED  )
CCCCCC
 1120 FORMAT(1H0,5X,48,A10,4(8X,A8,A10)/
     *  1H0,10X,FR,3,4(1HX,FR,3),1X,7HMICRONS /
     *  1H0,8X,1HX,10X,1HY,4(14X,1HX,10X,1HY)/
     *  2X,5(5X,1HD,4X,2HTF,3X,2HVF,2X,5HE*100,2H /)//)
CCCCCC
 1130 FORMAT(2X,5(F10.2,F11.2,5X )/2X,5(3X,F5.0,F6.0,F5.0,F5.0,2H / ))
 1150 FORMAT (8H DROPLET   13,19H HAS HIT UPPER WALL     )
 1160 FORMAT (8H DROPLET   13,19H HAS HIT RIGHT WALL     )
 1170 FORMAT (8H DROPLET   13,15H HAS EVAPORATED       )
 1180 FORMAT  (26HOLAST DROPLET CONDITIONS--      /
     1  6X,4HDROP,5X,2HTF,13X,2HVF,14X,1HD,14X,1HE  /
     2    5 (5X,I5,4E15.5 /) /)
      END
*DECK 03
      OVERLAY (IMPACT,3,0)
      PROGRAM ARBFLD
C
C     PROGRAM TO CALCULATE TRAJECTORIES FOR PNEUMATIC IMPACT ATOMIZER
C     THIS VERSION ASSUMES RUNNING WITH GOSMAN OUTPUT TAPE
C
      COMMON / TRAJ1 / X1STRT,X2STRT,TMETST
C
      COMMON / TRAJ / VFUEL,TFUEL,TFUELF,SGF,FMU,RHOF,PS,PT,TS,TT,
     1 RHO41R,A1RMU,G,VA1R,SHD1
     *  ,XMAX,YMAX
      COMMON / INPUT / KFUEL,DEQ,GAP,PPH,TITLE(8)
C
      COMMON/ TABLES / T1(7),V1SA1R(7),T2(2,4),SGFUEL(2,4),T3(12,4),
     1V1SFUL(12,4),NTAB1,NTAB2,NTAB3,NFUELS
      COMMON / TABLES / T5(10),SGTAB5(4),SRFTNS(10,4),NTAB5T,NTAB5S,
     1 D1ASHO(5),ND1ASH,RNTAB(7),FTAB(7),NTABRF,T4R(11),PRATAB(11),NTAB4
      COMMON/TABLES/ TAB(8),TKTAB(8),NTABH,T9R(10),CPTAB(10),NTAB9
      DIMENSION DIA(5)
      COMMON XL1,XL2,D1A1,D1A2,SLOPE1,SLOPE2
      COMMON NXXXX,AX1SHJ(10),AX1SHN(10),XXXX(10)
      COMMON / DEVAP/ DUMMY(20),D(5),TF(5),VF(5),VREL(5),      RN(5),
     1 CD(5),DRAG(5),FN(5),      CP(5),DELQ(5),SG(5),FRHO(5),DELTF(5),
     2 TIMS(5),FMASS(5),ALPHA(5),DELV(5),E(5),DX,W(5),VFSAVE(5),TFSAVE(5
     3 ),DSAVE(5),ESAVE(5),DSTART(5),SGSGD0(5),SGD0(5),DELM(5)
     4,OPTION,SPACE(6)
     *  ,WST(5),EW(5)
C
C
C     INPUT DATA
C
C     KFUEL= FUEL TYPE (1,2,3,4)
C     TFUELR= FUEL TEMPERATURE (R)
C     P3= AIR PRESSURE (PSIA)
C     T3R= AIR TEMPERATURE (R)
C     PPH= FUEL FLOW RATE (LB/HR)
C     DELP= DELTA PRESSURE (PSIA)
C
C
      TITLE(8)= 10HMODEL NO 3
C                                                    2714=O NT H01 =)8(ELTIT 2
      WRITE (61,1010) TITLE
      OPTION=0.
      READ (60,1201) VAG,KFUEL,TFUELR,P3,T3R,PPH,DELP,TGAS,DIA4
      WRITE(61,1202) VAG,KFUEL,TFUELR,P3,T3R,PPH,DELP,TGAS,DIA4
```

TABLE XXII. (CONTD)

```
 1201 FORMAT (F9.0,I1,7F10.0)
 1202 FORMAT (1IH0  VA GUESS . 5H FUEL,4X,6HTFUELR ,8X,2HP3 ,7X,3HT3R ,
     1 7X, 3HPPR , 6X,4HDELP ,6X,4HTGAS ,6X,4HDIA4 / 1X,F10.4,I5,7F10.4)
C      GEOMETRY PARAMETERS (IN)
       READ (60,1210)FJETID,DIAI,DIA2,DIA3,XLI,XL2,SUM,FJETOD
       WRITE(61,1290)FJETID,DIAI,DIA2,DIA3,XL1,XL2,    FJETOD
       NXXXX= 0
       IF (DIA2 .NE. 0.) GO TO 190
C      READ TABLE OF X VS. MAJOR AXIS AND MINOR AXIS
       NXXXX= DIA1
       READ (60,1210) (XXXX(I),I=1,NXXXX)
       WRITE(61,1370) (XXXX(I),I=1,NXXXX)
       READ (60,1210) (AXISMJ(I),I=1,NXXXX)
       WRITE(61,1370) (AXISMJ(I),I=1,NXXXX)
       READ (60,1210) (AXISMN(I),I=1,NXXXX)
       WRITE(61,1370) (AXISMN(I),I=1,NXXXX)
       DUMMY(1)= 3600.
       DO 140 I=1,NXXXX
       IF (AXISMN(I) .EQ. 0.) AXISMN(I)= AXISMJ(I)
       DUMMY(2)= AXISMN(I) * AXISMJ(I)
       IF (DUMMY(2) .GT. DUMMY(1)) GO TO 140
       DUMMY(1)= DUMMY(2)
       J=I
  140 AXISMJ(I)= SQRT(DUMMY(2))
       DIA1= AXISMJ(1)
       DIA2= AXISMJ(J)
       DIA3= AXISMJ(NXXXX)
       XL1= XXXX(J)
       XL2= XXXX(NXXXX) - XL1
       DO 150 I=1,NXXXX
       XXXX(I)= XXXX(I) / 12.
  150 AXISMJ(I)= AXISMJ(I) / 12.
  190 CONTINUE
       DEQ= DIA3
       READ (60,1210) X1STRT,X2STRT,THETST,GAP,CDGAP,XMAX,YMAX
       WRITE(61,1400) X1STRT,X2STRT,THETST,GAP,CDGAP,XMAX,YMAX
 1400 FORMAT (1H0,6X,4HXLIP,6X,4HYLIP,2X,8HTHET LIP,7X,3HGAP,5X,5HCDGAP,
     1 6X,4HXMAX,6X,4HYMAX / 1X, 8F10.4 )
C      RATBUP= CONSTANT FOR BREAK-UP LENGTH
       RATBUP= 2.40
       PI= 3.14159
       PI04= PI*.25
       PI0576= PI04/ 144.
       ZA=PI04*(DIA1**2-FJETOD**2)
C      CONVERT  DIAMETERS, LENGTHS TO FEET
       DIAI= DIA1 /12.
       DIA2= DIA2 /12.
       DIA3= DIA3 /12.
       DIA4= DIA4 /12.
       AGAP= CDGAP * PI * DIA4 * GAP / 12.
       XLI= XLI /12.
       XL2= XL2 /12.
       TFUELF= TFUELR- 459.69
       T3F= T3R- 459.69
C      FUEL SPECIFIC GRAVITY (DMLS)
       SGF= TAB(TFUELF,T2(1,KFUEL),SGFUEL(1,KFUEL),NTAB2)
       SG60F  =TAB(60.,T2(I,KFUEL),SGFUEL(I,KFUEL),NTAB2)
C      FUEL VISCOSITY (CENTISTOKES)
       FMU= TAB(TFUELF,T3(1,KFUEL),VISFUL(1,KFUEL),NTAB3)
C      AIR VISCOSITY (LB/SEC/FT)
       AMU= TAB(T3F,T1,VISAIR,NTAB1)
       WRITE (61,1140) SGF,FMU,AMU
       RHOA= 2.69917 * (P3 -DELP) / T3R
       RHOF= 62.428 * SGF
C      CALCULATE GUESS FOR V (AIR).
       VAIRG= VAG
```

TABLE XXII. (CONTD)

```
      IF (VAG .EQ. 0.) VAIRG= SQRT( 9266. * DELP / RHOA)
      KNTVA=0
      GAMMA=1.4
      C4= GAMMA-1.
      C1= C4*.5
      C2= GAMMA/ C4
      C3= GAMMA *.5
      C15= (GAMMA + 1.) / C4
      C5= C15 * .5
      C16= C15 - 1.
      Z1= 453.59/ 1728. / 2.54**3
      Z2= PI0576*FJETID **2 *3600.
      Z3= Z8 * 3600. / 144.
      Z4= 2.54 *12.
      SL= .5 *FJETID * 2.54
      Z5= 39.37E-6 /12.
      DX= .02 /12.
      XEND=  XL1 +XL2
      SLOPE1= (DIA2 - DIA1) / XL1
      SLOPE2= (DIA3 - DIA2) / XL2
      Z7= .2*PPH/3600.
      Z9=RHOF*P104/1.5
      G=32.174
      Z 0=G*GAMMA*53.35
      Z11= FJETID*.5
      VFUEL= PPH / Z2 / RHOF
C     SURFACE TENSION (DYNE/CM)
      DO 310 I=1,NTAB5S
  310 DUMMY(I)= TAB(TFUELF,T5,SRFTNS(1,I),NTAB5T)
      TAU= TAB(SG60F   ,SGTAB5,DUMMY,NTAB5S)
      ETAR= FMU * SGF
      RHOG= Z1 * RHOA
      VT= Z4 * VFUEL
      KPRINT=0
C
C     BEGIN CALC. WITH GUESSED VALUE FOR V 'AIR)
C
  300 KNTVA= KNTVA+1
      QMA= RHOA * Z3 * VAIRG
      QMR= QMA /PPH
      VR= VAIRG / VFUEL
      SMD1= SMDF (TAU,ETAR,RHOG,QMR,SL,VT,VR)
C
C                                   2714-D NT ASAN ,2 ,ON LEDOK NOITASIMOTA     C
C
C                                                        ;UAT(TRQS =)1(YMMUD
C       / RV / 276000. * FGS * UMF * )1(YMMUD( TRQS * DITEJF * 6E05. =1DMS
C                                                              ) RMQ  1
C
C
      WRITE (61,1110) VAIRG, KNTVA ,SMD1
C     INITIALIZE FOR CALCULATIONS THROUGH THE FUEL TUBE
      DO 320 I=1,5
      DIA(I)= DIASMD(I)* SMD1
      D(I)= DIA(I) * Z5
C     DROPLET MASS.  CONSTANT THROUGHOUT FUEL TUBE.
      FMASS(I)=D(I)**3*Z9
      E(I)=0.
      W(I)=FMASS(1)
      WST(I)=FMASS(I)
      FN(I)=Z7/FMASS(I)
      TF(I)= TFUELR
  320 VF(I)= VFUEL
      BRUPL=RATRUP* SMD1
      XN= BRUPL * Z5
      XSTART= XN
```

TABLE XXII. (CONTD)

```
      XFRACT= XSTART + Z11
      FRACTN= 0.
      TT=T3R
      PT=P3
      VAIR= VAIR
      DUMMY= VAIR**2 / TT
      FMACH2= DUMMY / (Z10 - DUMMY * C1)
      C7= 1. + C1 * FMACH2
      TS= TT / C7
      PS= PT / C7 **C2
      RHOA= 2.69917 * PS / TS
      WAIR= RHOA * Z8 / 144. * VAIR
      WTOI=WAIR
      KK=0
      RHOAIR= RHOA
      DDUCT= DIAMTR (XN)
      AIRMU= AMU
      ADUCT= PI04 * DDUCT**2
      INTER=1
      FDW=0.
      DELTO=0.
      DPOOPO= 0.
      FFM= 0.
      C11=(ADUCT-Z8/144.)/(Z8/144.)
C
C     BEGIN CALCULATIONS OVER INTERVAL DX
C
  330 CONTINUE
  331 C7= 1. + C1*FMACH2
      IF(KPRINT.NE.0) WRITE(61,2500)
 2500 FORMAT(1H0)
      BIGK=C7/(1.-FMACH2)
      FMACH2=FMACH2*(1.+BIGK*(-2.*C11+2.*FFM/WTOT*DELTO/TT-2.*DP00P0))
  335 FMACH= SQRT(FMACH2)
  336 KK=1
      TS= TT/C7
      PS= PT/ C7**C2
      VAIR= FMACH* SQRT(Z10 * TS)
      RHOAIR= 2.69917*PS/TS
      IF (KPRINT .EQ. 0) GO TO 337
      DUMMY(I)= XN * 12.
      WRITE (61,1250) TS,PS,TT,PT,FMACH ,VAIR,DUMMY(1)
  337 IF (XN .GE. XEND) GO TO 500
      TEMPB= RHOAIR/AIRMU
      RNAIR= VAIR *DDUCT * TEMPB
C     FRICTION FACTOR F
      IF (RNAIR .LT. RNTAB (1)) GO TO 340
      F= TAB(RNAIR,RNTAB ,FTAB  ,NTABRF)
      GO TO 350
  340 F= 16./ RNAIR
  350 TEMPA= RHOAIR / 9266.
      CPAIR= TAB(TT,T9R,CPTAB,NTAB9)
      DQ=0.
      TOTDRG=0.
      FL=0.
      FDW=0.
      FFM=0.
      NDCLAS=0
      DO 360 I=1,5
      IF(E(I).GT..989999) GO TO 360
      CALL EVAP (INTER,I)
      DIA(I)=D(I)/Z5
      DQ= DQ + FN(I) * DELQ(I)
      TOTDRG=TOTDRG +FN(I)*DRAG(I) * TIMS(I)
      FL = FL + VREL(I) * TIMS(I)
      FDW=FDW+2.*(1.-VF(I)/VAIR)*DELM(I)*FN(I)/WTOT
```

TABLE XXII. (CONTD)

```
      FFM=FFM+DELM(I)*FN(I)
  360 CONTINUE
      INTER=2
C     ADJUST DRAG AND HEAT FOR FRACTION OF FUEL INVOLVED
      TOTDRG= TOTDRG * FRACTN
      DQ= DQ * FRACTN
      FDW=FDW*FRACTN
      FFM=FFM*FRACTN
      IF(NOCLAS.GT.0) FL=FL/NOCLAS
      WTOT=WTOT+FFM
      WAIRST= ADUCT * RHOAIR * FL
      XNP1= XN + DX
      IF (XNP1 .LE. XEND) GO TO 380
      XNP1= XEND
  380 DDUCTP= DIAMTR (XNP1)
      ADUCTP= PID4 * DDUCTP**2
      DAREA= ADUCTP- ADUCT
      C6= FMACH2
      C11= DAREA / ADUCT
      C12= 4. * F * DX / DDUCT
      C13= TDTDRG /(C3* PS    * ADUCT *C6) / 144. +C12
      DELTQ= -DQ       /WTOT/CPAIR
      DP0DP0=-C3*C6*(DELTQ/TT+C13+FDW)
C     SET AIR PARAMETERS AT END OF INTERVAL
      PT= PT *(1.+ DP0DP0)
      TT= TT + DELTQ
C     ADJUST FUEL PARAMETERS FOR FRACTION INVOLVED
      FRACT1= 1.
      IF (XNP) .LT. XFRACT) FRACT1= 1. - (1. -(XNP1-XSTART)/Z11)**2
      TEMP1= FRACT1 - FRACTN
      DO 401 I=1,5
      IF(E(I).GT..989999) GO TO 401
      TF(I)= (FRACTN*TF(I) + TEMP1*TFUELR )/ FRACT1
      SGRESD= SGFCT (FSAVE(I))
      SG(I)= SGFCT (TF(I), SGRESD)
      SG60(I)= SGFCT (519.69,SGRESD)
      W2= W(I) - DELM(I) * FRACTN
      IF(W2.LT.).E-30) W2=1.E-30
      D(I)=(6.* W2 / PI / SG(I) / 62.428)**.3333333333
      IF(D(I).LT.1.E-10) D(I)=1.E-10
      E(I)= 1. - ( D(I) / DSTART(I) )**3 * SG(I) / SG60(I)/ SGSG60(I)
      IF(E(I).GT..99) E(I)=.99
      IF (E(I) .LT. 0.) E(I)=0.
  400 VF(I)= (FRACTN*VF(I) + TEMP1*VFUEL  )/ FRACT1
      W(I)=W2
      EW(I)=1.-W(I)/WST(I)
  401 CONTINUE
  405 IF (KPRINT .EQ. 0) GO TO 410
      WRITE (61,1260) TF
      WRITE (61,1270) VF
      WRITE(61,1350) E
      WRITE(61,2402) EW
      WRITE(61,2401) DIA
      WRITE(61,2403) W
 1350 FORMAT(4H E = 5F15.5)
 2402 FORMAT(4H EW= 5F15.5 )
 2401 FORMAT(4H D = 5F15.5)
 2403 FORMAT(4H W = 5E15.5)
  410 XN= XNP1
      AIRMU= TAB (TT  -459.69,T1,VISAIR,NTAB1)
      DDUCT= DDUCTP
      ADUCT= ADUCTP
      FRACTN= FRACT1
      GO TO 330
C
C     FUEL TUBE CALC. COMPLETE
```

TABLE XXII. (CONTD)

```
C
C     CALC. EFFECT OF GAP
  500 CONTINUE
      AGAPVC= PI * DIA3 * GAP / I2. * CDGAP
      AGAPE= PI * DIA4 * GAP / I2.
      FMGAP= FMACH
      IF (AGAPVC .GE. ADUCTP) AGAPVC= ADUCTP
      IF (AGAPVC .GE. ADUCTP) GO TO 502
      AGAP= AGAPVC
      FMGAP= FMACH * ADUCTP / AGAP
      IF (FMGAP .LT. I.) GO TO 501
      WRITE (6I,14I0) FMGAP
      CALL EXIT
  501 FMAVE2= (FMACH + FMGAP) **2 * .25
      DUMMY(I)= (I. + CI * FMAVE2) / (I. - FMAVE2)
      FMGAP= EXP (DUMMY(I) * ALOG(ADUCTP/AGAP) ) * FMACH
      C7= 1. + C1 * FMGAP**2
      TS= TT / C7
      PS= PT / C7**C2
      VAIR= FMGAP * SQRT(ZI0 * TS)
  502 CONTINUE
      PRINT I250,TS,PS,TT,PT,FMGAP,VAIR
      IF (DIA4 .LE. DIA3 + 6. * GAP / I2.) GO TO 503
      QGAP= RHOAIR * VAIR * VAIR / 9 66.
      CPID= (1. - 1. / (AGAPE / AGAPVC)**2 )
      ETAD= .5
      DPT= CPID * (I. - ETAD) * QGAP
      PT= PT - DPT
      PS= PS + CPID * ETAD * QGAP
      VAIR= VAIR * AGAPVC / AGAPE
      FMGAP= VAIR / SQRT (ZI0 * TS)
  503 CONTINUE
      PRINT I250,TS,PS,TT,PT,FMGAP,VAIR
C     CHECK IF GUESSED V(AIR) WAS O.K.
      DELPC= P3 - PS
      WRITE (6I,I220) DELP,DELPC,KNTVA
      IF (ABS(DELPC- DELP) .LE.  .020* DELP) GO TO 520
C     NOT WITHIN TOLERANCE
  510 VAIRG= VAIRG *SQRT(DELP/DELPC)
      IF (KNTVA .LT. I0) GO TO 300
      WRITE (6I,1I00) KNTVA
      CALL EXIT
  520 IF (KPRINT .NE. 0) GO TO 550
      KPRINT=I
      GO TO 5I0
C
C     CALC. AVERAGE FUEL VELOCITY AND TEMPERATURE
C
  550 VFUEL=(VF(1)+VF(2)+VF(3)+VF(4)+VF(5) )*.2
      TFUEL=(TF(1)+TF(2)+TF(3)+TF(4)+TF(5) )*.2
      WRITE (6I,I300) E
      WRITE (6I,I250) TS,PS,TT,PT,FMGAP,VAIR
      QMR= WAIR / PPH  * 3600.
      QCD= .00632229* WAIR   /P3/ ADUCTP * SQRT( T3P / DELP * PS)
      WRITE (6I,I515)      WAIR,QCD,QMR
      IF (F(I) .GT. .0I) GO TO 580
  570 TFUELF=TFUEL-459.69
      SGF=TAB(TFUELF,T2(I,KFUEL),SGFUEL(I,KFUEL),NTAB2)
      FMU= TAB(TFUELF,T3(I,KFUEL),VISFUL(I,KFUEL),NTAB3)
      RHOF=62.428*SGF
      DO 560 I=1,NTAB5S
  560 DUMMY(I)= TAB(TFUELF,T5,SRFTNS(I,I),NTAB5T)
      TAU= TAB(SG60F   ,SGTAB5,DUMMY,NTAB5S)
      ETAR= FMU * SGF
      RHOG= Z1 * RHOAIR
      VT= Z4 * VFUEL
```

TABLE XXII. (CONTD)

```
      VR= VAIR / VFUEL
      PPH= PPH * (1. - (EW(1)+EW(2)+EW(3)+EW(4)+EW(5))*.2)
      SL= PPH / (3600. * RHOF * VFUEL * PI * DIA4) * 4
      SLM= SL / 74 / 3.281E-6
      SMD1= SMDF (TAU,ETAR,RHOG,OMR,SL,VT,VR)
      FUELP=RHOF*VFUEL**2/9266.
      WRITE (61,230) VFUEL,TFUEL,VAIR,TT,FUELP,SMD1,PPH,SLM
C     CALCULATE TRAJECTORIES
      IF (XMAX .GT. 0.) CALL TRAJ3 (DIASMD)
      GO TO 1
  580 SUM= 0.
      SUM1= 0.
      DO 590 I=1,5
      SUM= SUM + W(I)
  590 SUM1= SUM1 + (TF(I) - TF(3)) * W(I) * (CP(I) + CP(3))
      TFUEL= SUM1 * .5 / SUM / CP(3)  + TF(3)
      GO TO 570
  700 WRITE (61,1240)
      CALL EXIT
    1 CONTINUE
C
 1010 FORMAT (1H1,8A10  /)
 1100 FORMAT (21HOND CONVERGENCE AFTER  ,I5,10HITERATIONS    )
 1110 FORMAT ( 8H0V(AIR)= F12.3,I10,5X,4HSMD=  F6.2)
 1140 FORMAT (4H0SG=  E12.4.7H (OHLS) ,4X,10HVISC FUEL=  E12.4,12H CENTI
     1STOKES  ,4X,10HVISC AIR =  E12.4,10H LB/SEC/FT       )
 1200 FORMAT (I10,7F10.2)
 1210 FORMAT (8F10.3)
 1220 FORMAT ( 6H0DELP= F10.4,4X, 6HDELPC= F10.4,4X, 6HCOUNT=  I5)
 1230 FORMAT ( 7H0VFUEL= F6.2,2X,6HTFUEL= F6.2,2X,5HVAIR= F6.2,2X,3HTT=
     1 F6.1,2X,6HFUELP= F6.2,2X,4HSMD= F6.2,2X,4HPPH= F10.4,2X,4HSLM=
     2 F7.3 )
 1240 FORMAT (26H0MACH NO ITERATION FAILURE      )
 1250 FORMAT (4H TS= F8.2,3X,3HPS= F8.4,3X,3HTT= F8.2,3X,3HPT= F8.4,3X,
     1 2HM= F8.5,3X,5HVAIR= F8.2,3X,4HXIN=  F8.5)
 1260 FORMAT (4H TF= 5F15.2)
 1270 FORMAT (4H VF= 5F15.2)
 1280 FORMAT (5H0FUEL ,4X,6HTFUELR ,8X,2HP3 ,7X,3HT3R ,7X,3HPPH,6X,4HDEL
     1P ,7X,3H     ,6X,4HDIA4    /  I5,5F10.4,10X,F10.4)
 1290 FORMAT (1H0,4X,5HJETID ,6X,4HDIA) ,6X,4HDIA2,6X,4HDIA3,7X,3HXL1,7X
     1 ,3HXL2           ,5X, 5HJETDD      / 8F10.4)
 1300 FORMAT (3H0E=  5F15.5)
 1370 FORMAT (1H0,10F10.3)
 1410 FORMAT (13H0GAP MACH NO=      F10.5)
 1515 FORMAT (15H0AIR FLOW RATE=  F11.5,4H PPS,5X,17HDISCHARGE COEFF.=
     1 F8.4 ,5X,)5HAIR-FUEL RATIO=     F10.4)
      END
      SUBROUTINE TRAJ3 (DIASMD)
C
C     PROGRAM TO CALCULATE TRAJECTORIES FOR IMPACT INJECTORS
C     CHANGES AND ADDITIONS MADE 7/31/7)  FOR GOSMAN COMPATIBILITY
C
C     OUTPUT OF ROUTINE IS LOCATION OF E= .1,.2,.3,.....9 FOR EACH OF 5
C           DROPLET GROUPS
      COMMON / OUTPT / X1E(5,10), X2E(5,10)
      COMMON / KIMH / X1(21),X2(21),G1(21,21),G2(21,21),RO(21,21),T(21,
     1 21), IN, JN, R(21), FEVAP(21,21)
      COMMON / TRAJ1 / A1STRT,X2STRT,THETST
C
      COMMON / TRAJ / VFUEL,TFUELR,TFUELF,SQ,FHU,RHOFUL,PS,PT,TS,TT,
     1RHOAIR,AMU,G,VAIRST,SMD,XMAX,YMAX
      COMMON / INPUT / KFUEL,OEQ,GAP,PPH,TITLE(8)
      COMMON / QEVAP/ DUMMY(20),D(5),TF(5),VF(5),VREL(5),      RN(5),
     1 CD(5),DRAG(5),FN(5),      CP(5),DELQ(5),SG(5),FRHO(5),DELTF(5),
     2 TIMS(5),FMASS(5),ALPHA(5),DELV(5),E(5),DX,W(5),VFSAVE(5),TFSAVE(5
     3 ),DSAVE(5),ESAVE(5),DSTART(5),SGSGGV(5),SGGU(5),DELM(5)
```

TABLE XXII. (CONTD)

```
     4,OPTION,VAIRH,VAIRV,SINT,COST,DUM1,DUM2
     5, WST(5),EW(5)
      COMMON /PLOTNG / KP_OT
C
      DIMENSION X(102,5),Y(102,5),NNN(5),LABELS(6),DIASMD(5),DIA(5)
      DIMENSION LABELF(4)
      DIMENSION DRD(102,5),EVP(102,5),TTF(102,5),VEF(102,5)
C
      DATA LABELF/ 10HSHELLDYN H ,10HJP5---JP8  ,10HJET A-1    ,3HJP4/
      DATA LABELS/ 8H 0 -  20,8H20 -  40, 8H40 -  60, 8H60 -  80,
     1 8H80 - 100, 10H / VOLUME  /
C
C
      REWIND 1
      READ(1) IN, JN, X1, X2, R
      READ (1)
      READ (1) G1
      READ (1) G2
      READ (1) RO
      READ (1)
      READ (1) T
      REWIND 1
      OPTION=1.
      DO 3  I=1,510
      X(I)=0.
    3 Y(I)=0.
      REWIND 2
      DO 10 I=1,441
   10 EVAP(I)= 0.
C     CONSTANTS FOR CALCULATIONS
      SI= .01
      ELIM= .96
      S=SI/12.
      DX=S
      CONV= 39.37E-6 /12.
C     CALCULATIONS BEGIN * * * * * * * * *
      XX= X1STRT / 12.
      YY= X2STRT / 12.
      CALL AIRPRP (XX,YY,VAIRH1,VAIRV1,TS1)
      THETA1= - THETST / 57.29578
      SINT1=SIN(THETA1)
      COST1=COS(THETA1)
      MAXK=0
      DO 150 I=1,5
C     DIA IS IN MICRONS
      DIA(I)= DIASMD(I) * SMD
C     D  IS IN FEET
      D(I)= DIA(I) * CONV
      E(I)= 0.
      EW(I)= 0.
      W(I)= D(I)**3*RHOFUL*3.14159265 / 4. / 1.5
      WST(I)= W(I)
      VF(I)= VFUEL
      TF(I)= TFUELR
      INTER=1
      KKK=1
C **  THETA= THETA1
      VAIRH= VAIRH1
      VAIRV= VAIRV1
      TS= TS1
      SINT=SINT1
      COST=COST1
      X(I,1)=XX
      Y(1,1)=YY
      K1= 0
      EW1= EW(I)
```

TABLE XXII. (CONTD)

```
      CALL FEVAPC (XX, YY, KI, EWI,EW(I))
      DRD(1,I)=D(I)/CON9
      EVP(I,1)=0.
      TTF(1,I)=TFUELR
      VEF(1,I)=VFUEL
      KOVER=I
      KOUNT= 1
  100 KOUNT= KOUNT +1
      IF (KOUNT .GT. 100) GO TO 110
  101 IF (F(I) .LT. ELIM) CALL EVAP (INTER,I)
      IF (INTER .LT. 0) GO TO 120
      INTEP=2
      J= KOUNT - 1
C     X, Y IN FEET
      X(KOUNT,I)= X(J,I) +S * COST
      Y(KOUNT,I)= Y(J,I) -S * SINT
      W(I)= W(I) - DELM(I)
      EW(I)= 1. - W(I) / WST(I)
      CALL FEVAPC (X(KOUNT,I), Y(KOUNT,I), KI, EWI,EW(I))
      DRD(KOUNT,I)= D(I)/CON9
      EVP(KOUNT,I)= EW(I) * 100.
      IF(E(I).LT. .001) EVP(KOUNT,I)=0.
      TTF(KOUNT,I)=TF(I)
      VEF(KOUNT,I)=VF(I)
C     CHECK IF THIS INTERVAL CROSSED EVAP. STORE POINT
      K= KKK
      DO 600 L=K,10
      KKK= L
      EP= FLOAT(L) * .1
      IF (L .EQ. 10) EP= .95
      IF (ESAVE(I) .GE. EP .OR. E(I) .LT. EP) GO TO 610
C     INTERPOLATE FOR (X1,X2) IN FEET
      DUM= 0.
      TEMP= E(I) - ESAVE(I)
      IF (TEMP .NE. 0.) DUM= (EP - ESAVE(I) ) / TEMP
      X1E(I,L)=          X(J,I) + DUM * (X(KOUNT,I) - X(J,I) )
      X2E(I,L)=          Y(J,I) + DUM * (Y(KOUNT,I) - Y(J,I) )
      X1F(I,L)= X1E(I,L) * 12.
      X2E(I,L)= X2E(I,L) * 12.
  600 WRITE (61,2010) L,EP,X1F(I,L),X2E(I,L)
      GO TO 120
C     CHECK IF HAVE HIT A BNDRY
  610 IF (X(KOUNT,I) .GE. X1(1) ) GO TO 620
      DUM= 4HLEFT
      GO TO 650
  620 IF (X(KOUNT,I) .LE. X1(IN)) GO TO 630
      DUM= 5HRIGHT
      GO TO 650
  630 IF (Y(KOUNT,I) .GE. X2(I) ) GO TO 640
      DUM= 6HBOTTOM
      GO TO 650
  640 IF (Y(KOUNT,I) .LE. X2(JN)) GO TO 105
      DUM= 3HTOP
  650 WRITE (61,2000) I,DUM
  655 DO 660 L=KKK,10
      X1E(I,L)= X(KOUNT,I)
  660 X2E(I,L)= Y(KOUNT,I)
      GO TO 120
  105 IF (INTER .LT. 0) GO TO 655
C **  THETA= ATAN2(DUM1,DUM2)
      SINT= DUM1 / VF(I)
      COST= DUM2 / VF(I)
      CALL AIRPRP (X(KOUNT,I),Y(KOUNT,I),VAIRH,VAIRV,TS)
      GO TO 100
  110 KOVER=KOVER+I
      IF (KOVER .LT. 10) GO TO 111
```

TABLE XXII. (CONTD)

```
      WRITE (61,1100) 1
      KOUNT= KOUNT-1
      GO TO 655
C     COMPRESS 100 PTS INTO 50 AND CONTINUE
  111 DO 112 J=4,100,2
      K=J/2
      DRD(K,1)=DRD(J,I)
      EVP(K,1)=EVP(J,1)
      TTF(K,1)=TTF(J,1)
      VEF(K,1)=VEF(J,1)
      X(K,1)=X(J,1)
  112 Y(K,I)=Y(J,1)
      KOUNT=50
      GO TO 100
  120 NNN(I)= KOUNT
      K1= -1
      CALL FEVAPC (X(KOUNT,1),Y(KOUNT,1),K1,EW1,EW(I))
      IF (MAXK .LT. KOUNT) MAXK=KOUNT
  150 CONTINUE
      WRITE (61,1200) FEVAP
 1200 FORMAT (7H0FEVAP= / 2(1H0,7E12.4 / 2(1X,7E12.4/) ) )
      WRITE (2) FEVAP
      REWIND 2
      WRITE (61,1180) (I,TF(I),VF(I),D(I),E(I),I=1,5)
      WRITE (61,1120) (LABELS(I),LABELS(6),I=1,5),(DIA(I),I=1,5)
      DO 158 I=1,5
      N= NNN(I) + 1
      IF (N .GT. MAXK) GO TO 158
      DO 156 J=N,MAXK
      DRD(J,1)= 0.
      TTF(J,1)= 0.
      VEF(J,1)= 0.
      EVP(J,1)= 0.
      X(J,I)=0.
  156 Y(J,1)= 0.
  158 CONTINUE
      DO 160 J=1,MAXK
C     CONVERT TO INCHES FOR PLOTTING AND PRINTING
      DO 169 I=1,5
      X(J,I)= X(J,I) * 12.
  169 Y(J,1)= Y(J,1) * 12.
      WRITE(6),1130) (X(J,I),Y(J,I),I=1,5),(DRD(J,I),TTF(J,1),VEF(J,I)
     * ,EVP(J,I),I=1,5)
  160 CONTINUE
C     PLOTTING
      CALL PLOT (1.,1.,-3)
      Q=1.
      IF(YMAX.GT.1.1.OR.XMAX.GT.1.4) Q=2
      IF(YMAX.GT.2.1.OR.XMAX.GT.2.8) Q=4
      IF(YMAX.GT.4.1.OR.XMAX.GT.5.8) Q=8
      IF(YMAX.GT.8.1.OR.XMAX.GT.11.5) Q=16
      XL= 1.50*Q
      YL=1.25*Q
      DELX=XL/12.
      DELY=YL/10.
      CALL AXIS(0.,0.,1HX,-1,12.,0.,0.,DELX)
      CALL  AXIS (0.,0.,1HY,1,10.,90.,0.,DELY)
      YL=8.5
      DO 180 I=1,5
      N=NNN(1)
      X(N+1,I)=0.
      Y(N+1,I)=0.
      X(N+2,I)=DELX
      Y(N+2,I)=DELY
      CALL LINE (X(1,1),Y(1,I),N,1,10,I)
      XL=4.5
```

TABLE XXII. (CONTD)

```
      CALL SYMBOL (XL,YL,.10,1,0.,-1)
      XL=XL+ .2
      CALL SYMBOL (XL,YL,.10,LABELS(I),0.,8)
      XL=XL+.80
      CALL SYMBOL (XL,YL,.10,46,0.,-1)
      XL=XL+.2
      CALL SYMBOL (XL,YL,.10,6HVOLUME,0.,6)
      XL=XL+1.
      CALL NUMBER(XL,YL,.1,D1A(1),0.,2)
      XL= XL + .8
      CALL SYMBOL(XL,YL,.1,7HMICRONS,0.,7)
      YL=YL+.2
  180 CONTINUE
      CALL PLOT (0.,-.5,-3)
      CALL SYMBOL (.5,10.5,.20,TITLE,0.,80)
      CALL SYMBOL (1.,10.,.10,21H1NJECTOR TRAJECTORIES ,0.,21)
      CALL SYMBOL (.5,9.4,.10,5HFUEL= ,0.,5)
      CALL SYMBOL (1.1,9.4,.10,LABELF(KFUEL),0.,10)
      CALL SYMBOL (2.5,9.4,.10,7HFUEL T= ,0.,7)
      CALL NUMBER (3.2,9.4,.10,TFUELR,0.,1)
      CALL SYMBOL (.5,9.2,.10,10HSTATIC P= ,0.,10)
      CALL NUMBER (1.7,9.2,.10,PS ,0.,1)
      CALL SYMBOL(.5,8.8,.1,4HSMD=,0.,4)
      CALL NUMBER(1.0,8.8,.1,SMD,0.,2)
      CALL SYMBOL(1.8,8.8,.1,7HMICRONS,0.,7)
  230 IF (KPLOT .EQ. 0) GO TO 240
      KPLOT=0
      CALL PLOT(16.,-12.5,-3)
      GO TO 250
  240 KPLOT=1
      CALL PLOT(-1.,11.5,-3)
  250 RETURN
 1100 FORMAT (42H0ITERATION REACHED MAX. OF 500 FOR DROPLET ,I5,
     121H, CALCULATION STOPPED )
 1120 FORMAT (1H0,5X,A8,A10,4(8X,A8,A10) /
     1 1H0,10X,F8.3,4(18X,F8.3),1X,7HMICRONS /
     2 1H0,8X,1HX,10X,1HY,4(14X,1HX,10X,1HY) /
     3 2X,5(5X,1HD,4X,2HTF,3X,2HVF,2X,5HE*100,2H /) //)
 1130 FORMAT(2X,5(F10.7,F11.2,5X,)/2X,5(3X,F5.0,F6.0,F5.0,F5.0,2H / ))
 1180 FORMAT (26H0LAST DROPLET CONDITIONS-- /
     1 6X,4HDROP,5X,2HTF,13X,2HVF,14X,1HD,14X,1HE /
     2 5 (5X,15,4E15.5 /) /)
 2000 FORMAT (13H0**** DROPLET ,13, 9H HAS HIT ,A7, 8HBOUNDARY )
 2010 FORMAT (8H0DROPLET ,13,3H E= F4.2,5X,8H X1, X2= 2F9.5,4H IN)
      END
      SUBROUTINE FEVAPC (X , Y , K1, EW1, EW)
      COMMON / K1HH / X1(21),X2(21),G1(21,21),G2(21,21),RO(21,21),T(21,
     1 21), IN, JN, R(21), FEVAP(21,21)
      COMMON / INPUT/ KFUEL, DEQ, GAP, PPH
C     CALC. AND STORE FUEL EVAPORATION RATE FOR GOSMAN PROGRAM
C
      IF (K1 .LT. 0) GO TO 50
C     DETERMINE WHICH ELEMENT VOLUME
      JN1= JN - 1
      DO 10 JJ= 2,JN1
      S1= (X2(JJ) + X2(JJ-1)) * .5
      S2= (X2(JJ) + X2(JJ+1)) * .5
      IF ( Y .LT. S1 .OR. Y .GE. S2) GO TO 10
      J= JJ
      GO TO 20
   10 CONTINUE
      GO TO 40
   20 IN1= IN - 1
      DO 30 II= 2,IN1
      S1= (X1(II) + X1(II-1)) * .5
      S2= (X1(II) + X1(II+1)) * .5
```

TABLE XXII. (CONTD)

```
      IF (X .LT. S1 .OR. X .GT. S2) GO TO 30
      I= II
      GO TO 100
   30 CONTINUE
C     NOT IN A VOLUME
   40 IF (K1 .EQ. 0) RETURN
      IF (ISAVE .EQ. 0) RETURN
      I= 0
C     CALC. FEVAP(I,J) FOR ISAVE, JSAVE
   50 VOL= (X1(ISAVE+1) - X1(ISAVE-1)) * (X2(JSAVE+1)-X2(JSAVE-1)) * .25
     1 * R(JSAVE)
      IF (R(JSAVE) .NE. 1. .OR. R(JSAVE+1) .NE. 1.) VOL= VOL * 6.28318
      DEW= EW - EW1
      FEVAP(ISAVE,JSAVE)= FEVAP(ISAVE,JSAVE) + DEW * PPH / 18000. / VOL
      EW1= EW
      IF (I .NE. 0) GO TO 60
      ISAVE= 0
      K1= 0
      RETURN
   60 ISAVE= I
      JSAVE= J
   70 RETURN
  100 IF (K1 .NE. 0) GO TO 110
      K1= 1
      GO TO 60
  110 IF (I .EQ. ISAVE .AND. J .EQ. JSAVE) GO TO 70
      GO TO 50
      END
      SUBROUTINE AIRPRP (X,Y,VAIRH,VAIRV,TS)
      COMMON / KIMH / X1(21),X2(21),G1(21,21),G2(21,21),RO(21,21),T(21,
     1 21), IN , JN
C     NOTE-- COORD. SYSTEM OF EVAP IS HORIZ. + TO RIGHT, VERTICAL + TO
C              BOTTOM
      DO 10 J=1,JN
      I=J
      IF (X2(J) - Y) 10,70,20
   10 CONTINUE
   20 IF (I .EQ. 1) I=2
      KKK=1
   40 T1 = TAB(X,X1,T (1,I),IN)
      G11= TAB(X,X1,G1(1,I),IN)
      G21= TAB(X,X1,G2(1,I),IN)
      RO1= TAB(X,X1,RO(1,I),IN)
      IF (KKK) 40,80,50
   50 J=I
      I= I - 1
      KKK= -1
      T2= T1
      G12= G11
      G22= G21
      RO2= RO1
      GO TO 40
   60 DEL= (Y - X2(I) ) / (X2(J) - X2(I))
      TS   =      T1 + (T2  - T1 ) * DEL
      DUM  =     RO1 + (RO2 - RO1) * DEL
      VAIRH=    (G11 + (G12 - G11) * DEL ) / DUM
      VAIRV= - (G21 + (G22 - G21) * DEL ) / DUM
   65 RETURN
   70 KKK=0
      GO TO 40
   80 TS= T1
      VAIRH= G11 / RO1
      VAIRV= - G21 / RO1
      GO TO 65
      END
*DECK D2
```

TABLE XXII. (CONTD)

```
      OVERLAY (IMPACT,2,0)
      PROGRAM SPRYST
C
C     PROGRAM TO CALCULATE TRAJECTORIES FOR PNEUMATIC IMPACT ATOMIZER
C
C
      COMMON / TRAJ / VFUEL,TFUEL,TFUELF,SGF,FMU,RHOF,PS,PT,TS,TT,
     1 RHOAIR,AIRMU,G,VAIR,SMD1
     * ,XMAX,YMAX
      COMMON / INPUT / KFUEL,DEQ,GAP,PPH,TITLE(8)
C
      COMMON/ TABLES / T1(7),V1SAIR(7),T2(2,4),SGFUEL(2,4),T3(12,4),
     1VISFUL(12,4),NTAB1,NTAB2,NTAB3,NFUELS
      COMMON / TABLES / T5(10),SGTAB5(4),SRFTNS(10,4),NTAB5T,NTAB5S,
     1 D1ASMD(5),NDIASM,RNTAB(7),FTAB(7),NTABRF,T4R(11),PRATAB(11),NTAB4
      COMMON/TABLES/ T8R(8),TKTAB(8),NTAB8,T9R(10),CPTAB(10),NTAB9
      DIMENSION DIA(5)
      COMMON XL1,XL2,D1A1,D1A2,SLOPE1,SLOPE2
      COMMON NXXXX,AXISMJ(10),AXISMN(10),XXXX(10)
      COMMON / DEVAP/ DUMMY(20),D(5),TF(5),VF(5),VREL(5),      RN(5),
     1 CD(5),DRAG(5),FN(5),      CP(5),DELQ(5),SG(5),FRMD(5),DELTF(5),
     2 TIMS(5),FMASS(5),ALPHA(5),DELV(5),E(5),DX,W(5),VFSAVE(5),TFSAVE(5
     3 ),USAVE(5),ESAVE(5),DSTART(5),SGSG60(5),SD60(5),DELM(5)
     4,OPTION,SPACE(6)
     * ,WST(5),EW(5)
C
C
C     INPUT DATA
C
C     KFUEL= FUEL TYPE (1,2,3,4)
C     TFUELR= FUEL TEMPERATURE (R)
C     P3= AIR PRESSURE (PSIA)
C     T3R= AIR TEMPERATURE (R)
C     PPH= FUEL FLOW RATE (LB/HR)
C     DELP= DELTA PRESSURE (PSIA)
C
C
      TITLE(8)= 10HMODEL NO 2
C                                                    2714-D NT M01 =)8(ELTIT 2
      WRITE (61,1010) TITLE
      OPTION=0.
      READ (60,1201) VAG,KFUEL,TFUELR,P3,T3R,PPH,DELP,TGAS,DIA4
      WRITE(61,1202) VAG,KFUEL,TFUELR,P3,T3R,PPH,DELP,TGAS,DIA4
 1201 FORMAT (F9.0,I1,7F10.0)
 1202 FORMAT (11H0  VA GUESS , 5H FUEL,4X,6HTFUELR ,8X,2HP3  7X,3HT3R ,
     1 7X, 3HPPH , 6X,4HDELP ,6X,4HTGAS ,6X,4HDIA4 / 1X,F10.4,I5,7F10.4)
C     GEOMETRY PARAMETERS (IN)
      READ (60,1210)FJETID,D1A1,D1A2,D1A3,XL1,XL2,SUM,FJETDD
      WRITE(61,1290)FJETID,D1A1,D1A2,D1A3,XL1,XL2,    FJETDD
      NXXXX= 0
      IF (DIA2 .NE. 0.) GO TO 190
C     READ TABLE OF X VS. MAJOR AXIS AND MINOR AXIS
      NXXXX= DIA1
      READ (60,1210) (XXXX(I),I=1,NXXXX)
      WRITE(61,1370) (XXXX(I),I=1,NXXXX)
 1370 FORMAT (1H0,10F10.3)
      READ (60,1210) (AXISMJ(I),I=1,NXXXX)
      WRITE(61,1370) (AXISMJ(I),I=1,NXXXX)
      READ (60,1210) (AXISMN(I),I=1,NXXXX)
      WRITE(61,1370) (AXISMN(I),I=1,NXXXX)
      DUMMY(1)= 3600.
      DO 140 I=1,NXXXX
      IF (AXISMN(I) .EQ. 0.) AXISMN(I)= AXISMJ(I)
      DUMMY(2)= AXISMN(I) * AXISMJ(I)
      IF (DUMMY(2) .GT. DUMMY(1)) GO TO 140
      DUMMY(1)= DUMMY(2)
```

TABLE XXII. (CONTD)

```
      J=I
  140 AXISMJ(I)= SQRT(DUMMY(2))
      DIA1= AXISMJ(I)
      DIA2= AXISMJ(J)
      DIA3= AXISMJ(NXXXX)
      XL1= XXXX(J)
      XL2= XXXX(NXXXX) - XL1
      DO 150 I=I,NXXXX
      XXXX(I)= XXXX(I) / 12.
  150 AXISMJ(I)= AXISMJ(I) / 12.
  190 CONTINUE
      READ (60,1210) X1STRT,X2STRT,THETST,GAP,COGAP,XMAX,YMAX
      WRITE(61,1400) X1STRT,X2STRT,THETST,GAP,COGAP,XMAX,YMAX
 1400 FORMAT (1H0,6X,4HXLIP,6X,4HYLIP,2X,8HTHET LIP,7X,3HGAP,5X,5HCOGAP,
     1 6X,4HXMAX,6X,4HYMAX / 1X, 8F10.4 )
      DEQ= DIA3
C     RATBUP= CONSTANT FOR BREAK-UP LENGTH
      RATBUP= 2.40
      PI= 3.14159
      PI04= PI*.25
      PI0576= PI04/ 144.
      Z8=PI04*(DIA1**2-FJETOD**2)
C     CONVERT  DIAMETERS, LENGTHS TO FEET
      DIA1= DIA1 /12.
      DIA2= DIA2 /12.
      DIA3= DIA3 /12.
      DIA4= DIA4 /12.
      AGAP= COGAP * PI * DIA4 * GAP / 12.
      XL1= XL1 /12.
      XL2= XL2 /12.
      TFUELF= TFUELR- 459.69
      T3F= T3R- 459.69
C     FUEL SPECIFIC GRAVITY (OMLS)
      SGF= TAB(TFUELF,T2(1,KFUEL),SGFUEL(1,KFUEL),NTAB2)
      SG60F  =TAB(60.,T2(1,KFUEL),SGFUEL(1,KFUEL),NTAB2)
C     FUEL VISCOSITY (CENTISTOKES)
      FMU= TAB(TFUELF,T3(1,KFUEL),VISFUL(1,KFUEL),NTAB3)
C     AIR VISCOSITY (LB/SEC/FT)
      AMU= TAB(T3F,T ,VISAIR,NTAB1)
      WRITE (61,1140) SGF,FMU,AMU
      RHOA= 2.69917 * (P3 -DELP) / T3R
      RHOF= 62.428 * SGF
C     CALCULATE GUESS FOR V (AIR).
      VAIRG= VAG
      IF (VAG .EQ. 0.) VAIRG= SQRT( 9266. * DELP / RHOA)
      KNTVA=0
      GAMMA=1.4
      C4= GAMMA-1.
      C1= C4*.5
      C2= GAMMA/ C4
      C3= GAMMA *.5
      C15= (GAMMA + 1.) / C4
      C5= C15 * .5
      C16= C15 - 1.
      Z1= 453.59/ 1728. / 2.54**3
      Z2= PI0576*FJETID **2 *3600.
      Z3= Z8 * 3600. / 144.
      Z4= 2.54 *12.
      SL= .5 *FJETID * 2.54
      Z5= 39.37E-6 /12.
      DX= .02 /12.
      XEND=  XL1 +XL2
      SLOPE1= (DIA2 - DIA1) / XL1
      SLOPE2= (DIA3 - DIA2) / XL2
      Z7= .2*PPH/3600.
      Z9=RHOF*PI04/1.5
```

TABLE XXII. (CONTD)

```
      G=32.174
      Z10=G*GAMMA*53.35
      Z11= FJETID*.5
      VFUEL= PPH / Z2 / RHOF
C     SURFACE TENSION (DYNE/CM)
      OD 310 I=1,NTABSS
  310 DUMMY(I)= TAB(TFUELF,T5,SRFTNS(1,I),NTABST)
      TAU= TAB(SGDC   ,SGTABS,DUMMY,NTABSS)
      ETAR= FMU * SGF
      RHOG= Z1 * RHOA
      VT= Z4 * VFUEL
      KPRINT=0
C
C     BEGIN CALC. WITH GUESSED VALUE FOR V (AIR)
C
  300 KNTVA= KNTVA+1
      QMA= RHOA * Z3 * VAIRG
      QMR= QMA /PPH
      VR= VAIRG / VFUEL
      SMD1= SMDF (TAU,ETAR,RHOG,QMR,SL,VT,VR)
C
C                                   2714-D NT ASAN ,2 .ON LEDDM NOITASIMDTA      C
C
C                                                        )UAT(TRQS =)1(YMMUD
C       / RV / 276000. * FGS * UMF * )1(YMMUD( TRQS * DITEJF * 6E05. =1DMS
C                                                                ) RMQ  1
C
C
      WRITE (61,1110) VAIRG, KNTVA ,SMD1
C     INITIALIZE FOR CALCULATIONS THROUGH THE FUEL TUBE
      DO 320 I=1,5
      D1A(I)= DIASMD(I)* SMD1
      D(I)= D1A(I) * Z5
C     DROPLET MASS.  CONSTANT THROUGHOUT FUEL TUBE.
      FMASS(I)=D(I)**3*Z9
      W(I)=FMASS(I)
      WST(I)=FMASS(I)
      E(I)=0.
      FN(I)=Z7/FMASS(I)
      TF(I)= TFUELR
  320 VF(I)= VFUEL
      BRUPL=RATRUP* SMD1
      XN= BRUPL * Z5
      XSTART= XN
      XFRACT= XSTART + Z11
      FRACTN= 0.
      TT=T3R
      PT=P3
      VAIR= VAIRG
      DUMMY= VAIR**2 / TT
      FMACH2= DUMMY / (Z10 - DUMMY * C1)
      C7= 1. + C1 * FMACH2
      TS= TT / C7
      PS= PT / C7 **C2
      RHOA= 2.69917 * PS / TS
      WAIR= RHOA * Z8 / 144. * VAIR
      WTOT=WAIR
      KK=0
      RHOAIR= RHOA
      DDUCT= DIAMTR (XN)
      AIRMU= AMU
      ADUCT= PI04 * DDUCT**2
      INTER=1
      FDW=0.
      DELTO=0.
      DPOOPO= 0.
```

TABLE XXII. (CONTD)

```
      FFM= 0.
      C11=(ADUCT-Z8/144.)/(Z8/144.)
C
C     BEGIN CALCULATIONS OVER INTERVAL DX
C
  330 CONTINUE
  331 C7= 1. + C1*FMACH2
      IF(KPRINT.NE.0) WRITE(61,2500)
 2500 FORMAT(1H0)
      BIGK=C7/(1.-FMACH2)
      FMACH2=FMACH2*(1.+BIGK*(-2.*C11+2.*FFM/WTOT*DELTO/TT-2.*DP00P0))
  335 FMACH= SQRT(FMACH2)
  336 KK=1
      TS= TT/C7
      PS= PT/ C7**C2
      VAIR= FMACH* SQRT(Z10 * TS)
      RHOAIR= 2.69917*PS/TS
      IF (KPRINT .EQ. 0) GO TO 337
      DUMMY(1)= XN * 12.
      WRITE (61,1250) TS,PS,TT,PT,FMACH ,VAIR,DUMMY(1)
  337 IF (XN .GE. XEND) GO TO 500
      TEMPB= RHOAIR/AIRMU
      RNAIR= VAIR *DDUCT * TEMPB
C     FRICTION FACTOR F
      IF (RNAIR .LT. RNTAB (1)) GO TO 340
      F= TAB(RNAIR,RNTAB ,FTAB  ,NTABRF)
      GO TO 350
  340 F= 16./ RNAIR
  350 TEMPA= RHOAIR / 9266.
      CPAIR= TAB(TT,TOR,CPTAB,NTAB9)
      DQ=0.
      TOTDRG=0.
      FL=0.
      FDW=0.
      FFM=0.
      NDCLAS=0
      DO 360 I=1,5
      IF(E(I).GT..989999) GO TO 360
      CALL EVAP (INTER,1)
      DIA(I)=D(1)/75
      DQ= DQ + FN(I) * DELQ(I)
      TOTDRG=TOTDRG +FN(I)*DRAG(I) * TIMS(I)
      FL = FL + VRFL(I) * TIMS(I)
      FDW=FDW+2.*(1.-VF(I)/VAIR)*DELM(I)*FN(I)/WTOT
      FFM=FFM+DELM(1)*FN(I)
  360 CONTINUE
      INTER=2
C     ADJUST DRAG AND HEAT FOR FRACTION OF FUEL INVOLVED
      TOTDRG= TOTDRG * FRACTN
      DQ= DQ * FRACTN
      FDW=FDW*FRACTN
      FFM=FFM*FRACTN
      IF(NDCLAS.GT.0) FL=FL/NDCLAS
      WTOT=WTOT+FFM
      WAIRST= ADUCT * RHOAIR * FL
      XNP1= XN + DX
      IF (XNP1 .LE. XEND) GO TO 380
      XNP1= XEND
  380 DDUCTP= DIAMTR (XNP1)
      ADUCTP= P104 * DDUCTP**2
      DAREA= ADUCTP- ADUCT
      C6= FMACH2
      C11= DAREA / ADUCT
      C12= 4. * F * DX / DDUCT
      C13= TOTDRG /(C3* PS    * ADUCT *C6) / 144. *C12
      DELTO= -DQ       /WTOT/CPAIR
```

TABLE XXII. (CONTD)

```
      DP00P0=-C3*C6*(DELTO/TT+CI3+FDW)
C     SET AIR PARAMETERS AT END OF INTERVAL
      PT= PT *(1.+ DP00P0)
      TT= TT + DELTO
C     ADJUST FUEL PARAMETERS FOR FRACTION INVOLVED
      FRACTI= I.
      IF (XNPI .LT. XFRACT) FRACTI= I. - (I. -(XNPI-XSTART)/Z11)**2
      TEMP1= FRACT1 - FRACTN
      DO 401 I=1,5
      IF(E(I).GT..999999) GO TO 401
      TF(I)= (FRACTN*TF(I) + TEMP1*TFUELR )/ FRACT1
      SGRESD= SGRFCT (ESAVE(I))
      SG(I)= SGFCT (TF(I), SGRESD)
      SG60(I)= SGFCT (519.69,SGRESD)
      W2= W(I) - DELM(I) * FRACTN
      IF(W2.LT.1.E-30) W2=1.E-30
      D(I)=(6.* W2 / PI / SG(I) / 62.428)**.3333333333
      IF(D(I).LT.1.E-10) D(I)=1.E-10
      E(I)= 1. - ( D(I) / DSTART(I) )**3 * SG(I) / SG60(I)/ SGSG60(I)
      IF(E(I).GT..99) E(I)=.99
      IF (F(I) .LT. 0.) F(I)=0.
  400 VF(I)= (FRACTN*VF(I) + TEMP1*VFUEL  )/ FRACT1
      W(I)=W2
      EW(I)=1.-W(I)/WST(I)
  401 CONTINUE
  405 IF (KPRINT .EQ. 0) GO TO 410
      WRITE (61,1260) TF
      WRITE (61,1270) VF
      WRITE(61,1350) E
      WRITE(61,2402) EW
      WRITE(61,2401) DIA
      WRITE(61,2403) W
 1350 FORMAT(4H E = 5F15.5)
 2402 FORMAT(4H EW= 5F15.5 )
 2401 FORMAT(4H D = 5F15.5)
 2403 FORMAT(4H W = 5E15.5)
  410 XN= XNPI
      AIRMU= TAB (TT  -459.69,TI,VISAIR,NTAB1)
      DDUCT= DDUCTP
      ADUCT= ADUCTP
      FRACTN= FRACT1
      GO TO 330
C
C     FUEL TUBE CALC. COMPLETE
C
C     CALC. EFFECT OF GAP
  500 CONTINUE
      AGAPVC= PI * DIA3 * GAP / I2. * CDGAP
      AGAPE= PI * DIA4 * GAP / I2.
      FMGAP= FMACH
      IF (AGAPVC .GE. ADUCTP) AGAPVC= ADUCTP
      IF (AGAPVC .GE. ADUCTP) GO TO 502
      AGAP= AGAPVC
      FMGAP= FMACH * ADUCTP / AGAP
      IF (FMGAP .LT. I.) GO TO 501
      WRITE (61,1410) FMGAP
      CALL EXIT
  501 FMAVE2= (FMACH + FMGAP) **2 * .25
      DUMMY(I)=  (1. + C1 * FMAVE2) / (I. - FMAVE2)
      FMGAP= EXP (DUMMY(I) * ALOG(ADUCTP/AGAP) ) * FMACH
      C7= 1. + CI * FMGAP**2
      TS= TT / C7
      PS= PT / C7**C2
      VAIR= FMGAP * SQRT(Z10 * TS)
  502 CONTINUE
      PRINT 1250,TS,PS,TT,PT,FMGAP,VAIR
```

TABLE XXII. (CONTD)

```
      IF (DIA4 .LE. DIA3 + 6. * GAP / 12.) GO TO 503
      QGAP= RHOAIR * VAIR * VAIR / 9 66.
      CPID= (1. - I. / (AGAPE / AGAPVC)**2 )
      ETAD= .5
      DPT= CPID * (1. - ETAD) * QGAP
      PT= PT - DPT
      PS= PS + CPID * ETAD * QGAP
      VAIR= VAIR * AGAPVC / AGAPE
      FMGAP= VAIR / SQRT (Z10 * TS)
  503 CONTINUE
      PRINT I250,TS,PS,TT,PT,FMGAP,VAIR
C     CHECK IF GUESSED V(AIR) WAS O.K.
      DELPC= P3 - PS
      WRITE (61,1220) DELP,DELPC,KNTVA
      IF (ABS(DELPC- DELP) .LE.  .020* DELP) GO TO 520
C     NOT WITHIN TOLERANCE
  510 VAIRG= VAIRG *SQRT(DELP/DELPC)
      IF (KNTVA .LT. 10) GO TO 300
      WRITE (61,1100) KNTVA
      CALL EXIT
  520 IF (KPRINT .NE. 0) GO TO 550
      KPRINT=I
      GO TO 510
C
C     CALC. AVERAGE FUEL VELOCITY AND TEMPERATURE
C
  550 VFUEL=(VF(1)+VF(2)+VF(3)+VF(4)+VF(5) )*.2
      TFUEL=(TF(1)+TF(2)+TF(3)+TF(4)+TF(5) )*.2
      WRITE (61,1300) E
      WRITE (61,1250) TS,PS,TT,PT,FMGAP,VAIR
      QMR= WAIR / PPH  * 3600.
      QCD= .00632299* WAIR   /P3/ ADUCTP * SQRT( T3R / DELP * PS)
      WRITE (61,1515)      WAIR,QCD,QMR
      IF (F(1) .GT. .01) GO TO 580
  570 TFUELF=TFUEL-459.69
      SGF=TAB(TFUELF,T2(I,KFUEL),SGFUEL(I,KFUEL),NTAB2)
      FMU= TAB(TFUELF,T3(I,KFUEL),VISFUL(I,KFUEL),NTAB3)
      RHOF=62.428*SGF
      DO 560 I=1,NTAB5S
  560 DUMMY(I)= TAB(TFUELF,T5,SRFTNS(I,I),NTAB5T)
      TAU= TAB(SG60F   ,SGTAB5,DUMMY,NTAB5S)
      ETAR= FMU * SGF
      RHOG= Z1 * RHOAIR
      VT= Z4 * VFUEL
      VR= VAIR  / VFUEL
      PPH= PPH * (1. - (EW(1)+EW(2)+EW(3)+EW(4)+EW(5))*.2)
      SL= PPH / (3600. * RHOF * VFUEL * PI * DIA4) * Z4
      SLM= SL / Z4 / 3. 81E-6
      SMDI= SMDF (TAU,ETAR,RHOG,QMR,SL,VT,VR)
      FUELP=RHOF*VFUEL**2/9266.
      WRITE (61,1230) VFUEL,TFUEL,VAIR,TT,FUELP,SMDI,PPH,SLM
C     CALCULATE TRAJECTORIES
      IF (XMAX .GT. 0.) CALL TRAJ  (DIASMD)
      GO TO I
  580 SUM= 0.
      SUMI= 0.
      DO 590 I=1,5
      SUM= SUM + W(I)
  590 SUMI= SUMI + (TF(I) - TF(3)) * W(I) * (CP(I) + CP(3))
      TFUEL= SUMI * .5 / SUM / CP(3)  + TF(3)
      GO TO 570
  700 WRITE (61,1240)
      CALL EXIT
    I CONTINUE
C
 1010 FORMAT (1HI,8A10  /)
```

TABLE XXI1. (CONTD)

```
1100 FORMAT (27HONO CONVERGENCE AFTER  ,I5,10H1TERATIONS    )
1110 FORMAT ( 8H0V(A1R)= F12.3,110,5X,4HSMO=  F6.2)
1140 FORMAT (4H0SG=  E12.4,7H (OMLS) ,4X,10HV1SC FUEL=  E12.4,12H CENT1
    1STOKES  ,4X,10HV1SC A1R =  E12.4,10H LB/SEC/FT       )
1200 FORMAT (110,7F10.2)
1210 FORMAT (8F)0.3)
1220 FORMAT ( 4H0DELP= F10.4,4X, 6H0ELPC= F10.4,4X, 6HCOUNT=  I5)
1230 FORMAT ( 7H0VFUEL= F6.2,2X,6HTFUEL= F6.2,2X,5HVAIR= F6.2,2X,3HTT=
    1 F6.1,2X,6HFUELP= F6.2,2X,4HSMO= F6.2,2X,4HPPH= F1 .4,2X,4HSLM=
    2 F7.3 )
1240 FORMAT  26H0MACH NO ITERATION FAILURE      )
1250 FORMAT (4H TS= F8.2,3X,3HPS= F8.4,3X,3HTT= F8.2,3X,3HPT= F8.4,3X,
    1 2HM= F8.5,3X,5HVAIR= F8.2,3X,4HX1N=  F8.5)
1260 FORMAT (4H TF= 5F15.2)
1270 FORMAT (4H VF= 5F15.2)
1280 FORMAT (5H0FUEL ,4X,6HTFUELR ,8X,2HP3 ,7X,3HT3R ,7X,3HPPH,6X,4HDEL
    1P ,7X,3H    ,6X,4HDIA=   /  I5,5F10.4,10X,F10.4)
1290 FORMAT (1H0.4X,5HJET1D ,6X,4HD1A1 ,6X,4HD1A2,6X,4HD1A3,7X,3HXL1,7X
    1 ,3HXL2           ,5X, 5HJET0D     / 8F10.4)
1300 FORMAT (3H0E=  5F15.5)
1410 FORMAT (13H0GAP MACH NO=     F10.5)
1515 FORMAT (15H0A1R FLOW RATE=  F11.5,4H PPS,5X,17H01SCHARGE COEFF.=
    1 F8.4 ,5X,15HAIR-FUEL RAT:0=    F10.4)
     END
     SUBROUTINE TRAJ (D1ASMO)
C
C    PROGRAM TO CALCULATE TRAJECTORIES FOR IMPACT INJECTORS
C
     COMMON / TRAJ / VFUEL,TFUELR,TFUELF,SQ,FMU,RHOFUL,PS,PT,TS,TT,
    1RHO/1R,AMU,G,VA1RST,SMD,XMAX,YMAX
     COMMON / INPUT / KFUEL,NEQ,GAP,PPH,TITLE(8)
     COMMON / QEVAP/ DUMMY(20),D(5),TF(5),VF(5),VREL(5),      RN(5),
    1 CO(5),DRAG(5),FN(5),      CP(5),DELQ(5),SG(5),FRHO(5),DELTF(5),
    2 TIMS(5),FMASS(5),ALPHA(5),OELV(5),E(5),DX,W(5),VFSAVE(5),TFSAVE(5
    3 ),OSAVE(5),ESAVE(5),OSTART(5),SGSG6V(5),SG6U(5),OELM(5)
    4,OPTION,VA1RH,VA1RV,SINT,COST,DUM1,DUM2
    5, WST(5),EW(5)
     COMMON /PLOTNG / KPLOT
C
     DIMENSION X(102,5),Y(102,5),NNN(5),LABELS(6),D1ASMD(5),DIA(5)
     DIMENSION LABELF(4)
     DIMENSION DRO(102,5),EVP(102,5),TTF(102,5),VEF(102,5)
C
     DATA LABELF/ 10HSHELLDYN H ,10HJP5---JP8  ,10HJET A-1    ,3HJP4/
     DATA LABELS/ 8H 0 -  20,8H20 -  40, 8H40 -  60, 8H60 -  80,
    1 8H80 - 100, 10H / VOLUME  /
C
     OPTION=1.
     DO 3  I=1,510
     X(I)=0.
   3 Y(I)=0.
C    CONSTANTS FOR CALCULATIONS
     SI= .01
     ELIM= .96
     S=SI/12.
     DX=S
     CON9= 39.37E-6 /12.
C    CALCULATIONS BEGIN * * * * * * * * *
C    DEFINE INITIAL (XX,YY) AND VAIR   (DISTANCE IN INCHES)
     XX= 5. * SMD * CON9 * 12.
     L=0
     CALL A1RFLW (XX,YY,VA1RST,L,VA1RH1,VAIRV1)
     THETA1= ATAN2 (VA1RV1,VA1RH1)
     ANGLIM= 1.39626
     VELLIM= 1.0
     XLIMIT=8.
```

TABLE XXII. (CONTD)

```
      XLIMIT= YMAX
      YLIMIT= XMAX
      SINT1=SIN(THETA1)
      COST1=COS(THETA1)
      MAXK=0
      DO 150 I=1,5
C     DIA IS IN MICRONS
      DIA(I)= DIASMD(I) * SMD
C     D  IS IN FEET
      D(I)= DIA(I) * CON9
      E(I)= 0.
      EW(I)= 0.
      W(I)= D(I)**3*RHOFUL*3.14159265 / 4. / 1.5
      WST(I)= W(I)
      VF(I)= VFUEL
      TF(I)= TFUELR
      INTER=I
      THETA= THETAI
      VAIRH= VAIRH1
      VAIRV= VAIRV1
      SINT=SINT1
      COST=COST1
      X(1,I)=XX
      Y(1,I)=YY
      ORD(1,I)=D(I)/CON9
      EVP(1,I)=0.
      TTF(1,I)=TFUELR
      VEF(1,I)=VFUEL
      KOVER=1
      KOUNT= 1
      NO=0
  100 KOUNT= KOUNT +1
      IF (KOUNT .GT. 100) GO TO 110
  101 IF (E(I) .LT. ELIM) CALL EVAP (INTER,I)
      IF (INTER .LT. 0) GO TO 120
      INTER=2
      J= KOUNT
      IF (NO .EQ. 0) J= KOUNT - 1
      X(KOUNT,I)= X(J,I) +SI* COST
      Y(KOUNT,I)= Y(J,I) +SI* SINT
      W(I)= W(I) - DELM(I)
      EW(I)= 1. - W(I) / WST(I)
      ORD(KOUNT,I)= D(I)/CON9
      EVP(KOUNT,I)= EW(I) * 100.
      IF(E(I).LT. .001) EVP(KOUNT,I)=0.
      TTF(KOUNT,I)=TF(I)
      VEF(KOUNT,I)=VF(I)
      IF (E(I) .GE. ELIM) GO TO 118
      IF (X(KOUNT,I) .GT. XLIMIT) GO TO 119
      IF (Y(KOUNT,I) .GT. YLIMIT) GO TO 117
      IF (Y(KOUNT,I) .GE. 0.) GO TO 105
      WRITE (6,1150) I
      Y(KOUNT,I)=0.
  105 THETA= ATAN (DUM1/DUM2)
      SINT= DUM1 / VF(I)
      COST= DUM2 / VF(I)
C     NEW AIR VELOCITY
      L=1
      CALL AIRFLW (X(KOUNT,I),Y(KOUNT,I), VAIRST, L , VAIRH,VAIRV)
      IF (L .EQ. 1) GO TO 108
C     FUEL FOLLOWS VAIR DIRECTION OUT TO XCORE
      THETA= ATAN2 (VAIRV,VAIRH)
      SINT= SIN(THETA)
      COST= COS(THETA)
  108 NO= NO +1
      IF (NO .GT. 3) NO=0
```

TABLE XXII. (CONTD)

```
      IF (NO .NE. 0) GO TO 101
      GO TO 100
  110 KOVER=KOVER+1
      IF (KOVER .LT. 10) GO TO 111
      WRITE (61,1100) I
      KOUNT= KOUNT-1
      GO TO 120
C     COMPRESS 100 PTS INTO 50 AND CONTINUE
  111 DO 112 J=4,100,2
      K=J/2
      ORD(K,1)=ORD(J,1)
      EVP(K,I)=EVP(J,I)
      TTF(K,1)=TTF(J,I)
      VEF(K,I)=VEF(J,I)
      X(K,I)=X(J,I)
  112 Y(K,I)=Y(J,I)
      KOUNT=50
      GO TO 100
  117 WRITE (61,1151) I
 1151 FORMAT ( 8H DROPLET   I3,19H WAS HIT LOWER WALL  )
      GO TO 120
  118 WRITE (61,1170) I
      GO TO 120
  119 WRITE (61,1160) I
  120 NNN(I)= KOUNT
      IF (MAXK .LT. KOUNT) MAXK=KOUNT
  150 CONTINUE
      WRITE (61,1180) (I,TF(I),VF(I),D(I),E(I),I=1,5)
      WRITE (61,1120) (LABELS(I),LABELS(6),I=I,5),(DIA(I),I=I,5)
      DO 158 I=1,5
      N= NNN(I) + 1
      IF (N .GT. MAXK) GO TO 158
      DO 156 J=N,MAXK
      ORD(J,1)= 0.
      TTF(J,I)= 0.
      VEF(J,I)= 0.
      EVP(J,1)= 0.
      X(J,I)=0.
  156 Y(J,1)= 0.
  158 CONTINUE
      DO 160 J=1,MAXK
      WRITE(61,1130) (X(J,I),Y(J,I),I=),5),(DRD(J,I),TTF(J,I),VEF(J,I)
     + ,EVP(J,1),I=1,5)
  160 CONTINUE
C     PLOTTING
      CALL PLOT (1.,1.,-3)
  170 CONTINUE
      Q=1.
      IF(YMAX.GT.1.1.OR.XMAX.GT.I.4) Q=2
      IF(YMAX.GT.2.1.OR.XMAX.GT.2.8) Q=4
      IF(YMAX.GT.4.1.OR.XMAX.GT.5.8) Q=8
      IF(YMAX.GT.8.1.OR.XMAX.GT.11.5) Q=16
      XL= 1.50*Q
      YL=1.25*Q
      DELX=XL/12.
      DELY=YL/10.
      CALL AXIS(0.,0.,1HX,-1,12.,0.,0.,DELX)
      CALL  AXIS (0.,0.,IHY,I,I0.,90.,0.,DELY)
      YL=8.5
      DO 180 I=I,5
      N=NNN(I)
      X(N+1,I)=0.
      Y(N+I,I)=0.
      X(N+2,I)=DELX
      Y(N+2,I)=DELY
      CALL LINE (X(I,I),Y(I,I),N,1,I0,I)
```

TABLE XXII. (CONTD)

```
      XL=4.5
      CALL SYMBOL (XL,YL,.10,I,0.,-1)
      XL=XL+ .2
      CALL SYMBOL (XL,YL,.10,LABELS(I),0.,8)
      XL=XL+.80
      CALL SYMBOL (XL,YL,.10,46,0.,-1)
      XL=XL+.2
      CALL SYMBOL (XL,YL,.10,6HVOLUME,0.,6)
      XL=XL+1.
      CALL NUMBER(XL,YL,.1,DIA(I),0.,2)
      XL= XL + .8
      CALL SYMBOL(XL,YL,.1,7HMICRONS,0.,7)
      YL=YL+.2
  180 CONTINUE
      CALL PLOT (0.,-.5,-3)
      CALL SYMBOL (.5,10.5,.20,TITLE,0.,80)
      CALL SYMBOL (1.,10.,.10,21HINJECTOR TRAJECTORIES ,0.,21)
      CALL SYMBOL (.5,9.4,.10,5HFUEL= ,0.,5)
      CALL SYMBOL (1.1,9.4,.10,LABELF(KFUEL),0.,10)
      CALL SYMBOL (2.5,9.4,.10,7HFUEL T=  ,0.,7)
      DUM1=TFUELR
      CALL NUMBER (3.2,9.4,.10,DUM1,0.,1)
      CALL SYMBOL (.5,9.2,.10,10HSTATIC  P=  ,0.,10)
      CALL NUMBER (1.7,9.2,.10,PS  ,0.,1)
      CALL SYMBOL (2.5,9.2,.10,4H, T=  ,0.,4)
      CALL NUMBER (3.1,9.2,.10,TT  ,0.,1)
      CALL SYMBOL (.5,9.0,.10,13HAIR VELOCITY=  ,0.,13)
      CALL NUMBER (1.9,9.0,.10,VAIRST,0.,1)
      CALL SYMBOL(.5,8.8,.1,4HSMO=,0.,4)
      CALL NUMBER(1.0,8.8,.1,SMD,0.,2)
      CALL SYMBOL(1.8,8.8,.1,7HMICRONS,0.,7)
  230 IF (KPLOT .EQ. 0) GO TO 240
      KPLOT=0
      CALL PLOT(16.,-12.5,-3)
      GO TO 250
  240 KPLOT=1
      CALL PLOT(-1.,11.5,-3)
  250 RETURN
 1100 FORMAT (42H0ITERATION REACHED MAX. OF 500 FOR DROPLET ,I5,
     121H, CALCULATION STOPPED  )
 1120 FORMAT (1H0,5X,A8,A10,4(8X,A8,A10)  /
     1 1H0,10X,F8.3,4(18X,F8.3),1X,7HMICRONS  /
     2 1H0,8X,1HX,10X,1HY,4(14X,1HX,10X,1HY)  /
     3 24,5(5X,1HO,4X,2HTF,3X,2HVF,2X,5HE*100,2H /)  //)
 1130 FORMAT(2X,5(F10.2,F11.2,5X,)/2X,5(3X,F5.0,F6.0,F5.0,F5.0,2H /  ))
 1150 FORMAT (8H DROPLET   I3,19H HAS HIT UPPER WALL     )
 1160 FORMAT (8H DROPLET   I3,19H HAS HIT RIGHT WALL     )
 1170 FORMAT (8H DROPLET   I3,15H HAS EVAPORATED       )
 1180 FORMAT  (24HOLAST DROPLET CONDITIONS--      /
     1  6X,4HDROP,5X,2HTF,13X,2HVF,14X,1HD,14X,1HE  /
     2    5 (5X,I5,4E15.5 /) /)
      END
      SUBROUTINE AIRFLW (XX,ZZ,UJ,KKK,UUH,UUV)
C     ROUTINE TO CALCULATE          AIR FLOW FIELD FOR IMPACT INJECTOR
C
      COMMON / INPUT / KFUEL,DEQ,GAP,PPH,TITLE(8)
      DIMENSION TEMPA(3)
      COMMON / TAB1 / ZZU50(10),ULUMAX(10),XX1(9),Z50G(9),UUMAXC(3),
     1 NTAB6,NTAB7,NTAB8,NTAB9,SINTAB(5),COSTAB(5)
      DATA ZZU50 / .025,.05,.1,.2,.3,.4,.5,.75,1.0,1.57 / ,
     1 ULUMAX / .70,.85,.97,   1.0,.98,.95,.90,.72,.50,0. /
      DATA XX1 / 0.,.13,.26,.39,.52,.65,.78,.91,1.0 /
     1 ,          Z50G / 1.,.647,.511,.533,.644,.845,1.0,1.18,1.33 /
      DATA SINTAB / -.148,-.109,-.030,0.,0, /,COSTAB /.989,.994,.9996,
     1  1.,1. /, NTAB9 /5/
      DATA UUMAXC / 1.,.5,0. / , NTAB6,NTAB7,NTAB8 / 10,9,3 /
```

TABLE XXII. (CONTD)

```
C * * * * * * * * * * * * * * * * * * * * * * * * * * * * * * * * * * *
C     ALL X AND Z VALUES ARE IN INCHES
C * * * * * * * * * * * * * * * * * * * * * * * * * * * * * * * * * * *
      IF (KKK .NE. 0) GO TO 100
      XCORE= DEQ * (1.0923) ** (100./112.)
      X1CORE= XCORE * 2.5
      CONSTK= .0782 * X1CORE ** .06
      CON1= 1.0923 * UJ
      CON2= GAP * .76  /X1CORE
      CON3= GAP * 1.07 / X1CORE
  100 IF (XX .LE.  XCORE ) GO TO 175
      UMAX= CON1 / (XX/DEQ) ** 1.12
      SINP= 0.
      COSP= 1.
      IF (XX .LE. X1CORE ) GO TO 200
      ZU50= CONSTK * XX ** .94
      IF (KKK .NE. 0) GO TO 150
C     FUEL BEGINS ON U50 LINE
      ZZ= ZU50
  150 DUMMY= ZZ / ZU50
      UU= TAB(DUMMY,ZZU50,ULUMAX,NTAB6) * UMAX
      GO TO 400
  175 UMAX= UJ
      DUMMY= XX / X1CORE
      SINP= TAB(DUMMY,XX1,SINTAB,NTAB9)
      COSP= TAB(DUMMY,XX1,COSTAB,NTAB9)
      GO TO 250
  200 DUMMY= XX / X1CORE
  250 RATIO= TAB (DUMMY,XX1,Z50G,NTAB7)
      TEMPA(2)= RATIO * GAP
      TEMPA(3)= TEMPA(2) + XX * CON2
      TEMPA(1)= TEMPA(2) - XX * CON3
      IF (KKK .NE. 0  .AND.  XX .GT. XCORE) GO TO 300
C     FUEL BEGINS ON U50 LINE AND STAYS OUT TO XCORE
      ZZ= TEMPA(2)                                                    C
  300 UU= TAB(ZZ,TEMPA,UUMAX,NTAB8) * UMAX
  400 CONTINUE
C     PROTECT AGAINST BEING OUTSIDE TABLES
      IF (UU .LT. 0.) UU=0.
      IF (UU .GT. UMAX) UU=UMAX
C     COMPONENTS
      UUH= UU * COSP
      UUV= UU * SINP
      IF (XX .LE. XCORE) KKK= -1                                      C
      RETURN
      END
```

4.0 PROGRAM USAGE

Injector performance can be computed at critical engine conditions, such as light-off, maximum loading, idle points, and the maximum power point. The venturi and impact plate diameters and gap width can be varied to determine resultant drop sizes. If X_{max} and Y_{max} on the last data card are set to zero, calculations will stop after the SMD is computed, with no trajectory calculations. After a satisfactory geometry is determined, spray trajectories and evaporation lengths can be computed with the use of the three flow options.

Assume, for example, that a typical flow field has been established with the Gosman 2-D program. Spray trajectories are then computed with Option 3. The length required for the largest drop size group to reach 95 percent evaporation can be used to determine injector spacing. Rates of evaporation along the trajectories can also be used to assess the amount of fuel that could be expected to impinge on the combustor walls.

As shown on the data sheet, an L-pipe spraying into a swirler cup can be modeled by appropriate input to obtain spray, SMD, and evaporation rates. This program, however, does not compute L-pipe temperatures (see Program 1529).

5.0 PROGRAM OUTPUT

A copy of a typical program output is presented in Table XXIII. A plot tape is written to plot the trajectories for each of the five drop groups.

When Option 3 is specified, an output tape, identified as TAPE2, is written containing the total evaporation rates in $lb/sec/ft^3/radian$ at each of the grid nodes for the Gosman program solution that supplied the two-dimensional flow field. This program and the Gosman program can be run separately with input and output tapes saved between runs. The two programs can also be run together in a combined sequential run for repetitive iteration of the two program solutions.

TABLE XXIII. PROGRAM NO. 1528 OUTPUT

```
3 IMPACT 1 TEST CASE - ARBITRARY FIELD OPTION                    MODEL NO 3

  VA GUESS FUEL    TFUELR        P3        T3R       PPH      DELP      T8AS      DI44
   -0.0000    4  530.0000  235.2000  660.0000   20.0000    7.1200   -0.0000    .4500

    JET10     D1A1     D1A2     D1A3      XL1      XL2     JET00
    .0450    .2400    .1930    .2000    .5000    .2000    .0620

     XL1P     YL1P  THET L1P      GAP    CDGAP     XMAX     YMAX
    .2000    .6000   90.0000    .1000    .6000   5.0000   4.0000

SG=   .7684E+00 (DMLS)    VISC FUEL=   .1132E-01 CENTISTOKES    VISC AIR =   .1401E-04 LB/SEC/FT

V(AIR)=     265.950          1     SMD= 28.85
TS=  641.63   PS=230.3956   TT=  644.48   PT=233.9996   M=  .14907   VAIR=  185.11   XIN=
TS=  641.63   PS=230.3956   TT=  644.48   PT=233.9996   M=  .14907   VAIR=  185.11   XIN=

DELP=    7.1200    DELPC=    4.8044    COUNT=    1

V(AIR)=     323.759          2     SMD= 24.63
TS=  642.53   PS=228.3235   TT=  646.67   PT=233.5224   M=  .17963   VAIR=  223.21   XIN=
TS=  642.53   PS=228.3235   TT=  646.67   PT=233.5224   M=  .17963   VAIR=  223.21   XIN=

DELP=    7.1200    DELPC=    6.8765    COUNT=    2

V(AIR)=     329.442          3     SMD= 24.30
TS=  642.58   PS=228.1046   TT=  646.86   PT=233.4711   M=  .18257   VAIR=  226.86   XIN=
TS=  642.58   PS=228.1046   TT=  646.86   PT=233.4711   M=  .18257   VAIR=  226.86   XIN=

DELP=    7.1200    DELPC=    7.0954    COUNT=    3

V(AIR)=     330.013          4     SMD= 24.27

TS=  650.94   PS=224.0874   TT=  660.00   PT=235.2000   M=  .26303   VAIR=  303.96   XIN=  .00229
TF=          530.00           530.00           530.00           530.00           530.00
VF=           10.49            10.49            10.49            10.49            10.49
E =           .00337           .00337           .00337           .00337           .00337
EW=          0.00000          0.00000          0.00000          0.00000          0.00000
D =        15.87267         19.35316         24.00455         31.64201         42.09409
W =     .37622E-11       .70933E-11       .14677E-10       .30030E-10       .69711E-10
DROP GROUP       (1)              (2)              (3)              (4)              (5)

TS=  652.29   PS=225.7150   TT=  660.00   PT=235.1057   M=  .24709   VAIR=  309.36   XIN=  .02229
TF=          536.96           535.96           534.96           534.09           533.28
VF=           43.62            34.95            30.78            25.96            21.56
E =           .01684           .01488           .01294           .01130           .00968
EW=           .01289           .01092           .00897           .00733           .00570
D =        15.59116         19.37194         24.02372         31.60137         42.11410
W =     .37137E-11       .70159E-11       .14545E-10       .29519E-10       .69314E-10

TS=  651.51   PS=225.3662   TT=  659.47   PT=235.1469   M=  .25134   VAIR=  314.49   XIN=  .04229
TF=          539.27           538.19           537.05           536.02           534.92
VF=           60.37            51.10            42.31            35.28            28.72
E =           .03557           .03100           .02647           .02263           .01878
EW=           .02924           .02501           .02080           .01724           .01360
D =        15.71354         19.49330         24.94164         31.77277         42.21303
W =     .36522E-11       .69159E-11       .14372E-10       .29512E-10       .68750E-10
```

OPTION

INPUT DATA

ITERATE FOR V (AIR) TO MATCH DELP

SMD FROM FUEL TUBE

VENTURI CONDITIONS

VOL FRAC EVAP WEIGHT

MICRONS

DROP MASS

LENGTH ALONG VENTURI CENTERLINE

TABLE XXIII. (CONTD)

TS= 650.60	PS=224.9916	TT= 654.82	PT=235.0009	M= .25473	VAIR= 319.76	X1N= .04229	
TF= 542.11	540.59	539.06	537.74	536.17			
VF= 73.74	62.47	51.44	42.09	34.64			
E = .05591	.04894	.04186	.03577	.02949			
EW= .04634	.04014	.03383	.02839	.02287			
D = 15.71840	19.49022	24.02959	31.75204	42.18191			
W = .35070E-11	.64086E-11	.14180E-10	.29178E-10	.60117E-10			

VENTURI COND. CONT'D

TS= 649.58	PS=224.5953	TT= 653.08	PT=235.0465	M= .26076	VAIR= 325.17	X1N= .08729	
TF= 545.58	543.39	541.29	539.55	537.81			
VF= 85.58	72.51	59.93	49.68	39.95			
E = .07527	.06455	.05745	.04962	.04109			
EW= .06231	.05672	.04670	.03976	.03249			
D = 15.69012	19.45028	24.07667	31.68646	42.10156			
W = .35270E-11	.67092E-11	.13990E-10	.28816E-10	.67446E-10			

TS= 648.81	PS=224.1804	TT= 652.29	PT=234.9909	M= .26490	VAIR= 330.69	X1N= .10229	
TF= 549.61	546.66	543.79	541.53	539.36			
VF= 96.38	81.82	67.64	56.83	44.93			
E = .08208	.06246	.07207	.06262	.05255			
EW= .07594	.06773	.05088	.05065	.04197			
D = 15.65262	19.39091	24.00890	31.60267	41.99086			
W = .34705E-11	.64129E-11	.13814E-10	.28509E-10	.66705E-10			

TS= 647.41	PS=223.7467	TT= 656.50	PT=234.9336	M= .26966	VAIR= 336.35	X1N= .12229	
TF= 550.04	550.16	546.56	543.69	540.97			
VF= 106.78	90.75	75.06	62.14	49.75			
E = .10587	.09595	.08506	.07476	.06345			
EW= .08677	.07866	.06939	.06061	.05094			
D = 15.61762	19.34029	24.73992	31.51603	41.88059			
W = .34398E-11	.63954E-11	.13658E-10	.28210E-10	.66160E-10			

TS= 646.31	PS=223.3610	TT= 659.71	PT=236.8755	M= .27453	VAIR= 342.14	X1N= .14229	
TF= 550.09	553.95	549.53	546.02	542.73			
VF= 116.83	99.48	82.30	68.16	54.50			
E = .11714	.10091	.08860	.08551	.07347			
EW= .09628	.08730	.07830	.06930	.05915			
D = 15.57538	19.30497	24.67687	31.43123	41.77989			
W = .34000E-11	.66735E-11	.13527E-10	.27947E-10	.65580E-10			

TS= 645.23	PS=222.8372	TT= 654.95	PT=234.8167	M= .27953	VAIR= 348.07	X1N= .16229	
TF= 561.23	557.27	552.65	548.50	544.60			
VF= 126.77	108.15	89.62	74.19	59.28			
E = .12878	.11668	.10515	.09474	.08243			
EW= .10621	.09559	.08566	.07689	.06648			
D = 15.51979	19.25334	24.62346	31.35651	41.67841			
W = .33626E-11	.64193E-11	.13428E-10	.27721E-10	.65077E-10			

TS= 644.17	PS=222.3556	TT= 654.23	PT=234.7571	M= .28468	VAIR= 354.19	X1N= .18229	
TF= 563.84	560.02	555.53	551.89	548.58			
VF= 136.77	116.88	96.98	80.32	64.14			
E = .14050	.12653	.11331	.10248	.09028			
EW= .11627	.10399	.09243	.08317	.07208			
D = 15.46034	19.19419	24.56748	31.29283	41.58730			
W = .33240E-11	.63557E-11	.13320E-10	.27513E-10	.64630E-10			

TS= 643.13	PS=221.8542	TT= 653.56	PT=234.6967	M= .28998	VAIR= 360.58	X1N= .20229	
TF= 566.15	562.43	558.03	553.64	549.65			
VF= 146.97	125.01	104.54	86.64	69.16			

TABLE XXIII. (CONTD)

E =	.15200	.13635	.12136	.10922	.09703
Ew=	.12620	.11238	.09926	.08870	.07839
D =	15.30920	19.13239	24.50606	31.23434	41.50029
W =	.32874E-11	.62962E-11	.13220E-10	.27346E-10	.64247E-10

TS=	642.13	PS=221.3314	TT= 652.93	PT=234.6356	M= .29547	VAIR= 367.02	XIN= .22229
TF=	568.29	564.63	560.30	555.95	550.82		
VF=	157.56	135.11	112.40	93.22	74.42		
E =	.16330	.14596	.12930	.11575	.10277		
Ew=	.13584	.12060	.10603	.09423	.08306		
D =	15.33832	19.06984	24.44293	31.17179	41.44144		
W =	.32512E-11	.62378E-11	.13121E-10	.27201E-10	.63921E-10		

TS=	641.15	PS=220.7860	TT= 652.35	PT=234.5741	M= .30111	VAIR= 373.76	XIN= .24229
TF=	570.37	566.75	562.46	558.13	552.90		
VF=	168.73	144.92	120.72	100.19	80.80		
E =	.17402	.15524	.13704	.12215	.10791		
Ew=	.14506	.12855	.11262	.09965	.08732		
D =	15.27878	19.00806	24.37977	31.10846	41.37955		
W =	.32165E-11	.61815E-11	.13024E-10	.27030E-10	.63624E-10		

TS=	640.21	PS=220.2166	TT= 651.81	PT=234.5126	M= .30495	VAIR= 380.73	XIN= .26229
TF=	572.42	568.82	564.55	560.22	555.03		
VF=	180.45	155.25	129.58	107.55	85.89		
E =	.18412	.16408	.14448	.12834	.11284		
Ew=	.15377	.13612	.11896	.10498	.09147		
D =	15.22172	18.94826	24.31799	31.04592	41.31754		
W =	.31837E-11	.61270E-11	.12931E-10	.26880E-10	.63335E-10		

TS=	639.29	PS=219.6220	TT= 651.34	PT=234.4512	M= .31299	VAIR= 387.94	XIN= .28229
TF=	574.15	570.58	566.35	562.04	556.84		
VF=	191.49	165.03	137.86	114.60	91.56		
E =	.19355	.17240	.15154	.13427	.11758		
Ew=	.16191	.14326	.12508	.10993	.09546		
D =	15.16780	18.89126	24.25856	30.98527	41.25690		
W =	.31531E-11	.60771E-11	.12842E-10	.26729E-10	.63056E-10		

TS=	638.40	PS=219.0000	TT= 650.91	PT=234.3903	M= .31924	VAIR= 395.41	XIN= .30229
TF=	575.60	572.07	567.80	563.60	558.42		
VF=	201.80	174.23	145.76	121.28	96.96		
E =	.20236	.18023	.15820	.13994	.12214		
Ew=	.16954	.15088	.13074	.11475	.09932		
D =	15.11661	18.83666	24.20109	30.92611	41.19728		
W =	.31244E-11	.60293E-11	.12758E-10	.26584E-10	.62707E-10		

TS=	637.53	PS=218.3511	TT= 650.52	PT=234.3294	M= .32571	VAIR= 403.15	XIN= .32229
TF=	576.83	573.33	569.19	564.96	559.01		
VF=	211.52	182.95	153.28	127.67	102.14		
E =	.21060	.18763	.16467	.14537	.12653		
Ew=	.17671	.15639	.13623	.11939	.10305		
D =	15.06788	18.78425	24.14541	30.86032	41.13018		
W =	.30974E-11	.59840E-11	.12678E-10	.26445E-10	.62527E-10		

TS=	636.66	PS=217.6706	TT= 650.17	PT=234.2602	M= .33240	VAIR= 411.15	XIN= .34229
TF=	577.88	574.43	570.34	566.16	561.05		
VF=	220.79	191.29	160.51	133.03	107.14		
E =	.21836	.19464	.17078	.15060	.13079		
Ew=	.18349	.16247	.14148	.12305	.10666		
D =	15.02160	18.73788	24.09144	30.81188	41.08062		

VENTURI CONDITIONS CONT'D

TABLE XXIII. (CONTD)

W =	.38719E-11	.59409E-11	.12600E-10	.26311E-10	.62275E-10

TS=	635.79	PS=216.9571	TT= 649.84	PT=234.2847	M= .33934	V&IR= 419.44	XIN= .36229
TF=	578.80	575.38	571.34	567.21	562.15		
VF=	229.68	199.32	167.48	139.78	111.99		
E =	.22568	.20130	.17642	.15562	.13490		
Ew=	.10091	.14826	.14452	.12814	.11017		
D =	14.87699	18.68541	24.03814	30.75474	41.02338		
W =	.38477E-11	.58998E-11	.12526E-10	.26181E-10	.62031E-10		

VENTURI CONDITIONS CONT'D

TS=	634.82	PS=216.2081	TT= 649.55	PT=234.1431	M= .34453	V&IR= 428.64	XIN= .39229
TF=	579.68	576.21	572.23	568.15	563.14		
VF=	238.28	207.10	176.24	145.58	116.72		
E =	.23261	.20764	.18222	.16047	.13890		
Ew=	.19681	.17380	.15136	.13233	.11358		
D =	14.93448	18.63872	23.98837	30.70290	40.96725		
W =	.38240E-11	.58605E-11	.12455E-10	.26056E-10	.61784E-10		

TS=	634.84	PS=215.4218	TT= 649.27	PT=234.0788	M= .35399	V&IR= 436.95	XIN= .40229
TF=	580.31	576.94	573.01	568.99	564.03		
VF=	248.63	214.67	180.86	151.25	121.36		
E =	.23918	.21369	.18759	.16515	.14278		
Ew=	.20181	.17989	.15603	.13635	.11689		
D =	14.89378	18.59367	23.93986	30.65827	40.91201		
W =	.38836E-11	.58230E-11	.12387E-10	.25835E-10	.61562E-10		

TS=	633.14	PS=214.5828	TT= 649.01	PT=234.0128	M= .36173	V&IR= 446.18	XIN= .42229
TF=	580.93	577.59	573.78	569.73	564.43		
VF=	254.78	222.88	187.34	156.80	125.90		
E =	.24543	.21948	.19276	.16968	.14658		
Ew=	.20735	.18417	.16052	.14026	.12012		
D =	14.85493	18.55615	23.89113	30.59882	40.85765		
W =	.39021E-11	.57869E-11	.12321E-10	.25810E-10	.61337E-10		

TS=	632.22	PS=213.7264	TT= 648.76	PT=233.9449	M= .36978	V&IR= 455.79	XIN= .44228
TF=	581.49	578.17	574.32	570.40	565.56		
VF=	262.79	229.35	193.78	162.27	130.39		
E =	.25139	.22503	.19775	.17406	.15022		
Ew=	.21265	.18985	.16486	.14485	.12327		
D =	14.81484	18.50807	23.84452	30.54848	40.80413		
W =	.39622E-11	.57523E-11	.12257E-10	.25706E-10	.61118E-10		

TS=	631.27	PS=212.8805	TT= 648.53	PT=233.8749	M= .37816	V&IR= 465.76	XIN= .46229
TF=	581.97	578.67	574.87	571.00	566.22		
VF=	278.68	236.53	199.98	167.67	136.82		
E =	.25789	.23035	.20255	.17831	.15388		
Ew=	.21772	.18374	.16906	.14773	.12634		
D =	14.78852	18.46733	23.79913	30.49922	40.75145		
W =	.39431E-11	.57190E-11	.12196E-10	.25584E-10	.60804E-10		

TS=	636.29	PS=211.8292	TT= 648.32	PT=233.8425	M= .38688	V&IR= 476.13	XIN= .48228
TF=	582.40	579.12	575.33	571.53	566.81		
VF=	278.48	243.62	206.29	173.82	138.21		
E =	.26254	.23566	.20718	.18243	.15729		
Ew=	.22259	.18827	.17313	.15130	.12934		
D =	14.74547	18.42703	23.75492	30.45088	40.69956		
W =	.39248E-11	.56868E-11	.12136E-10	.25486E-10	.60694E-10		

TABLE XXIII. (CONTD)

VENTURI CONDITIONS CONT'D

TS= 629.27	PS=210.8025	TT= 648.11	PT=233.7274	M= .39024	VAIR= 479.91	XIN= .60229	
TF=	582.77	579.50	575.77	572.08	567.34		
VF=	285.93	250.43	212.14	178.18	143.46		
E =	.26770	.24033	.21184	.18648	.16066		
EW=	.22720	.20258	.17782	.15475	.13225		
D =	14.71207	18.30997	23.71227	30.48619	40.64891		
W =	.29074E-11	.56564E-11	.12079E-10	.25343E-10	.60492E-10		
TS= 628.77	PS=210.3588	TT= 647.92	PT=233.6523	M= .34493	VAIR= 423.14	XIN= .62229	
TF=	583.05	579.81	576.12	572.39	567.75		
VF=	290.68	255.85	214.56	182.85	146.74		
E =	.27203	.24452	.21554	.18993	.16371		
EW=	.23099	.20621	.18038	.15777	.13483		
D =	14.68958	18.35792	23.67533	30.36297	40.00362		
W =	.28932E-11	.56306E-11	.12036E-10	.25292E-10	.60312E-10		
TS= 632.76	PS=215.2132	TT= 647.76	PT=233.5999	M= .30732	VAIR= 378.96	XIN= .64229	
TF=	583.43	580.20	576.53	572.53	568.27		
VF=	293.38	258.16	219.64	185.88	149.34		
E =	.27556	.24866	.21893	.19306	.16644		
EW=	.23487	.20928	.15338	.16044	.13715		
D =	14.66654	18.33630	23.64364	30.32697	40.56345		
W =	.28816E-11	.56088E-11	.11907E-10	.25212E-10	.60150E-10		
TS= 635.66	PS=218.7957	TT= 647.61	PT=233.5638	M= .27684	VAIR= 342.14	XIN= .66229	
TF=	583.78	580.66	576.96	573.29	568.76		
VF=	294.77	260.12	221.88	187.25	151.68		
E =	.27836	.25103	.22157	.19583	.16891		
EW=	.23649	.21186	.18584	.16292	.13928		
D =	14.64844	18.31322	23.62176	30.29520	40.52768		
W =	.28725E-11	.55965E-11	.11949E-10	.25141E-10	.60004E-10		
TS= 637.70	PS=221.6282	TT= 647.67	PT=233.5368	M= .25115	VAIR= 310.91	XIN= .68229	
TF=	584.04	580.96	577.37	573.73	569.23		
VF=	295.16	261.22	223.61	188.93	153.04		
E =	.28032	.25346	.22442	.19830	.17115		
EW=	.23815	.21396	.18864	.16494	.14116		
D =	14.63844	18.29439	23.60767	30.27293	40.49498		
W =	.28643E-11	.55757E-11	.11917E-10	.25077E-10	.59871E-10		
TS= 639.29	PS=223.6924	TT= 647.36	PT=233.5171	M= .22919	VAIR= 284.07	XIN= .70229	
TF=	584.28	581.23	577.73	574.14	569.68		
VF=	294.91	261.65	224.48	190.17	154.33		
E =	.28200	.25530	.22659	.20040	.17315		
EW=	.23963	.21553	.18998	.16682	.14200		
D =	14.62477	18.28065	23.57679	30.24736	40.47185		
W =	.28607E-11	.55645E-11	.11898E-10	.25021E-10	.59750E-10		
TS= 640.53	PS=225.1160	TT= 647.26	PT=233.5025	M= .21619	VAIR= 268.77	XIN= .72229	
TF=	584.70	581.32	578.04	574.51	570.09		
VF=	293.98	261.64	224.94	191.04	155.34		
E =	.28422	.25628	.22838	.20240	.17582		
EW=	.24173	.21827	.19143	.16847	.14447		
D =	14.61871	18.27226	23.55974	30.22490	40.44449		
W =	.28520E-11	.55592E-11	.11867E-10	.24971E-10	.59643E-10		
TS= 641.50	PS=226.4116	TT= 647.17	PT=233.4909	M= .19359	VAIR= 240.36	XIN= .74229	
TF=	585.24	581.62	578.25	574.83	570.47		
VF=	292.41	261.24	225.14	191.61	156.11		

TABLE XXIII. (CONTD)

```
E =          .28685          .25787          .22972          .20407          .17649
Ew=          .24418          .21779          .19256          .14989          .14589
D =        14.59404        18.26014        23.54679        30.20545        40.41975
W =     .28436E-11      .55485E-11      .11851E-10      .2492AE-10      .59561E-10

TS=  642.26   PS=227.4588   TT=  647.07   PT=233.4813   M=  .17A9A   VAIR=  222.36   XIN=  .68229
TF=        585.86          582.02          578.37          575.10          570.82
VF=        290.24          260.43          225.11          191.94          154.49
E =          .23978          .25988          .23060          .20546          .1781A
Ew=          .2A698          .21966          .19327          .17107          .14717
D =        14.57345        18.24483        23.53822        30.18911        40.39748
W =     .28333E-11      .55352E-11      .11A48E-10      .24893E-10      .59452E-10

TS=  642.86   PS=228.3121   TT=  646.98   PT=233.4731   M=  .16604   VAIR=  206.37   XIN=  .68229
TF=        586.56          582.58          578.62          575.29          571.12
VF=        287.54          259.24          224.86          192.88          157.18
E =          .29295          .26218          .23188          .20654          .17981
Ew=          .24982          .22178          .19447          .17197          .14838
D =        14.55535        18.22729        23.52615        30.17634        40.37769
W =     .28223E-11      .55201E-11      .11823E-10      .24866E-10      .59373E-10

TS=  643.33   PS=229.0157   TT=  646.88   PT=233.4659   M=  .15589   VAIR=  193.83   XIN=  .70888
TS=  642.58   PS=228.0825   TT=  646.88   PT=233.4659   M=  .18286   VAIR=  227.23   XIN=
TS=  642.58   PS=228.0825   TT=  646.88   PT=233.4659   M=  .18286   VAIR=  227.23   XIN=

DELP=    7.1200    DELPC=    7.1175    COUN7=    4

E=           .29295          .26218          .23188          .20654          .17981
TS=  642.58   PS=228.0825   TT=  646.88   PT=233.4659   M=  .18286   VAIR=  227.23   XIN=

AIR FLOW RATE=     .08991 PPS     DISCHARGE COEFF.=   .8219     ATR-FUEL RATIO=   16.1833

VFUEL=224.16  TFUEL=573.99  VAIR=227.23  TT= 646.9  FUELP=253.72  SMD=  7.88  PPM=   16.0846  SLM=  1.188

DROPLET  1 E= .10      X1, X2=   .20000    .60781 IN
DROPLET  1 E= .20      X1, X2=   .20033    .63111 IN
DROPLET  1 E= .30      X1, X2=   .20160    .64987 IN
DROPLET  1 E= .40      X1, X2=   .20542    .65962 IN
DROPLET  1 E= .50      X1, X2=   .21109    .65942 IN
DROPLET  1 E= .60      X1, X2=   .21939    .65862 IN
DROPLET  1 E= .70      X1, X2=   .22878    .65734 IN
DROPLET  1 E= .80      X1, X2=   .24488    .65521 IN
DROPLET  1 E= .90      X1, X2=   .24947    .65457 IN
DROPLET  1 E= .95      X1, X2=   .25177    .65425 IN
DROPLET  2 E= .10      X1, X2=   .20001    .61162 IN
DROPLET  2 E= .20      X1, X2=   .20058    .64505 IN
DROPLET  2 E= .30      X1, X2=   .20234    .66930 IN
DROPLET  2 E= .40      X1, X2=   .20753    .68371 IN
DROPLET  2 E= .50      X1, X2=   .21584    .68704 IN
```

END OF VENTURI

} GAP FLOW COND.

SHEET THICKNESS, MICRONS

POINTS IN GOSMAN FIELD FOR FRACTIONS EVAPORATED

TABLE XXIII. (CONTD)

DROPLET	2 E= .60	X1, X2=	.22704	.68574 IN
DROPLET	2 E= .70	X1, X2=	.24229	.68396 IN
DROPLET	2 E= .80	X1, X2=	.26779	.68084 IN
DROPLET	2 E= .90	X1, X2=	.29375	.67741 IN
DROPLET	2 E= .95	X1, X2=	.29807	.67681 IN
DROPLET	3 E= .10	X1, X2=	.20003	.62000 IN
DROPLET	3 E= .20	X1, X2=	.20000	.66638 IN
DROPLET	3 E= .30	X1, X2=	.20335	.70121 IN
DROPLET	3 E= .40	X1, X2=	.20900	.72334 IN
DROPLET	3 E= .50	X1, X2=	.22160	.72721 IN
DROPLET	3 E= .60	X1, X2=	.23985	.72592 IN
DROPLET	3 E= .70	X1, X2=	.26247	.72402 IN
DROPLET	3 E= .80	X1, X2=	.29933	.72051 IN
DROPLET	3 E= .90	X1, X2=	.37216	.71142 IN
DROPLET	3 E= .95	X1, X2=	.43322	.70127 IN
DROPLET	4 E= .10	X1, X2=	.20000	.63190 IN
DROPLET	4 E= .20	X1, X2=	.20120	.69693 IN
DROPLET	4 E= .30	X1, X2=	.20450	.74814 IN
DROPLET	4 E= .40	X1, X2=	.21277	.78219 IN
DROPLET	4 E= .50	X1, X2=	.23005	.79193 IN
DROPLET	4 E= .60	X1, X2=	.25532	.78879 IN
DROPLET	4 E= .70	X1, X2=	.29053	.78441 IN
DROPLET	4 E= .80	X1, X2=	.34441	.77772 IN
DROPLET	4 E= .90	X1, X2=	.45041	.76317 IN
DROPLET	4 E= .95	X1, X2=	.56920	.73956 IN
DROPLET	5 E= .10	X1, X2=	.20015	.65254 IN
DROPLET	5 E= .20	X1, X2=	.20107	.75205 IN
DROPLET	5 E= .30	X1, X2=	.20656	.83391 IN
DROPLET	5 E= .40	X1, X2=	.21760	.89120 IN
DROPLET	5 E= .50	X1, X2=	.24263	.91470 IN
DROPLET	5 E= .60	X1, X2=	.28264	.91534 IN
DROPLET	5 E= .70	X1, X2=	.33602	.91327 IN
DROPLET	5 E= .80	X1, X2=	.41475	.90960 IN

TABLE XXIII (CONTD)

DNOPLET S E= .90 X1, X2= .56855 .90327 IA

DNOPLET S E= .95 X1, X2= .73500 .80581 IA

FEVAP=

I=1	I=2	3	4	5	6	7	
0.	0.	0.	0.	0.	0.	0.	J=1
0.	0.	0.	0.	0.	0.	0.	
0.	0.	0.	0.	0.	0.	0.	
0.	0.	0.	0.	0.	0.	0.	2
0.	0.	0.	0.	0.	0.	0.	
0.	0.	0.	0.	0.	0.	0.	
0.	0.	0.	0.	0.	0.	0.	3
0.	0.	0.	0.	0.	0.	0.	
0.	0.	0.	0.	0.	0.	0.	
0.	0.	0.	0.	0.	0.	0.	4
0.	0.	0.	0.	0.	0.	0.	
0.	0.	0.	0.	0.	0.	0.	
0.	0.	0.	0.	0.	0.	0.	5
0.	0.	0.	0.	0.	0.	0.	
0.	0.	0.	0.	0.	0.	0.	
0.	0.	0.	0.	0.	0.	0.	6
0.	0.	0.	0.	0.	0.	0.	
0.	.1330E+02	0.	0.	0.	0.	0.	
0.	0.	0.	0.	0.	0.	0.	7
0.	0.	0.	0.	0.	0.	0.	
0.	.3136E+02	.1393E+01	0.	0.	0.	0.	
0.	0.	0.	0.	0.	0.	0.	8
0.	0.	0.	0.	0.	0.	0.	
0.	.7311E+01	.1051E+01	0.	0.	0.	0.	
0.	0.	0.	0.	0.	0.	0.	9
0.	0.	0.	0.	0.	0.	0.	
0.	.4255E+01	.1758E+01	.0200E-01	0.	0.	0.	
0.	0.	0.	0.	0.	0.	0.	10
0.	0.	0.	0.	0.	0.	0.	
0.	0.	0.	0.	0.	0.	0.	
0.	0.	0.	0.	0.	0.	0.	11
0.	0.	0.	0.	0.	0.	0.	
0.	0.	0.	0.	0.	0.	0.	
0.	0.	0.	0.	0.	0.	0.	12
0.	0.	0.	0.	0.	0.	0.	
0.	0.	0.	0.	0.	0.	0.	
0.	0.	0.	0.	0.	0.	0.	13
0.	0.	0.	0.	0.	0.	0.	
0.	0.	0.	0.	0.	0.	0.	
0.	0.	0.	0.	0.	0.	0.	14
0.	0.	0.	0.	0.	0.	0.	
0.	0.	0.	0.	0.	0.	0.	
0.	0.	0.	0.	0.	0.	0.	15
0.	0.	0.	0.	0.	0.	0.	

FEVAP (21, 21)

EVAPORATION RATES
LB/SEC/FT³/RADIAN
AT NODE POINTS
IN GOSMAN FIELD

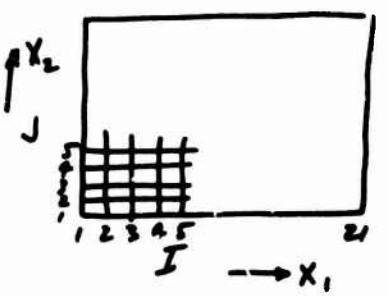


TABLE XXIII. (CONTD)

0. 0. 0. 0. 0. 0. 0. J=16
0. 0. 0. 0. 0. 0. 0.
0. 0. 0. 0. 0. 0. 0.

0. 0. 0. 0. 0. 0. 0. 17
0. 0. 0. 0. 0. 0. 0.
0. 0. 0. 0. 0. 0. 0.

0. 0. 0. 0. 0. 0. 0. 18
0. 0. 0. 0. 0. 0. 0.
0. 0. 0. 0. 0. 0. 0.

0. 0. 0. 0. 0. 0. 0. 19
0. 0. 0. 0. 0. 0. 0.
0. 0. 0. 0. 0. 0. 0.

0. 0. 0. 0. 0. 0. 0. 20
0. 0. 0. 0. 0. 0. 0.
0. 0. 0. 0. 0. 0. 0.

0. 0. 0. 0. 0. 0. 0. 21
0. 0. 0. 0. 0. 0. 0.
0. 0. 0. 0. 0. 0. 0.

LAST DROPLET CONDITIONS--

DROP	TF	VF	D	E
1	.28225E+03	.75720E+01	.13000E-09	.99000E+00
2	.37214E+03	.72046E+01	.56776E-05	.97053E+00
3	.26099E+03	.66555E+01	.10000E-09	.99000E+00
4	.65208E+03	.59257E+01	.11365E-04	.95839E+00
5	.65271E+03	.46694E+01	.14049E-04	.95138E+00

SPRAY TRAJECTORY — VGAS ≈ 8 FT/SEC

0 - 20 / VOLUME 4.671					20 - 40 / VOLUME 5.771					40 - 60 / VOLUME 7.353					60 - 80 / VOLUME 9.335					80 - 100 / VOLUME 12.361 MICRONS				
D	X TF	VF	Y E+100	/	D	X TF	VF	Y E+100	/	D	X TF	VF	Y E+100	/	D	X TF	VF	Y E+100	/	D	X TF	VF	Y E+100	/
.20			.60		.20			.60		.20			.60		.20			.60		.20			.60	
5.	574.	224.	0.	/	6.	574.	224.	0.	/	7.	574.	224.	0.	/	9.	574.	224.	0.	/	12.	574.	224.	0.	/
.20			.61		.20			.61		.20			.61		.20			.61		.20			.61	
4.	560.	183.	10.	/	6.	564.	196.	7.	/	7.	567.	205.	5.	/	9.	569.	212.	4.	/	12.	571.	217.	2.	/
.20			.62		.20			.62		.20			.62		.20			.62		.20			.62	
4.	573.	141.	13.	/	6.	571.	166.	10.	/	7.	560.	186.	8.	/	9.	568.	200.	6.	/	12.	569.	209.	4.	/
.20			.63		.20			.63		.20			.63		.20			.63		.20			.63	
4.	583.	101.	16.	/	5.	570.	137.	12.	/	7.	573.	167.	9.	/	9.	569.	187.	8.	/	12.	569.	202.	6.	/
.20			.64		.20			.64		.20			.64		.20			.64		.20			.64	
4.	591.	63.	20.	/	5.	584.	109.	15.	/	7.	577.	148.	11.	/	9.	572.	176.	9.	/	12.	569.	194.	7.	/
.20			.65		.20			.65		.20			.65		.20			.65		.20			.65	
4.	599.	20.	25.	/	5.	589.	82.	18.	/	7.	581.	129.	13.	/	9.	575.	162.	10.	/	12.	571.	187.	8.	/
.20			.66		.20			.66		.20			.66		.20			.66		.20			.66	
4.	608.	0.	32.	/	5.	594.	55.	22.	/	7.	585.	111.	15.	/	9.	578.	149.	11.	/	12.	573.	179.	8.	/
.21			.66		.20			.67		.20			.67		.20			.67		.20			.67	
4.	611.	8.	50.	/	5.	599.	31.	26.	/	7.	588.	92.	17.	/	9.	581.	137.	13.	/	12.	574.	171.	9.	/
.22			.66		.20			.68		.20			.68		.20			.68		.20			.68	
3.	446.	8.	50.	/	5.	606.	12.	31.	/	7.	591.	74.	20.	/	9.	583.	124.	14.	/	12.	576.	164.	10.	/
.23			.66		.21			.69		.20			.69		.20			.69		.20			.69	
3.	585.	0.	72.	/	5.	611.	7.	39.	/	7.	595.	57.	22.	/	9.	584.	112.	15.	/	12.	578.	154.	11.	/
.24			.66		.22			.69		.20			.70		.20			.70		.20			.70	
3.	760.	8.	74.	/	4.	618.	7.	50.	/	7.	599.	40.	25.	/	9.	584.	100.	17.	/	12.	580.	149.	12.	/

TABLE XXIII. (CONTD)

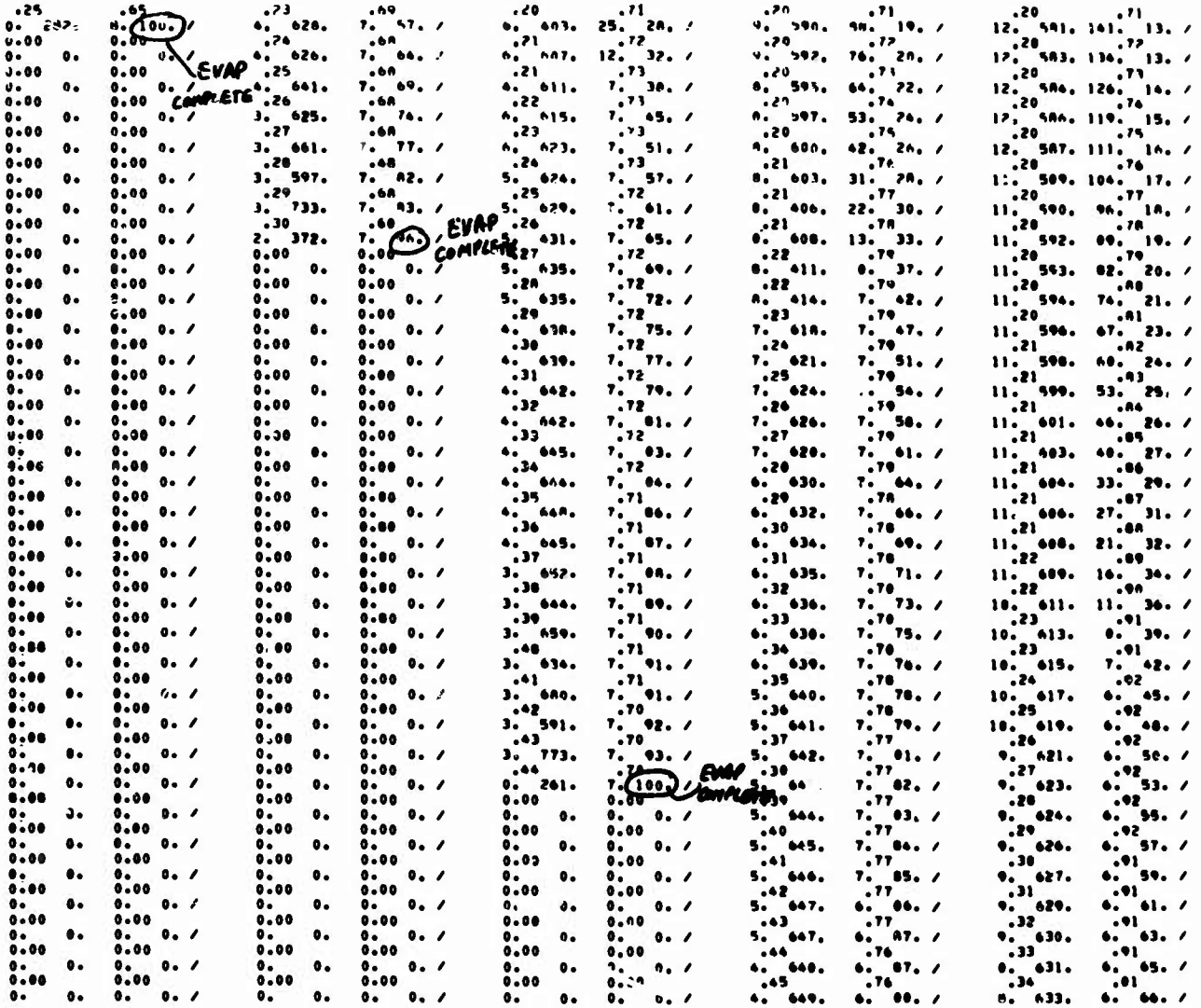


TABLE XXIII. (CONTD)

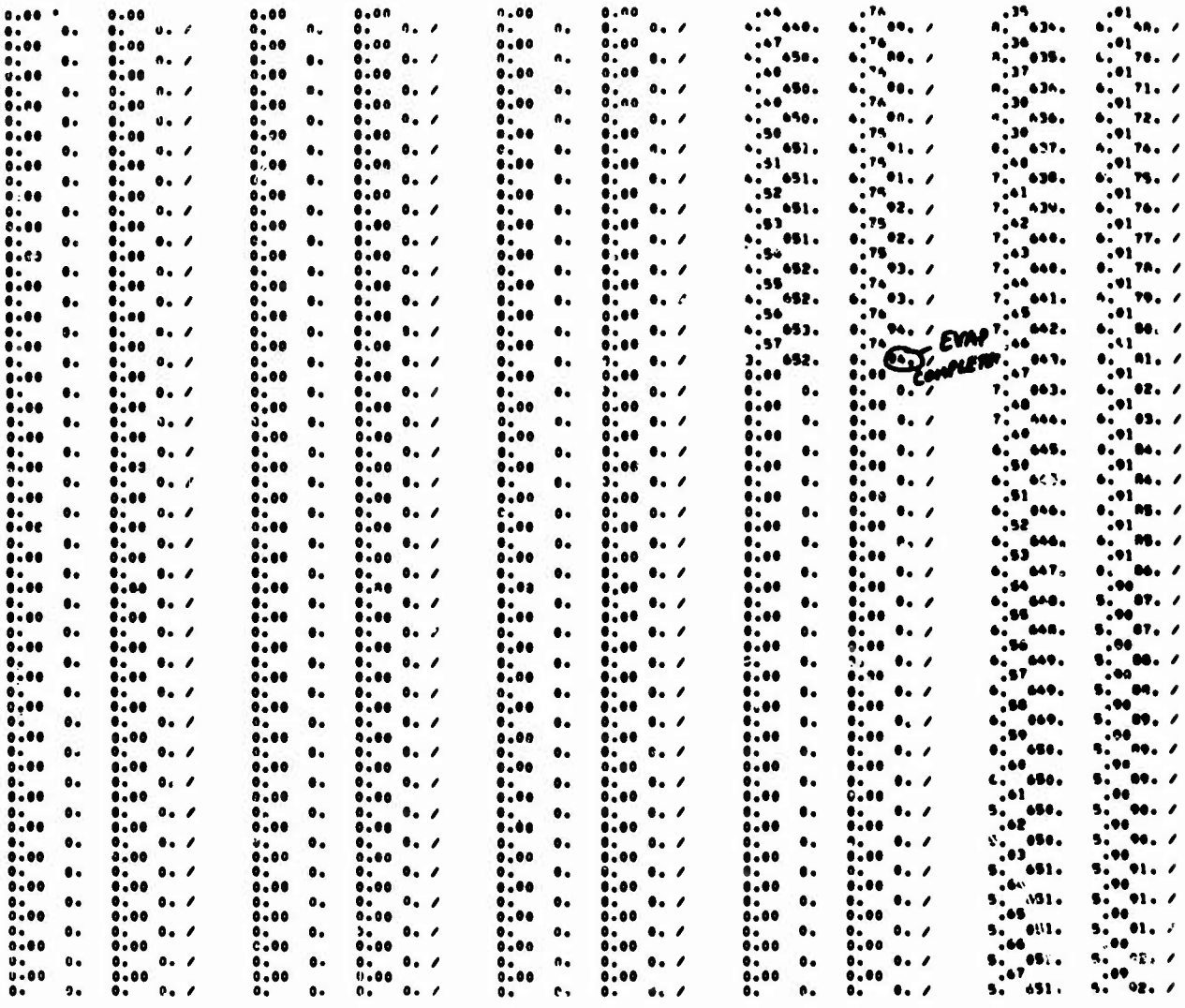


TABLE XXIII. (CONTD)

0.00		0.00		0.00		0.00		0.00		0.00		0.00		0.00		.64		.69	
0.	0.	0.	0. /	0.	0.	0.	0. /	0.	0.	0.	0. /	0.	0.	0.	0. /	5.	652.	5.	92. /
0.00		0.00		0.00		0.00		0.00		0.00		0.00		0.00		.69		.69	
0.	0.	0.	0. /	0.	0.	0.	0. /	0.	0.	0.	0. /	0.	0.	0.	0. /	5.	652.	5.	93. /
0.00		0.00		0.00		0.00		0.00		0.00		0.00		0.00		.70		.69	
0.	0.	0.	0. /	0.	0.	0.	0. /	0.	0.	0.	0. /	0.	0.	0.	0. /	5.	652.	5.	93. /
0.00		0.00		0.00		0.00		0.00		0.00		0.00		0.00		.71		.69	
0.	0.	0.	0. /	0.	0.	0.	0. /	0.	0.	0.	0. /	0.	0.	0.	0. /	5.	652.	5.	93. /
0.00		0.00		0.00		0.00		0.00		0.00		0.00		0.00		.72		.69	
0.	0.	0.	0. /	0.	0.	0.	0. /	0.	0.	0.	0. /	0.	0.	0.	0. /	5.	652.	5.	94. /
0.00		0.00		0.00		0.00		0.00		0.00		0.00		0.00		.73		.69	
0.	0.	0.	0. /	0.	0.	0.	0. /	0.	0.	0.	0. /	0.	0.	0.	0. /	5.	653.	5.	94. /
0.00		0.00		0.00		0.00		0.00		0.00		0.00		0.00		.74		.69	
0.	0.	0.	0. /	0.	0.	0.	0. /	0.	0.	0.	0. /	0.	0.	0.	0. /	5.	653.	5.	95. /

LEVAL COMPLETE

APPENDIX III

AIR-BLAST FILM VAPORIZER COMPUTER PROGRAM 1529

1.0 INTRODUCTION

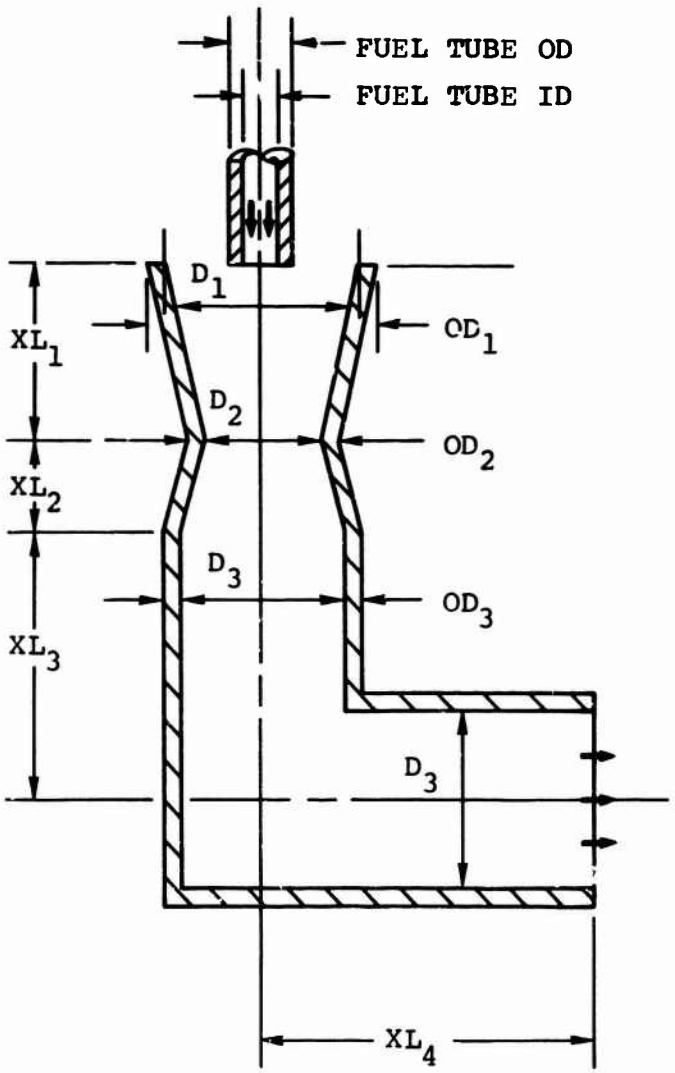
The air-blast film vaporizer program computes flow conditions in a pipe used to inject fuel onto the wall of the combustor for the purpose of generating a fuel film. Pipe airflow, fraction of fuel evaporated, and pipe temperature are calculated. Upon completion of the pipe calculations, the unevaporated fuel-film formation on the combustor dome, film thickness, and evaporation rates are computed. Input options include a noncircular pipe (Option A) and provisions for bypassing the pipe calculation to provide a means for computing only the film evaporation (Option B). Film evaporation can be computed for radial flow or constant width flow, as on a flat plate or cylindrical wall.

2.0 PROGRAM INPUT WITH L-PIPE (OPTION A)

For Option A, geometric definition of a circular L-pipe is shown in Figure 171. Dimensional data is entered on the Option A Data Sheet, Figure 172, Cards 3 and 4. Figure 173 shows the required geometries for entering a configuration with noncircular portions approximated as ellipses. Cards 8A through 11B are entered only if the noncircular input is desired (this is indicated by D_2 blank or zero).

Other data used in calculations pertaining to the L-pipe only include:

		Data Card No.
(a)	Fuel code (JP-4 or JP-5)	2
(b)	Fuel temperature, °R	2
(c)	L-pipe inlet pressure, psia	2
(d)	L-pipe inlet air temperature, °R	2
(e)	Fuel flow, lb/hr	2
(f)	L-pipe pressure drop, psi	2
(g)	L-pipe external flow temperature and velocity	5, 6, 7



INPUTS FOR CIRCULAR PIPE FOR CONSTANT DIAMETER

$OD_1 = OD_2 = OD_3$ (OUTSIDE DIAMETER)

$D_1 = D_2 = D_3$ (INSIDE DIAMETER)

FUEL TUBE EXIT IS AT D_1

Figure 171. L-Pipe Air-Blast Vaporizer Circular Pipe Geometry.

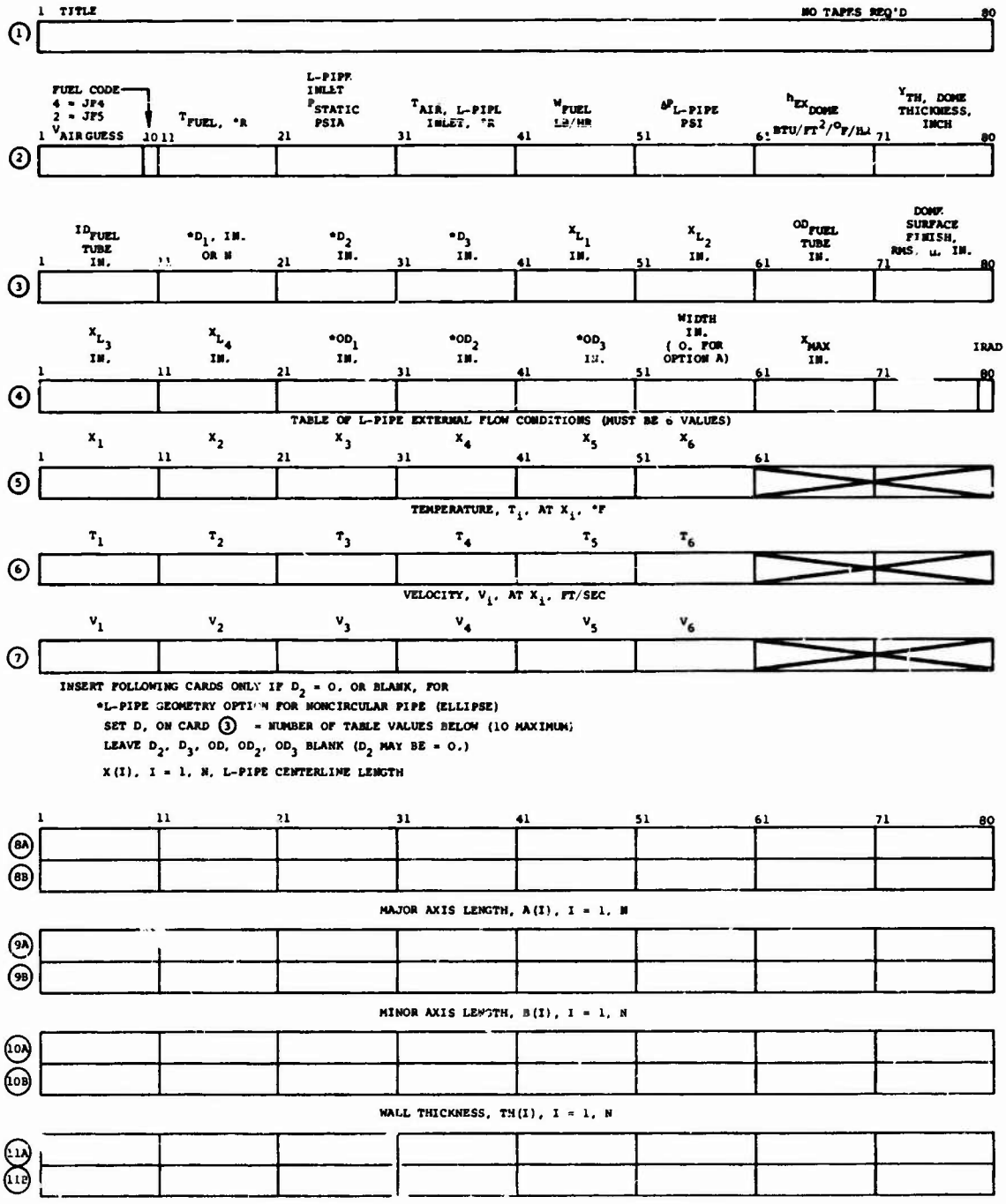


Figure 172. Film Vaporization Program, Air-Blast; Option A (With L-Pipe), Program No. 1529 Input Data.

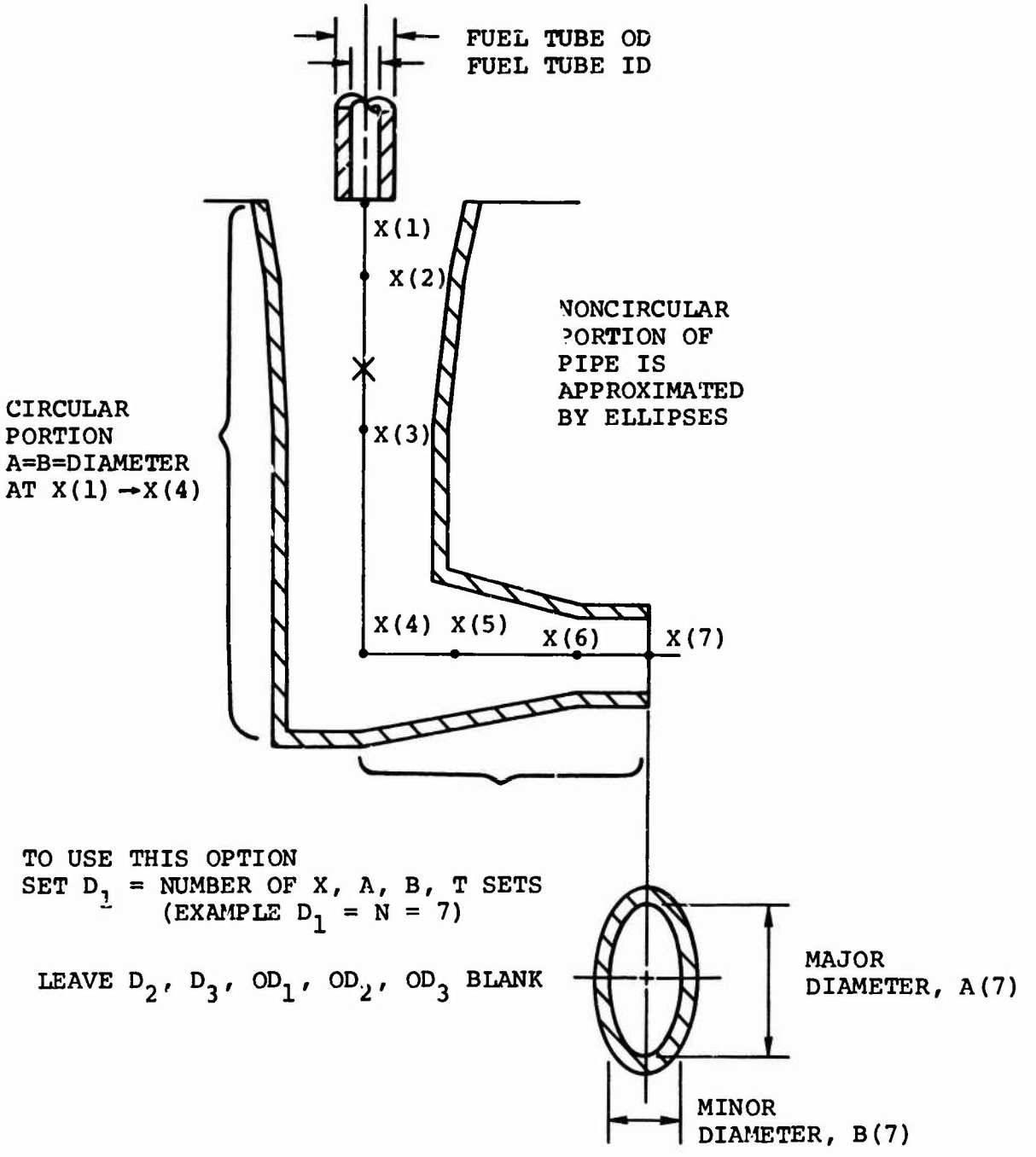


Figure 173. L-Pipe Air-Blast Vaporizer Noncircular Pipe.

The last item , g, is a tabulation of flow conditions around the L-pipe for use in calculating L-pipe temperature. Six sets of X, T, and V are entered. The values are estimated from primary-zone flow conditions, or can be parameterized to determine L-pipe temperature as a function of external conditions.

Remaining items on the data cards pertain to the film evaporation calculation and include:

		Data Card No.
(a)	h_{ex}, external dome heat-transfer coefficient	2
(b)	y_{th}, dome wall thickness, inches	2
(c)	Dome surface finish, microinches	3
(d)	Width for film spread, inches	4
(e)	X_{max}, length limit for evaporation calculation, inches	4
(f)	IRAD, indicator for flame radiation IRAD = 0, no radiation IRAD = 1, radiation included	4

Each of these is discussed as follows. The external heat transfer coefficient can be entered directly, if known. The program incorporates an equation for the heat-transfer coefficient in an annulus and requires an annulus velocity and hydraulic diameter. This equation is activated by inputting the velocity and hydraulic diameter as a negative combined number in the card space reserved for h_{ex}. For example, if the annulus velocity is 200 feet per second and the hydraulic diameter (2 annulus widths) is 0.5 in., a negative combined number of -200.5 is entered. The integer part of the number is the velocity, and the decimal part is the hydraulic diameter. Note that hydraulic diameter is limited to less than 1 inch. The value of h_{ex}, combustor dome thickness y_{th}, and surface finish influence the heat transfer from the wall to the film. This influence has been found to have only a minor effect on evaporation, since internal gas heat transfer predominates. Accuracy of these values is not critical.

Item (d) listed above is the width for fuel spreading. In a normal L-pipe calculation (Option A) this is set to 0.0, and the film is assumed to spread radially from the impingement

point. Gas flow conditions over the evaporating film are computed for a radial wall jet starting with L-pipe exit conditions. The primary-zone gas temperature is taken as the maximum of the 6 temperatures tabulated on Card 6. Radial-wall jet temperature stays constant for a short potential core length, then mixes gradually from L-pipe exit temperature toward gas temperature as a function of radius. Wall jet velocity decays toward zero.

Item (e), X_{max}, stops the calculation when this radial distance is reached. Item (f), IRAD, set to 1 causes a radiation input to the film heat balance. All radiation conditions are calculated within the program.

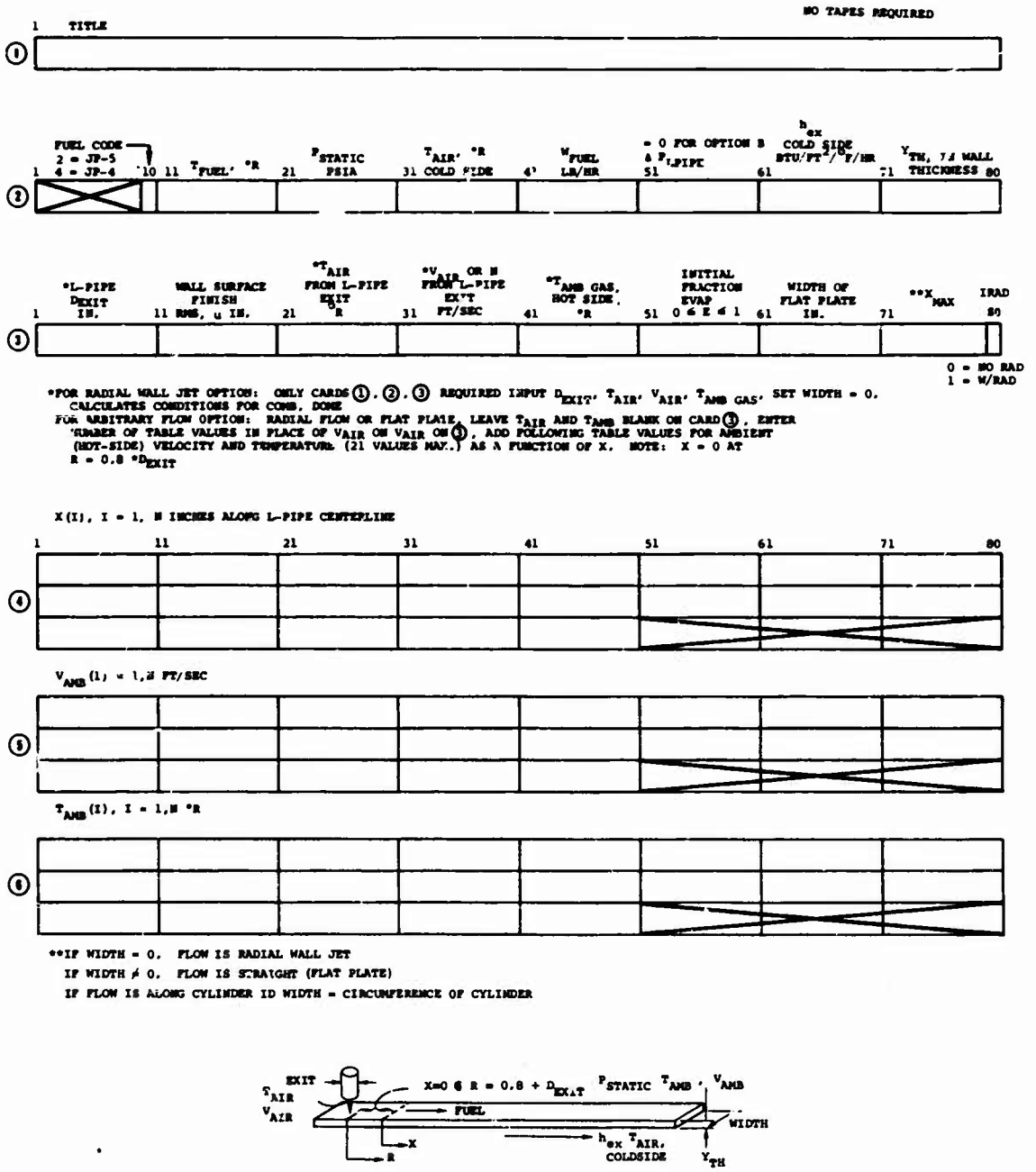
3.0 PROGRAM INPUT WITHOUT L-PIPE (OPTION B)

This option provides for film evaporation calculations independent of L-pipe output. The input for Option B is shown in Figure 174. Cards 1 and 2 are identical to that described in Section 2.0. Option B is activated by setting the L-pipe pressure drop to 0.0 on Card 2.

The fuel film can be considered to flow radially from a central point (as in Option A, width = 0), or along a constant width flat plate (enter plate width on Card 3). Flow conditions can be specified for a radial wall jet or an arbitrary input. For the radial wall jet conditions, the L-pipe exit temperature, velocity, and hot-side ambient gas temperature are entered on Card 3. For the arbitrary flow condition, T_{air} and T_{gas} (Card 3) are left blank. Tabulated sets of plate distance, X, air velocity, V, and air temperature, T, are entered on Cards 4, 5, and 6. The number of sets of X, V, and T is entered on Card 3 in place of V_{air}.

4.0 PROGRAM COMPUTATIONS

The listing for the program is given in Table XXIV. For Option A the calculation starts at the L-pipe inlet. Fuel from the fuel-injection tube is atomized and divided into five drop groups. Flow conditions along the L-pipe are computed considering drop evaporation, drag, friction loss, heat transfer, and area change. The airflow is iterated until the input pressure drop is matched. The main output information that is desired is the L-pipe airflow and discharge coefficient, fraction of the fuel evaporated in the L-pipe, and the L-pipe temperature.



*FOR RADIAL WALL JET OPTION: ONLY CARDS ①, ②, ③ REQUIRED INPUT D_{EXIT}, T_{AIR}, V_{AIR}, $T_{AMB\ GAS}$, SET WIDTH = 0. CALCULATES CONDITIONS FOR COMB. DOME
FOR ARBITRARY FLOW OPTION: RADIAL FLOW OR FLAT PLATE, LEAVE T_{AIR} AND T_{AMB} BLANK ON CARD ③. ENTER NUMBER OF TABLE VALUES IN PLACE OF V_{AIR} ON V_{AIR} ON ④, ADD FOLLOWING TABLE VALUES FOR AMBIENT (HOT-SIDE) VELOCITY AND TEMPERATURE (21 VALUES MAX.) AS A FUNCTION OF X. NOTE: X = 0 AT R = 0.8 *D_{EXIT}

**IF WIDTH = 0. FLOW IS RADIAL WALL JET
IF WIDTH ≠ 0. FLOW IS STRAIGHT (FLAT PLATE)
IF FLOW IS ALONG CYLINDER ID WIDTH = CIRCUMFERENCE OF CYLINDER

Figure 174. Film Vaporization Program, Air-Blast; Option B (Without L-Pipe), Program No. 1529 Input Data.

Film evaporation on the wall is computed by considering a turbulent velocity profile and integrated liquid flow rate to obtain a film thickness. Heat input from the air and wall is balanced against fuel temperature rise and evaporation. The main output desired is the rate of fuel evaporation, dome temperature, and final length for complete evaporation.

The main references for the computations are given in Shapiro[29], Priem[6], and Kinney[30]. Evaporation procedures of Priem were extended to provide for actual fuel distillation range as opposed to the single boiling-point approximation used in most references on evaporation.

5.0 PROGRAM OUTPUT

A typical program output for Option A is presented in Table XXV. Initial conditions are printed, followed by flow conditions at points along the L-pipe. This is followed by the film evaporation conditions as a function of length or radius on the dome

TABLE XXIV. LISTING OF PROGRAM NO. 1529

```
$$$
```

TABLE XXIV. (CONTD)

```
      DATA RNTAB / 3.E3,1.E4,3.E4,1.E5,3.E5,1.E6,1.E7  /,
     1 FTAB /.011,.008,.00625,.005,.00445,.0041,.0040  /
      DATA T9R /500.,600.,700.,800.,900.,1000.,1100.,1200.,1400.,1600./,
     1 CPTAB /.2405,.2410,.2422,.2440,.2462,.2490,.2519,.2550,.2613,
     2 .2670/
      DATA NTAB9 / 10 /
      DATA TDTAB / 660., 1060.,1460., 1860., 2260. /, NKMETL / 5 /,
     1   TABKMT / 76., 100., 130., 166., 195. /
      DATA RNLG10 / 0., 1., 2., 3., 4., 5., 5.39794 /, NUTABN / 7/,
     1 TABNU / .84, 1.83, 5.10, 15.7, 56.5, 245., 520./
C
    1 READ (60,1000) TITLE
      IF (EOF(60)) 999,2
  999 CALL EXIT
    2 CONTINUE
      WRITE (61,1010) TITLE
CCCCCCC
      NTABVT=0
      OPTION=0.
CCCCCC
      READ(60,1201) VAG,KFUEL,TFUELR,P3,T3R,PPM,DELP,HEX,YTH
      WRITE (61,1280) KFUEL,TFUELR,P3,T3R,PPM,DELP,HEX,YTH
 1201 FORMAT(F9.0,I1,7F10.2)
C     CHECK IF FUEL TUBE IS TO BE OMITTED
      IF (DELP .EQ. 0.) GO TO 800
C     GEOMETRY PARAMETERS (IN)
      READ (60,1210)FJET1D,D1A1,D1A2,D1A3,XL1,XL2,FJETOD,RMS
      WRITE(61,1290)FJET1D,D1A1,D1A2,D1A3,XL1,XL2,FJETOD,RMS
C     CONVERT RMS FROM MICROINCHES TO FT.
      RMS= RMS / 12.E6
      READ(60,1211) XL3,XL4,OD1,OD2,OD3,W1DTH,XLIMXX,DUME,IRAD
      WRITE(61,1340) XL3,XL4,OD1,OD2,OD3,W1DTH,XLIMXX
     * ,IRAD
      READ (60,1210) XTAB
      WRITE (61,1310) XTAB
      READ (60,1210) TAMB
      WRITE (61,1320) TAMB
      READ (60,1210) VAMB
      WRITE (61,1330) VAMB
      NXXXX= 0
      IF (D1A2 .NE. 0.) GO TO 190
C     READ TABLE OF X VS. MAJOR AXIS AND MINOR AXIS
      NXXXX= D1A1
      READ (60,1210) (XXXX(I),I=1,NXXXX)
      WRITE(61,1370) (XXXX(I),I=1,NXXXX)
      READ (60,1210) (AXISMJ(I),I=1,NXXXX)
      WRITE(61,1370) (AXISMJ(I),I=1,NXXXX)
      READ (60,1210) (AXISMN(I),I=1,NXXXX)
      WRITE(61,1370) (AXISMN(I),I=1,NXXXX)
      DO 140 I=1,NXXXX
      IF (AXISMN(I) .EQ. 0.) AXISMN(I)= AXISMJ(1)
      DUMMY(2)= AXISMN(I) * AXISMJ(I)
  140 AXISMJ(I)= SQRT(DUMMY(2))
      D1A1= AXISMJ(1)
C     SET OTHER PARAMETERS TO AVOID MODE ERROR
      D1A2= D1A1
      D1A3= D1A1
      OD1= D1A1
      OD2= D1A1
      OD3= D1A1
C     WALL THICKNESSES
      READ (60,1210) (AXISMN(I),I=1,NXXXX)
      WRITE(61,1370) (AXISMN(I),I=1,NXXXX)
      DO 150 I=1,NXXXX
      XXXX(I)= XXXX(I) / 12.
      AXISMN(I)= AXISMN(I) / 12.
```

TABLE XXIV. (CONTD)

```
  150 AXISMJ(I)= AXISMJ(I) / 12.
  190 CONTINUE
C     RATBUP= CONSTANT FOR BREAK-UP LENGTH
      RATBUP= 2.40
      TAMBMX= TAMB(1)
      DO 100 I=2,6
      IF (TAMBMX .LT. TAMB(I) ) TAMBMX= TAMB(I)
  100 CONTINUE
      PI= 3.14159
      PI04= PI*.25
      PI0576= PI04/ 144.
      Z8=PI04*(DIA1**2-FJETOD**2)
C     CONVERT  DIAMETERS, LENGTHS TO FEET
      DIA1= DIA1 /12.
      DIA2= DIA2 /12.
      DIA3= DIA3 /12.
      XL1= XL1 /12.
      XL2= XL2 /12.
      XL3= XL3 / 12.
      XL4= XL4 / 12.
      OD1= OD1 / 12.
      OD2= OD2 / 12.
      OD3= OD3 / 12.
      XL1MXX=XLTMXX/12.
      P4S= P3 - DELP
      TFUELF= TFUELR- 459.69
      T3F= T3R- 459.69
C     FUEL SPECIFIC GRAVITY (DMLS)
      SGF= TAB(TFUELF,T2(),KFUEL),SGFUEL(I,KFUEL),NTAB2)
      SG60F  =TAB(60.,T2(1,KFUEL),SGFUEL(1,KFUEL),NTAB2)
C     FUEL VISCOSITY (CENTISTOKES)
      FMU= TAB(TFUELF,T3(1,KFUEL),VISFUL(I,KFUEL),NTAB3)
C     AIR VISCOSITY (LB/SEC/FT)
      AMU= TAB(T3F,T',VISAIR,NTAB1)
      WRITE (61,1140) SGF,FMU,AMU
      RHOA= 2.69917 * (P3 -DELP) / T3R
      RHOF= 62.428 * SGF
C     CALCULATE GUESS FOR V (AIR).
CCCCCC
      VAIRG=VAG
CCCCCC
      IF(VAG.EQ.0.) VAIRG=SQRT(9266.*DELP/RHOA)
      KNTVA=0
      GAMMA=1.4
      C4= GAMMA-1.
      C1= C4*.5
      C2= GAMMA/ C4
      C3= GAMMA *.5
      C15= (GAMMA + 1.) / C4
      C16= C15 - 1.
      Z1= 453.59/ 1728. / 2.54**3
      Z2= PI0576*FJETID **2 *3600.
      Z3= Z8 * 3600. / 144.
      Z4= 2.54 *12.
      SL= .5 *FJETID * 2.54
      Z5= 39.37E-6 /12.
      DX= .02 /12.
      XTOB= XL1 + XL2 + XL3
      XEND= XTOB + XL4
      SLOPE1= (DIA2 - DIA1) / XL1
      SLOPE2= (DIA3 - DIA2) / XL2
      TLOPE1= (OD2 - OD1) / XL1
      TLOPE2= (OD3 - OD2 ) / XL2
      Z7= .2*PPH/3600.
      Z9=RHOF*PI04/1.5
      G=32.174
```

TABLE XXIV. (CONTD)

```
      Z10=G*GAMMA*53.35
      Z11= FJET10*.5
      VFUEL= PPH / Z2 / RHOF
C     SURFACE TENSION (DYNE/CM)
      DO 310 I=I,NTABSS
  310 DUMMY(I)= TAB(TFUELF,T5,SRFTNS(1,I),NTABST)
      TAU= TAB(SG60F  ,SGTAB5,DUMMY,NTABSS)
      ETAR= FMU * SGF
      RHOG= Z1 * RHOA
      VT= Z4 * VFUEL
      KPRINT=0
C
C     BEGIN CALC. WITH GUESSED VALUE FOR V (AIR)
C
  300 KNTVA= KNTVA+1
      QMA= RHOA * Z3 * VAIRG
      QMR= QMA /PPH
      VR= VAIRG / VFUEL
      SMD1= SMDF (TAU,ETAR,RHOG,QMR,SL,VT,VR)
      WRITE (61,1110) VAIRG, KNTVA ,SMD1
C     INITIALIZE FOR CALCULATIONS THROUGH THE FUEL TUBE
      DO 320 I=1,5
      DIA(I)= DIASMD(I)* SMD1
      D(I)= DIA(I) * Z5
C     DROPLET MASS.  CONSTANT THROUGHOUT FUEL TUBE.
      FMASS(1)=D(1)**3*Z9
CCCCCC
      W(1)=FMASS(I)
CCCCCC
      WST(I)=FMASS(I)
      E(I)=0.
      FN(1)=Z7/FMASS(1)
      TF(1)= TFUELR
  320 VF(1)= VFUEL
      BRUPL=RATBUP* SMD1
      XN= BRUPL * Z5
      XSTART= XN
      XFRACT= XSTART + Z11
      FRACTN= 0.
      TT=T3R
      PT=P3
      TDUCT= TT
      VAIR= VAIRG
CCCCCC
      DUMMY(1)=VAIR**2/TT
CCCCCC
      FMACH2=DUMMY(1)/(Z10-DUMMY(1)*C1)
      C7= 1. + C1 * FMACH2
      TS= TT / C7
      PS= PT / C7 **C2
      RHOA= 2.69917 * PS / TS
      WAIR= RHOA * Z8 / 144. * VAIR
CCCC
      WTOT=WAIR
      KK=0
      RHOAIR= RHOA
      CALL GEOM (XN,DDUCT,TH,DDUCT)
      TH= TH * 12.
      AIRMU= AMU
      ADUCT= PI04 * DDUCT**2
      INTER=1
      BFLAG= 0.
CC
      FDW=0.
CCCCCC
      DELT0=0.
```

TABLE XXIV. (CONTD)

```
CCCCCC
      DP00P0=0.
CCCCCC
      FFM=0.
CCCCCC
      C11=(ADUCT-ZB/144.)/(ZB/144.)
CCCCCC
      NSKP=4
CCCCCC
      NPRINT=1
C
C     BEGIN CALCULATIONS OVER INTERVAL DX
C
CCCC
  330 CONTINUE
CCCCCC
      IF(KPRINT.NE.0.AND.NPRINT.EQ.1) WRITE(61,2500)
 2500 FORMAT(1H0)
CCCC
      BIGK=C7/(1.-FMACH2)
CCCC
      FMACH2=FMACH2*(1.+BIGK*(-2.*C11+2.*FFM/WTOT*DELTO/TT-2.*DP00P0))
CCCC
  331 C7= 1. + C1*FMACH2
CCCC
  335 FMACH= SQRT(FMACH2)
  336 KK=1
      TS= TT/C7
      PS= PT/ C7**C2
      VAIR= FMACH* SQRT(Z10 * TS)
      RHOAIR= 2.69917*PS/TS
CCCCCC
CCCCCC
      IF(XN.GE.XEND) NPRINT=1
      IF(KPRINT.EQ.0.OR.NPRINT.NE.1) GO TO 337
      DUMMY(I)= XN * 12.
CCCCCC
      WRITE(61,1250)TS,PS,TT,PT,FMACH,VAIR,DUMMY(1),TDUCT
  337 TEMPB= RHOAIR/AIRMU
CCCCCC
      IF (XN .GE. XEND) GO TO 500
      RNAIR= VAIR *DDUCT * TEMPB
C     FRICTION FACTOR F
      IF (RNAIR .LT. RNTAB (I)) GO TO 340
      F= TAB(RNAIR,RNTAB ,FTAB  ,NTABRF)
      GO TO 350
  340 F= 16./ RNAIR
  350 TEMPA= RHOAIR / 9266.
      CPAIR= TAB(TT,T9R,CPTAB,NTAB9)
      DQ=0.
      TOTDRG=0.
      FL=0.
CCCC
      FDW=0.
CCCC
      FFM=0.
      NDCLAS=0
      DO 360 I=1,5
CCCC
CCCCCC
      IF(E(I).GT..989999) GO TO 360
      CALL EVAP (INTER,I)
      DIA(I)=D(I)/Z5
CCCCCC
      DQ=DQ+FN(I)*DELQ(I)
      TOTDRG=TOTDRG +FN(I)*DRAG(I) * TIMS(I)
```

```
      FL = FL + VREL(I) * TIMS(I)
CCCC
      FDW=FDW+2.*(1.-VF(I)/VAIR)*DELM(I)*FN(I)/WTOT
CCCC
      FFM=FFM+DELM(I)*FN(I)
      NOCLAS=NOCLAS+1
  360 CONTINUE
      INTER=2
C     ADJUST DRAG AND HEAT FOR FRACTION OF FUEL INVOLVED
      TOTDRG= TOTDRG * FRACTN
      DQ= DQ * FRACTN
CCCC
      FDW=FDW*FRACTN
CCCC
      FFM=FFM*FRACTN
CCCC
      IF(NOCLAS.GT.0) FL=FL/NOCLAS
CCCC
      WTOT=WTOT+FFM
      WAIRST= ADUCT * RHOAIR * FL
      XNP1= XN + DX
      IF (XNP1 .LT. XTOB .OR. BFLAG .NE. 0.) GO TO 370
      XNP1= XTOB
      BFLAG=1
  370 IF (XNP1 .LE. XEND) GO TO 380
      XNP1 = XEND
CCCCCC
      NPRINT=1
  380 CALL GEOM (XNP1,DDUCTP,THP,ODOCTP)
      THP= THP * 12.
      ADUCTP= PI04 * DDUCTP**2
      DAREA= ADUCTP- ADUCT
      C6= FMACH2
      C11= DAREA / ADUCT
      C12= 4. * F * DX / DDUCT
      C13= TOTDRG /(C3* PS    * ADUCT *C6) / 144. +C12
CCCCC
C     ADJUST FUEL PARAMETERS FOR FRACTION INVOLVED
      FRACT1= 1.
      IF (XNP1 .LT. XFRACT) FRACT1= 1. - (1. -(XNP1-XSTART)/Z11)**2
      TEMP1= FRACT1 - FRACTN
CCCC
      DO 401 I=1,5
CCCC
        IF(E(I).GT..989999) GO TO 401
      TF(I)= (FRACTN*TF(I) + TEMP1*TFUELR )/ FRACT1
      SGRESD= SGRFCT (ESAVE(I))
      SG(I)= SGFCT (TF(I), SGRESD)
      SG60(I)= SGFCT (519.69,SGRESD)
      W2=W(I)-DELM(I)*FRACTN
CCCC
      IF(W2.LT.1.E-30) W2=1.E-30
      D(I)=(6.* W2 / PI / SG(I) / 62.428)**.3333333333
CCCC
      IF(D(I).LT.1.E-10) D2=1.E-10
      E(I)= 1. - ( D(I) / DSTART(I) )**3 * SG(I) / SG60(I)/ SGSG60(I)
CCCC
      IF(E(I).GT. .99) E(I)=.99
      IF (E(I) .LT. 0.) E(I)=0.
  400 VF(I)= (FRACTN*VF(I) + TEMP1*VFUEL  )/ FRACT1
CCCCCC
      W(I)=W2
CCCCCC
      EW(I)=1.-W(I)/WST(I)
CCCCCC
  401 CONTINUE
```

```
CCCCC
C     CALC. OF DELQD= HEAT THROUGH DUCT WALL
      DUMMY(1)= XN * 12.
      VAMBX= TAB (DUMMY, XTAB,VAMB,6)
      TAMBX= TAB(DUMMY, XTAB,TAMB,6)
      RAMBX= 2.69917 * PBS / TAMBX
      DUMMY(1)= (TAMBX + TDUCT ) / 2.5
      VISCX= TAB (DUMMY,TAIRTB,AIRMUT,NTABAR)
      AIRKX= TAB (DUMMY,TAIRTB,AIRKTB,NTABAR)
      RNX= VAMBX * DDUCT * RAMBX / VISCX
      DUMMY(2)= ALOG(RNX) * .4342944819
      QNU= TAB (DUMMY(2),RNLG10,TABNU,NUTABN)
      HX=QNU * AIRKX / DDUCT
      VISCY= TAB (TT,TAIRTB,AIRMUT,NTABAR)
      AIRKY= TAB (TS,TAIRTB,AIRKTB,NTABAR)
      RNY= QMA / PID / DDUCT / VISCY / 3600.
      CPY= TAB (TT,TAIRTB,AIRCPT,NTABAR)
CCCC
      PRY=  CPY * VISCY / AIRKY * 3600.
      H= .023 * RNY **.8 * PRY **.4 * AIRKY / DDUCT
      HY= H * (1. + .144 * SQRT( SQRT(RNY) ) *DDUCT / XN)
      IF (XK .LE. XL1+XL2 ) GO TO 390
      DUMMY(1)= QMA / 2.69917 / PS * TT
      DUMMY(3)= (FRHO(1) + FRHO(2) + FRHO(3) + FRHO(4) + FRHO(5) ) * .2
      DUMMY(4)= (E   (1) + E   (2) + E   (3) + E   (4) + E   (5) ) * .2
      DUMMY(5)= (VF  (1) + VF  (2) + VF  (3) + VF  (4) + VF  (5) ) * .2
      TFAVE   = (TF  (1) + TF  (2) + TF  (3) + TF  (4) + TF  (5) ) * .2
      DUMMY(2)= PPH * (1. - DUMMY(4) ) / DUMMY(3)
      DUMMY(7)= TAB( TFAVE-459.69,T3(1,KFUEL),VISFUL(1,KFUEL),NTAB3)
     1 * DUMMY(3) / 62.428 * .000672
      DUMMY(8)= SGRECT (DUMMY(4))
      DUMMY(9)= CPFCT (TFAVE,DUMMY(8))
      DUMMY(10)= FLIQKF (TFAVE)
      DUMMY(6)= DUMMY(5) * DDUCT * DUMMY(3) / DUMMY(7)
      DUMMY(11)= DUMMY(9) * DUMMY(7) / DUMMY(10) * 3600.
      DUMMY(12)= .0214 * DUMMY(6) **.8 * DUMMY(11) **.4
      HH= DUMMY(12) * DUMMY(10) / DDUCT
      HY= ( HY * DUMMY(1) +   HH  * DUMMY(2)) / (DUMMY(1) + DUMMY(2))
  390 FKMET= TAB (TDUCT,TDTAB,TABKMT,NKMETL)
      DELTAT= (TAMBX - TT ) / (1. + FKMET / TH * (1./ HX / DDDCT + 1./
     1 HY / DDUCT ) )
      TDUCT= DELTAT * FKMET / TH / HY / DDUCT + TT
CCCCCC
      DELQD= HY * PI * DDUCT * DX * (TDUCT - TT) / 3600.
CCCC
CCCC
      DELTO=(DELQD-DQ)/WTDT/CPAIR
      PTMPS= PT - PS
CCCC
      DP00P0=-C3*C6*(DELTO/TT+C13*FDW)
CCCC
      IF(XN.EQ.XTOH) DP00P0=DP00P0-1.1*PTMPS/PT
C     SET AIR PARAMETERS AT END OF INTERVAL
      PT= PT *(1.+ DP00P0)
CC
      TT=TT+DELTO
CCCCCC
CCCCCC
  405 IF(KPRINT.EQ.0.OR.NPRINT.NE.1) GO TO 410
      WRITE (61,1260) TF
      WRITE (61,1270) VF
      WRITE (61,1350) E
CCCC
      WRITE(61,2402) EW
 2402 FORMAT(4H EW= 5F15.5)
CCCCCC
```

TABLE XXIV. (CONTD)

```
      WRITE(61,2601) D1A
 2601 FORMAT(4H D = 5F15.5)
  410 XN= XNF1
CCCCCC
      IF(NPRINT.EQ.NSKP+1) NPRINT=0
CCCCCC
      NPRINT=NPRINT+1
      AIRMU= TAB (TT  -459.69,T1,VISAIR,NTAB1)
CCCCCC
      ODUCT= ODUCTP
      ADUCT= ADUCTP
      TH= THP
      ODDCT= ODDCTP
      FRACTN= FRACT1
CCCC
      GO TO 330
C
C     FUEL TUBE CALC. COMPLETED. CHECK IF GUESSED V (AIR) WAS OK.
C
  500 DELPC= P3 - PS
      WRITE (61,1220) DELP,DELPC,KNTVA
      IF (ABS(DELPC- DELP) .LE.  .020* DELP) GO TO 520
C     NOT WITHIN TOLERANCE
  510 VAIRG= VAIRG *SQRT(DELP/DELPC)
      IF (KNTVA .LT. 10) GO TO 300
      WRITE (61,1100) KNTVA
      CALL EXIT
  520 IF (KPRINT .NE. 0) GO TO 550
      KPRINT=1
      GO TO 510
C
C     CALC. AVERAGE FUEL VELOCITY AND TEMPERATURE
C
  550 VFUEL=(VF(1)+VF(2)+VF(3)+VF(4)+VF(5) )*.2
      TFUEL=(TF(1)+TF(2)+TF(3)+TF(4)+TF(5) )*.2
      EAVE =(E (1)+E (2)+E (3)+E (4)+E (5) )*.2
      DEQ= ODUCTP * 12.
CCCCCCCCCCCC
      EWAVE=(EW(1)+EW(2)+EW(3)+EW(4)+EW(5))*.2
      QMR= WAIR / PPH  * 3600.
      QCD= .0063229* WAIR   /P3/ ADUCTP * SQRT( T3R / DELP * PS)
      WRITE (61,1515)      WAIR,QCD,QMR
      IF (E(1) .GT. .01) GO TO 580
  570 TFUELF=TFUEL-459.69
      SGF=TAB(TFUELF,T2(1,KFUEL),SGFUEL(1,KFUEL),NTAB2)
      RHOF=62.428*SGF
      FUELP=RHOF*VFUEL**2/9266.
      WRITE (61, 230) VFUEL,TFUEL,VAIR,TT,FUELP,EAVE
CCCC
      IF(EWAVE.LT..99) CALL FLMVAP(EWAVE,EAVE,WIDTH)
      GO TO 1
  580 SUM= 0.
      SUM1= 0.
      DO 590 I=1,5
      SUM= SUM + W(I)
  590 SUM1= SUM1 + (TF(I) - TF(3)) * W(I) * (CP(I) + CP(3))
      TFUEL= SUM1 * .5 / SUM / CP(3)  + TF(3)
      GO TO 570
  700 WRITE (61,1240)
      CALL EXIT
C     INPUT FOR FLMVAP
  800 TFUEL= TFUELH
      PS= P3
      READ(60,1211)DEQ,RMS,TT,VAIR,TAMBMX,EAVE,WIDTH,XLIMXX,IRAD
      WRITE(61,1380) DEQ,RMS,TT,VAIR,TAMBMX,EAVE,WIDTH,XLIMXX
     + ,IRAD
```

TABLE XXIV. (CONTD)

```
      XL1MXX=XL1MXX/12.
      RMS= RMS / 12.E6
      NTABVT= 0
      IF (TT .NE. 0.) GO TO 810
      NTABVT= VAIR
      READ (60,1210) (XWALLTB(I),I=1,NTABVT)
      WRITE(61,1390) (XWALLTB(I),I=1,NTABVT)
      READ (60,1210) (VWALLTB(I),I=1,NTABVT)
      WRITE(61,1400) (VWALLTB(I),I=1,NTABVT)
      READ (60,1210) (TWALLTB(I),I=1,NTABVT)
      WRITE(61,1410) (TWALLTB(I),I=1,NTABVT)
      GO TO 820
  810 RHOAIR= 2.69917 * PS / TT
CCCCCC
  820 CALL FLMVAP(EAVE,EAVE,WIDTH)
      GO TO 1
C
 1000 FORMAT (8A10)
 1010 FORMAT (1H1,8A10  /)
 1100 FORMAT (21HONO CONVERGENCE AFTER  ,I5,10H1TERATIONS    )
 1110 FORMAT ( 9H0V(AIR)= F12.3,I10,5X,4HSMD=  F6.2)
 1140 FORMAT (4H0SG=  E12.4,7H (OMLS) ,4X,10HVISC FUEL=  E12.4,12H CENTI
     1STOKES  ,4X,10HVISC AIR =  E12.4,10H LB/SEC/FT        )
 1200 FORMAT (I10,7F10.2)
 1210 FORMAT (8F10.3)
 1211 FORMAT(7F10.3,F9.3,I1)
 1220 FORMAT (1H0,2F13.4,I5)
 1230 FORMAT (7H0VFUEL= F6.2,2X,6HTFUEL= F6.2,2X,5HVAIR= F6.2,2X,3HTT=
     1 F8.1,2X,6HFUELP= F6.2,2X,2HE=  F7.5)
 1240 FORMAT (26H0MACH NO ITERATION FAILURE      )
 1250 FORMAT (4H TS= F8.2,3X,3HPS= F8.4,3X,3HTT= F8.2,3X,3HPT= F8.4,3X,
CCCCCC
     1 2HM= F8.5,3X,5HVAIR= F8.2,3X,4HXIN= F8.5,4X,4HTD=  F8.2)
 1260 FORMAT (4H TF= 5F15.2)
 1270 FORMAT (4H VF= 5F15.2)
 1280 FORMAT (5H0FUEL ,4X,6HTFUELR ,8X,2HP3 ,7X,3HT3R ,7X,3HPPM,6X,4HOEL
     1P,7X,3HHEX,8X,2HY        /  15,7F10.4      )
 1290 FORMAT (1H0,4X,5HJETID ,6X,4HDIA1 ,6X,4HDIA2,6X,4HDIA3,7X,3HXLI,7X
     1 ,3HXL2,5X,5HJETOD,7X,3HRMS        / 8F10.4)
 1310 FORMAT (6H0   X=    ,6F12.3)
 1320 FORMAT (6H0TAMB=    ,6F12.3)
 1330 FORMAT (6H0VAMB=    ,6F12.3)
 1340 FORMAT (1H0,3X,3HXL3,7X,3HXL4,7X,3HOD1,7X,3HOD2,7X,3HOD3,5X,5HWIDT
     1H,5X,5HX MAX,5X,5HI RAD / 7F10.4,I10)
 1350 FORMAT (4H  E= 5F15.5)
 1360 FORMAT (1H+,100X,3HTD= F8.2)
 1370 FORMAT (1H0,10F10.3)
 1380 FORMAT (1H0,6X,3HOEQ,7X,3HRMS,8X,2HTT,6X,4HVAIR,6X,4HTAMB,9X,1HE
     1 ,5X,5HWIDTH,5X,5HX MAX,5X,5HI RAD / 8F10.4,I10)
 1390 FORMAT (3H0X=     8F10.3 / (3X,8F10.3) )
 1400 FORMAT (3H0V=     8F10.3 / (3X,8F10.3) )
 1410 FORMAT (3H0T=     8F10.3 / (3X,8F10.3) )
 1515 FORMAT (15H0AIR FLOW RATE=  F11.5,4H PPS,5X,17H0ISCHARGE COEFF.=
     1 F8.4 ,5X,15HAIR-FUEL RATIO=    F10.4)
      END
      SUBROUTINE GEOM (X,DIAMTR,T,OD)
      COMMON XL1,XL2,DIA1,DIA2,SLOPE1,SLOPE2
     1, DIA3,OD1,OD2,OD3,TLOPE1,TLOPE2
      COMMON NXXXX,AXISMJ(10),AXISMN(10),XXXX(10)
      IF (NXXXX .NE. 0) GO TO 100
      IF (X .GT. XL1) GO TO 20
      DIAMTR= DIA1 + SLOPE1 * X
      OD= OD1 + TLOPE1 * X
   10 T= (OD - DIAMTR) * .5
      RETURN
   20 IF (X .GE. XL1 + XL2) GO TO 30
```

TABLE XXIV. (CONTD)

```
      DIAMTR= DIA2 + SLOPE2 *(X- XL1)
      OD= OD2 + TLOPE2 * (X - XL1)
      GO TO 10
   30 DIAMTR= DIA3
      OD= OD3
      GO TO 10
  100 DIAMTR= TAB(X,XXXX,AXISMJ,NXXXX)
      T     = TAB(X,XXXX,AXISMN,NXXXX)
      OD= DIAMTR + 2. * T
      GO TO 10
      END
      FUNCTION SMDF (TAU,ETAR,RHOG,QMR,SL,VT,VR)
      SMDF= 6. +1.4E4 *SQRT(TAU/RHOG)*ETAR**.21 *(1.+ .065/QMR/SQRT(QMR)
     1  ,*
     1SQRT( SL/ (VT**2 *( VR *(.5 *VR -1.) +1.) )  )
      RETURN
      END
      FUNCTION TAB (X,XX,YY,NTAB)
      DIMENSION XX(1), YY(1)
      F=1.
      IF (XX(I).GT.XX(2)) F=-F
      DO 10 J=I,NTAB
      I=J
      IF (F*(XX(I)-X)) 10,40,20
   10 CONTINUE
   20 IF (I.NE.1) GO TO 30
      I=2
   30 J=I-1
      DEL=XX(I)-XX(J)
      IF (DEL.EQ.0.) GO TO 50
      TAB=(YY(I)*(X-XX(J))-YY(J)*(X-XX(I)))/DEL
      RETURN
   40 TAB=YY(I)
      RETURN
   50 WRITE(6I,60) X,I,J
      CALL EXIT
   60 FORMAT (24H0***ERROR IN ROUTINE TAB,E15.4,2I5)
      END
*DECK B
      SUBROUTINE FLMVAP(EWAVE,EAVE,WIDTH)
C
C     FILM VAPORIZER MODEL FOR AIR BLAST INJECTOR
C
      COMMON / QFLMVAP / XWALLTB(21),VWALLTB(21),TWALLTB(2I),NTABVT
     * ,XLIMXX,IRAD
      COMMON / TRAJ / VFUEL,TFUEL,TFUELF,SGF,FMU,RHOF,PS,PT,TS,TT,
     1 RHOAIR,AIRMU,G,VAIR,SMDJ,TAMBMX
      COMMON / INPUT / KFUEL,NEQ,GAP,PPH,TITLE(8),HEX,YTH,T3R,RMS
      COMMON / QEVAP/ DUMMY(20),D(5),TF(5),VF(5),VREL(5),      RN(5),
     I CD(5),DRAG(5),FN(5),      CP(5),DELQ(5),SG(5),FRHO(5),DELTF(5),
     2 TIMS(5),FMASS(5),ALPHA(5),DELV(5),E(5),DX,W(5),VFSAVE(5),TFSAVE(5
     3 ),DSAVE(5),ESAVE(5),DSTART(5),SGSG60(3),SG60(5),DELM(5)
     4,OPTION,SPACE(6)
     * ,WST(5),ZWSPAC(5)
      COMMON/ TABLES / T1(7),VISAIR(7),T2(2,4),SGFUEL(2,4),T3(14,4),
     1VISFUL(I4,4),NTAB1,NTAB2,NTAB3,NFUELS
      COMMON /QEVAPI/ TAIRTB(7),AIRKTB(7),AIRMUT(7),AIRCPT(7),NTABAR
      DIMENSION WPTAB(6),YPTAB(6),UPTAB(6)
      DIMENSION TMTTAB(5),TKMTAB(5)
      DATA WPTAB / 1., 10., 30., 202., 300., 1300. /, NPWYU/6/
      DATA YPTAB / 1.45, 4.6, 8.2, 25., 32.8, 100. /
      DATA TMTTAB / 660., 1060., 1460., 1860., 2260. /, NTKMTL /5/
      DATA TKMTAB /  76.,  100.,  136.,  166.,  195. /
      DATA UPTAB / 1.15, 4.3, 6.6,12.5,13.25, 16.5 /
      DATA TWOPI / 6.2831853 /, R /1545.327 /
      WRITE(6),1200)
```

TABLE XXIV. (CONTD)

```
CCCC
      ELIMX=.955
      EPMT=.95
      EXX=.96
      HYD=14.
      LUM=.567*(17.-HYD)
      BEAM=2./12.
      FUAR=.0676
      TFLM=3460.
      PATM=PS/14.7
      EGAS=1.-EXP(-3.9E4*LUM*PATM*SQRT(FUAR*BEAM)/TFLM**1.5 )
      SFG=P=(1.+.8)/2.*EGAS*1.714E-9
      QFLM=SFGWP*TFLM**4
      IF(HEX.GT. .) GO TO 20
      NVEX=-HEX
      VEXT=NVEX
      DEXT=(-HEX-VEXT)/12.
      REXT=2040.*PS/14.7*VEXT*DEXT/(T3R/1000)**1.65
      RHOEXT=2.69917*PS/T3R
      HEX=.2**RHOEXT*VEXT*.034/(REXT**.2)*3600.
      WRITE(61,1015)VEXT,DEXT,REXT,HEX
 1015 FORMAT(20H0VEXT,DEXT,REXT,HEX=  ,F6.1,F6.3,E15.5,F7.2 )
   20 CONTINUE
CCCC
      FIDX= DEQ / 12.
      CON1= 3600. * 62.428
      CON2= 3600. * TWOPI
      WIDTH= WIDTH / 12.
      XX=0.
      RR= .80  * FIDX
      IF (NTABVT .EQ. 0) GO TO 4
      DO 2 I=1,NTABVT
    2 XWALLTB(I)= XWALLTB(I) / 12.
      TT=  TAB(XX,XWALLTB,TWALLTB,NTABVT)
      VAIR=TAB(XX,XWALLTB,VWALLTB,NTABVT)
      RHOAIR= 2.69917 * PS / TT
    4 CONTINUE
      SGRESD= SGFCT (0.)
      SG60F= SGFCT(519.69,SGRESD)
      VOLSTR= PPH / CON1 / SG60F
      PPHN= PPH * (1. - EAVE)
      SGRESD= SGFCT (EAVE )
      SGF   = SGFCT (519.69, SGRESD)
CCCCCC
      PPHN=PPH*(1.-EWAVE)
CCCCCC
      EW=EWAVE
      VN= PPHN / CON1 / SGF
      E(I)=(VOLSTR - VN) / VOLSTR
CCCCCC
      WRITE(61,1000)E(I)
      WRITE(61,1010)EW
      RRIN= RR * 12.
CCCCCC
      DO 8 I=1,10
      KKK=I
CCCCCC
      EP=I*.1
CCCCCC
      IF(EP.GT..9) EP=ELIMX
CCCCCC
      IF(EW.LT.EP) GO TO 9
    8 WRITE(61,1020)XX,RRIN,EP
    9 CONTINUE
      AIRK= TAB(TT,TAIRTB,AIRKTB,NTABAR)
      AIRMU= TAB(TT,TAIRTB,AIRMUT,NTABAR)
```

TABLE XXIV. (CONTD)

```
      AIRCP= TABTTT(TAIRTB,AIRCPT,NTABAR)
      RNJ= VAIR * FIDX * RHOAIR / AIRMU
      PRJ= AIRCP * AIRMU / AIRK * 3600.
      CON2= .368 * RNJ **.566* PRJ **.36
      CON3= SQRT(RNJ) / 43.5 / CON2
      DX=.01 /12.
      TM= TT
      VM= VAIR
      TF(1)= TFUEL
      X1= XX
      AS= DX * WIDTH
      KNT= 0
      INTER=1
      R1= RR
      KOUNTD=0
      LL= 0
      DELTF(1)=0.
      GO TO 40
   10 LL=1
      UL= UL2
      YL= YL2
      DUMMY(1)= YL * 12.
      WRITE (61,1040) UL,DUMMY(1)
      WRITE(61,1300)
C
C     BEGIN CALCS. OVER INTERVAL DX
C
   30 IF (NTABVT .EQ. 0) GO TO 35
      TM= TAB(XX,XWALLTB,TWALLTB,NTABVT)
      VM= TAB(XX,XWALLTB,VWALLTB,NTABVT)
      GO TO 38
   35 CALL FIELD1       (12.*XX, TM, VM)
   38 CONTINUE
CCCCCC
      DXS=DX
      DXC=.01/12.
      DXY=YL*4.
      DX=AMIN1(DXY,DXC)
      IF(EW2.GT.ELIMX) DX=1./12.
      KOUNTF=0
   39 CONTINUE
      AS=DX*WIDTH
CCCCCC
      R1= RR+ DX
      X1= XX+ DX
      IF (WIDTH .EQ. 0.) AS= TWOPI * RR * DX
   40 I=1
      RHOG= 2.69914 * PS / TM
C
      AIRM= 28.966
C     CHECK FOR FIRST ENTRY TO ROUTINE (INTER=1)
      IF (INTER .NE. 1) GO TO 50
C     ESTIMATE NEXT STATION CONDITIONS
      PPH2= PPHN
      TF2= TF(1)
      E2=  E(1)
CCCCCC
      EW2=EW
      GO TO 55
C     ESTIMATE NEXT STATION CONDITIONS
   50 CONTINUE
      PPH2= 2. * PPHN - PPHSV
      TF2= 2. * TF(1) - TFSAVE(I)
CCCCCC
      E2=E(1)+(E(1)-ESAVE(1))*DX/DXS
CCCCCC
```

TABLE XXIV. (CONTD)

```
      EW2=EW+(EW-EWSAVE)*DX/DXS
CCCCCCCCC
      TF2=TF(I)
CCCCCCCCC
      IF(E2.GE.ELIMX) E2=EXX
CCCCCC
      IF(EW2.GE.ELIMX) EW2=EXX
C     INITIALIZE FOR ITERATION ON E
   55 KOUNTC= 1
CCCCCC
      DELEG=EW2-EW
   60 KOUNTB= 1
C     INITIALIZE FOR ITERATION ON TF
      DELTFG= TF2 - TF(I)
      EZ= (E(I) + E2) * .5
      VAPM= VAPMF (EZ)
      SGRESD= SGRFCT (EZ)
C     AVERAGE TEMPERATURES, CALC. PROPERTIES
   70 TFZ= (TF(I) + TF2) * .5
CCCCCC
      TFZ=TF(I)
      TMX= (TM + TFZ) * .5
      PAS= PASF(TFZ,EZ)
      IF (PAS .LT. PS-.01) GO TO 80
C     AT BOILING POINT.
      PAS= PS - .01
      IF (KOUNTD .NE. 0) GO TO 80
      KOUNTD=1
      DUMMY(1)= X1 * 12.
      WRITE (61,1110) DUMMY(1)
   80 VAPK= VAPKF(TMX,VAPM)
      VAPMU= VAPMUF(TMX)
CCCC
      VAPLAM=VAPLMF(TFZ)
      CP(I)= CPFCT(TFZ,SGRESD)
      VAPCP= VAPCPF(TMX)
      SG(I)= SGFCT(TFZ,SGRESD)
      RHO(I)= SG(I) * 62.428
      FLIQK= FLIQKF (TFZ)
      VAPD= VAPDF(TMX,PS)
      IF (VAPD .LT. .00005) VAPD= .00005
      ALP= PS / PAS * ALOG(PS / (PS - PAS) )
C     AIR PROPERTIES
      AIRK=TAB(TMX,TAIRTB,AIRKTB,NTABAR)
      AIRMU=TAB(TMX,TAIRTB,AIRMUT,NTABAR)
      AIRCP=TAB(TMX,TAIRTB,AIRCPT,NTABAR)
C     DIFFUSION ZONE PROPERTIES
      QK= PAS / PS * .5
      QJ= 1. - QK
      QKMX= QJ * AIRK + QK * VAPK
      QMUMX= QJ * AIRMU + QK * VAPMU
      QMMX= QJ * AIRM + QK * VAPM
      QCPMX= (QJ * AIRM * AIRCP + QK * VAPM * VAPCP) / QMMX
      QRHOMX= PS * QMMX * 144. / R / TMX
      SC= QMUMX / VAPD / QRHOMX
      PR= QCPMX * QMUMX / QKMX * 3600.
      KOUNTA= 0
      FULMU2= TAB(TF2-459.69,T3(I,KFUEL),VISFUL(1,KFUEL),NTAB3) * 1.075E
     I -5
      SGRESD= SGRFCT (E2)
      SG2= SGFCT (TF2,SGRESD)
      RHUL= 62.428 * SG2
      DLPPHG= PPH2 - PPHN
      DUMMY(I)=WIDTH
      IF(WIDTH.EQ.0.) DUMMY(I)=TWOPI*RR
      FMUL=TAB(TF(1)-459.69,T3(I,KFUEL),VISFUL(I,KFUEL),NTAB3)*1.075E-5
```

TABLE XXIV. (CONTD)

```
      SGR1=SGNFCT(E(I))
      SPG1=SGFCT(TF(I),SGR1)
      WP1=PPHN/(3600.*DUMMY(1)*FMUI*SPGI*62.428)
      YP1=TAB(WP1,WPTAB,YPTAB,NPWYU)
  100 DUMM(I)=*IDTH
      IF (WIDTH .EQ. 0.) DUMMY(1)= TWOPI * R1
      WP2=PPH2 /(3600. * DUMMY(1)    * FULMU2 * RHOL)
      YP2= TAB (WP2,WPTAB,YPTAB,NPWYU)
      UP2= TAB (WP2,WPTAB,UPTAB,NPWYU)
CCCC
C * * * * * TEMPORARY ONLY  * * * * * * * * *
      REX=VM*R1*QRHOMX/QMUMX
      IF(NTABVT.EQ.0) QNUH=CON2*(RI/FIDX)**.134
      IF(NTABVT.NE.0) QNUH=.0295*PR**.6*REX**.8
      HMULT=1.0
      IF(NTABVT.EQ.0.AND.YPI.GE.21)
     * HMULT=1.+(40.*PPHN/CON3/RI)
      IF(NTABVT.NE.0.AND.YPI.GE.21)
     * HMULT=1.+(40.*PPHN/3600/WIDTH)
      QNUH=QNUH*HMULT
CCCC
C * * * * * TEMPORARY ONLY  * * * * * * * * *
      HIN= QNUH * QKMX / FIDX
CCCC
      IF(NTABVT.NE.0) HIN=QNUH*QKMX/RI
      F2= 2. * HIN / QRHOMX / VM / QCPMX / 3600.
     * /HMULT
      UL2=UP2 * SQRT (F2 * .5 * RHOG / RHOL) * VM
      YL2=YP2                * UP2 / UL2 * FULMU2
      IF (LL .EQ. 0) GO TO 10
      QNUM= QNUH * (SC / PR) **.4
      FIOT= QNUH * QKMX / HIN
      UL2= (UL + UL2) * .5
      TME= DX / UL2
C     CHECK IF DELW IS BEING CALCED BY BOILING EQUS
      IF (KOUNTD .GT. 1 .OR. (KOUNTD .EQ. 1 .AND. INTER .EQ. 2) ) GO TO
     1    300
      DELW= VAPD * VAPM * AS * QNUM * PAS * ALP /    R     / TMX / FIOT
CCCCCCC
     * *144.
CCCCCC
      IF(EW2.GE.ELIMX)DELW=0.
      IF(EW2.GE.FLIMX, EW2=EXX
      IF (KOUNTD .EQ. 1) GO TO 300
      PPH2= PPHN - DELW * 3600.
      IF (PPH2 .LT. 0.) PPH2= 0.
      DLPPHN= PPH2 - PPHN
      IF (ABS(DLPPHN - DLPPHG) .LE. .01 * ABS(DLPPHN) ) GO TO 300
      DLPPHG= DLPPHN
      KOUNTA= KOUNTA +1
      IF (KOUNTA .LT. 25) GO TO 100
CCCCCC
  250 WRITE(61,1100)KOUNTA,KOUNTB,KOUNTC,KOUNTD,KOUNTE,RR,E2,EW2
      DX=DX/4.
      KOUNTF=KOUNTF+1
      IF(KOUNTF.LT.10) GO TO 99
      GO TO 900
  300 KOUNTE= 0
      YZ= (YL + YL2) * .5
      TMETG= T3R
  320 FKMET= TAB (TMETG,TMTTAB,TKMTAB,NTKMTL)
CCCC
      AGEG=(TFLM/TMETG)**1.5
      DUMMY(I)=AGEG*EGAS
      IF(DUMMY(1).GT.1.0) DUMMY(I)=1.0
      AGEG=DUMMY(1)/EGAS
```

TABLE XXIV. (CONTD)

```
      QR=0.
      IF(IRAD.EQ.1) QR= QFLM-SFGWP*AGEG*TMETG**4
      U3M=1./(1./HEX+.5*YTH/FKMET)
CCCCCC
      IF(EW2.GE.ELIMX) GO TO 321
      UMF=1./(.5*YTH/FKMET+(.5*YZ+RMS)/FLIQK)
      THOT=TFZ
      GO TO 322
  321 CONTINUE
      UMF=1./(.5*YTH/FKMET+1./HIN)
      THOT=TM
  322 CONTINUE
      TMET=(QR+U3M*T3R+UMF*THOT)/(U3M+UMF)
CCCC
      IF ( ABS (TMETG - TMET) .LT. .0001 * TMETG ) GO TO 350
      TMETG= TMET
      KOUNTE= KOUNTE +1
      IF (KOUNTE .GT. 25) GO TO 250
      GO TO 320
CCCC
  350 Q1=UMF*AS*(TMET-THOT)
  360 Z= DELW * VAPCP * FIOT / QKMX / QNUM / AS
      ZZ= 1.
      IF (Z .GT. .00001) ZZ= Z / (EXP(Z) - 1.)
      Q2= AS * QKMX * QNUM * (TM - TFZ) * ZZ / FIDT
      QVZ= (Q1 + Q2) / 3600.
      IF (KOUNTD .NE. 0) GO TO 750
CCCCCC
      DELTF(1)=(QVZ-DELW*VAPLAM)*TME/AS/YZ/CP(1)
CCCC
CCCCCC
      IF(EW2.GE.ELIMX) DELTF(1)=0.
      TF2= TF(1) + DELTF(1)
CCCCCCC
      IF(KFUEL.EQ.4.AND.TF2.GT.1092.8) TF2=1092.8
CCCCCCC
      IF(KFUEL.NE.4.AND.TF2.GT.1210.4) TF2=1210.4
CCCCCC
CCCCCC
      DELTF(I)=TF2-TF(I)
CCCCCC
 2000 FORMAT(1X,10E12.4)
  375 IF (ABS( DELTF(1) - DELTFG) .LE. .01 * ABS(DELTF(1))) GO TO 400
      DELTFG = DELTF(1)
      IF (ABS(DELTFG) .LT. 1.) GO TO 400
      KOUNTH= KOUNTH +1
      IF (KOUNTH .LT. 25) GO TO 70
      GO TO 250
  400 SGRESD= SGHFCT (E2)
      SG60(1)= SGFCT (519.69,SGRESD)
      VOLNP1= PPH2 / CON1 / SG60(1)
      E2SV= E2
CCCCCC
      EW2SV=EW2
      E2=(VOLSTR - VOLNP1) / VOLSTR
CCCCCC
      IF(DELW.NE.0.) EW2=(PPH-PPH2)/PPH
CCCCCC
      IF(E2.GE.ELIMX)E2=EXX
CCCCCC
      IF(EW2.GE.ELIMX)EW2=EXX
CCCCCC
      DELE=EW2-EW
CCCCCC
      IF(ABS(DELEG-DELE).LE. .1*ABS(DELE)) GO TO 500
      DELEG= DELE
```

TABLE XXIV. (CONTD)

```
      IF (ABS(DELEG) .LT. 1.E-8) GO TO 500
      E2= (E2 + E2SV) * .5
CCCCCC
      EW2=(EW2+EW2SV)*.5
CCCCCC
      DELEG=EW2-EW
  450 KOUNTC= KOUNTC + 1
      IF (KOUNTC .LT. 25) GO TO 60
      GO TO 250
  500 TFSAVE(I)= TF(I)
      ESAVE(I)= E(I)
CCCCCC
      EWSAVE=EW
      PPHSV= PPHN
      TF(I)= TF2
      IF (E2 .LT. E(I) ) E2= E(I)
      E(I)= E2
CCCCCC
      EW=EW2
      PPHN= PPH2
      UL= UL2
      YL= YL2
      INTER= 2
      RSAVE= RR
      RR= R
      XX= X1
      IF(KNT.NE.0.AND.EW2.LT.ELIMX.AND.KOUNTF.EQ.0) GO TO 550
      DUMMY(1)= XX * 12.
      DUMMY(2)= YL2 * 12.
CCCC
      RS=R1*12.
      WLC=WIDTH
      IF(WLC.EQ.0.) WLC=TWOPI*R1
      WFPUL=PPH2/WLC
CCCC
      WRITE(6I,1120)DUMMY(I),RS,DUMMY(2),UL2,PPH2,E2,THET,TF2,TM,VM
CCCC
     * ,WFPUL,EW2
  550 KNT= KNT + I
      IF (KNT .GT. 9) KNT= 0
C     PRINT IF THIS INTERVAL CROSSED EVAP. PRINT AMOUNT
      J= KKK
      DO 600 I=J,I0
      KKK= I
CCCC
      EP=I*.1
CCCC
      IF(EP.GT..9) EP=EPRT
CCCCCC
      IF(EWSAVE.GE.EP.OR.EW.LT.EP) GO TO 6I0
CCCCCC
      RS=RSAVE+(EP-EWSAVE)/(EW-EWSAVE)*(RR-RSAVE)
      RS= RS * 12.
      DUMMY(1)=XX*12.
  600 WRITE(6I,I020) DUMMY(1),RS,EP
CCCC
  6I0 IF(XX.LT.XLIMXX) GO TO 30
      XLIMXX=XLIMXX*12.
      WRITE(6I,1030)XLIMXX,EW2
      GO TO 900
C     BOILING. ITERATE ON DELW, INSTEAD OF PPH2 AND TF2
  750 TF2= PASF (-PS,E2)
      DELTF(I)= TF2 - TF(I)
      DUMMY(1)= TM - TF2
      IF (DUMMY(I) .GE. 0.) GO TO 755
      DELWN=0.
```

TABLE XXIV. (CONTD)

```
      GO TO 756
  755 IF (    DUMMY(1)  .LT. 1.) DUMMY(1)= 1.
CCCCCC
      DELWN=(QVZ-DELTF(1)*AS*YZ*CP(1)/TME)/VAPLAM
  756 CONTINUE
CCCC
      IF(EW2.GE.ELIMX) DELWN=0.
      PPH2=PPHN - DELWN * 3600.
      IF (ABS(DELWN - OELW) .LE. 1.E-5* ABS(OELW) ) GO TO 760
      DEL= DELWN
      KOUNTD= KOUNTD + 1
      IF (KOUNTD .LT. 40) GO TO 70
      GO TO 250
  760 KOUNTD= 2
      GO TO 900
  900 RETURN
 1000 FORMAT (1H0,50(1H*) / 10H0E(START)= F8.5 )
CCCCCC
 1010 FORMAT(12H0EW (START)= F8.5 )
 1020 FORMAT(3H0X= ,F10.4,9H IN.,  R= ,F10.4,4H IN.,3X,
     + *FOR WEIGHT FRACTION EVAP, EW= *,F5.2)
 1030 FORMAT(22H0CALC. STOPPED AT X =   ,F9.2,14H INCHES, EW=  ,F7.5)
 1040 FORMAT(1H0,*INITIAL FILM VEL, FPS= *,F9.4,3X,
     + *FILM THICKNESS, IN.= *,F12.7)
 1100 FORMAT (15H0FLMVAP FAILURE   , 5I5,5X,3HRR=  F10.4,5X,2HE=  F10.5
CCCCCC
     + ,5X,3HEW=  F10.5 )
 1110 FORMAT (21H0H01LING STARTS AT X=   F8.3/)
CCCCCC
 1120 FORMAT(1H0,F5.2,F6.2,F8.5,F8.3,F9.3,F8.4,3F6.0,F8.2,E10.3,F8.4)
 1200 FORMAT (3H0  ,*FILM EVAPORATION*)
CCCCCC
 1300 FORMAT(3H0  ,2H X,T11,1HR, T14, 7HFILM-TH, T23, 6HFILM-V, T31,
     + 6HWF-PPH, T39, 7HFRAC-FV, T48, 3HT-W, T54, 3HT-F, T60, 3HT-G,
     + T67, 3HV-G, T73, 6HWF /FT ,T85,2HEW )
      END
      SUBROUTINE FIELD1      (X,TMAX,UMAX)
C     ROUTINE TO CALCULATE UMAX AND TMAX FOR A RADIAL WALL JET
C *** TJ .LE. TAMB
C
C *** DIMENSIONS IN INCHES
C
      COMMON / INPUT / KFUEL,DEQ,GAP
      COMMON / TRAJ / DUM1(9),TJ,DUM2(3),UJ,DUM3,TAMB
      CON4= SQRT (TAMB / TJ)
      CON5= 100. / 112.
      CON7= 1.0923 * CON4
      XCORE= DEQ * CON7**CON5
      CON1= CON7 * UJ
      CON8 = .91025 * CON4
      TCORE= DEQ * CON8**CON5
      CON6= (TAMB - TJ) * CON8
C     CALC. VELOCITY V, TEMPERATURE
      UMAX= UJ
      DUMM1= (X / DEQ) *  1.12
      IF (X .GT. XCORE)  UMAX= CON1 / DUMM1
      TMAX= TJ
      IF (X .GT. TCORE)  TMAX= TAMB - CON6 / DUMM1
  500 RETURN
      END
*DECK C
      SUBROUTINE EVAP (INTER,I)
C     DROPLET EVAPORATION,
C     PROGRAMMED 1-22-71 BY M. TANI,
C
C     D,TF,VF,E       ARE INPUT FOR DROP NO. I
```

TABLE XXIV. (CONTD)

```
C**** NOTE-- FUEL PROPERTY EQUATIONS ARE ONLY FOR JP4 AND JP57JP8 ****
C
      COMMON /DUMP / KPRINT
      COMMON / INPUT / KFUEL DEQ,GAP,PPH,TITLE(8)
      COMMON / DEVAP/ DUMMY(10),D(5),TF(5),VF(5),VREL(5),      RN(5),
     1 CD(5),DRAG(5),FN(5),      CP(5),DELQ(5),SG(5),FMMD(5),DELTF(5),
     2 TIMS(5),FMASS(5),ALPHA(5),DELV(5),E(5),DX,W(5),VFSAVE(5),TFSAVE(5
     3 ),DSAVE(5),ESAVE(5),DSTART(5),SGSG6V(5),SG6V(5),DELM(5)
     4,DPTION,VAIRH,VAIRV,SINT,COST,DUMI,DUM2
     * ,WST(5),EW(5)
      COMMON / TRAJ / VFUEL,TFUEL,TFUELF,SGF,FMU,RHOF,PS,PT,TS,TT,
     1DUMMZQ(3),VAIR
      COMMON /DEVAP1/ TAIRTH(7),AIRKTH(7),AIRMUT(7),AIRCPT(7),NTABAR
      DATA TAIRTH / 400.,600.,1000.,1500.,2000.,2500.,3000. /
     1, AIRKTH / .0114,.0165,.0252,.0344,.0422,.0486,.0547 /
     2,AIRMUT /1.E-5,1.3E-5,1.885E-5,2.5E-5,3.015E-5,3.48E-5,3.9E-5 /
     3, AIRCPT /.240*,.2409,.249,.2622,.2772,.2868,.2931 /,NTABAR/7/
      DATA G,GAMMA,R,PI04,GOGMI,GM102,PI /32.174,1.4,1545.327,.7853982,
     1 3.5,.2, 3.1415927 /
C
      AIRM= 28.966
      CONSTI= G * GAMMA * R * TS / AIRM
C     CHECK FOR FIRST ENTRY TO ROUTINE (INTER=I)
      IF (INTER .NE. 1) GO TO 50
C     ESTIMATE NEXT STATION CONDITIONS
      VF2= VF(I)
      TF2= TF(I)
      D2=  D(I)
      E2=  E(I)
      DSTART(I)= D(I)
      GO TO 55
C     ESTIMATE NEXT STATION CONDITIONS
CCCCCC
   50 CONTINUE
      VF2=VF(I)
      TF2=TF(I)
      D2=D(I)
      E2=E(I)
CCCCCC
      IF (D2 .LT. 1.E-10) D2= 1.E-10
      IF (E2 .GT. .99) E2= .99
      IF (E2 .LT. 0.) E2= 0.
C     INITIALIZE FOR ITERATION ON D
   55 KOUNTC= 1
      SGRESD= SGRFCT (E(I))
      SG(I)= SGFCT (TF(I),SGRESD)
      SG60(I)= SGFCT (519.69,SGRESD)
      IF (INTER .EQ. 1) SGSG60(I)= SG(I) / SG60(I)
CCCCCC
      DELDG= D2 - D(I)
      KOUNTD=0
   60 KOUNTD= 1
      DZ= (D(I) + D2) * .5
      CIRCUM= PI * DZ
      TEMPA= PI04 * DZ**2
      TEMPD= TEMPA * DZ / 1.5
C     INITIALIZE FOR ITERATION ON TF
      DELTFG= TF2 - TF(I)
      EZ= (E(I) + E2) * .5
      VAPM= VAPMF (EZ)
      SGRESD= SGRFCT (EZ)
C     AVERAGE TEMPERATURES, CALC. PROPERTIES
   70 TFZ= (TF(I) + TF2) * .5
      TMX= (TS + TFZ) * .5
      PAS= PASF(TFZ,EZ)
      IF (PAS .LT. PS-.01) GO TO 80
```

TABLE XXIV. (CONTD)

```
C     AT BOILING POINT.
      PAS= PS - .01
      KOUNTD=1
   80 VAPK= VAPKF(TMX,VAPM)
      VAPMU= VAPMUF(TMX)
      VAPLAM= VAPLMF(TFZ)
      CP(I)= CPFCT(TFZ,SGRESD)
      VAPCP= VAPCPF(TMX)
      SG(I)= SGFCT(TFZ,SGRESD)
      FRHO(I)= SG(I) * 62.428
      VAPD= VAPDF(TMX,PS)
      IF (VAPD .LT. .00005) VAPD= .00005
      ALP= PS / PAS * ALOG(PS / (PS - PAS) )
C     AIR PROPERTIES
      AIRK=TAB(TMX,TAIRTB,AIRKTB,NTABAR)
      AIRMU=TAB(TMX,TAIRTB,AIRMUT,NTABAR)
      AIRCP=TAB(TMX,TAIRTB,AIRCPT,NTABAR)
C     DIFFUSION ZONE PROPERTIES
      QK= PAS / PS * .5
      QJ= 1. - QK
      QKMX= QJ * AIRK + QK * VAPK
      QMUMX= QJ * AIRMU + QK * VAPMU
      QMMX= QJ * AIRM + QK * VAPM
      QCPMX= (QJ * AIRM * AIRCP + QK * VAPM * VAPCP) / QMMX
      QRHOMX= PS * QMMX * 144. / R / TMX
      SC= QMUMX / VAPD / QRHOMX
      PR= QCPMX * QMUMX / QKMX * 3600.
      TEMPE= DZ * QRHOMX / QMUMX
      QMASS= TEMPD * SG(I) * 62.428
      TEMPF= .6 * SC**.3333333333
CCCCCCC
      TEMPG=CIRCUM*VAPD*VAPM*PAS*ALP/R/TMX*144.
      TEMPH= .6 * PR**.3333333333
      TEMPI= VAPCP / CIRCUM / QKMX
      TEMPJ= CIRCUM * QKMX * (TS - TFZ) / 3600.
      TEMPK = TEMPD * SG(I) * CP(I) * 62.428
C     INITIALIZE FOR ITERATION ON VF
      DELVG= VF2 - VF(I)
      KOUNTA= 1
C     CALCULATE DELTA V FOR DROP
  100 VFZ= (VF(I) + VF2) * .5
      IF (OPTION .EQ. 0.) GO TO 115
      VRV= VFZ    * SINT - VAIRV
      VRH= VFZ    * COST - VAIRH
      VREL(I)= SQRT(VRV**2 + VRH**2)
      SPHI= VRV / VREL(I)
      CPHI= VRH / VREL(I)
      VSIGN= 1.
      GO TO 120
  115 VREL(I)= VAIR - VFZ
      VSIGN= 1.
      IF (VREL(I) .GE. 0.) GO TO 120
      VREL(I)= - VREL(I)
      VSIGN= -VSIGN
CCCCCC
  120 CONTINUE
CCCCCC
      IF(VREL(I).LT.1.) VREL(I)=1.
CCCCCC
      RN(I)=VREL(I)*TEMPE
      CD(I)= 27. / RN(I)**.84
      FMACH2= VREL(I)**2 / CONST1
      TEMPB= PS * ( (1. + GM102 * FMACH2)**GOGM1 - 1.)
CCCCCC
      IF(TEMPB.LE.0.) TEMPB=1.E-20
      DRAG(I) = TEMPB * CD(I) * TEMPA * 144.
```

```
      ALPHA(I)= DRAG(I)  / QMASS * VSIGN * G
      IF (OPTION .EQ. 0.) GO TO 140
C     MODIFY FOR EFFECT OF G
      DUM1= G - ALPHA(I) * SPHI
      DUM2= -ALPHA(I) * CPHI
      ALPHA(I)= SQRT (DUM1**2 + DUM2**2)
      SINB= DUM1 / ALPHA(I)
      COSB= DUM2 / ALPHA(I)
  140 TIMS(I)= DX / VF(I)
      DUMMY1= VF(I)**2
      DUMMY2= 2. * DX * ALPHA(I)
C     CHECK IF ROUND/OFF ERROR I S A PROBLEM
      IF (ABS(DUMMY2 / DUMMY1)  .LT. 1.E-7) GO TO 180
      TIMS(I)= (SQRT(DUMMY1 + DUMMY2) - VF(I) ) / ALPHA(I)
  180 DELV(I)= ALPHA(I) * TIMS( )
CCCCCC
      IF(ABS(DELV(I)).GT.VREL(I)) DELV(I)=VSIGN*(VREL(I)-1.)
      IF (OPTION .EQ. 0.) GO TO 185
      VRV= VRV + DELV(I) * SINB
      VRH= VRH + DELV(I) * COSB
      DUM1= VRV + VAIRV
      DUM2= VRH + VAIRH
      VF2= SQRT(DUM1**2 + DUM2**2)
      GO TO 186
  185 VF2= VF(I) + DELV(I)
C     CHECK IF WITHIN TOLERANCE
CCCCCC
  186 IF(ABS(DELV(I)-DELVG).LE. .01*ABS(DELV(I))) GO TO 200
      DELVG= DELV(I)
      IF ( ABS(DELVG) .LT..01) GO TO 200
      KOUNTA= KOUNTA + 1
      IF (KOUNTA .LT. 25) GO TO 100
  190 WRITE (61,1000) KOUNTA, KOUNTB, KOUNTC, KOUNTD, I
 1000 FORMAT(18H0**** EVAP FAILURE    ,4I5,5X,7HDROPLET  I5)
      WRITE (61,1001) TF2,VF2,D2,E2
 1001 FORMAT (4E15.5)
      INTER= -1
      IF (OPTION .NE. 0.) GO TO 300
      CALL EXIT
C     HAVE CONVERGED ON VF2.  NOW CALC. DELTA TF, WF
  200 TEMPC= SQRT(RN(I))
      QNUM= 2. * TEMPF * TEMPC
      DELW = QNUM * TEMPG
CCCC
      IF((DELW*TIMS(I)).GT.QMASS) DELW=QMASS/TIMS(I)
      QNUM= 2. * TEMPH * TEMPC
  210 Z= DELW / QNUM * TEMP1
      ZZ= Z / (EXP(Z) - 1.)
      QVZ= QNUM * ZZ * TEMPJ
      IF (KOUNTD .EQ. 0) GO TO 240
C     AT BOILING POINT.  ASSUME DELTF= 0.
      IF (VAPLAM .EQ. 0.) GO TO 190
      DELWN= QVZ / VAPLAM
CCCC
      IF((DELWN*TIMS(I)).GT.QMASS) DELWN=QMASS/TIMS(I)
      IF (ABS(DELWN  - DELW) .LE. .001 * ABS(DELW) ) GO TO 220
      DELW= DELWN
      KOUNTD= KOUNTD + 1
      IF (KOUNTD .LT. 25) GO TO 210
      GO TO 190
  220 IJK=1
      KOUNTD=1
C     AT BOILING POINT, CALC TF2 BASED ON PS AND E2
  230 TF2= PASF (-PS, E2)
      DELTF(I)= TF2 - TF(I)
      GO TO 250
```

TABLE XXIV. (CONTD)

```
  240 DELTF(I)= QDVZ - DELW * VAPL(TM) * TIMS(I) / TEMPK
      TF2= TF(I) + DELTF(I)
CCCC
      IF(KFUEL.EQ.4.AND.TF2.GT.1092.8) TF2=1092.8
CCCC
      IF(KFUEL.NE.4.AND.TF2.GT.1210.4) TF2=1210.4
CCCCCC
      DEL(F(I)=TF2-TF(I)
C     CHECK IF WITHIN TOLERANCE
  250 IF (ABS( DELTF(I) - DELTFG) .LE.  .01*ABS(DELTF(1)) ) GO TO 260
      DELTFG= DELTF(I)
      IF ( ABS(DELTFG) .LT. 1.) GO TO 260
      KOUNTB= KOUNTB + 1
      IF (KOUNTB .LT. 25) GO TO 70
      GO TO 190
C     HAVE CONVERGED ON TF2.  NOW CALC. DELTA D
  260 IJK=0
  270 W2= W(I) - DELW * TIMS(1)
      IF (W2 .LT. 1.E-30) W2= 1.E-30
      SGRESD= SGRFCT (E2)
      SG(I)= SGFCT(TF2,SGRESD)
      SG60(1)= SGFCT (519.69,SGRESD)
      D2= (6. * W2 / PI / SG(I) / 62.428)**.3333333333
      IF (D2 .LT. 1.E-10) D2= 1.E-10
      E2= 1. - (D2 / DSTART(I))**3 * SG(I) / SG60(1)/ SGSG60(I)
      IF (E2 .GT. .99) E2= .99
      IF (E2 .LT. 0.) E2= 0.
      DELD= D2 - D(I)
C     CHECK IF WITHIN TOLERANCE
CCCCCC
      IF(ABS(DELD-DELDG).LE. .01*ABS(DELD)) GO TO 300
      DELDG= DELD
      IF (ABS(DELDG) .LT. 1.E-7) GO TO 300
      KOUNTC= KOUNTC + 1
      IF (KOUNTC .LT. 20) GO TO 60
      GO TO 190
C     HAVE CONVERGED ON ALL PARAMETERS FOR THIS INTERVAL
C     SAVE OLD CONDITIONS, SET NEW ONES
  300 VFSAVE(I)= VF(I)
      VF(1)= VF2
      TFSAVE(I)= TF(I)
      TF(1)= TF2
      DSAVE(I)= D(I)
      D(I)= D2
      ESAVE(I)= E(1)
      E(I)= E2
      DELW(I)= QVZ * TIMS(I)
      DELM(I)= DELW * TIMS(1)
      RETURN
      END
*DECK D
      FUNCTION PASF (T,E)
C     T= TEMPER. (R), E= FRACTION EVAPORATED
C     PASF= FUEL VAPOR PRESSURE (PSIA) FOR JP4, JPS/JP8
      COMMON / INPUT / KFUEL,DEQ,GAP,PPH,TITLE(8)
      DIMENSION CK1(7,4), CK2(7,4), ETAB(7)
      DATA ETAB / 0.,.1, .3, .5, .7, .9 ,1.0 /
     1, CK1 / 0., 0., 0., 0., 0., 0., 0.,
     2 155810.,386390.,585230.,817550.,1321200.,3175400.,10497000.,
     3 0., 0., 0., 0., 0., 0., 0.,
     4       40497.,136750.,286430.,604200.,1399600.,704410C.,77680000./
     5, CK2 / 0., 0., 0., 0., 0., 0., 0.,
     6 7414.8,8548.4,9066.7,9484.0,10083.,11178.,12670.,
     7 0., 0., 0., 0., 0., 0., 0.,
     8        4816.,6269.,7151.,8042.,9045.,10974.,13839. /
C
```

TABLE XXIV. (CONTD)

```
      IF (KFUEL .NE. 2 .AND. KFUEL .NE. 4) GO TO 150
C     IF (T .LT. 0 , ARGUMENT IS (-PS).  FIND AND RETURN CORRES. TEMPERATURE
      PSTAT=-T
      DO 50 J=1,7
      I=J
      IF (E - ETAB(J)) 60,90,50
   50 CONTINUE
      GO TO 70
   60 IF (I .EQ. 1) I=2
   70 K=1
   80 IF (PSTAT .LT. 0.) GO TO 83
      PASF= CK2(I,KFUEL) /  ALOG(CK1(I,KFUEL) / PSTAT )
      GO TO 84
   83 PASF=CK1(I,KFUEL) * EXP( -CK2(I,KFUEL) / T )
   84 IF (K) 110,100,85
   85 PSAVE= PASF
      J=I
      I= I - 1
      K= -1
      GO TO 80
   90 K=0
      GO TO 80
  100 RETURN
  110 PASF= PASF + (PSAVE - PASF) / (ETAB(J) - ETAB(I)) * (E - ETAB(I))
      GO TO 100
  150 WRITE (61,1000) KFUEL
 1000 FORMAT (25H0PASF CANNOT HANDLE FUEL=     I5)
      CALL EXIT
      END
      FUNCTION VAPCPF (T)
C     T= TEMPER. (R), VAPCPF= CP FOR JP4, JP5/JP8 FUEL VAPOR
      COMMON / INPUT / KFUEL,DEQ,GAP,PPH,TITLE(8)
      IF (KFUEL .EQ. 2) GO TO 50
      VAPCPF= .180 + .000565 * T
      GO TO 100
   50 VAPCPF= .069 + .000530 * T
  100 RETURN
      END
      FUNCTION VAPMUF (T)
C     T= TEMPER. (R), VAPMUF= MU FOR JP4, JP5/JP8 FUEL VAPOR
      COMMON / INPUT / KFUEL,DEQ,GAP,PPH,TITLE(8)
      IF (KFUEL .EQ. 2) GO TO 50
      VAPMUF=   808.E-9 + 7.64E-9 * T
      GO TO 100
   50 VAPMUF= 248.E-9 + 6.31E-9 * T
  100 RETURN
      END
      FUNCTION VAPKF(T,W)
C     T= TEMPER. (R), VAPKF= K FOR FUEL VAPOR
C     W= MOLECULAR WEIGHT
      DIMENSION WTAB(4),ATAB(4),BTAB(4),TABK(4)
      DATA WTAB/50., 100., 150., 300, /, NTAB /4/,
     1 ATAB / -.006362,-.006358,-.006284,-.006010 /,
     2 BTAB / .0000297,.0000273,.0000259,.0000235 /
C
      DO 10 I=1,NTAB
   10 TABK(I)= ATAB(I) + BTAB(I) * T
      VAPKF= TAB (W,WTAB,TABK,NTAB)
      RETURN
      END
      FUNCTION SGFCT (T,SG60R)
C     SG60R =  SG RESIDUE AT 60 DEG F
C     T= TEMPER. (R), SGFCT= SG FOR JP4 AND JP5 LIQUID FUEL
      SGFCT= SG60R + .208 - .0004* T
      RETURN
      END
```

TABLE XXIV. (CONTD)

```
      FUNCTION SGRECT (E)
C     E= FRACTION EVAPORATED. SG60= SG AT 60 DEG F
C     SGRECT= SG RESIDUE AT 60 DEG F FOR JP4, JP5/JP8 LIQUID FUEL
      COMMON / INPUT / KFUEL,DEQ,GAP,PPH,TITLE(8)
      DATA SG60 / .775 / , SG6058 / .806 /
      SG60= SG6004
      IF (KFUEL .NE. 4) SG60= SG6058
      SGRECT= 1.076 / ( (1.076 / SG60 - 1.) * (1. - .67 * E) + 1. )
      RETURN
      END
      FUNCTION VAPDF (T,P)
C     T= TEMPER. (R) . P= STATIC PRESSURE
C     VAPDF= DIFFUSIVITY FOR HEPTANE-OXYGEN
      VAPDF= 2.043 / P  * (T * (T * 1.1319E-9 + 1.973E-6) - 9.815E-4)
      RETURN
      END
      FUNCTION VAPMF (E)
C     E= FRACTION EVAPORATED. VAPMF= MOLECULAR WEIGHT OF JP4, JP5/JP8
C                    FUEL VAPOR
      COMMON / INPUT / KFUEL,DEQ,GAP,PPH,TITLE(8)
      DIMENSION ETAB(7), TABMV(7,4)
      DATA ETAB / 0., .1, .3, .5, .7, .9, 1.0 /, NTAB /7/,
     1 TABMV / 0., 0., 0., 0., 0., 0., 0.,
     2 148.12,163.29,169.88,175.04,182.25,194.86,211.07,
     3          0., 0., 0., 0., 0., 0., 0.,
     4          93.26, 114.60, 126.61, 138.16, 150.59, 173.21, 204.76 /
C
      VAPMF= TAB(E, ETAB, TABMV(1,KFUEL), NTAB)
      RETURN
      END
      FUNCTION VAPLMF(T)
C     T= TEMPER (R), VAPLMF= LATENT HEAT OF VAPORISATION FOR JP4,BTU/LB
C                ALSO, JP5/JP8
      COMMON / INPUT / KFUEL,DEQ,GAP,PPH,TITLE(8)
      IF (KFUEL .EQ. 2) GO TO 50
      VAPLMF= 0.
      IF (T .LT. 1092.88) VAPLMF= 13.20 * (1092.88 - T) **.39
      GO TO 100
   50 VAPLMF= 0.
      IF (T .LT. 1210.45) VAPLMF= 10.75 * (1210.45 - T) **.41
  100 RETURN
      END
      FUNCTION CPFCT (T,SGR60)
C     T= TEMPER (R). CPFCT, CP FOR LIQUID JP4, JP5/JP8
C     SGR60= SG RESIDUE AT 60 DEG F FOR JP4
      CPFCT= ( .181 + .00045 * T) / SQRT(SGR60)
      RETURN
      END
      FUNCTION FLIQKF (T)
C     T= TEMPER (R), FLIQKF= THERMAL CONDUCT. FOR LIQUID JP4, OR JP5/JP8
      FLIQKF= .093 - .000026 * T
      RETURN
      END
```

TABLE XXV. PROGRAM NO. 1529 OUTPUT

```
AVL4HS L-PIPE DESIGN POINT

FUEL    TFUELA        P3        T3R        PPH       DELP        HEX         Y
   4  530.0000  235.0000 1290.0000   35.2000    7.0500 -100.5060      .0200

    JET1D      DIA1      DIA2      DIA3       XL1       XL2      JETOO       RMS
    .0450      .1600     .1300     .1300     .3000     .3000     .0450   25.0000

    XL3       XL4       OD1       OD2       OD3     WIDTH     X MAX     I RAD
    .1600     .3030     .1700     .1700     .1700    0.0000    1.5000         1

   X=        0.000       .200       .400       .800       .600      1.000

TAMB=    3000.000   3000.000   3000.000   3000.000   3000.000   3000.000

VAMB=      20.000     20.000     20.000     20.000     20.000     20.000

S0=   .7064E+00 (DMLS)    VISC FUEL=   .1132E+01 CENTISTOKES    VISC AIR =   .2244E-04 LB/SEC/FT

V(AIR)=     370.084         1     SMD= 29.67

    .7050E+01    .3493E+02    1

V(AIR)=     166.260         2     SMD= 64.60

    .7050E+01    .6686E+01    2

V(AIR)=     166.230         3     SMD= 63.68

    .7050E+01    .7065E+01    3

V(AIR)=     168.855         4     SMD= 63.75

TS= 1286.55   PS=234.0737   TT= 1290.00   PT=235.0000   M=  .07513   VAIR=  132.21   XIN=  .00602   TD=  1290.00
TF=         530.00          530.00          530.00          530.00          530.00
VF=          18.46           18.46           18.46           18.46           18.46
 E=         .00337          .00337          .00337          .00337          .00337
EW=        0.00000         0.00000         0.00000         0.00000         0.00000
D =       42.55201        52.58354        66.99804        85.02241       112.53484

TS= 1205.04   PS=233.7863   TT= 1207.35   PT=234.9503   M=  .08426   VAIR=  143.42   XIN=  .10602   TD=  1369.99
TF=         640.60          622.42          603.43          587.10          571.17
VF=          32.72           29.20           26.06           23.75           21.84
 E=         .07163          .05303          .03638          .02503          .01652
EW=         .05991          .04330          .02656          .01650          .01097
D =       42.11843        52.27941        66.86319        85.04077       112.73153

TS= 1065.09   PS=233.2963   TT= 1067.86   PT=234.8041   M=  .09598   VAIR=  153.60   XIN=  .20602   TD=  1329.44
TF=         664.55          665.13          642.27          620.66          598.73
VF=          45.43           39.62           33.61           29.49           25.74
 E=         .19276          .14321          .10411          .07659          .05043
EW=         .16394          .11984          .08540          .06192          .03955
D =       40.59337        51.02320        65.76952        84.02643       111.89299

TS=  973.53   PS=232.5448   TT=  975.96   PT=234.5759   M=  .11153   VAIR=  170.59   XIN=  .30602   TD=  1293.63
TF=         712.69          694.14          672.23          649.78          623.42
VF=          60.83           51.95           43.56           36.96           30.99
```

INPUT DATA

ITERATE TO MATCH DELP

DROP GRP ① ② ③ ④ ⑤

FUEL TEMP, °R
FUEL VELOCITY, FPS
VOLUME FRAC EVAP
WEIGHT FRAC EVAP
DROP SIZE, MICRONS

L-PIPE INTERNAL FLOW

L-PIPE TEMP °R

TABLE XXV. (CONTD)

```
 E=        .31384        .24115        .17346        .12546        .08867
EW=        .27167        .20549        .14516        .10385        .07139
D =      38.62354      49.21487      64.31890      82.91876     110.82440

TS=  924.99   PS=232.1931   TT=  927.41   PT=234.3285   M=  .11444   VAIR=  170.61   XIN=  .60602   TO=  1287.07
TF=       723.89        706.99        686.76        665.90        640.22
VF=        73.98         62.85         52.21         43.75         35.98
 E=        .40453        .32051        .23872        .17349        .11930
EW=        .35556        .27647        .20226        .14437        .09715
D =      38.90291      47.53422      62.73096      81.59184     109.89469

TS=  896.67   PS=231.8747   TT=  899.14   PT=234.1160   M=  .11731   VAIR=  172.20   XIN=  .60602   TO=  1291.71
TF=       726.55        712.50        694.14        674.75        650.63
VF=        84.62         71.87         59.52         49.58         40.35
 E=        .44899        .39129        .29150        .21681        .14895
EW=        .41720        .33291        .24946        .18219        .12254
D =      35.53756      46.11164      61.31902      80.25644     108.83698

TS=  870.18   PS=231.5921   TT=  880.63   PT=233.9302   M=  .11998   VAIR=  174.14   XIN=  .60602   TO=  1298.68
TF=       727.90        714.71        698.63        680.28        657.68
VF=        93.71         79.71         65.98         54.79         44.31
 E=        .51616        .42877        .33431        .25425        .17704
EW=        .46348        .37786        .28855        .21538        .14683
D =      34.45596      44.91316      60.09564      79.02545     107.74930

TS=  865.14   PS=231.3378   TT=  867.73   PT=233.7637   M=  .12217   VAIR=  176.15   XIN=  .70000   TO=  1276.88
TF=       728.15        716.88        700.95        684.14        662.40
VF=       101.68         88.78         71.81         59.55         47.97
 E=        .55307        .46649        .37051        .28629        .20296
EW=        .50841        .41423        .32218        .24418        .16946
D =      33.55317      43.90655      59.00398      77.92231     106.69142

TS=  855.57   PS=228.4672   TT=  858.27   PT=230.9412   M=  .12564   VAIR=  180.16   XIN=  .80000   TO=  1279.47
TF=       727.89        716.80        702.54        687.01        666.38
VF=       108.97         93.19         77.26         64.84         51.44
 E=        .58317        .49732        .40150        .31406        .22672
EW=        .53899        .44443        .35138        .26947        .19040
D =      32.77670      43.04465      58.02835      76.92908     105.60269

TS=  848.42   PS=228.1908   TT=  851.18   PT=230.7985   M=  .12751   VAIR=  182.07   XIN=  .90000   TO=  1283.34
TF=       727.54        717.32        703.68        689.12        669.48
VF=       115.53         99.12         82.32         68.24         54.71
 E=        .60799        .52311        .42807        .33803        .24828
EW=        .55652        .47003        .37672        .29229        .20957
D =      32.10711      42.29426      57.16156      76.01218     104.73907

TS=  842.96   PS=227.9896   TT=  845.77   PT=230.6553   M=  .12921   VAIR=  183.90   XIN= 1.00000   TO=  1287.66
TF=       727.23        717.59        704.59        690.74        671.91
VF=       121.49        104.59         87.04         72.18         57.82
 E=        .62889        .54541        .45111        .36108        .26785
EW=        .57824        .49239        .39893        .31298        .22712
D =      31.52120      41.62191      56.38671      75.16302     103.96000
TS=  842.03   PS=227.9509   TT=  844.85   PT=230.6396   M=  .12953   VAIR=  184.26   XIN= 1.00000   TO=  1287.78

    .7050E+01    .7049E+01    4

AIR FLOW RATE=     .00959 PPS     DISCHARGE COEFF.=   .5717     AIR-FUEL RATIO=     .9808

VFUEL= 88.62  TFUEL=682.53  VAIR=184.26  TT= 844.9  FUELP= 37.19  E= .45047
```

L-PIPE EXIT CONDITIONS

TABLE XXV. (CONTD)

FILM EVAPORATION

VEXT,DEXT,REXT,REX= 100.0 .042 .46590E+05 144.21

****

E(START)= .45247 VOLUME } FRACTION EVAP AT L-PIPE EXIT

EW (START)= .40193 WEIGHT }

X= 0.0000 IN., R= .1040 IN. FOR WEIGHT FRACTION EVAP, EW= .10

X= 0.0000 IN., R= .1040 IN. FOR WEIGHT FRACTION EVAP, EW= .20

X= 0.0000 IN., R= .1040 IN. FOR WEIGHT FRACTION EVAP, EW= .30

X= 0.0000 IN., R= .1040 IN. FOR WEIGHT FRACTION EVAP, EW= .40

INITIAL FILM VEL, FPS= 14.6434 FILM THICKNESS, IN.= .0074018

X IN.	R IN.	FILM-TH IN.	FILM-V FPS	WF-PPH	FRAC-EV (VOLUME)	T-I °R	T-F °R	T-G °R	V-G FPS	WF /FT LB/HR/FT	EW (WEIGHT)
.01	.11	.00212	15.194	21.005	.4540	851.	720.	845.	184.26	.353E+03	.4033
.08	.18	.00138	15.487	20.106	.4802	857.	745.	845.	184.26	.210E+03	.4288
.13	.23	.00108	15.633	19.246	.5050	843.	751.	845.	184.26	.159E+03	.4533
.17	.27	.00090	15.138	18.434	.5281	836.	755.	845.	184.26	.130E+03	.4763
.20	.30	.00077	14.685	17.713	.5485	831.	768.	845.	184.26	.111E+03	.4968
X= .2069 IN., R= .3104 IN. FOR WEIGHT FRACTION EVAP, EW= .50											
.23	.33	.00072	14.147	16.960	.5696	871.	814.	1025.	184.26	.969E+02	.5182
.26	.36	.00076	11.500	14.969	.4245	954.	899.	1275.	176.95	.786E+02	.5747
X= .2689 IN., R= .3725 IN. FOR WEIGHT FRACTION EVAP, EW= .60											
.29	.39	.00073	8.216	11.243	.7239	1018.	967.	1478.	156.12	.545E+02	.6806
X= .2959 IN., R= .3984 IN. FOR WEIGHT FRACTION EVAP, EW= .70											
.32	.42	.00057	5.964	7.178	.8277	1056.	1024.	1625.	141.11	.326E+02	.7961
X= .3190 IN., R= .4215 IN. FOR WEIGHT FRACTION EVAP, EW= .80											
BOILING STARTS AT X= .327											
X= .3347 IN., R= .4376 IN. FOR WEIGHT FRACTION EVAP, EW= .90											
.34	.44	.00035	3.575	2.779	.9349	1098.	1070.	1718.	131.50	.121E+02	.9211
.34	.44	.00029	3.179	1.943	.9547	1722.	1076.	1736.	129.70	.836E+01	.9600
X= .3400 IN., R= .4433 IN. FOR WEIGHT FRACTION EVAP, EW= .95 ← EVAPORATION COMPLETE											
1.34	1.44	.00012	2.745	1.943	.9547	1731.	1076.	1741.	129.21	.257E+01	.9600
2.34	2.44	.00019	1.094	1.943	.9547	2660.	1075.	2729.	27.81	.152E+01	.9600

CALC. STOPPED AT X = 1.50 INCHES, EW= .96000

APPENDIX IV
PRIMARY-ZONE MODEL
COMPUTER PROGRAM NO. 1338

1.0 INTRODUCTION

Computer Program No. 1338 provides a method for solving a number of finite-difference fluid flow equations. The program was set up mainly to analyze the primary zone of a gas turbine combustor but can also be used for many other two-dimensional flow fields.

This appendix describes the grid geometry setup, selection of equations to be solved, definition of fluid properties, inlet conditions, iteration controls, and input and output options.

2.0 FINITE-DIFFERENCE PROCEDURE

The program is a finite-difference method in which a flow field is represented by a grid of finite-element nodes and elemental volumes around each node. Derivation of the equations and finite-difference procedures is given in the text by Gosman et al.[37] The whole purpose of the mathematical derivations is to arrange all pertinent equations in an identical form so that all can be solved by the same computer coding. To use the program, it is not necessary to understand all the details of each equation, but the number and type of equations to be solved must be defined for each application.

The basic steps required in obtaining a solution are:

(a) Define grid geometry

(b) Define equations to be solved

(c) Define the fluid properties

(d) Define inlet conditions

(e) Define iteration controls

(f) Select program output options

(g) Determine input and output file options

Each of these steps will be discussed in terms of the input required for the data sheets shown in Figures 175 through 179.

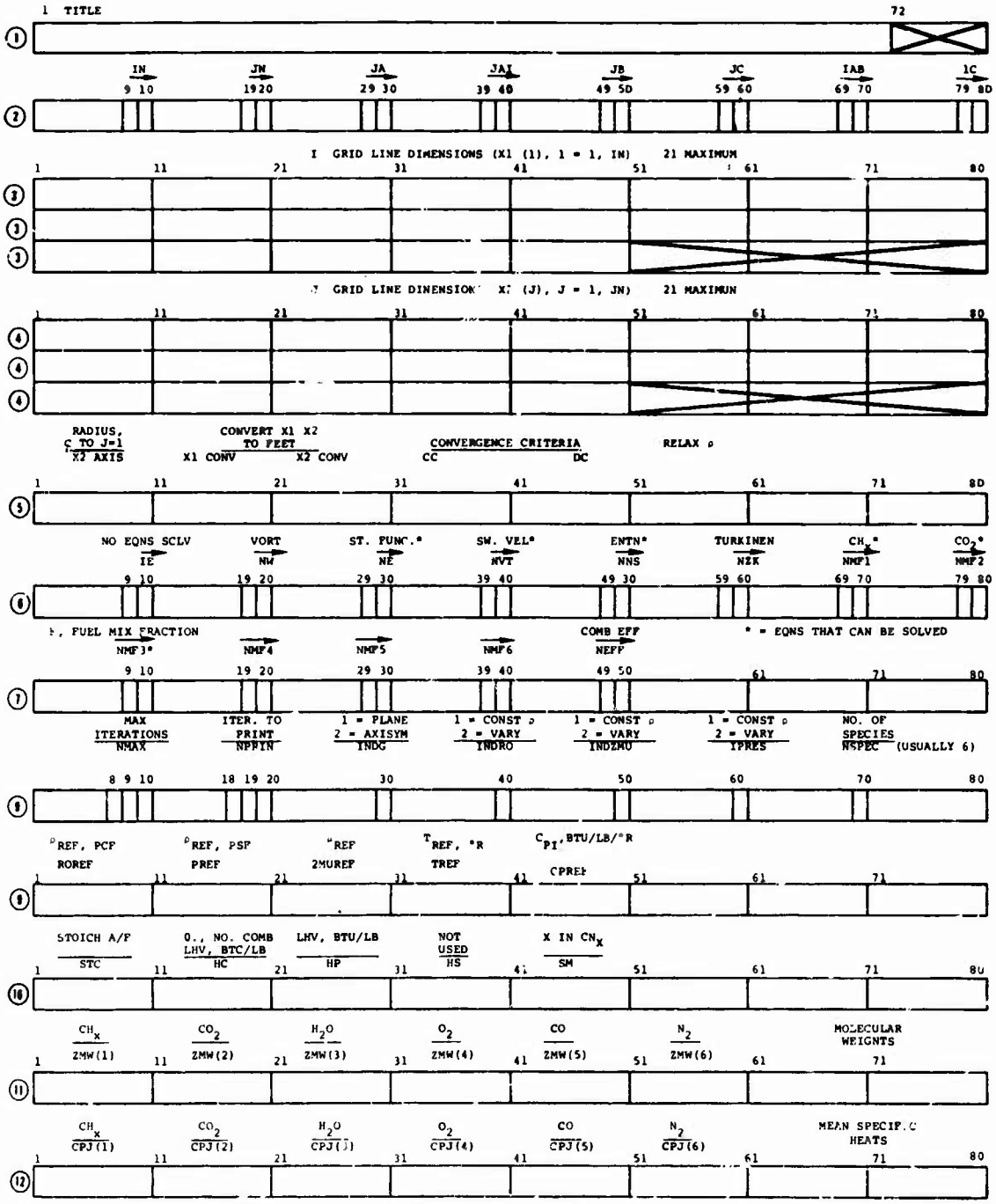


Figure 175. Two-Dimensional Flow, Program No. 1338 Input Data, Sheet 1.

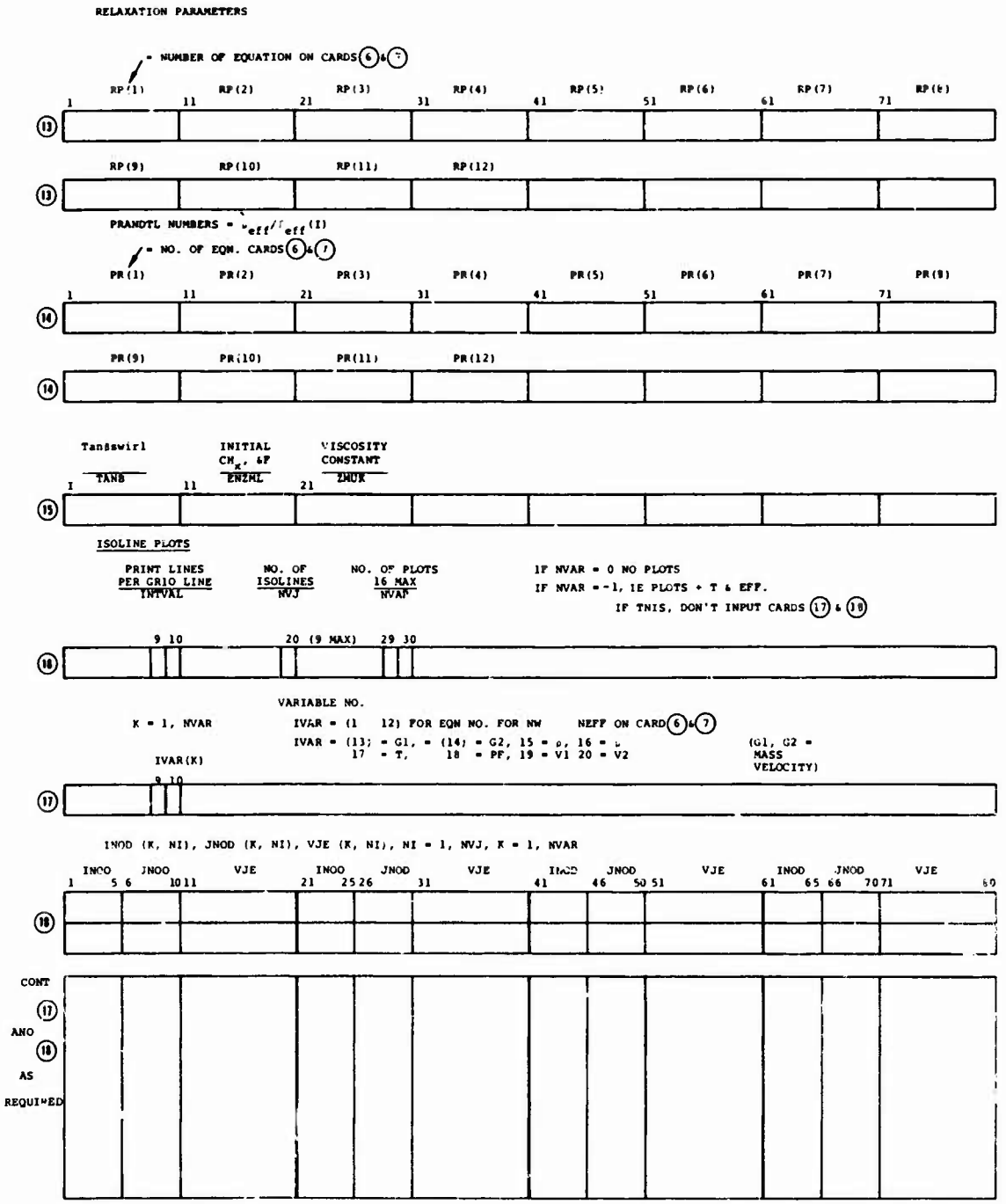
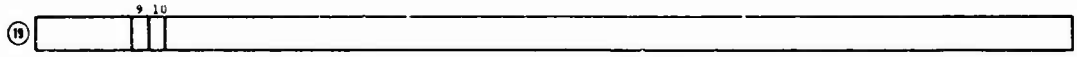
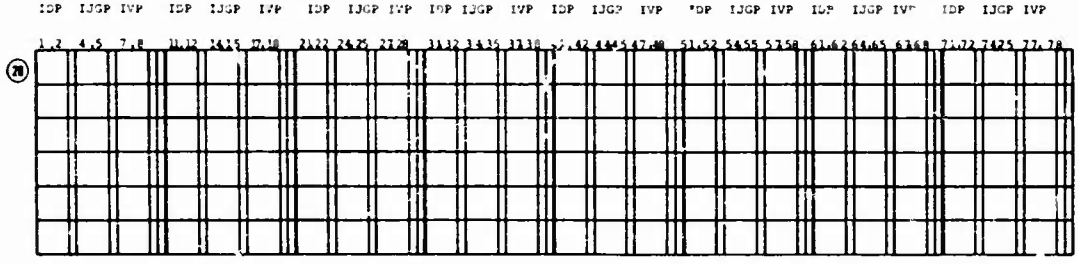


Figure 176. Two-Dimensional Flow, Program No. 1338 Input Data, Sheet 2.

PROFILE GRID LINE PLOTS

NVP, NO. OF PLOTS (42 MAXIMUM)



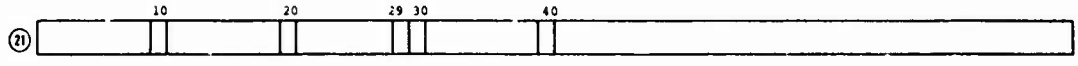


IDP = 01 FOR A J GRID LINE
= 02 FOR A I GRID LINE

IJGP = I OR J GRID LINE

IVP = VARIABLE NO. 1 12 FOR NW NEFF PER CARD 6 & 7
13 = G1 14 = G2 15 = ρ 16 = μ
17 = TEMP 18 = PF 19 = V1 20 = V2

INPUT FILE IOLD	OUTPUT FILE INEW	NO-NO_2 INDICATOR INOX	FUEL EVAP FILE IVAP



FILE NUMBERS (TAPE OR DISK) MUST BE = 1, 2, OR 3 AND IDENTIFIED BY LOCAL FILE NAMES, TAPE1, TAPE2, TAPE3

IOLD = OLD FILE NO. FOR INPUT SOLN. IF = 0 NO FILE
IF < PLOT ONLY - NO ITERATE

INEW = NEW FILE NO. FOR SOLN OUTPUT, IF = 0 NO FILE

IVAP = FILE FOR FUEL EVAPORATION RATES

NO & NO_2 SOLUTION

INOX = 0 NO "NO" OR "NO_2" } MAIN ITERATION DONE
= 1 "NO" ONLY
= 2 "NO" + "NO_2"
= -1 "NO" ONLY - NO MAIN ITERATION
= -2 "NO" + "NO_2" ONLY - NO MAIN ITERATION

Figure 177. Two-Dimensional Flow, Program No. 1338 Input Data, Sheet 3.

LEFT BOUNDARY (I=1) INLET CONDITIONS

NVARI = NO. OF VARIABLES TO BE INPUT

9 10

(22)

READ NVARI SETS OF IOVAR & (VAR(J), J = 1, JB)

ENTER EACH "IDVAR" ON A SEPARATE CARD, FIRST FIELD, RIGHT JUSTIFIED
FOLLOWED BY CARDS WITH INLET VALUES FOR THAT IDVAR

VALUES OF "VAR" MUST BE ENTERED FOR ALL NODES 1 ——→ JB EVEN THOUGH SOME NODES ARE ON A WALL (JA → JAI)

ONLY THE FOLLOWING VARIABLES CAN BE SET:

NMF1, NMF2, NMF3, NMF4, NMF5, NMF6, NHS, NZK
(IDVAR = EQN NO. FROM CARDS (6) & (7))

17 = TEMP, 19 = VI

IF NOT ENTERED, ALL ABOVE ARE = $1*10^{-30}$ EXCEPT TEMP=TREF

9 10

(23)

IDVAR

OR VAR (1) VAR VAR VAR VAR VAR VAR VAR

1 9 10 11 21 31 41 51 61 71 80

(24)

Figure 178. Two-Dimensional Flow, Program No. 1338 Input Data, Sheet 4.

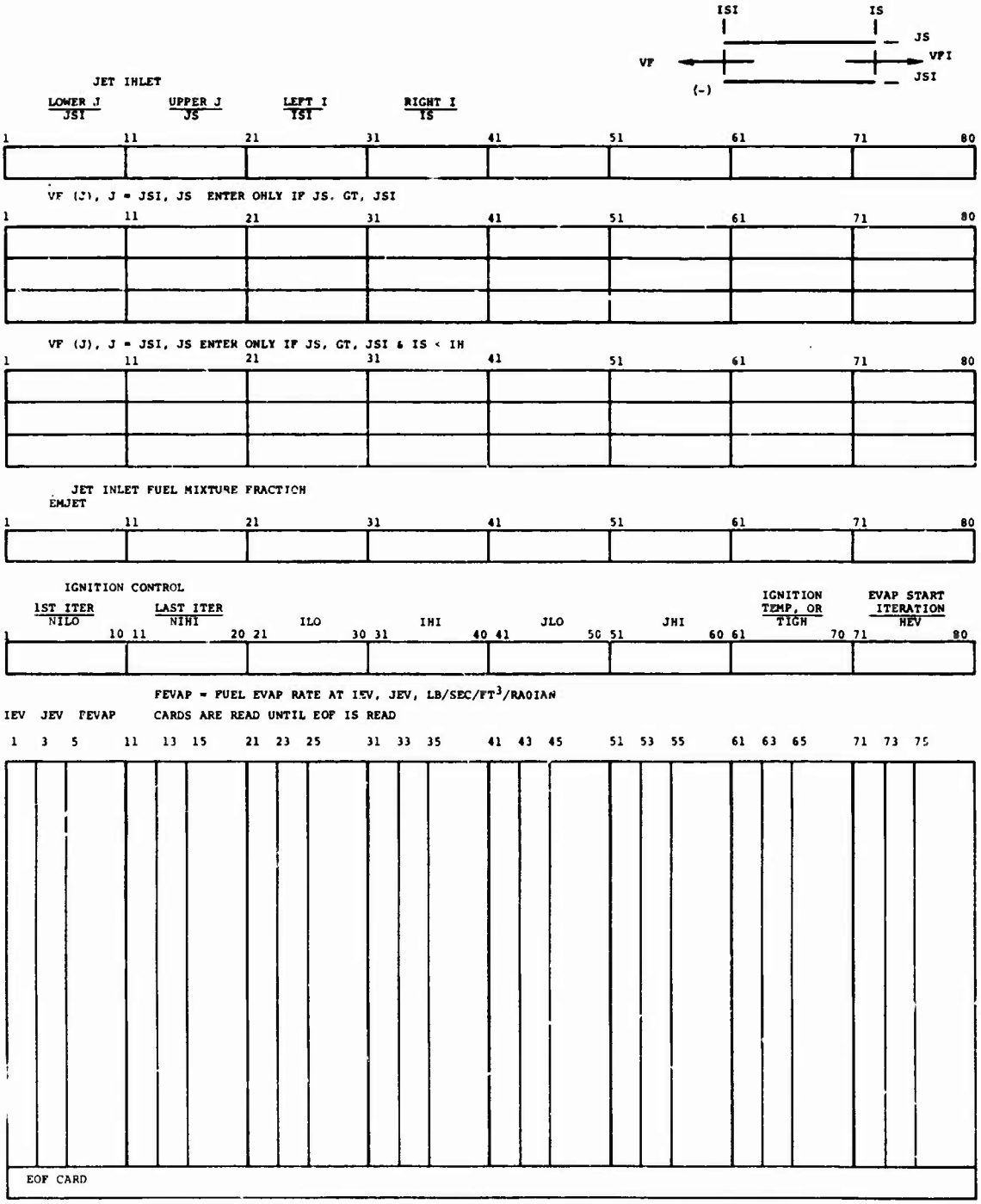


Figure 179. Two-Dimensional Flow, Program No. 1338 Input Data, Sheet 5.

3.0 GRID GEOMETRY DEFINITION

Figure 180 shows the basic grid geometry in this program. Figure 181 shows the wide variety of configurations that can be obtained by adjusting the various input parameters. In general, all flow inlet is at the left boundary, and flow exits across the right boundary.

The first step is to define the upper and lower boundaries. The lower boundary can be an axis of symmetry or a solid wall. The upper boundary must be a solid wall.

The next step is to define the inlets at the left wall. Two inlets are provided. One, called the primary inlet, extends up from the lower boundary, and is fixed to the lower boundary. The other, called the secondary inlet, can float anywhere between the primary inlet and the upper boundary. Either inlet can be extended to cover the full width of the left boundary, but they must not overlap. Swirl can be introduced at the secondary inlet.

Two other inlets were added to the original program and protrude up from the lower boundary. The left-hand inlet can be used for upstream injection, as from an L-pipe, or to simulate air recirculating from air jets impinging at the centerline.

With upper and lower boundaries and inlet dimensions defined, the grid mesh is established. Figure 182 illustrates this process.

4.0 EQUATIONS TO BE SOLVED

A listing of this program is given in Table XXVI. Up to seven equations can be solved. These are:

(a) Vorticity (NW)

(b) Stream function (NF)

(c) Swirl velocity (NVT) for INDG = 2 only

(d) Enthalpy (NHS)

(e) Unburned fuel, CH_x (NMF1)

(f) Carbon dioxide (NMF2)

(g) Fuel-mixture fraction, F (NMF3)

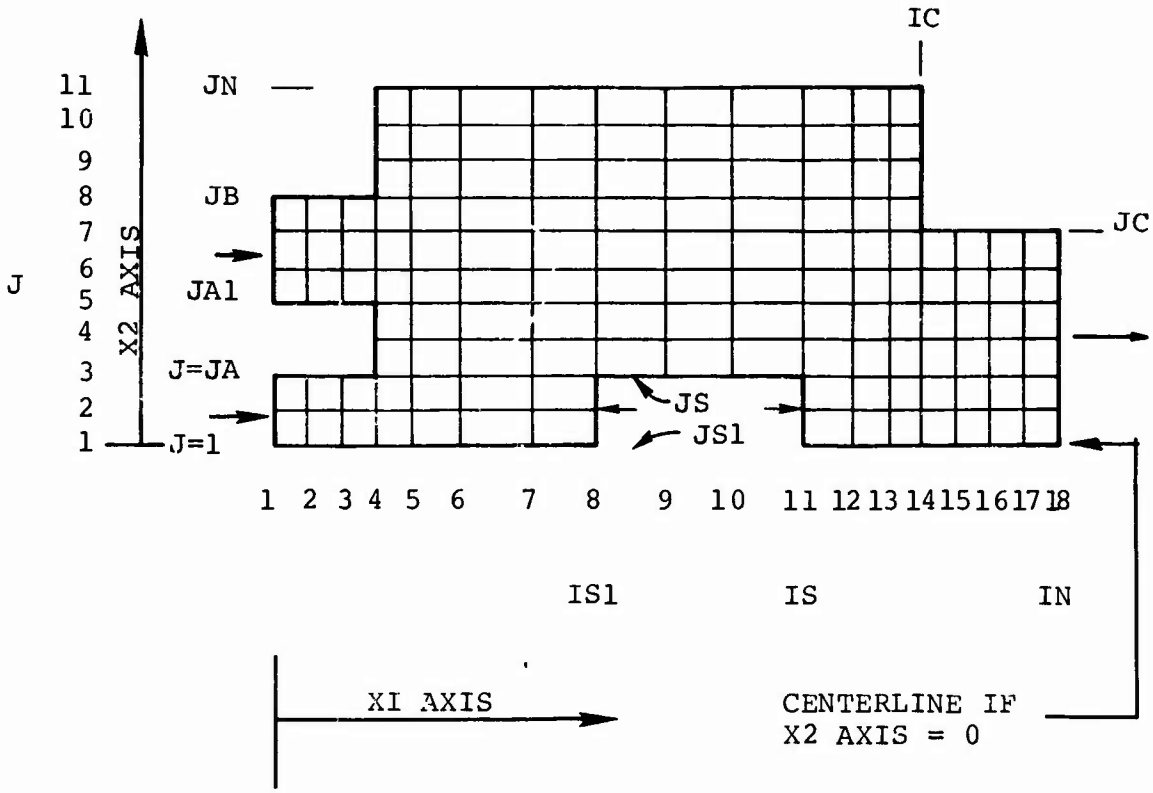


Figure 180. Grid Line Parameters.

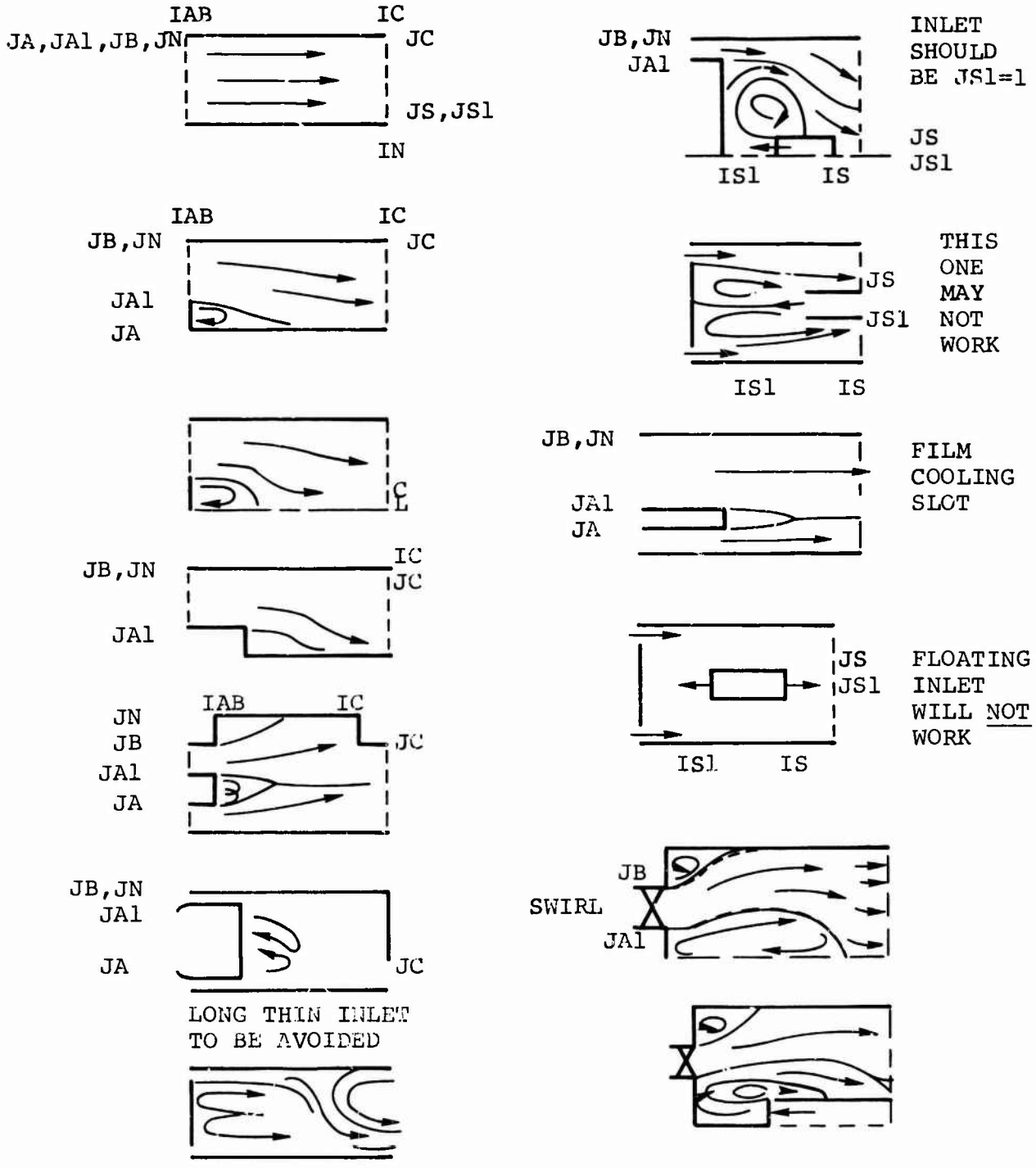


Figure 181. Various Grid Configurations.

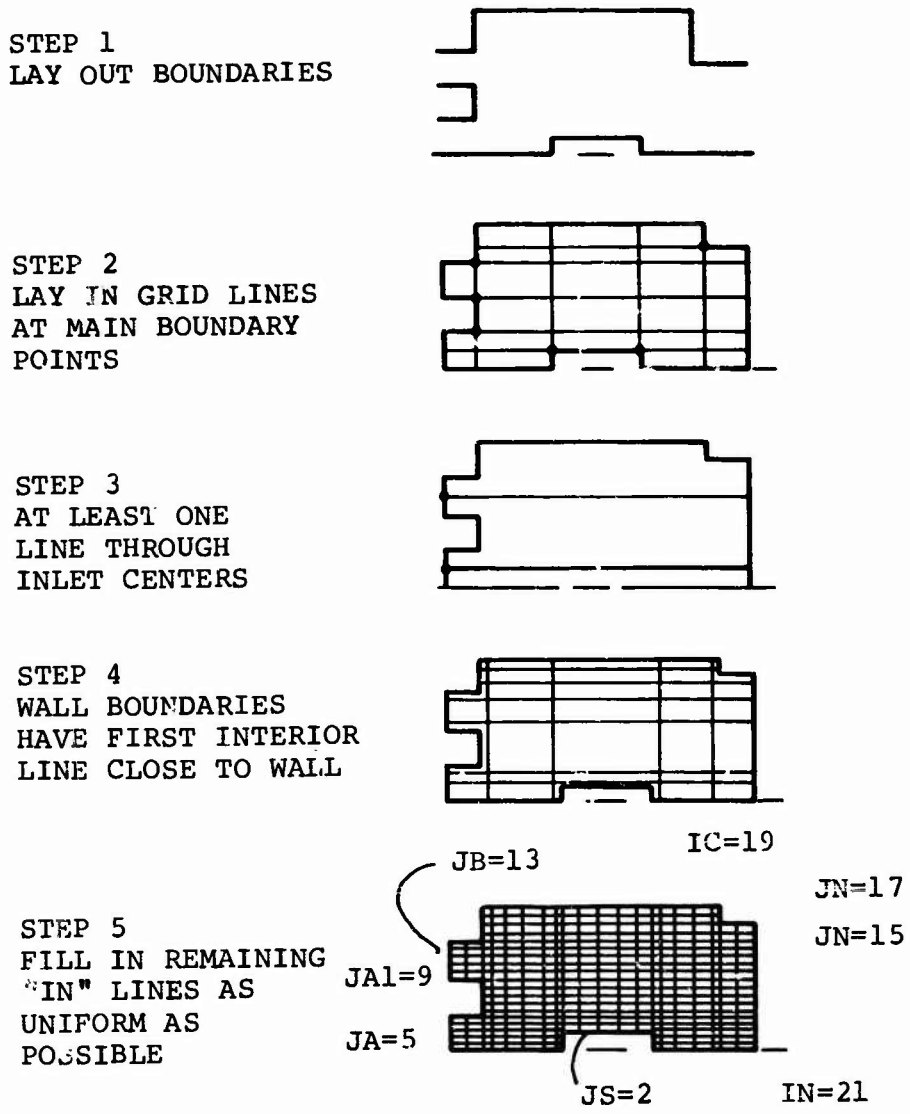


Figure 182. Grid Layout Procedure.

Two additional equations can be solved for NO and NO_2 after the above equations are converged.

Vorticity represents the combined X and Y momentum component equations and eliminates the need to solve for pressure variations. Vorticity is related to velocity gradients and will be high where velocity gradients are high and will be zero in uniform velocity regions.

The stream function represents continuity of mass and is essentially an integration of ρ AV.

The fuel mixture fraction primarily keeps track of the total atomic balance of C, H, N, and O atoms. The difference between NMF3 and NMF1 represents the fuel burned at a given node. Rates of fuel burning and CO_2 production are determined from reaction kinetics.

Iteration starts with all temperatures set to TREF. If this is less than approximately 3000°R, solutions with combustion will remain unreacted. A means for starting reactions, i.e., lighting off, is provided on Data Sheet 5, Figure 179. An artificial temperature is imposed on the reaction rate source terms. A value of 4000°R is recommended. Five iterations are generally sufficient to obtain ignition. Iteration will proceed, and combustion will either die back to a cold flow condition (blowout), or converge to a stable burning solution. Combustion efficiency is calculated at each node point from the CH_x and CO unburned. An integrated efficiency at the exit is printed after the final printout.

To solve for NO or NO_2 set INOX on Data Page 3 equal to 1 for NO only, or 2 for both NO and NO_2. These equations are solved after the main solution has converged.

TABLE XXVI. LISTING FOR PROGRAM NO 1338

```
$$$
```

TABLE XXVI. (Cont)

```
      NOXSOL=.FALSE.                                                    07/26/71
175   CONTINUE                                                          07/26/71
      IF(INEW .EQ.0) GO TO 1003
      REWIND INEW
      WRITE(INEW)IN,JN,X1,X2,R
      WRITE(INEW)A
      WRITE(INEW) G1
      WRITE(INEW) G2
      WRITE(INEW) HO
      WRITE(INEW) ZMU
      WRITE(INEW)T
      WRITE(INEW) PF
 1003 CONTINUE
  179 CALL OVERLAY(3HOUT,4,0)
      STOP
      END
*DECK PR
      SUBROUTINE PRINCI
*CALL CMU
      DIMENSION AQ(21,21,18)
      DIMENSION W(21)
C...KVB...                                                              08/09/71
      DIMENSION KLIST(20)                                               08/09/71
      EQUIVALENCE (A(1,1,1),AQ(1,1,1))
C*****************************************************************
C   **PRINT** SUBROUTINE
C   THIS SUBR. PRINTS OUT PART OF THE RESULTS FOR EASY EXAMINATION
C*****************************************************************
      IT=IE
C...KVB...                                                              08/09/71
      DO 30 KK=I,IE                                                     08/09/71
30    KLIST(KK)=KK                                                      08/09/71
      IF(NOXSOL) GO TO 46
      IF(IOLD.GE.0.AND.NMAIN.GT.0.AND.NNOX.EQ.0.AND.HC.GT.0.)GO TO 34
      IF(NNOX.GT.0)GO TO 34
      GO TO 36
   34 IT=IT+I
      KLIST(IT)=NMF5                                                    08/09/71
      IF(NNOX.GT.0.AND.IABS(INOX).NE.2) GO TO 36
      IT=IT+1                                                           08/09/71
      KLIST(IT)=NMF6                                                    08/09/71
36    CONTINUE                                                          08/09/71
      IF(IPRES.NE.2) GO TO 40                                           08/09/71
      IT=IT+1                                                           08/09/71
      KLIST(IT)=NUMA*6                                                  08/09/71
40    IF(INDRO.NE.2) GO TO 46                                           08/09/71
      IT=IT+1                                                           08/09/71
      KLIST(IT)=NUMA*5                                                  08/09/71
      IF(HC.EQ.0.)GO TO 46
      IT=IT+1
      KLIST(IT)=NEFF
46    CONTINUE                                                          08/09/71
C***  REMOVED ANAME,ASYMBL SET FOR NP AND TEMP - DONE IN BLOCK1
   60 CONTINUE
      IX=1
      IF (1.GT.IT)GO TO 15
      DO 190 KK=I,IT
      K=KLIST(KK)                                                       08/09/71
      WRITE(6,200) NMAIN,NNOX,K,(ANAME(L,K),L=1,6)
C***KVB***                                                              08/09/71
      DO 180 IP=1,2
      III=II
      IEMPTY=0
      IF (IP.EQ.1)IEND=10
      IF(IN.LT.10)IEND=IN                                               07/26/71
      IF (IP.EQ.2)IEND=IN
```

TABLE XXVI. (Cont)

```
      IF (I.GT.JN)GO TO 25
      DO 170 JJ=1,JN
      J=JN+1-JJ
      IF (IP.EQ.2.AND.IMAX(J).LT.11)GO TO 170
      IF (IP.EQ.1)II1=IMIN(J)
      IF (IP.EQ.1)IEMPTY=(II1-1)/IX
      II2=IMAX(J)
      IF (IP.EQ.1.AND.II2.GT.10)II2=10
      IF (K.NE.NW.AND.(INDE(K).NE.1.OR.K.NE.NVT))GO TO 80
      IF (II1.GT.II2)GO TO 35
      DO 70 I=II1,II2,IX
      W(I)=AQ(I,J,K)
      IF (K.EQ.NW)A(I,J,NW)=W(I)*R(J)
      IF (K.EQ.NVT.AND.R(J).GT.0.0)A(I,J,NVT)=W(I)/R(J)
   70 CONTINUE
   35 CONTINUE
   80 CONTINUE
      IF (IEMPTY.GE.1)GO TO 90
      WRITE (6,210)J,(AQ(I,J,K),I=II1,II2,IX)
      GO TO 150
   90 ICKCGT=IEMPTY
      IF (ICKCGT.LE.1)GO TO 100
      IF (ICKCGT.GE.5)GO TO 140
      GO TO (100,110,120,130,140),ICKCGT
  100 WRITE (6,240)J,(AQ(I,J,K),I=II1,II2,IX)
      GO TO 150
  110 WRITE (6,250)J,(AQ(I,J,K),I=II1,II2,IX)
      GO TO 150
  120 WRITE (6,260)J,(AQ(I,J,K),I=II1,II2,IX)
      GO TO 150
  130 WRITE (6,270)J,(AQ(I,J,K),I=II1,II2,IX)
      GO TO 150
  140 WRITE (6,280)J,(AQ(I,J,K),I=II1,II2,IX)
  150 CONTINUE
      IF (K.NE.NW.AND.(INDE(K).NE.1.OR.K.NE.NVT))GO TO 170
      IF (II1.GT.II2)GO TO 45
      DO 160 I=II1,II2,IX
  160 A(I,J,K)=W(I)
   45 CONTINUE
  170 CONTINUE
   25 CONTINUE
      IF (IP.EQ.1)WRITE (6,220)(I,I=1,IEND)
      IF(IP.EQ.2.AND.IN.LT.11)GO TO 180                                  07/26/71
      IF (IP.EQ.2)WRITE (6,220)(I,I=11,IEND)
      WRITE (6,230)
  180 CONTINUE
  190 CONTINUE
   15 CONTINUE
C*** REVISED RENO TO PREVENT DIVIDE BY ZERO, FIRST ITERATION
      RENO=0.0
      IF (ZMU(1,1).NE.0.0) RENO=-12.567*A(1,1,NF)/ZMU(1,1)
      WRITE(6,300)RENO
      WRITE (6,290)VEXIT
      RETURN
C
  200 FORMAT(11H1MAIN ITER=,I3,11H  NOX ITER=,I3,4H  K=,I2,          08/13/71
     *2X,6A6)                                                        08/13/71
  210 FORMAT (1H ,I2,2X,1PE11.3,1PE11.3,1PE11.3,1PE11.3,1PE11.3,1PE11.3,
     *1PE11.3,1PE11.3,1PE11.3,1PE11.3,1PE11.3,1PE11.3)
  220 FORMAT (1H0,/11111///)
  230 FORMAT (1H0,///)
  240 FORMAT (1H ,I2,2X,11X,1PE11.3,1PE11.3,1PE11.3,1PE11.3,1PE11.3,1PE1
     *1.3,1PE11.3,1PE11.3,1PE11.3,1PE11.3,1PE11.3)
  250 FORMAT (1H ,I2,2X,22X,1PE11.3,1PE11.3,1PE11.3,1PE11.3,1PE11.3,1PE1
     *1.3,1PE11.3,1PE11.3,1PE11.3,1PE11.3)
  260 FORMAT (1H ,I2,2X,33X,1PE11.3,1PE11.3,1PE11.3,1PE11.3,1PE11.3,1PE1
```

TABLE XXVI. (Cont)

```
     *1.3,1PE11.3,1PE11.3)
  270 FORMAT (1H ,I2,2X,44X,1PE11.3,1PE11.3,1PE11.3,1PE11.3,1PE11.3,1PE1
     *1.3,1PE11
  280 FORMAT (1  ,I2,2X,55X,1PE11.3,1PE11.3,1PE11.3,1PE11.3,1PE11.3,1PE1
     *1.3)
  290 FORMAT (9H VEXIT = ,1PE11.3)
  300 FORMAT(//# REYNOLDS NUMBER=#,G12.4)                                  07/26/71
      END
*DECK AO
      FUNCTION ADF(I,J,LX,KQ)
*CALL CMO
      DIMENSION AQ(21,21,18)
      DIMENSION BENQ(21),BWSR(21),BP(21)
      EQUIVALENCE (A(1,1,1),AQ(1,1,1))
      OF(PN,BENQ,BWSR,BP,XENQ,XWSR)=((XENQ*XENQ-XWSR*XWSR)*BP+XWSR*XWSR*
     *BENQ-XENQ*XENQ*BWSR)/(XENQ*XWSR*(PN*XENQ+XWSR))
C*************************************************************************
C   THIS FUNCTION EVALUATES FIRST DERVIATIVES ACCORDING
C   TO THE THREE-POINT QUADRATIC APPROXIMATION
C*************************************************************************
C
C****    DEPENDING ON THE POSITION OF THE POINT (I,J), THERE
C****    ARE FIVE DIFFERENT EXPRESSIONS FOR THE DERIVATIVE
C
C***  REVISED AOF TO ELIMINATE  GO XXX L=1,14
      LG1=NUMA+1
      LG2=NUMA+2
      LRO=NUMA+3
      LV1=NUMA+7
      LV2=NUMA+8
      L=KQ
      IF(KQ.NE.LV1.AND.KQ.NE.LV2) GO TO 5                                  08/09/71
      L=LRO
      GO TO 5
  310 IF (KQ.EQ.LV1) L=LG1
      IF(KQ.EQ.LV2) L=LG2
    5 M=1
      IF (I.LT.IAB.AND.I.GE.1)GO TO 10
      IF (J.EQ.1)GO TO 20
      IF (I.EQ.IAB)GO TO 30
      IF (J.EQ.JN.OR.(J.EQ.JC.AND.I.LE.IN.AND.I.GE.IC))GO TO 40
      IF(J.EQ.JS.AND.I.GE.IS1.AND.I.LE.IS ) GO TO 20
      IF(I.EQ.IS1.AND.J.GE.JS1.AND.J.LE.JS) M=5
      IF(I.EQ.IS.AND.J.GE.JS1.AND.J.LE.JS) GO TO 30
      IF ((I.EQ.IC.AND.J.LE.JN.AND.J.GE.JC).OR.(I.EQ.IN.AND.J.LE.JC.AND.
     *J.GE.1))M=5
      GO TO 50
   10 IF (J.EQ.1.OR.J.EQ.JA1)GO TO 20
      IF (I.EQ.1)GO TO 30
      IF (J.EQ.JB.OR.J.EQ.JA)GO TO 40
      GO TO 50
   20 M=2
      GO TO 50
   30 M=3
      GO TO 50
   40 M=4
   50 CONTINUE
      ICKCGT=M
      IF (ICKCGT.LE.1)GO TO 60
      IF (ICKCGT.GE.5)GO TO 190
      GO TO (60,100,130,160,190),ICKCGT
C****    M=1....FOR POINTS NOT ON ANY OF THE BOUNDARIES
   60 PN=1.
      IF (LX.EQ.1)GO TO 80
      IF (J.EQ.1.OR.J.EQ.JA1)GO TO 110
      IF (J.EQ.JN.OR.(J.EQ.JC.AND.I.EQ.IN).OR.(I.LT.IAB.AND.(J.EQ.JB.OR.
```

TABLE XXVI. (Cont)

```
     *J.EQ.JA))GO TO 170
C***
      BENQ(L)=AQ(I,J+1,L)

      BWSR(L)=AQ(I,J-1,L)
   70 BP(L)=AQ(I,J,L)
      XENQ=X2(J+1)-X2(J)
      XWSR=X2(J)-X2(J-1)
      GO TO 220
   80 IF (I.EQ.IAB.OR.I.EQ.1)GO TO 140
      IF ((I.EQ.IC.AND.J.EQ.JN).OR.I.EQ.IN)GO TO 200
C***
      BENQ(L)=AQ(I+1,J,L)
      BWSR(L)=AQ(I-1,J,L)
   90 BP(L)=AQ(I,J,L)
      XENQ=X1(I+1)-X1(I)
      XWSR=X1(I)-X1(I-1)
      GO TO 220
C****    M=2....FOR POINTS ON THE BOUNDARY J=1
  100 IF (LX.EQ.1)GO TO 60
  110 PN=-1.
C***
      BENQ(L)=AQ(I,J+1,L)
      BWSR(L)=AQ(I,J+2,L)
  120 BP(L)=AQ(I,J,L)
      XENQ=X2(J+1)-X2(J)
      XWSR=X2(J+2)-X2(J)
      GO TO 220
C****    M=3....FOR POINTS ON THE IAB-PLANE
  130 IF (LX.NE.1)GO TO 60
  140 PN=-1.
C***
      BENQ(L)=AQ(I+1,J,L)
      BWSR(L)=AQ(I+2,J,L)
  150 BP(L)=AQ(I,J,L)
      XENQ=X1(I+1)-X1(I)
      XWSR=X1(I+2)-X1(I)
      GO TO 220
C****    M=4....FOR POINTS ON ALL WALLS PARALLEL TO THE J-LINES,
C****    BEYONN THE IAB-PLANE
  160 IF (LX.EQ.1)GO TO 60
  170 PN=-1.
C***
      BENQ(L)=AQ(I,J-1,L)
      BWSR(L)=AQ(I,J-2,L)
  180 BP(L)=AQ(I,J,L)
      XENQ=X2(J-1)-X2(J)
      XWSR=X2(J-2)-X2(J)
      GO TO 220
C****    M=5....FOR POINTS ON THE WALL OF I=IC AND THOSE ON THE EXIT
  190 IF (LX.NE.1)GO TO 60
  200 PN=-1.
C***
      BENQ(L)=AQ(I-1,J,L)
      BWSR(L)=AQ(I-2,J,L)
  210 BP(L)=AQ(I,J,L)
      XENQ=X1(I-1)-X1(I)
      XWSR=X1(I-2)-X1(I)
  220 CONTINUE
C****    EVALUATION OF DERIVATIVES FOR V1   (KQ=15) AND V2  (KQ=16)
C***
      IF(KQ.NE.LV1.AND.KQ.NE.LV2) GO TO 240                          08/09/71
      IF (L.EQ.LRO) GO TO 310
      IF (L.EQ.LG2) GO TO 230
      BENQ(LV1)=BENQ(LG1)/BENQ(LRO)
      BWSR(LV1)=BWSR(LG1)/BWSR(LRO)
```

TABLE XXVI. (Cont)

```
  301 CONTINUE
      X2AXIS=X2AXIS*X2CONV
  302 CONTINUE
C***   END CONVERSION
C***  CHANGE COMPLETE
C
      IF (2.GT.INM)GO TO 5
      DO 30 I=2,INM
   30 DELX1(I)=0.5*(X1(I+1)-X1(I-1))
    5 CONTINUE
      IF (2.GT.JNM)GO TO 15
      DO 40 J=2,JNM
   40 DELX2(J)=0.5*(X2(J+1)-X2(J-1))
   15 CONTINUE
      IF (1.GT.JN)GO TO 25
      DO 50 J=1,JN
      IF (INOG.EQ.1)R(J)=1.0
      IF (INOG.EQ.2)R(J)=X2(J)+X2AXIS
   50 CONTINUE
   25 CONTINUE
      IF (INOG.NE.1)GO TO 60
C   FOR PLANE FLOWS PUT THE CHAMBER RADII EQUAL UNITY
C***  ADDED X2AXIS =1.0
      IF (X2AXIS.GT.0.0) X2AXIS=1.0
      RADA=1.0
      RADA1=1.0
      RADB=1.0
      RADC=1.0
      RADN=1.0
      GO TO 70
C**** SPECIFYING CHAMBER DIMENSIONS
   60 RADA=X2(JA)+X2AXIS
      RADA1=X2(JA1)+X2AXIS
      RADB=X2(JB)+X2AXIS
      RADC=X2(JC)+X2AXIS
      RADN=X2(JN)+X2AXIS
   70 DA=X1(IAB)
      DA1=X1(IAB)
      DB=X1(IAB)
      DCN=X1(IC)
      DN=X1(IN)
C**** SPECIFYING INDES
      IF (1.GT.IE)GO TO 35
      DO 80 L=1,IE
   80 INDE(L)=1
   35 CONTINUE
      IE1=IE+1
      IF(IE1.GT.NUMA) GO TO 45
      DO 90 L=IE1,NUMA
   90 INDE(L)=9
   45 CONTINUE
C**** SPECIFYING IMIN S AND IMAX S
C***  CORRECTED GOSMAN IN REGION JA TO JA1 BETWEEN INLETS TO SET
C***  IMIN=IAB RATHER THAN 1.0
      IF(JB.EQ.JN) GO TO 55
      JB1=JB+1
      DO 100 J=JB1,JN
      IMIN(J)=IAB
  100 CONTINUE
   55 CONTINUE
      DO 200 J=JA1,JB
      IMIN(J)=1
  200 CONTINUE
      IF(JA.EQ.JA1) GO TO 202
      JA1DUM=JA1-1
      DO 201 J=JA,JA1DUM
```

TABLE XXVI. (Cont)

```
      BP(LV1)=BP(LG1)/BP(LRO)
      GO TO 240
  230 CONTINUE
      BENQ(LV2)=BENQ(LG2)/BENQ(LRO)
      BWSR(LV2)=BWSR(LG1)/BWSR(LRO)
      BP(LV2)=BP(LG2)/BP(LRO)
  240 CONTINUE
C***
      ADF=DF(PN,BENQ(KQ),BWSR(KQ),BP(KQ),XENQ,XWSR)
      END
*DECK GO
      OVERLAY (INIT,1,0)
      PROGRAM GOSNOX
*CALL CMD
C...KVB...                                                          08/09/71
      DIMENSION AQ(21,21,18)                                        08/09/71
C***KVB***                                                          08/09/71
      EQUIVALENCE (A(1,1,1),AQ(1,1,1))
C*********************************************************************
C
C   MULTI-COMPONENT FLOW...WITH CHEMICAL REACTION...WITH SWIRL
C   REACTION IS THE SINGLE-STEP TYPE AND IS PHYSICALLY CONTROLLED
C
C***  THIS PROGRAM WAS PREPARED BY S.C.HUNTER AND S.PATWARDHAN.
C***  FOR AIRESEARCH-PHOENIX BASED ON THE CHAPTER 6 VERSION IN GOSMAN
C***  TEXT.  CHANGES MADE ARE INDICATED BY  C*** AND INCLUDE CHANGE OF
C***  ALL INPUT DATA TO READ INSTEAD OF BLOCK DATA, CHANGE OF INLET
C***  CONDITIONS TO VARIABLE PROFILES RATHER THAN CONSTANT, ADDITION OF
C***  A PICTORIAL INLET AND EXIT PROFILE PLOT.
C***  DENSITY AND TEMPERATURE CALCULATIONS WERE MADE MORE GENERAL.
C***  TEMPERATURE STORED IN AQ(I,J,14) - NEW TEMPORARY STORAGE
C***    CREATED IN AOF AND PRESC1
C***  GENERAL CHANGES NOT INDICATED REQUIRED FOR CDC6400 INCLUDE
C***  DO LOOP BYPASS FOR VARIABLE LOOP INDICES AND ELIMINATION OF IF
C***  STATEMENTS AT END OF DO LOOPS.
C*********************************************************************
C...KVB...G.SOTTER,V.QUAN,C.BODEEN OF KVB ENGINEERING,INC.           07/26/71
C...KVB...HAVE MODIFIED THIS PROGRAM DURING JUNE-AUGUST 1971         07/26/71
C...KVB...TO INCLUDE CALCULATION OF (NO) AND (NO2)                   07/26/71
C...KVB...    OTHER CHANGES...                                       07/26/71
C...KVB...                                                          07/26/71
C...KVB...        NEW INPUT CARD JUST BEFORE INLET BDY VALUES        07/26/71
C...KVB...           IOLD  LOGICAL UNIT TO RECOVER AQ MATRIX        07/26/71
C...KVB...           INEW  LOGICAL UNIT TO SAVE AQ MATRIX           07/26/71
C...KVB...           INDX  1=NOX SOLUTION DESIRED                   07/26/71
C...KVB...             ANY OF ABOVE=0 MEANS DON'T DO IT             07/26/71
C...KVB...                                                          07/26/71
C...KVB...   KVB COMMENTS ARE OBVIOUS                              07/26/71
C...KVB...   KVB FORTRAN INSERTIONS BEGIN WITH ...KVB...           07/26/71
C...KVB...    AND END WITH ***KVB***                                07/26/71
      DIMENSION DAY(2),TIME(2)                                      07/26/71
      DATA NUMA/12/
      CALL BLOCKK                                                   07/26/71
C***  MOVE READ ATITLE,ASYMBL,ANAME AND ROWF TO BLOCK.
      INM=IN-1
      JNM=JN-1
C
C***  MOVED X1,X2 TO BLOCK, ADDED X1CONV,X2CONV FOR UNIT CONVERSION.
C***   CONVERT THE GRID DIMENSIONS INTO THE DESIRED VALUES
C
      IF (1.GT.IN) GO TO 302
      DO 300 I=1,IN
      X1(I)=X1(I)*X1CONV
  300 CONTINUE
      DO 301 J=1,JN
      X2(J)=X2(J)*X2CONV
```

TABLE XXVI. (Cont)

```
      IMIN(J)=IAB
  201 CONTINUE
  202 CONTINUE
      IF(JA.EQ.1) GO TO 204
      DO 203 J=1,JA
      IMIN(J)=1
  203 CONTINUE
  204 CONTINUE
C***  CHANGE COMPLETE.
   65 CONTINUE
      IF (1.GT.JC)GO TO 75
      DO 120 L=1,JC
  120 IMAX(L)=IN
   75 CONTINUE
      JC1=JC+1
      IF (JC1.GT.JN)GO TO 85
      DO 130 L=JC1,JN
  130 IMAX(L)=IC
C***  MOVED ALL INITIAL VALUES TO BLOCK.
   85 CONTINUE
      IF(IS.LT.IN.OR.JS1.GT.JS.OR.JS.EQ.1)GO TO 175
      JSM1=JS-1
      DO 1000 J=JS1,JSM1
 1000 IMAX(J)=IS1
  175 CONTINUE
       IF (INOX .LT. 0 .OR. IOLO .LT.0)GO TO 170                          08/13/71
      DO 400 J=JA1,JB
  400 A(1,J,NVT)=A(1,J,NVT)*R(J)
  170 CONTINUE
      CALL HEADC1
      END
*DECK BL
      SUBROUTINE BLOCKK                                                  07/26/71
*CALL CMD
      COMMON/BLHE/TANB,SM
C...KVB...                                                               08/09/71
      DIMENSION AQ(21,21,18)                                             08/09/71
      DIMENSION BTITLE(12)                                               08/09/71
      INTEGER BTITLE                                                     08/09/71
C...KVB...                                                               07/26/71
      DIMENSION DATEIN(2),TIMEIN(2)                                      07/26/71
      LOGICAL PLONLY                                                     06/13/71
C***KVB***                                                               07/26/71
      DIMENSION ISYMBL(20),INAME(6,20)
      DIMENSION VT(21)
      DIMENSION VAR(21)
      DIMENSION IEV(8),JEV(8),OUM(8)
      EQUIVALENCE (A(1,1,1),AQ(1,1,1))
      DATA (ISYMBL(I),I=1,20) /   6HVORT  ,6HSTRM  ,6HVSWL  ,6HENTH  ,
     * 6HTBKE  ,6HMF 1  ,6HMF 2  ,6HMF 3  ,6HMF 4  ,6HMF 5  ,6HMF 6  ,
     * 6HEFF   ,6HG1    ,6HG2    ,6HRHO   ,6HVISC  ,6HTEMP  ,6HPRES  ,
     * 6HVEL1  ,6HVEL2   /
      DATA((INAME(I,J),I=1,6),J=1,5)/
     * 6HVORTIC,6HITY  -,6H A(I,J,6H,NW)  ,6H      ,6H      ,
     * 6HSTREAM,6H FUNCT,6HION - ,6HA(I,J,,6HNF)   ,6H      ,
     * 6HSWIRL ,6HVELOCI,6HTY - A,6H(I,J,N,6HVT)   ,6H      ,
     * 6HENTHAL,6HPY - A,6H(I,J,N,6HHS)   ,6H      ,6H      ,
     * 6HTURBUL,6HENT KI,6HNETIC ,6HENERGY,6H =A(I,,6HJ,NZK)/
      DATA((INAME(I,J),I=1,6),J=6,12)/
     * 6HMASS F,6HRACTIO,6HN NO 1,6H      ,6H      ,6H      ,
     * 6HMASS F,6HRACTIO,6HN NO 2,6H      ,6H      ,6H      ,
     * 6HMASS F,6HRACTIO,6HN NO 3,6H      ,6H      ,6H      ,
     * 6HMASS F,6HRACTIO,6HN NO 4,6H      ,6H      ,6H      ,
     * 6HMASS F,6HRACTIO,6HN NO 5,6H      ,6H      ,6H      ,
     * 6HMASS F,6HRACTIO,6HN NO 6,6H      ,6H      ,6H      ,
     * 6HEFFICI,6HENCY  ,6H      ,6H      ,6H      ,6H      /
```

TABLE XXVI. (Cont)

```
      DATA((INAME(I,J),I=1,6),J=13,20)/
     * 6HMASS V,6HELOCIT,6HY DIRE,6HC. 1 -,6H G1(I,,6H      ,
     * 6HMASS V,6HELOCIT,6HY DIRE,6HC. 2 -,6H G2(I,,6H      ,
     * 6HDENSIT,6HY - RO,6H(I,J) ,6H       ,6H       ,6H      ,
     * 6HVISCOS,6HITY - ,6HZMU(I,,6HJ)     ,6H       ,6H      ,
     * 6HTEMPER,6HATURE ,6H       ,6H       ,6H       ,6H      ,
     * 6HPRESSU,6HRE     ,6H       ,6H       ,6H       ,6H      ,
     * 6HVELOCI,6HTY - U,6HIRECTI,6HON 1 -,6H V1    ,6H      ,
     * 6HVELOCI,6HTY - U,6HIRECTI,6HON 2 -,6H V2    ,6H      /
C***   UNIVERSAL CONSTANTS
      DATA GCPM,GC,ZJC/1545.0,32.2,778.0/
      DATA O2,EN/,209495,,790505/
C*********************************************************************
C
C***  THIS SUBROUTINE CHANGED FROM BLOCK DATA TYPE TO READ AND INITIAL
C***  ALL INPUT DATA.
C
C*********************************************************************
C   FOR SINGLE COMPONENT FLOW PUT JA AND JAI EQUAL JB
C   JC CAN BE PUT EQUAL TO JN AND IC EQUAL IN
C   WHEN NO REACTION IS REQUIRED PUT HC=0
C*********************************************************************
      NAQ=NUMA+8
      KK=NUMA+1
C****   READ THE DATA
C****
C***   TITLE
      READ(5,10) ATITLE
C***   GRID
      READ(5,20) IN,JN,JA,JAI,JB,JC,IAB,IC
      READ(5,21) (X1(K1),K1=1,IN)
      READ(5,21) (X2(K2),K2=1,JN)
      READ(5,21)X2AXIS,X1CONV,X2CONV,CC,DC,ROWF
C***   EQUATIONS
      READ(5,20)IE,(NEQ(I),I=1,NUMA)
      NW=NEQ(1)
      NF=NEQ(2)
      NVI=NEQ(3)
      NHS=NEQ(4)
      NZK=NEQ(5)
      NMF1=NEQ(6)
      NMF2=NEQ(7)
      NMF3=NEQ(8)
      NMF4=NEQ(9)
      NMF5=NEQ(10)
      NMF6=NEQ(11)
      NEFF=NEQ(12)
      NZML=NMF1
      NZMH=NMF6
      READ(5,20)NMAX,NPRIN,INDG,INORO,INDZMU,IPRES,NSPEC
C***   REF. PROPERTIES
      READ(5,21) ROREF,PREF,ZMUREF,TREF,CPREF
C***   COMB. PARAMS.
      READ(5,21) STC,HC,HP,HS,SM
      XH=SM
      IF(SM.LT.1.0) XH=12.01*SM/1.008
      ZWF=12.01+1.008*XH
      X02=32./ZWF*(.5+XH/4.)
      XH20=18.016*XH/ZWF/2.
      XC0=28.01/ZWF
      ZWA=28.85
      Y02=16./44.01
      YC0=28.01/44.01
      Z02=02*32./ZWA/X02
      EMA=(1.+XH/4.)/02*ZWA
      FSD=ZWF/EMA
```

TABLE XXVI. (Cont)

```
      STC=1./FSD
      XN2=.768554
      XN2=1.-ZD2-XD2
C***   PROPERTIES
      READ(5,21) (ZMW(L),L=1,NSPEC)
      ZMW(1)=ZWF
      READ(5,21) (CPJ(L),L=1,NSPEC)
C***   NON-DIM. NOS.
      READ(5,21) (RP(K3),K3=1,NUMA)
      READ(5,21) (PR(K4),K4=1,NUMA)
C***   INITIAL CONDITIONS
      READ(5,21) TANB,ENZML,ZMUK
C***   VALUES FOR THE PLOTCT
      DO 200 K=1,KAQ
      IVAR(K)=K
      INDD(K,1)=99
  200 CONTINUE
      IT=IE+1
      IVAR(IT)=NMF5
      IT=IT+1
      IVAR(IT)=NMF6
      READ(5,20) INTVAL,NVJ,NVAR
      IF (1.GT.NVAR) GO TO 71
      DO 70 LL=1,NVAR
      READ(5,20) IVAR(LL)
      K=IVAR(LL)
      READ(5,22) (INDO(K,NI),JNDO(K,NI),VJE(K,NI),N1=1,4)
      IF(INDD(K,1).LE.1N.AND.NVJ.GT.4) READ(5,22)
     + (INDD(K,NI),JNDD(K,NI),VJE(K,NI),N1=5,NVJ)
   70 CONTINUE
   71 CONTINUE
C***   READ VELPLT INDICIES
      READ(5,20) NVP
      IF (1.GT.NVP) GO TO 75
      READ(5,24) (IDP(I),IJGP(I),IVP(I),I=1,NVP)
   75 CONTINUE
C      REARRANGE ANAME AND ASYMBL FOR EQUATION SOLVING ORDER
      DO 95 K=1,NUMA
      KNEW=NEQ(K)
      ASYMBL(KNEQ)=ISYMBL(K)
      DO 95 I=1,6
      ANAME(I,KNEQ)=INAME(I,K)
   95 CONTINUE
      DO 90 J=KK,KAQ
      ASYMBL(J)=ISYMBL(J)
      DO 90 I=1,6
      ANAME(I,J)=INAME(I,J)
   90 CONTINUE
C...KVB...                                                    07/26/71
      READ(5,1000)IOLO,INEW,INOX,IVAP
 1000 FORMAT(4I10)
      PLONLY=IOLD.LT.0                                        08/13/71
      IOLD=IABS(IOLD)                                         08/13/71
      IF(NVAR.GE.0) GO TO 800
      NVAR=IE+IABS(INOX)
  800 CONTINUE
      WRITE(6,999)IOLD,INEW,INOX,IVAP
  999 FORMAT(1H1,* IOLD, INEW, INOX, IVAP = *,4I3)
      IF(IOLD.EQ.0) GO TO 998
      REWIND IOLD
      READ(IOLO)
      READ(IOLO) A
      READ(IOLD) G1
      READ(IOLO) G2
      READ(IOLD) RO
      READ(IOLD) ZMJ
```

TABLE XXVI. (Cont)

```
      READ(IOLD) T
      READ(IOLD) PF
  998 CONTINUE
C***KVB***                                                    07/26/71
C***   SET THE INTIAL VALUES FOR THE INLET VELOCITIES.
C***
C***   SET THE INITIAL VALUES
      DO 100 LMN=1,JN
      VIN(LMN)=0.0
  100 CONTINUE
C...KVB...                                                    07/26/71
C***KVB***                                                    07/26/71
      DO 30 J=1,JN
      DO 30 I=1,IN
      IF(IOLO.NE.0) GO TO 35
      DO 60 K=I,NUMA
      A(I,J,K)=1.E-30                                         07/26/71
      IF(K.EQ.NMF1) A(I,J,K)=ENZML
      IF(K.EQ.NMF3) A(I,J,K)=ENZML
C...KVB...REMOVED USE OF NMF4,NMF5.........NMF3 REPRESENTS #F#  08/09/71
      IF(K.EQ.NHS) A(I,J,K)=CPREF*(TREF-536.67)
      IF (K.EQ.NVT) A(I,J,NVT)=0.0
   60 CONTINUE
C***
      PF(I,J)=0.0
      RO(I,J)=ROREF
      G1(I,J)=0.0
      G2(I,J)=0.0
      ZMU(I,J)=ZMUREF
      T(I,J)=TREF
   35 CONTINUE
      FEVAP(I,J)=0.
   30 CONTINUE
C...KVB...                                                    07/26/71
31    CONTINUE                                                07/26/71
C***KVB***                                                    07/26/71
C***  READ INITIAL CONDITIONS FOR ANY VARIABLE
      READ(5,20) NVARI
      LV1=NUMA+7
      LV2=NUMA+8
      IF (1.GT.NVARI) GO TO 141
      DO 140 IIV=1,NVARI
  110 READ(5,23) IDVAR,(VAR(J),J=1,J8)
      DO 140 J=I,JB
      IF(IDVAR.EQ.LV1) GO TO 120
      IF(IDVAR.EQ.LV2) GO TO 140
      IF(INOX.GE.0.AND.(J.LE.JA.OR.(J.GE.JAI.AND.J.LE.JB)))
     *  AQ(I,J,IDVAR)=VAR(J)
      GO TO 140
  120 VIN(J)=VAR(J)
  140 CONTINUE
  141 CONTINUE
      READ(5,20)JS1,JS,IS1,IS
      DO 201 J=I,21
      VF(J)=0.
  201 VF1(J)=0.
      IF(JS.GT.JSI) READ(5,21)(VF(LO),LO=JS1,JS)
      IF(IS.LT.IN.AND.JS.GT.JS1) READ(5,21) (VF1(LO),LO=JS1,JS)
      EMJET=ENZML
      IF(JS.GT.JSI) READ(5,21) EMJET
      DO 202 J=JS1,JS
      A(IS1,J,NMFI)=EMJET
      A(IS,J,NMF1)=EMJET
      A(ISI,J,NMF3)=EMJET
      A(IS,J,NMF3)=EMJET
  202 CONTINUE
```

TABLE XXVI. (Cont)

```
C***   SWIRL VELOCITY
C...KVB...
      IF(PLONLY) IOLD= -IOLD                                          08/13/71
      IF(PLONLY.OR.INOX.LT.0) GO TO 1050
C***KVB***
      DO 50 J=JA1,JB
      VT(J)=TANB*VIN(J)
      IF(JA1.EQ.JB) GO TO 40
      A(I,J,NVT)=VT(J)
   40 CONTINUE
   50 CONTINUE
      READ(5,26) NILO,NIHI,ILO,IHI,JLO,JHI,TIGN,NEV
   26 FORMAT(6I10,F10.0,I10)
      IF(ILO.EQ.0) ILO=IAB
      IF(IHI.EQ.0) IHI=IN
      IF(JLO.EQ.0) JLO=I
      IF(JHI.EQ.0) JHI=JC
  300 READ(5,25)(IEV(I),JEV(I),DUM(I),I=1,8)
   25 FORMAT(8(2I2,F6.0))
      IF(EOF(5)) 330,310
  310 CONTINUE
      DO 320 II=1,8
      I=IEV(II)
      IF(I.EQ.0) GO TO 330
      J=JEV(II)
      FEVAP(I,J)=DUM(II)
  320 CONTINUE
      GO TO 300
  330 CONTINUE
      IF(IVAP.GT.0) REWIND IVAP
      IF(IVAP.GT.0) READ(IVAP)FEVAP
      IF(IVAP.GT.0) REWIND IVAP
      RETURN
1050  CONTINUE
      IF(JA1.GE.JB) GO TO 1070
      DO 1060 J=JA1,JB
      VT(J)=A(I,J,NVT)
1060  CONTINUE
1070  CONTINUE
C***KVB***
C***
   10 FORMAT '12A6)
   20 FORMAT (8I10)
   21 FORMAT (8F10.0)
   22 FORMAT (4(2I5,F10.0))
   23 FORMAT (I10/(8F10.0))
   24 FORMAT (8(I2,1X,I2,1X,I2,2X))
      END
*DECK HE
      SUBROUTINE HEADCI
*CALL CMD
      COMMON/BLHE/TANB,SM
C***  ADDED FUNCTION ACYL
      ACYL(R2,R1)=(R2-R1)*(R2+R1)/2.
C*****************************************************************
C   ##HEADING## SUBROUTINE
C   THIS SUBR. PRINTS OUT SOME OF THE INFORMATION FED IN
C*****************************************************************
      WRITE (6,80)ATITLE
      WRITE(6,400)NW,NF,NVT,NHS,NZK,NMF1,NMF2,NMF3,NMF4,NMF5,NMF6,NEFF
  400 FORMAT(* EQUATION NUMBER ORDER */
     ** NW    NF   NVT   NHS   NZK  NMF1  NMF2  NMF3  NMF4  NMF5  NMF6
     * NEFF*/2X,I2(I2,4X)//
     ** OTHER VARIABLE NUMBERS*/
     ** G1    G2    R0    ZMU    T    PF    VI    V2*/
     ** 13    14    15    16    17    18    19    20*//
```

TABLE XXVI. (Cont)

```
     +*  DURING MAIN ITERATION     NMF5= O2    NMF6= CO*/
     +*  DURING NOX  ITERATION     NMF5= NO    NMF6= NO2*/
     +*  FOR FINAL PRINT +INOX=0   NMF5= O2    NMF6=CO*/
     +*                   INOX=1   NMF5=NO    NMF6= CO*/
     +*                   INOX=2   NMF5= NO    NMF6= NO2*/)
      IF (INOG.EQ.2)GO TO 10
      WRITE (6,270)
      GO TO 20
   10 WRITE (6,280)
   20 IF (INOZMU.EQ.2)GO TO 30
      WRITE (6,90)
      GO TO 40
   30 WRITE (6,100)
   40 IF (INORO.EQ.2)GO TO 50
      WRITE (6,110)
      GO TO 60
   50 WRITE (6,120)
   60 IF (IPRES.EQ.2) GO TO 65
      WRITE(6,300)
      GO TO 67
   65 WRITE(6,310)
   67 WRITE(6,130)
      IF (1.GT.IE)GO TO 5
      DO 70 K=1,IE
      IF(INOE(K).EQ.1) WRITE(6,)40)(ANAME(L,K),L=1,6)
   70 CONTINUE
    5 CONTINUE
      WRITE (6,150)JN,IN,(J,IMIN(J),IMAX(J),J=1,JN)
      WRITE (6,210)JA,JA1,JB,JC,IAB,IC,RAOA,RAOA1,RAOB,RAOC,RAON,OA,DA1,
     +OB,DCN,ON
      WRITE(6,290) X2AXIS,X1CONV,X2CONV
      WRITE(6,1000)CC,OC,ROWF
C...KVB...
        IJMX=MAX0(IN,JN)                                          07/26/71
      WRITE(6,220)(I,X1(I),X2(I),I=1,IJMX)                        07/26/71
C***KVB***
C***  CALCULATE MEAN INLET VELOCITIES
C*****
      VINPM=0.0
      VINSM=0.0
      IF(JA.EQ.1) GO TO 501
      FLOW=0.0
      ROMP=0.0
      DO 500 J=1,JA
      ROMP=ROMP+RO(1,J)
      IF(J.EQ.1) GO TO 500
      RSP=(RO(1,J)+RO(1,J-1))/2.
      VSP=(VIN(J)+VIN(J-1))/2.
      DX2=X2(J)-X2(J-1)
      IF (INOG.EQ.2) DX2=ACYL(R(J),R(J-I))
      FLOW=FLOW+RSP*VSP*DX2
  500 CONTINUE
      ROMP=ROMP/FLOAT(JA)
      DAREA=X2(JA)-X2(1)
      IF(INDG.EQ.2) DAREA=ACYL(R(JA),R(1))
      VINPM=FLOW/(ROMP*DAREA)
C***
  501 CONTINUE
      IF(JA1.EQ.JB) GO TO 503
      FLOW=0.0
      ROMS=0.0
      DO 502 J=JA1,JB
      ROMS=ROMS+RO(1,J)
      IF(J.EQ.JA1) GO TO 502
      RSP=(RO(1,J)+RO(1,J-1))/2.
      VSP=(VIN(J)+VIN(J-1))/2.
```

TABLE XXVI. (Cont)

```
      DX2=X2(J)-X2(J-1)
      IF (INOG.EQ.2) DX2=ACYL(R(J),R(J-1))
      FLOW=FLOW+RSP*VSP*DX2
  502 CONTINUE
      ROMS=ROMS/FLOAT(JB-JA1+1)
      DAREA=X2(JB)-X2(JA1)
      IF(INDG.EQ.2) DAREA=ACYL(R(JB),R(JA1))
      VINSM=FLOW/(ROMS*DAREA)
C***
  503 CONTINUE
      VINJM=0.
      VSP=0.
      VINJM1=0.
      VSP1=0.
      IF(JS.EQ.JS1) GO TO 610
       FLOW=0.
       ROMJ=0.
      ROMJ=ROREF
      RSP=ROREF
      FLOW1=0.
      ROMJ1=0.
      ROMJ1=ROREF
      RSP1=ROREF
      DO 600 J=JS1,JS
C     ROMJ1=ROMJ1+RO(IS,J)
C     ROMJ=ROMJ+RO(IS1,J)
      IF(J.EQ.JS1) GO TO 600
      DX2=X2(J)-X2(J-1)
      IF(INDG.EQ.2) DX2=ACYL(R(J),R(J-1))
C     RSP=(RO(IS1,J)+RO(IS1,J-1))/2.
      VSP=(VF(J)+VF(J-1))/2.
      FLOW=FLOW+RSP*VSP*DX2
      IF(IS.EQ.IN) GO TO 600
C     RSP1=(RO(IS,J)+RO(IS,J-1))/2.
      VSP1=(VF1(J)+VF1(J-1))/2.
      FLOW1=FLOW1+RSP1*VSP1*DX2
  600 CONTINUE
      DAREA=X2(JS)-X2(JS1)
      IF(INDG.EQ.2) DAREA=ACYL(R(JS),R(JS1))
C     ROMJ=ROMJ/(JS-JS1+1)
      VINJM=FLOW/(ROMJ*DAREA)
C     ROMJ1=ROMJ1/(JS-JS1+1)
      VINJM1=FLOW1/(ROMJ1*DAREA)
  610 CONTINUE
      WRITE(6,160)VINPM,VINSM,VINJM,VINJM1,
     * ROREF,PREF,ZMUREF,TREF,CPREF,GC,ZJC
      IF(INOZMU.EQ.2) WRITE(6,800)ZMUK
  800 FORMAT(1X,4HZMUK,2X,G12.5)
      WRITE(6,2000)TANB,ENZML,EMJET
      WRITE(6,260)STC,HC,HP,HS,SM
C***  ZA,ZB,ZC ARE UNDEFINED
C***  IF(INOE(NZK.EQ.1) WRITE(6,1/0) ZA,ZB,ZC,PR(NZK)
      WRITE(6,180)NSPEC,(ZMW(I),I=1,NSPEC)
      WRITE(6,3000) (CPJ(I),I=1,NSPEC)
      WRITE(6,4000)NILO,NIHI,ILO,IHI,JLO,JHI,TIGN,NEV
      WRITE(6,5000) (RP(I),I=1,12),(PR(I),I=1,12)
C...KVB...
80    FORMAT(1X,12A6)                                          07/26/71
90    FORMAT(1X,#LAMINAR#)                                     07/26/71
100   FORMAT(1X,#TURBULENT#)                                   07/26/71
110   FORMAT(1X,#INCOMPRESSIBLE#)                              07/26/71
120   FORMAT(1X,#NON-UNIFORM DENSITY#)                         07/26/71
130   FORMAT(1X,#DEP VARIABLES ARE #)
140   FORMAT(4X,6A6)                                           07/26/71
150   FORMAT(1X,#GEOMETRY #/# #,I3,# ROWS  #,I3,# COLUMNS#/
     * 3X,#J#,5X,#IMIN#,5X,#IMAX#/(1X,I3,2I9))                 07/26/71
```

TABLE XXVI. (Cont)

```
160   FORMAT(1X,#PHYSICAL DATA #/
     * 4X,#V PR1 #,G12.4,3X,#V SEC #,G12.4/                                  07/26/71
     * 4X,#V JM  #,G12.4,3X,#V JM1 #,G12.4/
     * 4X,#ROREF #,G12.4,3X,#P REF #,G12.4/                                  07/26/71
     * 4X,#ZMUREF#,G12.4,3X,#T REF #,G12.4/                                  07/26/71
     * 4X,#CP REF#,G12.4,3X,                                                 07/26/71
     */4X,#GC    #,G12.4,3X,#ZJC   #,G12.4/                                  07/26/71
     *)                                                                      07/26/71
170   FORMAT(                                                                07/26/71
     * 4X,#ZA    #,G12.4,3X,#ZB    #,G12.4/                                  07/26/71
     * 4X,#ZC    #,G12.4,3X,#PR NZK#,G12.4/)                                 07/26/71
 180 FORMAT(* NUM SPECIES= *,I2/* MOLEC WTS,ZMW= *,6F12.3)
3000 FORMAT(* SPECIFIC HEATS,CPJ= *,6F12.5)
190   FORMAT(4X,#NSPEC#,I3/                                                  07/26/71
     * 4X,#ZMW   #,6G12.4/                                                   07/26/71
     * 4X,#CP J  #,6G12.4/                                                   07/26/71
     * 4X,#PR    #,6G12.4)                                                   07/26/71
200   FORMAT(1X,#OTHER DATA #/                                               07/26/71
     * 4X,#CC    #,G12.4,3X,#OC    #,G12.4/                                  07/26/71
     * 4X,#NMAX  #,I4)                                                       07/26/71
210   FORMAT(1X,# JA,JA1, JB, JC,JAB, IC#/                                   07/26/71
     *  1X,I3,5I4/                                                          07/26/71
     *1X,#        RADA,       RADA1,       RADB,       RADC,    RADN#      07/26/71
     */ 1X,5G12.4/                                                          07/26/71
     * 1X,#          DA,         DA1,         DB,         DCN,      DN#     07/26/71
     */ 1X,5G12.4/)                                                         07/26/71
220   FORMAT(1X,#I OR J       X1(I)       X2(J)#/                          07/26/71
     *  (1X,I6,2G12.4))                                                     07/26/71
260   FORMAT(4X,#STC   #,G12.4,3X,#HC    #,G12.5/                          07/26/71
     *4X,*HP =  *,G12.5,3X,*HS =  *,G12.5/4X,*SM =  *,G12.5/)
270   FORMAT(1X,#CARTESIAN#)                                                 07/26/71
280   FORMAT(1X,#CYLINDRICAL#)                                               07/26/71
290   FORMAT(1X,#       X2AXIS       X1CONV       X2CONV#/                  07/26/71
     * 1X,3G12.4)                                                           07/26/71
300   FORMAT(1X,#CONSTANT PRESSURE#)                                         07/26/71
310   FORMAT(1X,#NON-UNIFORM PRESSURE#)                                      07/26/71
1000  FORMAT(4X,*CC = *,F12.8,3X,*DC = *,F12.5,3X,*ROWF = *,F12.5/)
2000  FORMAT(4X,*TANGENT SWIRL,TANB= *,F12.5/
     * 4X,*INT FUEL FRAC,ENZML= *,F12.5,3X,*JET FUEL FRAC,ENJET= *,
     *F12.5/)
4000  FORMAT(* IGNITION- NILO= *,I4,*  NIHI= *,I4/11X,*ILO= *,I2,*  IHI=
     * *,I2,*  JLO= *,I2,*  JHI= *,I ,*  IGN TEMP,TIGN= *,F12.4//
     * * ITERATION FOR START OF EVAPORATION, NEV= *,I4/)
5000  FORMAT(* RELAXATION PARAMETERS,RP =*,6F8.5/27X,6F8.5/
     *       * EQUATION PRANDTL NOS.,PR =*,6F8.5/27X,6F8.5/)
      END                                                                     07/26/71
*DECK SV
      OVERLAY(SOLV,2,0)
      PROGRAM SOLVCK
*CALL CMD
C*****************************************************************************
C   ##SOLVE## SUBROUTINE
C   THIS SUBR. CONTROLS THE ITERATION PROCEDURE
C*****************************************************************************
      IF(NOXSOL) GO TO 205
C...KVB...CONTROL WILL COME BACK TO NEXT STATEMENT AFTER CORE                 07/26/71
C...KVB...HAS BEEN SET UP FOR THE NOX SOLUTIONS                               07/26/71
4     CONTINUE                                                                07/26/71
C***KVB***                                                                    07/26/71
      KEQ=NUMA+3
      IF(INDRO.EQ.2.AND.(.NOT.NOXSOL)) CALL DENSC1
      KEQ=NF
      IF(.NOT.NOXSOL) CALL BOUNC1
      KEQ=NW
      IF(.NOT.NOXSOL) CALL BOUNC1
      WRITE(6,919)
```

TABLE XXVI. (Cont)

```
  919 FORMAT(///1X,# INITIAL BOUNDARY VALUES FOLLOW #//)
      CALL PRINCI
      WRITE (6,100)
      IF (1.GT.IE)GO TO 5
      DO 10 K=1,IE
      IF(INDE(K).EQ.1) WRITE(6,110)K,(ANAME(L,K),L=1,6)
      PHIMN(K)=0.
      RSOU(K)=0.
   10 CONTINUE
    5 CONTINUE
      WRITE (6,120)(ASYMBL(K),K=1,IE)
      NITER=1
      NNN=NPRIN
      KVORT=0
      ICONV=0
   20 IF(NOXSOL) GO TO 21                                          07/26/71
      KEQ=1
      IF(INORO.EQ.2) CALL DENSC1
      CALL MVELCT
      CALL MVACC1
      CALL VISCC1
   21 CONTINUE                                                     07/26/71
      IF (1.GT.IE)GO TO 15                                         07/26/71
      DO 30 K=1,IE                                                 07/26/71
      IF(NITER.GT.40.AND.ABS(RSOU(K)).LT.CC.AND.ICONV.EQ.0) GO TO 30
      DIFMAX(K)=0.                                                 07/26/71
      RSOU(K)=0.                                                   07/26/71
C***KVB***                                                         07/26/71
      KEQ=K
      IF(INDE(K).EQ.1) CALL FOEQC1
      IF(INDE(K).EQ.1) CALL BOUNC1
   30 CONTINUE
   15 CONTINUE
      WRITE (6,130)NITER,(RSOU(K),K=1,IE)
      WRITE (6,150)(DIFMAX(K),K=1,IE)
      WRITE(6,200) (IRS(K),JRS(K),K=1,IE)
  200 FORMAT (10X,20I6/)
      RES=RSOU(1)
      IF (2.GT.IE)GO TO 25
      DO 40 K=2,IE
      IF(ABS(RSOU(K)).GT.ABS(RES)) RES=RSOU(K)
   40 CONTINUE
   25 CONTINUE
      IF(.NOT.NOXSOL) NMAIN=NITER
      IF(.NOT.NOXSOL) NNOX=0
      IF(NOXSOL.AND.(INOX.LT.0)) NMAIN=0
      IF(NOXSOL) NNOX=NITER
      IF (NITER.GT.NMAX)GO TO 90
C***  ADDED PRINT OUT OF FIRST FOUR ITERATIONS TO ALLOW CHECK OF INITIAL
C***  BOUNDARY CONDITIONS
   50 CONTINUE
      IF(NITER.EQ.1) GO TO 70
      IF (NITER-NNN)80,60,60
   60 NNN=NNN+NPRIN
   70 CONTINUE
      KVORT=1
C...KVB...                                                         07/26/71
      IF(.NOT.NOXSOL) KEQ=NW
      IF(.NOT.NOXSOL) CALL BOUNC1
C***KVB***                                                         07/26/71
      CALL PRINC1
      WRITE (6,120)(ASYMBL(K),K=1,IE)
      KVORT=0
   80 CONTINUE
      NITER=NITER+1
      IF(ABS(RES).GT.CC.OR.NITER.LE.10) GO TO 20
```

TABLE XXVI. (Cont)

```
      IF(ICONV.EQ.1) GO TO 85
      ICONV=1
      GO TO 20
   85 CONTINUE
      KVORT=1
C...KVB...                                                          07/26/71
      IF(.NOT.NOXSOL) KEQ=NW
      IF(.NOT.NOXSOL) CALL BOUNC1
C***KVB***                                                          07/26/71
      IF(NOXSOL) GO TO 206
      GO TO 355
   90 WRITE (6,140)NITER
      IF(NOXSOL) GO TO 206
      GO TO 355
C...KVB...SET UP FOR NOX SOLUTION AFTER REGULAR PROBLEM HAS CONVGD  07/26/71
205   CONTINUE                                                      07/26/71
C...KVB...FLIP THE FIRST TWO ITEMS IN THE EQUATION ORDER LIST       07/26/71
C...KVB...WITH THE ITEMS RESERVED FOR NO AND NO2...NAMELY NMF5      07/26/71
C...KVB...AND NMF6                                                  07/26/71
      IES=IE                                                        08/13/71
      IE=IABS(INOX)                                                 08/13/71
      DO 220 J=1,JN                                                 07/26/71
      I1=IMIN(J)                                                    07/26/71
      I2=IMAX(J)                                                    07/26/71
      DO 210 I=I1,I2                                                07/26/71
      TA=A(I,J,NMF5)                                                07/26/71
      A(I,J,NMF5)=A(I,J,1)                                          07/26/71
      A(I,J,1)=TA                                                   07/26/71
      TA=A(I,J,NMF6)                                                07/26/71
      A(I,J,NMF6)=A(I,J,2)                                          07/26/71
      A(I,J,2)=TA                                                   07/26/71
      IF(IE.EQ.1) A(I,J,2)=0.                                       08/13/71
210   CONTINUE                                                      07/26/71
220   CONTINUE                                                      07/26/71
      DO 230 L=1,6                                                  07/26/71
      IAT=ANAME(L,NMF5)                                             07/26/71
      ANAME(L,NMF5)=ANAME(L,1)                                      07/26/71
      ANAME(L,1)=IAT                                                07/26/71
      IAT=ANAME(L,2)                                                07/26/71
      ANAME(L,2)=ANAME(L,NMF6)                                      07/26/71
      ANAME(L,NMF6)=IAT                                             07/26/71
230   CONTINUE                                                      07/26/71
      IAT=ASYMBL(NMF5)                                              07/26/71
      ASYMBL(NMF5)=ASYMBL(1)                                        07/26/71
      ASYMBL(1)=IAT                                                 07/26/71
      IAT=ASYMBL(NMF6)                                              07/26/71
      ASYMBL(NMF6)=ASYMBL(2)                                        07/26/71
      ASYMBL(2)=IAT                                                 07/26/71
C...KVB...FLIP THE EQUATION INDICATORS                              07/26/71
      IF(NW.EQ.1)NW=NMF5                                            07/26/71
      IF(NW.EQ.2)NW=NMF6                                            07/26/71
      IF(NF.EQ.1)NF=NMF5                                            07/26/71
      IF(NF.EQ.2)NF=NMF6                                            07/26/71
      IF(NMF1.EQ.1)NMF1=NMF5                                        07/26/71
      IF(NMF1.EQ.2)NMF1=NMF6                                        07/26/71
      IF(NMF2.EQ.1)NMF2=NMF5                                        07/26/71
      IF(NHS.EQ.1)NHS=NMF5                                          07/26/71
      IF(NMF2.EQ.2)NMF2=NMF6                                        07/26/71
      IF(NHS.EQ.2)NHS=NMF6                                          07/26/71
      IF(NMF3.EQ.1)NMF3=NMF5                                        07/26/71
      IF(NVT.EQ.1)NVT=NMF5                                          07/26/71
      IF(NMF3.EQ.2)NMF3=NMF6                                        07/26/71
      IF(NVT.EQ.2)NVT=NMF6                                          07/26/71
      IF(NMF4.EQ.1)NMF4=NMF5                                        07/26/71
      IF(NZK.EQ.1)NZK=NMF5                                          07/26/71
      IF(NMF4.EQ.2)NMF4=NMF6                                        07/26/71
```

TABLE XXVI. (Cont)

```
      IF(NZK.EQ.2)NZK=NMF6                                              07/26/71
      NMF5=1                                                            07/26/71
      NMF6=2                                                            07/26/71
      DO 240 L=1,9                                                      07/26/71
      INDE(L)=9                                                         07/26/71
240   CONTINUE                                                          07/26/71
      INDE(1)=1                                                         07/26/71
      INDE(2)=1                                                         07/26/71
      GO TO 4                                                           07/26/71
C***KVB***
  206 CONTINUE
C...KVB...THIS ENTRY IS REALLY A SEPARATE SUBROUTINE, BUT IT            07/26/71
C...KVB...IS INCLUDED HERE BECAUSE IT DOES JUST THE OPPOSITE            07/26/71
C...KVB...OF THE SECTION BETWEEN 200-250 ABOVE.                         07/26/71
300   CONTINUE                                                          07/26/71
C...KVB...RESTORE NW,,ETC LIST                                          07/26/71
      NW=NEQ(1)                                                         07/26/71
      NF=NEQ(2)                                                         07/26/71
      NVT=NEQ(3)                                                        07/26/71
      NHS=NEQ(4)                                                        07/26/71
      NZK=NEQ(5)                                                        07/26/71
      NMF1=NEQ(6)                                                       07/26/71
      NMF2=NEQ(7)                                                       07/26/71
      NMF3=NEQ(8)                                                       07/26/71
      NMF4=NEQ(9)                                                       07/26/71
      NMF5=NEQ(10)                                                      07/26/71
      NMF6=NEQ(11)                                                      07/26/71
      NEFF=NEQ(12)                                                      07/26/71
      NZML=NMF1                                                         07/26/71
      NZMH=NMF6                                                         07/26/71
      IE=IES
      DO 320 J=1,JN                                                     07/26/71
      I1=IMIN(J)                                                        07/26/71
      I2=IMAX(J)                                                        07/26/71
      DO 310 I=I1,I2                                                    07/26/71
      TA=A(I,J,1)                                                       07/26/71
      A(I,J,1)=A(I,J,NMF5)                                              07/26/71
      A(I,J,NMF5)=TA                                                    07/26/71
      TA=A(I,J,2)                                                       07/26/71
      A(I,J,2)=A(I,J,NMF6)                                              07/26/71
      A(I,J,NMF6)=TA                                                    07/26/71
310   CONTINUE                                                          07/26/71
320   CONTINUE                                                          07/26/71
      DO 330 L=1,6                                                      07/26/71
      IAT=ANAME(L,1)                                                    07/26/71
      ANAME(L,1)=ANAME(L,NMF5)                                          07/26/71
      ANAME(L,NMF5)=IAT                                                 07/26/71
      IAT=ANAME(L,NMF6)                                                 07/26/71
      ANAME(L,NMF6)=ANAME(L,2)                                          07/26/71
      ANAME(L,2)=IAT                                                    07/26/71
330   CONTINUE                                                          07/26/71
      IAT=ASYMBL(1)                                                     07/26/71
      ASYMBL(1)=ASYMBL(NMF5)                                            07/26/71
      ASYMBL(NMF5)=IAT                                                  07/26/71
      IAT=ASYMBL(2)
      ASYMBL(2)=ASYMBL(NMF6)                                            07/26/71
      ASYMBL(NMF6)=IAT                                                  07/26/71
      DO 340 L=IE,9                                                     07/26/71
      INDE(L)=9                                                         07/26/71
340   CONTINUE                                                          07/26/71
      DO 350 L=1,IE                                                     07/26/71
      INDE(L)=1                                                         07/26/71
350   CONTINUE                                                          07/26/71
C
  100 FORMAT (1H1,///10X,45HTHE FOLLOWING ARE MAXIMUM RESIDUES IN THE FI
     *E,41HLD OF INTEGRATION AT EACH ITERATION FOR...///)
```

TABLE XXVI. (Cont)

```
 110 FORMAT (1H ,40X,I2,3H.  ,6A6)
 120 FORMAT (////1H0,30X,35H..NOTE.. PREFIX #R# DENOTES RESIDUE,//117H0
    *....NOTE.....LEFT-HAND-COLUMNS FOR FRACTIONAL DIFFERENCES, RIGHT-H
    *AND-COLUMNS FOR CORRESPONDING ABSOLUTE DIFFERENCES,///6X,5HNITER,
    * 10(5X,1HR,A6)/(11X,10(5X,1HR,A6)/))
 130 FORMAT(1H ,6X,I3,10(1PE12.3)/(10X,10(1PE12.3)/))
 140 FORMAT (32H0THE PROCESS DID NOT CONVERGE IN,I5,13H   ITERATIONS)
 150 FORMAT(14X,10(1PE12.3)/)
 355 CONTINUE
     END
*DECK BC
     SUBROUTINE BDUNC1
*CALL CMD
     ACYL(R2,R1)=(R2-R1)*(R2+R1)/2.
     WP(XI2)=0.0*XI2
     WS(XI2)=0.0*XI2
     WVW(DELF,WQ,ROP,DELRO,ETA2)=-(DELF/((ETA2*DX1)**2)*WQ*(ROP/6.+DELR
    *O/8.))/(ROP/3.+5.*DELRO/24.)
     WHW(WK,DELF,WQ,ROP,DELRO,RAD)=-(DELF/(DX2*DX2)*WQ*(RAD+WK*DX2)*(RO
    *P+(RAD/6.+WK*DX2/8.)+DELRO*(RAD/8.+WK*DX2/10.)))/(RAD*(RDP*(RAD/3.
    *+5.*WK*DX2/24.)+DELRO*(5.*RAD/24.+3.*WK*DX2/20.)))
     YY(YN,YP)=1./(1.-(P/YN)**2)
C*****************************************************************
C   ##BOUNDARY## - CONDITIONS SUBROUTINE
C***BOUNDARY VALUES FOR
C***     STREAM FUNCTION
C***     VORTICITY
C***     MIXTURE FRACTIONS
C***     ENTHALPY
C***     SWIRL VELOCITY
C*****************************************************************
C
C
C*****************************************************************
C   ZERO AXIAL GRADIENTS FOR ALL DEPENDENT VARIABLES AT EXIT
C   QUADRATIC PROFILE NEAR #ADIABATIC# BOUNDARIES
C*****************************************************************
     K=KEQ
     RR=PREF/(GCPM*TREF)
     ROP=ZMW(1)*RR
     RDS=ZMW(2)*RR
C***  REVISED ROUTING
     IF (K.EQ.NW) GO TO 290
     IF (K.EQ.NF) GO TO 10
     IF (K.EQ.NVT) GO TO 430
     GO TO 130
C*************************************************
C   FOR STREAM FUNCTION..... A(I,J,NF)
C*************************************************
  10 CONTINUE
     IF(NITER.GE.3) GO TO 110
     ANF=1.
     IF(NITER.EQ.0.AND.IDLD.GT.0) ANF=A(1,1,NF)
C***   MODIFICATION FOR THE STREAM FUNCTION CALCULATIONS
C      FROM THE GIVEN VELOCITY PROFILE
C
C
     IF(JA1.GE.JB) GO TO 21
     DO 20 J4=JA1,JB
     VPSIM=0.0
     J=JB-(J4-JA1)
     IF(J.GE.JB) GO TO 22
     DO 23 J5=J,JB
     IF(J5.EQ.JB) GO TO 23
     DAREA=X2(J5+1)-X2(J5)
     IF(INDG.EQ.2) DAREA=ACYL(R(J5+1),R(J5))
```

TABLE XXVI. (Cont)

```
      VPSIM=VPSIM+(0.5*(RO(I,J5)+RO(I,J5+1)))*(0.5*
     * (VIN(J5)+VIN(J5+1)))*DAREA
   23 CONTINUE
   22 CONTINUE
      A(1,J,NF)=-VPSIM
   20 CONTINUE
   21 CONTINUE
      IF(JAI.GE.JB) FBASE=0.0
      IF(JAI.LT.JB) FBASE=A(I,JAI,NF)
C***
      IF(JA.LE.I) GO TO 25
      DO 30 L4=I,JA
      VPSIM=0.0
      J=JA-(L4-I)
      IF(J.GE.JA) GO TO 32
      DO 33 L5=J,JA
      IF(L5.EQ.JA) GO TO 33
      DAREA=X2(L5+1)-X2(L5)
      IF(INOG.EQ.2) DAREA=ACYL(R(L5+I),R(L5))
      VPSIM=VPSIM+(0.5*(RO(I,L5)+RO(1,L5+I)))*(0.5*(VIN(L5)+
     * VIN(L5+I)))*DAREA
   33 CONTINUE
   32 CONTINUE
      A(1,J,NF)=FBASE-VPSIM
   30 CONTINUE
   31 CONTINUE
C***   END STRM CALCULATIONS FOR INLETS
   15 CONTINUE
C
C
      IF (1.GT.IN)GO TO 25
      DO 40 I=1,IN
   40 A(I,1,NF)=A(1,1,NF)
   25 CONTINUE
      IF (IAB.GT.IC)GO TO 35
      DO 50 I=IAB,IC
   50 A(I,JN,NF)=0.
   35 CONTINUE
      IF (1.GT.IAB)GO TO 45
      DO 60 I=1,IAB
      A(I,JB,NF)=0.
      A(I,JA1,NF)=A(I,JA1,NF)
   60 A(I,JA,NF)=A(I,JAI,NF)
   45 CONTINUE
      IF (IC.GT.IN)GO TO 55
      DO 70 I=IC,IN
   70 A(I,JC,NF)=0.
   55 CONTINUE
      IF (JA.GT.JAI)GO TO 65
      DO 80 J=JA,JA1
   80 A(IAB,J,NF)=A(1,JAI,NF)
   65 CONTINUE
      IF (JB.GT.JN)GO TO 75
      DO 90 J=JB,JN
   90 A(IAB,J,NF)=0.
   75 CONTINUE
      IF (JC.GT.JN)GO TO 85
      DO 100 J=JC,JN
  100 A(IC,J,NF)=0.
   85 CONTINUE
C
C   MOD FOR JET INLETS
C
      IF(JA.NE.1) GO TO 601
      DO 602 I=IAB,IN
      A(I,1,NF)=A(IAB,JA,NF)
```

TABLE XXVI. (Cont)

```
  602 CONTINUE
  601 CONTINUE
      IF(2.GT.JS)GO TO 600
      JSPI=JSI+1
      IF(JSP1.GT.JS) GO TO 600
      DO 610 J=JSP1,JS
      A(IS1,J,NF)=A(IS1,J-1,NF)
     + +((RO(J)+RO(J-1))/2.)*((VF(J-I)+VF(J))/2.)*(X2(J)-X2(J-1))*
     + ((R(J)+R(J-1))/2.)
  610 CONTINUE
      IF(IS1.GT.IS.OR.ISI.EQ.IN) GO TO 612
      DO 611 I=IS1,IS
  611 A(I,JS,NF)=A(IS1,JS,NF)
  612 CONTINUE
      IF(JS1.GE.JS.OR.IS1.EQ.IS.OR.IS.EQ.IN) GO TO 616
      DO 615 J4=JS1,JS
      J=JS-(J4-1)
      IF(J.EQ.JS) GO TO 615
      A(IS,J,NF)=A(IS,J+1,NF)-(RO(J)+RO(J+1))*(VF1(J)+VF1(J+1))
     + *(R(J)+R(J+I))/8.*(X2(J+I)-X2(J))
  615 CONTINUE
  616 CONTINUE
      IF(JS1.NE.1) GO TO 621
      DO 620 I=IS,IN
  620 A(I,1,NF)=A(IS,JS1,NF)
  621 CONTINUE
  600 CONTINUE
C    INITIALIZE INTERIOR GRID NODES
      IF(NITER.GT.0) GO TO 2900
      DO 934 J=2,JNM
      IL=IMIN(J)+1
      IH=IMAX(J)-I
      DO 934 I=IL,IH
      IF(I.GE.IS1.AND.I.LE.IS.AND.J.GE.JSI.AND.J.LE.JS) GO TO 934
      IF(IOLO.GT.0) GO TO 52
      IF(JS.LT.JA1.AND.J.LE.JB.AND.J.GE.JAI)A(I,J,NF)=A(1,J,NF)
      IF(JS.EQ.I.AND.JA.GT.1.AND.J.LE.JA)A(I,J,NF)=A(1,J,NF)
C
      GO TO 934
   52 A(I,J,NF)=A(I,J,NF)/ANF*A(1,1,NF)
  934 CONTINUE
 2900 CONTINUE
  110 CONTINUE
      BB=YY(2.*OELXI(IN-I),X1(IN)-X1(IN-I))
      JSP1=JS+I
      IF(IS.LT.IN)JSPI=1
      IF(JSP1.GT.JC) GO TO 95
      DO 120 J=JSP1,JC
  120 A(IN,J,NF)=BB*A(IN-1,J,NF)-(BB-I.)*A(IN-2,J,NF)
   95 CONTINUE
      GO TO 999
C***  REMOVED INLET B.C. CALCULATIONS. THESE ARE SET IN BLOCK1
C*****************************************************
C***  GENERAL ADIABATIC, IMPERMEABLE, INERT BOUNDARY CONDITIONS WITH
C***  ZERO GRADIENT AT WALLS AND EXIT FOR ANY VARIABLE L.
C*****************************************************
  130 L=K
  170 CONTINUE
      IF (IAB.LE.2)GO TO 200
      IF (1.GT.IAB)GO TO 125
      DO 190 I=I,IAB
      BB=YY(2.0*OELX2(JB-I),X2(JB)-X2(JB-I))
      A(I,JB,L)=BB*A(I,JB-1,L)-(BB-I.0)*A(I,JB-2,L)
      IF (JB.EQ.JAI)GO TO 180
      BB=YY(2.0*OELX2(JAI+I),X2(JA1+1)-X2(JA1))
      A(I,JA1,L)=BB*A(I,JA1+1,L)-(BB-1.0)*A(I,JA1+2,L)
```

TABLE XXVI. (Cont)

```
  180 IF (JA1.EQ.JA)GO TO 190
      BB=YY(2.0*DELX2(JA-1),X2(JA)-X2(JA-1))
      A(I,JA,L)=BB*A(I,JA-1,L)-(BB-1.0)*A(I,JA-2,L)
  190 CONTINUE
  125 CONTINUE
  200 CONTINUE
      BB=YY(2.*DELX1(IAB+1),X1(IAB+1)-X1(IAB))
      IF (JA.EQ.JA1.OR.(JA1-JA).LE.1)GO TO 220
      JJA=JA+1
      JJA1=JA1-1
      IF (JJA.GT.JJA1)GO TO 135
      DO 210 J=JJA,JJA1
  210 A(IAB,J,L)=BB*A(IAB+1,J,L)-(BB-1.)*A(IAB+2,J,L)
  135 CONTINUE
  220 CONTINUE
      JBB=JB+1
      IF (JBB.GT.JN)GO TO 145
      DO 230 J=JBB,JN
  230 A(IAB,J,L)=BB*A(IAB+1,J,L)-(BB-1.)*A(IAB+2,J,L)
  145 CONTINUE
      BB=YY(2.*DELX2(JN-1),X2(JN)-X2(JN-1))
      IF (IAB.GT.IC)GO TO 155
      DO 240 I=IAB,IC
  240 A(I,JN,L)=BB*A(I,JN-1,L)-(BB-1.)*A(I,JN-2,L)
  155 CONTINUE
      BB=YY(2.*DELX1(IC-1),X1(IC)-X1(IC-1))
      IF (JC.GT.JN)GO TO 165
      DO 250 J=JC,JN
  250 A(IC,J,L)=BB*A(IC-1,J,L)-(BB-1.)*A(IC-2,J,L)
  165 CONTINUE
      BB=YY(2.*DELX2(JC-1),X2(JC)-X2(JC-1))
      IF (IC.GT.IN)GO TO 175
      DO 260 I=IC,IN
  260 A(I,JC,L)=BB*A(I,JC-1,L)-(BB-1.)*A(I,JC-2,L)
  175 CONTINUE
      BB=YY(2.*DELX2(2),X2(2)-X2(1))
      IF (1.GT.IN)GO TO 185
      DO 270 I=1,IN
      A(I,1,L)=BB*A(I,2,L)-(BB-1.)*A(I,3,L)
  270 CONTINUE
  185 CONTINUE
      BB=YY(2.*DELX1(IN-1),X1(IN)-X1(IN-1))
      IF (1.GT.JC)GO TO 195
      DO 280 J=1,JC
      IF(IS.EQ.IN.AND.J.LE.JS.AND.JS.NE.1) GO TO 280
      A(IN,J,L)=BB*A(IN-1,J,L)-(BB-1.)*A(IN-2,J,L)
      IF(G1(IN,J).LE.0..AND.(K.EQ.NMF1.OR.K.EQ.NMF2.OR.K.EQ.NMF3.OR.
     *K.EQ.NMF4.OR.K.EQ.NMF5.OR.K.EQ.NMF6)) A(IN,J,L)=0.
  280 CONTINUE
  195 CONTINUE
      IF(JS.EQ.1) GO TO 899
      BB=YY(2.*DELX1(IS1-1),X1(IS1)-X1(IS1-1))
      DO 800 J=JS1,JS
      IF(VF(J).EQ.0.) A(IS1,J,L)=BB*A(IS1-1,J,L)-(BB-1.)*A(IS1-2,J,L)
      IF(VF1(J).EQ.0..AND.IS.LT.(IN-1)) A(IS,J,L)=BB*A(IS+1,J,L)
     * -(BB-1.)*A(IS+1,J,L)
  800 CONTINUE
      IF(JS1.GT.3) BB1=YY(2.*DELX2(JS1-1),X2(JS1)-X2(JS-1))
      BB=YY(2.*DELX2(JS+1),X2(JS+1)-X2(JS))
      IS1P1=IS1+1
      DO 810 I=IS1P1,IS
      A(I,JS,L)=BB*A(I,JS+1,L)-(BB-1)*A(I,JS+2,L)
      IF(JS1.GT.3) A(I,JS1,L)=BB1*A(I,JS1-1,L)-(BB1-1)*A(I,JS1-2,L)
  810 CONTINUE
  899 CONTINUE
C...KVB...LIMIT  MASS FRACTION TO + VALUES                          09/10/71
```

TABLE XXVI. (Cont)

```
      IF(K.NE.NMF1.AND.K.NE.NMF2.AND.K.NE.NMF3.AND.K.NE.NMF4.AND.
     * K.NE.NMF5.AND.K.NE.NMF6) GO TO 999
      DO 1285 J=1,JN                                                    09/10/71
      DO 1285 I=1,IN                                                    09/10/71
      IF(A(I,J,K).LT.0.) A(I,J,K)=0.                                    09/10/71
 1285 CONTINUE                                                          09/10/71
C***K.V.B.***                                                           09/10/71
      GO TO 999
C*********************************************
C   FOR VORTICITY.... A(I,J,NW)
C*********************************************
  290 CONTINUE
      RK=FLOAT(INOG-1)
      IF (KVORT.NE.1)GO TO 370
C***  CALCULATE WALL VORTICITIES BEFORE PRINTING (KVORT=1)
      DX2=X2(JN)-X2(JN-1)
      IF (IAB.GT.IC)GO TO 205
      DO 300 I=IAB,IC
  300 A(I,JN,NW)=WHW(-WK,A(I,JN-1,NF),A(I,JN-1,NW),RO(I,JN),RO(I,JN-1)-R
     *O(I,JN),RADN)
  205 CONTINUE
      DX1=X1(IAB+1)-X1(IAB)
      IF (JA.GT.JA1)GO TO 215
      DO 310 J=JA,JA1
      IF(J.EQ.1) GO TO 3000
      A(IAB,J,NW)=WVW(A(IAB+1,J,NF)-A(IAB,J,NF),A(IAB+1,J,NW),RO(IAB,J),
     *RO(IAB+I,J)-RO(IAB,J),R(J))
 3000 CONTINUE
  310 CONTINUE
  215 CONTINUE
C***  CORRECTED GOSMAN PROG TO SEPARATE JA AND JA1 CALCULATIONS
      IF (I.GT.IAB)GO TO 225
      IF (JA.EQ.1) GO TO 319
      DX2=X2(JA)-X2(JA-1)
      DO 318 I=1,IAB
      A(I,JA,NW)=WHW(-WK,A(I,JA-1,NF)-A(I,JA,NF),A(I,JA-1,NW),RO(I,JA),R
     *O(I,JA-1)-RO(I,JA),RADA)
  318 CONTINUE
  319 CONTINUE
      IF(JA1.EQ.JN.OR.JA1.EQ.1) GO TO 225
      DX2=X2(JA1+1)-X2(JA1)
      DO 320 I=1,IAB
  320 A(I,JA1,NW)=WHW(WK,A(I,JA1+1,NF)-A(I,JA1,NF),A(I,JA1+I,NW),RO(I,JA
     *1),RO(I,JA1+1)-RO(I,JA1),RADAI)
  225 CONTINUE
      DX1=X1(IAB+1)-X1(IAB)
      IF (JB.GT.JN)GO TO 235
      DO 330 J=JB,JN
      IF(J.EQ.1) GO TO 3001
      A(IAB,J,NW)=WVW(A(IAB+1,J,NF),A(IAB+1,J,NW),RO(IAB,J),RO(IAB+I,J)-
     *RO(IAB,J),R(J))
 3001 CONTINUE
  330 CONTINUE
  235 CONTINUE
      IF(JB.EQ.1) GO TO 245
      DX2=X2(JB)-X2(JB-I)
      IF (I.GT.IAB)GO TO 245
      DO 340 I=1,IAB
  340 A(I,JB,NW)=WHW(-WK,A(I,JB-1,NF),A(I,JB-1,NW),RO(I,JB),RO(I,JB-1)-R
     *O(I,JB),RADB)
  245 CONTINUE
      DX1=X1(IC)-X1(IC-1)
      IF (JC.GT.JN)GO TO 255
      DO 350 J=JC,JN
      IF(J.EQ.1) GO TO 3002
      A(IC,J,NW)=WVW(A(IC-1,J,NF),A(IC-1,J,NW),RO(IC,J),RO(IC-1,J)-RO(IC
```

TABLE XXVI. (Cont)

```
     +,J),R(J))
 3002 CONTINUE
  350 CONTINUE
  255 CONTINUE
      IF(JC.EQ.1) GO TO 265
      DX2=X2(JC)-X2(JC-1)
      IF (IC.GT.IN)GO TO 265
      DO 360 I=IC,IN
  360 A(I,JC,NW)=WHW(-WK,A(I,JC-1,NF),A(I,JC-1,NW),RO(I,JC),RO(I,JC-1),R
     +O(I,JC),RAOC)
  265 CONTINUE
      IF(JS.EQ.1) GO TO 3005
      DX2=X2(JS+1)-X2(JS)
      DO 3004 I=IS1,IS
      A(I,JS,NW)=WHW(WK,A(I,JS+1,NF),A(I,JS,NF),A(I,JS+1,NW),RO(I,JS),
     +RO(I,JS+1)-RO(I,JS),R(JS))
 3004 CONTINUE
 3005 CONTINUE
C*** CALCULATE INLET, EXIT AND CENTERLINE VORTICITIES DURING ITERATION
C***** WHEN CYLINDRICAL COORDINATES ARE USED, I.E. INDG=2,
C***** OBTAIN W/R (VORTICITY/RAD) AT AXIS FROM THE QUADRATIC EXP
C***** W=A*R + B*R*R, A AND B BEING FUNCTIONS OF R(2) AND R(3)
  370 IF (1.GT.IN)GO TO 275
      DO 390 I=1,IN
      IF (X2AXIS.GT.0.0)GO TO 380
      IF (INDG.EQ.1)A(I,1,NW)=0.0
      IF (INDG.EQ.2)A(I,1,NW)=A(I,2,NW)+(X2(2)/(X2(3)-X2(2)))*(A(I,2,NW)
     +-A(I,3,NW))
      GO TO 390
  380 DX2=X2(2)-X2(1)
      A(I,1,NW)=WHW(WK,A(I,2,NF)-A(I,1,NF),A(I,2,NW),RO(I,1),RO(I,2)-RO(
     +I,1),X2AXIS)
  390 CONTINUE
  275 CONTINUE
      JAA=JA-1
      IF(2.GT.JAA) GO TO 285
      DO 400 J=2,JAA
      IF(NITER.LE.1) A(1,J,NW)=0.
      LV1=NUMA+7
      IF(NITER.GT.1) A(1,J,NW)=-ADF(1,J,2,LV1)/R(J)
  400 CONTINUE
  285 CONTINUE
      JAA=JA1+1
      JBB=JB-1
      IF(JAA.GT.JBB) GO TO 295
      DO 410 J=JAA,JBB
      IF(NITER.LE.1) A(1,J,NW)=0.
      LV1=NUMA+7
      IF(NITER.GT.1) A(1,J,NW)=-ADF(1,J,2,LV1)/R(J)
  410 CONTINUE
  295 CONTINUE
      IF(2.GT.JS) GO TO 701
      IF(JS.EQ.1) GO TO 701
      JS1P1=JS1+1
      JSM1=JS-1
      IF(JS1P1.GT.JSM1) GO TO 701
      DO 700 J=JS1P1,JSM1
      A(IS1,J,NW)=0.
  700 A(IS,J,NW)=0.
  701 CONTINUE
      BB=YY(2.*DELX1(IN-1),X1(IN)-X1(IN-1))
      JCM1=JC-1
      DO 420 J=2,JCM1
      IF(J.GE.JS1.AND.J.LE.JS.AND.IS.EQ.IN) GO TO 420
      LV1=NUMA+7
      IF(G1(IN,J).LE.0..AND.NITER.GT.1)A(IN,J,NW)=-ADF(IN,J,2,LV1)/R(J)
```

TABLE XXVI. (Cont)

```
      IF(G1(IN,J).LE.0..AND.NITER.LE.1) A(IN,J,NW)=0.
      IF(G1(IN,J).GT.0.) A(IN,J,NW)=BB*A(IN-1,J,NW)-(BB-1.)*A(IN-2,J,NW)
      IF(G1(IN,J).LE.0.) A(IN,J,NW)=0.
  420 CONTINUE
  305 CONTINUE
      GO TO 999
C*************************************************
C   FOR SWIRL VELOCITY
C*************************************************
  430 CONTINUE
      BB=YY(2.*DELX1(IN-1),X1(IN)-X1(IN-1))
      IF (1.GT.JC)GO TO 315
      DO 440 J=I,JC
  440 A(IN,J,NVT)=BB*A(IN-1,J,NVT)-(BB-1.)*A(IN-2,J,NVT)
  315 CONTINUE
  999 CONTINUE
      RETURN
      END
*DECK MB
      SUBROUTINE MVBCCI
*CALL CMD
      DIMENSION AQ(21,21,18)
      EQUIVALENCE (A(1,1,1),AQ(1,1,1))
C*****************************************************************************
C   **MASS-VELOCITY-BOUNDARY-CONDITION** SUBROUTINE
C   THIS SUBR. CALCULATES G1, G2 ON THE BOUNDARIES
C*****************************************************************************
C
C*****************************************************************************
C   UNIFORM INLET-VELOCITY DISTRIBUTIONS...
C   ZERO AXIAL GRADIENTS OF STREAM FUNCTION AND VORTICITY AT EXIT
C   VEXIT IS THE MEAN VELOCITY AT EXIT
C*****************************************************************************
      RR=PREF/(GCPM*TREF)
      ROP=ZMW(1)*RR
      IF (JA.EQ.JB)ROP=RO(1,1)
      ROS=ZMW(2)*RR
      IF (1.GT.JA)GO TO 5
      DO 10 J=1,JA
C***   REVISED G1 FOR VARIABLE INLET PROFILES AT PRIMARY INLET
      G1(1,J)=RO(1,J)*VIN(J)
   10 G2(1,J)=0.
    5 CONTINUE
      IF (JA1.GT.JB)GO TO 15
      DO 20 J=JA1,JB
C***   REVISED G1 FOR VARIABLE INLET PROFILES AT SECONDARY INLET
      G1(1,J)=RO(1,J)*VIN(J)
   20 G2(1,J)=0.
   15 CONTINUE
      JJC=JC-1
      IF (2.GT.JJC)GO TO 25
      DO 30 J=2,JJC
      G1(IN,J)=ADF(IN,J,2,NF)/R(J)
      G2(IN,J)=0.0
   30 CONTINUE
   25 CONTINUE
      JSIMI=JSI-1
      IF(2.GT.JSIMI) GO TO 210
      DO 200 J=2,JSIMI
  200 G1(IN,J)=ADF(IN,J,2,NF)/R(J)
      G2(IN,J)=0.
  210 CONTINUE
      IF(JS1.GE.JS) GO TO 230
      DO 220 J=JS1,JS
      G2(IS1,J)=0.
      G1(IS1,J)=RO(IS1,J)*VF(J)
```

TABLE XXVI. (Cont)

```
      IF (ISI.NE.IS) G1(IS,J)=RO(IS,J)*VFI(J)
      G2(IS,J)=0.
      IF(IS.LT.IN.AND.J.LT.JC) G1(IN,J)=ADF(IN,J,2,NF)/R(J)
      G2(IN,J)=0.
  220 CONTINUE
  230 CONTINUE
      JSP1=JS+1
      JCC=JC-1
      IF(JSP1.GT.JCC) GO TO 250
      DO 240 J=JSP1,JCC
      G2(IN,J)=0.
      G1(IN,J)=ADF(IN,J,2,NF)/R(J)
  240 CONTINUE
  250 CONTINUE
      DX2=X2(2)-X2(1)
      BB=1./(1.-((X2(2)-X2(1))/(X2(3)-X2(1)))**2)
      IF (2.GT.IN)GO TO 35
      DO 40 I=2,IN
      IF (X2AXIS.EQ.0.0)GI(I,1)=BB*G1(I,2)-(BB-1.)*GI(I,3)
      IF (X2AXIS.GT.0.0)GI(I,1)=0.0
   40 G2(I,1)=0.
   35 CONTINUE
      ROSUM=0.0
      IF (1.GT.JC)GO TO 45
      DO 50 J=1,JC
   50 ROSUM=ROSUM+RO(IN,J)
   45 CONTINUE
      ROMEAN=ROSUM/FLOAT(JC)
      IF (INDG.EQ.1)VEXIT=-A(IN,I,NF)/(X2(JC)*ROMEAN)
      IF (INDG.EQ.2)VEXIT=-2.*A(IN,1,NF)/((RADC*RADC-X2AXIS*X2AXIS)*ROME
     *AN)
      RETURN
      END
*DECK ME
      SUBROUTINE MVEL.CT
*CALL CMD
      DIMENSION AQ(21,21,18)
      EQUIVALENCE (A(1,1,1),AQ(1,1,1))
C*****************************************************************
C   **MASS-VELOCITY** SUBROUTINE
C   THIS SUBR. CALCULATES G1 AND G2 AT ALL POINTS NOT ON THE BOUND.
C*****************************************************************
      IF (2.GT.JNM)GO TO 5
      DO 20 J=2,JNM
      IL=IMIN(J)+1
      IH=IMAX(J)-1
      IF (JA.EQ.JA1)GO TO 10
      IF (J.EQ.JA.OR.J.EQ.JA1)IL=IAB+1
   10 CONTINUE
      IF (J.EQ.JB)IL=IAB+1
      IF (J.EQ.JC)IH=IC-1
      DO 20 I=IL,IH
      IF(J.GE.JS .AND.J.LE.JS.AND.I.GE.ISI.AND.I.LE.IS) GO TO 30
      G1(I,J)=ADF(I,J,2,NF)/R(J)
      G2(I,J)=-ADF(I,J,1,NF)/R(J)
      GO TO 20
   30 GI(I,J)=0.
      G2(I,J)=0.
   20 CONTINUE
    5 CONTINUE
      RETURN
      END
*DECK VI
      SUBROUTINE VISCC1
*CALL CMD
C*****************************************************************
```

TABLE XXVI. (Cont)

```
C   **VISCOSITY** SUBROUTINE
C*****************************************************************
      LOGICAL INLET
      DATA C3,CA,CB,ZC,XSL,CL2,CKV/.016,.005,10.,  .22,  20.,  .2,  .02/
      IF (INDZMU.EQ.1)GO TO 20
      ZMFU=2.*(A(IAB,JA,NF)-A(IAB,1,NF))
      ZMAIR=2.*(A(IAB,JB,NF)-A(IAB,JA1,NF))
      ZMJ=2.*(A(ISI,JS1,NF)-A(ISI,JS,NF))
      ZMJ1=2.*(A(IS,JS,NF)-A(IS,JS1,NF))
      IF( INDG.EQ.2)ZMJ=ZMJ*3.14159
      IF( INDG.EQ.2)ZMJ1=ZMJ1*3.14159
      IF (INDG.EQ.2)ZMFU=ZMFU*3.14162
      IF (INDG.EQ.2)ZMAIR=ZMAIR*3.14162
C***  REVISED ZMVV FOR MEAN VELOCITIES
      ZMVV=ZMFU*VINPM*VINPM+ZMAIR*VINSM*VINSM
      ZMVV=ZMVV+ZMJ*VINJM*VINJM+ZMJ1*VINJM1*VINJM1
      IF (INDE(NVT).EQ.1)ZMVV=ZMVV+ZMAIR*(A(I,JB-I,NVT)**2)
      ZMVV=ZMVV**0.33333
      AA=ZMUK*((2.*X2(JN))**0.666667)*ZMVV/((DCN-DA)**0.33333)
      S=X2(JA)-X2(1)
      SI=X2(JB)-X2(JSI)
      IF(X2AXIS.EQ.0.) S=2.*S
      SJ=X2(JS)-X2(JS1)
      IF(X2AXIS.EQ.0.) SJ=2.*SJ
      ILIM=(ISI-IAB)/2+IAB
      JLIM=(JA1-JA)/2+JA
      IF(S.EQ.0)JLIM=0
      IF(SI.EQ.0) JLIM=JN
      IF(ZMUK.GT.0.)CKV=ZMUK
      IF (I.GT.JN)GO TO 5
      DO 10 J=I,JN
      IL=IMIN(J)
      IH=IMAX(J)
      IF(J.GT.JLIM) GO TO 50
      SL=S
      YL=X2(J)
      AK=ABS(CKV*VINPM*VINPM)
      GO TO 60
   50 SL=SI
      AK=ABS(CKV*VINSM*VINSM)
      YL=X2(JN)-X2(J)
   60 CONTINUE
      DO 10 I=IL,IH
      XS=X1(I)-X1(IAB)
      ELAM=CA*(CB+XSL)
      IF(XS/SL.LT.XSL) ELAM=CA*(CB+XS/SL)
C   FOR NODES AT INLET USE INITIAL INPUT VALUES OF NZK
      INLET=.F.
      IF(I.EQ.1.AND.J.LT.JB.AND.J.GT.JA1)INLET=.T.
      IF(I.EQ.I.AND.J.LT.JA)INLET=.T.
      IF(I.EQ.ISI.AND.J.LT.JS.AND.J.GT.JS1.AND.VF(J)  .NE.0.)INLET=.T.
      IF(I.EQ.IS.AND.J.LT.JS.AND.J.GT.JSI.AND.VF1(J)  .NE.0.)INLET=.T.
      IF(INLET)GO TO 80
C    FOR NODES NEXT TO WALL AK=0
      IF(J.GE.JN-1)GO TO 65
      IF(I.LE.IAB+I.AND.J.GE.JB-1)GO TO 65
      IF(I.LE.IAB+1.AND.J.GE.JA-1.AND.J.LE.JA1+I)GO TO 65
      IF(I.GE.IC-1.AND.J.GE.JC-1) GO TO 65
      IF(J.LE.JS+1.AND.J.GE.JSI-1.AND.I.GE.ISI-1.AND.I.LE.IS +1)GOTO65
      IF(J.LE.2.AND.X2AXIS.NE.0.) GO TO 65
      GO TO 70
   65 A(I,J,NZK)=0.
      GO TO 80
   70 A(I,J,NZK)=AK
   80 CONTINUE
      IF(A(I,J,NZK).LT.0.) A(I,J,NZK)=0.
```

TABLE XXVI. (Cont)

```
      ZL=ELAM*YL
      ZMU(I,J)=ZC*SQRT(A(I,J,NZK))*RD(I,J)*ZL+ZMUREF
   10 CONTINUE
    5 CONTINUE
      GO TO 40
   20 IF (1.GT.JN)GO TO 15
      DO 30 J=1,JN
      IL=IMIN(J)
      IH=IMAX(J)
      DO 30 I=IL,IH
      ZMU(I,J)=ZMUREF
   30 CONTINUE
   15 CONTINUE
   40 CONTINUE
      RETURN
      END
*DECK DE
      SUBROUTINE OENSC1
*CALL CMD
      DIMENSION HF(7),EMF(6)
      LOGICAL INLET
      DIMENSION AHR(6,6),CCL(6,6),CHL(6,6),CCM(6),CHM(6),ALR(6,6)
     *  ,CCH(6,6),CHH(6,6)
      DATA (HF(LL),LL=1,6)/-2007.1,-3846.7,-5774.7,0.,-1697.5,0./
      DATA ((ALR(N,L),N=1,6),L=1,6) /
     +4.24977,-6.91266E-3,31.6021E-06,-29.7154E-09,9.51036E-12,-10186.6,
     +2.1701,10.3781E-03,-10.7339E-06,6.34592E-09,1.62807E-12,-48352.6,
     +4.15650,-1.72443E-03,5.69823E-06,4.593E-09,1.42337E-12,-30288.8,
     +3.71899,-2.51673E-03,8.58374E-06,-8.29987E-9,2.78082E-12,-1057.67,
     +3.78713,-2.17095E-03,5.07573E-06,-3.47377E-9,.772168E-12,-14363.5,
     +3.69161,-1.33326E-03,2.65031E-06,-.976883E-9,-.099772E-12,-1062.8/
      DATA ((AHR(N,L),N=1,6),L=1,6) /
     +1.17957,10.9505E-03,-4.06221E-6,.713703E-9,-.0474904E-12,-9855.66,
     +4.41293,3.19229E-3,-1.29782E-6,.241474E-9,-.01674299E-12,-48944.0,
     +2.67075,3.03172E-3,-.853516E-6,.117908E-9,-.00619736E-12,-29888.9,
     +3.59761,.781456E-3,-.223867E-6,.042490E-9,-.00334602E-12,-1192.79,
     +2.95115,1.55256E-3,-.619114E-6,.113503E-9,-.00778827E-12,-14231.8,
     +2.85458,1.59763E-3,-.625663E-6,.113158E-9,-.00788971E-12,-890.174/
C*****************************************************************************
C   **OENSITY** SUBROUTINE
C   MIXTURE DENSITY CALCULATION
C*****************************************************************************
      IF(NITER.GT.2) GO TO 610
      EHC=HC
      IF(HC.EQ.0.)EHC=HP
      DO 605 L=1,6
      RM=1.98726/ZMW(L)
      DO 600 N=1,5
      CCL(N,L)=ALR(N,L)*RM/(1.8**(N-1))
      CCH(N,L)=AHR(N,L)*RM/(1.8**(N-1))
      CHL(N,L)=CCL(N,L)/N
      CHH(N,L)=CCH(N,L)/N
  600 CONTINUE
      CHL(6,L)= ALR(6,L)*RM*1.8
      CHH(6,L)= AHR(6,L)*RM*1.8
  605 CONTINUE
  610 CONTINUE
      CHL(6,1)=EHC+XCD/YCD*HF(2)+XH2O*HF(3)-264.2
      CHH(6,1)=CHL(6,1)+72.883
      TVAP=530.
      HS=HF(1)-264.2+TVAP*(CHL(1,1)+TVAP*(CHL(2,1)+TVAP*(CHL(3,1)
     ++TVAP*(CHL(4,1)+TVAP*(CHL(5,1))))))
      RR=PREF/GCPM
      IF (1.GT.JN)GO TO 5
      DO 40 J=1,JN
      IL=IMIN(J)
```

TABLE XXVI. (Cont)

```
      IH=IMAX(JJ)
      DO 40 I=IL,IH
      INLET=.F.
      IF(I.EQ.1.AND.J.LE.JA.AND.VINPM.NE.0.) INLET=.T.
      IF(I.EQ.1.AND.(J.GE.JA1.AND.J.LE.J8 ).AND.VINSM.NE.0.) INLET=.T.
      IF(I.EQ.IS.AND.(J.GE.JS1.AND.J.LE.JS).AND.VINJM1.NE.0.) INLET=.T.
      IF(I.EQ.IS).AND.(J.GE.JS1.AND.J.LE.JS).AND.VINJM.NE.0)  INLET=.T.
C****
      P=PREF
C     CALCULATE MIXTURE FRACTIONS
      F=A(I,J,NMF3)
      FO2=ZO2*XO2*(1.-F)
      IF(MC.EQ.0.) A(I,J,NMF1)=F
      EMCHX=A(I,J,NMF1)
      EMCO2=A(I,J,NMF2)
      EMH2O=XH2O*(F-EMCHX)
      EMO2=FO2-XO2*(F-EMCHX)-YO2*EMCO2
      EMCO=(XCO+XO2*YCO/YO2)*(F-EMCHX)-YCO/YO2*(FO2-EMO2)
      EMF(1)=EMCHX
      EMF(2)=EMCO2
      EMF(3)=EMH2O
      EMF(4)=EMO2
      EMF(5)=EMCO
      EMF(6)=1.-EMF(1)-EMF(2)-EMF(3)-EMF(4)-EMF(5)
      DO 200 KK=1,NSPEC
      IF (EMF(KK).LT.0.) EMF(KK)=0.
      IF (EMF(KK).GT.1.) EMF(KK)=1.
  200 CONTINUE
      EMF(6)=1.-EMF(1)-EMF(2)-EMF(3)-EMF(4)-EMF(5)
      DO 615 N=1,6
      CHM(N)=0.
      CCM(N)=0.
      DO 615 L=1,6
      IF(T(I,J).LT.1800.) CHM(N)=CHM(N)+CHL(N,L)*EMF(L)
      IF(T(I,J).GE.1800.) CHM(N)=CHM(N)+CHH(N,L)*EMF(L)
      IF(N.LT.6.AND.T(I,J).LT.1800.) CCM(N)=CCM(N)+CCL(N,L)*EMF(L)
      IF(N.LT.6.AND.T(I,J).GE.1800.) CCM(N)=CCM(N)+CCH(N,L)*EMF(L)
  615 CONTINUE
C     CALCULATE MOLECULAR WEIGHT
   90 CONTINUE
      SUM=0.0
      IF(1.GT.NSPEC) GO TO 105
      DO 100 NJ=1,NSPEC
  100 SUM=SUM+EMF(NJ)/ZMW(NJ)
  105 CONTINUE
      IF(SUM.LE.0.0) SUM=1./ZMW(1)                                    08/13/71
      AMOLW=1./SUM
C     CALCULATE TEMPERATURE
      CPBAR=0.
      IF (1.GT.NSPEC) GO TO 35
      DO 30 L=1,NSPEC
   30 CPBAR=CPBAR+CPJ(L)*EMF(L)
   35 CONTINUE
      IF(T(I,J).GT.2660.) EHC=HC-.2187*T(I,J)+581.742
      HF(1)=EHC+XCO/YCO*HF(2)+XH2O*HF(3)
      CPIN=F*CPJ(1)+(1.-F)*(ZO2*XO2*CPJ(4)+XN2*CPJ(6))
      AH=CPIN*(TREF-536.67)+F*HF(1)
      SHF=0.
      DO 500 LL=1,6
      SHF=EMF(LL)*HF(LL)+SHF
  500 CONTINUE
      T(I,J)=536.67+(AH-SHF)/CPBAR
      TREFH=TREF
      IF(INOE(NHS).EQ.1.AND.INLET) TREFH=T(I,J)
      HCHX=HF(1)-264.2+TREF*(CHL(1,1)+TREF*(CHL(2,1)+TREF*(CHL(3,1)
     + +TREF*(CHL(4,1)+TREF*CHL(5,1)))))
```

TABLE XXVI. (Cont)

```
      HO2 =CHL(6,6)    +TREF*(CHL(1,4)+TREF*(CHL(2,4)+TREF*(CHL(3,4)
     + +TREF*(CHL(4,4)+TREF*CHL(5,4)))))
      HN2 =CHL(6,6)    +TREF*(CHL(1,6)+TREF*(CHL(2,6)+TREF*(CHL(3,6)
     + +TREF*(CHL(4,6)+TREF*CHL(5,6)))))
      TREF=TREFM
      IF(INLET) A(I,J,NHS)=F*HCHX+FO2*HO2+XN2*(1.-F)*HN2
      HTOT=A(I,J,NHS)
      IF(INDE(NHS).NE.1)HTOT=F*HCHX+FO2*HO2+XN2*(1.-F)*HN2
      TR=T(I,J)
      NCHK=0
  620 CONTINUE
      NCHK=NCHK+1
      CPBAR=CCM(1)+TR*(CCM(2)+TR*(CCM(3)+TR*(CCM(4)+TR*(CCM(5)))))
      OHO=CHM(6)-HTOT+TR*(CHM(1)+TR*(CHM(2)+TR*(CHM(3)+TR*(CHM(4)
     + +TR*CHM(5)))))
      TR=TR-OHO/CPBAR
      IF(NCHK.GT.10) GO TO 625
      IF(ABS(OHO/HTOT).GT..001) GO TO 620
      GO TO 630
  625 WRITE(6,640) I,J,NCHK
  640 FORMAT(1X,# I J NCHK IN OENS #,3I5)
  630 CONTINUE
      T(I,J)=TR
510   CONTINUE
      A(I,J,NEFF)=0.
      IF(F.GT.0..AND.HC.GT.0.) A(I,J,NEFF)=(HF(1)-SHF/F)/HC
C     CALCULATE DENSITY
      IF (IPRES.EQ.2) P=(1.+PF(I,J))*PREF
   20 DENSTY=P*AMOLW/(GCPM*T(I,J))
      RO(I,J)=ROWF*DENSTY+(1.-ROWF)*RO(I,J)
   40 CONTINUE
    5 CONTINUE
      RETURN
      END
*OECK FD
      SUBROUTINE FDEQC1
*CALL CMD
      WC1H(WK,OELF,ROP,DELRO,RAO)=-(DELF/(DX2*DX2))/(RAO*(ROP*(RAO/3.+5.
     +*WK*DX2/24.)+OELRO*(5.*RAO/24.+3.*WK*DX2/20.)))
      WC2H(WK,ROP,DELRO,RAO)=-(RAO+WK*DX2)*(ROP*(RAO/6.+WK*DX2/8.)+DELRO
     +*(RAO/8.+WK*DX2/10.))/(RAO*(ROP*(RAO/3.+5.*WK*DX2/24.)+OELRO*(5.*R
     +AO/24.+3.*WK*DX2/20.)))
      WC1V(DELF,ROP,DELRO,ETA2)=-DELF/(((ETA2*DX1)**2)*(ROP/3.+5.*DELRO/
     +24.))
      WC2V(ROP,DELRO)=-(ROP/6.+DELRO/8.)/(ROP/3.+5.*DELRO/24.)
C*****************************************************************
C   **FINITE-DIFFERENCE-EQUATION** SUBROUTINE
C*****************************************************************
      K=KEQ
      IF (2.GT.JNM)GO TO 5
      PHIMAX=0.
      EMLIM=0.
      DO 180 J=2,JNM
      IL=IMIN(J)+1
      IH=IMAX(J)-1
      IF (JA.EQ.JA1)GO TO 10
      IF (J.EQ.JA.OR.J.EQ.JA1)IL=IAB+1
   10 CONTINUE
      IF (J.EQ.JB)IL=IAB+1
      IF (J.EQ.JC)IH=IC-1
      DO 180 I=IL,IH
      IF(I.GE.IS1.AND.I.LE.IS.AND.J.GE.JS1.AND.J.LE.JS) GO TO 180
      IF(K.EQ.NW.AND.(J.EQ.JS.OR.J.EQ.JS1).AND.(I.EQ.(IS1-1).OR.I.EQ.
     + (IS+1)).AND.(JS.GT.1)) GO TO 20
      IF (K.EQ.NW.AND.(J.EQ.JA.AND.I.EQ.(IAB+1)))GO TO 20
      IF (K.EQ.NW.AND.(J.EQ.JA1.AND.I.EQ.(IAB+1)))GO TO 20
```

TABLE XXVI. (Cont)

```
      IF (K.EQ.NK.AND.(J.EQ.JB.AND.I.EQ.(IAB+1)))GO TO 20
      GO TO 30
C***** CAL. VORTICITIES AT PTS. ONE MESH AWAY FROM PROTRUDING CORNERS
   20 CALL COEFCT (I,J,NF)
      YY=A(I,J,NF)*(CE+CW+CN+CS)
      YY=YY-(CE*A(I+1,J,NF)+CW*A(I-1,J,NF)+CN*A(I,J+1,NF)+CS*A(I,J-1,NF)
     +)
      Z=A(I,J,NW)
      A(I,J,NW)=YY/R(J)
      GO TO 170
   30 CONTINUE
      CALL SORCCK(I,J,K,SOURCE,ZQ,EMLIM)
      CALL COEFCT(I,J,K)
      IF (K.NE.NW)GO TO 140
C**** INCORPORATING B.C. FOR VORTICITY IN THE FINITE DIFF. FORMULATION
C****    UP TO STATEMENT NUMBER 130
      ZW=0.
      ZWMU=0.0
      IF (I.EQ.IL.AND.(J.GE.JB.OR.(J.LE.JA1.AND.J.GE.JA)))GO TO 40
      IF (I.EQ.IH.AND.J.GE.JC)GO TO 70
      GO TO 80
   40 CONTINUE
      IF (J.EQ.JB.OR.J.EQ.JA1.OR.J.EQ.JA)GO TO 130
      LIEW=I-1
      CQEW=CW
      GO TO 90
   50 LJNS=J+1
      WKNS=FLOAT(1-INDG)
      IF (J.EQ.JNM)RADNS=RAOM
      IF (J.EQ.(JB-1))RADNS=RAOB
      IF (J.EQ.(JA-1))RAONS=RAOA
      IF (J.EQ.(JC-1))RAONS=RAOC
      CQNS=CN
      ZWHALF=ZW
      GO TO 100
   60 LJNS=J-1
      WKNS=FLOAT(INOG-1)
      RADNS=R(LJNS)
      CQNS=CS
      GO TO 100
   70 LIEW=I+1
      CQEW=CE
      GO TO 90
   80 IF (J.EQ.JNM)GO TO 50
      IF (J.EQ.(JA-1).AND.I.LE.IAB)GO TO 50
      IF (J.EQ.(JC-1).AND.I.GE.IC)GO TO 50
      IF (J.EQ.(JA1+1).AND.I.LE.IAB)GO TO 60
      IF(I.GE.IS1.AND.I.LE.IS.AND.J.EQ.(JS+1)) GO TO 60
      IF ((JB-JA1).GT.2.AND.(J.EQ.(JB-1).AND.I.LE.IAB))GO TO 50
      IF(JS1.GT.1.AND.I.LE.IS.AND.I.GE.IS1.AND.J.EQ.(JS1-1)) GO TO 50
      GO TO 130
   90 OX1=ABS(X1(LIEW)-X1(I))
      A(LIEW,J,NW)=WC1V(A(I,J,NF)-A(LIEW,J,NF),RO(LIEW,J),RO(I,J)-RO(LIE
     +W,J),R(J))
      ZW=CQEW*WC2V(RO(LIEW,J),RO(I,J)-RO(LIEW,J))
      ZWMU=ZWMU+ZW*ZMU(LIEW,J)
      GO TO 110
  100 OX2=ABS(X2(LJNS)-X2(J))
      A(I,LJNS,NW)=WC1H(WKNS,A(I,J,NF)-A(I,LJNS,NF),RO(I,LJNS),RO(I,J)-R
     +O(I,LJNS),RADNS)
      ZW=CQNS*WC2H(WKNS,RO(I,LJNS),RO(I,J)-RO(I,LJNS),RAONS)
      ZWMU=ZWMU+ZW*ZMU(I,LJNS)
      IF (LJNS.EQ.(J+1))GO TO 130
      GO TO 120
  110 IF (I.EQ.(IAB+1).AND.J.EQ.JNM)GO TO 50
      IF (I.EQ.(IC-1).AND.J.EQ.JNM)GO TO 50
```

TABLE XXVI. (Cont)

```
      GO TO 130
  120 IF ((JB-JA1).EQ.2.AND.(J.EQ.(JB-1).AND.I.LE.IAB))GO TO 50
  130 CONTINUE
C**** END VORTICITY B.C. SPECIAL FORMULATION
  140 IF (K.NE.NF) GO TO 160
      IF(JS.LE.1) GO TO 200
      IF(K.NE.NF) GO TO 160
      IF((J.EQ.JS.OR.J.EQ.JS1).AND.I.EQ.(IS+1))
     + GO TO 150
      IF((J.EQ.JS.OR.J.EQ.JS1).AND.I.EQ.(IS1-1).AND.VF(J).NE.0.)
     + GO TO 151
  200 CONTINUE
      IF (K.EQ.NF.AND.(J.EQ.JA.AND.I.EQ.(IAB+1)))GO TO 150
      IF (K.EQ.NF.AND.(J.EQ.JA1.AND.I.EQ.(IAB+1)))GO TO 150
      IF (K.EQ.NF.AND.(J.EQ.JB.AND.I.EQ.(IAB+1)))GO TO 150
      GO TO 160
  151 A(I,J,NF)=A(I+1,J,NF)
      GO TO 180
  152 A(I,J,NF)=A(I,J-1,NF)
      GO TO 180
  150 A(I,J,NF)=A(I-1,J,NF)
      GO TO 180
  160 CONTINUE
      CALL CONVEC(I,J,K,AU,ZU)
      IF (K.EQ.NW)AU=AU*R(J)*R(J)
      IF (K.EQ.NW)ZU=ZU*R(J)*R(J)
      ANUM=CE*C(2)*A(I+1,J,K)+CW*C(4)*A(I-1,J,K)+CN*C(3)*A(I,J+1,K)+CS*C
     +(5)*A(I,J-1,K)+AU+SOURCE
      ADNM=(CE+CW+CN+CS)*C(1)+ZU+ZQ
      IF (K.EQ.NW)ADNM=ADNM-ZWMU
C  CHANGE SCH
      IF (ADNM.EQ.0..OR.ANUM.EQ.0.)GO TO 180
      Z=A(I,J,K)
      A(I,J,K)=ANUM/ADNM
      IF(K.EQ.NMF2.AND.A(I,J,K).LT.0.) A(I,J,K)=0.
      IF((K.EQ.NMF5.OR.K.EQ.NMF6).AND.A(I,J,K).LT.0.) A(I,J,K)=0.        09/10/71
      IF(K.EQ.NMF1.AND.A(I,J,K).LT.EMLIM) A(I,J,K)=EMLIM
      IF(K.EQ.NMF2.AND.A(I,J,K).GT.EMLIM) A(I,J,K)=EMLIM
  170 CONTINUE
      DIF=A(I,J,K)-Z
      A(I,J,K)=Z+RP(K)*DIF
C***  ADDED AB
      AB=0.25*(A(I+1,J,K)+A(I-1,J,K)+A(I,J+1,K)+A(I,J-1,K))
C***  BYPASS DIVIDE BY ZERO
      IF (A(I,J,K).EQ.0.OR.AB.EQ.0.)GO TO 180
      RS=DIF/A(I,J,K)
C   CHANGE  SCH
      RSM=DIF/AB
      RS2=1.E30
      IF(PHIMN(K).NE.0.) RS2=DIF/PHIMN(K)
      IF (ABS(RSM).LT.ABS(RS))RS=RSM
      IF(ABS(RS2).LT.ABS(RS/DC)) RS=RS2
      IF (ABS(RS).GT.ABS(RSDU(K))) IRS(K)=I
      IF (ABS(RS).GT.ABS(RSDU(K))) JRS(K)=J
      IF (ABS(RS).GT.ABS(RSDU(K)))RSDU(K)=RS
      IF (ABS(DIF).GT.ABS(DIFMAX(K)))DIFMAX(K)=DIF
      AABS=ABS(A(I,J,K))
      PHIMAX=AMAX1(PHIMAX,AABS)
  180 CONTINUE
    5 CONTINUE
      PHIMN(K)=PHIMAX
      RETURN
      END
*DECK CF
      SUBROUTINE CDEFCT (I,J,K)
*CALL CMD
```

TABLE XXVI. (Cont)

```
C**********************************************************************
C   **COEFFICIENT** (FOR DIFFUSION TERMS) SUBROUTINE
C**********************************************************************
C*****  SUBSCRIPTS 1,2,3,4,5  REFER TO POINTS P,E,N,W,S RESPECTIVELY
      DIMENSION B(5)
      DO 10 L=1,5
   10 C(L)=1.0
      IF (K.NE.NW) GO TO 20
C***** FOR VORTICITY
      B(1)=R(J)**3
      B(2)=B(1)
      B(3)=R(J+1)**3
      B(4)=B(1)
      B(5)=R(J-1)**3
      C(1)=ZMU(I,J)
      C(2)=ZMU(I+1,J)
      C(3)=ZMU(I,J+1)
      C(4)=ZMU(I-1,J)
      C(5)=ZMU(I,J-1)
      GO TO 50
   20 IF (K.NE.NF)GO TO 30
C*****  FOR STREAM FUNCTION
      B(1)=1./(R(J)*RO(I,J))
      B(2)=1./(R(J)*RO(I+1,J))
      B(3)=8.0/((R(J)+R(J+1))*(RO(I,J)+RO(I,J+I)))-B(I)
      B(4)=1./(R(J)*RO(I-1,J))
      B(5)=8.0/((R(J)+R'J-1))*(RO(I,J)+RO(I,J-I)))-B(I)
      GO TO 50
   30 IF (K.NE.NVT)GO TO 40
C*****  FOR SWIRL VELOCITY
      B(1)=ZMU(I,J)*R(J)**3
      B(2)=ZMU(I+1,J)*R(J)**3
      B(3)=ZMU(I,J+1)*R(J+1)**3
      B(4)=ZMU(I-1,J)*R(J)**3
      B(5)=ZMU(I,J-I)*R(J-1)**3
      C(1)=1./(R(J)*R(J))
      C(2)=C(1)
      C(3)=I./(R(J+1)*R(J+1))
      C(4)=C(1)
      IF (R(J-1).GT.0.0)C(5)=1./(R(J-1)*R(J-I))
      IF (R(J-1).EQ.0.0)C(5)=0.0
      GO TO 50
C*****  FOR MIXTURE FRACTION AND ENTHALPY
   40 B(1)=ZMU(I,J)*R(J)/PR(K)
      B(2)=ZMU(I+1,J)*R(J)/PR(K)
      B(3)=ZMU(I,J+I)*R(J+1)/PR(K)
      B(4)=ZMU(I-1,J)*R(J)/PR(K)
      B(5)=ZMU(I,J-1)*R(J-1)/PR(K)
   50 CONTINUE
C*****  FOR ALL DEPENDENT VARIABLES
      CE=(B(2)+B(1))/((X1(I+1)-X1(I))*2.*DELX1(I))
      CW=(B(1)+B(4))/((X1(I)-X1(I-1))*2.*DELXI(I))
      CN=(B(3)+B(1))/((X2(J+1)-X2(J))*2.*DELX2(J))
      CS=(B(1)+B(5))/((X2(J)-X2(J-I))*2.*DELX2(J))
      RETURN
      END
*DECK CV
      SUBROUTINE CONVEC(I,J,K,AU,ZU)
*CALL CMO
C**********************************************************************
C   **CONVECTION** - TERM  SUBROUTINE
C   TANK-AND-TUBE FORMULATION OF THE CONVECTION TERMS
C**********************************************************************
      AU=0.
      ZU=0.
      IF (K.EQ.NF)GO TO I20
```

TABLE XXVI. (Cont)

```
      DX12=1./(4.*DELX1(I)*DELX2(J))
      GM1E=DX12*(A(I+1,J+1,NF)-A(I,J-1,NF)+A(I+1,J+I,NF)-A(I+I,J-1,NF))
      GM1W=DX12*(A(I,J+1,NF)-A(I-1,J-1,NF)+A(I-1,J+I,NF)-A(I-1,J-1,NF))
      GM2S=-DX12*(A(I+1,J,NF)-A(I-1,J,NF)+A(I+1,J-1,NF)-A(I-1,J-1,NF))
      GM2N=-DX12*(A(I+1,J,NF)-A(I-I,J,NF)+A(I+1,J+I,NF)-A(I-1,J+I,NF))
C
      IF (GM1W)10,30,20
   10 ZU=-GM1W
      GO TO 30
   20 AU=GM1W*A(I-I,J,K)
      IF (K.EQ.NW.AND.(I.EQ.IL.AND.(J.GE.JB.OR.(J.LE.JA1.AND.J.GE.JA))))
     *GO TO 130
   30 IF (GM2S)40,60,50
   40 ZU=ZU-GM2S
      GO TO 60
   50 AU=AU+GM2S*A(I,J-I,K)
      IF (K.EQ.NW.AND.J.EQ.(JA1+1).AND.I.LE.IAB)GO TO 140
   60 IF (GM1E)70,90,80
   70 AU=AU-GM1E*A(I+1,J,K)
      IF (K.EQ.NW.AND.(I.EQ.IH.AND.J.GE.JC))GO TO 150
      GO TO 90
   80 ZU=ZU+GM1E
   90 IF (GM2N)100,110,110
  100 AU=AU-GM2N*A(I,J+1,K)
      IF (K.EQ.NW.AND.(J.EQ.JNM.OR.J.EQ.(JB-I).OR.J.EQ.(JA-1).OR.J.EQ.(J
     *C-1)))GO TO 160
      RETURN
  110 ZU=ZU+GM2N
  120 RETURN
C
  130 IF (J.NE.JNM)ZU=ZU-GM1W*ZW/CW
      IF (J.EQ.JNM)ZU=ZU-GM1W*ZWHALF/CW
      GO TO 30
  140 IF ((JB-JA1).GT.2)ZU=ZU-GM2S*ZW/CS
      IF ((JB-JA1).EQ.2)ZU=ZU-GM2S*ZWHALF/CS
      GO TO 60
  150 IF (J.NE.JNM)ZU=ZU+GM1E*ZW/CE
      IF (J.EQ.JNM)ZU=ZU+GM1E*ZWHALF/CE
      GO TO 90
  160 IF (J.EQ.JNM)GO TO 170
      IF (J.EQ.(JC-1).OR.J.EQ.(JA-1))GO TO 170
      IF (J.EQ.(JB-1).AND.((JB-JA1).GE.2))GO TO 170
      RETURN
  170 ZU=ZU+GM2N*ZW/CN
      RETURN
      END
*DECK SC
      SUBROUTINE SORCCK(I,J,K,SOURCE,ZQ,EMLIM)
*CALL CMO
      DIMENSION QZ(21,21,8)                                          08/09/71
      EQUIVALENCE (QZ,Z1)                                            08/09/71
C...KVB...ABOVE DATA SPECIALIZED TO CH4                              08/09/71
C*********************************************************************
C   ##SOURCE## - TERMS SUBROUTINE
C   SOURCE TERMS IN FINITE DIFFERENCE FORM
C*********************************************************************
C...KVB...                                                           07/26/71
      IF(NOXSOL) GO TO 100                                           07/26/71
C***KVB***                                                           07/26/71
      IF (K.EQ.NW) GO TO 10
      IF (K.EQ.NF) GO TO 20
      IF (K.EQ.NVT) GO TO 40
      GO TO 30
C*****  FOR VORTICITY
   10 SOURCE=0.
      DEN=16.0*DELX1(I)*DELX2(J)/(R(J)**2)
```

TABLE XXVI. (Cont)

```
      S1=RO(I,J+1)+RO(I,J)
      S1=S1*(VS2(I+1,J)-VS2(I-1,J)+VS2(I+1,J+1)-VS2(I-1,J+1))
      S2=RO(I,J-1)+RO(I,J)
      S2=S2*(VS2(I-1,J)-VS2(I+1,J)+VS2(I-1,J-1)-VS2(I+1,J-1))
      S3=RO(I+1,J)+RO(I,J)
      S3=S3*(VS2(I,J-1)-VS2(I,J+1)+VS2(I+1,J-1)-VS2(I+1,J+1))
      S4=RO(I-1,J)+RO(I,J)
      S4=S4*(VS2(I,J+1)-VS2(I,J-1)+VS2(I-1,J+1)-VS2(I-1,J-1))
      SOURCE=SOURCE+(S1+S2+S3+S4)/DEN
      IF (INDE(NVT).EQ.1)SOURCE=SOURCE+(RO(I+1,J)*(A(I+1,J,NVT)**2)-RO(I
     +=1,J)*(A(I-1,J,NVT)**2))/((X1(I+1)-X1(I-1))*R(J))
      ZQ=0.
      RETURN
C*****  FOR STREAM FUNCTION
   20 SOURCE=A(I,J,NW)*R(J)
      ZQ=0.
      RETURN
C*****  FOR MIXTURE FRACTION AND ENTHALPY
   30 SOURCE=0.
      IF((K.EQ.NMF1.OR.K.EQ.NMF3).AND.NITER.GE.NEV) SOURCE=FEVAP(I,J)
     + *R(J)
      IF(K.EQ.NHS.AND.NITER.GE.NEV)SOURCE=R(J)*(-156+HS)*FEVAP(I,J)
      ZQ=0.
      IF(HC.EQ.0.) RETURN
      EMCHX=A(I,J,NMF1)                                          08/09/71
      EMCO2=A(I,J,NMF2)                                          08/09/71
      F     =A(I,J,NMF3)                                         08/09/71
      FO2=ZO2*XO2*(1.-F)
      IF(K.EQ.NMF1) EMLIM=F-FO2/XO2+YO2/XO2*EMCO2
      IF(K.EQ.NMF2) EMLIM=(FO2-XO2*(F-EMCHX))/YO2
      EMH2O=XH2O*(F-EMCHX)                                       08/09/71
      EMO2=FO2-XO2*(F-EMCHX)-YO2*EMCO2
      IF(EMO2.LT.0.)EMO2=0.
      EMCO=(XCO+XO2*YCO/YO2)*(F-EMCHX)-YCO/YO2*(FO2-EMO2)
      A(I,J,NMF5)=EMO2
      A(I,J,NMF6)=EMCO
C***KVB***                                                       08/09/71
      IF (EMH2O .LT.0.) EMH2O=0.
      IF(EMO2.LT.0.) EMO2=0.
      IF(EMCO.LT.0.) EMCO=0.
      IF((NITER.LT.NILO).OR.(NITER.GT.NIH1)) GO TO 101
      IF(I.GE.ILO.AND.I.LE.IHI.AND.J.GE.JLO.AND.J.LE.JHI) EMH2O=XH2O*F
      IF(I.GE.ILO.AND.I.LE.IHI.AND.J.GE.JLO.AND.J.LE.JHI) T(I,J)=TIGN
  101 CONTINUE
      IF(K.EQ.NMF1)ZQ=3.54E15*RO(I,J)**2*EXP(-51629/T(I,J))
     + *SQRT(EMO2*EMH2O)
      IF(K.EQ.NMF2)SOURCE=+1.88E10*RO(I,J)**2*EXP(-22647/T(I,J))
     + *SQRT(EMO2*EMH2O)
C...KVB...                                                       08/09/71
      DNMF1=F-EMCHX                                              08/09/71
      IF(K.EQ.NMF2.AND.DNMF1.LT.1.E-05) SOURCE=0.
      IF(K.EQ.NMF2.AND.EMO2.LT..001) SOURCE=0.
      IF(K.EQ.NMF2) ZQ=SOURCE*YCO
      IF(K.EQ.NMF2) SOURCE=SOURCE*XCO*(F-EMCHX)
      SOURCE=SOURCE*R(J)                                         08/09/71
      ZQ=ZQ*R(J)                                                 08/09/71
C***KVB***                                                       08/09/71
      RETURN
C*****  FOR SWIRL VELOCITY
   40 ZQ=0.
      SOURCE=0.0
      RETURN
C...KVB...                                                       07/26/71
100   CONTINUE                                                   07/26/71
      RHO=RO(I,J)                                                08/09/71
      CTNO=A(I,J,NMF5)*RHO/30.008                                08/09/71
```

TABLE XXVI. (Cont)

```
      CTNO2=A(I,J,NMF6)*RHO/46.008                                          08/09/71
      IF(CTNO.LT.0.)CTNO=0.
      IF(CTNO2.LT.0.) CTNO2=0.
      IF(K.EQ.NMF5) GO TO 200                                               07/26/71
      IF(K.EQ.NMF6) GO TO 300                                               07/26/71
      WRITE(6,1000)                                                         07/26/71
1000  FORMAT(45HOSORCCK CALLED FOR NOX WITH BAD VALUE OF K       )          07/26/71
      STOP                                                                  07/26/71
C...KV8...SOURCE TERM FOR (NO)                                              07/26/71
200   CONTINUE                                                              07/26/71
      ONOM=Z3(I,J)+Z1(I,J)*CTNO                                             09/10/71
      SOURCE=R(J)*30.008*(Z6(I,J)+Z7(I,J)*CTNO2+Z2(I,J)/ONOM)               09/10/71
      ZQ=R(J)*RHO*((Z5(I,J)+Z4(I,J)/ONOM)*CTNO+Z8(I,J))                     09/10/71
      RETURN                                                                07/26/71
C...KV8...SOURCE TERM FOR (NO2)                                             07/26/71
300   CONTINUE                                                              07/26/71
      SOURCE=R(J)*46.008*Z8(I,J)*CTNO                                       08/09/71
      ZQ=R(J)*RHO*Z7(I,J)                                                   09/10/71
      RETURN                                                                07/26/71
C***KV8***                                                                  07/26/71
      END
      FUNCTION VS2(I,J)
C***  THIS SUBROUTINE UNCHANGED
      COMMON /CVPCCC/ A(21,21,12),G1(21,21),G2(21,21),RO(21,21),
     *                ZMU(21,21),T(21,21),PF(21,21)
      VS2=(G1(I,J)*G1(I,J)+G2(I,J)*G2(I,J))/(RO(I,J)*RO(I,J))
      RETURN
      END
*DECK NX
      OVERLAY (NOX,3,0)
      PROGRAM NOXCON
*CALL CMD
      DIMENSION AQ(21,21,18)
      EQUIVALENCE (AQ,A)
      INTEGER BSYMBL(8)
      DIMENSION CT(13)
      EQUIVALENCE(CT,CTCHX)                                                 09/10/71
      DIMENSION EM(13)
      EQUIVALENCE(EM,EMCHX)
      DIMENSION FKF(8),FKB(8),FKEQ(11)
      EQUIVALENCE(FKEQ(9),FK15),(FKEQ(10),FK16),(FKEQ(11),FK17)
      DIMENSION QZ(21,21,8)
      EQUIVALENCE (QZ,Z1)
      DIMENSION AJ(8),ENJ(8),BJ(8)
      DIMENSION TEMPKP(5),FLOGKP(5,11)
      LOGICAL PASS2
      DATA IBLK/6H      /
      DATA AJ,ENJ,BJ
     */3.1E13,6.43E9,4.22E13,3.01E13,3.6E13,4.82E13,1.02E15,1.0E13,
     *  0.   ,  -1. ,   0.  ,  0.   ,   0. ,  0.   ,  0.   ,  0.  ,
     *  .334 , 6.25 ,   0.  , 5.439 ,12.084,12.084 , -1.870,  .6  /
      DATA AJ(7),BJ(4),BJ(5),BJ(6)/1.05E15,10.8,24.,24./                    08/13/71
      DATA AJ(4),AJ(5),AJ(6),BJ(4),BJ(5),BJ(6)/
     *2.95E13,3.82E13,4.58E13,10.77,24.1,24.1/
      DATA TEMPKP/1800.,2700.,3600.,4500.,5400./
      DATA FLOGKP/
     * 15.784,10.309,7.567,5.921,5.823,
     *  7.660,5.336 ,4.170,3.467,2.996,
     * 17.022,8.879,5.977,4.471,3.548,
     * 15.569,10.877,8.480,7.015,6.042,
     * 17.977,12.096,9.121,7.316,6.123,
     *  9.853, 7.123,5.723,4.863,4.277,
     * 13.782, 8.533,5.939,4.402,3.389,
     * 10.744, 7.347,5.631,4.595,3.900,
     *  2.687, 1.110,0.320,-0.128,-0.413,
     *  2.408, 1.219,0.641,0.301,0.081,
```

TABLE XXVI. (Cont)

```
     *  2.749, 1.490,0.866,0.502,0.2647
      DATA BSYMBL/6HREAC 1,6HREAC 2,6HREAC 3,6HREAC 4,6HREAC 5,
     * 6HREAC 6,6HREAC 7,6HREAC 8/
C...KVB...ABOVE DATA SPECIALIZED FOR CH4 .........
C...KVB...
      PASS2=.FALSE.
      CLOG=ALOG10(.0160185)
      DO 5 K=1,8
      AJ(K)=AJ(K)*0.0160185*(9./5.)**ENJ(K)
      IF(K.EQ.7) AJ(K)=AJ(K)*.0160185
      BJ(K)=BJ(K)/.001104
5     CONTINUE
      DO 10 K=1,5
      TEMPKP(K)=1./TEMPKP(K)
      FLOGKP(K,7)=FLOGKP(K,7) + CLOG
10    CONTINUE
      GO TO 20
C...KVB...
C...KVB...ENTRY #RATES# IS USED FOR POST MORTEM ANALYSIS
C     ENTRY RATES
C     PASS2=.TRUE.
20    CONTINUE
      IMID=(IAB+IC)/2                                              09/10/71
      JMID=JN/2                                                    09/10/71
      IF(INOG.EQ.1)AREA=X2(JN)-X2(1)                               09/10/71
      IF(INOG.EQ.2)AREA=X2(JN)**2-X2(1)**2                         09/10/71
      VEL=-A(1,1,NF)/(RO(IMID,JMID)*AREA)                          09/10/71
      RNO=.03*EXP(1./4500.)/EXP(1./T(IMID,JMID))                   09/10/71
      PRINT 25,IMID,JMID,RO(IMID,JMID),T(IMID,JMID),VEL,AREA,RNO   09/10/71
25    FORMAT(# IMID,JMID,RO,T,VEL,AREA,RNO#/1X,2I3,5G10.3)         09/10/71
      DO 100 J=1,JN
      IUP=IMAX(J)-1
      ILOW=IMIN(J)+1
      DO 100 I=ILOW,IUP
      IF(I.GE.IS1.AND.I.LE.IS.AND.J.GE.JS1.AND.J.LE.JS) GO TO 100
      TIME=(X1(I)-X1(IAB))/VEL                                     09/10/71
      A(I,J,NMF5)=1E-6
      A(I,J,NMF6)=A(I,J,NMF5)/100.                                 09/10/71
      IF(J.EQ.JMID) PRINT 26,I,TIME,A(I,J,NMF5)
26    FORMAT(# I,TIME,(NO)#/1X,I3,2G10.3)                          09/10/71
      TT=T(I,J)
      RT=1./TT
      CALL LININT(TEMPKP,FLOGKP(1,1),RT,FLOG,5)
      FKEQ(1)=10.**FLOG
      DO 30 K=2,11
      CALL MOREYS(TEMPKP,FLOGKP(1,K),RT,FLOG,5)
      FKEQ(K)=10.**FLOG
30    CONTINUE
      DO 40 K=1,8
      FKF(K)=AJ(K)*TT**(-ENJ(K))*EXP(-BJ(K)/TT)
      FKB(K)=FKF(K)/FKEQ(K)
40    CONTINUE

C...KVB...  EMX = MASS FRACTION OF X
C...KVB...  CTX = CONCENTRATION OF X    LB MOLE / FT3
      EMCHX=A(I,J,NMF1)
      EMCO2=A(I,J,NMF2)
      F    =A(I,J,NMF3)
      FO2=ZO2*XO2*(1.-F)
      EMNO =A(I,J,NMF5)
      EMNO2=A(I,J,NMF6)
C...KVB...
      EMH2O=XH2O*(F-EMCHX)
      EMO2=FO2-XO2*(F-EMCHX)-YO2*EMCO2
      EMCO=(XCO+XO2*YCO/YO2)*(F-EMCHX)-YCO/YO2*(FO2-EMO2)
      EMN2 =XN2*(1.-F)
```

TABLE XXVI. (Cont)

```
C...KVB...
      DO 45 L=1,8
      IF(EM(L).LT.0.) EM(L)=0.
 45   CONTINUE
      RHO=RO(I,J)
      CTCHX=EMCHX*RHO/ZMW(1)
      CTCO2=EMCO2*RHO/44.010
      CTH2O=EMH2O*RHO/18.016
      CTO2 =EMO2 *RHO/32.000                                          09/10/71
      CTCO =EMCO *RHO/28.010
      CTNO =EMNO *RHO/30.008
      CTNO2=EMNO2*RHO/46.006
      CTN2 =EMN2 *RHO/28.016
C...KVB...
      CTM  =PREF/(1545.*T(I,J)) * (1.+PF(I,J))
      IF(CTCO2.LT.1.E-30)GO TO 50
      CTO  =FK15/FK16 * CTCO *CTO2 / CTCO2
      CTOH=SQRT(CTH2O*CTO/FK17)
      CTH=FK15*CTCO*CTOH/CTCO2
      GO TO 55
50    CONTINUE
      CTO=0.
      CTH=0.
      CTOH=0.
55    CONTINUE
      CTN2O=0.
      CTN=0.
      DO 60 L=1,13
      IF(CT(L).LE.0.) CT(L)=1.E-30
60    CONTINUE
      IF(PASS2)GO TO 70
C...KVB...
      GG1=FKB(1)*CTN2*CTO                                             08/13/71
      GG2=FKB(2)*CTO+FKB(3)*CTH                                       08/13/71
      G3=FKF(2)*CTO2 + FKF(3)*CTOH
      G4=FKB(4)*CTN2*CTOH + FKB(5)*CTN2*CTO2
      G5=FKF(4)*CTH + FKF(5)*CTO
      G6=FKF(6)*CTO
      G7=FKB(7)*CTM + FKF(8)*CTO
      G8=FKF(7)*CTO*CTM + FKB(8)*CTO2
C...KVB...
      Z1(I,J)=FKF(1)
      Z2(I,J)=GG1*GJ*2.                                               08/13/71
      Z3(I,J)=G3
      Z4(I,J)=FKF(1)*GG2*2.                                           08/13/71
      Z5(I,J)=G5/(G5+G6) * FKB(6) * 2.
      Z6(I,J)=G4*G6/(G5+G6) *2.
      Z7(I,J)=G7
      Z8(I,J)=G8
C...KVB...
      GO TO 100
70    CONTINUE
      CTN2O=(FKB(4)*CTN2*CTOH+FKB(5)*CTN2*CTO2+FKB(6)*CTNO*CTNO)
     *     /(FKF(4)*CTH+FKF(5)*CTO+FKF(6)*CTO)
      CTN=(FKB(1)*CTN2*CTO+FKB(2)*CTNO*CTO+FKB(3)*CTNO*CTH)
     *       /(FKF(1)*CTNO+FKF(2)*CTO2+FKF(3)*CTOH)
      Z1(I,J)=FKF(1)*CTN*CTNO  -  FKB(1)*CTN2*CTO
      Z2(I,J)=FKF(2)*CTN*CTO2  -  FKB(2)*CTNO*CTO
      Z3(I,J)=FKF(3)*CTN*CTOH  -  FKB(3)*CTNO*CTH
      Z4(I,J)=FKF(4)*CTH*CTN2O -  FKB(4)*CTN2*CTOH
      Z5(I,J)=FKF(5)*CTO*CTN2O -  FKB(5)*CTN2*CTO2
      Z6(I,J)=FKF(6)*CTO*CTN2O -  FKB(6)*CTNO*CTNO
      Z7(I,J)=FKF(7)*CTM*CTNO*CTO -  FKB(7)*CTM*CTNO2
      Z8(I,J)=FKF(8)*CTNO2*CTO  -  FKB(8)*CTNO*CTO2
      DO 90 K=1,8
      AQ(I,J,K)=QZ(I,J,K)
```

TABLE XXVI. (Cont)

```
90      CONTINUE
        IE=8
        DO 110 K=1,8
        IVAR(K)=K
        INOD(K,1)=99
        VJE(K,1)=0.
        ASYMBL(K)=BSYMBL(K)
        ANAME(1,K)=BSYMBL(K)
        DO 109 KK=2,6
        ANAME(KK,K)=IBLK
109     CONTINUE
110     CONTINUE
        CALL PRINC1
        NVAR=8
C       CALL PLOTHR
100     CONTINUE
        END
*DECK LI
        SUBROUTINE LININT(XT,YT,X,Y,N)
C...KVB...SUB FOR LINEAR INTERPOLATION
C...KVB...ASSUMES XT IS MONATONIC
        DIMENSION XT(1),YT(1)
        IF(XT(1).LT.XT(2)) GO TO 9
        DO 5 I=1,N
        IF(X.GT.XT(I)) GO TO 20
5       CONTINUE
        GO TO 11
9       CONTINUE
        DO 10 I=1,N
        IF(X.LT.XT(I)) GO TO 20
10      CONTINUE
C...KVB...FALL THRU INDICATES X OFF TABLE ON HIGH I END
C...KVB...USE LAST VALUE IN TABLE RATHER THAN EXTRAPOLATE
11      I=N+1
        XFAC=0
        GO TO 30
20      IF(I.EQ.1)I=2                                          09/10/71
C...KVB...          EXTRAPOLATE OFF LOW END OF TABLE           09/10/71
        XFAC=(X-XT(I-1))/(XT(I)-XT(I-1))
30      CONTINUE
C...KVB... CDC VERSION NEXT CARD
        ENTRY MOREYS
        Y=(YT(I)-YT(I-1))*XFAC + YT(I-1)
C...KVB...ENTRY POINT PERMITS MORE DEPENDENT VARIABLES FROM
C...KVB...SAME INDEPENDENT VARIABLE TABLE
        RETURN
C...KVB...COME HERE IF X OFF TABLE ON LOW I END
C...KVB...USE FIRST VALUE IN TABLE RATHER THAN EXTRAPOLATE
        END
*DECK OU
        OVERLAY (OUT,4,0)
        PROGRAM OUTPUT
*CALL CMD
        IF(IOLO.LT.0) GO TO 100
        CALL PRINC1
        CALL TABUC1
  100   CONTINUE
        CALL PLOTC1
        IF(NVP.EQ.0) GO TO 181                                 07/26/71
        DO 180 II=1,NVP
  180   CALL VELPLT (IOP(II),IJGP(II),IVP(II))
181     CONTINUE                                               07/26/71
C...KVB...                                                     07/26/71
        XNO=0.                                                 08/13/71
        XNO2=0.                                                08/13/71
        EFF=0.
```

TABLE XXVI. (Cont)

```
      JSP1=JS+1
      IF(IS.LT.IN) JSP1=2
      JM1N=JSP1-1
      DO 500 J=JSP1,JC
      JJ=J-1
      AMOLW=RD(IN,J)*GCPM*T(IN,J)/PREF
      FLO=(A(IN,JJ,NF)-A(IN,J,NF))/(A(IN,JM1N,NF)*2.)
      EFF=EFF + FLO                                                    08/13/71
     *   *(A(IN,JJ,NEFF)+A(IN,J,NEFF))                                08/13/71
      XNO=XNO + FLO                                                    08/13/71
     *  *(A(IN,JJ,NMF5)+A(IN,J,NMF5))/30.008*AMOLW                     08/13/71
      XNO2=XNO2 + FLO                                                  08/13/71
     *  *(A(IN,JJ,NMF6) + A(IN,J,NMF6))/46.008*AMOLW
C***KVB***                                                             07/26/71
  500 CONTINUE
C...KVB...                                                             07/26/71
      XNO=XNO*1.E6
      XNO2=XNO2*1.E6
      XSUM=XNO+XNO2                                                    08/13/71
      WRITE(6,1010)EFF,XNO,XNO2,XSUM                                   08/13/71
1010  FORMAT(5(/),1X,18HEXIT EFFICIENCY=  ,E11.3/                      07/26/71
     *            1X,18HEXIT (NO)  PPM =  ,E11.3/                     08/13/71
     *            1X,18HEXIT (NO2) PPM =  ,E11.3/                     08/13/71
     *            1X,18HEXIT (NOX) PPM =  ,E11.3)                     08/13/71
C...KVB...CALL RATES    HERE                                           08/13/71
C***KVB***                                                             07/26/71
C
      END
*DECK PL
      SUBROUTINE PLOTC1
*CALL CMD
      DIMENSION AQ(21,21,18)
      DIMENSION X(120),XA(9),VJ(9),D(11),Y(41)
      EQUIVALENCE (A(1,1,1),AQ(1,1,1))
      DATA XEMTY/1H /,XBDUN/1H./,(XA(L),L=1,9)/1H1,1H2,1H3,1H4,1H5,1H6,
     +1H7,1H8,1H9/
C*************************************************************************
C   **PLOTTING** SUBROUTINE
C   THIS SUBR. GIVES APPROX. CONTOUR-PLOTS OF THE DEPENDENT VAR.
C   ALSO OF TEMPERATURE
C*************************************************************************
C
C****    INTVAL=NUMBER OF LINE-SPACING BETWEEN TWO J-LINES
C****    NVJ=NUMBER OF CONTOUR-LINES TO BE PLOTTED FOR EACH VARIABLE
C
      L6=NUMA+6
      L7=NUMA+7
      L8=NUMA+8
      IF (1.GT.JN)GO TO 5
      DO 10 J=1,JN
      DO 10 I=1,IN
      A(I,J,NW)=A(I,J,NW)*R(J)
      IF (INDE(NVT).EQ.1.AND.R(J).GT.0.0)A(1,J,NVT)=A(I,J,NVT)/R(J)
   10 CONTINUE
C...KVB...ADDED ENTRY FOR PLOTTING REACTION RATES                      08/09/71
      ENTRY PLOTRR                                                     08/09/71
C***KVB***                                                             08/09/71
    5 CONTINUE
      JX=1
      IF((JN*INTVAL-3).GT.44) JX=2
      IX=1
      IF((IN*10-9).GT.101) IX=2
      NVJS=NVJ
      IF (1.GT.NVAR) GO TO 15
      DO 340 KK=1,NVAR
      K=IVAR(KK)
```

TABLE XXVI. (Cont)

```
      IF(INOD(K,IT).LE.IN) GO TO 30
C****    FINDING MAX., MIN. AND MEAN VALUES IN THE FIELD AND
C****    HENCE DETERMINING THE INTERVALS
      VMIN=1.E+30                                                    07/26/71
      VMAX=-1E+30
      NVJ=9
      SUM=0.
      NSUM=0
      IF (1.GT.JN)GO TO 25
      DO 20 J=1,JN,JX
      III=IMIN(J)
      II2=IMAX(J)
      DO 20 I=III,II2,IX
      IF (AQ(I,J,K).GT.VMAX) VMAX=AQ(I,J,K)
      IF(AQ(I,J,K).LT.VMIN) VMIN=AQ(I,J,K)
      SUM=SUM+A(I,J,1)
   20 NSUM=NSUM+1
   25 CONTINUE
      VMEAN=SUM/FLOAT(NSUM)
      VSTEP1=(VMEAN-VMIN)/4.
      VSTEP2=(VMAX-VMEAN)/4.
      VJ(1)=VMIN+.05*ABS(VMIN)
      VJ(2)=VMIN+VSTEP1
      VJ(3)=VJ(2)+VSTEP1
      VJ(4)=VJ(3)+VSTEP1
      VJ(5)=VMEAN
      VJ(6)=VMEAN+VSTEP2
      VJ(7)=VJ(6)+VSTEP2
      VJ(8)=VJ(7)+VSTEP2
      VJ(9)=VMAX-.05*ABS(VMAX)
      IF(VJ(1).GE.VJ(2)) VJ(1)=(VJ(2)+VMIN)/2.
      IF(VJ(9).LE.VJ(8)) VJ(9)=(VMAX+VJ(8))/2.
      IF(K.EQ.NF) VJ(1)=AQ(IAB,JA,NF)
      GO TO 52
C
C***  CHANGED VJ TO READ IN BLOCK EITHER A GIVEN NODE OR A FIXED VALUE
C***       JNOD,INOD IS GRID NODE FOR ISOLINE CONSTANT
C***       VJE IS SPECIFIED VALUE FOR ISOLINE
C
   30 CONTINUE
      DO 40 NI=1,NVJ
      IF(JNOD(K,NI).EQ.0) GO TO 32
      IJK=INOD(K,NI)
      JIK=JNOD(K,NI)
      IF (K.EQ.L7.OR.K.EQ.L8) GO TO 31
      VJ(NI)=AQ(IJK,JIK,K)
      GO TO 40
   31 IF (K.EQ.L7) VJ(NI)=G1(IJK,JIK)/RO(IJK,JIK)
      IF (K.EQ.L8) VJ(NI)=G2(IJK,JIK)/RO(IJK,JIK)
      GO TO 40
   32 VJ(NI)=VJE(K,NI)
   40 CONTINUE
   50 CONTINUE
C    END SPECIAL VJ VALUES FOR C-T PROBLEM
C
C****    PRINT OUT CONSTANT VALUES TO BE PLOTTED
   52 WRITE(6,350) ASYMBL(K)
      WRITE (6,360)(VJ(L),L=1,NVJ)
      WRITE (6,410)
      IF (1.GT.JN)GO TO 35
      JNC=JN
      IF((JN.EQ.((JN/2)*2)).AND.JX.EQ.2) JNC=JNC+1
      DO 330 JJ=1,JNC,JX
      J=JN+1-JJ
      IF(J.LT.1)J=1
      III=IMIN(J)
```

TABLE XXVI. (Cont)

```
      II2=IMAX(J)
      L1=(IMIN(J)/IX-1/IX)*10+1
      L2=(IMAX(J)/IX-1/IX)*10+1
      IB=IX+IMIN(J)
C**** BOUNDARIES FOR THE PROBLEM
      IF (1.GT.INTVAL)GO TO 45
      DO 320 JJN=1,INTVAL
      DO 60 L=1,101
   60 X(L)=XEMTY
      X(L1)=XBOUN
      X(L2)=XBOUN
      IF (J.EQ.JN.AND.JJN.EQ.1)GO TO 70
      IF (J.EQ.1.AND.JJN.EQ.1)GO TO 70
      GO TO 90
   70 IF (L1.GT.L2)GO TO 55
      DO 80 L=L1,L2
   80 X(L)=XBOUN
   55 CONTINUE
      GO TO 160
   90 CONTINUE
C
C**** SPECIAL BOUNDARIES FOR THE COMBUSTION-CHAMBER PROBLEM
C
      IF (JA.EQ.JA1)GO TO 100
      IF (J.EQ.JA.AND.JJN.EQ.1)GO TO 110
      IF (J.LE.JA1.AND.J.GT.JA)GO TO 110
  100 CONTINUE
      IF (J.EQ.JB.AND.JJN.EQ.1)GO TO 110
      IF (J.EQ.JC.AND.JJN.EQ.1)GO TO 130
      GO TO 150
  110 L3=(IAB/IX-1/IX)*10+1
      IF (1.GT.L3)GO TO 65
      DO 120 L=1,L3
  120 X(L)=XBOUN
   65 CONTINUE
      IF ((JC.EQ.JB.OR.JC.EQ.JA.OR.JC.EQ.JA1).AND.JJN.EQ.1)GO TO 130
      GO TO 150
  130 IF (J.NE.JC)GO TO 150
      L3=(IC/IX)*10+1
      IF (L3.GT.L2)GO TO 75
      DO 140 L=L3,L2
  140 X(L)=XBOUN
   75 CONTINUE
  150 CONTINUE
  160 CONTINUE
      IF (J.LE.JA1.AND.J.GT.JA)IB=IAB+IX
C**** INTERPOLATION BETWEEN TWO CONSECUTIVE J-LINES
      J1=J-JX
      IF(J1.LT.1) J1=1
      IF (II1.GT.II2)GO TO 85
      DO 180 I=II1,II2
      IF (J.EQ.1)GO TO 170
      IF(K.LE.L6)DELAJ=(AQ(I,J1,K)-AQ(I,J,K))/FLOAT(INTVAL)
      IF(K.EQ.L7)DELAJ=(G1(I,J1)/RO(I,J1)-G1(I,J)/RO(I,J))/FLOAT(INTVAL)
      IF(K.EQ.L8)DELAJ=(G2(I,J1)/RO(I,J1)-G2(I,J)/RO(I,J))/FLOAT(INTVAL)
      GO TO 185
  170 DELAJ=0.
  185 IF(K.LE.L6)Y(I)=AQ(I,J,K)+FLOAT(JJN-1)*DELAJ
      IF(K.EQ.L7)Y(I)=G1(I,J)/RO(I,J)+FLOAT(JJN-1)*DELAJ
      IF(K.EQ.L8)Y(I)=G2(I,J)/RO(I,J)+FLOAT(JJN-1)*DELAJ
  180 CONTINUE
   85 CONTINUE
C**** INTERPOLATION BETWEEN TWO I-LINES
      IF (IB.GT.II2)GO TO 95
      II2C=II2
      IF((IN.EQ.((IN/2)*2)).AND.IX.EQ.2) II2C=II2C+1
```

TABLE XXVI. (Cont)

```
      DO 260 I=IB,II2C,IX
      I1=I-IX
      IF (IX.EQ.2)GO TO 190
      GO TO 220
  190 DELY1=(Y(I1+1)-Y(I1))/5.
      DO 200 IJK=1,6
  200 O(IJK)=Y(I1)+FLOAT(IJK-1)*DELY1
      DELY2=(Y(I)-Y(I1+1))/5.
      DO 210 IJK=7,11
  210 O(IJK)=Y(I1+1)+FLOAT(IJK-6)*DELY2
      GO TO 240
  220 CONTINUE
      DELY=(Y(I)-Y(I1))/10.
      DO 230 IJK=1,11
  230 O(IJK)=Y(I1)+FLOAT(IJK-1)*DELY
  240 CONTINUE
      IF (1.GT.NVJ)GO TO 105
      DO 250 KL=1,NVJ
      DO 250 IJK=1,10
      IF (IX.EQ.2.AND.IJK.LT.6)DELY=DELY1
      IF (IX.EQ.2.AND.IJK.GE.6)DELY=DELY2
      NN=0
      IF (VJ(KL).GE.O(IJK).AND.VJ(KL).LE.(O(IJK)+DELY/2.))NN=IJK
      IF (VJ(KL).GE.(O(IJK)+DELY/2.).AND.VJ(KL).LE.O(IJK+1))NN=IJK+1
      IF (VJ(KL).LE.O(IJK).AND.VJ(KL).GE.(O(IJK)+DELY/2.))NN=IJK
      IF (VJ(KL).LE.(O(IJK)+DELY/2.).AND.VJ(KL).GE.O(IJK+1))NN=IJK+1
      IF (NN.EQ.0)GO TO 250
      N1=(I1/IX-I/IX)*10
      N2=N1+NN
      X(N2)=XA(KL)
  250 CONTINUE
  105 CONTINUE
C**** PLOTTING OF ALL POINTS ON ONE J-LINE
  260 CONTINUE
   95 CONTINUE
      IF (JJN.EQ.1.AND.(J.NE.JN.AND.J.NE.1))GO TO 270
      GO TO 290
  270 IF (LI.GT.L2)GO TO 115
      DO 280 L4=L1,L2,10
      IF (X(L4).EQ.XEMTY) X(L4)=XBOUN
  280 CONTINUE
  115 CONTINUE
  290 CONTINUE
      IF (((J.EQ.JA.AND.JJN.EQ.1.OR.J.GT.JA).AND.J.LE.JA1).OR.((J.EQ.JB.
     +AND.JJN.EQ.1.OR.J.GT.JB).AND.J.LE.JN))GO TO 300
      IF (JJN.EQ.1)WRITE (6,370)J,(X(IP),IP=1,101)
      IF (JJN.NE.1)WRITE (6,380)(X(IP),IP=1,101)
      GO TO 310
  300 IF (JJN.EQ.1)WRITE (6,390)J,(X(IP),IP=1,101)
      IF (JJN.NE.1)WRITE (6,400)(X(IP),IP=1,101)
  310 IF (J.EQ.1)GO TO 330
  320 CONTINUE
   45 CONTINUE
  330 CONTINUE
   35 CONTINUE
      WRITE (6,420)(IZ,IZ=1,IN,IX)
      NVJ=NVJS
  340 CONTINUE
   15 CONTINUE
      DO 345 J=1,JN
      DO 345 I=1,IN
      IF(R(J).EQ.0.) GO TO 345
      A(I,J,NW)=A(I,J,NW)/R(J)
      IF(INOE(NVT).EQ.1)A(I,J,NVT)=A(I,J,NVT)*R(J)
  345 CONTINUE
      RETURN
```

TABLE XXVI. (Cont)

```
C
  350 FORMAT (25H1CONSTANT-VALUE PLOT OF  ,A6//23H NUMBERS REFER TO THE
     * ,39HCONSTANT-VALUES PLOTTED,VALUES BEING...,//)
  360 FORMAT (1H ,3H1= ,1PE12.4,3X,1H,,3H2= ,1PE12.4,3X,1H,,3H3= ,1PE12.
     *4,3X,1H,,3H4= ,1PE12.4,3X,1H,,3H5= ,1PE12.4/4H 6= ,1PE12.4,3X,1H,,
     *3H7= ,1PE12.4,3X,1H,,3H8= ,1PE12.4,3X,1H,,3H9= ,1PE12.4)
  370 FORMAT (1H ,I2,10X,101A1)
  380 FORMAT (1H ,12X,101A1)
  390 FORMAT (1H ,I2,4X,6H.......,101A1)
  400 FORMAT (1H ,6X,6H.......,101A1)
  410 FORMAT (1H0,///)
  420 FORMAT (1H0,//12X,I2,8X,I2,8X,I2,8X,I2,8X,I2,8X,I2,8X,I2,8X,I2,8X,I2,8X,
     *I2,8X,I2,8X,I2,8X,/)
      END
*DECK TA
      SUBROUTINE TABUC1
*CALL CMD
      DATA AB/6H
C*************************************************************************
C   **TABULATE** SUBROUTINE
C   THIS SUBR. TABULATES THE COMPLETE SET OF RESULTS
C*************************************************************************
C***  ADDED TESTS FOR TEMPERATURE AND PRESSURE
      L5=NUMA+5
      L6=NUMA+6
      IQ=IE
      I1=AB
      I2=AB
      AV1=0.0
      AV2=0.0
      IFG=1
      IF (INDRO.EQ.1.AND.IPRES.EQ.1) GO TO 1
      IF (INDRO.EQ.2.AND.IPRES.EQ.1) GO TO 2
      IF (INDRO.EQ.1.AND.IPRES.EQ.2) GO TO 3
      IF (INDRO.EQ.2.AND.IPRES.EQ.2) GO TO 14
      GO TO 1
    2 I1=ASYMBL(L5)
      IFG=2
      GO TO 1
    3 I1=ASYMBL(L6)
      IFG=3
      GO TO 1
   14 I1=ASYMBL(L5)
      I2=ASYMBL(L6)
      IFG=4
    1 WRITE (6,30)(ASYMBL(K),K=1,IE),I1,I2
      ILINE=0
      IF (1.GT.JN)GO TO 5
      DO 20 J=1,JN
      IL=IMIN(J)
      IH=IMAX(J)
      DO 20 I=1,IN
C***
      IF (IFG.EQ.2.OR.IFG.EQ.4) AV1=T(I,J)
      IF(IFG.EQ.3) AV1=PF(I,J)
      IF(IFG.EQ.4) AV2=PF(I,J)

      ILINE=ILINE+1
      IF (I.LT.IL.OR.I.GT.IH)WRITE (6,60)I,J
      IF (I.LT.IL.OR.I.GT.IH)GO TO 10
      W=A(I,J,NW)*R(J)
      V1=G1(I,J)/RO(I,J)
      V2=G2(I,J)/RO(I,J)
      IF (INDE(NVT).EQ.1)V3=A(I,J,NVT)
      IF (INDE(NVT).EQ.1.AND.R(J).GT.0.0)A(I,J,NVT)=V3/R(J)
C***  ADDED IFG AV1 AV2 I1 I2
```

TABLE XXVI. (Cont'd)

```
      IF (IFG.EQ.1)
     *WRITE (6,40)I,J,V1,V2,RO(I,J),ZMU(I,J),W,(A(I,J,K),K=2,IE)
      IF (IFG.EQ.2.OR.IFG.EQ.3)
     *WRITE (6,40)I,J,V1,V2,RO(I,J),ZMU(I,J),W,(A(I,J,K),K=2,IE),AV1
      IF (IFG.EQ.4)
     *WRITE (6,40)I,J,V1,V2,RO(I,J),ZMU(I,J),W,(A(I,J,K),K=2,IE),AV1,AV2
      IF (INOE(NVT).EQ.1)A(I,J,NVT)=V3
   10 CONTINUE
      IF (ILINE/IN*IN.EQ.ILINE)WRITE (6,50)
      IF (IN.LT.21.AND.ILINE/(4*IN).EQ.ILINE)WRITE (6,30)(ASYMBL(K),K=1,
     *IE),II,I2
      IF(IN.EQ.21.AND.ILINE/(2*IN)*(2*IN).EQ.ILINE) WRITE(6,30)(ASYMBL
     *(K),K=1,IE),I1,I2
   20 CONTINUE
    5 CONTINUE
C     1VISC  ,9(6X,A6))
      RETURN
C
   30 FORMAT(6HI  I  J,6X,2HV1,8X,2HV2,5X,7HDENSITY,5X,4HVISC,7X,
     * A6,5X,A6,5X,A6,5X,A6,5X,A6,5X,A6,5X,A6,5X,A6,5X,A6/
     * (47X,8(5X,A6)/))
   40 FORMAT(1H ,I2,1X,I2,1X,2F10.3,F9.5,1X,1PE11.3,1PE11.3,1PE11.3,
     * 1PE11.3,1PE11.3,1PE11.3,1PE11.3,1PE11.3/
     * (48X,8(1PE11.3)/))
   50 FORMAT (1H )
   60 FORMAT(1H ,I2,1X,I2)
      END
*DECK VE
      SUBROUTINE VELPLT (IO,IJG,IV)
*CALL CMO
C***  THIS IS A NEW SUBROUTINE TO PLOT PROFILES OF ANY VARIABLE
C***  ALONG AN I OR J GRID LINE.  PLOT CONTROL IS CONTAINED IN
C***  COMMON CVPLOT
C***       IO = 1 FOR PROFILE IN I DIRECTION ALONG J=IJG GRID LINE
C***          = 2 FOR PROFILE IN J DIRECTION ALONG I=IJG GRID LINE
C***      IJG = I OR J GRID LINE TO BE PLOTTED
C***       IV = VARIABLE TO BE PLOTTED FROM AQ ARRAY
C***      NVP = TOTAL NUMBER OF VARIABLES TO BE PLOTTED
      DIMENSION IAS(81),VAR(21)
      DIMENSION AQ(21,21,18)
      EQUIVALENCE (A(1,1,1),AQ(1,1,1))
      L7=NUMA+7
      L8=NUMA+8
      IF (IO.EQ.1) GO TO 60
C
C     PLOT AN I GRID LINE
C
      WRITE (6,1000) (ANAME(L,IV),L=1,6),IJG,ASYMBL(IV)
 1000 FORMAT(1HI,9X,16HDISTRIBUTION OF ,6A6/
     * 10X,25HIN J DIRECTION ALONG I = ,I2//
     * 6X,1HJ,10X,A6//)
      IFLAG=1
      VARMAX=0.
      DO 40 J=1,JN
      IF (IJG.GT.IC.AND.J.GT.JC) GO TO 45
      IF(IJG.LT.IA8.AND.((J.GT.JA.AND.J.LT.JA1).OR.(J.GT.JB))) GO TO 45
      IF (IV.EQ.L7) GO TO 10
      IF (IV.EQ.L8) GO TO 5
      IF (IV.EQ.NVT) GO TO 20
      VAR(J)=AQ(IJG,J,IV)
      GO TO 30
    5 VAR(J)=G2(IJG,J)/RO(IJG,J)
      GO TO30
   10 VAR(J)=G1(IJG,J)/RO(IJG,J)
      GO TO 30
   20 IF (INDE(NVT).EQ.1.AND.R(J).GT.0.) VAR(J)=A(IJG,J,IV)/R(J)
```

TABLE XXVI. (Cont)

```
      GO TO 30
   45 VAR(J)=0.0
   30 VARA=ABS(VAR(J))
      VARMAX=AMAX1(VARMAX,VARA)
      IF (VAR(J).LT.0) IFLAG=-I
   40 CONTINUE
      DO 50 JR=1,JN
      J=JN+1-JR
      NAR=41
      IF (IFLAG.LT.0) NAR=81
      CALL LINPLT (NAR,40,VAR(J),VARMAX,IAS)
      WRITE(6,2000) J,VAR(J),(IAS(LK),LK=I,NAR)
 2000 FORMAT(5X,I2,6X,GII.4,8X,81A1)
   50 CONTINUE
      GO TO I20
C
C     PLOT A J GRID LINE
C
   60 CONTINUE
      WRITE (6,3000) (ANAME (L,IV),L=1,6),IJG,ASYMBL(IV)
 3000 FORMAT(1H1,9X,16HDISTRIBUTION OF ,6A6/
     + 10X,25HIN I DIRECTION ALONG J = ,I2//
     + 6X,1HI,10X,A6//)
      IFLAG=1
      VARMAX=0.
      DO I00 I=1,IN
      IF (IJG.GT.JC.AND.I.GT.IC) GO TO 95
      IF(I  .LT.IAB.AND.((IJG.GT.JA.AND.IJG.LT.JAI).OR.(IJG.GT.JB)))
     + GO TO 95
      IF (IV.EQ.L7) GO TO 75
      IF (IV.EQ.L8) GO TO 70
      IF (IV.EQ.NVT) GO TO 80
      VAR(I)=AQ(I,IJG,IV)
      GO TO 90
   75 VAR(I)=G1(I,IJG)/RO(I,IJG)
      GO TO 90
   70 VAR(I)=G2(I,IJG)/RO(I,IJG)
      GO TO 90
   80 IF (INDE(NVT).EQ.I.AND.R(IJG).GT.0.) VAR(I)=A(I,IJG,IV)/R(IJG)
      GO TO 90
   95 VAR(I)=0.0
   90 VARA=ABS(VAR(I))
      VARMAX=AMAX1(VARMAX,VARA)
      IF (VAR(I).LT.0) IFLAG=-1
  100 CONTINUE
      DO II0 IR=I,IN
      I=IN+I-IR
      NAR=41
      IF (IFLAG.LT.0) NAR=81
      CALL LINPLT (NAR,40,VAR(I),VARMAX,IAS)
      WRITE (6,2000) I,VAR(I),(IAS(LK),LK=I,NAR)
  110 CONTINUE
  120 RETURN
      END
*DECK LP
      SUBROUTINE LINPLT (NAR,NT,V,VAMAX,IR)
C        ROUTINE TO GENERATE ARRAY IR OF SYMBOLS ,(BLANK,-,OR,+)
C        FOR PRINT PLOT OF VARIATION OF VARIABLE ARRAY V, WITH ABSOLUTE
C        MAXIMUM VALUE OF VAMAX.
C             NAR = TOTAL NUMBER (MUST BE OOO) OF IR VALUES
C                 = TOTAL WIDTH OF PLOT IN PRINTING SPACES.
C             NT  = MAXIMUM NUMBER OF PLOT SPACES ON POSITIVE SIDE OF NO
C                   MUST BE GREATER THAN 10 OR ZERO IF V ALL NEGATIVE
C             NO  = SPACE IR FOR V = 0., = NAR-NT
C        IF ONLY POSITIVE VALUES OF V EXPECTED SET NT=NAR-I
C        IF ONLY NEGATIVE VALUES OF V EXPECTED, SET NT=0
```

TABLE XXVI. (Cont)

```
C       IF BOTH - AND + VALUES EXPECTED SET NT= (NAR-1)/2
C       PRINT THE IR SYMBOLS IN AN #A# TYPE FORMAT WITH NAR-1) PRINT
      DIMENSION IR(NAR)
      DATA ISIGA,ISIGP,ISIGM,ISIGS/1H ,1H+,1H-,1H*/
      NO=NAR-NT
      NC=(NAR-1)/2+1
      IF (NO.LE.NC) NTP=NT
      IF (NO.GT.NC) NTP=NO-1
      IF(VAMAX.LE.0.0) VAMAX=1.
      LR=V/(VAMAX*.999999)*NTP
      LR=LR+NO
      LMIN=NO
      LMAX=LR
      IF (LR.LT.NO.AND.LR.GT.0) LMIN=LR
      IF (LR.LT.NO.AND.LR.GT.0) LMAX=NO
      IF (LR.LE.0.OR.LR.GT.NAR) GO TO 20
      DO 10 J=1,NAR
      IR(J)=ISIGB
      IF (J.GE.LMIN.AND.J.LE.LMAX.AND.LR.LT.NO) IR(J)=ISIGM
      IF (J.GE.LMIN.AND.J.LE.LMAX.AND.LR.GE.NO) IR(J)=ISIGP
   10 CONTINUE
      RETURN
   20 WRITE(6,100)
  100 FORMAT (1X,99HIN LINPLT SUBROUTINE, ABSOLUTE VALUE OF VARIABLE EXC
     +EEDS PLOT LIMITS.  CHECK FOR ERROR IN NT VALUE.)
      DO 30 J=1,NAR
   30 IR(J)=ISIGS
      RETURN
      END
```

5.0 FLUID PROPERTIES

The input data cards were shown in Figures 175 through 179. The fluid density can be constant or variable. For all cases with fuel mixture, with or without combustion, density should be variable. A reference density is entered for constant density and is used for initializing variable-density cases. Variable ROWF controls density variation during iteration. Values different from 1.0 will over- or under-relax the density, but this has never proved necessary in any cases run.

The fluid viscosity can be constant (INDZMU= 1) at the value entered for ZMUREF, or the viscosity can vary (INDZMU=2). For turbulent flow, the variation of viscosity over the grid has a predominant effect on the solution. The program has a viscosity computation built in, but this should be closely examined for each new case. Parameter ZMUK is redefined from the constant in the Gosman text, Chapter 6, to be the fraction of turbulent kinetic energy divided by the square of the inlet velocity. If entered as 0.0, ZMUK is set to 0.02.

The current program provides only constant pressure (IPRES = 1) as most cases of interest are nearly constant pressure. Conversion of the pressure subroutine to the new program format must be accomplished, if required.

The number of species (NSPEC) should always be entered as 6. Species 1 through 6, in order, are CH_x, CO_2, $H2O$, O_2, CO, and N_2. Molecular weights are entered as ZMW(1) to ZMW(6). Mean specific heats CPJ(1) to CPJ(6) are used for initial temperature estimates only, and should be selected at an estimated mean field temperature.

Fluid viscosity defines the mixing rate for momentum. Mixing of other quantities is related to viscosity through dimensionless Prandtl numbers (PR) on Data Sheet 2. For example, a PR of 0.5 for NMF1 will double the fuel mixing rate compared with momentum. For most uses, all PR values can be set to 1.0 initially, and then revised to obtain better agreement as required. The Gosman text discusses values for the various equations (text symbol for PR is σ).

Fuel properties are described in terms of the lower heating value and the H/C atomic ratio. The tenth card on Data Sheet 1 shows variables STC, HC, HP, HS, and SM. STC is the stoichiometric air-fuel ratio, but is now computed in the program, and entered values are ignored. The fuel lower heating value is entered in HC if combustion is desired, or in HP if fuel mixing and enthalpy are solved without combustion (HC must be 0.0). HS is now ignored and the fuel H/C atomic ratio is entered in SM.

6.0 INLET CONDITIONS AND FUEL EVAPORATION

Inlet temperatures and velocities must be specified. Inlet conditions for some of the equation variables may also be specified if desired. All node temperatures are initialized to TREF. Data Sheet 4 has provisions for entering left boundary inlet conditions. Values for all nodes from J = 1 to JB must be entered even though JA to JA1 is between the two inlets. All variables are identified by a number, IDVAR. Of the equation variables, only NMF1 to NMF6, NHS, and NZK can be initialized. The variable number to be used is the same number entered for the variable on Cards 6 and 7, Data Sheet 1. Velocity is identified as variable No. 17 and temperature is No. 19. Values can be the same for all nodes (uniform profiles), or variable profiles can be entered. The variable number, IDVAR, is entered alone on one card, followed by cards with variable values (VAR). The total number of variables being entered is indicated by NVARI on a separate card.

For the central jets, the temperature is constant at TREF and the velocities are entered on Data Sheet 5. Note that for the left inlet at IS1, the velocity must be negative for flow into the grid system. Jet inlet premixed fuel mixture fraction (EMJET) is also entered on Data Sheet 5.

When fuel is to be evaporated within the grid, two optional procedures can be used to introduce the fuel, by data cards or by a tape generated by fuel-insertion programs for the air-assist atomizer (Program 1527) or pneumatic-impact atomizer (Program 1528). Fuel is introduced at a grid node in terms of mass flow per unit volume in $lb/sec/ft^3/radian$. This variable, FEVAP(I, J), is printed out by the fuel insertion programs. The values can be entered on Data Sheet 5 along with the applicable IEV = I and JEV = J grid lines. The alternate tape input procedure is discussed in Section 9.0. Application of evaporation rates during iteration is controlled by NEV, the iteration at which evaporation starts. Evaporation should be delayed 10 to 20 iterations to allow cold flow to be established, but must overlap the ignition sequence to ensure adequate fuel for ignition.

The inlet condition for swirl velocity is specified by TANB, Data Sheet 2, and is the tangent of the swirl angle. This applies only to the secondary inlet (JA1 to JB).

The variable ENZML initializes the entire grid fuel-mixture fraction and is used as an initial guess to reduce iteration.

7.0 ITERATION CONTROLS

The maximum number of iterations is set by NMAX. It has been found that with the program compiled on OPT = 2, it takes 0.0022 second per node (IN x JN) per equation (IE) per iteration. The total time required for NITER iterations is:

Time = 0.0022 x IN x JN x IE x NITER.

The number of iterations possible in 400 seconds is given in Table XXVII.

TABLE XXVII. NUMBER OF ITERATIONS POSSIBLE

No. of Equations IE	I Grid Lines IN	J Grid Lines JN	Total Nodes IN x JN	No. of Iterations NITER
2	21		441	206
2	11	11	121	750
4	21	21	441	103
4	11	11	121	375
7	21	21	441	59
7	11	11	121	214

During iteration, the output will be printed every NPRIN number of iterations. A value of 20 to 50 is recommended. The output is also printed three times at the start of the program: (1) input of saved tape solution, (2) initialized values, and (3) after the first iteration.

The values CC and DC, Data Sheel 1, control the convergence criteria. These criteria are defined on page 134 of the Gosman text. From the Gosman text CC is λ of equation 3.43-8 and DC is $\lambda_1\lambda_2$. The text recommends a CC of 0.001 to 0.005 and a DC of 100. It has been found that a CC of 0.01 and a DC of 10 is good for initial runs to get a rough solution reducing to the text values for final predictions.

The rate of convergence can be affected by relaxation. This is discussed on page 135 of the Gosman text. The relaxation parameters, RP (1-12), are entered on Data Sheet 2 for the equations and ROWF for density on Data Sheet 1.

8.0 PROGRAM OPTIONS

The output is of four types: (1) the values at each node are printed in an array pattern similar to the grid node pattern; (2) all results are tabulated in column form; (3) grid isoline plots are made for any selected variable that show lines of constant values (like an isctherm); and (4) profile plots are shown along selected grid lines for any variable. Plotting is done on the printed output, not the CalComp plotter. Items (1) and (2) above are always printed.

Control of Item (3), isoline plots, is governed by input on Data Sheet 2. The value INTVAL specifies the number of printer spaces for each grid line. Values of 2 to 4 are recommended. If the output size would exceed the paper page, the plot is reduced by 1/2. Value NVJ specifies the number of isolines to be printed, which can be up to 9 maximum. NVAR is the number of variables to be plotted. If NVAR is set to -1, all the IE equations solved are plotted, and if 0, no plots are made; however, if greater than zero, additional cards are read in to specify the variables to be plotted and values for each plot line. The plot line values can be specified in one of two ways: (1) the converged value at a given node can be selected by entering INOD, JNOD grid line numbers, or (2) the actual desired value can be entered as VJE. The variable number is entered as IVAR on one card followed by NVJ values of either (INOD, JNOD) or VJE. An additional option is activated by setting the first value of INOD to 99. Other values for INOD, JNOD on the card should be set to 0 for all NVJ values. This uses a preset method of equal spacing of the isoline values between the minimum and maximum values in the field.

Note that if the NVAR = -1 option is used, only IE plots of the solved variables are plotted, plus the temperature and efficiency, if density is variable (INDRO = 2). If it is desired to plot any other variable, such as velocity, density, or viscosity, all the variables to be plotted must be specified with the IVAR cards.

Profile plots along a grid line are specified on Data Sheet 3. NVP is the number of plots (grid lines) and is set to zero if no plots are desired. IDP = 01 selects a J grid line and IDP = 02 selects an I grid line. IJGP is the number

of the I or J grid line desired, and IVP identifies the variable. For example, IDP = 02. IJGP = 04, IVP = 19 will plot the horizontal velocity V1 along grid line I = 4.

9.0 INPUT AND OUTPUT FILE OPTIONS

The program provides three tapes (or disk files): TAPE1, TAPE2, and TAPE3. Use of the tapes is controlled by variables IOLD, INEW, and IVAP. IOLD is the input tape containing a saved solution from a previous run. If IOLD = 1, 2, or 3, a new solution will be generated starting with the solution from the specified tape. Normally IOLD = 1. If zero, no tape input is required. If IOLD is entered negative, a new solution is not generated, but the saved solution is plotted with the grid isoline plots. This provides for replotting a solution with new values of INOD, JNOD, or VJE to gain a better view of the field.

INEW is the output tape to which a new solution is written. If zero, no tape is written. If INEW = IOLD, then the new solution is written over the old solution.

IVAP is an input tape containing values of FEVAP, fuel evaporation rates at all 21 x 21 grid nodes. Set IVAP to zero if no tape is needed. The tape must be generated with the use of fuel insertion Program 1527, Air Assist Atomizer, or Program 1528, Pneumatic-Impact Atomizer.

The Gosman program can be run together with one of the fuel insertion programs on the same computer run. The Gosman program is run first to generate a flow field saved on file TAPE1 (INEW = 1). The fuel insertion program is then run with input from TAPE1 and generates a fuel evaporation rate file TAPE2. Fuel insertion program run time is about one-half that of the Gosman program. However, by proper shuffling of the tape files and copying the input data cards to disk files, a multistep run could be made.

10.0 PROGRAM APPLICATIONS

Figure 183 illustrates eight grid configurations to which the program has been applied. Configurations A and B were for development of program options. The upstream inlet was incorporated and used in Configurations F and G. The nonrectangular option of Configuration B was successful but is not yet incorporated in the final program, as no specific applications deemed it necessary. Configuration C was used primarily to verify the ability to compute combustion efficiency and water-model flow patterns. Configuration D was used to predict recirculation zones and velocities in a water model.

Configuration E models a fuel-insertion tunnel and was used to verify the communication between the fuel-insertion evaporation programs and the Gosman program. Configuration F represents an L-pipe primary zone used for NO_x prediction. Configuration G represents the L-pipe swirler primary zone. Computations were initiated recently to combine swirl, upstream injection, and fuel evaporation as a means of predicting primary-zone performance. Configuration H represents dilution-zone mixing beyond the jet injection point as a means of predicting pattern-factor decay.

Operation of the program with these configurations has shown that the various patterns can be solved. Failures of the solutions can usually be traced to improper eddy viscosity, excessive grid mode nonuniformity, and difficulties with source terms in the CO_x and CO_2 mass-fraction source terms.

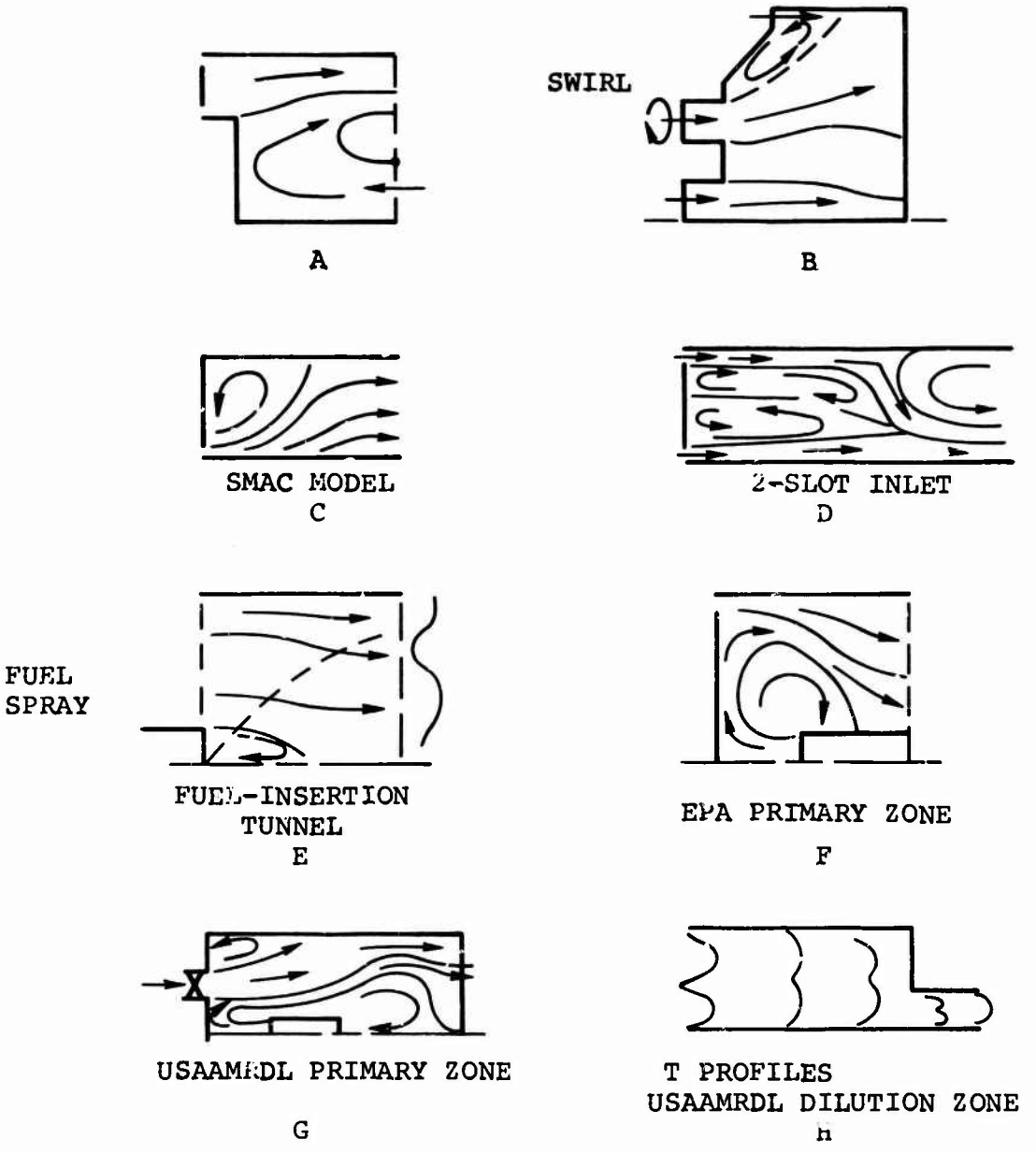


Figure 183. Tested Configurations.

APPENDIX V

IMPINGEMENT-JET, PRIMARY-ZONE RECIRCULATION MODEL COMPUTER PROGRAM NO. 1526

1.0 INTRODUCTION

This appendix describes a computer program for computation of primary-zone recirculation created by centrally impinging air jets. The analysis is based on the work of Verduzio and Campanaro.[38] The main result of the program is the computation of the flow fraction of the impinging jet flow that flows upstream into the primary zone. With this program it is possible to optimize the number and size of primary-zone holes.

Although the analysis is somewhat involved, the final equations required for calculation are fairly simple and the program is quite short.

2.0 PROGRAM INPUT VARIABLES

The following variables are entered on a single card with the format

3F10.0, I3, 7X, 4F10.0

Cards for additional cases can be run at one time, and the program will terminate when an EOF card is encountered.

Program Symbol	Parameter Symbol	Units	Description
BETA	--	Degrees	Initial jet efflux angle through primary-zone holes; 90 degrees is along jet axis; 0 degrees is in downstream direction; β_o in analysis = 90 - BETA.
DO	$2R_o$	Inch	Combustor diameter (single-can) or annulus width (annular) at orifice point.
SDO	d_o	Inch	Diameter of primary holes.
NH	N	-	Number of primary holes (must be two for annular combustor).
TAU	τ	-	Ratio of inlet air density to hot primary-zone gas density. Can be estimated as ratio of T stoichiometric/T inlet.
FPZ	f_p	-	Primary-zone fuel-air ratio for mass addition only.
TANA	tan α	-	Tangent of α, jet spreading angle (see Figure 184). Recommend value of 0.1 be used.
V	V	-	Ratio of flow through combustor dome to flow through primary holes. Can be effective-area ratio or obtain from Annulus Loss Model No. 5.

3.0 COMPUTATION PROCEDURE

A listing of the program is presented in Table XXVIII. The basic equation to be solved results from a pressure-drop and momentum balance for the central impingement region and expresses the fraction, k, of jet flow that flows upstream. Note that if there is no dome flow, very low primary-zone velocities, and straight jet injection, the flow fraction would be 0.50--i.e., half the flow upstream and half downstream.

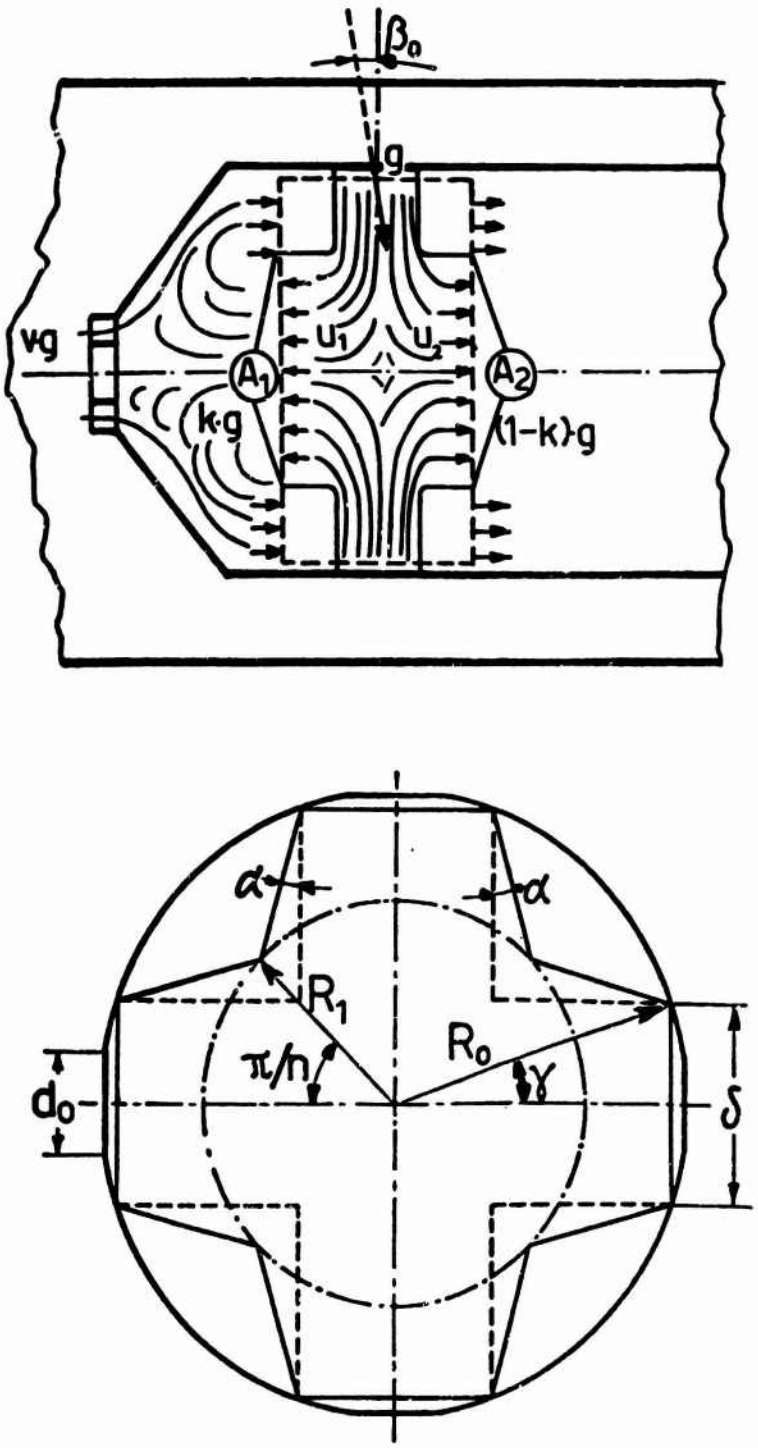


Figure 184. Recirculation Model.

TABLE XXVIII. LISTING OF PROGRAM NO. 1526

```
$$$
```

The equation to be solved is

$$k = -\left(V + \frac{1}{2C_2}\right) + \sqrt{\left(V + \frac{1}{2C_2}\right) - \left(V^2 - \frac{C_1}{C_2}\right)} \quad (150)$$

where

$$C_1 = 0.5 - \frac{\tan(\beta_o)\, B_i^2}{2n}\left(\frac{D_o}{d_o}\right)^2 \quad (151)$$

$$C_2 = \frac{\tau\,(1+f)^2\, B_i^2}{4\left(1 - B_i^2\right)^2}\left(\frac{A_3}{A_r} - 1\right)^2 \quad (152)$$

Values in this equation are inputs, with the exception of B_i and A_3/A_r. B_i is the ratio of the impingement-zone radius to the combustor radius. The impingement-zone radius, R_1, is computed as the radius that encompasses the points at which adjacent jets intersect as shown in Figure 184. Trigonometry yields

$$B_i = \frac{\left(\frac{\delta}{2R_o} + \tan\alpha\cos\gamma\right)}{\left(\sin\frac{\pi}{n} + \tan\alpha\cos\frac{\pi}{n}\right)} \quad (153)$$

Everything is given but α and γ. δ is the initial jet width with the jet deformed by the primary exit flow. This is obtained from an empirical relation

$$\frac{\delta}{d_o} = 1 + \frac{F}{n^2}\cos^2\beta_o \quad (154)$$

where $F = 16 - 0.45 \cdot \beta_o$

The angle $\gamma = \arcsin\frac{\delta}{2R_o}$

This completes calculation of β_i.

In addition to calculating the flow fraction, k, a parameter is derived which characterizes the recirculation so that optimum designs can be selected. For a fixed pressure drop, combustor diameter, and number of holes, the mass flow recirculated (g_r) is a function of orifice diameter. As the diameter increases, flow ratio (k) decreases but orifice flow (g) increases so that recirculated flow passes through a maximum. The optimization parameter is computed as

$$E - k\ n\ \pi\left(\frac{d_o}{2R_o}\right)^2 \qquad (155)$$

4.0 PROGRAM USAGE

A typical program output is presented in Table XXIX. In addition to using the program results alone, the recirculating-flow rate (g_r) and diameter of impingement zone (R_o) can be used for input to the Gosman-Spalding primary-zone two-dimensional flow program.

PROGRAM 1526 OUTPUT

TABLE XXIX. PROGRAM NO. 1526 OUTPUT

PROGRAM IMPINGE - PRIMARY ZONE RECIRCULATION

BETA O =	0.000	LINER DO=	5.000	ORIF D =	1.000	NO HOLES=	8	DEN RATIO=	1.000	F/A PZ =	0.00000
V RATIO=	0.0000	R I =	.7300	R 1 =	1.8251	F PARAM=	16.000	GAMMA =	.25268	A3/AR =	4.80966
C 1 =	.50000	C 2 =	8.8659	TAN ALPH=	.1000			K FRAC =	.18769	E PARAM=	.18868
BETA O =	0.000	LINER DO=	5.000	ORIF D =	.500	NO HOLES=	8	DEN RATIO=	1.000	F/A PZ =	0.00000
V RATIO=	0.0000	R I =	.4720	R 1 =	1.1799	F PARAM=	16.000	GAMMA =	.12533	A3/AR =	2.13923
C 1 =	.50000	C 2 =	.1195	TAN ALPH=	.1000			K FRAC =	.47321	E PARAM=	.11893
BETA O =	0.000	LINER DO=	5.000	ORIF D =	1.000	NO HOLES=	4	DEN RATIO=	1.000	F/A PZ =	0.00000
V RATIO=	0.0000	R I =	.6321	R 1 =	1.5802	F PARAM=	16.000	GAMMA =	.41152	A3/AR =	3.29749
C 1 =	.50000	C 2 =	1.4522	TAN ALPH=	.1000			K FRAC =	.33546	E PARAM=	.16862
BETA O =	0.000	LINER DO=	5.000	ORIF D =	1.000	NO HOLES=	6	DEN RATIO=	1.000	F/A PZ =	0.00000
V RATIO=	0.0000	R I =	.6557	R 1 =	1.6392	F PARAM=	16.000	GAMMA =	.29307	A3/AR =	3.69826
C 1 =	.50000	C 2 =	2.4078	TAN ALPH=	.1000			K FRAC =	.29312	E PARAM=	.22101
BETA O =	0.000	LINER DO=	5.000	ORIF D =	1.000	NO HOLES=	8	DEN RATIO=	4.000	F/A PZ =	0.00000
V RATIO=	0.0000	R I =	.7300	R 1 =	1.8251	F PARAM=	16.000	GAMMA =	.25268	A3/AR =	4.80966
C 1 =	.50000	C 2 =	53.1954	TAN ALPH=	.1000			K FRAC =	.08001	E PARAM=	.08047
BETA O =	0.000	LINER DO=	5.000	ORIF D =	1.000	NO HOLES=	8	DEN RATIO=	4.000	F/A PZ =	0.00000
V RATIO=	0.0000	R I =	.7300	R 1 =	1.8251	F PARAM=	16.000	GAMMA =	.25268	A3/AR =	4.80966
C 1 =	.50000	C 2 =	35.4636	TAN ALPH=	.1000			K FRAC =	.10547	E PARAM=	.10603
BETA O =	0.000	LINER DO=	5.000	ORIF D =	1.000	NO HOLES=	8	DEN RATIO=	1.000	F/A PZ =	0.00000
V RATIO=	.8000	R I =	.7300	R 1 =	1.8251	F PARAM=	16.000	GAMMA =	.25268	A3/AR =	4.80966
C 1 =	.50000	C 2 =	8.8659	TAN ALPH=	.1000			K FRAC =	.74360	E PARAM=	.74755
BETA O =	0.000	LINER DO=	5.000	ORIF D =	1.000	NO HOLES=	8	DEN RATIO=	1.000	F/A PZ =	0.00000
V RATIO=	.4000	R I =	.7300	R 1 =	1.8251	F PARAM=	16.000	GAMMA =	.25268	A3/AR =	4.80964
C 1 =	.50000	C 2 =	8.8659	TAN ALPH=	.1000			K FRAC =	.46385	E PARAM=	.46632
BETA O =	10.000	LINER DO=	5.000	ORIF D =	1.000	NO HOLES=	8	DEN RATIO=	1.000	F/A PZ =	0.00000
V RATIO=	0.0000	R I =	.6990	R 1 =	1.7474	F PARAM=	11.500	GAMMA =	.23707	A3/AR =	4.24718
C 1 =	.36540	C 2 =	4.9232	TAN ALPH=	.1000			K FRAC =	.18919	E PARAM=	.19019
BETA O =	30.000	LINER DO=	5.000	ORIF D =	1.000	NO HOLES=	8	DEN RATIO=	1.000	F/A PZ =	0.00000
V RATIO=	0.0000	R I =	.6393	R 1 =	1.5983	F PARAM=	2.500	GAMMA =	.20734	A3/AR =	3.43821
C 1 =	.13129	C 2 =	1.7375	TAN ALPH=	.1000			K FRAC =	.11020	E PARAM=	.11078

APPENDIX VI

DILUTION-ZONE JET-TRAJECTORY CALCULATION COMPUTER PROGRAM NO. 1530

1.0 INTRODUCTION

This appendix describes a computer program for computation of air-jet injection trajectories into a gas stream with nonuniform velocity and temperature profiles. The procedure is used for optimizing dilution orifice sizing. The program can be used alone to aid in orifice sizing, or can be used together with the Gosman-Spalding program to estimate mixing rates and pattern factor.

There are many reports of analytical and empirical correlations for jet trajectories in uniform streams. The purpose of developing this program was to incorporate the effects of mainstream velocity and temperature profiles, duct area change, and mass addition effects. The program analyzes a single circular jet; however, with proper input of mass addition effects, this program can simulate a multiple-jet arrangement.

2.0 PROGRAM STRUCTURE

A listing of the program is presented in Table XXX. The program consists of nine subroutines that perform the following functions:

- TRAJEC - Main program controls the finite difference step process in the cross-stream direction. Calculation is stepped in increments of jet diameter. Results are saved for trajectory plotting.
- INREAD - Reads in data cards.
- STEP - Calculates the change in trajectory angle for each step.
- OUTPRT - Prints out results.
- PATHPL - Plots initial effective velocity ratio profile and jet trajectory. Plotting is done on the output printer, not the CalComp plotter.
- LINPLT - Used by PATHPL to generate velocity ratio plot symbols.

TABLE XXX. LISTING OF PROGRAM NO. 1530

```
$$$
```

TABLE XXX. (CONTD)

```
      XS=XDOS*DO
      CALL INTERP(2,NXP,XA,AF,XS,AFS,JJ)
      VGM=VGM/AFS/(1.-ABLK)
      VEM=SQRT(ROGM/EMO)*VGM
      VA=ABS(VEM)
      CALL INTERP(2,NVKT,VKT,SKFT,VA,SKM,JJ)
      PARAM=CONS*SKM*VEM*ABS(VEM)
      CALL STEP
      SDOS=SDOS+DSDO
      XDOS=XDOS+DXDO
      HDOS=HDOS+DSDO*SKM
      APS=APS+HDOS*DYDOS*DO*DO
      WJWJOS=1.+SQRT(ROGM/ROJ)*APS*VA /AO
      IF (JS.LT.NSAV) GO TO 30
      YS=YDOS*DO
      CALL INTERP (2,NYP,YP,ROGP,YS,ROGS,JJ)
      CALL INTERP (2,NYP,YP,VGP,YS,VGS,JJ)
      XS=XDOS*DO
      CALL INTERP (2,NXP,XA,AF,XS,AFS,JJ)
      VGS=VGS/AFS/(1.-ABLK)
      VES=SQRT(ROGS/EMO)*VGS
      VA=ABS(VES)
      CALL INTERP(2,NVKT,VKT,SKFT,VA,SKS,JJ)
      JS=0
      J=J+1
   25 BETA(J)=BETAS
      SDD(J)=SDOS
      S(J)=SDOS*DO
      HDD(J)=HDOS
      H(J)=HDOS*DO
      YDD(J)=YDOS
      Y(J)=YDOS*DO
      DYDD(J)=DYDOS
      XDD(J)=XDOS
      X(J)=XDOS*DO
      AP(J)=APS
      SK(J)=SKS
      V(J)=VES
      ROG(J)=ROGS
      VG(J)=VGS
      WJWJO(J)=WJWJOS
      ROR=ROGS/ROJ
      SROR=SQRT(ROR)
      VD=0.
      IF(VA*SROR.EQ.1)GO TO 28
      VD=(WJWJOS/(.192*(SDOS+AVIRT)**2)-2.625*VA*SROR)
     * /(ROR*(1.-VA*SROR)*.826)
   28 CONTINUE
      VDS=VD
      IF(VD.GT.1.0) VDS=1.0
      IF(VD.LT.0.)VDS=0.
      VCL(J)=VGS+VDS*(ABS(VJO)-ABS(VGS))
      CALL INTERP(2,NYP,YP,TOGP,Y(J),TG,JJ)
      TD=VD*.74
      IF(TD.GT.1.0) TD=1.0
      IF(TD.LT.0.)TD=0.
      TCL(J)=TG+TD*(TJO-TG)
      VDP(J)=VDS
      TDP(J)=TD
      CALL OUTPRT(J)
      IF (J.EQ.1) GO TO 20
   30 JS=JS+1
      BETAI1=BETAI
      BETAI=BETAS
      IF (Y(J).GE.YMAX.OR.J.GE.100) GO TO 40
      IF (BETAS.LT.90..AND.BETAS.LE.BETMIN) GO TO 40
```

TABLE XXX. (CONTD)

```
      IF (BETAS.GT.90..AND.(180.-BETAS).LT.BETMIN) GO TO 40
      GO TO 20
   40 CALL PATHPL(J)
      GO TO 10
      END
      SUBROUTINE INREAD
      COMMON/JETINT/ROJ,VJO,OH,OO,BETAO,AVIRT,AO,WJO,CDJ,TJO,PO,NTYP
     * ,EMO
      COMMON/PROFIL/NYP,YP(100),RDGP(100),VGP(100),TOGP(100),ABLK
      COMMON/FUNCKV/NVKT,SKFT(10),VKT(10),NVK(10),SKFR(10,10),VK(10,10)
      COMMON /STEPCN/ DYRDO,YMAX,BETMIN,NSAV,PLIM,IPLT
      COMMON/AFAC/NXP,XA(100),AF(100)
      DIMENSION XDAT(8)
      DATA TJO,VJO,PO,OH,BETAO,AVIRT,NTYP,CDJ/540.,1.,25.19933,1.,90.,
     * .8,1,1.0/
      DATA NYP,YP(1),YP(2),TOGP(1),TOGP(2),VGP(1),VGP(2),ABLK/
     *      2,   0.. 1000.,540.,    540.,   1.0,   1.0,   0./
      DATA NXP,XA(1),XA(2),AF(1),AF(2)/2,0.,1000.,1.,1./
      DATA DYRDO,YMAX,BETMIN,NSAV,PLIM/.0125,10.,2.,10, .06/
      DATA IPLT/1/
      DATA NVKT,SKFT(1),SKFT(2),VKT(1),VKT(2)/2,1.,1.,-1000.,1000./
      DATA NVK(1),(SKFR(I,1),I=1,2),(VK(I,1),I=1,2)/
     * 2, 1.0,1.0,   -1000.,1000./
      DATA NVK(2),(SKFR(I,2),I=1,10),(VK(I,2),I=1,10)/10,
     * .32,.45  ,.7  ,.9  ,1.03,1.06,1.06,.85 ,.8  ,.8  ,
     * .01,.067, .1  ,.125,.167,.2  ,.25 ,.5  ,1.  ,100./
      DATA NVK(3),(SKFR(I,3),I=1,10),(VK(I,3),I=1,10)/10,
     * .32,.525 ,.6  ,.67 ,.725,.76 ,.78 ,.79 ,.8  ,.8  ,
     * .00 ,.1  ,.2  ,.3  ,.4  ,.5  ,.6  ,.7  ,.8  ,100./
C     READ INPUT DATA
    2 CONTINUE
      READ(5,100)ICARD,XDAT
  100 FORMAT(I1,F9.0,7F10.0)
      IF (EOF(5)) 999,5
    5 CONTINUE
      REWIND 7
      WRITE(7) XDAT
      REWIND 7
      IF(ICARD.LT.1) GO TO 10
      IF(ICARD.GT.6) GO TO 60
      GO TO (10,20,30,40,50,60),ICARD
   10 READ(7)TYP,TJO,VJO,PO,OH,BETAO,CDJ
      NTYP=TYP
      GO TO 2
   20 NYP=XDAT(1)
      ABLK=XDAT(2)
      READ(5,300)(YP(J),TOGP(J),VGP(J),J=1,NYP)
  200 FORMAT(9F8.0)
      GO TO 2
   30 NXP=XDAT(1)
      READ(5,300) (XA(J),AF(J),J=1,NXP)
  300 FORMAT(8F10.0)
      GO TO 2
   40 READ(7)DYRDO,YMAX,BETMIN,SAVN,PLIM,PLT
      IPLT=PLT
      NSAV=SAVN
      GO TO 2
   50 N=NTYP
      NVKT=XDAT(1)
      READ(5,300)(SKFT(I),VKT(I),I=1,NVKT)
      GO TO 2
   60 RETURN
  999 STOP
      END
      SUBROUTINE STEP
      COMMON /STEPCC/ BETAI,BETAI1,PARAM,A,SDOS,DYDOS,BETAS,OSDO,DXDO
```

TABLE XXX. (CONTD)

```
      RAD=57.29578
      COTBI=0.
      COTBI1=0.
      COTBA=0.
      IF (BETAI.EQ.90..AND.BETAI1.EQ.90.) GO TO 30
      IF (BETAI.EQ.90.) GO TO 10
      RBI=BETAI/RAD
      COTBI=1./TAN(RBI)
   10 IF (BETAI1.EQ.90.) GO TO 20
      RBI1=BETAI1/RAD
      COTBI1=1./TAN(RBI1)
   20 COTBA=(3.*COTBI-COTBI1)/2.
   30 OSDO=SQRT(1.+COTBA*COTBA)*DYDOS
      COTB=COTBI+PARAM*(2.*A+SOOS+OSOO)*DYDOS
      DXOO=(COTBI+COTB)/2.*DYDOS
      IF (COTB.EQ.0.) GO TO 40
      BETAS=ATAN(1./COTB)
      BETAS=BETAS*RAD
      IF (BETAS.LT.0.) BETAS=180.+BETAS
      RETURN
   40 BETAS=90.
      RETURN
      END
      SUBROUTINE OUTPRT(J)
      COMMON /OUTSAV/ BETA(100),SDO(100),S(100),HOO(100),H(100),
     * YOO(100),Y(100),DYDO(100),XOO(100),X(100),AP(100),SK(100),V(100),
     *ROG(100),VG(100),WJWJO(100)
     *,VDP(100),TOP(100),VCL(100),TCL(100)
      COMMON/JETINT/ROJ,VJO,DH,DO,BETAO,AVIRT,AO,WJO,COJ,TJO,PO,NTYP
     * ,EMO
      COMMON/PROFIL/NYP,YP(100),ROGP(100),VGP(100),TOGP(100),ABLK
      COMMON/FUNCKV/NVKT,SKFT(10),VKT(10),NVK(10),SKFR(10,10),VK(10,10)
      COMMON /STEPCN/ DYRDO,YMAX,BETMIN,NSAV,PLIM,IPLT
      COMMON/AFAC/NXP,XA(100),AF(100)
      DIMENSION AL(50)
      DATA (AL(I),I=1,40)/
     * 10HDENSITY,  ,10HLB/FT3    =,10HDELTA Y/R ,10HDO        =,
     * 10HVELOCITY, ,10HFT/SEC    =,10HY MAX, IN.,10H          =,
     * 10HJET DIAM.,,10HOO, IN.   =,10HBETA MIN. , 10H         =,
     * 10HEFFLUX ANG,10HLE, DEG.  =,10HNO. OF STE,10HPS TO PRIN,3HT =,
     * 10HVIRTUAL SO,10HURCE      =,10HJET AREA, ,10HSQ. IN.   =,
     * 10HJET MOMEN,,10H LB/F/S2  =,10HFLOW RATE,,10H LB/SEC   =,
     * 10HY, IN.     ,10HTEMP, F    ,10HVELOCITY  , 2HVE,1HK,
     * 10HTEMPERATUR,10HE, F      =,10HPRESSURE, ,10HATMOS     =,
     * 10HDISCHARGE ,10HCOEF.     =,10HHOLE DIAM.,10H,OH, IN. =,
     * 10HPLOT SMOOT,10HH LIMIT   =/
       IF (J.GT.0) GO TO 30
      WRITE (6,100)
  100 FORMAT  (27H1JET TRAJECTORY CALCULATION,// 5X,10HINPUT DATA// ,
     *7X,18HINITIAL JET DATA =,35X,19HSTEP CONTROL DATA =)
      WRITE (6,200) AL(1),AL(2),ROJ,AL(3),AL(4),DYRDO
      WRITE (6,200) AL(5),AL(6),VJO,AL(7),AL(8),YMAX
      WRITE (6,200) AL(9),AL(10),DO,AL(11),AL(12),BETMIN
      WRITE (6,300) AL(13),AL(14),BETAO,AL(15),AL(16),AL(17),NSAV
      WRITE(6,200)AL(31),AL(32),TJO,AL(39),AL(40),PLIM
      WRITE(6,400)AL(33),AL(34),PO
      WRITE(6,400)AL(35),AL(36),COJ
      WRITE(6,400)AL(37),AL(38),DH
      WRITE (6,400) AL(18),AL(19),AVIRT
      WRITE (6,400) AL(20),AL(21),AO
      WRITE (6,500) AL(22),AL(23),EMO
      WRITE (6,400) AL(24),AL(25),WJO
      WRITE(6,870)NTYP,ABLK
  870 FORMAT(9X,*ORIFICE TYPE NO.  = *,I6,25X,*DUCT AREA FRACTION BLOCKE
     *D BY JETS = *,F11.5)
      WRITE (6,600) AL(26),AL(27),AL(28),AL(29),AL(30)
```

```
      L=1
   10 JR=L
      IF(L.LE.NYP)WRITE(6,700)YP(JR),TDGP(JR),VGP(JR),ROGP(JR)
      IF(L.GT.NYP)WRITE(6,860)
  860 FORMAT(1H )
      IF(L.LE.NVKT)WRITE(6,800)VKT(JR),SKFT(JR)
      IF(L.LE.NXP)WRITE(6,850) XA(JR),AF(JR)
      IF(L.GE.NYP.AND.L.GE.NVKT.AND.L.GE.NXP) GO TO 20
      L=L+1
      GO TO 10
   20 WRITE (6,900)
      RETURN
  200 FORMAT (9X,2A10,F13.6,20X,2A10,2X,F8.4)
  300 FORMAT (9X,2A10,F13.6,20X,2A10,A3,1X,I4)
  400 FORMAT (9X,2A10,F13.6)
  500 FORMAT (9X,2A10,F13.1)
  600 FORMAT (1H0,7X,23HUPSTREAM PROFILE DATA -,20X,
     + 31HSPREAD RATE PARAMETER VERSUS VE,10X,9HDUCT AREA RATIO//
     +10X,3A10,10HDENSITY    ,12X,A2,10X,A1,17X,1HX,9X,10HAREA RATIO )
  700 FORMAT(7X,F8.3,5X,F6.1,4X,F7.2,3X,F8.5)
  800 FORMAT(1H+,57X,F9.3,5X,F7.4)
  850 FORMAT(2H+ ,86X,F10.3,5X,F11.5)
  900 FORMAT(1H1,T5,1HY,T12,4HY/DO,T21,1HX,T27,4HX/DO,T35,1HS,T42,4HS/DO
     +,T50,1HN,T56,4HN/DO,T64,2HVE,T70,2HVG,T77,3HVDP,T83,5HVJ CL,
     + T91,3HTDP,T97,5HTJ CL,T104,4HBETA,T110,6HWJ/WJC,T120,1HK)
   30 WRITE(6,1000)Y(J),YDO(J),X(J),XDO(J),S(J),SDO(J),H(J),HDO(J),V(J),
     + VG(J),VDP(J),VCL(J),TDP(J),TCL(J),BETA(J),WJWJD(J),SK(J)
 1000 FORMAT(1X,F7.3,F7.2,F8.3,F7.2,F8.3,F7.2,F7.2,F7.2,F7.3,F7.1,F7.3,
     + F7.1,F7.3,F7.0,F7.2,F7.2,F7.4)
      RETURN
      END
      SUBROUTINE PATMPL(NPT)
      COMMON /OUTSAV/ BETA(100),SDO(100),S(100),HDO(100),H(100),
     + YDO(100),Y(100),OYOD(100),XDO(100),X(100),AP(100),SK(100),V(100),
     +ROG(100),VG(100),WJWJO(100)
     +,VDP(100),TDP(100),VCL(100),TCL(100)
      COMMON/JETINT/ROJ,VJO,DM,DO,BETAD,AVIRT,AD,WJD,CDJ,TJD,PO,NTYP
     + ,EMD
      COMMON /STEPCN/ DYRDD,YMAX,BETMIN,NSAV,PLIM,IPLT
      DIMENSION IP(101),IAL(19),IAR(21)
      DATA ISIGB,ISIGP,ISIGM/1H ,1H+,1H-/
      DATA(IAL(I),I=1,19)/4H-8.0,4H-7.0,4H-6.0,4H-5.0,4H-4.0,4H-3.0,
     + 4H-2.0,4H-1.0,4H 0.0,4H 1.0,4H 2.0,4H 3.0,4H 4.0, 4H 5.0,4H 6.0,
     + 4H 7.0,4H 8.0,4H 9.0,4H10.0/
      DATA LAB1/4H X  /,LAB2/4HX/DO/,LAB3/4H  Y /,LAB4/4HY/DO/
C     IPLT=0,PLOT AS X/DO,Y/DO -- IPLT=1 PLOT AS X,Y
      XMIN=0.
      XMAX=0.
      VEMAX=0.
      DO 10 J=1,NPT
      VEAB=ABS(V(J))
      VEMAX=AMAX1(VEMAX,VEAB)
      IF (VEAB.EQ.VEMAX) VEMAXD=V(J)
      IF (Y(J).GT.YMAX) GO TO 20
      IF(IPLT.EQ.1) GO TO 5
      XMIN=AMIN1(XMIN,XDO(J))
      XMAX=AMAX1(XMAX,XDO(J))
      GO TO 10
    5 XMIN=AMIN1(XMIN,X(J))
      XMAX=AMAX1(XMAX,X(J))
   10 CONTINUE
   20 IF (XMIN.GE.0.) NORIG=0
      X2=-2.
      IF (XMIN.LT.0..AND.XMIN.GE.X2) NORIG=2
      X4=-4.
      IF(XMIN.LT.X2.AND.XMIN.GE.X4) NORIG=4
```

```
      X6=-6.
      IF(XMIN.LT.X4.AND.XMIN.GE.X6) NORIG=6
      X8=-8.
      IF(XMIN.LT.X6) NORIG=8
      NLO=9-NORIG
      NHI=NLO+10
      IF(IPLT.EQ.0)WRITE(6,100)VEMAXO,BETAO,LAB4,LAB2
      IF(IPLT.EQ.1)WRITE(6,100)VEMAXO,BETAO,LAB3,LAB1
  100 FORMAT(1H1,*JET PATH PLOT*,10X,*VE MAX = *,F10.5,10X
     +,*INITIAL JET ANGLE = *,F10.2/// 1X,T8,9HVE/VE MAX,T24,A4,T74,A4)
      WRITE(6,200) (IAL(I),I=NLO,NHI)
  200 FORMAT(1H0,21X,11(6X,A4)//1X,2H-1,8X,1H0,9X,1H1,8X,1HI,10(9H------
     +---,1HI))
      DO 30 I=1,101
   30 IP(I)=ISIGB
      J=0
      YP=0
   40 LP=(YP+.000001)*10
      IF(IPLT.EQ.1) GO TO 44
      CALL INTERP (2,NPT,YDO,V,YP,VEP,JJ)
      CALL INTERP (2,NPT,YDO,XDO,YP,XP,JJ)
      GO TO 46
   44 CALL INTERP(2,NPT,Y,V,YP,VEP,JJ)
      CALL INTERP(2,NPT,Y,X,YP,XP,JJ)
   46 CONTINUE
      CALL LINPLT (21,10,VEP,VEMAX,IAR)
   50 CONTINUE
      NCT=NORIG*10+1
      LXT=XP*10.+NCT
      LXH=XP*100.+NCT*10
      LXTT=LXT*10
      DL=LXH-LXTT
      DX=ABS(DL)/100.
      IF (DX.GT.PLIM.AND.XP.LT.0..AND.LXTT.GT.LXH) LXTT=LXTT-10
      IF (DX.GT.PLIM.AND.XP.GT.0..AND.LXH.GT.LXTT) LXTT=LXTT+10
      DL=LXH-LXTT
      DX=ABS(DL)/100.
      LX=LXTT/10
      IF (LX.GT.101.OR.LX.LT.0) RETURN
      IF (DX.LT.PLIM.AND.LX.LE.101) IP(LX)=ISIGP
      JP=J/6*10
      JPP=JP/10
      IF (LP.EQ.JP) WRITE(6,300) (IAR(JR),JR=1,21),JPP,(IP(JR),JR=1,LX)
      IF (LP.NE.JP) WRITE(6,400) (IAR(JR),JR=1,21),ISIGM,
     + (IP(JR),JR=1,LX)
  300 FORMAT (1X,21A1,3X,I1,4X,101A1)
  400 FORMAT (1X,21A1,3X,A1,4X,101A1)
      YCH=YP*00
      IF(IPLT.EQ.1) YCH=YP
      YP=YP+1./6.
      IF(YP.GT.9.OR.YCH.GE.YMAX) RETURN
      J=J+1
      IP(LX)=ISIGB
      GO TO 40
      END
      SUBROUTINE LINPLT (NAR,NT,V,VAMAX,IR)
C        ROUTINE TO GENERATE ARRAY IR OF SYMBOLS ,(BLANK,-,OR,+)
C        FOR PRINT PLOT OF VARIATION OF VARIABLE ARRAY V, WITH ABSOLUTE
C        MAXIMUM VALUE OF VAMAX.
C             NAR = TOTAL NUMBER (MUST BE ODD) OF IR VALUES
C                 = TOTAL WIDTH OF PLOT IN PRINTING SPACES.
C             NT  = MAXIMUM NUMBER OF PLOT SPACES ON POSITIVE SIDE OF NO
C                   MUST BE GREATER THAN 10 OR ZERO IF V ALL NEGATIVE
C             NO  = SPACE IR FOR V = 0., = NAR-NT
C        IF ONLY POSITIVE VALUES OF V EXPECTED SET NT=NAR-1
C        IF ONLY NEGATIVE VALUES OF V EXPECTED, SET NT=0
```

TABLE XXX. (CONTD)

```
C        IF BOTH - AND + VALUES EXPECTED SET NT= (NAR-1)/2
C        PRINT THE IH SYMBOLS IN AN #A# TYPE FORMAT WITH NAR*1I PRINT
      DIMENSION IR(NAR)
      DATA ISIGB,ISIGP,ISIGM,ISIGS/1H ,1H+,1H-,1H*/
      NO=NAR-NT
      NC=(NAR-1)/2+1
      IF (NO.LE.NC) NTP=NT
      IF (NO.GT.NC) NTP=NO-1
      IF(VAMAX.LE.0.0) VAMAX=1.
      LR=V/(VAMAX*.999999)*NTP
      LR=LR+NO
      LMIN=NO
      LMAX=LR
      IF (LR.LT.NO.AND.LR.GT.0) LMIN=LR
      IF (LR.LT.NO.AND.LR.GT.0) LMAX=NO
      IF (LR.LE.0.OR.LR.GT.NAR) GO TO 20
      DO 10 J=1,NAR
      IR(J)=ISIGB
      IF (J.GE.LMIN.AND.J.LE.LMAX.AND.LR.LT.NO) IR(J)=ISIGM
      IF (J.GE.LMIN.AND.J.LE.LMAX.AND.LR.GE.NO) IR(J)=ISIGP
   10 CONTINUE
      RETURN
   20 WRITE(6,100)
  100 FORMAT (1X,99HIN LINPLT SUBROUTINE, ABSOLUTE VALUE OF VARIABLE EXC
     +EEDS PLOT LIMITS.  CHECK FOR ERROR IN NT VALUE.)
      DO 30 J=1,NAR
   30 IR(J)=ISIGS
      RETURN
      END
      SUBROUTINE INTERP (ID,N,PN,WA,P,ZZ,JJ)
      DIMENSION PN(100),WA(100),A(5),B(5)
      CALL HILOW  (PN,P,N,IL,IH,JJ)
      IF(JJ-1)2,30,50
    2 IF(IL-IH)20,10,20
   10 ZZ=WA(IL)
      RETURN
   20 IF(IL-1)30,30,40
   30 CALL LAGRNG (ID,PN,WA,P,Z)
      ZZ=Z
      RETURN
   40 IF(IH-N)80,50,80
   50 K1=N-ID
   60 DO 70 I=1,ID
      J=I+K1
      A(I)=PN(J)
   70 B(I)=WA(J)
      CALL LAGRNG(ID,A,B,P,Z)
      ZZ=Z
      RETURN
   80 IF( ABS(P-PN(IL))- ABS(P-PN(IH)))90,90,100
   90 K1=IL-ID+1
      GO TO 60
  100 K1=IL-I
      GO TO 60
      END
      SUBROUTINE HILOW  (Y,X,N,IL,IH,J)
      DIMENSION Y(100)
      J=0
      S=1
      S= SIGN(S,Y(N)-Y(1))
      IL=1
      IH=N
      I=1
      IF(S*(X-Y(1))) 7,30,6
    6 I=N
      IF(S*(X-Y(N)))10,30,8
```

TABLE XXX. (CONTD)

```
 7 IH=1
   J=1
   RETURN
 8 IL=N
   J=2
   RETURN
10 I=(IL+IH)/2
   IF(S*(X-Y(I)))20,30,40
20 IH=I
   GO TO 50
30 IL=I
   IH=I
   RETURN
40 IL=I
50 IF(IL+1-IH)10,60,60
60 RETURN
   END
   SUBROUTINE LAGRNG (N,X,Y,W,Z)
   DIMENSION X(5),Y(5)
   Z=0.
   DO 40 J=1,N
   P=1.
   DO 30 I=1,N
   IF(I-J)20,10,20
10 P=P*Y(J)
   GO TO 30
20 P=P*(W-X(I))/(X(J)-X(I))
30 CONTINUE
40 Z=Z+P
   END
```

- o INTERP - Sets up tabular data for Lagrangian interpolation.
- o HILOW - Used by INTERP to select high and low point for interpolation.
- o LAGRNG - Performs 2- or 3-point Lagrangian interpolation.

3.0 PROGRAM INPUT

Input data format is shown in Figures 185 and 186. The input is divided into 6 sections. The first card of each section is numbered in the first column. All data is preset in the program, and the preset values are used if a particular card set is not entered in the data deck. If a given card set is entered, all values in that set replace the preset values and the entered values remain for following cases. Therefore, for repeated cases, only those card sets for which values change need to be entered. Except for the card set number in Column 1, all numbers entered require a decimal point.

3.1 Card Set 1 - Jet Data

This card set consists of one card containing all data pertaining to the orifice initial-injection conditions. Data required is shown on Data Sheet 1. The orifice type, NTYP, describes the spreading rate parameter function to be used. Orifice types available are listed at the bottom of Data Sheet 2. Other data on the card is self-explanatory.

3.2 Card Set 2 - Mainstream Gas Profile Data

The mainstream gas profile immediately upstream of the orifice centerline is defined by temperature (TOGP) and velocity (VGP) at NYP number of points, each a distance YP away from the wall through which the jet is injected. Up to 100 points can be entered, depending on the severity of the profile. Linear interpolation is used between points. Gas velocity is positive in the mainstream flow direction. Negative values of gas velocity can be entered if regions of reverse flow exist.

An area blockage factor, ABLK, is included to account for the increase in mainstream gas velocity as the result of jet mass flow addition. ABLK is calculated as

$$ABLK = \frac{D_h * YMAX * N}{ADIL} \qquad (156)$$

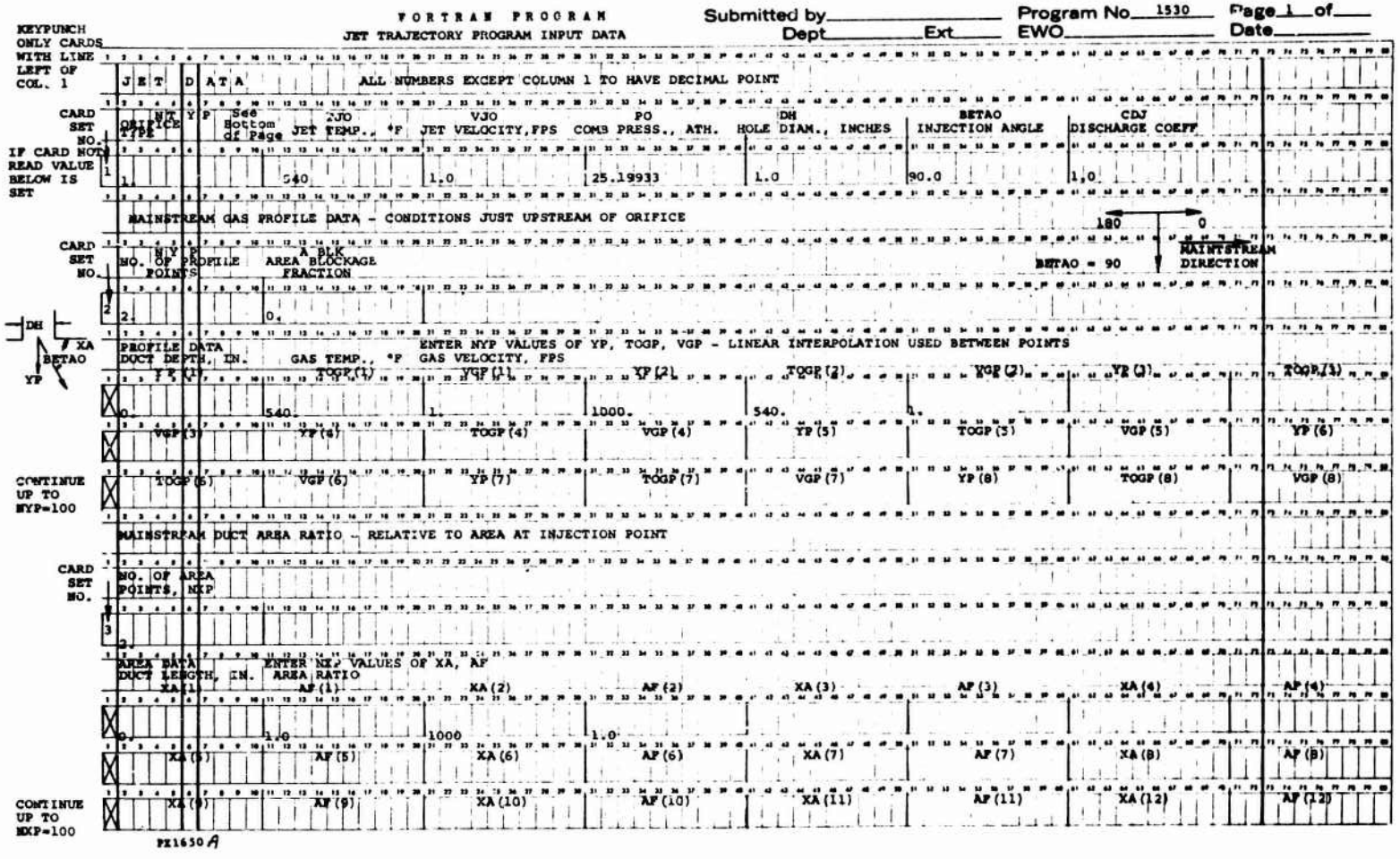


Figure 186. Input Data for Program No. 1530, Sheet 1.

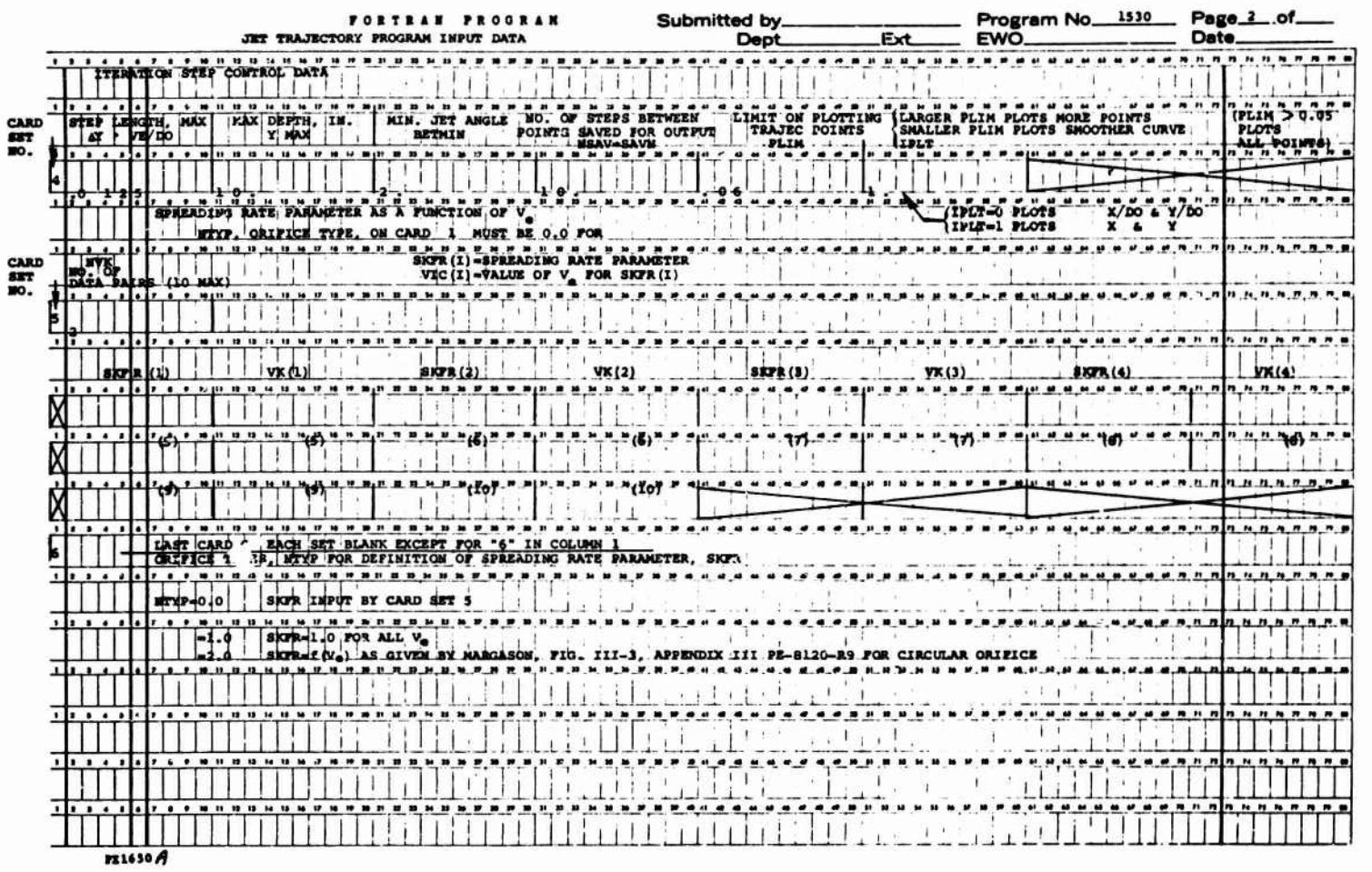


Figure 186. Input Data for Program No. 1530, Sheet 2.

where D_h = orifice diameter or width

YMAX = dilution-zone width or estimated jet penetration depth

N = number of orifices

ADIL = dilution-zone total cross-section area at injection point

If swirl is present in the mainstream gas, velocity VGP should be the absolute velocity magnitude and ADIL above is the axial cross section times the cosine of the swirl angle.

3.3 Card Set 3 - Mainstream Duct Area Ratio

The combustor area is input as a fraction, AF, of the area at the injection point as a function of distance, XA, downstream of the injection point at NXP number of points up to 100. If this card set is left out the area remains constant.

3.4 Card Set 4 - Iteration Step Control

This card will usually not have to be entered, as preset values will normally be acceptable. If the card is input for the purpose of changing one of the values, all of the remaining values must be entered even if unchanged from preset values.

Dilution-zone width, YMAX, has no effect on the trajectory and only serves to stop calculation. A smaller value can be used to reduce computer time. Iteration proceeds until YMAX or BETAMIN, minimum trajectory angle, is reached. PLIM can be used to smooth out the plots by using values between 0.01 and 0.05. IPLT is used to generate trajectory plots versus actual dimensions X and Y or nondimensionally relative to jet diameter.

3.5 Card Set 5 - Spreading Rate Parameter

The change in trajectory angle is calculated by the following equation. (Symbols are defined in Table XXXI of nomenclature.)

$$\cot \beta_2 = \cot \beta_1 + \frac{4 V_e^2}{\pi \sin \beta_o} K \left(2a + \frac{s_2}{D_h}\right)\frac{\Delta Y}{D_h} \qquad (157)$$

TABLE XXXI. NOMENCLATURE

a = virtual origin of jet, diameters

A_p = primary-zone exit area, sq in.

A_r = reference area, sq in.

A_t = total orifice geometry area in one row, sq in.

C = combustor mean circumference (annular) or outer diameter (cans)

D_h = orifice hole diameter, in.

D_o = jet diameter at vena contracta, in.

H = jet spreading width, in.

K = jet empirical spreading rate parameter

N = number of holes per row

s = jet trajectory path length, in.

s_2 = s at downstream end of current trajectory step

T_3 = combustor inlet temperature, ^oR

V_e = effective velocity ratio = $\sqrt{\frac{\rho_g}{\rho_{jo}}} \quad \frac{V_g}{V_{jo}}$

V_j = jet velocity, ft/sec

V_{jo} = jet initial injection velocity, ft/sec

V_p = primary-zone exit velocity, ft/sec

V_r = reference velocity, ft/sec

w_p = primary-zone exit airflow rate, lb/sec

w_t = combustor total airflow rate, lb/sec

$\Delta P/P$ = combustor fractional pressure loss

ΔY = trajectory step depth, in.

β_o = initial jet injection angle, deg

β_1 = trajectory angle from previous step

β_2 = trajectory angle calculated for current step

ρ_{jo} = initial jet density, lb/cu ft

ρ_g = mainstream gas density, lb/cu ft

ρ_p = primary-zone exit density, lb/cu ft

The term $K\left(2a + \frac{s_2}{D_h}\right)$ represents the width (in jet diameters) of the jet out to points on either side of the centerline where the velocity difference has decreased to one-tenth of the initial velocity difference. The trajectory calculation is, therefore, directly dependent on the spreading rate parameter, K. Analysis indicates that K is of the order of 1.0, but empirical values must be employed to obtain exact agreement. Dilution-zone test results will be used to generate improved functions of K. If specific data is not available to the user, set NTYP = 2.0 on Card Set 1 and do not enter Card Set 5. This will use tabulated values of K as a function of v_e derived from test data for a circular orifice.

The parameter V_e is the basic correlating parameter for the calculation and is defined as an effective velocity ratio

$$V_e = \sqrt{\frac{\rho_q}{\rho_{jo}}}\ \frac{V_q}{V_{jo}} \tag{158}$$

Empirical relations for K are then derived as a function of V_e for specific orifice types.

3.6 Card Set 6 - End of Case

A card, blank except for 6 in Column 1, signifies the end of the case.

3.7 Multiple and Nondimensional Cases

Execution time is between 5 and 10 seconds per case. Multiple cases can be run. The run is terminated with an EOF card after Card 6 of the last case. A test case using all of the preset data values can be run by inputting only Card 6. For this case $V_e = 1.0$, and all velocities and densities are nondimensionally equal to 1.0. Pressure is set to 25.19933 atmospheres with temperatures set to 540°F (1000°R) to produce a density of 1.0. Nondimensional cases can be run, for example, by leaving out Card 1 and entering mainstream velocities as ratios of the jet velocity. The mainstream density is nondimensionalized through the gas temperatures TOGP(I). The jet temperature is preset to 540°F (1000°R). If TOGP is input as 2540°F (3000°R), the mainstream to jet density ratio will be 1/3. Cases can also be run by leaving out the mainstream profile Card Set 2 and entering jet data, Card 1, in nondimensional form. In this case the mainstream

is uniform. The advantage of nondimensionalizing is that a library of runs can be generated and saved for future use. It also simplifies computation of different operating conditions for a given dilution-zone configuration.

4.0 PROGRAM OUTPUT

The output for each case is printed on three pages shown in Table XXXII. The first page lists the input parameters for initial jet data, step control data, mainstream profile, spreading rate parameter function, and duct area ratio.

The second sheet lists the calculated results. Values printed out include:

Y = jet penetration depth, inches
X = axial length from injection point, inches
S = length along jet trajectory path, inches
H = total width of jet, inches

Also listed are the above values divided by the jet diameter, DO. Note that DO is not the geometric orifice diameter, DH, but is the actual jet vena contracta diameter, and DO = SQRT (CDJ) * DH. CDJ is the jet discharge coefficient. Additional values listed are:

VE = effective velocity ratio

VG = mainstream gas velocity, ft/sec

VDF = jet centerline velocity decay parameter,
= (VJ CL - VG)/(VJO - VG)

VJ CL = jet centerline velocity, ft/sec

TDP = jet centerline temperature decay parameter,
= (TJ CL - TOGP)/(TJO - TOGP)

TJ CL = jet centerline temperature, °F

BETA = jet centerline trajectory angle, deg

VJ/WJO = mass flow entrainment ratio

K = spreading rate parameter

The third output sheet is a plot of the jet centerline trajectory. A nondimensional representation of the mainstream V_e profile is printed on the left side. The trajectory is plotted in coordinates of X and Y or X/DO and Y/DO as specified by the input Card 4. For injection angles between 0 and 90 degrees the plot will be made with X = 0 at the left side. For upstream injection the origin is shifted to the right as required to contain the trajectory on the plot.

TABLE XXXII. OUTPUT FOR PROGRAM NO. 1530

JET TRAJECTORY CALCULATION

INPUT DATA

INITIAL JET DATA -

DENSITY, LB/FT3	=	.492200
VELOCITY, FT/SEC	=	304.000000
JET DIAM.,DO, IN.	=	.146833
EFFLUX ANGLE, DEG.	=	68.490000
TEMPERATURE, F	=	830.000000
PRESSURE, ATMOS	=	16.000000
DISCHARGE COEF.	=	.539000
HOLE DIAM.,DH, IN.	=	.200000
VIRTUAL SOURCE	=	.800000
JET AREA, SQ. IN.	=	.016933
JET MOMEN, LB/F/S2	=	45487.1
FLOW RATE, LB/SEC	=	.017595
ORIFICE TYPE NO.	=	2

STEP CONTROL DATA -

DELTA Y/R DO	=	.0125
Y MAX, IN.	=	10.0000
BETA MIN.	=	2.0000
NO. OF STEPS TO PRINT	=	10
PLOT SMOOTH LIMIT	=	.0600

DUCT AREA FRACTION BLOCKED BY JETS = .10000

UPSTREAM PROFILE DATA -

Y, IN.	TEMP, F	VELOCITY	DENSITY
0.000	3230.0	39.10	.17207
2.000	3230.0	39.10	.17207

SPREAD RATE PARAMETER VERSUS VE

VE	K
.010	.3200
.067	.4500
.100	.7000
.125	.9000
.167	1.0300
.200	1.0600
.250	1.0600
.500	.8500
1.000	.8000
100.000	.8000

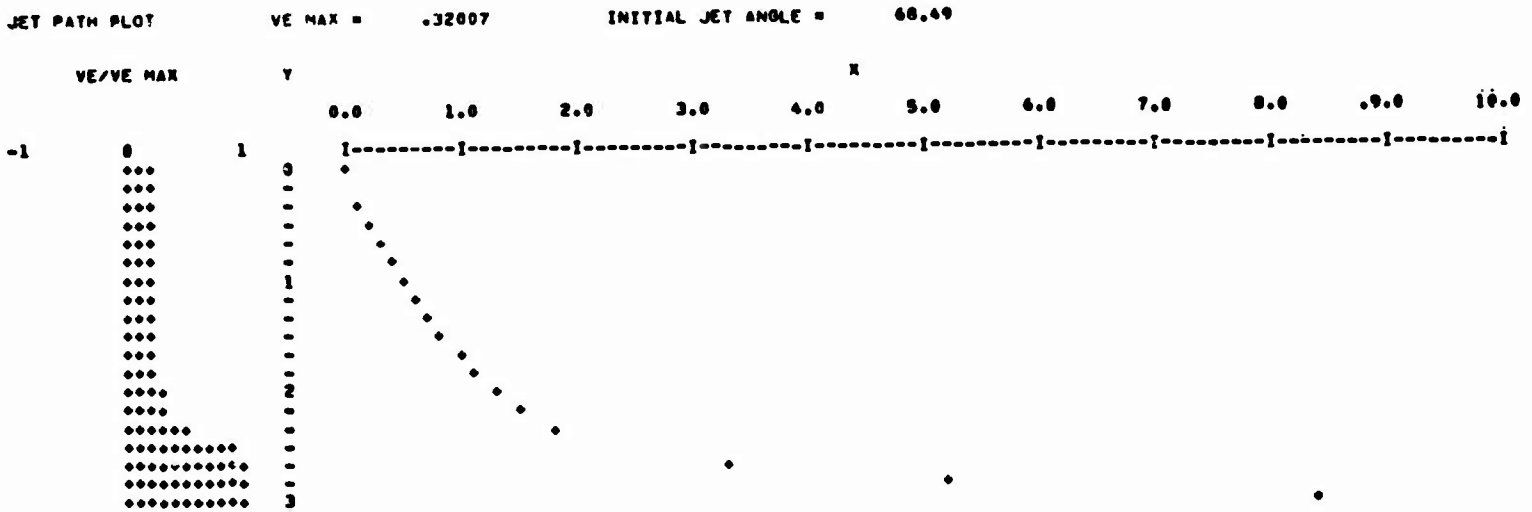
DUCT AREA RATIO

X	AREA RATIO
0.000	1.00000
1.800	1.00000
2.200	.26400
10.000	.26400

TABLE XXXII. (CONTD)

Y	Y/DO	X	X/DO	S	S/DO	H	H/DO	VE	VG	VDP	VJ CL	TDP	TJ CL	BETA	WJ/WJO	K
0.000	0.00	0.000	0.00	0.000	0.00	.12	.83	.076	39.1	1.000	304.0	1.000	830.	69.49	1.00	.5185
.147	1.00	.059	.40	.158	1.08	.21	1.46	.084	43.4	1.000	304.0	1.000	830.	67.87	1.07	.5826
.294	2.00	.120	.82	.317	2.16	.31	2.09	.084	43.4	1.000	304.0	1.000	830.	66.96	1.19	.5826
.440	3.00	.184	1.25	.477	3.25	.40	2.72	.084	43.4	1.000	304.0	.797	1317.	65.77	1.34	.5826
.587	4.00	.252	1.72	.639	4.35	.49	3.37	.084	43.4	.623	205.7	.461	2124.	64.31	1.54	.5826
.734	5.00	.325	2.22	.803	5.47	.59	4.02	.084	43.4	.380	142.4	.281	2556.	62.59	1.78	.5826
.881	6.00	.405	2.76	.970	6.61	.69	4.68	.084	43.4	.233	104.2	.172	2816.	60.65	2.06	.5826
1.028	7.00	.491	3.34	1.141	7.77	.79	5.35	.084	43.4	.137	79.1	.101	2947.	58.51	2.38	.5826
1.175	8.00	.585	3.98	1.315	8.96	.89	6.05	.084	43.4	.069	61.4	.051	3108.	56.19	2.74	.5826
1.321	9.00	.688	4.68	1.494	10.18	.99	6.76	.084	43.4	.018	48.3	.014	3197.	53.74	3.15	.5826
1.468	10.00	.801	5.45	1.679	11.44	1.10	7.49	.084	43.4	0.000	43.4	0.000	3230.	51.18	3.61	.5826
1.615	11.00	.925	6.30	1.872	12.75	1.21	8.25	.084	43.4	0.000	43.4	0.000	3230.	48.56	4.11	.5826
1.762	12.00	1.060	7.22	2.072	14.11	1.33	9.05	.084	43.4	0.000	43.4	0.000	3230.	45.91	4.66	.5826
1.909	13.00	1.210	8.24	2.281	15.54	1.46	9.91	.092	47.5	0.000	47.5	0.000	3230.	42.98	5.61	.6422
2.056	14.00	1.378	9.39	2.505	17.06	1.61	10.95	.105	54.0	0.000	54.0	0.000	3230.	39.01	7.05	.7408
2.202	15.00	1.578	10.75	2.752	18.75	1.81	12.32	.126	64.6	0.000	64.6	0.000	3230.	33.42	9.26	.9019
2.283	15.55	1.710	11.65	2.907	19.80	1.95	13.29	.144	74.2	0.000	74.2	0.000	3230.	29.39	11.70	.9595
2.357	16.05	1.853	12.62	3.068	20.89	2.11	14.38	.172	88.3	0.000	88.3	0.000	3230.	25.06	14.07	1.0343
2.430	16.55	2.030	13.83	3.260	22.20	2.31	15.76	.225	115.7	0.000	115.7	0.000	3230.	19.91	19.14	1.0600
2.481	16.90	2.191	14.92	3.429	23.35	2.49	16.96	.313	161.0	0.000	161.0	0.000	3230.	15.59	27.63	1.0069
2.518	17.15	2.339	15.93	3.581	24.39	2.64	18.00	.320	164.6	0.000	164.6	0.000	3230.	12.60	30.19	1.0011
2.555	17.40	2.520	17.16	3.766	25.65	2.83	19.26	.320	164.6	0.000	164.6	0.000	3230.	10.47	31.25	1.0011
2.592	17.65	2.737	18.64	3.985	27.14	3.05	20.75	.320	164.6	0.000	164.6	0.000	3230.	8.89	32.46	1.0011
2.628	17.90	2.990	20.37	4.242	28.89	3.30	22.50	.320	164.6	0.000	164.6	0.000	3230.	7.66	33.77	1.0011
2.665	18.15	3.283	22.36	4.537	30.90	3.60	24.52	.320	164.6	0.000	164.6	0.000	3230.	6.68	35.19	1.0011
2.702	18.40	3.619	24.64	4.874	33.20	3.94	26.81	.320	164.6	0.000	164.6	0.000	3230.	5.87	36.74	1.0011
2.738	18.65	3.999	27.23	5.256	35.80	4.32	29.42	.320	164.6	0.000	164.6	0.000	3230.	5.20	38.44	1.0011
2.775	18.90	4.427	30.15	5.686	38.73	4.75	32.35	.320	164.6	0.000	164.6	0.000	3230.	4.62	40.31	1.0011
2.812	19.15	4.908	33.42	6.168	42.01	5.23	35.64	.320	164.6	0.000	164.6	0.000	3230.	4.13	42.36	1.0011
2.849	19.40	5.445	37.08	6.707	45.67	5.77	39.31	.320	164.6	0.000	164.6	0.000	3230.	3.71	44.63	1.0011
2.885	19.65	6.043	41.16	7.306	49.76	6.37	43.40	.320	164.6	0.000	164.6	0.000	3230.	3.33	47.13	1.0011
2.922	19.90	6.708	45.69	7.972	54.29	7.04	47.93	.320	164.6	0.000	164.6	0.000	3230.	3.00	49.89	1.0011
2.959	20.15	7.445	50.71	8.710	59.32	7.78	52.97	.320	164.6	0.000	164.6	0.000	3230.	2.71	52.95	1.0011
2.995	20.40	8.261	56.26	9.527	64.88	8.59	58.54	.320	164.6	0.000	164.6	0.000	3230.	2.45	56.32	1.0011
3.032	20.65	9.163	62.41	10.429	71.03	9.50	64.69	.320	164.6	0.000	164.6	0.000	3230.	2.22	60.04	1.0011
3.069	20.90	10.160	69.19	11.426	77.82	10.50	71.49	.320	164.6	0.000	164.6	0.000	3230.	2.01	64.16	1.0011

TABLE XXXII. (CONTD)



5.0 PROGRAM APPLICATION

The main objective in dilution-zone design is to optimize the dilution air injection to obtain maximum mixing in a minimum length. The ultimate goal is to be able to predict the pattern factor and the effects of geometric combustor changes to improve the pattern factor. The analytical model can be used at several levels of complexity to assist in achieving these goals.

The level of complexity is dependent on the information available about the primary-zone exit conditions. For small annular combustors, the width of the annulus is primarily determined by fuel nozzle spacing and primary-zone considerations. The airflow available for dilution is generally that which is left after requirements for primary and wall cooling air are established. The major design parameters to be established for the dilution zone are the distribution, the configuration and size of orifices, and the length.

From the analysis the main correlating parameter, V_e, can be used to characterize the dilution-zone design. Refer to the table of nomenclature for symbol definition.

$$V_e = \text{SQRT } (\rho_p/\rho_{jo}) \times V_p/V_{jo} \tag{159}$$

This relation can be related to the main combustor design parameters as follows: the primary-zone exit velocity can be related to reference velocity by area, density, and weight-flow ratios. The jet velocity can be related to combustor pressure drop. With these substitutions, the equation for V_e becomes

$$V_e = 0.01707 \frac{\text{SQRT } (\rho_{jo}/\rho_p)}{\text{SQRT } (T_3 \times \Delta P/P} \times V_r \cdot \frac{A_r}{A_p} \times \frac{w_p}{w_t} \tag{160}$$

With the exception of densities, all variables in this equation are defined by other considerations. The jet density can be estimated as combustor inlet density. The primary-zone exit density can be computed from the adiabatic temperature rise at primary-zone fuel-air ratio with some assumed primary-zone combustion efficiency. If no information is available, an assumption of 80 percent is probably reasonable.

Table XXXII shows a jet trajectory calculation for a test case and will be used to illustrate the procedure for applying the method. Input conditions were taken from the results of the AiResearch Annulus Loss Model, Program 1173. The trajectory calculation applies to the first dilution orifice. The V_e parameter has a value of 0.076.

Consideration of the typical ranges of the various parameters in the V_e can range from 0.02 to 0.8. For typical annular reverse-flow combustors with a reference velocity of 25 feet per second, a pressure drop of 3 percent, an inlet temperature of 600°F, a reference-to-liner-area ratio of 1.6, and a primary flow fraction of 0.35, the V_e parameter is 0.04. Values of V_e should probably be kept below about 0.25 for good penetration.

From Table XXXII, Sheet 2 it is seen that the jet temperature decay parameter, TDP, drops to 0.1 within a path length, S/DO, 7.77 jet diameters so that mixing is essentially complete at that point. This point occurs at a penetration depth, Y, of 1.028 inches, which is 75 percent of the 1.37-inch annulus width of the combustor and at a length of 0.5 inch from the injection point. If it is assumed that peak temperatures occur at the annulus centerline, it is apparent that this orifice is sized to reach beyond the centerline and may be somewhat oversized.

With regard to orifice spacing, the centerline circumference of the combustor is 27 inches. For the 12 orifices originally selected, the spacing is 2.25 inches, or 11.25 orifice diameters. Table XXXII, Sheet 2 shows the jet spreading, H/DO, to be 5.35 jet diameters (4 orifice diameters) at the end of mixing (TDP = 0.1). Spreading is therefore insufficient to obtain full coverage. The number of holes could be increased with reduced diameters, or the downstream dilution ports could be located between those upstream.

Experience has shown that 3 to 4 dilution holes per fuel injector should be used. With 8 injectors in the test case combustor, an increase from 12 to 24 holes would be reasonable. The following parameter can be used to characterize the spreading:

$$\frac{C}{NH} = \frac{\Pi}{4} \frac{C\ D_h}{A_t\ (H/D_h)} = \frac{\pi}{4} \frac{C\ D_h}{A_t\ (H/D_o)\ \sqrt{C_d}} \qquad (161)$$

A value of 1.0 would indicate complete spreading. For 12 holes, the value is 2.81, decreasing to 1.98 and 1.725 for 24 and 32 holes, respectively. Further increase in the number of holes would probably result in inadequate penetration. The process of checking penetration and spreading should be iterated until a satisfactory compromise is achieved.

The procedure just described is applied to each dilution row in succession. Downstream rows should be located at the distance, X, from the previous row where the temperature decay parameter had reached 0.1. Gas stream conditions for the downstream rows should be estimated by adjusting the primary zone exit velocity and temperature by the flow mixing in from the upstream rows and including an increase in combustion efficiency.

With regard to orifice configuration, initial design computations should be made with circular orifices assumed (lowest cost). When V_e is relatively high and adequate penetration cannot be achieved, rectangular orifices can be considered with the long dimension aligned with the flow. If V_e values are very low, a circular jet will probably impinge on the opposite wall before mixing is completed. Consideration can then be given to a rectangular orifice with the long dimension at a right angle to the mainstream. Also, when annulus velocities are sufficiently high to result in jet injection angles less than 70 degrees, orifices should be plunged. Tests have shown that plunged orifices have injection angles of 80 to 90 degrees regardless of annulus velocity. This also occurs if the ratio of the orifice diameter to the wall thickness is less than about 4.

With regard to prediction of pattern factor, the jet trajectory program cannot be used alone, since it deals with a jet mixing into an infinite stream. The maximum gas temperature and resultant pattern factor, therefore, remain constant up to the point at which spreading of adjacent jets begins to overlap.

The output of the jet trajectory analysis can be used as input to the Gosman program to compute temperature profile decay rates as a function of duct length. Preliminary indications are that after the initial jet mixing length, the pattern factor decays very slowly. The final turbine inlet pattern factor is, therefore, highly dependent on the primary-zone exit pattern factor.

In summary, the various applications of the procedure include the use of the V_e parameter in terms of combustor design parameters to characterize the dilution-zone design.

If V_e differs greatly from the range of 0.1 to 0.5, consideration should be given to raising or lowering the pressure drop or changing geometry. With geometry established, the trajectory analysis can be applied to determine optimum orifice sizes, configuration, and spacing. Finally, the Gosman program can be employed to estimate pattern-factor decay.